

BLACK HOLES IN HIGHER DIMENSIONS

Black holes are one of the most remarkable predictions of Einstein's general relativity. Now widely accepted by the scientific community, most work has focused on black holes in our familiar four spacetime dimensions. In recent years, however, ideas in brane-world cosmology, string theory, and gauge/gravity duality have all motivated a study of black holes in more than four dimensions, with surprising results. In higher dimensions, black holes exist with exotic shapes and unusual dynamics.

Edited by leading expert Gary Horowitz, this exciting book is the first devoted to this new field. The major discoveries are explained by the people who made them: for example, Rob Myers describes the Myers–Perry solutions that represent rotating black holes in higher dimensions; Ruth Gregory describes the Gregory–Laflamme instability of black strings; and Juan Maldacena introduces gauge/gravity duality, the remarkable correspondence that relates a gravitational theory to nongravitational physics. There are two additional chapters on this duality, explaining how black holes can be used to describe relativistic fluids and aspects of condensed matter physics.

Accessible to anyone who has taken a standard graduate course in general relativity, this book provides an important resource for graduate students and for researchers in general relativity, string theory, and high energy physics.

GARY T. HOROWITZ is a professor of physics at the University of California, Santa Barbara. He has made numerous contributions to classical and quantum gravity. In particular, he (co-)discovered a class of higher-dimensional black holes called “black branes”. Professor Horowitz is a member of the National Academy of Science, a Fellow of the American Physical Society, and a member of the International Committee for the General Relativity and Gravitation Society. He has won the Xanthopoulos Prize in general relativity and has written over 150 research articles.

BLACK HOLES IN HIGHER DIMENSIONS

Edited by

GARY T. HOROWITZ



CAMBRIDGE
UNIVERSITY PRESS

CAMBRIDGE UNIVERSITY PRESS
Cambridge, New York, Melbourne, Madrid, Cape Town,
Singapore, São Paulo, Delhi, Mexico City

Cambridge University Press
The Edinburgh Building, Cambridge CB2 8RU, UK

Published in the United States of America by Cambridge University Press, New York

www.cambridge.org
Information on this title: www.cambridge.org/9781107013452

© Cambridge University Press 2012

This publication is in copyright. Subject to statutory exception
and to the provisions of relevant collective licensing agreements,
no reproduction of any part may take place without the written
permission of Cambridge University Press.

First published 2012

Printed in the United Kingdom at the University Press, Cambridge

A catalogue record for this publication is available from the British Library

Library of Congress Cataloguing in Publication data
Black holes in higher dimensions / edited by Gary T. Horowitz.
p. cm.

ISBN 978-1-107-01345-2 (hardback)
Black holes (Astronomy) – Mathematical models. 2. Hyperspace. I. Horowitz, Gary T., 1955–
QB843.B55.B5878 2012
523.8'875 – dc23 2011053168

ISBN 978-1-107-01345-2 Hardback

Cambridge University Press has no responsibility for the persistence or
accuracy of URLs for external or third-party internet websites referred to
in this publication, and does not guarantee that any content on such
websites is, or will remain, accurate or appropriate.

Contents

	page
<i>List of contributors</i>	ix
<i>Preface</i>	xi
Part I Introduction	1
1 Black holes in four dimensions	3
GARY T. HOROWITZ	
1.1 Schwarzschild solution	3
1.2 Reissner–Nordström solution	6
1.3 Kerr solution	10
1.4 Black holes with nonzero cosmological constant	14
1.5 General properties of four-dimensional black holes	16
1.6 Black hole thermodynamics	20
Part II Kaluza–Klein theory	27
2 The Gregory–Laflamme instability	29
RUTH GREGORY	
2.1 Overview	29
2.2 Black holes in higher dimensions	30
2.3 A thermodynamic argument for instability	32
2.4 Perturbing the black string	33
2.5 Consequences of the instability	40
3 Final state of Gregory–Laflamme instability	44
LUIS LEHNER AND FRANS PRETORIUS	
3.1 Overview	44
3.2 Background	45
3.3 Numerical approach	46

	<i>Contents</i>	
3.4	Evolution of an unstable black string	54
3.5	Speculations and open questions	60
4	General black holes in Kaluza–Klein theory <small>GARY T. HOROWITZ AND TOBY WISEMAN</small>	69
4.1	Energy in Kaluza–Klein theory	69
4.2	Homogeneous black hole solutions	72
4.3	Inhomogeneous black hole solutions	81
Part III Asymptotically flat solutions		99
5	Myers–Perry black holes <small>ROBERT C. MYERS</small>	101
5.1	Static black holes	101
5.2	Spinning black holes	103
5.3	Appendix A: Mass and angular momentum	126
5.4	Appendix B: A case study of $d = 5$	128
6	Black rings <small>ROBERTO EMPARAN AND HARVEY S. REALL</small>	134
6.1	Introduction	134
6.2	Ring coordinates	135
6.3	Singly spinning black ring solution	138
6.4	Black ring with two angular momenta	145
6.5	Multiple black hole solutions	148
6.6	Stability	152
Part IV General properties		157
7	Constraints on the topology of higher-dimensional black holes <small>GREGORY J. GALLOWAY</small>	159
7.1	Introduction	159
7.2	Hawking’s theorem on black hole topology	160
7.3	Marginally outer-trapped surfaces	161
7.4	A generalization of Hawking’s theorem and some topological restrictions	164
7.5	The proof of Theorem 7.4.1	166
7.6	The borderline case	170
7.7	Effect of the cosmological constant	171
7.8	Further constraints on black hole topology	173
7.9	Final remarks	176

	<i>Contents</i>	
8	Blackfolds <small>ROBERTO EMPARAN</small>	180
8.1	Introduction	180
8.2	Effective theory for black hole motion	181
8.3	Effective blackfold theory	184
8.4	Stationary blackfolds, action principle, and thermodynamics	190
8.5	Examples of blackfold solutions	196
8.6	Gregory–Laflamme instability and black brane viscosity	204
8.7	Extensions	208
8.8	Appendix: Geometry of submanifolds	209
9	Algebraically special solutions in higher dimensions <small>HARVEY S. REALL</small>	213
9.1	Introduction	213
9.2	CMPP classification	214
9.3	De Smet classification	224
9.4	Other approaches	227
9.5	Outlook	229
10	Numerical construction of static and stationary black holes <small>TOBY WISEMAN</small>	233
10.1	Introduction	233
10.2	Static vacuum black holes	236
10.3	Stationary vacuum solutions	257
Part V Advanced topics		271
11	Black holes and branes in supergravity <small>DONALD MAROLF</small>	273
11.1	Introduction	273
11.2	Supergravity in eleven dimensions	274
11.3	M-branes: the BPS solutions	285
11.4	Kaluza–Klein and dimensional reduction	296
11.5	Branes in 9+1 type II supergravity	304
11.6	Some remarks on string perturbation theory	313
12	The gauge/gravity duality <small>JUAN MALDACENA</small>	325
12.1	Scalar field in AdS	332
12.2	The $\mathcal{N} = 4$ super Yang–Mills/AdS ₅ × S ⁵ example	335
12.3	The spectrum of states or operators	342
12.4	The radial direction	343

13	The fluid/gravity correspondence VERONIKA E. HUBENY, SHIRAZ MINWALLA, MUKUND RANGAMANI	348
13.1	Introduction	348
13.2	Relativistic fluid dynamics	353
13.3	Perturbative construction of gravity solutions	359
13.4	Results at second order	363
13.5	Specific fluid flows and their gravitational analogue	370
13.6	Extensions beyond conformal fluids	374
13.7	Relation to other developments	380
13.8	Summary	382
13.9	Epilogue: Einstein and Boltzmann	383
14	Horizons, holography and condensed matter SEAN A. HARTNOLL	387
14.1	Introduction	387
14.2	Preliminary holographic notions	388
14.3	Brief condensed matter motivation	392
14.4	Holography with a chemical potential	396
14.5	The planar Reissner–Nordström–AdS black hole	397
14.6	Holographic superconductors	400
14.7	Electron stars	405
14.8	Dilatonic scalars: Lifshitz and beyond	410
14.9	Horizons, fractionalisation and black hole information	412
<i>Index</i>		420

Contributors

Roberto Emparan

Institució Catalana de Recerca i Estudis Avançats (ICREA), Passeig Lluís Companys 23, E-08010 Barcelona, Spain; Departament de Física Fonamental and Institut de Ciències del Cosmos, Universitat de Barcelona, Martí i Franquès 1, E-08028 Barcelona, Spain

Gregory J. Galloway

Department of Mathematics, University of Miami, Coral Gables, FL 33124, USA

Ruth Gregory

Centre for Particle Theory, Durham University, Durham, DH1 3LE, UK

Sean A. Hartnoll

Department of Physics, Stanford University, Stanford, CA 94305, USA

Gary T. Horowitz

Department of Physics, University of California at Santa Barbara, Santa Barbara, CA 93106, USA

Veronika E. Hubeny

Centre for Particle Theory, Durham University, Durham, DH1 3LE, UK

Luis Lehner

Perimeter Institute, Waterloo, Ontario N2L 2Y5, Canada; Department of Physics, University of Guelph, Ontario N1G 2W1, Canada

Juan Maldacena

Institute for Advanced Study, Princeton, NJ 08540, USA

Donald Marolf

Department of Physics, University of California at Santa Barbara, Santa Barbara, CA 93106, USA

Shiraz Minwalla

Tata Institute of Fundamental Research, Homi Bhabha Rd, Mumbai 400005, India

Robert C. Myers

Perimeter Institute, Waterloo, Ontario N2L 2Y5, Canada

Frans Pretorius

Department of Physics, Princeton University, Princeton, NJ 08544, USA

Mukund Rangamani

Centre for Particle Theory, Durham University, Durham, DH1 3LE, UK

Harvey S. Reall

Department of Applied Mathematics and Theoretical Physics, Cambridge University, Cambridge, CB3 0WA, UK

Toby Wiseman

Theoretical Physics Group, Blackett Laboratory, Imperial College, London SW7 2AZ, UK

Preface

Black holes are one of the most striking predictions of general relativity. Their main classical properties were understood by the 1970s. In particular, it had been shown that they are very simple objects: stationary vacuum black holes are uniquely characterized by their mass and angular momentum. Astrophysical evidence for black holes has improved dramatically over the past decade and it is now widely accepted that black holes are ubiquitous in our universe.

Naturally enough, the work through the 1970s was focused on black holes in our familiar four spacetime dimensions ($D = 4$). Recently, there has been an explosion of interest in higher-dimensional black holes. There are at least four reasons for this.

(1) As mentioned above, black holes in $D = 4$ are special: they must be spherical, specified by a few parameters, always stable, etc. It is natural to ask whether these properties are characteristic of black holes in general or just a result of four spacetime dimensions.

(2) Recent brane-world ideas suggest that our familiar three spatial dimensions might just be a surface in a higher-dimensional space. In these theories, nongravitational forces are confined to the brane but gravity is higher dimensional. So black holes extend into the extra dimensions.

(3) String theory, one of the most promising approaches to quantum gravity, predicts that spacetime has more than four dimensions. This incorporates older ideas of unification based on the idea that extra dimensions are curled up into a small ball. So, in string theory we must consider higher-dimensional black holes.

(4) Gauge/gravity duality, which has emerged from string theory, relates certain strongly coupled nongravitational theories to higher-dimensional theories with gravity. Under this duality, thermal equilibrium in some (3+1)-dimensional non-gravitational systems is described by a higher-dimensional black hole.

Over the past two decades we have learned that higher-dimensional black holes are much less constrained than their cousins in $D = 4$. They do not have to be

spherical, and they are not uniquely determined by their mass and angular momentum. In addition, they have more interesting dynamics, since some stationary black holes are unstable. This instability causes the horizon to pinch off in finite time, producing a singularity that is visible from infinity, i.e., a naked singularity. So while there is strong evidence that naked singularities cannot form generically in four-dimensional general relativity, they do form generically in higher dimensions.

Given all these exciting results, the time is right for a book devoted to higher-dimensional black holes and some of their applications. I have asked people who have made significant contributions to this subject to explain them for this edited volume. The book is not an exact-solutions manual, with all known $D > 4$ black hole solutions included. Since the field is still progressing, that would quickly become obsolete. Instead, while it includes the most important explicitly known solutions, it focuses on general properties of higher-dimensional black holes and their recent applications to other areas of physics.

The book is divided into five parts. The first gives a brief introduction, reviewing the familiar four-dimensional black holes. The next part is devoted to five-dimensional Kaluza–Klein theory. This is the oldest approach to higher dimensions, in which one adds a single compact extra dimension to general relativity. This is the simplest setting in which to introduce the Gregory–Laflamme instability (described in a chapter by Ruth Gregory) and the resulting pinch-off of the horizon (explained by Luis Lehner and Frans Pretorius). There is also a chapter (by Toby Wiseman and Gary Horowitz) on general Kaluza–Klein black holes, including solutions that are homogeneous in the extra dimension and those that are not.

In Part III some asymptotically flat higher dimensional black holes are described. The higher-dimensional analogues of the Kerr solution are Myers–Perry black holes (described in a chapter by Rob Myers). The first nonspherical black hole was the black ring discovered by (and explained by) Roberto Emparan and Harvey Reall. After these analytic solutions, the next part focuses on more general higher-dimensional black holes. There is a chapter by Greg Galloway on the possible topologies of higher-dimensional horizons, and a chapter by Roberto Emparan on blackfolds – a way of approximately constructing higher-dimensional black holes that realize some of these nontrivial topologies. Harvey Reall describes algebraically special solutions in higher dimensions and Toby Wiseman explains how to numerically construct general static and stationary black holes.

Essentially everything up to this point is based on the (higher-dimensional) Einstein equation with zero matter. The final section (which is more than a third of the book) adds some interesting matter fields and describes the recent applications of black holes to other areas of physics. It starts with a chapter by Don Marolf introducing the black holes and branes of ten- and eleven-dimensional supergravity. Juan Maldacena then explains the basic ideas behind the remarkable gauge/gravity

duality, which allows us to relate general relativity to nongravitational physics. Taking the long-wavelength limit of this duality yields a fluid/gravity correspondence (described in a chapter by Veronika Hubeny, Shiraz Minwalla, and Mukund Rangamani). Finally, Sean Hartnoll explains some aspects of the most recent application of gauge/gravity duality, namely to condensed matter physics.

A common theme is the connection between black hole horizons and fluid dynamics. This had already been noticed in the 1980s, with the development of the membrane paradigm, but it has become much more refined in recent years. Similarities to fluids are found in the way the horizon pinches off (Chapter 3), in the effective dynamics of black branes (Chapter 8) and, of course, the fluid/gravity correspondence (Chapter 13).

The book is pedagogical in style, and in most chapters it is assumed only that the reader has taken a standard course on general relativity. (Some chapters in the last part perhaps require a somewhat broader background.) The book should be a useful reference for students and researchers in string theory, high energy theory, and gravitational physics. Owing to the developments described in the final chapter, it may also be of interest to some condensed matter physicists.

I would like to thank the chapter authors for agreeing to contribute to this project and for writing excellent introductions or reviews of their respective topics. They made my job as editor as painless as possible. I also thank the National Science Foundation for providing funding for my research. Finally, I wish to thank my wife, Corinne, for her constant support.

Gary T. Horowitz

Part I

Introduction

Black holes in four dimensions

GARY T. HOROWITZ

In this chapter we briefly review black holes in four spacetime dimensions. (For more details see any standard textbook in general relativity such as [1, 2] and for a guide to the extensive literature see [3, 4].) We begin with some explicit solutions and then discuss their general properties. This will set the stage for our exploration of higher-dimensional black holes in the rest of the book.

1.1 Schwarzschild solution

Within months of Einstein's final formulation of general relativity in 1915, Schwarzschild found an exact solution given by

$$ds^2 = - \left(1 - \frac{2M}{r}\right) dt^2 + \left(1 - \frac{2M}{r}\right)^{-1} dr^2 + r^2 d\Omega^2 \quad (1.1)$$

where $d\Omega^2$ is shorthand for $d\theta^2 + \sin^2\theta d\phi^2$. The parameter M represents the total mass in units with $G = 1 = c$. This metric solves Einstein's equation with $T_{\mu\nu} = 0$, so it is called a vacuum solution. Since the metric is static and spherically symmetric, it was originally interpreted as describing the geometry outside a static spherical star.

The metric (1.1) clearly has a problem at $r = 2M$. For ordinary stars this is a few kilometers, which is much smaller than the radius of the star, so this problem can be ignored. However, it is known that after a star uses up its nuclear fuel it undergoes gravitational collapse. A sufficiently massive star will continue to collapse to essentially zero volume. If the star is spherically symmetric, the geometry outside is given by the Schwarzschild solution. So in this case, we can no longer ignore the problem at $r = 2M$.

In general relativity, one must distinguish between curvature singularities and coordinate singularities. As its name suggests, a curvature singularity is a genuine singularity in spacetime at which the curvature diverges. In contrast, a coordinate singularity is a place where the curvature is perfectly fine but the metric components diverge owing to a bad choice of coordinates. If one computes the square of the Riemann tensor, $R_{\mu\nu\rho\sigma}R^{\mu\nu\rho\sigma}$, for the Schwarzschild solution, one finds that it is proportional to M^2/r^6 . This suggests that $r = 2M$ is just a coordinate singularity (and $r = 0$ is a real curvature singularity).

To find good coordinates across $r = 2M$ it is convenient to base them on the motion of physical particles. One possibility is to use ingoing radial photons. These satisfy

$$v_0 - t = \int \left(1 - \frac{2M}{r}\right)^{-1} dr = r + 2M \ln(r - 2M) \equiv r_* \quad (1.2)$$

where v_0 is a constant labeling the different ingoing radial photons. Setting $v = t + r_*$ and using v as a new time coordinate, the Schwarzschild metric takes the form

$$ds^2 = -\left(1 - \frac{2M}{r}\right) dv^2 + 2dvdr + r^2 d\Omega^2. \quad (1.3)$$

These are called ingoing Eddington–Finkelstein coordinates. The metric is now nonsingular at $r = 2M$. The fact that $g_{vv} = 0$ there just means that the $\partial/\partial v$ Killing field changes from being timelike for $r > 2M$ to spacelike for $r < 2M$. The metric remains invertible and does not change signature. It is clear from (1.2) that $t \rightarrow \infty$ at $r = 2M$, which is why there is a coordinate singularity in the original form of the Schwarzschild solution.

By construction, ingoing light rays follow curves of constant v . Outgoing light rays satisfy

$$\frac{dr}{dv} = \frac{1}{2} \left(1 - \frac{2M}{r}\right). \quad (1.4)$$

For $r > 2M$ the right-hand side is positive, so outgoing light rays move to larger values of r as expected. For $r = 2M$ the right-hand side vanishes, so these are outgoing light rays. For $r < 2M$ the right-hand side is negative, so even outgoing light rays are dragged to smaller radii. This means that any observer following a timelike worldline must decrease r and eventually hit the singularity. The surface $r = 2M$ is called the *event horizon* and the entire region $r \leq 2M$ is a *black hole*.

Surfaces of constant $r < 2M$ are spacelike. Thus, the singularity at $r = 0$ is also spacelike. In other words, the singularity is not at a particular location in space, but

rather at a particular time. Inside the black hole, the singularity is in your future and cannot be avoided.

If we do not include matter then (1.3) does not cover the entire spacetime, even if we let $-\infty < v < \infty$, $0 < r < \infty$. One can show that $e^{v/4M}$ is an affine parameter along the outgoing null geodesics, so the affine parameter never reaches minus infinity in (1.3). Similarly, setting $u = t - r_*$, one can show that $e^{-u/4M}$ is an affine parameter along ingoing null geodesics. To construct the maximally extended spacetime, we introduce Kruskal coordinates X, T based on these affine parameters:

$$\begin{aligned} X &= \frac{1}{2}(e^{v/4M} + e^{-u/4M}) = (r - 2M)^{1/2} e^{r/4M} \cosh \frac{t}{4M}, \\ T &= \frac{1}{2}(e^{v/4M} - e^{-u/4M}) = (r - 2M)^{1/2} e^{r/4M} \sinh \frac{t}{4M}. \end{aligned} \quad (1.5)$$

The Schwarzschild metric becomes

$$ds^2 = \frac{32M^3}{r} e^{-r/2M} (-dT^2 + dX^2) + r^2 d\Omega^2 \quad (1.6)$$

where r is now a function of T and X defined implicitly by

$$X^2 - T^2 = (r - 2M)e^{r/2M}. \quad (1.7)$$

The first thing to note about these new coordinates is that each surface of constant r is represented twice in the (X, T) -plane. There are two hyperbolas with the same value of r . In particular, there are two $r = 0$ singularities (one with $T > 0$ and one with $T < 0$), two asymptotic regions (one with $X \gg 0$ and one with $X \ll 0$), and two event horizons ($T = X$ and $T = -X$).

A convenient way to represent the causal structure of a spacetime is via a Penrose diagram. This is obtained upon conformally rescaling the metric $\tilde{g}_{\mu\nu} = \Omega^2 g_{\mu\nu}$ by a function that goes to zero at infinity, so that infinity is brought to a finite distance in the unphysical metric $\tilde{g}_{\mu\nu}$. If one does this for Minkowski spacetime, one finds that the boundary at infinity consists of two null surfaces, \mathcal{I}^\pm , called future and past null infinity, and three points representing spatial infinity and future and past timelike infinity. The conformal rescaling does not change causal relations. In a Penrose diagram, light cones are drawn at 45 degrees just as in Minkowski spacetime, so these causal relations are easy to see.

After conformally rescaling the metric (1.6) to bring infinity to a finite distance, we get the Penrose diagram shown in Fig. 1.1. Each point in this two-dimensional figure represents a two-sphere of radius r . Region I is the original asymptotically flat region and region II is the black hole. The ingoing Eddington–Finkelstein coordinates cover regions I and II. Region III is the time reverse of a black hole,

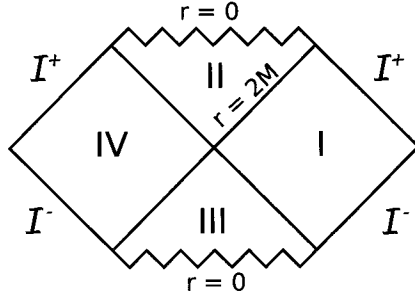


Figure 1.1 Penrose diagram of the maximally extended Schwarzschild solution. There are two asymptotically flat regions (I and IV), a black hole (II), and a white hole (III).

called a white hole. Material can come out of a white hole, but nothing can fall in. Region IV is another asymptotically flat region of spacetime similar to region I. However, it is clear that these two regions are causally disconnected. There is no way for someone in region I to communicate with someone in region IV. A spacelike surface stretching from one asymptotically flat region to the other has the geometry of a wormhole.

To summarize, we have seen that the simple-looking Schwarzschild solution (1.1) is full of surprises. Although originally viewed as the geometry outside a spherical star, it also describes a black hole, a white hole, and a second asymptotic region causally disconnected from the original one. However, one should keep in mind that the maximally extended vacuum spacetime is not very physical. A black hole that forms from a collapsing star does not have regions III or IV.

1.2 Reissner–Nordström solution

A few years after Schwarzschild found his solution, the generalization to the charged case was found by Reissner and Nordström. The metric takes a form similar to (1.1):

$$ds^2 = - \left(1 - \frac{2M}{r} + \frac{Q^2}{r^2} \right) dt^2 + \left(1 - \frac{2M}{r} + \frac{Q^2}{r^2} \right)^{-1} dr^2 + r^2 d\Omega^2 \quad (1.8)$$

where M is again the mass and Q is the charge. For an electrically charged black hole, the only nonzero component of the Maxwell field is $F_{rt} = Q/r^2$. For a magnetically charged black hole, the only nonzero component is $F_{\theta\phi} = Q \sin\theta$. This solves the Einstein–Maxwell equations, which follow from the action

$$S = \int d^4x \sqrt{-g} (R - F_{\mu\nu}F^{\mu\nu}) . \quad (1.9)$$

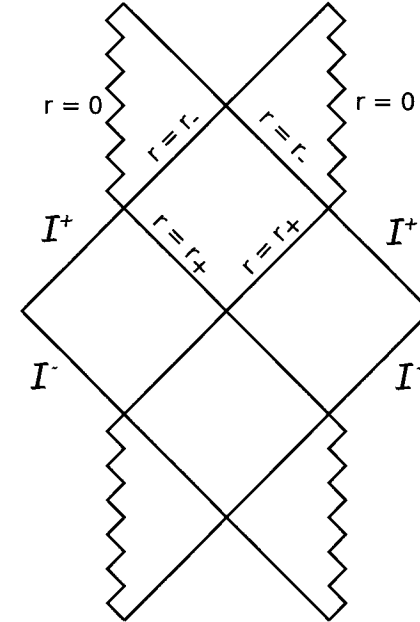


Figure 1.2 The Penrose diagram for the maximally extended Reissner–Nordström solution with $Q < M$. The diagram repeats infinitely often in the vertical direction.

There are three cases to consider, depending on the relative size of M and Q (we will assume $Q > 0$). One might wonder how we can compare mass and charge since they seem to have different units. The answer is to write everything in Planck units. Setting $\hbar = 1$ (as well as $G = c = 1$), the fundamental unit of electric charge is given by $e^2 = 1/137$, so $e \sim (1/10)m_{\text{Planck}} \sim 10^{-6}$ gm.

We consider first the case $M > Q$. It is convenient to write

$$1 - \frac{2M}{r} + \frac{Q^2}{r^2} = \frac{(r - r_+)(r - r_-)}{r^2} \quad (1.10)$$

where $r_{\pm} = M \pm \sqrt{M^2 - Q^2}$. The metric components are singular at $r = r_{\pm}$ and $r = 0$, but only $r = 0$ is a curvature singularity. The surfaces of constant r are timelike for $r < r_-$ so, unlike the Schwarzschild solution, the singularity is timelike. In other words, here the singularity occurs at a location in space and not in time, so it can be avoided. In fact this solution is timelike geodesically complete, so no freely falling observer hits the singularity. The complete spacetime is shown in Fig. 1.2. Note that an arbitrarily small charge Q causes a qualitative change in the causal structure of the solution.

The surface $r = r_+$ is the event horizon and the surface $r = r_-$ is the inner horizon or Cauchy horizon. The Cauchy horizon marks the limit where initial data

on a spacelike surface stretching from one asymptotic region to the other has a unique evolution. Past this horizon the evolution can be modified by unknown boundary conditions at the singularity.

The inner horizon has been shown to be unstable: the slightest perturbation causes the curvature to diverge. To see why, notice that an observer crossing the inner horizon can look back and see the entire future of the asymptotically flat spacetime he or she left behind. Consider a star that is radiating at a fixed distance from the black hole. It will send radiation across the event horizon that gets blueshifted and builds up on the inner horizon. If the star radiates forever, an infinite amount of radiation piles up near $r = r_-$. Of course stars do not radiate forever, but it has been shown that any perturbation outside the horizon causes enough radiation to fall into the black hole for the curvature to diverge at the inner horizon [5, 6]. Interestingly, the singularity that forms is initially rather weak. It is null (not spacelike) and the metric is continuous (but not differentiable) across it. This means that even though the tidal forces diverge, the total tidal distortion remains finite. Whether someone could actually survive a journey across the inner horizon is not clear. There is good evidence that the aforementioned singularity eventually turns into a much stronger spacelike curvature singularity.

Since there is no charged matter, the charge enclosed inside a sphere of radius r is independent of r . Hence one can view the charge as residing at the singularity. The two singularities actually have charges of opposite sign. The reason is that the electric field seen by a family of observers is a spacelike vector pointing from left to right everywhere in Fig. 1.2. The singularity on the left has charge $Q > 0$, and the one on the right has charge $-Q$.

The case $M = Q$ is called the extremal limit. This is the maximum charge that one can put on a black hole of mass M . In this case $r_+ = r_- = Q$, so the spacetime has a single horizon that is degenerate, i.e., g_{tt} has a double zero. The metric takes the form

$$ds^2 = -\left(1 - \frac{Q}{r}\right)^2 dt^2 + \left(1 - \frac{Q}{r}\right)^{-2} dr^2 + r^2 d\Omega^2. \quad (1.11)$$

(Recall that we are assuming charges are positive.) The causal structure is shown in Fig. 1.3.

The proper distance to the horizon from any point $r > Q$ along a surface of constant t is infinite. This may lead you to suspect that the black hole has receded to an infinite distance, but it has not: infalling observers reach the horizon in finite proper time. Similarly, radial null geodesics reach the horizon in finite affine parameter. Letting $\rho = r - Q$, the solution becomes

$$ds^2 = -h^{-2}(\rho)dt^2 + h^2(\rho)(d\rho^2 + \rho^2 d\Omega^2), \quad A_t = h^{-1}, \quad (1.12)$$

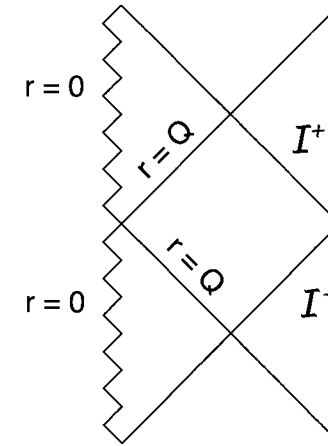


Figure 1.3 The Penrose diagram for the extreme charged black hole. The diagram repeats infinitely often in the vertical direction.

where $h = 1 + Q/\rho$. The horizon is now at $\rho = 0$. In fact, the entire set of Einstein–Maxwell equations reduce to a simple (flat-space!) Laplace equation on h : $\partial^2 h = 0$. Since this is a linear equation, one can superpose solutions. For example, introducing Cartesian coordinates \vec{x} instead of the spherical coordinates ρ, θ, ϕ , the solution

$$h(\vec{x}) = 1 + \sum \frac{Q_i}{|\vec{x} - \vec{x}_i|} \quad (1.13)$$

describes a static collection of extremal black holes with charges Q_i and positions \vec{x}_i . There is no force between extremal black holes since the gravitational attraction is exactly balanced by the Coulomb repulsion. These are known as the Majumdar–Papapetrou solutions.

The fact that the proper distance to the horizon is infinite on a surface of constant t allows one to extract a limiting geometry near the horizon. Starting with (1.12) with $h = 1 + Q/\rho$, write $\rho = \epsilon \tilde{\rho}$, $t = \tilde{t} Q^2/\epsilon$, and take the limit $\epsilon \rightarrow 0$ with the tilded coordinates held fixed. The metric becomes

$$ds^2 = Q^2 \left(-\tilde{\rho}^2 d\tilde{t}^2 + \frac{d\tilde{\rho}^2}{\tilde{\rho}^2} + d\Omega^2 \right). \quad (1.14)$$

This is the product of a two-sphere and a two-dimensional spacetime of constant negative curvature called the anti-de Sitter spacetime (AdS_2). Both these spaces have radius of curvature Q . This near-horizon geometry has more symmetry than the original spacetime. The time-translation symmetry is enhanced to $SO(2, 1)$,

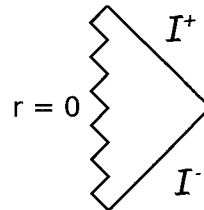


Figure 1.4 The Penrose diagram for the $Q > M$ Reissner–Nordström solution. This is also the Penrose diagram for the Schwarzschild solution with $M < 0$.

which is the symmetry group of AdS_2 . We will talk more about anti-de Sitter spacetime in section 1.4, and extremal black holes will be discussed further in Chapter 11.

Finally, the case $Q > M$ does not describe a black hole at all (see Fig. 1.4). Here $g_{tt} < 0$ everywhere, so $r = 0$ is a timelike singularity that is naked, i.e., visible to distant observers. Can one form such a singularity from smooth initial conditions? It is easy to construct a ball of charged dust with $Q > M$ (recall that the fundamental unit of electric charge corresponds to 10^{-6} gm), but this will not collapse to $r = 0$. The Coulomb repulsion exceeds the gravitational attraction so it would take an infinite amount of energy to compress it to zero volume. We will discuss the possibility of forming naked singularities further in section 1.5.

1.3 Kerr solution

Although the Schwarzschild solution was found just months after the discovery of general relativity and the Reissner–Nordström solution was found a couple years later, it took almost 50 years before the analogous solution for a rotating black hole was found by Kerr. One reason for the delay was that the metric is considerably more complicated:

$$\begin{aligned} ds^2 = & - \left(1 - \frac{2Mr}{\Sigma} \right) dt^2 - \frac{4Mar \sin^2 \theta}{\Sigma} dt d\phi + \frac{\Sigma}{\Delta} dr^2 + \Sigma d\theta^2 \\ & + \left[\frac{(r^2 + a^2)^2 - \Delta a^2 \sin^2 \theta}{\Sigma} \right] \sin^2 \theta d\phi^2, \end{aligned} \quad (1.15)$$

where

$$\Sigma = r^2 + a^2 \cos^2 \theta, \quad \Delta = r^2 - 2Mr + a^2. \quad (1.16)$$

This metric solves the vacuum Einstein equation; it depends on two parameters, the mass M and the angular momentum $J = Ma$. Setting $a = 0$ yields the

Schwarzschild metric and setting $M = 0$ yields flat spacetime in unusual coordinates. The metric is independent of t and ϕ , so the spacetime is stationary and axisymmetric. It is not static, like the Schwarzschild metric, since it is not invariant under $t \rightarrow -t$, but it is invariant under simultaneous reflection in t and ϕ .

A key difference between this metric and those we have studied so far is that $g_{t\phi} \neq 0$. This is true for all rotating objects and has an important consequence. Consider an observer whose four-momentum is orthogonal to a constant- t surface. This observer is “at rest” with respect to the surface of constant t and has zero angular momentum (since $L = P_\mu (\partial/\partial\phi)^\mu$ and the rotational Killing field is tangent to the surface of constant t). Nevertheless, the observer must be rotating with respect to infinity. This can be seen as follows. The observer’s four-momentum takes the form $P^\mu \propto (\partial/\partial t)^\mu + \Omega(\partial/\partial\phi)^\mu$, where Ω can be determined from $0 = P_\mu (\partial/\partial\phi)^\mu \propto g_{t\phi} + \Omega g_{\phi\phi}$. Since we also know that $P^\mu = i(\partial/\partial t)^\mu + \dot{\phi}(\partial/\partial\phi)^\mu$, the coordinate angular velocity is nonzero:

$$\frac{d\phi}{dt} = \Omega = -\frac{g_{t\phi}}{g_{\phi\phi}} = \frac{2Mra}{(r^2 + a^2)^2 - \Delta a^2 \sin^2 \theta}. \quad (1.17)$$

The fact that observers locally at rest must rotate with respect to infinity can be interpreted as a “dragging of inertial frames”. This is a property not just of rotating black holes but of any rotating body in general relativity.

The metric components in (1.15) diverge when $\Sigma = 0$ or when $\Delta = 0$. Only the first is a true curvature singularity. Note that $\Sigma = 0$ implies $r = 0$ and $\theta = \pi/2$. Normally $r = 0$ is a point, and the values of the angular coordinates do not matter. The fact that the singularity only occurs when $r = 0$ and $\theta = \pi/2$ shows that these are not ordinary spherical coordinates. In terms of good coordinates, it turns out that constant- r surfaces (for small r) are ellipsoids that degenerate into a disk of proper radius a when $r = 0$. Surfaces of constant θ are hyperboloids that meet the ellipsoids orthogonally. The angle θ acts like a radial coordinate inside the disk $r = 0$. As a result, the singularity at $r = 0$ and $\theta = \pi/2$ is a ring. If one goes through the center of the ring, one finds another asymptotically flat region of spacetime whose metric is again given by (1.15) but now with $r < 0$.

In close analogy with the situation for the Reissner–Nordström metric, $\Delta = 0$ is a coordinate singularity. There are again three cases, depending on the ratio a/M . We discuss first the physically most interesting choice, $a < M$. In this case Δ has two roots, $r_\pm = M \pm \sqrt{M^2 - a^2}$. The larger root, r_+ , is the event horizon and the smaller root, r_- , is an inner horizon. Since the spacetime is not spherically symmetric, one cannot represent the causal structure completely by a two-dimensional Penrose diagram. However, if one looks at the geometry along a radial line in the equatorial plane, the causal structure is similar to that in Fig. 1.2. If you move

off the equatorial plane, the singularity at $r = 0$ is no longer present and there is another asymptotically flat region of spacetime.

A curious feature of the Kerr metric is the presence of closed timelike curves. Consider a curve parameterized by ϕ near the singularity on the other side of the $r = 0$ disk. Taking t constant, r small, and $\theta \approx \pi/2$, we have $g_{\phi\phi} \approx 2Mr a^2/(r^2 + a^2 \cos^2 \theta)$. But after going through the disk, $r < 0$. So $g_{\phi\phi} < 0$ and this is a closed timelike curve! In fact, one can show that there is a closed timelike curve through every point inside the inner horizon. Unfortunately, this time machine is probably unphysical since the inner horizon is unstable for reasons similar to those applying in the Reissner–Nordström case.

The Kerr solution has a new feature *outside* the black hole, which has important physical consequences: $\partial/\partial t$ becomes spacelike when $r^2 - 2Mr + a^2 \cos^2 \theta < 0$, and this region extends outside the event horizon. It is called the *ergoregion*. Since $g_{tt} > 0$ in this region, the condition $g_{\mu\nu} u^\mu u^\nu = -1$ on the four-velocity shows that every observer must rotate with respect to infinity: $d\phi/dt > 0$. In other words, the dragging of inertial frames becomes so strong in this region that all observers are dragged around, not just those at rest.

The Killing vector that becomes null at the event horizon is

$$\chi^\mu = (\partial/\partial t)^\mu + \Omega_H (\partial/\partial \phi)^\mu \quad (1.18)$$

where

$$\Omega_H = \frac{a}{2Mr_+} \quad (1.19)$$

is called the angular velocity of the black hole. Note that it agrees with (1.17) evaluated at the horizon.

As Penrose first showed, one can extract energy from a rotating black hole using the ergoregion. Suppose that we have a particle following a geodesic with four-momentum P_μ . It has conserved energy $E = -P_\mu(\partial/\partial t)^\mu$ and angular momentum $L = P_\mu(\partial/\partial \phi)^\mu$. Now suppose that the particle decays into two particles with momenta $P_\mu^{(1)}$ and $P_\mu^{(2)}$. Conservation of momentum requires that $P_\mu = P_\mu^{(1)} + P_\mu^{(2)}$, so $E = E^{(1)} + E^{(2)}$. The vectors $P_\mu^{(1)}$ and $P_\mu^{(2)}$ must be future directed and timelike (or null). Normally $(\partial/\partial t)^\mu$ is also future directed and timelike, which ensures that the energy is not negative, but in the ergoregion this is not the case. Since $(\partial/\partial t)^\mu$ is spacelike, there are geodesics with $E^{(1)} < 0$. These geodesics fall into the black hole, decreasing M , while the remaining particle leaves the black hole with more energy than it had when it entered: $E^{(2)} > E$.

There is an analogue of this process for waves scattering off a rotating black hole. Owing to the symmetries of the Kerr metric, one can expand a scalar field in

modes $\phi(r, \theta)e^{-i\omega t}e^{im\phi}$. Consider the Klein–Gordon current

$$J_\mu = i(\phi \nabla_\mu \phi^* - \phi^* \nabla_\mu \phi). \quad (1.20)$$

This is conserved by virtue of the Klein–Gordon equation. The flux across the horizon is

$$-J_\mu \chi^\mu = 2(\omega - m\Omega_H)|\phi|^2 \quad (1.21)$$

where χ^μ is given in (1.18). This is negative for modes satisfying $\omega < m\Omega_H$. Thus these modes will reflect off the black hole with a larger amplitude than that with which they went in. This is called *superradiance*. It holds for electromagnetic waves and even gravitational waves, as well as for scalars. However, it does not hold for fermionic fields. The analogue of the current (1.20) is manifestly timelike or null for spinor fields, so the flux across the horizon is never negative.

The maximum angular momentum that a black hole of mass M can have is $J = M^2$. This corresponds to $a = M$ in (1.15) and is called the extremal limit. Since the inner and outer horizons have coalesced, there is now a closed timelike curve through every point inside the event horizon. The horizon is again infinitely far away on a surface of constant t (although only a finite distance away in timelike or null directions). One can again take a scaling limit and extract the near-horizon geometry. Set

$$r = M + \epsilon \tilde{r}, \quad t = \frac{\tilde{t}}{\epsilon}, \quad \phi = \tilde{\phi} + \frac{\tilde{t}}{2M\epsilon} \quad (1.22)$$

and take the limit $\epsilon \rightarrow 0$ keeping the tilded coordinates fixed. The shift from ϕ to $\tilde{\phi}$ makes $\partial/\partial \tilde{t}$ tangent to the horizon. In other words, the coordinates corotate with the horizon. The result is [7]

$$ds^2 = J(1 + \cos^2 \theta) \left(-\tilde{r}^2 d\tilde{t}^2 + \frac{d\tilde{r}^2}{\tilde{r}^2} + d\theta^2 \right) + 2J \sin^2 \theta (1 + \cos^2 \theta)^{-1} (d\tilde{\phi} + \tilde{r} d\tilde{t})^2. \quad (1.23)$$

This is a vacuum analogue of the $\text{AdS}_2 \times S^2$ near-horizon geometry found in the extremal Reissner–Nordström metric. As in that case, there is enhanced symmetry. The time translation $\partial/\partial t$ is again replaced by a full $SO(2, 1)$ symmetry group.

Finally, the case $a > M$ does not describe a black hole. The ring singularity at $r = 0, \theta = \pi/2$ is naked and there are closed timelike curves through every point in the spacetime.

1.4 Black holes with nonzero cosmological constant

In the absence of matter, Einstein's equation with nonzero cosmological constant is

$$R_{\mu\nu} - \frac{1}{2} R g_{\mu\nu} + \Lambda g_{\mu\nu} = 0. \quad (1.24)$$

Taking the trace, this equation reduces to $R_{\mu\nu} = \Lambda g_{\mu\nu}$.

If $\Lambda > 0$, the maximally symmetric solution is called de Sitter spacetime. It has constant curvature and can be obtained by considering a timelike hyperboloid in five-dimensional Minkowski spacetime:

$$-T^2 + X_1^2 + X_2^2 + X_3^2 + X_4^2 = L^2. \quad (1.25)$$

In globally valid coordinates, the induced metric on this surface takes the form

$$ds^2 = -d\tilde{t}^2 + L^2 \cosh^2(\tilde{t}/L) d\Omega_3^2, \quad (1.26)$$

where $d\Omega_3^2$ denotes the metric on a unit three-sphere. This solves Einstein's equation with $\Lambda = 3/L^2$. The symmetry group is $SO(1, 4)$. Letting t be a coordinate along one of the boost symmetries, we can write the metric in static coordinates:

$$ds^2 = -\left(1 - \frac{r^2}{L^2}\right) dt^2 + \left(1 - \frac{r^2}{L^2}\right)^{-1} dr^2 + r^2 d\Omega^2. \quad (1.27)$$

The surface $r = L$ is null and called the de Sitter horizon.

A (neutral, nonrotating) black hole in de Sitter space is given by

$$ds^2 = -\left(1 - \frac{r^2}{L^2} - \frac{2M}{r}\right) dt^2 + \left(1 - \frac{r^2}{L^2} - \frac{2M}{r}\right)^{-1} dr^2 + r^2 d\Omega^2. \quad (1.28)$$

This describes a black hole only if g_{tt} vanishes, i.e., only if the black hole horizon fits inside the de Sitter horizon. In other words, there is an upper limit to the mass of a black hole in de Sitter space: $M \leq L/3^{3/2}$. If M is bigger than this bound, the singularity at $r = 0$ is naked.

If $\Lambda < 0$, the maximally symmetric solution is anti-de Sitter space. It can be obtained by starting with a five-dimensional flat space with signature $(2, 3)$, for which

$$ds^2 = -dT_1^2 - dT_2^2 + dX_1^2 + dX_2^2 + dX_3^2, \quad (1.29)$$

and considering the metric induced on the surface

$$-T_1^2 - T_2^2 + X_1^2 + X_2^2 + X_3^2 = -L^2. \quad (1.30)$$

Setting $r^2 = X_i X^i$ and letting τ/L be the rotation angle in the (T_1, T_2) -plane, the metric becomes

$$ds^2 = -\left(\frac{r^2}{L^2} + 1\right) d\tau^2 + \left(\frac{r^2}{L^2} + 1\right)^{-1} dr^2 + r^2 d\Omega^2. \quad (1.31)$$

This solves Einstein's equation with $\Lambda = -3/L^2$. In this construction τ is periodic, but it is conventional to unwrap it and let $-\infty < \tau < \infty$, so that there are no closed timelike curves. These coordinates cover the entire spacetime, so anti-de Sitter spacetime is globally static and spherically symmetric. In fact, by construction the symmetry group is $SO(2, 3)$.

Another convenient coordinate system for anti-de Sitter spacetime is obtained by setting $\rho = T_1 - X_1$, $t = T_2 L/\rho$, and $x_i = X_i L/\rho$ for $i = 2, 3$. Then the metric takes the form

$$ds^2 = \frac{\rho^2}{L^2} (-dt^2 + dx_i dx^i) + \frac{L^2}{\rho^2} d\rho^2. \quad (1.32)$$

The coordinates ρ , t , and x_i are known as Poincaré coordinates. They are useful, since the surfaces of constant ρ are flat, but they do not cover the entire spacetime. The surface $\rho = 0$ is null and is called the Poincaré horizon.

A (neutral, nonrotating) black hole in anti-de Sitter spacetime is given by the metric

$$ds^2 = -\left(\frac{r^2}{L^2} + 1 - \frac{2M}{r}\right) d\tau^2 + \left(\frac{r^2}{L^2} + 1 - \frac{2M}{r}\right)^{-1} dr^2 + r^2 d\Omega^2. \quad (1.33)$$

For any $M > 0$, there is one value of r where $g_{tt} = 0$. This is the event horizon, $r = r_+$. Like the black holes we have discussed so far, this one has a spherical horizon. However, anti-de Sitter spacetime also admits black holes with a planar horizon [8]:

$$ds^2 = \frac{\rho^2}{L^2} \left[-\left(1 - \frac{\rho_+^3}{\rho^3}\right) dt^2 + dx_i dx^i \right] + \frac{L^2}{\rho^2} \left(1 - \frac{\rho_+^3}{\rho^3}\right)^{-1} d\rho^2. \quad (1.34)$$

The geometry of the event horizon at $\rho = \rho_+$ (and constant t) is clearly flat. By compactifying x_i we see that anti-de Sitter black holes can have toroidal topology. But we should note that since the identifications extend all the way out to infinity, toroidal black holes only exist in solutions that are locally, but not globally, anti-de Sitter at infinity. In addition there are black holes with a hyperbolic horizon, which are obtained by replacing the terms $+1$ with -1 in (1.33) and replacing $d\Omega^2$ by the metric on a unit hyperboloid. By compactifying the hyperboloid, one can obtain black holes with the topology of any genus g Riemann surface in spacetimes that are locally anti-de Sitter at infinity.

Solutions describing charged and rotating black holes in spacetimes with nonzero cosmological constant have also been found [9].

1.5 General properties of four-dimensional black holes

We now move from talking about specific black hole solutions to general properties of black holes in four dimensions. We will see later that the properties discussed in this section do not generalize to higher dimensions.

1.5.1 Uniqueness

Birkhoff showed that the Schwarzschild metric (1.1) was the only spherically symmetric vacuum solution. So, in the absence of matter a spherically symmetric spacetime must be static. This statement implies that there are no spherical gravitational waves. Birkhoff's theorem extends to the Einstein–Maxwell equations: the only spherically symmetric solution of these equations is the Reissner–Nordström metric (1.8), because there are no spherical electromagnetic waves either. In contrast, there is no analogue of the Birkhoff theorem for the Kerr metric. Axisymmetric spacetimes do not have to be stationary since there are axisymmetric gravitational waves. More importantly, the Kerr metric is not the only stationary axisymmetric vacuum solution. One can consider stationary axisymmetric mass distributions with arbitrary multipole moments, and there are vacuum solutions describing the gravitational field outside the matter.

If one requires an event horizon, the solutions are much more restricted. Israel showed that the only static, asymptotically flat, vacuum solution with a smooth event horizon is the Schwarzschild solution [10]. This came as a surprise since one can form a black hole in many ways, by collapsing matter with arbitrary multipole moments. Israel showed that, if a black hole is not rotating or charged, after it settles down it must be spherically symmetric and be given by the Schwarzschild metric. In other words, static black holes must be spherical. This complements the Birkhoff theorem, which says that spherically symmetric solutions must be static.

Israel extended his theorem to the Einstein–Maxwell equations: the only static, asymptotically flat, electrovac solution with smooth event horizon is the Reissner–Nordström solution. Finally, Robinson, following earlier work by Carter, Hawking, and others, showed that the only stationary, asymptotically flat, vacuum solution with smooth event horizon is the Kerr solution [11]. In particular, stationary vacuum black holes must be axisymmetric.

These results assume a nondegenerate horizon, corresponding to a nonextremal black hole. Indeed, we have seen earlier in the chapter that there are static solutions

consisting of several extremely charged black holes. However, if one restricts one's attention to solutions with a single connected horizon, the uniqueness theorems have recently been extended to the extremal case.

The net result of these uniqueness theorems is that stationary black holes in four-dimensional Einstein–Maxwell theory are uniquely characterized by conserved quantities at infinity, the mass M , charge Q , and angular momentum J . After these results were established, researchers started to consider black holes coupled to other matter fields, such as scalar fields. It was shown that in many cases there were no stationary black holes with nontrivial matter fields outside the horizon; intuitively, the reason is that the matter usually falls into the horizon or radiates out to infinity. These results became known as “no hair” theorems, following Wheeler's colorful description of the fact that black holes have no distinguishing characteristics other than the conserved quantities.

It was later realized, however, that various nonlinear matter fields can exist outside a black hole. For example, if the matter system admits a soliton solution in the absence of gravity then one can usually put a small black hole inside it without destroying the soliton. Nontrivial hair can exist even in theories without solitons. It was realized recently that static charged scalar fields can exist outside a charged black hole in anti-de Sitter spacetime [12]. In fact, near extremality the Reissner–Nordström anti-de Sitter solution is unstable to forming this scalar hair. This instability is the result of a charged analogue of superradiance combined with the fact that a negative cosmological constant acts like a confining box and reflects outgoing waves back toward the black hole.

1.5.2 Stability

The Schwarzschild and Reissner–Nordström solutions have been shown to be stable to linearized perturbations [13]. Black holes do not have ordinary normal modes of oscillation since energy can be lost via radiation out to infinity or via waves falling through the horizon. If one considers perturbations with a harmonic time dependence $e^{-i\omega t}$ and imposes boundary conditions that the modes are purely outgoing at infinity and ingoing at the horizon then one finds solutions for a discrete set of complex ω . These are called *quasinormal modes*. The imaginary part of ω is negative, so these modes oscillate with an exponentially decaying amplitude. A typical perturbation of the black hole decays exponentially for a while but falls off like a power law at late times. This is a result of backscattering of the perturbation off the curvature around the black hole.

The Kerr solution also is almost certainly stable to linearized perturbations, but this has not yet been rigorously established. Individual modes have been shown to be stable, but it is not known whether these modes are complete. A much

more difficult open question is whether black holes are stable to small but finite perturbations. Minkowski space is known to be stable in this strong sense, but the proof even in this case requires sophisticated global analysis. Since a perturbation could add a small angular momentum, one must allow the final state to be Kerr even if one started with a Schwarzschild solution. It is expected that four-dimensional black holes are stable even to nonlinear perturbations. Strong evidence for this comes from numerical relativity, where simulations of black hole collisions and black hole coalescence show that the final black hole settles down to a Kerr metric.

1.5.3 Topology of the event horizon

An asymptotically flat stationary black hole must have spherical topology. This was originally proved by Hawking, and his argument is reviewed in Chapter 7. An alternative proof is now available using *topological censorship* [14]. Roughly speaking, topological censorship amounts to the statement that an observer cannot probe nontrivial topology: all topological structures quickly collapse to a black hole. To make a more precise statement, recall that a causal curve is one whose tangent vector is everywhere timelike or null, and the *null energy condition* holds if $T_{\mu\nu}k^\mu k^\nu \geq 0$ for all null vectors k^μ . This is an inequality on the stress tensor that is satisfied for many interesting matter fields (e.g., Maxwell fields, scalar fields, etc.). Topological censorship states that, given an asymptotically flat spacetime satisfying the null energy condition, every causal curve from past null infinity to future null infinity can be continuously deformed (with fixed endpoints) to a curve in a simply connected neighborhood of null infinity.

To see how this constrains the topology of a four-dimensional black hole, note that a cross section of the event horizon must be a compact oriented two-manifold and hence must have the topology of a sphere with n handles. If $n > 0$ then one could construct a causal curve, from past null infinity to future null infinity, that goes around a handle. Such a curve could not be deformed to one near infinity without crossing the horizon but, once it enters the black hole, a causal curve cannot emerge from it. This contradicts topological censorship unless $n = 0$, i.e. the horizon is topologically S^2 .

We saw earlier that black holes with negative cosmological constant can have a more general topology, because infinity can have a more general topology. There is a version of topological censorship that applies in this case and relates the topology of the event horizon to the topology of (the analogue of null) infinity [15].

1.5.4 Cosmic censorship

The black hole solutions discussed above all have curvature singularities. It was

order to find exact solutions of Einstein's equations. Penrose showed that this was not the case [16]. Independently of any assumption of symmetry, he showed that once gravitational collapse reached a certain point it must continue until it forms a singularity. The “point of no return” is the formation of a *trapped surface*. This is a compact two-dimensional surface having the property that both the outgoing and ingoing null geodesics orthogonal to it are converging.

The singularity theorem does not show that the singularity is always inside an event horizon. There is the possibility of naked singularities, i.e., singularities that remain visible to distant observers. The assumption that naked singularities do not form generically from smooth initial data is known as *cosmic censorship*. The physics near a singularity is not governed by general relativity but rather by quantum gravity. If cosmic censorship holds then general relativity is sufficient to describe all gravitational phenomena outside black holes. If it fails then we have the possibility of observing the effects of quantum gravity directly.¹

To formulate a precise statement of cosmic censorship, one must specify the type of matter under consideration. A simple model of pressureless dust can easily produce naked singularities. These “shell crossing” or “shell focusing” singularities happen even in the absence of gravity, so they are not related to a gravitational instability. A reasonable approach is to consider only matter, such as Maxwell fields or scalar fields, that does not produce singularities when evolved in flat spacetime. One might be tempted to formulate cosmic censorship as the statement that gravity coupled to such matter fields never produces naked singularities.

To explore this, consider an ingoing spherical pulse of scalar field coupled to gravity. When the amplitude of the pulse is small, gravity remains weak and the pulse scatters and goes out to infinity. No singularities form. When the amplitude is large, the scalar field collapses and forms a large black hole. Since the amplitude can be varied continuously, a natural question is what happens at the threshold between these two behaviors. This was studied analytically by Christodoulou [17] and numerically by Choptuik [18]. They showed that for a critical value of the amplitude, which separates black hole formation from solutions with no black hole, the evolution produces a naked singularity. So the simple statement of cosmic censorship above is violated in general relativity. However, in this example the naked singularity is not generic since one has to fine-tune the amplitude. The amount of fine tuning is rather small (assuming spherical symmetry), since the shape of the initial pulse is arbitrary. In the infinite-dimensional space of spherically symmetric initial data, there is a codimension-1 surface that produces naked singularities.

Of more physical interest is a statement about generic solutions. So one might conjecture the following.

Cosmic censorship Generic initial data for gravity coupled to reasonable matter does not produce naked singularities.

It is not yet known whether this conjecture is true, but it seems likely in four dimensions. The evidence in favor of cosmic censorship starts with the stability of black holes discussed above. It has also been shown to hold for a class of solutions with two Killing fields known as the Gowdy spacetimes [19]. In addition, a class of potential counterexamples has been ruled out. Consider some initial data that contain a trapped surface S . Assuming cosmic censorship, one can show that there must be an event horizon surrounding S . Let $A_{\text{BH}}^{\text{in}}$ denote its area. We will show in the next section that the area of event horizons cannot decrease, so under evolution we expect the black hole to settle down to a stationary black hole with larger area A_{BH}^{f} . Since energy can be radiated away in the process, A_{BH}^{f} must be less than the area of the largest black hole with initial mass M , which is a Schwarzschild black hole. Putting this together, we have the “Penrose inequality”

$$A(S) \leq A_{\text{BH}}^{\text{in}} \leq A_{\text{BH}}^{\text{f}} \leq 16\pi M^2. \quad (1.35)$$

The interesting thing about this inequality is that, even though it was derived by assuming standard properties of black holes including cosmic censorship, the final result $A(S) \leq 16\pi M^2$ only involves properties of the initial data. Many people tried unsuccessfully to find initial data violating this inequality. A proof for time-symmetric initial data was eventually found [20, 21].

The evidence presented above for cosmic censorship is still rather weak. More evidence comes from the fact that numerical relativists now have full (3+1)-dimensional codes that can describe, e.g., the collision of black holes and the approach to cosmological singularities. No evidence for naked singularities has yet been seen, but a full analytic proof of cosmic censorship is still far off.

1.6 Black hole thermodynamics

Although we will continue to focus on four spacetime dimensions, the properties of general black holes discussed in this section hold in all dimensions $D \geq 4$.

We begin by defining the event horizon of a dynamical black hole more precisely. The past of a point p , $I^-(p)$, is the set of all events that can be connected to p by a future-directed timelike curve. For asymptotically flat spacetimes, one considers the past of all points on future null infinity $I^-[I^+]$ and defines the black hole to be the complement of this set. This consists of all events that cannot send signals to infinity. The boundary of the black hole, $\partial I^-[I^+]$, is the event horizon. The main advantage of this definition is that the boundary of a past set is always a null surface and is ruled by null geodesics which stay on the boundary. This makes it

easier to prove general properties of the horizon. The main disadvantage is that the event horizon cannot be determined locally. One needs the entire future of the spacetime to know where the event horizon is. Physically, this is reasonable since the collapse of a large massive shell of matter in the future will stop many events from communicating with distant observers. However, for practical reasons one might want a more local definition of a horizon, and there has been extensive work on defining a black hole more locally [22].

To discuss general properties of black holes we will need the following important result. Consider a spacelike two-surface S and a family of outgoing orthogonal null geodesics with tangent k^μ . Let λ be the affine parameter with $\lambda = 0$ on S , and let $h_{\mu\nu}$ be the induced metric on the constant- λ surfaces. Then the expansion θ and shear $\sigma_{\mu\nu}$ of the null geodesics are given by

$$\theta = h^{\mu\nu} \nabla_\mu k_\nu, \quad \sigma_{\mu\nu} = h_\mu^\alpha h_\nu^\beta \nabla_\alpha k_\beta - \frac{\theta}{2} h_{\mu\nu}. \quad (1.36)$$

The rate of change of θ along the geodesics is given by the Raychaudhuri equation:

$$\frac{d\theta}{d\lambda} = -\frac{\theta^2}{2} - \sigma_{\mu\nu}\sigma^{\mu\nu} - 8\pi T_{\mu\nu}k^\mu k^\nu. \quad (1.37)$$

When the null energy condition holds, $T_{\mu\nu}k^\mu k^\nu \geq 0$ and so $d\theta/d\lambda < -\theta^2/2$. If θ were to become negative, i.e., $\theta(0) = -\theta_0 < 0$, then

$$\theta(\lambda) < -\frac{2\theta_0}{2 - \theta_0\lambda} \quad (1.38)$$

and $\theta(\lambda) \rightarrow -\infty$ before $\lambda = 2/\theta_0$. This divergence in θ does not necessarily mean that the geodesics have hit a spacetime singularity. What it does mean is that nearby null geodesics have started to cross.

We now apply this to the null geodesics that lie on the event horizon. If their expansion were to become negative then they would have to cross. But, once null geodesics cross, points along the curve become timelike related and so the curve cannot stay on the boundary of a past set. This is a contradiction since the boundary of a past set (like the event horizon) must be ruled by null geodesics that stay on the boundary. Thus $\theta \geq 0$ everywhere on the horizon. This is the essence of the area theorem [23]. Consider a cross section of the horizon with induced metric $h_{\mu\nu}$ and area A . Then if $h = \det h_{\mu\nu}$, we have

$$\theta = \frac{1}{\sqrt{h}} \frac{d\sqrt{h}}{d\lambda}, \quad (1.39)$$

and so

$$\frac{dA}{d\lambda} = \int \frac{d\sqrt{h}}{d\lambda} d^2x = \int \theta \sqrt{h} d^2x . \quad (1.40)$$

Since $\theta \geq 0$, the area of the event horizon cannot decrease (assuming that the matter satisfies the null energy condition).

To continue our discussion of general properties of black holes, we need the notion of surface gravity. Consider a stationary black hole. Even though we are now allowing general matter fields outside the horizon, one can show that a stationary black hole must be axisymmetric (like the Kerr solution). In fact, the event horizon of a stationary black hole is a *Killing horizon*, i.e., a null hypersurface whose null geodesic generators are orbits of a Killing field χ^μ . Physically, this is expected because otherwise the horizon would change in time and radiate gravitational waves. Since $\chi^\mu \chi_\mu = 0$ on the horizon, $\nabla^\nu (\chi^\mu \chi_\mu)$ is normal to the horizon. But the vector normal to the null event horizon is χ^ν itself. So we must have $\nabla^\nu (\chi^\mu \chi_\mu) = -2\kappa \chi^\nu$ for some κ . Since χ^μ is a Killing field we have

$$\chi^\mu \nabla_\mu \chi^\nu = \kappa \chi^\nu . \quad (1.41)$$

In other words, χ^μ is tangent to a geodesic but is not affinely parameterized. It is related to k^μ (the tangent to the affinely parameterized null geodesic) by $\chi^\mu = (\kappa\lambda)k^\mu$. The quantity κ is called the *surface gravity* of the black hole. For a nonrotating black hole, it is the force you have to exert at infinity to hold a unit mass in place as it approaches the horizon.

A simple way to calculate the surface gravity is the following. Let $\chi^\mu \chi_\mu = -V^2$. Then one can show that

$$\kappa^2 = \lim \nabla_\mu V \nabla^\mu V , \quad (1.42)$$

where the limit is taken as you approach the horizon. For a static spherically symmetric spacetime such as Schwarzschild or Reissner–Nordström, with metric

$$ds^2 = -f(r)dt^2 + \frac{dr^2}{f(r)} + r^2 d\Omega^2 \quad (1.43)$$

and horizon at $r = r_+$, (1.42) reduces to $\kappa = f'(r_+)/2$. For an extremal black hole, f has a double zero at the degenerate event horizon and the surface gravity vanishes.

For the Kerr metric the surface gravity is given by

$$\kappa = \frac{\sqrt{M^2 - a^2}}{2Mr_+} . \quad (1.44)$$

Note that the surface gravity is constant on the horizon despite the fact that the black hole is not spherical. This can be shown to hold in general for any bifurcate Killing horizon. Such a horizon is one for which the Killing field χ^μ vanishes along a cross section, called the bifurcation surface. All nonextremal stationary black holes are expected to have bifurcate Killing horizons. In Fig. 1.1 the bifurcation surface is represented by the point where the two $r = 2M$ horizons meet, and in Fig. 1.2 the bifurcation surface is represented by the point where the two $r = r_+$ horizons meet.

Suppose that one adds a small amount of matter (characterized by $\delta T_{\mu\nu}$) to a stationary black hole with mass M , angular momentum J , and horizon area A . To first order in $\delta T_{\mu\nu}$, M and J will change by an amount given by an integral over the horizon of $\delta T_{\mu\nu}$ contracted with either the time translation or the rotation Killing vectors. More precisely, let k^μ be tangent to the affinely parameterized null geodesic generators of the horizon with affine parameter λ . Then

$$\begin{aligned} \delta M &= \int d\lambda \int dS \delta T_{\mu\nu} (\partial/\partial t)^\mu k^\nu , \\ \delta J &= - \int d\lambda \int dS \delta T_{\mu\nu} (\partial/\partial\varphi)^\mu k^\nu \end{aligned} \quad (1.45)$$

where the second integral is over a cross section of the horizon at constant λ . Now consider the Raychaudhuri equation (1.37). Since initially $\theta = 0$ and $\sigma_{\mu\nu} = 0$, to first order we have

$$\frac{d\theta}{d\lambda} = -8\pi T_{\mu\nu} k^\mu k^\nu . \quad (1.46)$$

Here k^μ is related to the Killing vector χ^μ by

$$k^\mu = \frac{1}{\kappa\lambda} \chi^\mu = \frac{1}{\kappa\lambda} \left(\frac{\partial}{\partial t} + \Omega_H \frac{\partial}{\partial\varphi} \right)^\mu . \quad (1.47)$$

Multiplying both sides of (1.46) by $-\kappa\lambda$ and integrating over the horizon yields

$$\begin{aligned} -\kappa \int d\lambda \int dS \lambda \frac{d\theta}{d\lambda} &= 8\pi \int d\lambda \int dS \delta T_{\mu\nu} (\partial/\partial t + \Omega_H \partial/\partial\varphi)^\mu k^\nu \\ &= 8\pi(\delta M - \Omega_H \delta J) . \end{aligned} \quad (1.48)$$

The left-hand side can be simplified by writing $\lambda d\theta/d\lambda = d(\lambda\theta)/d\lambda - \theta$. Inside the integral, the total derivative term does not contribute since $\theta = 0$ both before and after the matter is thrown in. From (1.40) the remaining integral is just the change in area. So we get

$$\delta M = \frac{\kappa}{8\pi} \delta A + \Omega_H \delta J . \quad (1.49)$$

We can summarize the properties of black holes discussed in this section in the following three laws of black hole mechanics, first derived by Bardeen, Carter, and Hawking [24]:

- (0) κ is constant over the horizon of a stationary black hole;
- (1) $\delta M = \kappa \delta A / 8\pi + \Omega_H \delta J$;
- (2) $\delta A \geq 0$.

There is clearly a close analogy between these three laws and the laws of thermodynamics, where κ plays the role of the temperature and A plays the role of the entropy. The fact that this is more than an analogy was made clear by Hawking, when he coupled quantum matter fields to a classical black hole and showed that they do indeed emit essentially thermal radiation at a temperature (setting \hbar and Boltzmann's constant equal to unity) given by

$$T = \frac{\kappa}{2\pi}. \quad (1.50)$$

Comparing (1.49) with the standard thermodynamic relation $\delta E = T \delta S - P \delta V$ shows that black holes have an entropy

$$S = \frac{A}{4} \quad (1.51)$$

in Planck units. The temperature of a Schwarzschild black hole is $T = 1/(8\pi M)$. Since the temperature increases as the black hole radiates energy, this system has negative specific heat. A solar-mass black hole has an extremely low temperature (10^{-7} K) and an enormous entropy – much greater than the entropy of the matter that collapsed to form it. This suggests that black holes have a large number of microstates. Finding a quantum description of these microstates and showing that there are e^S of them was a challenge for over two decades. It was finally achieved in the mid 1990s. A brief description is given at the end of Chapter 11.

It turns out that black holes in anti-de Sitter spacetime have thermodynamic properties different from those of the asymptotically flat Schwarzschild solution. The planar black hole (1.34) is of particular interest. Dropping the numerical factors, the Hawking temperature is $T \propto \rho_+$. The total energy is $E \propto \rho_+^3 V \propto T^3 V$ and the entropy is $S \propto A \sim \rho_+^2 V \propto T^2 V$. So not only is the specific heat positive, the energy and entropy are exactly like a thermal gas in 2+1 dimensions! This is the first indication that general relativity with anti-de Sitter boundary conditions can be related to nongravitational systems. This will be discussed further in Chapter 12.

References

- [1] S. M. Carroll, *Spacetime and Geometry: An Introduction to General Relativity*, Addison-Wesley (2004), 513 p.

- [2] R. M. Wald, *General Relativity*, Chicago University Press (1984).
- [3] S. Detweiler, Resource letter BH-1: black holes, *Am. J. Phys.* **49** (1981), 394–400.
- [4] E. Gallo and D. Marolf, Resource letter BH-2: black holes, *Am. J. Phys.* **77** (2009), 294–307 [arXiv:0806.2316 [astro-ph]].
- [5] E. Poisson and W. Israel, Internal structure of black holes, *Phys. Rev.* **D41** (1990), 1796–1809.
- [6] M. Dafermos, The interior of charged black holes and the problem of uniqueness in general relativity, *Commun. Pure Appl. Math.* **58** (2005), 445 [arXiv:gr-qc/0307013].
- [7] J. M. Bardeen and G. T. Horowitz, The extreme Kerr throat geometry: a vacuum analog of $AdS(2) \times S^{**2}$, *Phys. Rev.* **D60** (1999), 104030 [hep-th/9905099].
- [8] J. P. S. Lemos, Cylindrical black hole in general relativity, *Phys. Lett.* **B353** (1995), 46–51.
- [9] B. Carter, Hamilton–Jacobi and Schrödinger separable solutions of Einstein's equations, *Commun. Math. Phys.* **10** (1968), 280.
- [10] W. Israel, Event horizons in static vacuum space-times, *Phys. Rev.* **164** (1967), 1776–1779.
- [11] D. C. Robinson, Uniqueness of the Kerr black hole, *Phys. Rev. Lett.* **34** (1975), 905–906.
- [12] S. S. Gubser, Breaking an Abelian gauge symmetry near a black hole horizon, *Phys. Rev.* **D78** (2008), 065034 [arXiv:0801.2977 [hep-th]].
- [13] S. Chandrasekhar, *The Mathematical Theory of Black Holes*, Clarendon Press (1992).
- [14] J. L. Friedman, K. Schleich, and D. M. Witt, Topological censorship, *Phys. Rev. Lett.* **71** (1993), 1486–1489 [gr-qc/9305017].
- [15] G. J. Galloway, K. Schleich, D. M. Witt, and E. Woolgar, Topological censorship and higher genus black holes, *Phys. Rev.* **D60** (1999), 104039 [gr-qc/9902061].
- [16] R. Penrose, Gravitational collapse and space-time singularities, *Phys. Rev. Lett.* **14** (1965), 57–59.
- [17] D. Christodoulou, Examples of naked singularity formation in the gravitational collapse of a scalar field, *Ann. Math.* **140** (1994), 607–653.
- [18] M. W. Choptuik, Universality and scaling in gravitational collapse of a massless scalar field, *Phys. Rev. Lett.* **70** (1993), 9–12.
- [19] H. Ringstrom, Cosmic censorship for Gowdy spacetimes, *Living Rev. Rel.* **13** (2010), 2.
- [20] G. Huisken and T. Ilmanen, The inverse mean curvature flow and the Riemannian Penrose inequality, *J. Differential Geometry* **59** (2001), 353.
- [21] H. Bray, Proof of the Riemannian Penrose inequality using the positive mass theorem, *J. Differential Geometry* **59** (2001), 177.
- [22] A. Ashtekar and B. Krishnan, Isolated and dynamical horizons and their applications, *Living Rev. Rel.* **7** (2004), 10 [gr-qc/0407042].
- [23] S. W. Hawking, Gravitational radiation from colliding black holes, *Phys. Rev. Lett.* **26** (1971), 1344–1346.
- [24] J. M. Bardeen, B. Carter, and S. W. Hawking, The four laws of black hole mechanics, *Commun. Math. Phys.* **31** (1973), 161–170.

Part II

Kaluza–Klein theory

The Gregory–Laflamme instability

RUTH GREGORY

In this chapter we introduce the notion of higher-dimensional gravity in the context of one extra spatial dimension. We focus on the *black string*, a simple extension of the Schwarzschild solution to five dimensions. Here we will show that this solution is unstable to long-wavelength perturbations and discuss its implications and extensions.

2.1 Overview

Kaluza [1] and Klein [2], very shortly after Einstein’s general relativity had been verified by Eddington’s 1919 expedition, suggested that adding an extra dimension to our space could have an amazing consequence: “gravity” in five dimensions with the extra dimension stabilised has the appearance, in a four-dimensional slice, of Einstein–Maxwell theory. Kaluza–Klein theory, as it is now known, is a construction adding to space extra dimensions which are much smaller than scales we can directly physically probe and which thus contribute only a few long-range, or massless, additional forces to nature. Kaluza–Klein theory is reviewed in full in Chapter 4 but, for the purposes of this chapter, we will require only some very basic intuition. We will consider only solutions to vacuum gravity in five dimensions and focus on a particularly simple solution, the black string. We will describe the solution, discuss its properties and then demonstrate explicitly that it is unstable to linear perturbations. We conclude with a brief discussion of the more general situation.

2.2 Black holes in higher dimensions

The Schwarzschild solution in four dimensions is found by solving the vacuum Einstein equations

$$R_{\mu\nu} = 0, \quad (2.1)$$

subject to a physically motivated spherical symmetry restriction. It is known that in four dimensions the only possible static black hole solution must be spherically symmetric – but what happens if we live in four, or more, *spatial* dimensions? In particular, what happens if that final spatial dimension has finite extent and is very small?

In five dimensions, we obviously have to solve the same equation,¹

$$R_{ab} = 0. \quad (2.2)$$

However, we now have to choose an appropriate symmetry for the spacetime metric. An obvious generalisation of the Schwarzschild solution is a metric with a hyperspherically symmetric solution,

$$ds^2 = -V_5(r)dt^2 + V_5(r)^{-1}dr^2 + r^2d\Omega_3^2, \quad (2.3)$$

where V_5 is an appropriate generalisation of the four-dimensional Schwarzschild potential. This is indeed the case (see Chapter 5 or [3] for a discussion of general solutions) if the extra dimension is infinite, when V_5 is given explicitly by

$$V_5(r) = 1 - \frac{r_5^2}{r^2}, \quad (2.4)$$

where r_5 is the horizon radius and is related to the mass of the black hole via [3]

$$r_5^2 = \frac{8G_5M_5}{3\pi}. \quad (2.5)$$

Moreover, there is another simple solution that we can easily guess based on the properties of the Riemann tensor. If we assume that nothing depends on the extra dimension, we can consider a spacetime of the form

$$ds^2 = g_{\mu\nu}(x^\mu)dx^\mu dx^\nu + dz^2, \quad (2.6)$$

for which the Riemann tensor has only four-dimensional components. In this case, a solution of the four-dimensional Einstein equations will automatically be a solution of the five-dimensional Einstein equations, as $R_{5a} = 0$ by construction. Thus, we

¹ We reserve the labels μ, ν, \dots for purely four-dimensional indices, and use a, b, \dots for the full range of dimensions.

can extend the four-dimensional Schwarzschild solution uniformly into the extra dimension to obtain a black string:

$$ds^2 = -V(r)dt^2 + V(r)^{-1}dr^2 + r^2d\Omega_2^2 + dz^2, \quad (2.7)$$

where

$$V(r) = 1 - \frac{r_+}{r} \quad (2.8)$$

is the Schwarzschild potential introduced in the previous chapter ((1.1) with $r_+ = 2M$).

This may seem a rather unremarkable observation, as it is a straightforward solution to write down. Nevertheless, it is the first sign that gravity in higher dimensions may have distinctively new phenomena to offer. In four dimensions black holes are essentially unique, classified by very few parameters: mass, charge and angular momentum. Once these parameters are specified the solution is known and the horizon topology is always spherical. Here, by adding an extra dimension, with very little effort we have constructed two distinct black objects, one with a spherical and one with a cylindrical event horizon. Clearly, these black holes have different masses: the black string has (strictly) infinite mass and is not asymptotically flat. However, our simple construction shows that event horizons in higher dimensions need no longer be spherical [4]; in Chapter 7 we discuss the possible topologies of black objects. As we will see in Chapters 6 and 8, this first indication of the nonuniqueness of “black” solutions is the tip of the iceberg: many distinct black solutions with the same charges exist, see e.g. [5–7].

Now let us consider what happens if our extra dimension is compact, i.e., finite and of length L . This will give the black string a finite length, hence mass, and in fact corresponds to the traditional Kaluza–Klein picture. The black string therefore corresponds to a basic Kaluza–Klein black hole; there is no dependence of the geometry on the extra dimension, which remains a Killing symmetry of the full solution. From the four-dimensional viewpoint it looks just like a Schwarzschild black hole. At energies of order L^{-1} , new physics is expected to come into play – physics corresponding to the additional degrees of freedom of the extra dimension. In our case, as we are considering only vacuum Einstein gravity, our new degrees of freedom correspond to a dependence of the geometry on the extra dimension. Alternatively, from a four-dimensional perspective these can be interpreted as a tower of massive gravitons. We can therefore ask whether there are any alternative solutions to the black string that excite these extra degrees of freedom. An obvious starting point is the five-dimensional “Schwarzschild” solution (2.3). Once we have a finite spatial direction we do not expect exact hyperspherical symmetry, since the finite size of the extra dimension introduces an effective periodicity in one direction,

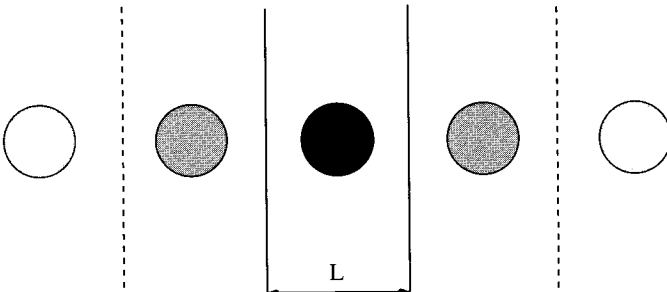


Figure 2.1 A sketch of the five-dimensional black hole confined within a finite extra dimension and its mirror images, with which it interacts.

and hence the black hole will ‘‘interact’’ with the mirror image black holes (see Fig. 2.1), altering the gravitational potential along the extra dimension. For $r_5 \ll L$ the five-dimensional potential (2.4) will be a good approximation to the solution, but for larger black holes the nonlinearity of gravity does not allow for an analytic solution and the geometry must be found numerically. As the mass of a black hole increases further, eventually it can no longer fit inside the extra dimension and must become a string-like solution. These solutions are known as *localised black holes* and *inhomogeneous black strings* and will be discussed further in Chapter 4 (see also [8–10]).

Therefore, within the context of five-dimensional Kaluza–Klein theory there seem to be various options for a simple uncharged black hole: it can be a homogeneous or inhomogeneous black string or a localised black hole. Which solution is the physically relevant one, or which will form in a collapse process? Are all these solutions possible or is there a selection process which rules out some?

The answer is provided by black string instability. Depending on the size of the extra dimension and the mass of the black hole, there is a unique stable solution and hence a unique preferred end state for gravitational collapse. The rest of this chapter is devoted to explaining why the instability is natural and proving that it exists.

2.3 A thermodynamic argument for instability

Typically, in nature, we decide which is the most likely state of a system by determining which has the lowest energy; however, in the case of black holes and black strings, both solutions can have the same energy and therefore a different physical principle must be used. In the last chapter we saw how black holes could be assigned thermodynamic properties, and in thermodynamics it is the state with largest entropy that is preferred. Thus, if there is an entropy

difference between the two states then we might expect that one is preferred over the other.

In the previous chapter the entropy of a black hole was shown to be proportional to its area: $S = A/4$ in Planck units. However, there is a subtlety if we are dealing with Kaluza–Klein theory; this formula for S actually contains a hidden Newton constant and so the Planck mass is dimension dependent in a compactification:

$$M_p^2 = V_{D-4} M_D^{D-2}, \quad (2.9)$$

where V_{D-4} is the volume of the internal space on which we are compactifying and D is the total number of dimensions. For the five-dimensional case that we are considering here, this gives

$$G_5 = L G_4 = L \quad (2.10)$$

(where we have set $G_4 = 1$ in the last step), and hence what we mean by the Planck scale is renormalised by a factor L . We therefore obtain for the entropies of the black hole and black string (assuming, for simplicity, that the black hole is approximated by its exact analytic form (2.3)):

$$S_{\text{BH}} = \frac{\pi^2 r_5^3}{2L}, \quad S_{\text{BS}} = \pi r_+^2, \quad (2.11)$$

where r_5 and r_+ are the horizon radii of the black hole and string respectively. We now need to compare these entropies for the same total mass of hole or string. The black string has mass $r_+/2$ and, using (2.5) and (2.10), the black hole mass is

$$M_5 = \frac{3\pi r_5^2}{8L}. \quad (2.12)$$

Hence, setting the masses equal the entropies can be re-expressed as

$$S_{\text{BH}} = 4\pi M^2 \sqrt{\frac{8L}{27\pi M}}, \quad S_{\text{BS}} = 4\pi M^2. \quad (2.13)$$

Clearly, if L becomes sufficiently large then the black hole will be thermodynamically preferred over the black string and hence the black string solution should have a long-wavelength instability. In order to prove this we have to look at perturbations around the black string solution.

2.4 Perturbing the black string

Now we will show explicitly that the black string is unstable. In order to do this, we perturb the metric (2.7) and solve the linearised Einstein equations to show that there is a growing mode.

There are several issues to bear in mind when considering perturbation theory in general relativity. First, a perturbation must be “small”; this may seem to be a statement of the obvious but when a change of coordinates can make the components of a tensor large we must be careful to interpret correctly what “small” means. Second, we need to specify an initial data surface for our perturbation problem; this, as we will see, ties in with the regularity of the perturbation and is easily resolved by choosing an appropriate Cauchy surface. Finally, gravity has an infinite gauge group, i.e., there are an infinite set of different coordinate transformations that we can perform on any particular geometry and thus there will be many perturbations that are pure gauge. In other words, the act of changing coordinates gives a perturbation to the metric, but one that is not physical. We must therefore be careful to ensure that our perturbation is physical.

2.4.1 Perturbation theory

We begin by defining the perturbation. In Einstein gravity, a small perturbation of a spacetime is represented by a change in metric

$$g_{ab} \rightarrow g_{ab} + h_{ab}, \quad (2.14)$$

under which the Ricci tensor acquires a perturbation

$$R_{ab} \rightarrow R_{ab} - \frac{1}{2}\Delta_L h_{ab}. \quad (2.15)$$

Here Δ_L is the Lichnerowicz operator,

$$\Delta_L h_{ab} = \square h_{ab} + 2R_{acbd}h^{cd} - 2R^c_{(a}h_{b)c} - 2\nabla_{(a}\nabla^ch_{b)c} + \nabla_a\nabla_b h, \quad (2.16)$$

the curved space wave operator for a spin-2 massless particle. Clearly a perturbation of a vacuum spacetime must obey $\Delta_L h_{ab} = 0$.

For the black string, the facts that the Ricci tensor is zero (as the string is a solution of the vacuum Einstein equations) and that there are no z components of the Riemann tensor will simplify the equations considerably. In addition, since we are in vacuum we can also choose the “transverse tracefree” gauge for h_{ab} ,

$$\nabla_a h_b^a = 0 = h, \quad (2.17)$$

which further simplifies (2.16) as follows:

$$\Delta_L h_{ab} \rightarrow \square h_{ab} + 2R_{acbd}h^{cd} = 0. \quad (2.18)$$

² If not in vacuum, we can still choose $\nabla_a h_b^a - \frac{1}{2}\nabla_b h = 0$, just not the individual parts separately.

It is now a matter of algebraic computation and manipulation to compute the perturbation equations component by component, using the above gauge choice to simplify equations where relevant.

As is standard practice, we use a separation of variables method and decompose the perturbation in terms of the symmetries, or Killing vectors, of the background geometry. The black string has both time- and z -translation invariances, as well as an $SO(3)$ isometry corresponding to the four-dimensional spherical symmetry of the Schwarzschild solution. For simplicity (and with the benefit of hindsight!) we will consider spherically symmetric perturbations since the entropy argument indicates that the instability should manifest itself at this level. This means that h_{ab} has no cross terms with an angular coordinate and has the form

$$h_{ab} = \begin{bmatrix} h_{tt} & h_{tr} & 0 & 0 & h_{tz} \\ h_{tr} & h_{rr} & 0 & 0 & h_{rz} \\ 0 & 0 & h_{\theta\theta} & 0 & 0 \\ 0 & 0 & 0 & h_{\theta\theta} \sin^2 \theta & 0 \\ h_{tz} & h_{rz} & 0 & 0 & h_{zz} \end{bmatrix}. \quad (2.19)$$

In addition, the t - and z -translation symmetries allow us to factor out an oscillatory e^{imz} behaviour and a growing $e^{\Omega t}$ mode corresponding to an unstable perturbation.

2.4.2 Finding the perturbation

The full set of equations is rather lengthy and not particularly illuminating, so we refer the reader to the original literature for the details, [11]. For the purposes of this review we note that the perturbations h_{zz} and $h_{z\mu}$ must vanish for any unstable mode. To see this is particularly straightforward for the h_{zz} perturbation, as the absence of Riemann components in the z -direction means that the equation for this component decouples. Writing $h_{zz} = e^{imz}e^{\Omega t}h$ we obtain

$$h'' + \left(\frac{2r - r_+}{r - r_+}\right)\frac{h'}{r} - [m^2r(r - r_+) + \Omega^2r^2]\frac{h}{(r - r_+)^2} = 0. \quad (2.20)$$

This equation has asymptotic solutions

$$h \sim e^{\pm\sqrt{\Omega^2+m^2}r} \quad \text{as} \quad r \rightarrow \infty, \\ h \sim (r - r_+)^{\pm\Omega r_+} \quad \text{as} \quad r \rightarrow r_+.$$

Clearly, therefore, any regular solution must vanish at the horizon and at infinity, with a turning point at some finite r at which $h''/h < 0$. However, examination of

(2.20) shows that $h''/h > 0$ at any turning point, hence no such solution exists. A similar argument shows that $h_{z\mu}$ must also vanish.

We are now left with a perturbation that has only four-dimensional components, $h_{\mu\nu} = e^{imz} e^{\Omega t} H_{\mu\nu}(r)$. After imposing the gauge constraints, the equations of motion reduce to a pair of first-order ODEs plus one constraint:

$$H_+ = \frac{H_-}{V} \frac{2r^2\Omega^2 + r^2m^2V - \frac{1}{2}(1-V^2)}{r^2m^2 + 1 - V} - \frac{rH}{\Omega} \frac{4\Omega^2 + m^2(1-3V)}{r^2m^2 + 1 - V}, \quad (2.21)$$

$$H' = \frac{\Omega(H_+ + H_-)}{2V} - \frac{(1+V)H}{rV}, \quad (2.22)$$

$$H'_- = \frac{m^2H}{\Omega} + \frac{H_+}{r} + \frac{(1-5V)H_-}{2rV}, \quad (2.23)$$

where

$$H_{\pm} = \frac{H_{tt}}{V} \pm VH_{rr}, \quad (2.24)$$

$$H = H_{tr}. \quad (2.25)$$

Once again, reading off the asymptotic behaviour gives

$$r \rightarrow \infty, \quad \begin{cases} H \sim \pm\sqrt{\Omega^2 + m^2} e^{\pm\sqrt{\Omega^2 + m^2}r}, \\ H_- \sim \frac{m^2}{\Omega} e^{\pm\sqrt{\Omega^2 + m^2}r}; \end{cases} \quad (2.26)$$

$$r \rightarrow r_+, \quad \begin{cases} H \sim \left(\pm\Omega r_+ - \frac{1}{2}\right) (r - r_+)^{\pm\Omega r_+-1}, \\ H_- \sim \left(\frac{m^2}{\Omega} \pm \frac{2}{r_+}\right) (r - r_+)^{\pm\Omega r_+}. \end{cases} \quad (2.27)$$

An instability therefore corresponds to a solution of (2.22), (2.23) that is regular at both the horizon and infinity, as determined by the asymptotic forms (2.26), (2.27).

2.4.3 Regularity conditions

In order to determine the regularity of the perturbation, we clearly need h_{ab} to tend to zero at large r , thus picking out the exponentially decaying branch of (2.26), and also to be regular at the horizon. Surprisingly, this latter constraint is not equivalent to the regularity of the perturbation in a local orthonormal system, as it is easy to see from (2.27) that $h_{\hat{r}\hat{r}} = h_{tr}$ blows up as $r \rightarrow r_+$ for $\Omega r_+ < 1$. Instead, we have to check the regularity in a locally regular coordinate system at the horizon.

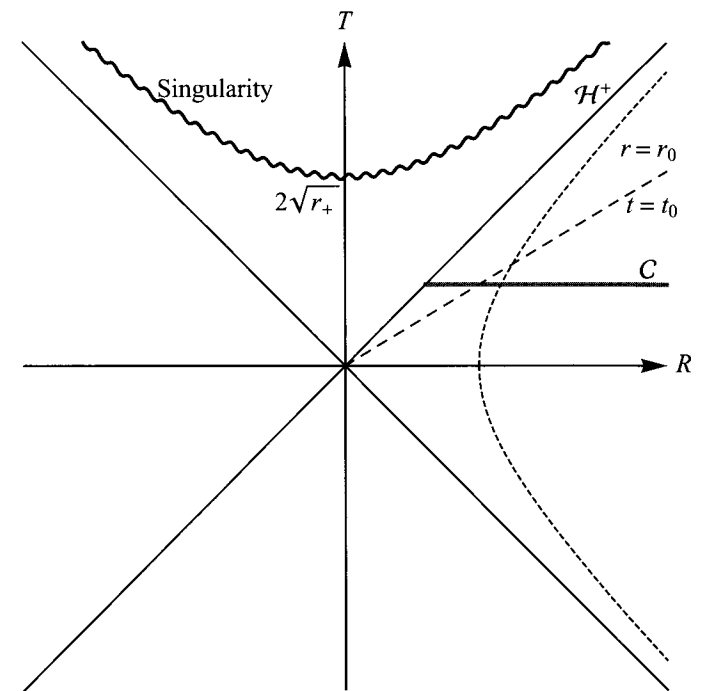


Figure 2.2 A diagram of the black hole spacetime in Kruskal-style coordinates (R, T) . The future event horizon \mathcal{H}^+ and the singularity are labelled, as well as the lines of constant t and r , the original Schwarzschild coordinates. The initial data surface \mathcal{C} from which we evolve the perturbation is also indicated schematically.

A convenient choice of coordinates is based on the Kruskal system:

$$T = 2e^{r_*/2r_+} \sinh\left(\frac{t}{2r_+}\right), \quad R = 2e^{r_*/2r_+} \cosh\left(\frac{t}{2r_+}\right), \quad (2.28)$$

where

$$r_* = r - r_+ + r_+ \log(r - r_+) \quad (2.29)$$

is the standard tortoise coordinate in the Schwarzschild metric (see Fig. 2.2).

Transforming to this new coordinate system, we see that

$$h_{TT} \sim \frac{\mathcal{U}(R, T)}{(R^2 - T^2)} (R^2 h_{\hat{r}\hat{r}} - 2RT h_{\hat{r}\hat{r}} + T^2 h_{\hat{r}\hat{r}}), \quad (2.30)$$

$$h_{TR} \sim \frac{\mathcal{U}(R, T)}{(R^2 - T^2)} (RT(h_{\hat{r}\hat{r}} + h_{\hat{r}\hat{r}}) - (T^2 + R^2)h_{\hat{r}\hat{r}}), \quad (2.31)$$

$$h_{RR} \sim \frac{\mathcal{U}(R, T)}{(R^2 - T^2)} (T^2 h_{\hat{r}\hat{r}} - 2RT h_{\hat{r}\hat{r}} + R^2 h_{\hat{r}\hat{r}}), \quad (2.32)$$

must be regular at the horizon, where $h_{\hat{t}\hat{t}} = h_{tt}/V$ refers to the components in a local orthonormal system and

$$\mathcal{U}(R, T) = \mathcal{U}(R^2 - T^2) = \frac{r_+^2}{r e^{(r-r_+)/r_+}} \quad (2.33)$$

is the new (nonsingular) Kruskal gravitational potential.

Substituting in the near-horizon behaviour gives

$$h_{TT} \simeq h_{RR} \propto \pm(R \pm T)^{\Omega r_+ - 2}, \quad (2.34)$$

$$h_{TR} \propto (R \pm T)^{\Omega r_+ - 2}, \quad (2.35)$$

and we see that the upper branch of (2.27) is always regular on the future event horizon ($R = T$) and the lower branch on the past event horizon. At the bifurcation point, where \mathcal{H}^+ and \mathcal{H}^- meet, corresponding to $r = r_+$ at finite t , neither branch is strictly regular and to exclude both would render the Lichnerowicz operator non-self-adjoint. For simplicity we consider perturbations that are regular on the future event horizon, as the black string is presumed to form from gravitational collapse and hence any initial data surface would have to be chosen to terminate on the future horizon. Figure 2.2 shows the black hole spacetime in Kruskal coordinates, together with the initial data surface.

2.4.4 The instability

To determine the existence of an instability we must numerically integrate the perturbation equations (2.22) and (2.23) between the horizon and infinity, looking for a solution that approaches the regular horizon branch and is exponentially decaying at infinity. We do not expect solutions for all Ω and m , since the thermodynamic argument indicates that an instability can only set in for $r_+ m < 32/27$. We expect a single characteristic frequency Ω_m for any wavelength; thus we must scan through the values of Ω for each m to check whether a solution exists. Figure 2.3 shows a plot of the frequency pairs (m, Ω) for which a regular solution, and hence an instability, exists, and Fig. 2.4 shows the behaviour of the perturbation.

Having found an unstable solution to the perturbation equations, in the final step of the argument we need to demonstrate that this is a physical instability of the black string and not just some unusual gauge mode. In fact, it is easy to demonstrate just by looking at (2.18). Since both the perturbation and the Riemann tensor vanish in the extra dimension ($h_{za} = 0 = R_{zabc}$), the five-dimensional Lichnerowicz operator reduces to the four-dimensional Lichnerowicz operator with a mass term:

$$\Delta_L^{(5)} h_{\mu\nu} = \Delta_L^{(4)} h_{\mu\nu} + \frac{\partial^2}{\partial z^2} h_{\mu\nu} = (\Delta_L^{(4)} - m^2) h_{\mu\nu}. \quad (2.36)$$

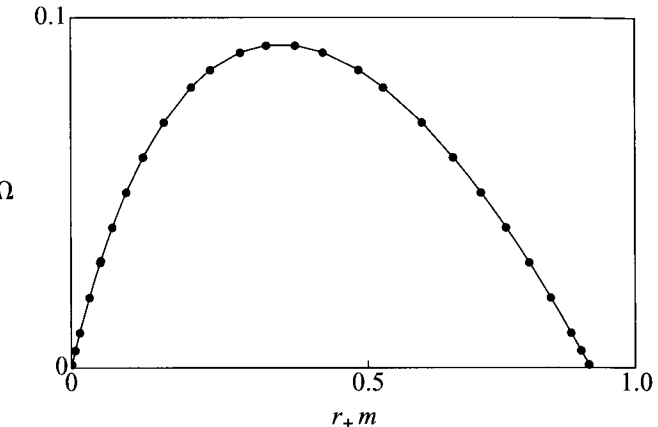


Figure 2.3 A plot of the eigenvalues (m, Ω) , scaled by r_+ , for which an instability is present.

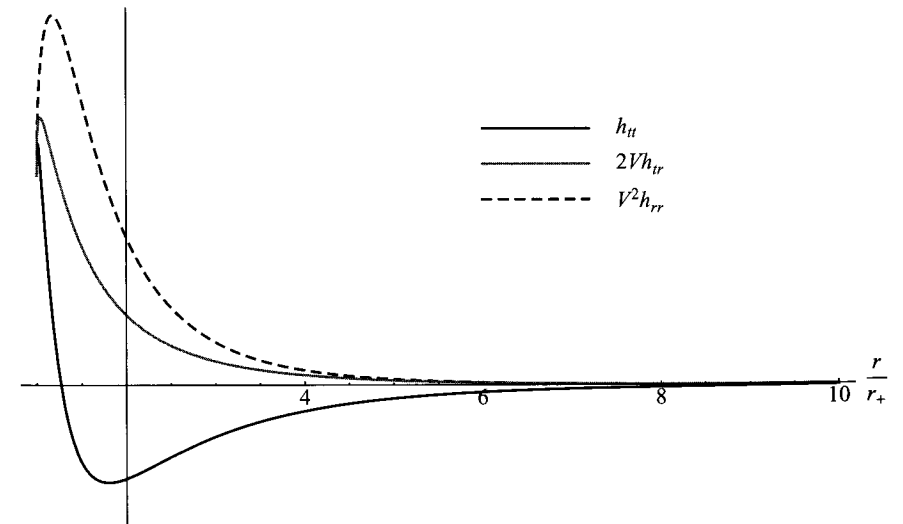


Figure 2.4 A plot of the metric perturbations h_{tt} , $2Vh_{tr}$ and V^2h_{rr} as a function of the radius.

However, if $h_{\mu\nu}$ is a gauge mode then it must correspond to a purely four-dimensional change of coordinates; in other words, it can have *no* dependence on z . Thus any solution of the *massive* four-dimensional Lichnerowicz operator must be a physical Kaluza–Klein instability.

2.4.5 More general instabilities

So far the discussion has been strictly in terms of five-dimensional vacuum Einstein gravity. This approach was chosen so that the mathematics and physics of the instability would be clearer, but of course if an instability exists with one extra dimension then it will also exist more generally. In [11–13], it was shown how black branes, objects with arbitrary numbers of extra dimensions, would be unstable; 1–6 extra dimensions were considered for the purpose of application to the string-theoretic solutions found by Horowitz and Strominger [14].

These instabilities look very similar to the five-dimensional case detailed here: an instability is once more restricted to a four-dimensional s-wave, where now the effective mass term in (2.36) is a general eigenvalue $\exp(m_i z^i)$ of the symmetries in the extra dimensions. The details of the (m, Ω) plot vary, but the qualitative shape and features are the same (see [11–13]). Instabilities of charged solutions, analogous to the four-dimensional Reissner–Nordstrom family of black holes (see Chapter 11), can also be found.

Interestingly, an instability does not require a translation invariance along the string or brane; it also applies to more general higher-dimensional spacetimes. Essentially, all that is required is some sort of factorizability of the metric and wave operator [15] so that we can decompose the perturbation in terms of effective four-dimensional quantities with suitable eigenfunctions of the extra dimensions:

$$h_{ab} \rightarrow h_{\mu\nu} = u_m(z^i) e^{\Omega t} H_{\mu\nu}(r), \quad (2.37)$$

where the Riemann tensor and wave operator also factorise so that a massive wave equation in the form of (2.36) is obtained for H .

2.5 Consequences of the instability

In the previous section, we proved that an instability of the black string exists, in that there is a linear perturbation of the black string solution which is exponentially growing in our coordinate time, t . However, it is not clear what the effect of this growing mode will be on the event horizon, which is a coordinate singularity, and in fact corresponds to $t \rightarrow \infty, r \rightarrow r_+$ in Schwarzschild coordinates.

To explore the effect of such an instability, we return to the Kruskal coordinates and check what happens to outgoing light rays near the original event horizon. In the unperturbed spacetime, null geodesics satisfy $R = \pm T + R_0$, $R = T$ being the future event horizon, as indicated in Fig. 2.2. In the perturbed spacetime, the

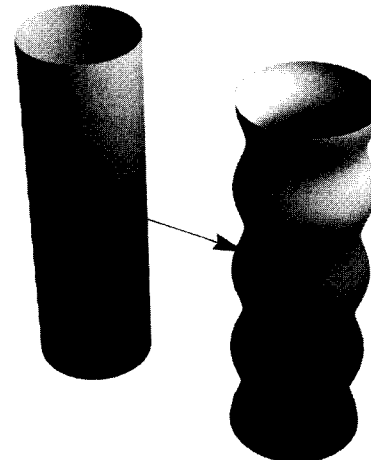


Figure 2.5 A representation of the effect of the instability on the black string horizon.

geodesic equation becomes

$$\left(\frac{dR}{dT}\right)^2 = 1 + \frac{1}{\mathcal{U}} (h_{TT} + 2h_{TR}\dot{R} + h_{RR}\dot{R}^2) \quad (2.38)$$

$$= 1 + \epsilon \cos mz (R + T)^{2r_+ \Omega - 2} \left(1 + \frac{dR}{dT}\right)^2, \quad (2.39)$$

where ϵ is an (arbitrary) small parameter representing the size of the initial perturbation. From this, we see that the event horizon is schematically shifted to

$$R = T + \epsilon \cos mz T^{2r_+ \Omega - 1} \quad (2.40)$$

or, in Schwarzschild coordinates,

$$r = r_+ + \epsilon T^{2\Omega} \cos mz. \quad (2.41)$$

In other words, the “horizon” begins to ripple (see Fig. 2.5).

This now has very interesting consequences. In four-dimensional gravity, the event horizon cannot shrink in any classical process without violating the positivity of energy. This black string instability is a classical process, so what is happening? Clearly, although the horizon is shrinking in some places along the black string, in other places it is growing; hence overall this classical process is increasing the total area, as we would expect from the thermodynamic argument of entropic instability. However, increasing the area of an event horizon is not the only classical relativistic constraint. If we follow the instability to its logical endpoint, dictated

by the entropy argument, we might expect that the black string will eventually fragment, forming a black hole caged within the larger fifth dimension. This is a simple conclusion, perhaps, but at the moment when the horizon pinches off the curvature at the horizon diverges, forming a naked singularity.

In the catalogue of four-dimensional relativity, a pattern emerges where, apart from in a few very well-known examples such as the big bang, singularities, and certainly singularities which form during a physical collapse, tend to be clothed by an event horizon. This led Penrose to conjecture [16] that a “censorship” applies in gravitational collapse which prevents any singularity forming that could be visible from infinity. Although a full proof of this conjecture remains elusive, any counterexamples that have been constructed are either unphysical in some way or highly nongeneric. Therefore the *cosmic censor* has been assumed to be an omnipotent authority in classical gravity. Yet here, within the bounds of classical gravity, a physical generic process has been shown to exist that strongly suggests a violation of cosmic censorship at the moment when a string fragments into a black hole. For this reason, for many years after the discovery of the black string instability, the final fate of the black string was viewed as an open question [17, 18], and cosmic censorship was an unknown factor in higher-dimensional gravity. The story of what happens to the black string and of how the instability proceeds requires a *tour de force* numerical simulation [19], a description of which forms the core of the next chapter.

References

- [1] T. Kaluza, Zum Unittsproblem der Physik, *Sitzungsber. Preussische Akad. Wiss.* **96** (1921), 69.
- [2] O. Klein, Quantentheorie und fünfdimensionale Relativitätstheorie, *Eur. Phys. J. A* **37** (1926), 895–906.
- [3] R. C. Myers and M. J. Perry, Black holes in higher dimensional space-times, *Ann. Phys.* **172** (1986), 304.
- [4] G. J. Galloway and R. Schoen, A generalization of Hawking’s black hole topology theorem to higher dimensions, *Commun. Math. Phys.* **266** (2006), 571 [[arXiv:gr-qc/0509107](#)].
- [5] R. Emparan and H. S. Reall, A rotating black ring solution in five-dimensions, *Phys. Rev. Lett.* **88** (2002), 101 101 [[arXiv:hep-th/0110260](#)].
- [6] R. Emparan, Blackfolds, [arXiv:1106.2021](#) [hep-th].
- [7] R. Emparan, T. Harmark, V. Niarchos, and N. A. Obers, Blackfolds in supergravity and string theory, [arXiv:1106.4428](#) [hep-th].
- [8] H. Kudoh and T. Wiseman, Properties of Kaluza–Klein black holes, *Prog. Theor. Phys.* **111** (2004), 475 [[arXiv:hep-th/0310104](#)].
- [9] T. Harmark and N. A. Obers, Phase structure of black holes and strings on cylinders, *Nucl. Phys. B* **684** (2004), 183 [[arXiv:hep-th/0309230](#)].
- [10] B. Kol, The phase transition between caged black holes and black strings: a review, *Phys. Rept.* **422** (2006), 119 [[arXiv:hep-th/0411240](#)].

- [11] R. Gregory and R. Laflamme, Black strings and p-branes are unstable, *Phys. Rev. Lett.* **70** (1993), 2837 [[arXiv:hep-th/9301052](#)].
- [12] R. Gregory and R. Laflamme, The instability of charged black strings and p-branes, *Nucl. Phys. B* **428** (1994), 399 [[arXiv:hep-th/9404071](#)].
- [13] R. Gregory and R. Laflamme, Evidence for stability of extremal black p-branes, *Phys. Rev. D* **51** (1995), 305 [[arXiv:hep-th/9410050](#)].
- [14] G. T. Horowitz and A. Strominger, Black strings and p-branes, *Nucl. Phys. B* **360** (1991), 197.
- [15] R. Gregory, Black string instabilities in Anti-de Sitter space, *Class. Quant. Grav.* **17** (2000), L125 [[arXiv:hep-th/0004101](#)].
- [16] R. Penrose, *Riv. Nuovo Cimento* **1** (1969), 252.
- [17] G. T. Horowitz and K. Maeda, Fate of the black string instability, *Phys. Rev. Lett.* **87** (2001), 131 301 [[arXiv:hep-th/0105111](#)].
- [18] D. Marolf, On the fate of black string instabilities: an observation, *Phys. Rev. D* **71** (2005), 127 504 [[arXiv:hep-th/0504045](#)].
- [19] L. Lehner and F. Pretorius, Black strings, low viscosity fluids, and violation of cosmic censorship, *Phys. Rev. Lett.* **105** (2010), 101 102 [[arXiv:1006.5960](#) [hep-th]].

3

Final state of Gregory–Laflamme instability

LUIS LEHNER AND FRANS PRETORIUS

3.1 Overview

The ultimate fate of black holes subject to the Gregory–Laflamme instability has been an open question for almost two decades. In this chapter we discuss the behavior of an unstable five-dimensional black string and elucidate its final state. Our studies reveal that the instability unfolds in a self-similar fashion, in which the horizon at any given time can be seen as thin strings connected by hyperspherical black holes of different radii. As the evolution proceeds pieces of the string shrink while others give rise to further spherical black holes, and consequently the horizon develops a fractal structure. At this stage its overall topology is still $\mathbb{R} \times S^2$; the fractal geometry arises along \mathbb{R} and has an estimated Hausdorff dimension $d \approx 1.05$. However, the ever-thinning string regions eventually shrink to zero size, revealing a (massless) naked singularity. Consequently, this spacetime provides a generic counterexample to the cosmic censorship conjecture, albeit in five dimensions. While we restrict to the five-dimensional case for reasons of computational cost, our observations are intuitively applicable to higher dimensions.

To capture the late-time nonlinear dynamics of the system correctly requires numerical solution of the full Einstein equations. In this chapter, following a brief historical account (section 3.2) we describe details of our numerical implementation (section 3.3) as well as the behavior of the obtained solution (section 3.4). We discuss some additional properties of the solution, including speculation on when quantum corrections are expected to become important, and future directions in section 3.5.

3.2 Background

The observation of Gregory and Laflamme that linearized perturbations of D -dimensional black strings ($D \geq 5$) are unstable for long wavelengths (see Chapter 2 or [1]) is in stark contrast with the known behavior of black holes in four dimensions [2]. On the basis of the nature of growing perturbations of black strings, together with entropy arguments, Gregory and Laflamme conjectured that black strings would bifurcate, thus inducing a topology change in the horizon to yield localized S^{D-2} black holes. However, black hole bifurcation necessarily implies, at the classical level, the formation of a naked singularity where the pinch-off occurs (see for example [3]). Assuming such behavior would be resolved by quantum gravity, the conjecture was taken as likely to be true for about a decade. In the early years after 2000, tension arose when Horowitz and Maeda proved that any bifurcation could only take place at infinite affine time along the generators of the horizon that cross the bifurcation point [4]. They dismissed this possibility as unlikely and conjectured the existence of stationary nonuniform black string solutions as the endpoint of the instability. Follow-up works presented approximate stationary solutions found perturbatively [5] or numerically [6–8] (see Chapter 4), though these had less entropy than the uniform string and so could not be the end-point of the system. Regarding these developments, interesting observations were made as to a possible reversal of this behavior for $D > D_{\text{crit}}$ [9], where the critical dimension D_{crit} depends on the boost of the black string [10] ($D_{\text{crit}} = 13$ for an unboosted black string and $D_{\text{crit}} = 0$ for sufficiently large boosts). Furthermore, it was pointed out that electrically charged black strings are more unstable than magnetically charged ones [11], and arguments were presented for a conical structure in the black-string–black-hole transition [12, 13].

This flurry of activity not only hinted at the possibility of rich phenomenology awaiting in the dynamics of the system but also at the need for a full analysis to uncover it. A first attempt to do so was presented in [14]. This study revealed that the development of a black string perturbed by a long-wavelength periodic mode progressed to a structure that could be described as a sequence of S^3 black holes joined by strings, though the final fate of the structure could not be uncovered since the code was unable to evolve the solution further. Detailed follow-up analysis of the results from this simulation showed that the affine time along the generators grew faster than a simple exponential in the asymptotic time [15], suggesting the consistency of a possible pinch-off with the theorem presented in [4]; see also [16].

Following these works, additional hints to the possible end state came from the analogy with fluid systems. The membrane paradigm [17] first suggested that event horizon dynamics could be described, to leading order, by the Navier–Stokes equations for a viscous fluid (albeit with some “unusual” properties, such as a

negative bulk viscosity). More recently, descriptions of black brane dynamics in asymptotically five-dimensional anti-de Sitter spacetime (see Chapter 13 or [18]), and an effective worldvolume theory of black holes (the “blackfolds” paradigm, see Chapter 8 or [19, 20]), use the Navier–Stokes equations. Cardoso and Dias noted the qualitative similarity between the dispersion relations of unstable modes of black strings and those of thin fluid streams subject to the Rayleigh–Plateau instability¹ and pointed out that if the similarities persisted beyond linear development then the black string solution could share the same fate as the fluid, which *does* pinch off [21]. Moreover, in the latter system, evolution to pinch-off can be accompanied by a phenomenon known as satellite formation, where one or more generations of ever smaller spherical “beads” form in the thinning stream; the lower the viscosity of the fluid, the more generations are observed (see for example [23]). In fact, as we describe here, this *is* qualitatively what is seen to occur in the black string [24]. The self-similar nature of this solution makes it impossible numerically to follow the evolution to arbitrary small scales, though following the trends, together with the fact that there is no intrinsic length scale in the field equations of general relativity, suggests that infinitely many generations of satellites will form (at the classical level). Interestingly, horizon–fluid analogues describe the horizon as a perfect fluid with a shear viscosity to entropy density ratio, η/s , of $1/(4\pi)$, implying a lower viscosity than that of any “real-world” fluid [25, 26].

3.3 Numerical approach

As mentioned above, we relied on numerical simulations to reveal the solution of an unstable black string. In this section we describe particularly relevant aspects of the numerical implementation adopted. We note that achieving a reliable implementation of Einstein’s equations for any given class of problem requires one to deal with many subtle issues. It is beyond the scope of this chapter to go into the full details (for textbook introductions to numerical relativity see [27–29]); however, since there is as of yet no universal approach to problems requiring numerical relativity, we find it useful to describe a method that has been successful in evolving the five-dimensional black string spacetime, focusing on details particular to this problem.²

In the class of not-so-subtle issues regarding successful solution of the initial boundary value problem are: solving the constraint equations for consistent initial

¹ Note, though, that the relationship is not exact; in particular in the limit of long wavelengths λ the growth rate Ω in Rayleigh–Plateau differs from Gregory–Laflamme as $\Omega \propto \lambda^{-1/2}$ versus $\Omega \propto \lambda^{-1}$ [21, 22]. However, as the results here show, the behavior of the system is determined by intermediate wavelengths; thus the infinitely-long-wavelength behavior is likely to be irrelevant as far as the late-time behavior of the string is concerned.

² For other examples of numerical relativity exploring dynamical scenarios in higher-dimensional settings see [14, 30–35].

data; using a mathematically well-posed formulation of the field equations that furthermore does not admit exponentially growing solutions from truncation-error-seeded constraint violations; dealing with the geometric singularity inside the black string; and using a stable numerical integration scheme that can adequately resolve all the relevant length scales. The initial data we use here is the same as in an earlier numerical study [14], and we will describe the ansatz and solution method in section 3.3.1. For evolution, the present study uses a harmonic approach [36]³ with constraint damping [41, 42], and this is described in section 3.3.2. We use the *excision* approach to remove the black string singularity from the computational domain. This relies on having a detailed description of the apparent horizon of the spacetime, which is also a key structure employed to analyze the dynamics of an unstable string. In section 3.3.3 we describe the basic properties of an apparent horizon and how the latter is found in the simulation. For our numerical scheme, we use finite difference techniques with adaptive mesh refinement (AMR). These methods will not be discussed here but, where appropriate, references to further information will be given.

Subtle issues of import to five-dimensional black string evolution will be discussed in the following sections as well, including the coordinates to be employed and the appropriate choice of constraint damping parameters.

3.3.1 Initial data

We are interested in studying the black string’s dynamics with respect to perturbations in vacuum. Here, rather than adopting generic perturbations we concentrate on those that break the symmetry only along the extra “string” direction w (henceforth we will refer to it as the “string-like” direction). As was shown in the original work [1, 43], perturbations in the $S^2(\theta, \phi)$ -sector lead, at the linear level, to subdominant modes with respect to those in w . Thus restricting attention to such a case should not affect the generality of the observed behavior and, as an important added bonus, allows us to restrict to a numerical implementation with only two relevant spatial coordinates.

In what follows we summarize the approach that has been adopted to define such data; for full details see [14]. To obtain consistent initial data we adopt a Cauchy 4+1 decomposition of the Einstein equations. At an initial ($t = 0$) hypersurface, its intrinsic metric γ_{ij} and extrinsic curvature K_{ij} provide suitable data if they satisfy the Hamiltonian and momentum constraints

$$H \equiv {}^{(4)}R + K^2 - K_{ij}K^{ij} = 0, \quad (3.1)$$

$$M_i \equiv D_j(K_i^j - \gamma_i^j K) = 0, \quad (3.2)$$

³ For additional examples of its use in numerical relativity see, e.g. [37–40].

where ${}^{(4)}R$ is the Ricci scalar associated with γ_{ij} , $K \equiv \gamma^{ij}K_{ij}$, and D_i is the covariant derivative compatible with γ_{ij} . We consider only perturbations depending on (r, w) and respecting the $SO(3)$ symmetry; then the general intrinsic metric can be expressed as

$${}^{(4)}ds^2 = \gamma_{rr}dr^2 + 2\gamma_{rw}drdw + \gamma_{ww}dw^2 + r^2\gamma_\Omega d\Omega^2, \quad (3.3)$$

where $d\Omega^2$ is the unit 2-sphere metric. With these assumptions $M_\theta = M_\phi = 0$, so the constraints provide three equations for eight variables. Thus three unknowns can be solved for provided that the remaining information is prescribed. To obtain this information, we notice that, using ingoing Eddington–Finkelstein coordinates, we have for the unperturbed black string

$$\gamma_{rr} = 1 + \frac{2M}{r}, \quad \gamma_{rw} = 0, \quad \gamma_{ww} = 1, \quad \gamma_\Omega = 1, \quad (3.4)$$

$$K_{rr} = -2M\frac{r+M}{r^3}\alpha, \quad K_{rw} = 0, \quad K_{ww} = 1, \quad K_{\theta\theta} = 2M\alpha, \quad (3.5)$$

with $\alpha = \sqrt{r/(r+2M)}$ and M the mass per unit length. We will thus adopt $\gamma_{rw} = \gamma_{ww} - 1 = K_{rw} = K_{ww} = 0$ and introduce a perturbation

$$\gamma_\Omega = 1 + A \sin\left(w\frac{2\pi q}{L}\right) e^{-(r-r_0)^2/\delta_r^2}. \quad (3.6)$$

Here A is a parameter controlling the overall strength of the perturbation, q is an integer defining its spatial frequency in the w direction, and r_0 and δ_r are parameters controlling the extent of the perturbation in the radial direction. For the results presented below $A = 0.1$, $q = 1$, $r_0 = 2.5$, and $\delta_r = 0.5$. The remaining variables are obtained numerically by solving the Hamiltonian and momentum constraints. To this end we adopt a finite difference approximation of the constraints on a uniform grid with $(r, w) \in [R_{\min}, R_{\max}] \times [0, L]$ and deal with the constraints as follows. The Hamiltonian constraint provides an equation for γ_{rr} that can be written schematically as

$$F_1\partial_r\gamma_{rr} + F_2\gamma_{rr}\partial_{ww}^2\gamma_{rr} + F_3\gamma_{rr}\partial_w\gamma_{rr} + F_4(\partial_w\gamma_{rr})^2 + F_5(\gamma_{rr})^2 + F_6\gamma_{rr} = 0, \quad (3.7)$$

the F_l ($l = 1, \dots, 6$) being functions that do not depend on γ_{rr} . This equation is integrated outwards from an inner boundary chosen well inside the unperturbed black string horizon ($R_{\min} = M$); the boundary data there is provided by the unperturbed value of γ_{rr} . A second-order-accurate radial integration is adopted, for which the presence of the w -derivatives makes the numerical problem a nonlinear, cyclic (owing to the w -periodicity), tridiagonal system for the unknowns $\gamma_{rr}|_{r_i, w_j}$. This system is solved using Newton’s method and a cyclic tridiagonal linear algorithm.

The momentum constraint along the r direction provides a first-order equation for $K_{\theta\theta}$ of the form

$$G_1\partial_r K_{\theta\theta} + G_2 K_{\theta\theta} + G_3 = 0, \quad (3.8)$$

the G_l ($l = 1, \dots, 3$) being functions that do not depend on $K_{\theta\theta}$. This is a simple ordinary differential equation (ODE), which is integrated along each line of constant w by employing second-order finite differences and boundary conditions at R_{\max} provided by the unperturbed black string solution. The momentum constraint along the w direction provides an equation for K_{rr} of the form

$$H_1\partial_w K_{rr} + H_2 K_{rr} + H_3 = 0, \quad (3.9)$$

the H_l ($l = 1, \dots, 3$) being functions that do not depend on K_{rr} . This is again a simple ODE that can be integrated to second-order accuracy along lines of constant r . Boundary conditions are specified along $w = w_{\min}$ using the unperturbed values.

The procedure above provides consistent data for our problem. We stress that it is by no means a general procedure to obtain consistent initial data for a black string problem; rather, it is a straightforward way of setting up a particular perturbation of the black string to study its subsequent evolution.⁴

The method described above provides data for $\{g_{ij}, K_{ij}\}$ ($i, j = r, \theta, \phi, w$). However, the data required for the harmonic formulation discussed in the following subsection consist of $\{g_{\mu\nu}, g_{\mu\nu,t}\}$. Note also that for the evolution we impose the harmonic condition with respect to the *Cartesian* coordinates (x, y, z, w) ; thus we first need to transform (r, θ, ϕ) to (x, y, z) via the standard relations between three-dimensional Cartesian and spherical polar coordinates. Data for $g_{\mu\nu}$ can be defined straightforwardly by making use of the relation between metrics provided by a standard 4+1 Cauchy decomposition:

$$g_{00} = -\alpha^2 + \gamma_{ij}\beta^i\beta^j, \quad g_{0i} = \gamma_{ij}\beta^j, \quad g_{ij} = \gamma_{ij}, \quad (3.10)$$

where we adopt the unperturbed values for the lapse α and shift β^i . Data for $g_{\mu\nu,t}$ are obtained by taking the time derivative of the expressions above and making use of the relation between K_{ij} and $\gamma_{ij,t}$,

$$-2\alpha K_{ij} = (\partial_t - \mathcal{L}_\beta)\gamma_{ij}, \quad (3.11)$$

and the harmonic coordinate condition, which in 4+1 form is

$$(\partial_t - \beta^i\partial_i)\alpha = -\alpha^2 K, \quad (3.12)$$

$$(\partial_t - \beta^i\partial_i)\beta^j = \alpha\gamma^{jl}(\alpha\gamma^{mn}{}^{(4)}\Gamma_{lmn} - \alpha_{,l}), \quad (3.13)$$

where ${}^{(4)}\Gamma_{lmn}$ are the Christoffel symbols of the 4-metric.

⁴ For alternatives see [6, 44, 45].

3.3.2 Evolution

The harmonic decomposition with constraint damping

In what follows we briefly review the harmonic formulation of Einstein's equations, in particular with regard to a numerical implementation (for more details see [39, 46]). *Harmonic coordinates* satisfy a set of gauge conditions that require each spacetime coordinate x^α independently to satisfy the covariant scalar wave equation

$$\nabla^\nu \nabla_\nu x^\mu = \frac{1}{\sqrt{-g}} \partial_\nu (\sqrt{-g} g^{\nu\xi} \partial_\xi x^\mu) \equiv 0. \quad (3.14)$$

Here g is the determinant of the spacetime metric $g_{\mu\nu}$.⁵ Harmonic coordinates have a long history in relativity and are well adapted to describing black strings since the metric in harmonic coordinates is regular on the horizon. More importantly, for numerical evolution, substitution of (3.14) (and its first covariant gradient) into the vacuum Einstein field equations $R_{\mu\nu} = 0$ yields for the metric a system of explicitly symmetric hyperbolic evolution equations,

$$\frac{1}{2} g^{\xi\chi} g_{\mu\nu,\xi\chi} + g^{\xi\chi}_{(\mu} g_{\nu)\chi,\xi} + \Gamma_{\nu\chi}^\xi \Gamma_{\mu\xi}^\chi = 0, \quad (3.15)$$

where $\Gamma_{\nu\chi}^\xi$ are the Christoffel symbols. By themselves these equations admit a larger class of solutions than is desired, and it is only the subset of solutions that satisfy what can now be considered the constraints, i.e.,

$$C_\mu \equiv g_{\mu\nu} \nabla^\xi \nabla_\xi x^\nu = 0, \quad (3.16)$$

that are of physical interest. The time derivatives of these constraints can be related to the traditional Hamiltonian and momentum constraints discussed in section 3.3.1. At the analytical level, Bianchi identities imply that initial data (the metric and its first time derivative) satisfying $C_\mu = 0$ as well as the traditional constraints will evolve via (3.15) to a solution where $C_\mu = 0$ for all time, *provided* that the boundary conditions are consistent with $C_\mu = 0$.

Numerically the situation is more complicated, as truncation error will generically source nonzero C_μ during evolution and typically C_μ grows exponentially (even in a convergent implementation), rendering it difficult to achieve long-time well-behaved evolution. The cure, following [41], is to add to the harmonic form of the Einstein equations (3.15) *constraint damping* terms, obtaining

$$\begin{aligned} & \frac{1}{2} g^{\xi\chi} g_{\mu\nu,\xi\chi} + g^{\xi\chi}_{(\mu} g_{\nu)\chi,\xi} + \Gamma_{\nu\chi}^\xi \Gamma_{\mu\xi}^\chi \\ & + \kappa (2n_{(\mu} C_{\nu)} - (1 + \rho) g_{\mu\nu} n^\chi C_\chi) = 0, \end{aligned} \quad (3.17)$$

where n^μ is a unit timelike vector, here chosen to be a vector normal to surfaces of constant harmonic time t , and (κ, ρ) are the constraint damping parameters. Notice that the extra terms are homogeneous in C_μ ; hence, when $C_\mu = 0$, (3.17) trivially reduces to the Einstein equations. If $C_\mu \neq 0$, perturbation analysis about Minkowski spacetime [41] reveals that, for $\kappa > 0, \rho > -1$, all Fourier modes of C_μ except a zero-wavelength mode are exponentially damped. Analytical results are not known for the efficacy of constraint damping in the strong-field nonlinear regime, though empirically it has been shown to work for generic compact binary systems in four dimensions (involving black holes and neutron stars) and the unstable black string in five dimensions. Typically, the value of κ that works well is $\kappa \approx 1/\ell$, where ℓ is some characteristic scale in the problem; here κ is set to $1/M$, where M is the initial mass per unit length of the unperturbed string. In all four-dimensional simulations to date, ρ has been set to zero; for the black string, a value of $\rho \in (-1, \dots, 0)$ is *essential* to damp a zero-wavelength mode growing along the string-like dimension w . The exact value, however, is not important, and we have chosen $\rho = -0.5$.

Regarding the boundary conditions in the numerical simulation, the domain was identified periodically in the w direction and, at the outer boundary, Dirichlet conditions were imposed for simplicity, with the metric fixed to the values of the initial data there. This latter condition is consistent with $C_\mu = 0$ only to leading order in $1/r_b$, where r_b is the radius of the outer boundary; hence to avoid any potential problems that might arise from this, r_b was chosen to be sufficiently large that the outer boundary is out of causal contact with the string horizon during the entire length of the simulation.

Symmetries and the cartoon method

Since the typical computational resources required to numerically solve a hyperbolic problem scale as N^D , where N represents the number of mesh points needed to resolve a feature of interest along one dimension and D is the total number of spacetime dimensions, it would be impossible to solve for a general perturbation of a five-(or higher-)dimensional black string on contemporary computer clusters. However, as mentioned before, the analysis in [1, 43] shows that only modes along the extra string-like direction w are unstable whereas perturbations within the S^2 cross sections decay exponentially. Hence it is reasonable to expect that one can obtain a correct picture of the final end state by restricting to spherical symmetry within each w -constant slice. In other words, we need to consider metrics of the form

$$ds^2 = {}^{(3)}g_{\mu\nu} dx^\mu dx^\nu + R^2 (d\theta^2 + \sin^2 \theta d\phi^2), \quad (3.18)$$

⁵ Generalized harmonic coordinates add an arbitrary set of source functions H^α to the right-hand side of (3.14) [47]; these can be chosen to implement different gauges. Here, though, we choose $H^\mu = 0$.

where $x^\mu = (x^0, x^1, x^2) = (t, r, w)$, where t is the harmonic time, r is the radial coordinate, and w is the string-like direction, and the 3-metric ${}^{(3)}g_{\mu\nu}$ and areal radius R depend only on the 3-coordinates x^μ .

It would seem that the natural way to proceed (as similarly done with the initial data) is to directly discretize the field equations with a metric ansatz of the form (3.18), reducing the problem to a (2+1)-dimensional simulation. However, we were not able to obtain long-term stable evolution within the harmonic formulation (i.e. while requiring that (t, r, w) be harmonic coordinates with appropriate gauge sources). Possible reasons for the difficulties experienced are related to the fact that the spherical coordinates are not harmonic and that the limited set of gauge source functions that we used to account for this did not yield well-behaved evolutions. Potentially related difficulties were reported in a study of harmonic evolution in four-dimensional spherical symmetry [48].

A way around this problem is to consider the full five-dimensional metric $g_{\mu\nu}$ in harmonic *Cartesian* coordinates (t, x, y, z, w) , as this strategy works well in four dimensions. The S^2 symmetry of the spacetime can then be imposed via the corresponding Killing vectors,

$$\xi_1^\mu = x \left(\frac{\partial}{\partial y} \right)^\mu - y \left(\frac{\partial}{\partial x} \right)^\mu, \quad (3.19)$$

$$\xi_2^\mu = y \left(\frac{\partial}{\partial z} \right)^\mu - z \left(\frac{\partial}{\partial y} \right)^\mu, \quad (3.20)$$

$$\xi_3^\mu = z \left(\frac{\partial}{\partial x} \right)^\mu - x \left(\frac{\partial}{\partial z} \right)^\mu. \quad (3.21)$$

Thus, a single $y = 0, z = 0$ (for example) slice of the spacetime is sufficient to reconstruct the entire spacetime by the action of the Killing vectors on the metric:

$$\mathcal{L}_{\xi_1} g_{\mu\nu} = \mathcal{L}_{\xi_2} g_{\mu\nu} = \mathcal{L}_{\xi_3} g_{\mu\nu} = 0. \quad (3.22)$$

The practical way to implement this in the code is to discretize the given three-dimensional slice of the five-dimensional metric and then use the Killing conditions (3.22) to replace derivatives orthogonal to the slice (i.e. in the y and z directions), as required in the harmonic evolution equations (3.17), with derivatives tangent to the slice (i.e. in the x direction). For example, expanding $\mathcal{L}_{\xi_3} g_{\mu\nu} = 0$ one can solve for the z -gradients of the metric elements as follows:

$$g_{\mu\nu,z} = \frac{1}{x} (z g_{\mu\nu,x} - 2\delta^z_{(\mu} g_{\nu)x} + 2\delta^x_{(\mu} g_{\nu)z}). \quad (3.23)$$

This is a variant [36] of the so-called *cartoon* method [49], originally applied to axisymmetric evolution in four-dimensional spacetime.

3.3.3 Apparent horizons

Crucial to understanding the dynamics of an unstable black string is understanding the behavior of its horizon. In a numerical simulation of finite length, at best one can recover an approximation to the actual event horizon. This can be done by, for example, looking at the boundary of the causal past of some region of the spacetime at the last time step of the simulation. Furthermore, in spacetimes with naked singularities, as implied by numerical solutions for this system an event horizon does not exist. A better local property of the spacetime to study is the apparent horizon (AH), defined as the outermost marginally outer-trapped surface (in other words, the outermost surface from which the outward null expansion is exactly zero and the inward null expansion is less than or equal to zero at each point on the surface). Even though apparent horizons are slicing dependent, the study [14] showed that the AH was essentially indistinguishable from the approximate event horizon everywhere, except at late times because of the ambiguity in defining the region of spacetime whose causal past defines the exterior of the event horizon. We thus focus on the AH, which incidentally also guides the excision technique used to remove the geometric singularity inside the black string from the computational domain.

For more information on how AHs are defined and searched for in a numerical evolution, see [50]; we use a *flow method* in our implementation.

3.3.4 Evolution code

The basics of the numerical evolution code employed can be briefly summarized as follows. The harmonic equations with constraint damping (3.17), reduced to first order in time by introducing the auxiliary variables $\dot{g}_{\mu\nu} \equiv \partial_t g_{\mu\nu}$, are discretized using fourth-order finite difference methods with adaptive mesh refinement (AMR) [51], as implemented in the PAMR/AMRD⁶ libraries (which also handle parallelization via a message-passing interface (MPI)). The time integration is via fourth-order Runge–Kutta. Standard centered spatial difference operators are used in the interior of the grid, while at the inner excision boundary (chosen to match the shape of the AH, but a fraction between 10% and 50% smaller in radius) centered difference operators are replaced with sideways operators as appropriate. A sixth-order Kreiss–Oliger-style dissipation filter is used to control the high-frequency truncation error [52].

⁶ <http://laplace.physics.ubc.ca/Group/Software.html>.

3.4 Evolution of an unstable black string

With the implementation described previously, we now concentrate on describing the results from the evolution of an unstable black string. We will concentrate on a single case, in which the unperturbed string has periodicity-length $20M$. Such an identification satisfies $L > L_c$, where L_c is the critical wavelength beyond which modes become unstable, yet allows only a single unstable mode initially. To study this case, we adopted the computational domain $(r, w) \in ([0, 320M] \times [0, 20M])$. For convenience we have relabelled the Cartesian coordinate x as r , though of course $x = r$ on the $y = z = 0$ slice of the spacetime. We adopted an initial grid that uniformly covers the entire domain with $(N_r, N_w) = (1025, 9)$ points. As the evolution proceeds and finer structure arises, the AMR algorithm introduces additional higher-resolution grids where needed, on the basis of a specified maximum truncation error tolerance.

A typical “low” resolution run had a coarsest radial mesh spacing of about $0.3/M$, which is the resolution at the outer boundary. Additional levels were added by the AMR algorithm (each refined with a $2 : 1$ ratio, in both r and w , of the parent level) in order to resolve the region of spacetime near the AH of the string. Initially three additional levels were added, and this grew to 16 additional levels by the time the simulation was terminated at $t \sim 229.0M$ (owing to the prohibitive computational costs that would have been required to continue). Medium and high resolutions, for convergence and error estimates, were specified by decreasing the maximum allowed (estimated) truncation error by factors 8 and 64 respectively. Owing to the longer run times needed with increasing resolution, the medium- and higher-resolution cases were not evolved as far. Specifically, the longest medium-resolution case was terminated at $t \sim 226.8M$ and the longest high-resolution case was terminated at $t \sim 217.9M$; the high-resolution run required around 100 000 CPU hours on the woodhen cluster at Princeton University.⁷ This translated into roughly two months of essentially continuous running on 100 processors.

3.4.1 Apparent horizon dynamics

To help understand the dynamics of the system we monitored several relevant quantities, in particular, the apparent horizon radius $R_{\text{AH}}(t, w)$, the total horizon area $A(t)$, its intrinsic geometry via a flat-space embedding diagram, and two space-time curvature invariants, $I = R_{\mu\nu\xi}R^{\mu\nu\xi}$ and $J = R_{\mu\nu\xi}R^{\xi\eta\sigma}R_{\eta\sigma}{}^{\mu\nu}$, evaluated

⁷ <http://www.princeton.edu/researchcomputing/computational-hardware/>.

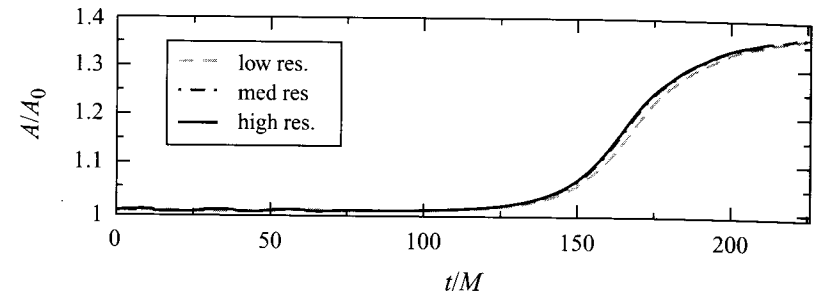


Figure 3.1 Apparent horizon area as a function of time for the perturbed black string. Shown is the area normalized to the initial area for simulations with three different resolutions (see the main text for a description of the resolutions).

on the horizon. Regarding the curvature invariants, we found it useful to rescale them as

$$K = IR_{\text{AH}}^4/12, \quad S = 27(12J^2I^{-3} - 1) + 1, \quad (3.24)$$

since such a rescaling yields $K = S = 6$ for an S^3 Schwarzschild–Tangherlini black hole while $K = S = 1$ for a uniform black string.

Figure 3.1 shows the total apparent horizon area A as a function of time for the evolution of our perturbed black string. As expected for a reasonable approximation to the event horizon, the area is nondecreasing with time. More interestingly, we note that at the end of the simulation corresponding to the lowest-resolution run (the run that was the longest in time) the total area was $A = (1.369 \pm 0.005)A_0$,⁸ where A_0 is the initial area; this value essentially reaches the value $1.374A_0$ that an exact five-dimensional black hole of the same total mass would have.

More insight into the dynamics of the horizon can be garnered by observing the evolution of its intrinsic geometry with time. Figure 3.2 shows several snapshots of embedding diagrams of the AH from the medium-resolution simulation run. As can be seen in the figure, the string initially evolves to a configuration resembling a hyperspherical black hole connected to a thin string segment, as reported in [14] (where the simulation ended at roughly $t \sim 164M$). However, as the evolution proceeds it is apparent that the string segments are themselves unstable: this pattern repeats in a self-similar manner to ever smaller scales.

Though the intrinsic geometry on the horizon resembles spheres connected by strings, this by itself does not imply that the local *spacetime* geometry is similar

⁸ The error in the area was estimated from convergence studies at the latest time that data were available from all simulations.

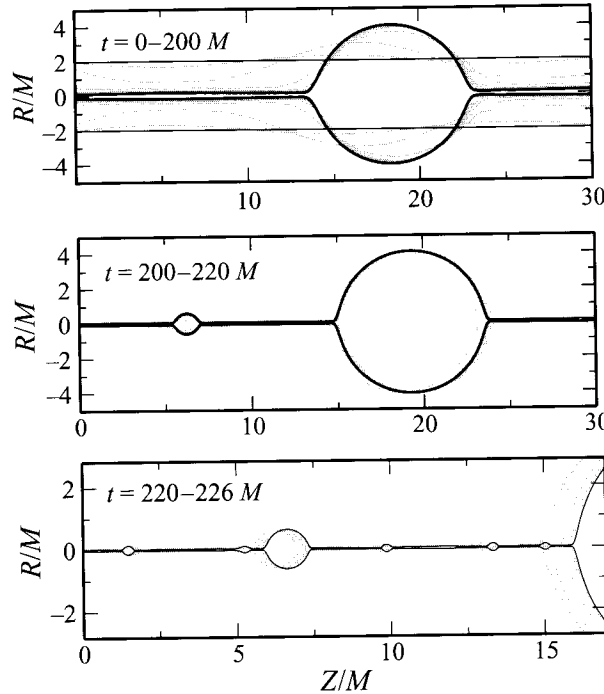


Figure 3.2 Embedding diagram of the apparent horizon at several instances in the evolution of the perturbed black string, from the medium-resolution run. The areal radius is R and the embedding coordinate Z is defined so that the proper length of the horizon in the spacetime w direction (for fixed t, θ, ϕ) is exactly equal to the Euclidean length of $R(Z)$ in the above figure. For visual aid, reflections of the curves about $R = 0$ are included. In the top panel, the thin black lines are from the initial time; in each of the top two panels the thick black lines are the last time from the time-segment depicted in the corresponding panel, whereas in the bottom panel the last time-snapshot has been drawn with a thin black line. Note that the vertical and horizontal axis scales have been changed in the bottom panel to better show the satellites that have formed at late times. The computational domain is periodic in w with period $\delta w = 20M$; at the initial (final) stage of the simulation, $\delta Z = 20M$ ($\delta Z = 27.2M$). See also Fig. 3.5.

to either five-dimensional spherical black holes or black strings, respectively. However, evaluation of the curvature invariants (3.24) on the horizon gives further insight into this question, and the results are shown in Fig. 3.3, taken from the last time step of the medium-resolution run. As seen in the figure, near the spherical-like sections the normalized invariants approach the value 6, in contrast with the string-like sections, where they are close to 1; thus, on the basis of these two invariant indicators at least, the near-horizon geometry does indeed resemble that of the solutions suggested by the shape of the AH.

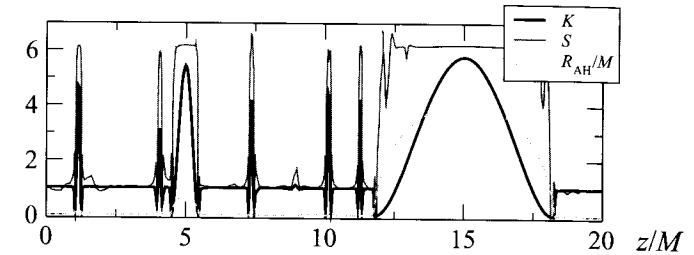


Figure 3.3 Curvature invariants evaluated on the apparent horizon at the last time of the medium-resolution simulation depicted in Fig. 3.2. The areal radius of the apparent horizon is also shown. The invariant K evaluates to 1 for an exact black string and to 6 for an exact spherical black hole; similarly for S (3.24).

3.4.2 Interpretation of the horizon dynamics

The shape of the AH in the embedding diagram and the fact that the invariants tend to the limits associated with pure black strings or black holes at corresponding locations on the AH suggest that it is reasonable to describe the local geometry as being similar to a sequence of black holes connected by black strings. This also strongly suggests that satellite formation will continue in a self-similar cascade, as each string segment locally resembles a uniform black string and is sufficiently thin and long to be unstable. Note that, even if at some point in the cascade thick segments were to form, this would generically not be a stable configuration since (except possibly in an exactly symmetric situation) the satellites will have some nonzero w -velocity; hence they would eventually merge, effectively lengthening the segments connecting the remaining satellites.

With this interpretation we can understand key features of the AH dynamics by sequencing its time evolution into generations of satellite formation. We assign a time t_i to the onset of a new generation, when the local instability has reached an “observable” level, *defined* here (somewhat arbitrarily) as the time when a nascent spherical region reaches an areal radius 1.5 times the surrounding string radius. For each generation we measure the number n_s of satellite black holes that form per string segment, their radii $R_{AH,f}$ as well as the corresponding string segment’s radii $R_{s,i}$ and lengths $L_{s,i}$. These features are summarized in Table 3.1, where the error bars come from convergence calculations.⁹ Only the first generation is in a sense nongeneric since, by construction, initially only one unstable mode

⁹ The global truncation error tends to grow with time; as mentioned, for the third generation we ran only the low- and medium-resolution cases far enough to uncover this fact and consequently (assuming convergence) the much larger errors there. Only the low-resolution run was continued for long enough to reveal a fourth generation; thus there is a lack of error estimates there.

Table 3.1 Properties of the black string's apparent horizon (see the main text for a discussion)

Generation	t_i/M	n_s	$R_{s,i}/M$	$R_{AH,f}/M$	$L_{s,i}/R_{s,i}$
1	118.1 ± 0.5	1	2.00	$4.09 \pm 0.5\%$	10.0
2	203.1 ± 0.5	1	$0.148 \pm 1\%$	$0.63 \pm 2\%$	$105 \pm 1\%$
3	223 ± 2	≥ 1	$0.05 \pm 20\%$	$0.1 - 0.2$	$\approx 10^2$
4	≈ 227	≥ 1	≈ 0.02	?	$\approx 10^2$

is allowed to develop. Generations after the first display string segments where the ratio $L_{s,i}/R_{s,i} \simeq 100$ is not only above the critical value ($\simeq 7.2$) but can in principle accommodate several unstable modes (although see the discussion in section 3.5.1 below). One would expect that the mode closest to the maximum in the dispersion relation would dominate in each segment and thus that *qualitatively* similar dynamics would unfold from one generation to the next. In particular, we see that the time scale for the development of the n th generation of the instability is essentially the same along each string segment, as are the radii of the corresponding strings and spheres that form. However, beyond the second generation we find a variation as a function of the resolution in the number n_s of satellites that form (hence the entries “ ≥ 1 ” in the table). This suggests that exactly which mode dominates depends sensitively on the initial conditions, sufficiently so that a small perturbation, here coming from the numerical truncation error,¹⁰ can change the *quantitative* details of the late-time dynamics. This is not unexpected since, from the Gregory–Laflamme dispersion relation, except for the mode exactly at the maximum there are two unstable modes with the same growth rate.

Extrapolation to the end state

The above observations of the solution properties allow us to extrapolate to the end state of the instability, estimating the time when this will occur and the structure of the horizon just prior to it. We will first calculate when the self-similar cascade ends, namely, the time when the connecting string segments reach zero radius, and then estimate the fractal dimension of the AH geometry just prior to this end.

The time when the first-generation satellite appears is controlled by the perturbation imparted by the initial data, which here is $T_0/M \approx 118$. Subsequent generations, however, should represent the generic development of the instability. From the data in Table 3.1, the time of growth of the first instability *beyond* that

¹⁰ In a slight abuse of terminology, as of course the truncation error does not in general correspond to any physical perturbation.

sourced by the initial data is $T_1/M \approx 80$. Beyond that, with the caveats that we have a small number of data points and poor control over the error at late times, the data *suggests* that each subsequent instability unfolds on a time scale X that is about one-quarter that of the preceding one. Again this is to be expected if the instability is qualitatively like the Gregory–Laflamme instability of the exact black string, where the time scale is proportional to the string radius. Then, the total time ΔT for the end state to be reached is roughly given by

$$\Delta T \approx T_0 + \sum_{i=0}^{\infty} T_1 X^i = T_0 + \frac{T_1}{1-X}. \quad (3.25)$$

For this case, then, $\Delta T/M \approx 231$. At this time¹¹ all string segments will reach zero radius. Since (harmonic) time is regular everywhere from some distance inside the AH outwards and corresponds to the time measured by stationary asymptotic observers (and since the Kretchman curvature invariant (3.24) just outside a string segment of radius r is proportional to r^{-4}), this indicates *the formation of a naked singularity and thus a violation of cosmic censorship*. Furthermore, it is generic in the sense that no fine-tuning of the initial data is required (i.e., *any* lengthwise perturbation exceeding the critical wavelength will have the same effect).

To give further evidence that the data supports the above conclusion, in Fig. 3.4 we show the time evolution of the radius for several representative cross sections of the AH, in logarithmic coordinates where time has been shifted by the estimated time of naked singularity formation. That the radius of string-like segments decreases *linearly* in shifted-logarithmic time is consistent with a self-similar scaling to zero radius at the corresponding finite asymptotic time. Another intriguing aspect of this self-similar scaling is that it is qualitatively the same as that observed in the approach to pinch-off of Raleigh–Plateau unstable fluid streams. In the fluid case a scaling solution is known [53, 54], and the radius R of the fluid column decreases linearly with time t to fluid break-up at $t = t_c$:

$$R \propto t_c - t. \quad (3.26)$$

Figure 3.4 shows that this relation, to a good approximation, also describes the shrinking regions of the black string.

A further consequence of the self-similar nature of the instability is that the AH shape will develop a fractal structure prior to pinch-off. This implies that for a fixed angular cross section ($\theta, \phi = \text{constant}$) of the horizon, the proper length

¹¹ The exact value of the time ΔT is expected to vary slightly along the length of the horizon with our chosen time coordinate and initial perturbation, though one should be able to define a time-slicing for which this time would be exactly the same everywhere along the string.

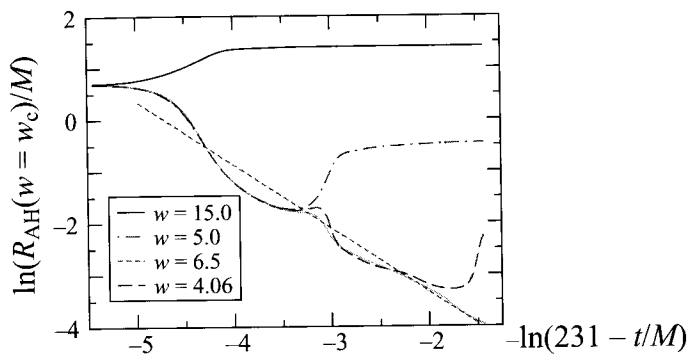


Figure 3.4 The logarithm of the areal radius vs. the logarithm of the shifted time for select points on the apparent horizon, from the medium-resolution run depicted in Fig. 3.2. We have shifted the time axis, *assuming* self-similar behavior; the putative naked singularity forms at asymptotic time $t/M \approx 231$. The coordinates at $w = 15, 5$ and 4.06 correspond to the maxima of the areal radii of the first- and second-generation satellites and one third-generation satellite at the time the simulation stopped (the w positions of the satellites do evolve slightly with time). The value $w = 6.5$ is a representative slice in the middle of a piece of the horizon that remains string-like throughout the evolution. For comparison with an analogous fluid pinch-off scaling solution (3.26), a line with slope equal to minus one has been added (broken line).

$L_p(t)$ (within the periodically identified domain) will grow with each subsequent generation, diverging at a rate related to the Hausdorff dimension d of the end-state shape. Assuming that there is a scaling relation of the form (3.26), that the additional length in each new generation is caused by every string segment developing (on average) the same number n_s of satellites, each with radii $R_{AH,f}$ following the scaling suggested in Table 3.1, and that $n_s R_{AH,f}/L_{s,i} \ll 1$, it can be shown that the following growth in $L_p(t)$ is expected:

$$L_p(t) \propto (t_c - t)^{(1-d)}. \quad (3.27)$$

Figure 3.5 shows a plot of $L_p(t)$ on a logarithmic scale. From the measured slope and the above relationship we find $d \simeq 1.05$, which as expected is greater than 1 (the value 1 corresponds to a nonfractal curve), but only slightly, as the fractal structure is obtained by repeatedly replacing a relatively long straight line with a similar length line plus a small semicircular protrusion.

3.5 Speculations and open questions

In this chapter we have described the evolution of an unstable black string in five dimensions, as far as is numerically feasible given the finite computational

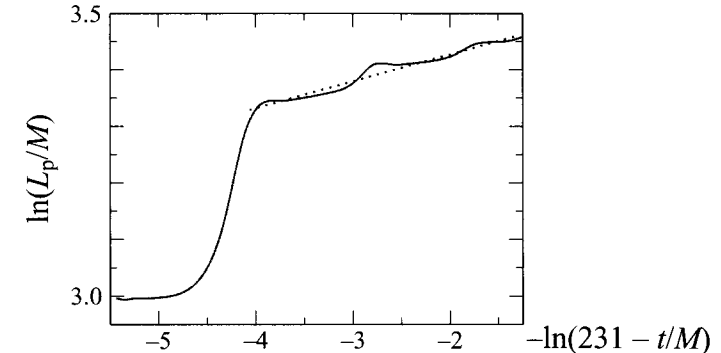


Figure 3.5 The proper length $L_p(t)$ vs. time for the apparent horizon, in logarithmic coordinates along a fixed azimuthal cross-section ($\theta = \phi = \text{constant}$ in spherical coordinates) and over one period of the spacetime in the w direction. The time coordinate is scaled as in Fig. 3.4. The dotted line is a visual linear fit to the late-time dynamics and has a slope ~ 0.048 .

resources, and extrapolated the observed behavior to describe the nature of the end state of the instability. This has provided a first insight into the fascinating dynamics of unstable horizons in higher dimensions and at the same time has raised many questions and opened up avenues for future work. In this concluding section we discuss in section 3.5.1 whether the Gregory–Laflamme linear perturbative analysis can be used to understand quantitatively the dynamics of subsequent generations of the string instability; in section 3.5.2 we estimate when quantum corrections are expected to become important as the string gets thinner; we end with a list of open questions for future directions in section 3.5.3.

3.5.1 Mode behavior

To gain more insight into what determines its observed dynamical behavior, we analyze the different modes in a string segment at the late stages of the first generation (see Table 3.1), which correspond to the early stages of growth of the second generation. In particular, we look at $R_{AH}(t, w)$ in $t \in (175M, 205M)$ when only one spherical region is clearly distinguishable; *in our coordinates*, this region has extent $w \in [10M, 20M]$. The string section corresponds to $w \in [0, 10M]$, and we decompose $R_{AH}(t, w)$ in this latter domain via the expansion

$$R_{AH}(t, w) = c_0 - \sum_{l=1}^{\infty} c_l \sin l\pi w \quad (3.28)$$

and extract the coefficients c_l up to $l = 6$. Figure 3.6 illustrates the values c_l/c_0 within this time frame, and we have plotted only the odd values of l as c_2, c_4, c_6

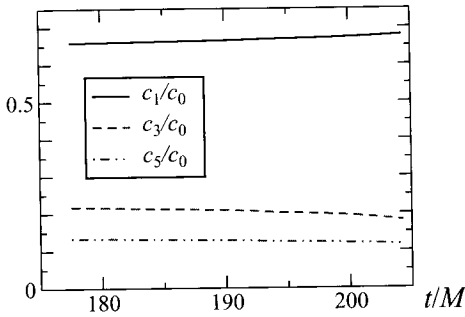


Figure 3.6 Values of the expansion coefficients for the string segment corresponding to the first generation. The even modes (except c_0) are a few orders of magnitude smaller than the odd modes.

are about two orders of magnitude smaller. This is consistent with the observed symmetry in the development of the single second-generation hypersphere within this segment, as it forms exactly in the middle of the string. Interestingly, of the odd modes only $l = 1$ displays a growing behavior even though the length/radius ratio of the string at this time would allow for several modes to be unstable according to the Gregory–Laflamme instability criterion. This may not be too surprising, however, as during this stage the solution is highly dynamical, shrinking in radius at a rate comparable with that at which the putative Gregory–Laflamme modes could grow. This suggests that a linear analysis perturbing about the static black string “background” is not applicable here and can capture only the qualitative nature of subsequent generations of instability. Note, though, that this is not in tension with the observation provided by the invariants K and S , as the string can shrink in a time-dependent fashion and still maintain $K \approx S \approx 1$.

3.5.2 Dynamics beyond the classical regime

As discussed, our *classical* description of the system reveals a cascading self-similar behavior of the horizon, with regions evolving to ever-shrinking cross-sectional radius. Such regions are asymptotic (in finite time) to a zero-mass naked singularity. Obviously, for small enough regions a classical description is no longer applicable and quantum phenomena must be taken into account. This is typically expected to happen when the cross-sectional radius r approaches some small length scale ℓ (e.g. the Planck length l_p or the string length l_s), though exactly when this happens will depend on the details of the leading-order corrections to the field equations. For example, string-type corrections predict this to be of the form

$$R_{\mu\nu} = \ell^2 R_{\mu\alpha\beta\gamma} R_\nu^{\alpha\beta\gamma} + \dots \quad (3.29)$$

Since each term in (3.29) has dimension 1/length², in a naive estimate the right-hand side becomes important when its magnitude becomes of order $1/r^2$, as r is the relevant length scale in the vicinity of a shrinking region of the horizon. Since $R_{\mu\alpha\beta\gamma} \sim 1/r^2$ there, this suggests that corrections to general relativity are important when $\ell^2/r^4 \sim 1/r^2$, i.e., if $\ell = l_p$ then this occurs when the radius shrinks to the Planck length.

Another effect that could in principle alter the classical picture before the Planck scale is reached is if the time scale of Hawking evaporation τ_H of the string segment becomes smaller than the Gregory–Laflamme time scale τ_{GL} . However, as the following argument shows, τ_H only becomes smaller than τ_{GL} beyond the Planck scale.

Assuming that a four-dimensional description of evaporation at a constant- w cross section of a string-like region gives a decent approximation to an evaporating string, we can estimate the time scale of Hawking evaporation and compare it with the time scale for development of the next generation within the self-similar cascade. From the simulation results, we have

$$\tau_{GL} \simeq 100 M_i G / c^3 , \quad (3.30)$$

while for the Hawking evaporation of a four-dimensional black hole of mass M_i we have

$$\tau_H = 10240 \pi^2 \left(\frac{c^5}{hG} \right) \left(\frac{GM_i}{c^3} \right)^3 . \quad (3.31)$$

Thus, for these two times to become comparable, we require that

$$M_i \simeq 10^{-1} \sqrt{\frac{\hbar c}{G}} = 10^{-1} M_p , \quad (3.32)$$

where M_p is the Planck mass. This suggests that if the length scale ℓ in (3.29) is of order the Planck length or larger then, in describing the leading-order alterations to the classical description of the instability, higher-curvature corrections will generically be more important than Hawking evaporation.

3.5.3 Future work

We conclude this chapter by listing some open questions and directions for future work, though this is by no means an exhaustive list.

First, one could consider a broader class of initial perturbations of the five-dimensional black string for which other unstable modes, and possibly linear combinations of modes with similar growth rates, are excited. We would not expect anything to change in a radical fashion, as the qualitative nature of the linear

growth of all these modes is similar. Nevertheless, a quantitative analysis of such scenarios would tell whether this expectation is borne out, and it would allow one to understand how (if at all) the initial perturbation affects the unfolding structure of subsequent generations of the instability. In a similar vein, exploring how adding angular momentum to the string changes the picture would be interesting. Again the qualitative picture should not change, since, as argued in [20] and shown at the linear level in [55], rotation does not suppress the instability. However, in [56] it was suggested that rotation could induce superradiant and gyrating instabilities; this would make for much richer dynamics in the approach to the end state. Allowing for angular momentum would imply less symmetry however, which would lead to more expensive numerical evolution.

Second, one could extract more details about the spacetime, such as the evolution of the generators of the horizon (as in [15]) and the gravitational waves that are emitted as the instability unfolds. Perhaps the most profound question raised by the results in this chapter is the striking qualitative similarity between the *non-linear* evolution of the instability and the Rayleigh–Plateau instability. Is this a coincidence or is it the consequence of a deeper relationship between Einstein and Navier–Stokes than already suggested by the membrane paradigm, black folds, and the other perturbative descriptions of horizon dynamics? What would be useful in trying to understand this is to identify and extract geometric characteristics of the dynamical horizon that would map to effective fluid properties. Such a map could also prove useful in using what is known about the Rayleigh–Plateau instability to learn more about Gregory–Laflamme; for example, translating the Eggers scaling solution [53] to an approximate solution for a thinning string segment.

Third, nonvacuum spacetimes could be considered; in particular, charged black strings would be interesting since charges modify the onset of instabilities in the system (see for example [11, 43]).

Fourth, the case where the spacetime is asymptotically flat in all spatial directions should be studied (the current study imposed periodicity in the fifth dimension). This would be required to provide an example of cosmic censorship violation in the five-dimensional asymptotically flat case. However, it is natural to expect the same behavior as seen here, on the basis of the following putative scenario. Consider a highly distorted S^3 horizon, namely one that is long and thin (i.e., cigar shaped), so that near its center it locally resembles an $S^2 \times \mathbb{R}$ black string. One may expect that this horizon would ring down via gravitational wave emission to a uniform S^3 horizon; however, if the dynamical time scale for the ring-down (which will be proportional to the light-crossing time in the prolate direction and so could be made arbitrarily long) is much longer than that of the Gregory–Laflamme instability of the central region then the latter should take over first, resulting in a pinch-off.

Fifth, black strings in higher-dimensional spacetimes could be explored, in particular to investigate the conjecture in [9] that a qualitatively different end state is expected for $D > 13$. Even if one continues to impose $SO(D - 2)$ symmetry, the problem can still be expressed in such a way as to depend only on (t, r, w) , making it tractable with current computational resources. However, as the fields decay as r^{D-3} or r^{D-2} when one moves away from the black hole or black string solutions respectively, the resolution and/or order of the numerical scheme would need to be higher than that used in this work to obtain results of a comparable accuracy.

Sixth, additional black objects subject to Gregory–Laflamme-like instabilities could be explored. For instance, rapidly rotating black holes have been shown to be subject to a similar instability [57]. Recent numerical work presented the first exploration of such systems [34], though there the radiation of angular momentum stabilizes the black holes considered. However, the growth rate of the instability in the cases studied was rather mild, and it is quite likely that choosing a more extreme scenario (where the time scale of the unstable modes is shorter than the dynamical time of gravitational radiation) would give rise to a pinch-off similar to those studied in this chapter.

Finally, unstable black strings (and other black objects) can be evolved within asymptotically anti-de Sitter (AdS) spacetime, and the consequences explored within the context of the AdS and conformal field theory (CFT) duality of string theory. This is in part related to the point mentioned above about further investigation of the intriguing connections between gravity and fluids, since certain states within a CFT will admit a hydrodynamic description. In any case, understanding the CFT duals to unstable black hole spacetimes is interesting in its own right and could have implications for the more recent applications of AdS/CFT in modeling certain condensed-matter and high-energy particle physics systems.

Acknowledgements

We thank A. Buchel, V. Cardoso, M. Choptuik, R. Emparan, D. Garfinkle, K. Lake, S. Gubser, G. Horowitz, D. Marolf, R. Myers, E. Poisson, W. Unruh, and R. Wald for stimulating discussions. This work was supported by NSERC (LL), CIFAR (LL), the Alfred P. Sloan Foundation (FP), and NSF grant PHY-0745779 (FP). Research at Perimeter Institute is supported through Industry Canada and by the Province of Ontario through the Ministry of Research & Innovation.

References

- [1] R. Gregory, and R. Laflamme, Black strings and p-branes are unstable, *Phys. Rev. Lett.* **70** (1993), 2837–2840.

- [2] R. H. Price, Nonspherical perturbations of relativistic gravitational collapse. I. Scalar and gravitational perturbations, *Phys. Rev.* **D5** (1972), 2419–2438.
- [3] S. W. Hawking and G. F. R. Ellis, *The Large Scale Structure of Space-Time*, Cambridge University Press (1973).
- [4] G. T. Horowitz and K. Maeda, Fate of the black string instability, *Phys. Rev. Lett.* **87** (2001), 131301.
- [5] Gubser, S. S., On non-uniform black branes, *Class. Quant. Grav.* **19** (2002), 4825–4844.
- [6] T. Wiseman, Static axisymmetric vacuum solutions and non-uniform black strings, *Class. Quant. Grav.* **20** (2003), 1137–1176.
- [7] H. Kudoh and T. Wiseman, Properties of Kaluza–Klein black holes, *Prog. Theor. Phys.* **111** (2004), 475–507.
- [8] B. Kleihaus, J. Kunz, and E. Radu, New nonuniform black string solutions, *JHEP* **0606** (2006), 016.
- [9] E. Sorkin, A critical dimension in the black-string phase transition, *Phys. Rev. Lett.* **93** (2004), 031601.
- [10] J. L. Hovdebo and R. C. Myers, Black rings, boosted strings and Gregory–Laflamme, *Phys. Rev.* **D73** (2006), 084013.
- [11] O. Sarbach and L. Lehner, Critical bubbles and implications for critical black strings, *Phys. Rev.* **D71** (2005), 026002.
- [12] B. Kol and T. Wiseman, Evidence that highly non-uniform black strings have a conical waist, *Class. Quant. Grav.* **20** (2003), 3493–3504.
- [13] B. Kol, The phase transition between caged black holes and black strings – a review, *Phys. Rept.* **422** (2006), 119–165.
- [14] M. W. Choptuik, L. Lehner, I. Olabarrieta, *et al.*, Towards the final fate of an unstable black string, *Phys. Rev.* **D68** (2003), 044001.
- [15] D. Garfinkle, L. Lehner, and F. Pretorius, A numerical examination of an evolving black string horizon, *Phys. Rev.* **D71** (2005), 064009.
- [16] D. Marolf, On the fate of black string instabilities: an observation, *Phys. Rev.* **D71** (2005), 127504.
- [17] K. S. Thorne, R. H. Price, and D. A. Macdonald, (eds.), *Black Holes: The Membrane Paradigm*, Yale University Press (1986).
- [18] S. Bhattacharyya, V. E. Hubeny, S. Minwalla, and M. Rangamani, Nonlinear fluid dynamics from gravity, *JHEP* **0802** (2008), 045.
- [19] R. Emparan, T. Harmark, V. Niarchos, and N. A. Obers, World-volume effective theory for higher-dimensional black holes, *Phys. Rev. Lett.* **102** (2009), 191301.
- [20] R. Emparan, T. Harmark, V. Niarchos, and N. A. Obers, Essentials of blackfold dynamics, *JHEP* **1003** (2010), 063.
- [21] V. Cardoso, and O. J. C. Dias, Gregory–Laflamme and Rayleigh–Plateau instabilities, *Phys. Rev. Lett.* **96** (2006), 181601.
- [22] J. Camps, R. Emparan, and N. Haddad, Black brane viscosity and the Gregory–Laflamme instability, *JHEP* **1005** (2010), 042.
- [23] J. Eggers, Nonlinear dynamics and breakup of free-surface flows, *Rev. Mod. Phys.* **69** (1997), 865–930.
- [24] L. Lehner and F. Pretorius, Black strings, low viscosity fluids, and violation of cosmic censorship, *Phys. Rev. Lett.* **105** (2010), 101102.
- [25] P. Kovtun, D. T. Son, and A. O. Starinets, Viscosity in strongly interacting quantum field theories from black hole physics, *Phys. Rev. Lett.* **94** (2005), 111601.
- [26] A. Buchel and J. T. Liu, Universality of the shear viscosity in supergravity, *Phys. Rev. Lett.* **93** (2004), 090602.

- [27] C. Bona and C. Palenzuela-Luque, *Elements of Numerical Relativity*, Springer-Verlag (2005).
- [28] M. Alcubierre, *Introduction to 3+1 Numerical Relativity*, Oxford Science Publications (2008).
- [29] T. W. Baumgarte, and S. L. Shapiro, *Numerical Relativity: Solving Einstein's Equations on the Computer*, Cambridge University Press (2010).
- [30] O. Sarbach and L. Lehner, No naked singularities in homogeneous, spherically symmetric bubble spacetimes?, *Phys. Rev.* **D69** (2004), 021901.
- [31] F. S. Guzman, L. Lehner, and O. Sarbach, Do unbounded bubbles ultimately become fenced inside a black hole?, *Phys. Rev.* **D76** (2007), 066003.
- [32] H. Witek, *et al.*, Numerical relativity for D dimensional space-times: head-on collisions of black holes and gravitational wave extraction, *Phys. Rev.* **D82** (2010), 104014.
- [33] H. Witek, *et al.*, Head-on collisions of unequal mass black holes in $D = 5$ dimensions, *Phys. Rev.* **D83** (2011), 044017.
- [34] M. Shibata and H. Yoshino, Bar-mode instability of rapidly spinning black hole in higher dimensions: numerical simulation in general relativity, *Phys. Rev.* **D81** (2010), 104035.
- [35] H. Okawa, K. Nakao, and M. Shibata, Is super-Planckian physics visible? – scattering of black holes in 5 dimensions, *Phys. Rev.* **D84** (2011), 064045.
- [36] F. Pretorius, Numerical relativity using a generalized harmonic decomposition, *Class. Quant. Grav.* **22** (2005), 425–452.
- [37] D. Garfinkle, Harmonic coordinate method for simulating generic singularities, *Phys. Rev.* **D65** (2002), 044029.
- [38] B. Szilagyi and J. Winicour, Well-posed initial-boundary evolution in general relativity, *Phys. Rev.* **D68** (2003), 041501.
- [39] L. Lindblom, M. A. Scheel, L. E. Kidder, R. Owen, and O. Rinne, A new generalized harmonic evolution system, *Class. Quant. Grav.* **23** (2006), S447–S462.
- [40] C. Palenzuela, M. Anderson, L. Lehner, S. L. Liebling, and D. Neilsen, Stirring, not shaking: binary black holes' effects on electromagnetic fields, *Phys. Rev. Lett.* **103** (2009), 081101.
- [41] C. Gundlach, J. M. Martin-Garcia, G. Calabrese, and I. Hinder, Constraint damping in the Z4 formulation and harmonic gauge, *Class. Quant. Grav.* **22** (2003), 3767–3774.
- [42] F. Pretorius, Evolution of binary black hole spacetimes, *Phys. Rev. Lett.* **95** (2005), 121101.
- [43] R. Gregory, and R. Laflamme, The instability of charged black strings and p-branes, *Nucl. Phys.* **B428** (1994), 399–434.
- [44] E. Sorkin and T. Piran, Initial data for black holes and black strings in 5d, *Phys. Rev. Lett.* **90** (2003), 171301.
- [45] M. Anderson, L. Lehner, and J. Pullin, Arbitrary black-string deformations in the black string–black hole transitions, *Phys. Rev.* **D73** (2006), 064011.
- [46] F. Pretorius, *Binary Black Hole Coalescence*, Springer (2007).
- [47] H. Friedrich, On the hyperdolicity of Einstein's and other gauge field equations, *Commun. Math. Phys.* **100** (1985), 525–543.
- [48] E. Sorkin and M. W. Choptuik, Generalized harmonic formulation in spherical symmetry, *Gen. Rel. Grav.* **42** (2010), 1239–1286.
- [49] M. Alcubierre, S. Brandt, B. Bruegmann, *et al.*, Symmetry without symmetry: numerical simulation of axisymmetric systems using Cartesian grids, *Int. J. Mod. Phys.* **D10** (2001), 273–290.

- [50] J. Thornburg, Event and apparent horizon finders for 3+1 numerical relativity, *Living Rev. Rel.* **10** (2007), 3.
- [51] M. J. Berger and J. Oliger, Adaptive mesh refinement for hyperbolic partial differential equations, *J. Comput. Phys.* **53** (1984), 484.
- [52] G. Calabrese, L. Lehner, O. Reula, O. Sarbach, and M. Tiglio, Summation by parts and dissipation for domains with excised regions, *Class. Quant. Grav.* **21** (2004), 5735–5758.
- [53] J. Eggers, Universal pinching of 3D axisymmetric free-surface flow, *Phys. Rev. Lett.* **71** (1993), 3458–3460.
- [54] U. Miyamoto, One-dimensional approximation of viscous flows, *JHEP* **10** (2010), 011.
- [55] O. J. C. Dias, P. Figueras, R. Monteiro, H. S. Reall, and J. E. Santos, An instability of higher-dimensional rotating black holes, *JHEP* **1005** (2010), 076.
- [56] D. Marolf and B. C. Palmer, Gyrating strings: a new instability of black strings?, *Phys. Rev.* **D70** (2004), 084045.
- [57] R. Emparan and R. C. Myers, Instability of ultra-spinning black holes, *JHEP* **09** (2003), 025.

4

General black holes in Kaluza–Klein theory

GARY T. HOROWITZ AND TOBY WISEMAN

One of the oldest ideas for unifying gravity and electromagnetism is to consider general relativity in five dimensions, with one dimension curled up into a small circle. In other words, one studies vacuum solutions in five dimensions that asymptotically approach $\mathbb{R}^4 \times S^1$ at infinity. This is known as Kaluza–Klein theory [1, 2]. We have already discussed the simplest black hole solution in this theory: the product of a Schwarzschild black hole and a circle. In this chapter we discuss more general Kaluza–Klein black holes. We begin by describing a surprising property of the total energy in this theory. After that we discuss black holes that are invariant under translations around the circle and then drop this restriction.

4.1 Energy in Kaluza–Klein theory

The total energy of an asymptotically flat five-dimensional spacetime is given by a direct generalization of the standard Arnowitt, Deser, and Misner (ADM) formula in four dimensions. Consider the metric on an asymptotically flat spacelike surface and let x^i be asymptotically Euclidean coordinates. Then

$$g_{ij} = \delta_{ij} + h_{ij}, \quad (4.1)$$

and the total mass is given by

$$M = \frac{1}{16\pi G_5} \oint (h_{ij,j} - h_{jj,i}) dS^i, \quad (4.2)$$

where the integral is over a surface at large r . In Kaluza–Klein theory an identical formula holds, but the integral is now over a surface with topology $S^2 \times S^1$, where

the S^2 (two-sphere) has radius r and the S^1 (circle) has length L . The Kaluza-Klein vacuum, the product of a circle and four-dimensional Minkowski space, has $M = 0$.

With standard asymptotically flat boundary conditions, there is a positive energy theorem that states, roughly speaking, that the solution with lowest total energy is Minkowski spacetime. More precisely, recall that the dominant-energy condition states that $T_{\mu\nu}t_1^\mu t_2^\nu \geq 0$ for any two future directed timelike vectors t_1^μ, t_2^ν . One can prove the following [3, 4].

Positive energy theorem Consider any nonsingular asymptotically flat initial data set satisfying the dominant-energy condition. Its total energy cannot be negative and vanishes only for flat Minkowski spacetime.

The condition that the initial data be nonsingular is required to rule out, e.g., the negative-mass Schwarzschild solution. This result holds in all dimensions $D \geq 4$ [5, 6], but only if the spacetime asymptotically approaches \mathbb{R}^D with the flat Minkowski metric.

If a five-dimensional spacetime asymptotically approaches $\mathbb{R}^4 \times S^1$ at infinity, as required in Kaluza–Klein theory, then this theorem does not hold [7]. To see this, consider the five-dimensional generalization of the Schwarzschild metric,

$$ds^2 = - \left(1 - \frac{r_0^2}{r^2}\right) dt^2 + \left(1 - \frac{r_0^2}{r^2}\right)^{-1} dr^2 + r^2(d\theta^2 + \sin^2 \theta d\Omega^2). \quad (4.3)$$

We now make the analytical continuations $t \rightarrow i\chi$ and $\theta \rightarrow \pi/2 + i\tau$. The result is

$$ds^2 = \left(1 - \frac{r_0^2}{r^2}\right) d\chi^2 + \left(1 - \frac{r_0^2}{r^2}\right)^{-1} dr^2 + r^2(-d\tau^2 + \cosh^2 \tau d\Omega^2). \quad (4.4)$$

Since (4.3) is Ricci flat, so is (4.4). To investigate the behavior near $r = r_0$, set $r = r_0 + \rho^2/(2r_0)$. Then, near $\rho = 0$ the (χ, r) part of the metric becomes

$$d\rho^2 + \rho^2 \frac{d\chi^2}{r_\alpha^2} . \quad (4.5)$$

So, if χ is periodic with period $2\pi r_0$ then $\rho = 0$ ($r = r_0$) is just the smooth origin of a rotational symmetry. Now consider the metric on the $\tau = 0$ surface. This spatial metric is asymptotically flat and, since χ is periodic, it satisfies Kaluza-Klein boundary conditions. What is the total energy of this solution? From (4.2) the energy comes from the $1/r$ correction to the metric, so if there is no $1/r$ correction then the total energy vanishes! This shows that $M_4 \times S^1$ is not the only zero-energy solution in the theory.

What is the interpretation of the solution (4.4)? Since the χ circle smoothly caps off at $r = r_0$, there is no spacetime for $r < r_0$. This is called a “bubble of nothing”, in analogy to the bubble of true vacuum that can nucleate inside a false vacuum in field theory. This “bubble of nothing” expands rapidly until it is moving close to the speed of light and eventually hits null infinity.

Not only are there nontrivial solutions with zero energy, one can find vacuum solutions with arbitrarily negative energy [8, 9]. Consider time-symmetric initial data, i.e., initial data with zero extrinsic curvature just like the $\tau = 0$ surface considered above. The only constraint on the spatial metric is that the scalar curvature vanishes. We now use the fact that the Reissner–Nordström metric must have zero scalar curvature since the stress tensor for a Maxwell field in four dimensions is traceless. Analytically continuing t to $i\chi$ and q to iq in the Reissner–Nordström metric yields

$$ds^2 = U(r)d\chi^2 + U^{-1}(r)dr^2 + r^2d\Omega^2, \quad (4.6)$$

with

$$U(r) = 1 - \frac{2m}{r} - \frac{q^2}{r^2}. \quad (4.7)$$

The function $U(r)$ vanishes when $r = r_+ \equiv m + \sqrt{m^2 + q^2}$, so we restrict the r coordinate to $r \geq r_+$. To avoid a conical singularity at $r = r_+$, we identify the coordinate x with period

$$L = \frac{4\pi}{U'(r_+)} = \frac{2\pi r_+^2}{r_+ - m} . \quad (4.8)$$

(Note that we are interested only in the metric and not the Maxwell field that is also a part of the usual Reissner–Nordström solution; we are constructing initial data for a five-dimensional vacuum solution. In particular, q should not be thought of as an electromagnetic charge.)

One can easily evaluate the energy (4.2) for this initial data and one finds that $G_5 M = mL/2$. The parameter m can be positive or negative in this construction since $r_+ > 0$ and the initial data remains nonsingular. Thus we have negative-energy solutions. (The special case $m = 0$ is precisely the initial data for the “bubble of nothing” solution discussed above.) By letting m tend to $-\infty$ and taking $a \approx (-m)^{3/4}$, one can make M arbitrarily negative while keeping L constant.

Given that there are solutions with arbitrarily negative energy in Kaluza–Klein theory, one might wonder why it is still taken seriously as a physical theory. The main reason is that all the solutions we have discussed that violate the positive-energy theorem have the property that spinors must be antiperiodic around a circle

at infinity. This is a problem for the following reason. One can expand any five-dimensional fermion in a Fourier series around the S^1 . The result is an infinite tower of four-dimensional fields with masses which are multiples of $1/L$. Since we want L to be small, the only light fermion is the zero mode. In a space in which all fermions are antiperiodic, there is no such zero mode; hence all fermions would be very massive, which contradicts the fact that we observe light fermions in nature. A realistic theory requires that we supplement the boundary condition with the requirement that fermions are periodic around the circle at infinity. With this added condition, one can prove a positive-energy theorem [5, 6]. All the solutions we discuss in the remainder of this chapter satisfy this condition.

4.2 Homogeneous black hole solutions

If a five-dimensional spacetime is invariant under translations around a small circle, it can be viewed as an effective four-dimensional spacetime coupled to certain matter fields. We begin by constructing the four-dimensional theory that governs these fields. Letting y be a periodic coordinate around the circle with period L , we can write the five-dimensional metric in the form

$$ds^2 = e^{-4\phi/\sqrt{3}}(dy + 2A_\mu dx^\mu)^2 + e^{2\phi/\sqrt{3}}g_{\mu\nu}dx^\mu dx^\nu, \quad (4.9)$$

where $\phi, A_\mu, g_{\mu\nu}$ depend on x^μ but not y . The reason for the factor $\sqrt{3}$ in the definition of the scalar ϕ will become clear shortly.

Note that under a coordinate transformation $y = \tilde{y} + 2\lambda(x^\mu)$ we have

$$dy + 2A_\mu dx^\mu = d\tilde{y} + 2\tilde{A}_\mu dx^\mu, \quad (4.10)$$

where $\tilde{A}_\mu = A_\mu + \partial_\mu\lambda$. So A_μ is like a four-dimensional Maxwell potential, and the usual five-dimensional coordinate transformations include ordinary gauge transformations for A_μ .

For the metric (4.9), $\sqrt{-^5g} = e^{2\phi/\sqrt{3}}\sqrt{-g}$, independently of A_μ , where 5g denotes the five-dimensional metric. If we evaluate the Einstein action for metrics of this form, we find (dropping a surface term):

$$\begin{aligned} S &= \frac{1}{16\pi G_5} \int dy d^4x \sqrt{-^5g} {}^5R \\ &= \frac{1}{16\pi G_4} \int d^4x \sqrt{-g} \left[R - 2(\nabla\phi)^2 - e^{-2\sqrt{3}\phi} F^2 \right], \end{aligned} \quad (4.11)$$

where $F_{\mu\nu} \equiv 2\nabla_{[\mu} A_{\nu]}$ is the Maxwell field associated with A_μ and $G_4 = G_5/L$.

Thus, for metrics that are independent of y , the five-dimensional Einstein action reduces to the action in four-dimensional general relativity, a Maxwell field, and

an extra scalar field ϕ . The strange-looking factors in (4.9) were chosen so that $g_{\mu\nu}$ has the standard four-dimensional Einstein action. The equations of motion that follow from this action are

$$\nabla_\mu \left(e^{-2\sqrt{3}\phi} F^{\mu\nu} \right) = 0, \quad (4.12)$$

$$\nabla^2\phi + \frac{\sqrt{3}}{2}e^{-2\sqrt{3}\phi} F^2 = 0, \quad (4.13)$$

$$\begin{aligned} G_{\mu\nu} &= 2\nabla_\mu\phi \nabla_\nu\phi - g_{\mu\nu}(\nabla\phi)^2 \\ &\quad + 2e^{-2\sqrt{3}\phi} F_{\mu\rho}F_\nu^\rho - \frac{1}{2}g_{\mu\nu}e^{-2\sqrt{3}\phi} F^2. \end{aligned} \quad (4.14)$$

The five-dimensional mass computed from (4.2) agrees with the standard mass computed from the four-dimensional metric $g_{\mu\nu}$.

One simple class of solutions to these equations is $\phi = \text{constant}$, $F_{\mu\nu} = 0$, $g_{\mu\nu}$ is any four-dimensional vacuum solution of Einstein's equation. This is just saying that if a four-dimensional metric ds_4^2 is Ricci flat then its product with S^1 ,

$$ds_5^2 = ds_4^2 + dy^2, \quad (4.15)$$

is also Ricci flat. In particular, if ds_4^2 is the Schwarzschild metric then we get the black string discussed in the previous two chapters.

The above relation between the four- and five-dimensional Newton constant helps explain a puzzle about black hole entropy. In five dimensions the entropy is proportional to the three-dimensional “area” of the event horizon. Since this clearly increases with the length of the circle, one might think that the five-dimensional black string can have many more microstates than the four-dimensional black hole. But in fact the five-dimensional entropy is the same as the four-dimensional entropy:

$$S_5 = \frac{A_5}{4G_5} = \frac{A_4 L}{4G_5} = \frac{A_4}{4G_4} = S_4. \quad (4.16)$$

4.2.1 Nonrotating charged black holes

We have seen that neutral black holes can be obtained by simply taking the product of the Schwarzschild solution and a circle. The same is not true for charged black holes. They are not simply related to the Reissner–Nordström solution since if $F_{\mu\nu} \neq 0$ it acts as a source for ϕ , and so ϕ cannot be constant. At first sight it seems difficult to find charged black hole solutions in this theory since the field equations involve exponentials of ϕ . However, one can use a trick. From the five-dimensional standpoint, one can generate a Maxwell field by a simple boost in the y direction. Indeed, the four-dimensional charge is simply the five-dimensional momentum. So

we start with the product of a Schwarzschild black hole and a line:

$$ds^2 = -\left(1 - \frac{2m}{r}\right)dt^2 + \left(1 - \frac{2m}{r}\right)^{-1}dr^2 + r^2d\Omega^2 + d\hat{y}^2. \quad (4.17)$$

We now boost this solution in the \hat{y} direction:

$$\begin{aligned} \hat{t} &= t \cosh \alpha - y \sinh \alpha, \\ \hat{y} &= y \cosh \alpha - t \sinh \alpha. \end{aligned} \quad (4.18)$$

Then¹

$$\begin{aligned} ds^2 &= -\left(1 - \frac{2m \cosh^2 \alpha}{r}\right)dt^2 + \left(1 + \frac{2m \sinh^2 \alpha}{r}\right)dy^2 \\ &\quad - \frac{4m \cosh \alpha \sinh \alpha}{r} dt dy + \left(1 - \frac{2m}{r}\right)^{-1}dr^2 + r^2d\Omega^2. \end{aligned} \quad (4.19)$$

We now compactify y and put this into standard Kaluza–Klein form by defining

$$e^{-4\phi/\sqrt{3}} = 1 + \frac{2m \sinh^2 \alpha}{r}, \quad (4.20)$$

$$A_t = -\frac{m \cosh \alpha \sinh \alpha}{r + 2m \sinh^2 \alpha}. \quad (4.21)$$

In defining the four-dimensional metric $g_{\mu\nu}$ one must remember to subtract the A_t^2 term from g_{tt} in (4.19). Setting

$$q = 2m \cosh^2 \alpha, \quad (4.22)$$

the result is

$$g_{\mu\nu}dx^\mu dx^\nu = -f dt^2 + \frac{dr^2}{f} + R^2 d\Omega^2 \quad (4.23)$$

where

$$f(r) = \frac{r - 2m}{[r^2 + (q - 2m)r]^{1/2}}, \quad R^2(r) = r[r^2 + (q - 2m)r]^{1/2}. \quad (4.24)$$

This describes a black hole with event horizon at $r = 2m$ and singularity at $r = 0$. Note that the boost and dimensional reduction have not changed the location of the horizon or singularity. Unlike the Reissner–Nordström case, these black

holes do *not* have a regular inner horizon. The singularity is spacelike, as for the Schwarzschild solution.

The total mass can be obtained by applying the general formula (4.2) to the five-dimensional metric (4.19), but an easier approach is to compare the four-dimensional metric (4.23) at large r with the Schwarzschild solution. Expanding the metric functions for large r , we have $R^2 = r^2 + r(q - 2m)/2 + \dots$ and $f = 1 - (q + 2m)/2r + \dots$. To compare with Schwarzschild, we take R to be our radial coordinate, so $f = 1 - (q + 2m)/(2R) = 1 - 2G_4M/R$. The total charge can be obtained by writing $A_t = -Q/R + \dots$. The results are

$$G_4M = \frac{q + 2m}{4}, \quad Q^2 = \frac{q(q - 2m)}{4}. \quad (4.25)$$

The extremal limit corresponds to the maximum possible charge for a given mass. This limit corresponds to $m \rightarrow 0$, so one obtains

$$Q \rightarrow \frac{q}{2}, \quad G_4M \rightarrow \frac{q}{4} \quad \Rightarrow \quad Q = 2G_4M. \quad (4.26)$$

Recall that the extremal Reissner–Nordström black hole has $Q = G_4M$, so on the face of it Kaluza–Klein black holes can carry twice as much charge. Actually, a Kaluza–Klein black hole cannot quite carry twice as much charge, since the extremal limit is singular. The event horizon is at $r = 2m$, so in the extremal limit ($m = 0$) the horizon becomes singular. Since the nonextremal black hole has a spacelike singularity, one might expect that in the extremal limit the singularity is either spacelike or null. However, the following calculation shows that the singularity is actually timelike. Consider a radial null geodesic that hits the singularity. It satisfies

$$dt = \frac{dr}{f} \approx q^{1/2} \frac{dr}{r^{1/2}}, \quad (4.27)$$

where the last expression is valid for small r . Since the ingoing radial null geodesic can reach the singularity at $r = 0$ in finite t , it can lie entirely to the past of an outgoing radial null geodesic. This shows that the singularity is timelike. If the singularity were null then t would diverge as $r \rightarrow 0$, just like geodesics approaching a horizon.

What is the five-dimensional description of an extreme black hole? Writing (4.19) in terms of $q = 2m \cosh^2 \alpha$ and taking the limit $m \rightarrow 0$ while keeping q fixed yields

$$ds^2 = -dt^2 + dy^2 + dr^2 + r^2d\Omega^2 + \frac{q}{r}(dt - dy)^2. \quad (4.28)$$

¹ These boosted black strings are also subject to Gregory–Laflamme instabilities [10].

This is a five-dimensional generalization of a plane-fronted gravitational wave. Setting $v = t + y$, $u = t - y$, plane-fronted waves take the form

$$ds^2 = -dudv + dx^i dx_i + F(u, x^i) du^2. \quad (4.29)$$

These metrics are Ricci flat if F satisfies the simple flat-space Laplace equation

$$\partial^i \partial_i F = 0, \quad (4.30)$$

where $i = 1, 2, 3$ in five dimensions. The u -dependence is arbitrary. The extremal black hole corresponds to a very simple plane-fronted wave that is independent of u . It is a higher-dimensional version of the Aichelberg–Sexl metric.

We have discussed electrically charged solutions. Magnetically charged solutions can be obtained by a duality rotation. Setting

$${}^*F_{\mu\nu} = \frac{1}{2} e^{-2\sqrt{3}\phi} \epsilon_{\mu\nu}^{\rho\sigma} F_{\rho\sigma}, \quad (4.31)$$

the field equations are invariant under $F \rightarrow {}^*F$, $\phi \rightarrow -\phi$. (A similar duality rotation can be used to obtain magnetically charged Reissner–Nordström black holes.) So, a magnetically charged black hole has the same four-dimensional metric (4.23), (4.24) but different matter fields. To emphasize that the solution is now magnetically charged we will replace q with p , i.e., set $p = 2m \cosh^2 \alpha$. Then

$$e^{4\phi/\sqrt{3}} = 1 + \frac{p - 2m}{r}, \quad (4.32)$$

$$A_\phi = P(1 - \cos \theta), \quad (4.33)$$

where

$$P^2 = \frac{p(p - 2m)}{4}; \quad (4.34)$$

P is the magnetic charge, since $F_{\theta\phi} = \partial_\theta A_\phi = P \sin \theta$, so

$$P = \frac{1}{4\pi} \int F_{\theta\phi} d\theta d\phi. \quad (4.35)$$

There is no globally defined vector potential for a magnetic monopole: if A were globally defined, we would have $\int_{S^2} dA = 0$. The vector potential in (4.33) is not well behaved at $\theta = \pi$ since $\int A_\phi d\phi \neq 0$ even when the circle shrinks to zero size. This is sometimes called a “Dirac string”. To avoid it, one can work with two separate regions on the sphere, using (4.33) on the northern hemisphere and setting $A_\phi = -P(1 + \cos \theta)$ on the southern hemisphere.

Let us reconstruct the five-dimensional metric corresponding to the magnetically charged black hole. Using the general formula (4.9) we get

$$ds^2 = \left(1 + \frac{p - 2m}{r}\right)^{-1} [dy + 2P(1 - \cos \theta)d\phi]^2 - \left(1 - \frac{2m}{r}\right)dt^2 + \left(1 + \frac{p - 2m}{r}\right)\left(1 - \frac{2m}{r}\right)^{-1}dr^2 + r^2 \left(1 + \frac{p - 2m}{r}\right)d\Omega^2 \quad (4.36)$$

Note that the square roots that are present in the four-dimensional metric have gone. This spacetime still has a horizon at $r = 2m$ and a singularity at $r = 0$. We now take the extremal limit: $m = 0$. Remarkably, $g_{tt} = -1$ so the metric reduces to a simple product of time and a four-dimensional positive definite metric. The four-dimensional metric still looks singular at $r = 0$, but if we set $\chi \equiv y/2P$ and

$$\rho \equiv 2(pr)^{1/2} \Rightarrow d\rho^2 = \frac{pdr^2}{r} \quad (4.37)$$

then near $r = 0$ the spatial metric is

$$d\rho^2 + \frac{\rho^2}{4} \left\{ [d\chi + (1 - \cos \theta)d\phi]^2 + d\theta^2 + \sin^2 \theta d\phi^2 \right\}. \quad (4.38)$$

If χ is periodic with period 4π , the quantity in brackets is the metric on S^3 with radius 2 expressed as a Hopf fibration. So, the metric is smooth at $\rho = 0$ (or $r = 0$) provided that y has period $8\pi P$; this fixes the period of the Kaluza–Klein circle in terms of the magnetic charge P . This nonsingular solution is called the *Kaluza–Klein monopole* [11, 12].

It is remarkable that Kaluza–Klein theory has a nonsingular magnetic monopole solution, since Einstein–Maxwell theory, for example, does not.² The spatial metric is called the Taub-NUT instanton and has topology \mathbb{R}^4 . Asymptotically it looks like $\mathbb{R}^3 \times S^1$ and satisfies the usual Kaluza–Klein boundary conditions, but at small r the S^1 combines with the S^2 of spherical symmetry to form an S^3 , which smoothly shrinks to zero at the origin of the four-dimensional space.

Since the four-dimensional metric is the same as in the electrically charged case, the extremal limit is singular. Thus we have an example of a four-dimensional spacetime with a curvature singularity that is resolved by lifting the solution to five dimensions. Conversely, one can see that the singularity in the four-dimensional

² Of course the five-dimensional metric is still a vacuum solution to Einstein’s equation. The magnetic charge arises in the reduction to four dimensions.

metric arises because $g_{yy} = 0$ at $r = 0$. In other words, the length of the circle along which we are reducing goes to zero there.

We have seen that the extremal limit of both the electrically charged and magnetically charged Kaluza–Klein black holes is singular in four dimensions. It turns out that black holes with both electric and magnetic charge (sometimes called dyonic black holes) have an extremal limit with a nonsingular horizon having nonzero area. We will not present it here since the solution is considerably more complicated [13] and is easily obtained from the more general rotating black holes to be discussed in the next section.

4.2.2 Rotating Kaluza–Klein black holes

To obtain a rotating, electrically charged, Kaluza–Klein solution, one can repeat the construction in the previous section, starting with the Kerr metric. In other words one takes the product of Kerr and a line, boosts along the line, and then compactifies the extra dimension. Rather than discuss this solution explicitly, we will jump ahead and give the most general known analytic family of black holes in Kaluza–Klein theory. These solutions are all stationary, axisymmetric, and invariant under translations in y . They depend on four parameters (m, q, p, a) which determine the mass M , the electric and magnetic charges Q, P , and the angular momentum J . The five-dimensional metric is given by

$$ds^2 = \frac{H_2}{H_1}(dy + 2\mathbf{A})^2 - \frac{\Delta_\theta}{H_2}(dt + \mathbf{B})^2 + H_1 \left(\frac{dr^2}{\Delta} + d\theta^2 + \frac{\Delta}{\Delta_\theta} \sin^2 \theta d\phi^2 \right), \quad (4.39)$$

where $H_1, H_2, \Delta_\theta, \Delta$ are all quadratic functions of r :

$$\begin{aligned} H_1 &= r^2 + a^2 \cos^2 \theta + r(p - 2m) + \frac{p}{p+q} \frac{(p-2m)(q-2m)}{2} \\ &\quad - \frac{p}{2m(p+q)} \sqrt{(q^2 - 4m^2)(p^2 - 4m^2)} a \cos \theta, \end{aligned} \quad (4.40)$$

$$\begin{aligned} H_2 &= r^2 + a^2 \cos^2 \theta + r(q - 2m) + \frac{q}{p+q} \frac{(p-2m)(q-2m)}{2} \\ &\quad + \frac{q}{2m(p+q)} \sqrt{(q^2 - 4m^2)(p^2 - 4m^2)} a \cos \theta, \end{aligned} \quad (4.41)$$

$$\Delta_\theta = r^2 - 2mr + a^2 \cos^2 \theta, \quad (4.42)$$

$$\Delta = r^2 - 2mr + a^2, \quad (4.43)$$

and the 1-forms \mathbf{A}, \mathbf{B} are given by

$$\begin{aligned} \mathbf{A} = & - \left[Q \left(r + \frac{p-2m}{2} \right) + \sqrt{\frac{q^3(p^2-4m^2)}{16m^2(p+q)}} a \cos \theta \right] H_2^{-1} dt \\ & - \left(P(H_2 + a^2 \sin^2 \theta) \cos \theta + \sqrt{\frac{p(q^2-4m^2)}{16m^2(p+q)^3}} \right. \\ & \left. \times \{(p+q)[pr-m(p-2m)]+q(p^2-4m^2)\} a \sin^2 \theta \right) H_2^{-1} d\phi \end{aligned} \quad (4.44)$$

$$\mathbf{B} = \sqrt{pq} \frac{(pq+4m^2)r - m(p-2m)(q-2m)}{2m(p+q)\Delta_\theta} a \sin^2 \theta d\phi. \quad (4.45)$$

The complicated solution (4.39)–(4.45) was found by a solution-generating technique that uses hidden symmetries of Einstein's equations with Killing fields [14–16].

After dimensional reduction the five-dimensional solution becomes a four-dimensional black hole with metric

$$ds^2 = -\frac{\Delta_\theta}{\sqrt{H_1 H_2}}(dt + \mathbf{B})^2 + \sqrt{H_1 H_2} \left(\frac{dr^2}{\Delta} + d\theta^2 + \frac{\Delta}{\Delta_\theta} \sin^2 \theta d\phi^2 \right). \quad (4.46)$$

The matter fields are the gauge field \mathbf{A} (4.44), and the dilaton, for which

$$e^{-4\phi/\sqrt{3}} = \frac{H_2}{H_1}. \quad (4.47)$$

The four parameters m, q, p, a appearing in the solution are related to the physical parameters M, Q, P, J by

$$G_4 M = \frac{p+q}{4}, \quad (4.48)$$

$$G_4 J = \frac{\sqrt{pq}(pq+4m^2)}{4(p+q)} \frac{a}{m}, \quad (4.49)$$

$$Q^2 = \frac{q(q^2-4m^2)}{4(p+q)}, \quad (4.50)$$

$$P^2 = \frac{p(p^2-4m^2)}{4(p+q)}. \quad (4.51)$$

The charge parameters Q, P have already appeared, in (4.44) and (4.45). Note that $q, p \geq 2m$; equality corresponds to the absence of electric or magnetic charge, respectively. The solutions discussed in the previous subsection correspond to $a = 0$ and either $p = 2m$ or $q = 2m$.

These rotating black holes have inner and outer horizons at $\Delta = 0$, i.e.,

$$r_{\pm} = m \pm \sqrt{m^2 - a^2}. \quad (4.52)$$

There are two qualitatively different types of extremal limit. Both yield black holes with smooth event horizons. The first is like Kerr: $a = m$. This is called the “fast rotation” case since $G_4 J > QP$. The other extremal limit is like that in the charged case discussed earlier: we take $m \rightarrow 0$ and $a \rightarrow 0$ but keep the ratio $a/m < 1$ fixed. This is the “slow rotation” case, since $G_4 J < QP$. In this limit,

$$Q^{2/3} + P^{2/3} = \left(\frac{q+p}{2}\right)^{2/3}, \quad (4.53)$$

and so the mass of the black hole can be expressed in terms of the charges:

$$2G_4 M = (Q^{2/3} + P^{2/3})^{3/2}. \quad (4.54)$$

The striking thing about this formula is that it is independent of the angular momentum J . As long as $G_4 J < QP$, one can add angular momentum to an extremal Kaluza–Klein black hole without changing the mass or making it nonextremal. Another surprising aspect of this extremal black hole is that the angular velocity of the horizon vanishes even though the angular momentum is nonzero. This implies that there is no ergoregion.

The black hole temperature vanishes in both extremal limits. The entropy takes a simple form. For the slowly rotating extremal solution ($G_4 J < QP$) the entropy is

$$S = 2\pi \sqrt{\frac{Q^2 P^2}{G_4^2} - J^2}, \quad (4.55)$$

while for the fast-rotation case ($G_4 J > QP$) the extremal entropy is

$$S = 2\pi \sqrt{J^2 - \frac{Q^2 P^2}{G_4^2}}. \quad (4.56)$$

The only difference is the overall sign inside the square root. When $G_4 J = QP$ the horizon area vanishes and the extremal solution is again singular. The solutions discussed in the previous subsection have $J = 0$ and only one nonzero charge, so their horizon area vanishes in the extremal limit as already discussed.

4.3 Inhomogeneous black hole solutions

For the remainder of this chapter we shall focus on static vacuum five-dimensional solutions to Kaluza–Klein theory but will drop the condition that the metric has an isometry associated with translations about the S^1 . With that isometry the only static black hole solution that asymptotes to the Kaluza–Klein vacuum is (4.36) [17, 18]. We further restrict our attention to solutions with no Kaluza–Klein magnetic charge, so that the only translationally invariant static black hole solution is the black string.

However, we shall see that the full space of static solutions without the circle isometry is very complicated indeed.³

Without the S^1 isometry the Einstein equations lead to partial differential equations, and it is currently unclear how to find exact solutions. Perturbative techniques give a window onto certain solutions, and we shall discuss these shortly. However, generally we require numerical methods such as those to be discussed in Chapter 10 to reveal the full and fascinating structure of the solution space.

4.3.1 Localized black holes

We will begin our exploration of the general static Kaluza–Klein black hole by taking the limit in which we can neglect the fact that the extra dimension is compact. A very small black hole, where by “small” we mean that its radius is much smaller than the size of the compact dimension, L , will appear to a nearby observer approximately like a five-dimensional Schwarzschild solution. The spherical symmetry of the black hole will be preserved near its horizon, but far away will be broken by the compactification of the spacetime. Conversely, the asymptotic S^1 translation invariance will be broken by the presence of this black hole, which is localized at some particular position on the circle. We term such a solution a “localized” black hole, and such solutions were first discussed in detail by Myers [21].

Consider a five-dimensional Schwarzschild solution. We may write this in isotropic coordinates as

$$ds_{\text{Sch}}^2 = -\left(\frac{\rho_0^2 - 4\rho^2}{\rho_0^2 + 4\rho^2}\right)^2 dt^2 + \left(1 + \frac{\rho_0^2}{4\rho^2}\right)^2 (d\rho^2 + \rho^2 d\Omega_3^2), \quad (4.57)$$

where the horizon radius is ρ_0 , although we note that the coordinate position of the horizon, ρ_h , is at $\rho_h = \rho_0/2$. Of course, far from the horizon, i.e., for $\rho \gg \rho_h$, this

³ Much literature exists on this topic, and there are many details and interesting avenues that we are not able to cover here. The interested reader is referred to two reviews on this topic [19, 20], although we note that there has been significant numerical progress since these were written.

solution becomes flat:

$$ds_{\text{Sch}}^2 = -dt^2 + dr^2 + r^2 d\Omega_2^2 + dy^2 + \frac{\rho_0^2}{2\rho^2} (2dt^2 + dr^2 + r^2 d\Omega_2^2 + dy^2) + O\left(\frac{\rho_0^4}{\rho^4}\right), \quad (4.58)$$

where we have chosen new coordinates, r and y , in which to write this asymptotic behaviour:

$$r = \rho \cos \theta, \quad y = \rho \sin \theta, \quad (4.59)$$

so that $\rho^2 = r^2 + y^2$. The leading term looks just like the Kaluza–Klein vacuum,

$$ds_{\text{vac}}^2 = -dt^2 + dr^2 + r^2 d\Omega_2^2 + dy^2, \quad (4.60)$$

except that we cannot make the identification $y \sim y + L$ as this is not compatible with the subleading term going as $\sim 1/\rho^2$ in (4.58).

Let us try to describe more precisely what happens to the metric away from the black hole. The method we will use is based on the ‘‘matched asymptotic expansion’’ approach of [22, 23]. We term the coordinates r, y the ‘‘far-field chart’’. These are adapted to the asymptotic translation symmetry, and $y \sim y + L$. The coordinates ρ, θ form the ‘‘near-field chart’’; they are adapted to the approximate spherical symmetry near the horizon of a small black hole. These two charts must overlap. Let us take the extents of the near and far field charts to be such that

$$\text{far field : } r^2 + y^2 > (1 - \Delta)\ell^2; \quad \text{near field : } \rho_h^2 < \rho^2 < (1 + \Delta)\ell^2, \quad (4.61)$$

where ℓ is a scale that is both parametrically larger than ρ_0 and smaller than L in the limit $\rho_0/L \rightarrow 0$. We might, for example, take $\ell^2 = \rho_0 L$. The constant Δ is $O(1)$ and ensures that the charts overlap: $0 < \Delta < 1$.

Far from the horizon the black hole appears to be a localized source of mass and, being static, we expect that it can be treated as a point mass source in Newtonian perturbation theory. For a point mass source at $r = y = 0$ in the vacuum (4.60), one may solve the linear problem to obtain the metric in the far field:

$$ds^2 \simeq ds_{\text{vac}}^2 + \Phi(2dt^2 + dr^2 + r^2 d\Omega_2^2 + dy^2), \quad (4.62)$$

where the Newtonian potential is explicitly given as

$$\Phi = \frac{4G_5 M}{3Lr} \frac{\sinh(2\pi r/L)}{\cosh(2\pi r/L) - \cos(2\pi y/L)}, \quad (4.63)$$

here M is the mass computed from (4.2) and Φ is a harmonic function on (4.60) with a delta function source at the origin [21]. In the overlap region, then, $\rho/L \ll 1$

and we may expand the potential Φ in the near-field coordinates as follows:

$$\Phi = \frac{4G_5 M}{3\pi\rho^2} \left[1 + \frac{\pi^2}{3} \frac{\rho^2}{L^2} + \frac{\pi^4(1 - 2\cos 2\theta)}{45} \frac{\rho^4}{L^4} + O\left(\frac{\rho^6}{L^6}\right) \right]. \quad (4.64)$$

Taking the two leading terms we write the metric in the overlap as

$$ds^2 \simeq ds_{\text{vac}}^2 + \frac{4G_5 M}{3\pi} \left(\frac{1}{\rho^2} + \frac{\pi^2}{3L^2} \right) (2dt^2 + d\rho^2 + \rho^2 d\Omega_3^2). \quad (4.65)$$

In the near field the matched asymptotic expansion method suggests that we consider perturbations of the five-dimensional Schwarzschild solution. However, for our discussion the perturbation that we require can be thought of simply as a global scaling together with a scaling of time. Hence the near-field solution remains Schwarzschild, and we can write it as

$$ds^2 = -(1 + c_t) \left(\frac{\rho_0^2 - 4\rho^2}{\rho_0^2 + 4\rho^2} \right)^2 dt^2 + (1 + c_y) \left(1 + \frac{\rho_0^2}{4\rho^2} \right)^2 (d\rho^2 + \rho^2 d\Omega_3^2), \quad (4.66)$$

where c_t and c_y are constants, with $|c_t|, |c_y| \ll 1$, which give the required perturbative scalings. Then, in the overlap, where $\rho \gg \rho_0$ the metric behaves similarly to the expansion (4.58):

$$ds^2 \simeq ds_{\text{vac}}^2 + \frac{\rho_0^2}{2\rho^2} (2dt^2 + d\rho^2 + \rho^2 d\Omega_3^2) - c_t dt^2 + c_y (d\rho^2 + \rho^2 d\Omega_3^2). \quad (4.67)$$

We see that in order to match the far- and near-field asymptotic expansions, (4.65) and (4.67), we must have

$$G_5 M = \frac{3\pi}{8} \rho_0^2, \quad -\frac{1}{2} c_t = c_y = \frac{\pi^2 \rho_0^2}{6L^2}. \quad (4.68)$$

Here we have matched the first two terms in the asymptotic expansions. Proceeding further, we see that the next term in (4.64) involves an angular dependence and cannot be matched simply by the Schwarzschild metric alone. One must perform static perturbation theory about the Schwarzschild metric and match this with a multipole expansion. In addition, in the far field one must go beyond the Newtonian order. This procedure is detailed in [22], which shows how to construct the metric in the near and far field, order by order in the perturbation parameter ρ_0/L . The simple behavior discussed above arises because the lowest multipole static perturbations of Schwarzschild (being spherically symmetric) can only be trivial global and time scalings, owing to Birkhoff’s theorem.

Having related the far-field parameter, the mass M , to the near-field parameters ρ_0 , c_t , and c_y , we may proceed to compute physical quantities. From the near-field solution we may compute the horizon area A and the surface gravity κ perturbatively in powers of ρ_0/L :

$$\begin{aligned} A &\simeq 2\pi^2 \rho_0^3 (1 + c_y)^{3/2} = 2\pi^2 \rho_0^3 \left[1 + \frac{\pi^2 \rho_0^2}{4L^2} + O\left(\frac{\rho_0^4}{L^4}\right) \right], \\ \kappa &\simeq \frac{1}{\rho_0} \left(\frac{1 + c_t}{1 + c_y} \right)^{1/2} = \frac{1}{\rho_0} \left[1 - \frac{\pi^2 \rho_0^2}{4L^2} + O\left(\frac{\rho_0^4}{L^4}\right) \right]. \end{aligned} \quad (4.69)$$

We know that the mass has leading behavior $M = (3\pi/8G_5)\rho_0^2$. However, we can compute the subleading correction to this using the first law of black hole mechanics (see the end of Chapter 1) at constant circle size L , giving $dM = (\kappa/8\pi G_5)dA$. Then, using the expressions for A and κ above yields

$$M = \frac{3\pi}{8G_5} \rho_0^2 \left[1 + \frac{\pi^2 \rho_0^2}{12L^2} + O\left(\frac{\rho_0^4}{L^4}\right) \right], \quad (4.70)$$

and hence we see that for small localized black holes we have the behavior

$$\begin{aligned} A &= 32(2\pi)^{1/2} \left(\frac{G_5 M}{3} \right)^{3/2} \left[1 + \frac{\pi G_5 M}{3L^2} + O\left(\frac{G_5^2 M^2}{L^4}\right) \right], \\ \kappa &= \left(\frac{8G_5 M}{3\pi} \right)^{-1/2} \left[1 - \frac{5\pi G_5 M}{9L^2} + O\left(\frac{G_5^2 M^2}{L^4}\right) \right], \end{aligned} \quad (4.71)$$

where the leading behavior is that predicted by Myers [21] and the subleading corrections were computed in [23, 24].

Another interesting quantity to compute is the proper distance between the poles of the horizon along the axis of rotational symmetry, L_{axis} . One might imagine that as the black hole size is increased there is a corresponding linear response, decreasing the length of the axis as $L_{\text{axis}} \simeq L(1 - \alpha\rho_0/L)$ for some constant $\alpha > 0$. This constant may be computed from our metrics above, and surprisingly one finds it precisely vanishes. There is no linear variation of L_{axis} , and this has been termed the “Archimedes effect” [22]. To leading order the geometry around the small black hole precisely expands to accommodate the latter.

Moving beyond perturbation theory we expect that localized black holes exist as solutions to the full Einstein equations, at least for $G_5 M \ll L^2$. Since the five-dimensional Schwarzschild solution is dynamically stable, we expect that the localized black hole solutions are similarly dynamically stable in this limit. An interesting question to which we shall return later is what happens to this branch of solutions as their mass M increases for fixed L . Presumably, when $G_5 M \sim L^2$,

so that their horizon size becomes of order the asymptotic circle size, they become strongly deformed from the Schwarzschild geometry. One possibility is that the interellar distance L_{axis} actually goes to zero at some finite mass, say M_* , so that the solution branch ends. Another possibility is that the Archimedes effect ensures that the geometry always accommodates an increasingly large horizon, and so there is no upper mass limit to these solutions. We shall return to this question later and find evidence that the former possibility actually occurs. However, before we discuss this we must introduce a rather exotic static black hole, the inhomogeneous black string.

4.3.2 Inhomogeneous black strings

Earlier we discussed the simplest static black hole in Kaluza–Klein theory, the black string, which is a straightforward product of the Schwarzschild metric and a circle. Let us write this solution in Schwarzschild form as

$$ds^2 = - \left(1 - \frac{r_0}{r} \right) dt^2 + \left(1 - \frac{r_0}{r} \right)^{-1} dr^2 + r^2 d\Omega_2^2 + dy^2. \quad (4.72)$$

We have seen that this solution is dynamically unstable to perturbations that have wavenumber k on the circle less than a critical wavenumber $k_c \simeq 0.876/r_0$. Let us choose our extra dimension to have length L , so that $y \sim y + L$, and take this length to be precisely the critical wavelength for marginal stability, $L = 2\pi/k_c$. Being marginally stable this black string has an exactly static linear perturbation, and Gregory and Laflamme realized that this might signal the existence of a new class of static solutions [25]. Gubser argued that this deformation does indeed lift to the full nonlinear theory, to generate an entirely new branch of solutions [26]. Since the perturbation explicitly breaks the translation invariance on the circle, these static solutions have the horizon topology of the black string but are inhomogeneous on the circle. We term them inhomogeneous black strings, in contrast with the solution (4.72) above to which we now refer as a homogeneous black string. Such inhomogeneous black strings were first discussed by Horowitz and Maeda as possible end states of the Gregory–Laflamme (GL) instability [27]; interestingly, at least for five-dimensional Kaluza–Klein theory, it appears that they are all unstable and therefore cannot serve as such an end state.

Just as for the localized solutions, these inhomogeneous black strings may be constructed perturbatively. For localized black holes the perturbative limit occurs when the horizon size is very small compared with L . For these inhomogeneous black strings the perturbative limit occurs when they are very weak deformations of the homogeneous marginally stable solution. We will now give an overview of this perturbative construction, essentially following the approach of Gubser [26]. For

this discussion we will perform an overall scaling of the solution such that $r_0 = 1$, so that $L = 2\pi/0.876$. We may then write the general metric with the isometries of the inhomogeneous black strings as

$$ds^2 = - \left(1 - \frac{1}{r}\right) e^{2A} dt^2 + e^{2B} \left[\left(1 - \frac{1}{r}\right)^{-1} dr^2 + dy^2 \right] + r^2 e^{2C} d\Omega_2^2, \quad (4.73)$$

where the functions A , B , C depend on r and also on y owing to the inhomogeneity. We require that the horizon at $r = 1$ is regular and that asymptotically $A, B, C \rightarrow 0$, which ensures that the static Killing vector $\partial/\partial t$ has unit normalization and the circle size is L .

At linear order in perturbation theory we have the marginal GL mode. This takes the form

$$A = \lambda a(r) \cos k_c y, \quad B = \lambda b(r) \cos k_c y, \quad C = \lambda c(r) \cos k_c y, \quad (4.74)$$

where λ is the perturbation parameter and a , b , and c are functions of r and must be determined numerically by solving ordinary differential equations. Gubser's method gives a systematic way to compute the backreaction of this mode. Nonlinear terms in the Einstein equations couple the various Fourier modes on the circle. The linear term squares to give a source at quadratic order and, since $\cos^2 k_c y = \frac{1}{2}(1 + \cos 2k_c y)$, one obtains contributions to the backreaction at $O(\lambda^2)$ that go as the constant mode and as $\cos 2k_c y$ on the circle. Similarly, since $\cos^3 k_c y$ decomposes into components $\cos k_c y$ and $\cos 3k_c y$, at cubic order $O(\lambda^3)$ one has a backreaction in these Fourier modes, and so on. Thus the full solution for A generated by the backreaction of the marginal GL mode takes the form

$$\begin{aligned} &+ \lambda a_{1,1} \cos k_c y \\ &+ \lambda^2 a_{2,0} + \lambda^2 a_{2,2} \cos 2k_c y \\ &+ \lambda^3 a_{3,1} \cos k_c y + \lambda^3 a_{3,3} \cos 3k_c y \\ &+ \lambda^4 a_{4,0} + \lambda^4 a_{4,2} \cos 2k_c y + \lambda^4 a_{4,4} \cos 4k_c y \\ &+ \dots \end{aligned} \quad (4.75)$$

where the $a_{n,m}$ are functions depending on r , and B and C have expansions taking the same form, with coefficient functions $b_{n,m}$ and $c_{n,m}$ respectively. We denote the level (n, m) as being at order $O(\lambda^n)$ and Fourier mode $\cos mk_c y$. The leading linear term is the level-(1, 1) marginal GL mode, so that $a_{1,1}(r) = a(r)$ in (4.74)

and similarly for $b_{1,1}$ and $c_{1,1}$. At the level (n, m) one must solve a problem that we represent schematically as $\mathcal{L}(a_{n,m}, b_{n,m}, c_{n,m}) = \mathcal{S}$, where, on the left-hand side, \mathcal{L} is a homogeneous linear differential operator acting on the level- (n, m) functions $a_{n,m}$, $b_{n,m}$, and $c_{n,m}$, and on the right-hand side \mathcal{S} is the source for this inhomogeneous linear problem. This source originates not only from the component of the n th power of the leading linear terms $a_{1,1}$, $b_{1,1}$, and $c_{1,1}$ in the m th Fourier mode but also from various combinations of the intermediate backreaction orders.

Solving these inhomogeneous linear systems is technical but straightforward, and we will not give the details here. The level- (n, m) linear system can be computed by numerically integrating ordinary differential equations provided that the previous orders $O(\lambda)$, $O(\lambda^2)$, ..., $O(\lambda^{n-1})$ have been computed. In practice, computing the levels (1, 1), (2, 0), (0, 2), and (3, 1) is quite straightforward and that is all we shall require for our discussion. Numerical computation gives the following data:

$$\begin{aligned} k_c &= 0.876, & a_{1,1}(1) &= b_{1,1}(1) = -0.55, & c_{1,1}(1) &= 1, \\ a_{2,0}(1) &= -0.28, & b_{2,0}(1) &= 0.77, & c_{2,0}(1) &= 0.80, \\ a_{2,2}(1) &= b_{2,2}(1) = 0.34, & c_{2,2}(1) &= -0.69, \\ a_{3,1}(1) &= b_{3,1}(1) = -0.24, & c_{3,1}(1) &= 0, \end{aligned} \quad (4.76)$$

which in principle specifies the solution to the levels (1, 1), (2, 0), (0, 2), and (3, 1) if one integrates these data from the horizon to infinity (although one would require more precision than the two significant figures given here).⁴ For these levels, asymptotically the functions $a_{n,m}$, $b_{n,m}$, and $c_{n,m}$ all decay exponentially except for (2, 0), which has a power law decay going as

$$\begin{aligned} b_{2,0} &= \frac{B_\infty}{r} + O\left(\frac{1}{r^2}\right), & c_{2,0} &= \frac{C_\infty \log r}{r} + O\left(\frac{1}{r}\right), \\ B_\infty &= 0.41, & C_\infty &= -0.11. \end{aligned} \quad (4.77)$$

The variations in the mass M , area A , and surface gravity κ for a nonuniform string take the form

$$\begin{aligned} M &= M_{\text{GL}} (1 + m_2 \lambda^2 + m_4 \lambda^4 + \dots), & A &= A_{\text{GL}} (1 + a_2 \lambda^2 + a_4 \lambda^4 + \dots), \\ \kappa &= \kappa_{\text{GL}} (1 + \kappa_2 \lambda^2 + \kappa_4 \lambda^4 + \dots), \end{aligned} \quad (4.78)$$

⁴ Note that we have chosen the constant-circle-size scheme of [26], so that the wavenumber in (4.75) is unperturbed at higher orders in λ .

where

$$M_{\text{GL}} = \frac{0.876L^2}{4\pi G_5}, \quad A_{\text{GL}} = \frac{0.876^2 L^3}{\pi}, \quad \kappa_{\text{GL}} = \frac{\pi}{0.876L}, \quad (4.79)$$

and we have thus rescaled our solution so that the circle size is L again. Note that the marginal GL perturbation of level $(1, 1)$ does not contribute to these values at order $O(\lambda)$, as it decays exponentially away from the horizon and, being a harmonic perturbation on the circle, does not change the horizon area at this order. In fact we see that corrections to these quantities arise only from even powers in λ . The quadratic variations are determined from the above data as

$$\begin{aligned} m_2 &= 3B_\infty - 2C_\infty = 1.45, \\ a_2 &= b_{2,0}(1) + 2c_{2,0}(1) + \frac{1}{4}b_{1,1}(1)^2 + b_{1,1}(1)c_{1,1}(1) + c_{1,1}(1)^2 = 2.90, \\ \kappa_2 &= a_{2,0}(1) - b_{2,0}(1) = -1.04, \end{aligned} \quad (4.80)$$

and thus, in a manner similar to that for the small localized solutions, we have computed the properties of the inhomogeneous string in a perturbative limit.

Let us consider the dynamical stability of the homogeneous black strings. Homogeneous strings with $M < M_{\text{GL}}$ are unstable to GL perturbations with wavelength L . Indeed for small enough mass, $M < M_{\text{GL}}/n$ for integer n , the wavelengths $L/2, L/3, \dots, L/n$ will also be unstable since the higher harmonics of the GL mode fit into the circle. For $M > M_{\text{GL}}$ the homogeneous black strings are stable since the unstable GL modes, having minimum wavelength $(M/M_{\text{GL}})L$, cannot fit into the circle.

Now let us consider the stability of the weakly inhomogeneous solutions, namely those with $\lambda \ll 1$ so that M is close to M_{GL} . We see that, since $m_2 > 0$, these inhomogeneous solutions have mass greater than M_{GL} and hence coexist at the same mass as a stable homogeneous black string. Let us compare the areas of these two solutions. Consider moving an infinitesimal distance $d\lambda$ along the inhomogeneous black string branch starting at $\lambda = 0$. Then the first law, $dM = \kappa dA/(8\pi G_5)$, for a fixed circle size implies at order $O(\lambda^2)$ that $2m_2 = a_2$, which, as we can see, is consistent with the numerical data above. At order $O(\lambda^4)$ it implies that $2m_4 - a_4 - \frac{1}{2}\kappa_2 a_2 = 0$. A homogeneous string has area $A_h = (16\pi G_5^2/L)M^2$ for a mass M , and so we can compute the fractional area difference between the inhomogeneous and homogeneous strings for a mass M as

$$\begin{aligned} \frac{\Delta A}{A_h} &= \frac{A - A_h}{A_h} = (a_2 - 2m_2)\lambda^2 + (a_4 - 2a_2m_2 + 3m_2^2 - 2m_4)\lambda^4 + O(\lambda^6) \\ &= -m_2(m_2 + \kappa_2)\lambda^4 + O(\lambda^6) \simeq -0.59\lambda^4, \end{aligned} \quad (4.81)$$

where the quadratic term vanishes, by the first law, and the quartic term is precisely determined by the data given above. We arrive at the result that at fixed mass and fixed circle size the weakly inhomogeneous string has a lower area than a stable homogeneous string of the same mass. Since area cannot decrease in a dynamical process this argument shows that weakly inhomogeneous strings are dynamically unstable to perturbations that preserve their mass and deform them into homogeneous strings. Currently, it has not been demonstrated whether this perturbative instability can be seen in linear perturbation theory or only at higher orders. However, we believe that it is likely to manifest itself as a linear dynamical instability and later we shall assume that this is the case. A reasonable supposition is that such a linear instability generates an evolution that ends at a stable homogeneous black string with similar mass.

As with the localized solutions, an interesting question is what happens to the branch of inhomogeneous solutions as one deforms past the weakly inhomogeneous regime, so that the above perturbative approach breaks down. In the next subsection we shall consider this.

4.3.3 The space of static black hole solutions

We have seen that homogeneous black strings exist for all masses, given a fixed circle size, but are stable only for a sufficiently large mass $M > M_{\text{GL}} \sim O(L^2/G_5)$. At low masses, $M \ll L^2/G_5$, we have another branch of solutions, localized black holes, which we expect to be dynamically stable. In the intermediate-mass range, for masses just above M_{GL} we also have inhomogeneous black strings, which we have argued are unstable. We already see that there is no uniqueness for static solutions to Kaluza–Klein theory for fixed mass and circle size.

We have posed the question of what happens to localized black holes as they become large, and also of what happens to inhomogeneous black strings as they become increasingly inhomogeneous. Harmark and Obers [28] argued that the localized black holes might connect continuously to the inhomogeneous black string solutions proposed by Horowitz and Maeda. Kol used a Morse-theory argument to deduce that in the simplest scenario the localized black holes do connect continuously to the inhomogeneous black string branch found by Gubser [29]. Furthermore Kol predicted that the two branches connect via a singular solution that mediates a topology change of the horizon. This is analogous to the topology change between hyperbolic and parabolic conic sections, which is mediated by a singular section taken through the apex of the cone. Indeed, there is a static, spherically symmetric, Ricci-flat conical geometry,

$$ds_{\text{cone}}^2 = d\alpha^2 + \frac{1}{3}\alpha^2(d\beta^2 - \sin^2\beta dt^2) + \frac{1}{3}\alpha^2 d\Omega_2^2, \quad (4.82)$$

which is singular at its apex, $\alpha = 0$. The base of the cone is the product of a two-sphere and a two-dimensional de Sitter space ($d\beta^2 - \sin^2 \beta dt^2$), with $\beta \in [0, \pi]$ where $\beta = 0$ and $\beta = \pi$ are Killing horizons with respect to $\partial/\partial t$. These horizons are connected (although not smoothly) at the apex of the cone, where the de Sitter factor has zero size. Kol proposed that this gives a local model for the geometry of the topology-changing solution at the singular point of the horizon. Moving away from the singular topology-changing solution to the inhomogeneous black string branch would resolve the sphere, so that it was finite in size at $\alpha = 0$. This would accord with the inhomogeneous strings having no exposed axis of symmetry, and the two components of the horizon with $\beta = 0$ and $\beta = \pi$ would be smoothly connected. Conversely, moving to the localized black hole branch would resolve the de Sitter factor, so that the horizons at $\beta = 0$ and $\beta = \pi$ would not touch and $\alpha = 0$ would be the exposed axis of symmetry.

In order to make progress in understanding the extension of the localized black hole and inhomogeneous black string branches we must resort to numerical work. Inhomogeneous black strings were first computed in [30] and localized black holes in [31, 32, 33]. Recently, a standard approach to constructing static vacuum solutions numerically has been developed [34] and will be discussed in Chapter 10. Unlike the previous methods employed (see for example [29]) this approach is geometrically elegant, being covariant, and may be applied to problems depending nontrivially on as many coordinates as one likes. In practice this new method works very well. The results presented here for both inhomogeneous black strings and localized black holes are those computed in [34].

As we shall now see, the results are compatible with Kol's prediction of a topology-changing merger of localized black holes and inhomogeneous black strings, discussed above. The numerical calculations have not yet been adapted to explore the singular potential merger point and inevitably break down for both the localized and inhomogeneous string branches as this point is approached. We note that it is still early days for these methods, and we fully expect that future work in coming years will significantly improve on the solutions reproduced here.

Let us begin by showing in Figs. 4.1 and 4.2 curves of area A and of surface gravity, plotted as inverse temperature $1/T = 2\pi/\kappa$, against mass M for fixed circle size L . The plotted quantities are made dimensionless using appropriate powers of the circle size L . We find a very interesting behavior for the localized black holes, namely that there is a maximum mass solution, with $G_5 M_{\max} \simeq 0.17L^2$. We note that, since $dM = \kappa dA/(8\pi G_5)$ for a fixed circle size L , any extremum of M will similarly be an extremum of A . Hence the area against mass curve has a cuspy profile at $M = M_{\max}$. We see from Fig. 4.2 that there is a minimum surface gravity (or, equivalently, minimum temperature) solution at $M = M_\kappa$. The actual value of M_κ is numerically close to that of M_{\max} , as is clear visually, but

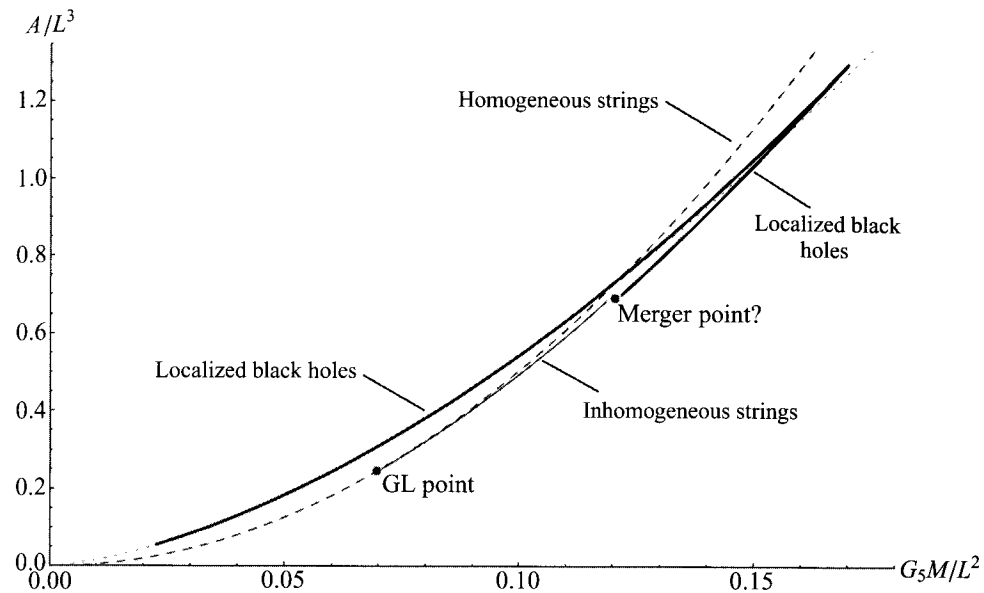


Figure 4.1 Plot of area A against mass M for fixed Kaluza-Klein circle size L for homogeneous (broken line) and inhomogeneous (thin solid line) black strings and for localized black holes (thick solid line). The curves for the latter two are numerical solutions from [34]. The inhomogeneous black string and localized black hole plots are compatible with a merger at $G_5 M_*/L^2 \simeq 0.12$ and there is a maximum-mass localized solution, with $G_5 M_{\max}/L^2 \simeq 0.17$. The dotted line gives the small localized black hole approximation (4.71), and we see that this approximation is excellent for increasing mass up to $M \sim M_{\max}$.

we emphasize that since the curve of $1/\kappa$ against M is smooth for the localized solutions about the maximum mass, as we expect and indeed see numerically, the points of maximum mass and minimum surface gravity cannot coincide, and $M_\kappa < M_{\max}$. This leads to the unexpected conclusion that the localized solutions in the narrow range $M_\kappa < M < M_{\max}$ actually have positive specific heat.

We confirm that the perturbative prediction computed above in (4.71) provides a good description of the localized behaviour for small mass. In both figures this approximation is plotted, and we see surprisingly good agreement for increasing mass up to M_{GL} and even past this point, to around $M \sim M_{\max}$. These approximations have no maximum mass and hence cannot agree past this point in the localized branch, and we expect nonperturbative effects to become important thereafter.

The inhomogeneous black string branch departs from the homogeneous branch at the GL point $M = M_{\text{GL}}$. Moving away from this point the deformation of the horizon becomes greater. The degree of inhomogeneity, measured by the ratio of the maximum and minimum two-sphere radii of the horizon, increases monotonically.

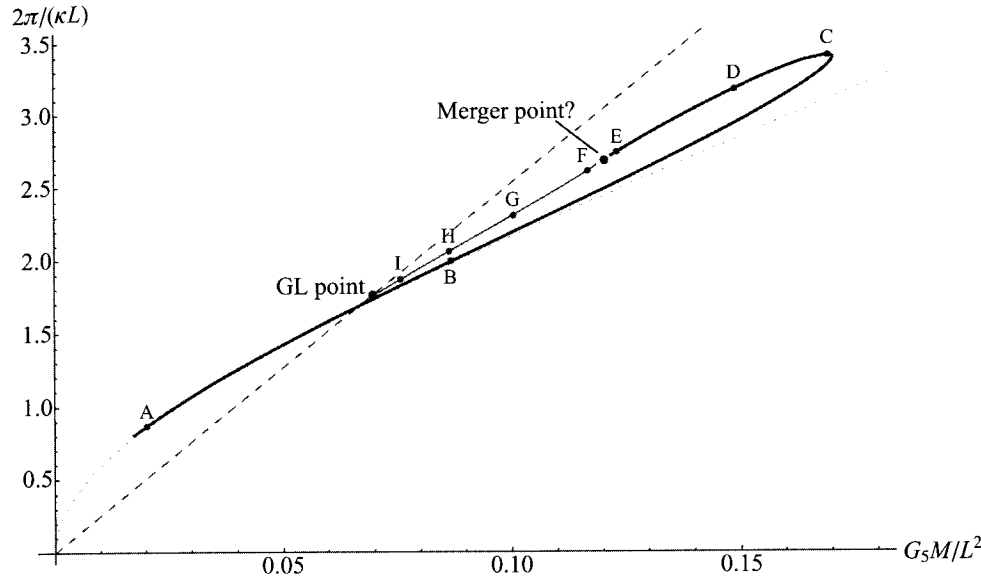


Figure 4.2 Plot of inverse temperature $2\pi/\kappa$ against mass M for fixed circle size L for the same solutions as in the previous figure. The labels A to I denote solutions whose horizon embeddings are displayed in the next figure. Again we see consistency with a merger. We also note that there is a minimum surface gravity solution at M_κ (near the label C) which is rather close to, but slightly less than M_{\max} . The perturbative approximation in (4.71) is also plotted (dotted line) and again very good agreement is seen for localized solutions with increasing mass up to around $M \sim M_{\max}$.

The most striking feature of these plots is that, moving as far along the localized and inhomogeneous branches as possible, both branches appear to be compatible with their joining at some mass M_* with $G_5 M_* \simeq 0.12L^2$. This is an indication that these branches do indeed both end at the same singular topology-changing solution. Plots for other physical quantities, not displayed here, also support this conclusion.

In Fig. 4.3 we show several embeddings of the horizon for various localized and inhomogeneous string solutions. We see graphical confirmation that the most inhomogeneous strings appear to be close to having the minimum two-spheres of their horizon go to zero size. The localized black holes also appear to be close to having their north and south poles meet as the axis of symmetry shrinks to zero length. Near the potential merger, lying between E and F, the geometries appear to be similar away from the singular region.

We note that by uncompactifying the solutions above and then recompactifying with circle size an integer multiple of L one can construct multi-centered localized black hole solutions, although presumably all such solutions would be unstable.

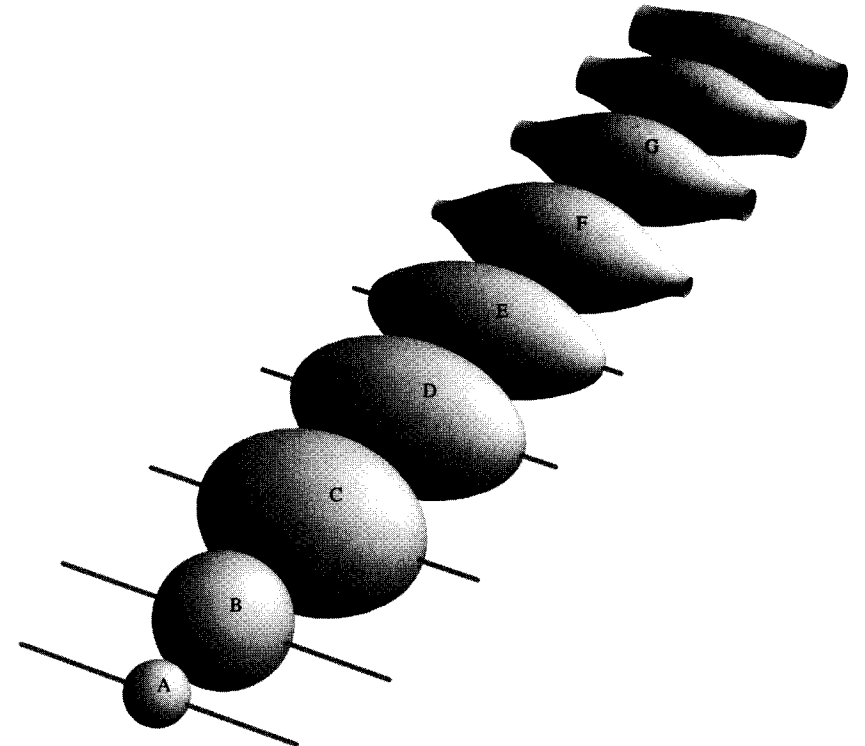


Figure 4.3 Figure showing the spatial geometry of the horizon for a number of localized black holes and inhomogeneous black strings, all with the same asymptotic circle size. The embeddings are labelled A to I and correspond to the solutions annotated in the previous figure. We emphasize that these geometries are those actually found in the numerical solutions in [34]. For the localized black holes the proper length of the axis of symmetry is also depicted.

The metric for inhomogeneous black strings has been tested to see explicitly whether the cone geometry advocated by Kol emerges, for solutions with $M \simeq M_*$, in the region surrounding the minimum radius of the horizon. Strings in various dimensions were found, and the appropriate cone geometries were indeed seen to emerge [35]. Similar tests have not yet been performed on the localized solutions but we believe it is very plausible that again this cone geometry will be seen.

4.3.4 Stability of the static black hole solutions

Having considered an elegant proposal for the space of static solutions and numerical evidence supporting it we now discuss the likely dynamical stability of these solutions. From Fig. 4.1 we see that for fixed circle size the localized solutions

dominate the area for a given mass when $M < M_{\text{crit}}$, where $G_5 M_{\text{crit}} \simeq 0.12 L^2$, and that the homogeneous black strings dominate the area for $M > M_{\text{crit}}$. Thus at fixed mass (the ‘‘microcanonical ensemble’’) we expect that the globally stable solution is a localized black hole for $M < M_{\text{crit}}$ and a homogeneous string for $M > M_{\text{crit}}$.

This does not tell us about the local dynamical stability of the solutions. For example, the homogeneous strings with $M_{\text{GL}} < M < M_{\text{crit}}$ are dynamically stable to small perturbations even though they do not globally dominate the area, and they can be deformed to a more stable solution with the same mass for a sufficiently large deformation.

Let us now consider this local stability. We have argued that the small localized solutions are perturbatively stable and the weakly inhomogeneous black strings are perturbatively unstable. Furthermore, it appears that these two branches should be thought of as one, joined together by a singular topology-changing solution. If these assertions are correct then the simplest situation is that either (i) the entire inhomogeneous branch and part of the localized branch are unstable to a single perturbation mode or, alternatively, (ii) the instability ends at some point along the inhomogeneous branch and so there are strongly deformed stable inhomogeneous solutions and all the localized black holes are stable. For either scenario to be true the instability should smoothly turn off as one moves in the space of solutions, and hence there will be a localized solution for scenario (i) or an inhomogeneous string for scenario (ii) with a marginal static perturbation.

The localized branch has precisely such a candidate marginal static perturbation, as we shall now argue, indicating that scenario (i) is realized. Since we are considering a microcanonical ensemble we require a static perturbation that leaves the mass invariant. (A static perturbation that changes the mass results in a different black hole, not a perturbation of the original black hole.) Take the perturbation of the metric for a localized solution to be that generated by moving infinitesimally along the branch of solutions (i.e. the perturbation is tangent to the space of solutions there). For a generic solution, such a perturbation will, to linear order, change the mass. However, precisely at the point $M = M_{\text{max}}$ the perturbation will leave the mass invariant at linear order. This then gives the required candidate static perturbation, which is both regular at the horizon and leaves the mass invariant.⁵ Physically we may gain some intuition into this change in stability at the maximum mass solution by considering taking a small (presumed stable) localized black hole and gradually dropping matter into it. Initially one may expect that the mass will grow as it absorbs the matter. However, when it reaches the localized maximum mass solution with $M = M_{\text{max}}$ (and correspondingly maximal area) it can no longer remain a stable solution. Adding more matter will force the area to increase during

the ensuing dynamics, implying that this solution cannot settle back to any solution near $M = M_{\text{max}}$ since these all have lower area.

Let us summarize our stability discussion. The numerical solutions imply that localized black holes with $M < M_{\text{crit}}$ are globally dynamically stable while homogeneous strings with $M > M_{\text{crit}}$ are globally stable. We have argued that the simplest picture of linear stability is that the localized black holes are linearly stable for small mass and remain stable as their mass is increased up to the value $M = M_{\text{max}}$. Moving further along this localized branch, these solutions become unstable to a single perturbation mode and this instability continues through the topology change and all the way along the inhomogeneous black string branch. A further comment is that whilst dynamically unstable solutions may be interesting in terms of understanding the moduli space of static vacuum solutions, presumably they play no physical role. Whilst we have had to resort to sophisticated numerical work to elucidate the full structure of solutions, from a physical perspective the interesting (i.e. stable) solutions are the simplest ones. We know the homogeneous black strings analytically and the stable localized solutions with $M < M_{\text{max}}$ appear to be rather well described by the perturbative construction given earlier.

Sorkin has shown that this picture changes remarkably in higher dimensions [36]. Treating the dimension as a continuous parameter D (previously in this chapter we have considered only $D = 5$), and again taking the case of a single compact Kaluza–Klein circle, one finds that the sign of m_2 in (4.78), and correspondingly that of the area difference in equation (4.81), changes above a critical dimension $D_* \simeq 13.5$. Now, weakly inhomogeneous strings have masses $M < M_{\text{GL}}$ and are expected to be stable and to be the end state of the GL instability of homogeneous strings with mass just below M_{GL} . Assuming that the localized solutions and inhomogeneous strings still merge at some mass M_* then, in the simplest picture, for $M < M_*$ localized black holes exist and dominate the area for fixed mass over homogeneous strings and for $M_* < M < M_{\text{GL}}$ inhomogeneous strings exist and dominate homogeneous strings. An interesting question is whether there are inhomogeneous black strings that are stable for $D < D_*$. We have argued for $D = 5$ they are likely to all be unstable. However, for D close to but less than D_* , continuity implies that strongly inhomogeneous black strings will remain stable even though weakly inhomogeneous black strings will become unstable. Whether stability persists for strongly inhomogeneous black strings down to $D = 10$ or $D = 11$, the maximum dimensions proposed in quantum theories of gravity, is currently unclear.

We conclude this discussion with the caveat that the picture advocated here is the simplest one compatible with the numerical data currently available. We may learn, however, that the situation is considerably more complicated than we expect at present: it is certainly possible that there are even more exotic static black hole solutions waiting to be discovered.

⁵ We thank Harvey Reall for an important discussion clarifying this issue.

References

- [1] T. Kaluza, On the problem of unity in physics, *Sitzungsber. Preuss. Akad. Wiss. Berlin (Math. Phys.)* **K1** (1921), 966–972.
- [2] O. Klein, Quantum theory and five-dimensional theory of relativity (in German and English), *Z. Phys.* **37** (1926), 895–906.
- [3] R. Schoen and S.-T. Yau, Positivity of the total mass of a general space-time, *Phys. Rev. Lett.* **43** (1979), 1457–1459.
- [4] E. Witten, A simple proof of the positive energy theorem, *Commun. Math. Phys.* **80** (1981), 381.
- [5] X.-Z. Dai, A positive mass theorem for spaces with asymptotic SUSY compactification, *Commun. Math. Phys.* **244** (2004), 335.
- [6] X.-Z. Dai, A note on positive energy theorem for spaces with asymptotic SUSY compactification, *J. Math. Phys.* **46** (2005), 042505 [math-ph/0406006].
- [7] E. Witten, Instability of the Kaluza–Klein vacuum, *Nucl. Phys.* **B195** (1982), 481.
- [8] D. Brill and H. Pfister, States of negative total energy in Kaluza–Klein theory, *Phys. Lett.* **B228** (1989), 359–362.
- [9] D. Brill and G. T. Horowitz, Negative energy in string theory, *Phys. Lett.* **B262** (1991), 437–443.
- [10] J. L. Hovdebo and R. C. Myers, Black rings, boosted strings and Gregory–Laflamme, *Phys. Rev.* **D73** (2006), 084013 [hep-th/0601079].
- [11] D. J. Gross and M. J. Perry, Magnetic monopoles in Kaluza–Klein theories, *Nucl. Phys.* **B226** (1983), 29.
- [12] R. D. Sorkin, Kaluza–Klein monopole, *Phys. Rev. Lett.* **51** (1983), 87–90.
- [13] G. W. Gibbons and D. L. Wiltshire, Black holes in Kaluza–Klein theory, *Ann. Phys.* **167** (1986), 201.
- [14] D. Rasheed, The rotating dyonic black holes of Kaluza–Klein theory, *Nucl. Phys.* **B454** (1995), 379–401 [hep-th/9505038].
- [15] T. Matos and C. Mora, Stationary dilatons with arbitrary electromagnetic field, *Class. Quant. Grav.* **14** (1997), 2331–2340 [hep-th/9610013].
- [16] F. Larsen, Rotating Kaluza–Klein black holes, *Nucl. Phys.* **B575** (2000), 211–230. [hep-th/9909102].
- [17] M. Mars and W. Simon, On uniqueness of static Einstein–Maxwell dilaton black holes, *Adv. Theor. Math. Phys.* **6** (2003), 279–305 [gr-qc/0105023].
- [18] G. W. Gibbons, D. Ida and T. Shiromizu, Uniqueness of (dilatonic) charged black holes and black p-branes in higher dimensions, *Phys. Rev.* **D66** (2002), 044010 [hep-th/0206136].
- [19] B. Kol, The phase transition between caged black holes and black strings: A review, *Phys. Rept.* **422** (2006), 119 [arXiv:hep-th/0411240].
- [20] T. Harmark, V. Niarchos, and N. A. Obers, *Class. Quant. Grav.* **24** (2007), R1 [arXiv:hep-th/0701022].
- [21] R. C. Myers, Higher dimensional black holes in compactified space-times, *Phys. Rev.* **D35** (1987), 455.
- [22] D. Gorbonos and B. Kol, A dialogue of multipoles: matched asymptotic expansion for caged black holes, *JHEP* **0406** (2004), 053 [arXiv:hep-th/0406002].
- [23] T. Harmark, Small black holes on cylinders, *Phys. Rev.* **D69** (2004), 104015 [arXiv:hep-th/0310259].
- [24] B. Kol, E. Sorkin, and T. Piran, Caged black holes: black holes in compactified space-times. 1. Theory, *Phys. Rev.* **D69** (2004), 064031 [arXiv:hep-th/0309190].

- [25] R. Gregory and R. Laflamme, Hypercylindrical black holes, *Phys. Rev.* **D37** (1988), 305.
- [26] S. S. Gubser, On nonuniform black branes, *Class. Quant. Grav.* **19** (2002), 4825 [arXiv:hep-th/0110193].
- [27] G. T. Horowitz and K. Maeda, Fate of the black string instability, *Phys. Rev. Lett.* **87** (2001), 131301 [arXiv:hep-th/0105111].
- [28] T. Harmark and N. A. Obers, Black holes on cylinders, *JHEP* **0205** (2002), 032 [arXiv:hep-th/0204047].
- [29] B. Kol, Topology change in general relativity, and the black hole black string transition, *JHEP* **0510** (2005), 049 [arXiv:hep-th/0206220].
- [30] T. Wiseman, Static axisymmetric vacuum solutions and nonuniform black strings, *Class. Quant. Grav.* **20** (2003), 1137–1176 [hep-th/0209051].
- [31] H. Kudoh and T. Wiseman, Properties of Kaluza–Klein black holes, *Prog. Theor. Phys.* **111** (2004), 475 [arXiv:hep-th/0310104].
- [32] E. Sorkin, B. Kol, and T. Piran, Caged black holes: black holes in compactified space-times. 2. 5-d numerical implementation, *Phys. Rev.* **D69** (2004), 064032 [hep-th/0310096].
- [33] H. Kudoh and T. Wiseman, Connecting black holes and black strings, *Phys. Rev. Lett.* **94** (2005), 161102 [arXiv:hep-th/0409111].
- [34] M. Headrick, S. Kitchen, and T. Wiseman, A new approach to static numerical relativity, and its application to Kaluza–Klein black holes, *Class. Quant. Grav.* **27** (2010), 035002 [arXiv:0905.1822].
- [35] E. Sorkin, Non-uniform black strings in various dimensions, *Phys. Rev.* **D74** (2006), 104027 [gr-qc/0608115].
- [36] E. Sorkin, A critical dimension in the black string phase transition, *Phys. Rev. Lett.* **93** (2004), 031601 [arXiv:hep-th/0402216].

Part III

Asymptotically flat solutions

Myers–Perry black holes

ROBERT C. MYERS

In this chapter we will continue the exploration of black holes in higher dimensions with an examination of asymptotically flat black holes with spherical horizons, i.e., in d spacetime dimensions the topology of the horizon and of spatial infinity is an S^{d-2} . In particular, we will focus on a family of vacuum solutions describing spinning black holes, known as Myers–Perry (MP) metrics. In many respects these solutions admit the same remarkable properties as the standard Kerr black hole in four dimensions. However, studying these solutions also begins to provide some insight into the new and unusual features of event horizons in higher dimensions.

These metrics were discovered in 1985 as a part of my thesis work as a Ph.D. student at Princeton [1]. My supervisor, Malcolm Perry, and I had been led to study black holes in higher dimensions, in part by the renewed excitement in superstring theory that had so dramatically emerged in the previous year. We anticipated that examining black holes in $d > 4$ dimensions would be important in obtaining a full understanding of these theories. I should add that, amongst the subsequent developments, this family of spinning black hole metrics was further generalized to include a cosmological constant as well as Newman, Unti, and Tamburino (NUT) parameters.¹ While I will not have space to discuss these extensions, the interested reader may find a description of the generalized solutions in [2].

5.1 Static black holes

Before considering spinning black holes, we note that the Schwarzschild solution is easily generalized to $d \geq 4$ dimensions as

$$ds^2 = -\left(1 - \frac{\mu}{r^{d-3}}\right) dt^2 + \left(1 - \frac{\mu}{r^{d-3}}\right)^{-1} dr^2 + r^2 d\Omega_{d-2}^2, \quad (5.1)$$

¹ There is more than one such parameter in higher dimensions.

where $d\Omega_{d-2}^2$ denotes the line element on the unit $(d-2)$ -sphere. While this vacuum solution of the d -dimensional Einstein equations was first found by Tangherlini in the early 1960s [3], it is still traditionally referred to as a Schwarzschild black hole. In part, this nomenclature probably arose because, for any value of $d > 4$, the features of the spacetime (5.1) are essentially unchanged from its four-dimensional predecessor.

In particular, the constant μ emerges as an integration constant in solving the Einstein equations. In Appendix A we derive expressions for the mass and angular momentum in a d -dimensional spacetime by examining the asymptotic structure of the metric. There one finds that μ fixes the mass M of the black hole (5.1) – see (5.65) – with

$$M = \frac{(d-2)\Omega_{d-2}}{16\pi G} \mu , \quad (5.2)$$

where Ω_{d-2} is the area of a unit $(d-2)$ -sphere, i.e.,

$$\Omega_{d-2} = \frac{2\pi^{(d-1)/2}}{\Gamma(\frac{d-1}{2})} . \quad (5.3)$$

As long as $\mu > 0$, the surface $r^{d-3} = \mu$ is an event horizon. It is a straightforward exercise to generalize the discussion presented in Chapter 1 by constructing good coordinates across this surface and finding the maximal analytic extension of the geometry. The corresponding Penrose diagram then takes precisely the same form as that in Fig. 1.1, but where each point now represents a $(d-2)$ -sphere.² Notably, there is a future (past) curvature singularity at $r = 0$ in region II (III), where $R_{\mu\nu\rho\sigma} R^{\mu\nu\rho\sigma} \propto \mu^2/r^{2(d-1)}$ as $r \rightarrow 0$. Of course, if $\mu < 0$ then the spacetime has a naked timelike singularity at $r = 0$ and the corresponding Penrose diagram matches that given in Fig. 1.4.

Another simple exercise is to extend Birkhoff's theorem to higher dimensions. That is, one can solve Einstein's vacuum equations in any $d \geq 4$ assuming that the geometry is asymptotically flat and spherically symmetric, i.e., the solution has an $SO(d-1)$ isometry, without assuming that the spacetime is static. The Schwarzschild–Tangherlini metric (5.1) remains the most general solution and so any spherically symmetric solution of $R_{\mu\nu} = 0$ must also be static. It is also possible to prove a uniqueness theorem indicating that the metric (5.1) is the only solution of the vacuum Einstein equations in higher dimensions if one assumes that the geometry is asymptotically flat and static [4, 5]. Hence all such static solutions are spherically symmetric and completely determined by their mass M .

² Of course, the past and future horizons should now be labeled as $r^{d-3} = \mu$.

The generalization of the four-dimensional Reissner–Nordström metric to solutions describing static charged black holes in higher dimensions is also straightforward. Again, the features of these solutions of the Einstein–Maxwell equations in $d > 4$ are essentially unchanged from those described for four dimensions in Chapter 1. Here it is of interest to extend the Majumdar–Papapetrou solutions, describing multiple extremely charged black holes in static equilibrium, to higher dimensions. With these solutions one can construct periodic arrays of such black holes, which can then be compactified using the Kaluza–Klein ansatz [6], discussed in Chapter 4. The resulting solutions provide simple analytic metrics describing black holes localized in the Kaluza–Klein dimensions.

5.2 Spinning black holes

Before writing down the metric for a spinning black hole, it is useful first to orient the discussion by writing the metric for flat space in higher dimensions. To begin, consider the case $d = 2n + 1$ (with $n \geq 2$), for which the flat-space metric can be written as

$$\begin{aligned} ds^2 &= -dt^2 + \sum_{i=1}^n (dx_i^2 + dy_i^2) \\ &= -dt^2 + dr^2 + r^2 \sum_{i=1}^n (d\mu_i^2 + \mu_i^2 d\phi_i^2) . \end{aligned} \quad (5.4)$$

In the first line we have paired the spatial coordinates as Cartesian coordinates x_i, y_i in n orthogonal planes. In the second line we have introduced polar coordinates, which can be expressed as

$$x_i = r\mu_i \cos \phi_i, \quad y_i = r\mu_i \sin \phi_i . \quad (5.5)$$

Implicitly, we are defining $r^2 = \sum_{i=1}^n (x_i^2 + y_i^2)$ and so the direction cosines μ_i are constrained to satisfy

$$\sum_{i=1}^n \mu_i^2 = 1 . \quad (5.6)$$

Hence not all the $d\mu_i^2$ in the flat-space metric (5.4) are independent and one such term can be eliminated using this constraint. However, we have left this replacement implicit for the sake of keeping the metric simple. For completeness, we note that the ranges of the coordinates are as follows: $t \in (-\infty, \infty)$, $r \in [0, \infty)$, $\mu_i \in [0, 1]$, and $\phi_i \in [0, 2\pi]$, where the latter are periodically identified by $\phi_i = \phi_i + 2\pi$. We will adopt polar coordinates analogous to those in (5.4) to present the MP metrics

for $d = 2n + 1$ below. In particular, then, the black hole geometry will approach the flat-space metric (5.4) asymptotically.

For an even number of dimensions, i.e., $d = 2n + 2$ (with $n \geq 1$), there will be an extra unpaired spatial coordinate

$$z = r\alpha, \quad \text{with } \alpha \in [-1, 1]. \quad (5.7)$$

Hence the flat-space metric becomes

$$ds^2 = -dt^2 + dr^2 + r^2 \sum_{i=1}^n (d\mu_i^2 + \mu_i^2 d\phi_i^2) + r^2 d\alpha^2, \quad (5.8)$$

while the constraint on the direction cosines becomes

$$\sum_{i=1}^n \mu_i^2 + \alpha^2 = 1. \quad (5.9)$$

Equation (5.8) exhibits the polar coordinates which we will adopt below for the MP metric with $d = 2n + 2$.

One outstanding feature of the polar coordinates in (5.4) and (5.8) is that there are n commuting Killing vectors in the angular directions ϕ_i . The corresponding rotations in each of the orthogonal planes (5.5) match the n generators of the Cartan subalgebra of the rotation groups $SO(2n)$ or $SO(2n+1)$, for odd and even d , respectively. This feature highlights the fact that in higher dimensions we must think of angular momentum as an antisymmetric two-tensor $J^{\mu\nu}$, e.g., see (5.62) below. In considering a general rotating body, we may simplify this angular momentum tensor by going to the center-of-mass frame, which eliminates the components having a time index. Then a suitable rotation of the spatial coordinates brings the remaining spatial components J^{ij} into the standard form

$$J^{ij} = \begin{pmatrix} 0 & J_1 & & & \\ -J_1 & 0 & & & \\ & 0 & J_2 & & \\ & -J_2 & 0 & & \\ & & & \ddots & \end{pmatrix}. \quad (5.10)$$

Here each J_i denotes the angular momentum associated with motions in the corresponding plane. Note that, for even d , the last row and column of the above matrix vanishes. Therefore a general angular momentum tensor is characterized by $n = \lfloor (d-1)/2 \rfloor$ independent parameters J_i . Hence the general spinning black hole metrics considered below will be specified by $n+1$ parameters: the mass M and the n commuting angular momenta $J^{y_i x_i}$. In four dimensions these parameters would completely fix the black hole solution but, as we will see in section 5.2.8

and in subsequent chapters, these parameters alone will not fix a unique black hole metric in higher dimensions.

5.2.1 Myers–Perry black hole metrics

As can be anticipated from (5.4) and (5.8), the form of the metrics differs slightly for odd and even dimensions. Hence let us begin with the metric describing a spinning black hole in an even number of spacetime dimensions, i.e., $d = 2n + 2$ with $d \geq 4$:

$$ds^2 = -dt^2 + \frac{\mu r}{\Pi F} \left(dt + \sum_{i=1}^n a_i \mu_i^2 d\phi_i \right)^2 + \frac{\Pi F}{\Pi - \mu r} dr^2 + \sum_{i=1}^n (r^2 + a_i^2) (d\mu_i^2 + \mu_i^2 d\phi_i^2) + r^2 d\alpha^2, \quad (5.11)$$

where

$$F = 1 - \sum_{i=1}^n \frac{a_i^2 \mu_i^2}{r^2 + a_i^2}, \quad (5.12)$$

$$\Pi = \prod_{i=1}^n (r^2 + a_i^2). \quad (5.13)$$

With $n = 1$, we have $d = 4$ and the above metric reduces to the well-known Kerr solution, discussed in Chapter 1.³ For $d = 2n + 1$ with $d \geq 5$, the metric becomes

$$ds^2 = -dt^2 + \frac{\mu r^2}{\Pi F} \left(dt + \sum_{i=1}^n a_i \mu_i^2 d\phi_i \right)^2 + \frac{\Pi F}{\Pi - \mu r^2} dr^2 + \sum_{i=1}^n (r^2 + a_i^2) (d\mu_i^2 + \mu_i^2 d\phi_i^2), \quad (5.14)$$

with F and Π again given by (5.12) and (5.13). Examining the asymptotic structure of these metrics – see (5.65) – one finds that the $n+1$ free parameters μ and a_i determine the mass and angular momentum of the black hole, with

$$M = \frac{(d-2)\Omega_{d-2}}{16\pi G} \mu, \quad (5.15)$$

$$J^{y_i x_i} = \frac{\Omega_{d-2}}{8\pi G} \mu a_i = \frac{2}{d-2} M a_i,$$

³ To make the connection more explicit, we would set $a_1 = a$, $\mu_1 = \sin \theta$, and $\alpha = \cos \theta$.

where Ω_{d-2} is the area of an S^{d-2} , given in (5.3). Setting all the spin parameters $a_i = 0$, both (5.11) and (5.14) reduce to the d -dimensional Schwarzschild metric (5.1). Now also setting $\mu = 0$ yields the flat-space metric in (5.4) and (5.8), respectively.

With general spin parameters a_i , both metrics have $n + 1$ commuting Killing symmetries corresponding to shifts in t and ϕ_i . These symmetries are enhanced when some spin parameters coincide. In particular, if $a_i = a$ for $i = 1, \dots, m$, the corresponding rotational symmetry is enhanced from $U(1)^m$ to $U(m)$, where the latter acts on the complex coordinates $z_i = \mu_i e^{i\phi_i}$ in the associated subspace. A particularly interesting case is $d = 2n + 1$, with all n spin parameters equal. Then, with the $U(n)$ symmetry the solution reduces to cohomogeneity 1, i.e., it depends on a single (radial) coordinate. Of course, if k spin parameters vanish then an $SO(2k)$ symmetry emerges in the corresponding subspace. When d is even, this enhanced rotational symmetry is extended to $SO(2k + 1)$ by including the z direction.

Of course, as with the Kerr metric, these geometries are stationary rather than static, reflecting the rotation of the corresponding black holes. In particular, the metric components $g_{t\phi_i}$ are nonvanishing when $a_i \neq 0$ and, as a result, one finds frame-dragging in these higher-dimensional spacetimes, just as was described in Chapter 1 for four dimensions. We might also note that (5.11) and (5.14) contain nonvanishing $g_{\phi_i\phi_k}$. Further, implicitly there are also nonvanishing $g_{\mu_i\mu_k}$ (as well as $g_{\mu_i\alpha}$ for even d), which would appear explicitly if one direction cosine were eliminated by means of (5.6) or (5.9).

5.2.2 Singularities

Various components of the metrics (5.11) and (5.14) will diverge if either $\Pi F/r^\gamma = 0$ or $\Pi - \mu r^\gamma = 0$, where $\gamma = 2$ and 1 for d for odd and even, respectively. The former indicates a true curvature singularity while the latter corresponds to an event horizon. To consider the former in more detail, one must examine a list of separate cases, i.e., for odd or even d and different numbers of vanishing spin parameters. In most cases one finds that $\Pi F/r^\gamma = 0$ at $r = 0$, and so this entire surface is singular. There are three exceptional cases, which we will consider in more detail below: (a) even d and all $a_i \neq 0$, (b) odd d and only one $a_i = 0$, and (c) odd d and all $a_i \neq 0$. We should add that all our comments with regard to curvature singularities can be confirmed by examining the behavior of the curvatures directly. For example, we examine the particular case of the $d = 5$ MP metric in detail in Appendix B, and our results there explicitly match those discussed in (b) and (c) below.

(a) Even d and all $a_i \neq 0$ This case includes the Kerr metric with $d = 4$ and the results are similar to those found for that case, described in Chapter 1. First, we

will use the constraint (5.9) to re-express (5.12) as

$$F = \alpha^2 + r^2 \sum_{i=1}^n \frac{\mu_i^2}{r^2 + a_i^2} \quad \text{for even } d . \quad (5.16)$$

From this expression, we can see that in order for $\Pi F/r$ to vanish we must have both $r = 0$ and $\alpha = 0$. Further intuition comes from noting that it is most appropriate to think of the surfaces of constant r as ellipsoids of the form

$$\frac{z^2}{r^2} + \sum_{i=1}^n \frac{x_i^2 + y_i^2}{r^2 + a_i^2} = 1 . \quad (5.17)$$

For example, if we set $\mu = 0$ in the black hole metric (5.11), the resulting metric describes flat space foliated by these surfaces. Hence, as we approach $r = 0$ these $(d - 2)$ -dimensional ellipsoids collapse to a $(d - 2)$ -dimensional ball in the hyperplane $z = 0$. Now, the direction cosine $\alpha = z/r$ acts as a radial coordinate in this ball; $\alpha = 1$ corresponds to the origin and $\alpha = 0$ to the boundary of the ball where the curvature diverges. Thus, in higher even dimensions, the ring-like singularity of the Kerr metric is elevated to a singularity on a $(d - 3)$ -sphere. The $(d - 2)$ -ball at $r = 0$ acts as a two-sided aperture. Passing through the aperture to negative values of r , we enter a new asymptotically flat space with negative mass (and no horizons). Further, as noted in Chapter 1 for the Kerr metric, this region also contains closed timelike curves. Passing through the aperture a second time in the same direction, we reach a space isometric to the original $r > 0$ region and, for simplicity, these two regions are usually identified.

(b) Odd d and only one $a_i = 0$ For simplicity, let us denote the vanishing spin parameter as a_1 . We begin by rewriting (5.12), this time using the constraint (5.6):

$$F = \mu_1^2 + r^2 \sum_{i=2}^n \frac{\mu_i^2}{r^2 + a_i^2} \quad \text{for odd } d \text{ and } a_1 = 0 . \quad (5.18)$$

Hence, in this case, for $\Pi F/r^2$ to vanish we require both $r = 0$ and $\mu_1 = 0$ – note that Π contributes a factor of r^2 here. The appropriate geometric intuition comes from regarding constant- r surfaces as ellipsoids of the form

$$\frac{x_1^2 + y_1^2}{r^2} + \sum_{i=2}^n \frac{x_i^2 + y_i^2}{r^2 + a_i^2} = 1 . \quad (5.19)$$

As we approach $r = 0$, these $(d - 2)$ -dimensional ellipsoids collapse to a ball in the hyperplane $x_1 = 0 = y_1$. As above, μ_1 acts as a radial coordinate in this ball; $\mu_1 = 0$ corresponds to the boundary of the ball, where the curvature diverges. However, a key difference from case (a) is that as $r \rightarrow 0$ the ellipsoids (5.19)

become very narrow and collapse to a point in the (x_1, y_1) -plane at $r = 0$. Hence the ball at $r = 0$ extends only in $d - 3$ dimensions. A careful examination of the geometry shows that there is also a conical singularity in the (x_1, y_1) -plane for any $\mu_1 \neq 0$.⁴ Consequently the entire $r = 0$ surface is in fact singular here, although with a milder singularity than in the generic cases.

(c) *Odd d and all $a_i \neq 0$* If we apply the constraint (5.6) then (5.12) becomes

$$F = r^2 \sum_{i=1}^n \frac{\mu_i^2}{r^2 + a_i^2} \quad \text{for odd } d. \quad (5.20)$$

In this case, we observe that Π approaches a finite constant at $r = 0$ and (5.6) does not allow all the μ_i to vanish simultaneously. Therefore $\Pi F/r^2$ remains finite at $r = 0$ and so there is no curvature singularity here. Nevertheless, the metric (5.11) remains problematic at this location since $g_{rr} \propto r^2$ as $r \rightarrow 0$. However, this is only a coordinate singularity and can be avoided by choosing a new radial coordinate $\rho = r^2$. Now, in passing to negative values of ρ , the function $\Pi F/r^2(\rho)$ eventually vanishes and a curvature singularity arises at $\rho = -a_s^2$, where a_s is the absolute value of the spin parameter(s) with the smallest magnitude. If more than one spin parameter has the value $\pm a_s$, the entire surface $\rho = -a_s^2$ is singular. If only one spin parameter, say a_1 , has the value $\pm a_s$, the singularity at $\rho = -a_s^2$ only appears at $\mu_1 = 0$. In this case, if $a_{s'}$ is the absolute value of the next smallest spin parameter then the geometry extends smoothly to values $-a_{s'}^2 \leq \rho \leq -a_s^2$ in certain directions. However, the curvature singularity extends throughout this range of ρ since F can vanish for certain angular directions. Hence ultimately all trajectories moving towards smaller values of ρ end on a singularity in this region.

5.2.3 Horizons

In considering the event horizons for these metrics, we must again consider separately the cases where the spacetime dimension is even and the cases where it is odd. Let us start with $d = 2n + 2$, which includes the Kerr metric for $d = 4$. The event horizons arise where g^{rr} vanishes, and so from (5.11) we require that

$$\Pi - \mu r = 0. \quad (5.21)$$

Thus the horizons correspond to the roots of a polynomial, which is of order $d - 2$ in r . Unfortunately, apart from $d = 4$ or 6 , there are no general analytic solutions (in terms of radical expressions) for the position of the horizon. Hence a complete set of necessary and sufficient conditions for the existence of a horizon is unavailable for higher d values. However, we can still make some general observations.

⁴ Of course, this statement assumes that the mass parameter μ is nonvanishing.

First, the horizon, if it exists, must have the topology of S^{d-2} since it is a surface of constant r . Further, to avoid a naked singularity we require the mass (i.e., μ) to be positive. The latter fact can be deduced from two observations: first, the singularity appears at $r = 0$ and, second, the function Π is everywhere positive (or zero) – recall the definition (5.13). Hence for (5.21) to have a root at positive r , we must have $\mu > 0$. With a closer examination of the polynomial in (5.21) we see that, in fact, it is large and positive for large $|r|$ and has a single minimum. We conclude that there are only three possible scenarios: two, one, or zero horizons. In this regard the higher-dimensional metrics (5.11) are the same as the familiar Kerr metric in $d = 4$. However, an interesting difference arises if one (or more) spin parameter vanishes. Recall that Π is monotonically increasing and grows as r^{2n} at large r . However, in this case Π vanishes at $r = 0$ and grows as r^{2m} for small r , with m vanishing spin parameters. Thus the right-hand side of (5.21) is negative for small r yet is large and positive for large r . Hence there must always be one nondegenerate root at positive r , corresponding to a single horizon. This result holds irrespective of how large the remaining spin parameters are, and so the event horizon appears even when the angular momentum grows arbitrarily large, as long as there is no rotation in at least one orthogonal plane. These solutions with very large angular momenta have been dubbed “ultra-spinning” black holes in [7]. As we will see in section 5.2.8, the latter have further interesting consequences.

For $d = 2n + 1$, the location of the horizon in (5.14) is determined by

$$\Pi - \mu r^2 = 0. \quad (5.22)$$

It is more useful to present this expression using the new radial coordinate $\rho = r^2$ introduced in the previous discussion of singularities. In terms of ρ , eq. (5.22) becomes

$$\prod_{i=1}^n (\rho + a_i^2) - \mu \rho = 0. \quad (5.23)$$

Hence we are looking for the roots of a polynomial of order n and so analytic solutions only exist for $n = 2, 3$, and 4 , i.e., $d = 5, 7$, and 9 . The solution for $d = 5$ is given in Appendix B. Of course, the horizon has the topology of S^{d-2} since it is a surface of constant ρ .⁵ Finding a root with $\rho > 0$ again requires positive μ . In fact, a positive root requires that

$$\mu > \sum_i \prod_{j \neq i} a_j^2, \quad (5.24)$$

⁵ Implicitly we are assuming that $\rho > 0$ here. See the additional discussion below of the case where all the spin parameters are nonvanishing.

which ensures that the coefficient of the linear term is negative in (5.23). This constraint is necessary but not sufficient for the absence of a naked singularity. Provided that μ is sufficiently large, we again find only one or two horizons with positive ρ , just as in the case of even d . Note that, for odd d , a single vanishing spin parameter is insufficient to guarantee the existence of a horizon since the constraint (5.24) remains nontrivial. However, if two or more spin parameters vanish, (5.23) has one positive root as well as a root at $\rho = 0$. Further, in this particular case we can have regular ultra-spinning solutions for which an event horizon appears, even when the remaining spin parameters become arbitrarily large.

Recall that the singularity structure distinguishes the case of odd d and all $a_i \neq 0$. In particular, in this case the surface $\rho = 0$ is nonsingular and the geometry extends to negative values of ρ . To avoid naked singularities, we require only that the outermost horizon, i.e., the largest root of (5.23), appears for $\rho > -a_s^2$, where the singularity appears.⁶ Now, with positive μ the only possibility is that the horizon appears at positive ρ provided that μ is sufficiently large, as described above. However, we have $\Pi(\rho = -a_s^2) = 0$ and hence for any negative μ a root appears in (5.23) in the range $-a_{s'}^2 < \rho < 0$. Below, we will see that these negative-mass solutions are even more pathological since they contain causality-violating regions extending beyond the horizon. To close this discussion, we recall that, when only one spin parameter has the minimal value, the geometry extends further into the range $-a_{s'}^2 < \rho < -a_s^2$. In this case, for small positive μ one finds two roots or one degenerate root in this new range. However, these surfaces intersect the singular surface and so the latter is not entirely concealed by these horizons. Further, if horizons occur in the range $-a_{s'}^2 < \rho < -a_s^2$ then one can show that no other horizons appear for positive ρ . Therefore these spacetimes contain naked singularities.

5.2.4 Ergosurfaces and causality violation

Turning now to ergosurfaces, we must determine the surfaces where g_{tt} vanishes. From the metrics in (5.11) and (5.14), the latter correspond to the roots of

$$\begin{aligned} F\Pi - \mu r &= 0, & \text{even } d, \\ F\Pi - \mu r^2 &= 0, & \text{odd } d, \end{aligned} \quad (5.25)$$

for $r > 0$. These surfaces still have the topology of S^{d-2} but, of course, the factor F introduces a more complicated directional dependence than appears for the horizons. As above, while there is no analytic solution for these equations, one is

⁶ As in the previous subsection, to discuss this case, we adopt the notation whereby a_s and $a_{s'}$ are the magnitudes of the smallest and second smallest spin parameters, respectively.

still able to deduce the general properties of the surfaces. In particular, one such surface always appears outside the outer horizon and another may appear inside the inner horizon if the latter exists. As can be seen from (5.26), the ergosurface will touch the horizons where $F = 1$. If m spin parameters vanish when d is even, then the latter corresponds to the $2m$ -dimensional sphere described by $1 = \alpha^2 + \sum_{k=1}^m \mu_k^2$, where the sum runs over the m indices for which $a_k = 0$. Hence if no spin parameters vanish, the two surfaces only touch at the two points on the horizon where $\alpha = \pm 1$, as was found for the four-dimensional Kerr metric. Similarly, if m spin parameters vanish when d is odd then the ergosurface and horizon will touch along the S^{2m-1} described by $1 = \sum_{k=1}^m \mu_k^2$. In particular, the two surfaces will not coincide anywhere if all the spin parameters are nonvanishing in the case of odd d . Further, in this case one finds that, for positive μ , there will be an ergosurface outside the outer horizon but no such surface inside the inner horizon. However, if μ is negative then no ergosurfaces exist at all.

As described in Chapter 1, the outer ergosurface marks the boundary within which particles cannot remain at rest with respect to infinity. Further, the spinning black holes in higher dimensions can be mined with Penrose processes, just as in four dimensions. Another analogy with $d = 4$ arises in the scattering waves propagating in these geometries, which produces superradiance for the MP solutions as in the Kerr metric.

We close this subsection by turning to the question of causality violation. For many of the black holes under consideration we need consider only $r > 0$, and in this domain the angular coordinates are perfectly well behaved. The exceptional cases requiring additional consideration correspond to the black holes where all $a_i \neq 0$. First, for even d , r can be extended to negative values in the second asymptotic region. In this region the metric components $g_{\phi_i \phi_i}$ can become negative, leading to closed time-like loops as occurs in the Kerr metric. For odd d and all $a_i \neq 0$, the geometry extends beyond $r = 0$ to negative values of $\rho = r^2$. In this case, for each angle ϕ_i , (5.14) gives

$$g_{\phi_i \phi_i} = (\rho + a_i^2) \left(1 + \frac{\mu a_i^2}{\Pi} \right) \quad (5.26)$$

in the plane $\mu_i = 1$. The above expression will become negative if the second factor has a zero, i.e., for radii inside that where $\Pi + \mu a_i^2 = 0$. Now recall that for $\mu < 0$ the horizon arises at the root of (5.23) that lies between $\rho = -a_s^2$ and 0. Hence the more important observation is that, for any angle ϕ_i for which the corresponding spin parameter satisfies $a_i^2 > a_s^2$, the above metric component will be negative for some values of ρ outside the horizon (since Π is a monotonically increasing function). That is, the negative-mass solutions typically contain causality-violating regions extending beyond the horizon – the only exception would be the case when

all the spin parameters are precisely equal. For completeness, we also note that in this case, with $\mu > 0$ and a single a_i taking the value $\pm a_s$, there is the possibility that (5.26) vanishes for $a_i = a_s$ in the range $-a_{s'}^2 < \rho < -a_s^2$.

5.2.5 Maximal analytic extension

In examining the maximal analytic extension of the solutions (5.11) and (5.14) one can use the standard techniques developed to study four-dimensional black holes, and the results are essentially the same as for $d = 4$. In particular, one finds two separate extensions of the spacetime at each horizon, i.e., an infalling coordinate patch that extends the geometry across the future horizon and an outgoing patch that smoothly traverses the past horizon. In the following, our discussion will focus on the case of even d and the extension of (5.11). However, with obvious changes, the same discussion is easily adapted to the case of odd d , and we will briefly examine this case near the end of this subsection.

In working towards the construction of the maximal analytic extension of these spacetime geometries, it is straightforward to construct Eddington-like coordinates

$$dt = dt_{\pm} \mp \frac{\mu r}{\Pi - \mu r} dr , \quad d\phi_i = d\phi_{\pm,i} \pm \frac{\Pi}{\Pi - \mu r} \frac{a_i dr}{r^2 + a_i^2} . \quad (5.27)$$

With these new coordinates the metric (5.11) becomes

$$ds^2 = -dt_{\pm}^2 + dr^2 + \sum_{i=1}^n (r^2 + a_i^2) (d\mu_i^2 + \mu_i^2 d\phi_{\pm,i}^2) + r^2 d\alpha^2$$

$$\pm 2 \sum_{i=1}^n a_i \mu_i^2 d\phi_{\pm,i} dr + \frac{\mu r}{\Pi F} \left(dt_{\pm} \pm dr + \sum_{i=1}^n a_i \mu_i^2 d\phi_{\pm,i} \right)^2 \quad (5.28)$$

Hence the metric is well behaved in either coordinate system at the horizons, i.e., $\Pi - \mu r = 0$. Of course, various metric components are still singular at $\Pi F/r = 0$ since the latter corresponds to a true curvature singularity. As can be seen from (5.28), each coordinate system is adapted to a particular family of radial geodesics following the null vectors

$$k_{\pm}^{\mu} \frac{\partial}{\partial x^{\mu}} = \frac{\partial}{\partial t} \mp \frac{\partial}{\partial r} . \quad (5.29)$$

That is, the $+$ and $-$ coordinates are well behaved along infalling and outgoing geodesics, respectively, which cross the horizons. Hence t_+ remains finite on the

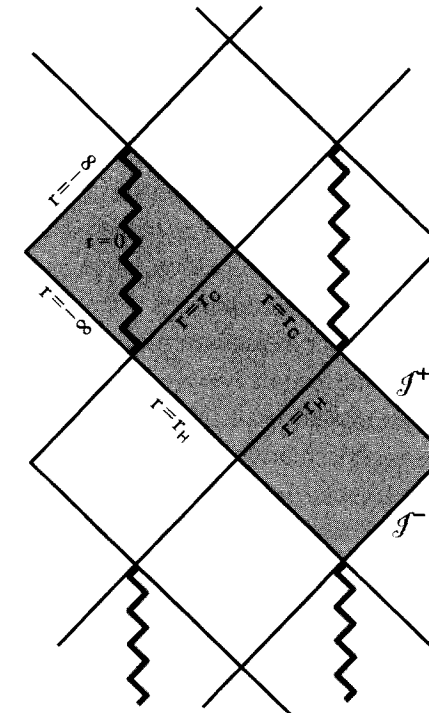


Figure 5.1 Penrose diagram for a spinning black hole with two horizons, for even d . The shaded regions indicate a single coordinate patch covered by infalling Eddington coordinates.

future horizon, where $r \rightarrow r_H$ and $t \rightarrow +\infty$, while t_- remains finite on the past horizon, where $r \rightarrow r_H$ and $t \rightarrow -\infty$.

The above Eddington-like coordinates (5.27) indicate that the structure of the horizons is essentially the same as that found in four dimensions. In particular, let us consider the case where (5.21) has two distinct roots at positive r – recall this requires that all the spin parameters are nonvanishing. Hence we have an outer event horizon at $r = r_H$ and an inner Cauchy horizon at $r = r_C (< r_H)$. The corresponding Penrose diagram is shown in Fig. 5.1. A typical Eddington coordinate patch covers three regions in this diagram: the asymptotically flat exterior region where $r > r_H$; the central region between the inner and outer horizons where $r_C < r < r_H$; and the inner region, where $r < r_C$, which contains a timelike “ring” singularity and which can be extended to an asymptotically flat region (with $r < 0$). If we consider the regions covered by the infalling coordinates $(t_+, \phi_{+,i})$ then each of these three regions can be separately extended by transforming to the outgoing coordinates, $(t_-, \phi_{-,i})$. Hence the maximally extended spacetime becomes a tower in which the basic geometry illustrated in Fig. 5.1 is repeated an infinite number of times. We

might note that, as illustrated in the figure, the horizons at $r = r_H$ and r_C have the characteristic "X" structure of a bifurcate Killing horizon. Here the various branches of the horizon are connected at the bifurcation surface at the center of the X, which corresponds to a fixed point of the associated Killing vector. Strictly speaking, in order to demonstrate that the regions of the various overlapping Eddington patches are in fact smoothly connected at the bifurcation surface one should find Kruskal-like coordinates, which are simultaneously well behaved across both the future and past horizons (as well as across the bifurcation surface). While this is certainly possible, the construction of these coordinates is a more involved exercise and we refer the interested reader to [1] for a discussion of this point.

As noted above, the inner horizon at $r = r_C$ is a Cauchy horizon, representing the boundary for the unique evolution of initial data on some space-like surface stretched across the Einstein–Rosen bridge joining two asymptotically flat regions. Now, we expect that these Cauchy horizons should be unstable since the simple arguments which indicate that such a surface is unstable in the four-dimensional Kerr metric can be applied equally well here in higher dimensions. However, it must be said that this issue has not been studied in the same detail as in four dimensions and so an accurate description of the resulting singularity remains lacking for higher dimensions.

Above, we considered the spinning black holes (5.11) (with all $a_i \neq 0$) in the regime where there were two distinct horizons. If the mass of this solution is fixed and some spin parameters are increased, eventually the two horizons will coalesce producing an extremal black hole. In this case, the individual Eddington coordinate patches cover the exterior region and the inner region, and connecting these patches results in the maximal extension illustrated in Fig. 5.2(a). In this case, the near-horizon analysis of [8] can also be extended to higher dimensions, to find that the throat region of the extremal black hole corresponds to an analogue of the geometry $\text{AdS}_2 \times S^n$ [9, 10]. If any spin parameter is increased further then the horizon disappears and one is left with a naked singularity, as shown in Fig. 5.2(b). Hence the extended black hole geometries described here and above provide a direct analogue in higher dimensions of the four-dimensional story for the Kerr solution, described in Chapter 1.

Another possibility, which we have not yet considered for even d , occurs when one or more spin parameters vanish. In this case there is a single horizon, which corresponds to a simple zero in (5.21). There will be a second root but it occurs at the singularity at $r = 0$. One finds that this singular surface is spacelike and so the Penrose diagram is similar to that of the Schwarzschild solution. In particular, there is no infinite tower of connected regions here but, rather, the singularities form spacelike boundaries for the future and past interior regions. Here an analogy might be drawn with the $d = 4$ Kerr metric in the limit $a \rightarrow 0$, where $r_C \rightarrow 0$ and the

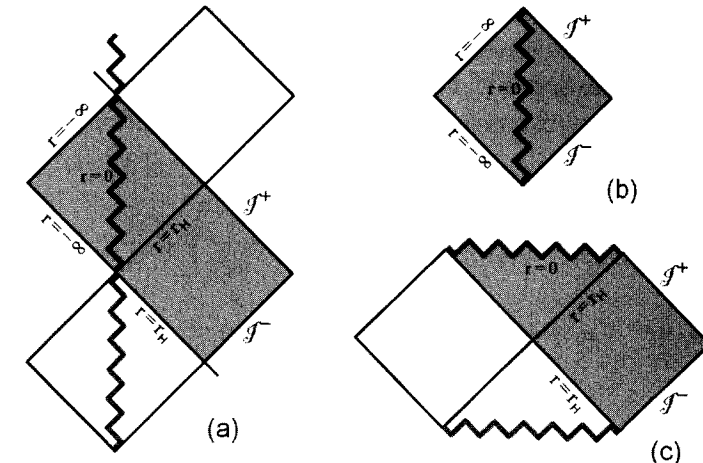


Figure 5.2 Further Penrose diagrams for even d : (a) an extremal spinning black hole with single degenerate horizon, (b) an over-rotating solution without a horizon, and (c) a spinning black hole with one or more $a_i = 0$. As before, the shaded regions indicate a single coordinate patch covered by infalling Eddington coordinates.

geometry reduces to that of the Schwarzschild solution. In higher dimensions there will still be other nonvanishing spin parameters, in general, but the structure of the spacetime remains unchanged irrespective of how large the remaining a_i become. Hence, as noted above, with one a_i equal to 0 (and d even) we can construct ultra-spinning black holes, carrying an arbitrary amount of angular momentum.

The above discussion was restricted to even d but there are no essential differences for the case of odd d . Of course, as mentioned in section 5.2.2, with all spin parameters nonvanishing the surface $r = 0$ is nonsingular and the geometry extends to negative values of $\rho = r^2$. Further, one finds a timelike singularity in the latter domain but there is no connection to a second asymptotically flat region. Another difference is that the cases where the Penrose diagram takes a Schwarzschild form include either two or more $a_i = 0$ and $\mu > 0$ or one $a_i = 0$ and $\mu > \sum_i \prod_{j \neq i} a_j^2$. The same structure also arises when all $a_i \neq 0$ and $\mu < 0$ but, as described above, these spacetimes are pathological since they contain causality-violating regions outside the horizon.

To close this subsection, let us make a few supplementary comments. First, we note that the metrics (5.28) actually have the so-called Kerr–Schild form:

$$g_{\mu\nu} = \eta_{\mu\nu} + h(k_{\pm})_{\mu}(k_{\pm})_{\nu}, \quad (5.30)$$

where $h = \mu r / (\Pi F)$. Of course, a further coordinate transformation would be required to introduce Cartesian coordinates, in which the flat-space line element would take the conventional form. Here I note that a remarkable feature of the

four-dimensional Kerr metric is that it can be written in this particular form [11]. Ultimately, it was the fact that the MP metrics can also be written in the Kerr–Schild form that allowed us to derive (5.11) and (5.14).

It is also interesting to examine the null vectors (5.29) in the original coordinate system of (5.11):

$$k_{\pm}^{\mu} \frac{\partial}{\partial x^{\mu}} = \frac{\Pi}{\Pi - \mu r} \left(\frac{\partial}{\partial t} - \sum_{i=1}^n \omega_i \frac{\partial}{\partial \phi_i} \right) \mp \frac{\partial}{\partial r}, \quad (5.31)$$

where $\omega_i = a_i/(r^2 + a_i^2)$. From these expressions we see that, upon approaching the horizon,

$$k_{\pm}^{\mu} \frac{\partial}{\partial x^{\mu}} \propto \frac{\partial}{\partial t} - \sum_{i=1}^n \Omega_i \frac{\partial}{\partial \phi_i}, \quad (5.32)$$

with $\Omega_i = a_i/(r_H^2 + a_i^2)$. That is, k_{-}^{μ} becomes the generator of the future horizon at $r = r_H$ in the infalling Eddington coordinate patch described by $(t_+, \phi_{+,i})$. Similarly, with infalling Eddington coordinates, k_{+}^{μ} matches the generator of the past horizon at $r = r_H$. A final comment is that these two vector fields given in (5.29) or (5.31) correspond to the principal null vectors that appear in the algebraic classification to be discussed in Chapter 9.

5.2.6 Hidden symmetries and geodesics

In the four-dimensional Kerr metric, particle motion is easily studied because the geodesics are completely soluble by quadratures. That is, there are four constants of motion, and this allows us to write the complete solution for geodesic motion in terms of a set of indefinite integrals. At first sight this is a rather remarkable property since the Killing symmetries and the fixed norm of the four-velocity provide only three such constants. The fourth constant is more subtle and relies on the existence of a Killing–Yano tensor in this particular background [12–14] – see below. The existence of this tensor is also responsible for the separability of the wave equations for fields with spin 0, 1/2, 1, or 2 in this background. Recent work has uncovered a rich structure of analogous relationships in higher dimensions, e.g., [15–19]. In particular, the required hidden symmetries were found for the Myers–Perry metrics [15], from which one can infer the integrability of geodesic motion in these backgrounds [16].

Central to this discussion is the existence of a rank-2 closed conformal Killing–Yano tensor (CCKY) $h_{\mu\nu}$, which is a two-form satisfying

$$\nabla_{(\mu} h_{\nu)\rho} = \frac{1}{d-1} (g_{\mu\nu} \nabla_{\sigma} h^{\sigma}_{\rho} - \nabla_{\sigma} h^{\sigma}_{(\mu} g_{\nu)\rho}). \quad (5.33)$$

As this two-form is closed it also satisfies $dh = 0$, and so at least locally there exists a one-form potential b such that $h = db$. In the case of the MP metrics (5.11) and (5.14), the CCKY tensor can be written explicitly using standard wedge products:

$$h = \sum_{i=1}^n a_i \mu_i d\mu_i \wedge [a_i dt + (r^2 + a_i^2) d\phi_i] \\ + r dr \wedge \left(dt + \sum_{i=1}^n a_i \mu_i^2 d\phi_i \right). \quad (5.34)$$

Following the standard construction in four dimensions, one obtains a second-rank Killing tensor [12–14]

$$K_{(\mu\nu)} = -h_{\mu}^{\sigma} h_{\nu\sigma} + \frac{1}{2} g_{\mu\nu} h_{\rho\sigma} h^{\rho\sigma}, \quad (5.35)$$

which then satisfies the identity

$$\nabla_{(\mu} K_{\nu\rho)} = 0. \quad (5.36)$$

Hence, along a geodesic described by the d -velocity u^{μ} the following is a constant of the motion: $K_{\mu\nu} u^{\mu} u^{\nu}$. In higher dimensions the latter is only the first in a series of new conserved quantities. We will not describe the above-mentioned construction here but merely give the results. One finds the following tower of second-rank Killing tensors [15–17]:

$$K^{(\ell)\mu}_{\nu} = \frac{(2\ell)!}{(2\ell \ell!)^2} (\delta^{\mu}_{\nu} h^{[\mu_1 \nu_1} \dots h^{\mu_{\ell} \nu_{\ell}]} h_{[\mu_1 \nu_1} \dots h_{\mu_{\ell} \nu_{\ell}]} \\ - 2\ell h^{\mu[\nu_1} \dots h^{\mu_{\ell} \nu_{\ell}]} h_{\nu_1} \dots h_{\mu_{\ell} \nu_{\ell}}). \quad (5.37)$$

Note that on comparing this expression with (5.35) we see that $K_{\mu\nu}^{(1)} = K_{\mu\nu}$. Now using (5.33) for the CCKY tensor, it follows that all these tensors satisfy the identity (5.36) and hence each provides a constant of the motion along a geodesic, $c_{\ell} = K_{\mu\nu}^{(\ell)} u^{\mu} u^{\nu}$.

On the one hand, from (5.37) it would appear that this construction extends to $\ell = 1, \dots, n+1$ for $d = 2n+2$; however, one finds for $\ell = n+1$ that the right-hand side vanishes as an identity. On the other hand, one can extend this series naturally to $\ell = 0$ with $K^{(0)\mu}_{\nu} = \delta^{\mu}_{\nu}$, in which case $c_0 = K_{\mu\nu}^{(0)} u^{\mu} u^{\nu} = g_{\mu\nu} u^{\mu} u^{\nu}$ is simply the norm of the d -velocity. Hence the Killing tensors provide $n+1$ constants of motion. An essential feature of this construction is that these constants are in fact all independent. The latter statement is related to the fact that the CCKY tensor contains $n+1$ independent “eigenvalues” for even d , when it is put in a standard form analogous to (5.10). Of course, the Killing symmetries (time translations and the n rotations in each ϕ_i) provide a further $n+1$ constants of the

motion. Hence in total there are $d = 2n + 2$ constants, which allows us to solve for the geodesics in quadratures.

For $d = 2n + 1$ there is a similar counting of the constants of motion. In this case, the Killing tensors provide $n + 1$ independent constants c_ℓ with $\ell = 0, 1, \dots, n$. Further, the Killing symmetries provide $n + 1$ independent constants. At this point it may seem that we have too many integration constants but, in the case of odd d , it turns out that c_n is reducible. That is, $c_{(n)} = (\xi^\nu g_{\mu\nu} u^\mu)^2$, where ξ^ν is a Killing vector [16, 17]. This result comes from describing (5.37) as the contraction of a CCKY tensor of rank $d - 2\ell$ (dual to the wedge product of ℓ h 's). Hence, for $\ell = n$ the latter tensor is a one-form for which the analogue of (5.33) reduces to Killing's equation. We conclude that this tensor is in fact simply a linear combination of the Killing vectors. Consequently, the total number of independent constants is precisely $d = 2n + 1$ and the geodesic motion is again completely integrable [16, 17].

We comment that it has also been shown that the Killing(-Yano) tensors also lead to the separability of the Klein-Gordon and Dirac equations as well as of the Hamilton-Jacobi equations in these backgrounds; see e.g. [19–21]. While we do not have room to describe these results in detail here, a key element in this analysis is to construct “symmetry operators” that commute with the appropriate wave operator. For example, in the case of the Klein-Gordon equation [18] we can start with simple operators constructed for each of the Killing coordinates, i.e., $i\partial_t$ and $i\partial_{\phi_i}$, each of which commutes with $\nabla^2 - m^2$. Various components of the separated solution of $(\nabla^2 - m^2)\psi = 0$ can then be identified as eigenfunctions of these operators, e.g., $e^{i\omega t}$ and $e^{im\phi_i}$. Now, the Killing tensors provide an additional set of symmetry operators $\hat{K}^{(\ell)} = \nabla_\mu(K^{(\ell)\mu\nu}\nabla_\nu)$, which also satisfy $[\nabla^2 - m^2, \hat{K}^{(\ell)}]$. Again, various separated components of the desired solutions can then be written as eigenfunctions of these new operators. It remains an open question whether a similar set of symmetry operators can be constructed for the equations of a Maxwell field or a field of linearized gravitons and whether separability extends to these equations. We note that some progress in analyzing linearized metric perturbations has been made for the particular case in which d is odd and all the a_i are equal [22].

5.2.7 Black hole thermodynamics

As already stated in Chapter 1, the basic framework of black hole thermodynamics extends from four to higher dimensions in a straightforward way. We might add that implicitly this relies on the fact that our discussion of higher-dimensional black holes is restricted to solutions of Einstein's equations. There have also been interesting extensions of black hole thermodynamics to include both higher-curvature actions and higher dimensions [23–25]. In any event, we will keep our comments here brief – see also the remarks in the following subsection.

The zeroth law, namely, that the surface gravity or temperature (i.e., $T = \kappa/(2\pi)$) is constant across any stationary event horizon, must hold if the corresponding black holes are to behave like a thermal bath. This result is easily established if the horizon is a bifurcate Killing horizon, which is certainly the case here, following the discussion of section 5.2.5. As noted there, the horizon generator is given by

$$\chi^\mu \partial_\mu = \partial_t - \sum_{i=1}^n \Omega_i \partial_{\phi_i}. \quad (5.38)$$

Recall that $\Omega_i = a_i/(r_H^2 + a_i^2)$. Hence, using $\chi^\sigma \nabla_\sigma \chi^\mu = \kappa \chi^\mu$ to evaluate the surface gravity, one finds

$$\kappa = \begin{cases} \frac{\partial_r \Pi - \mu}{2\mu r} \Big|_{r=r_H} & \text{for even } d, \\ \frac{\partial_r \Pi - 2\mu r}{2\mu r^2} \Big|_{r=r_H} & \text{for odd } d. \end{cases} \quad (5.39)$$

While these are somewhat formal expressions, they clearly illustrate that κ is constant across the entire horizon.

Of course, the first law takes precisely the same form as in four dimensions:

$$\delta M = \frac{\kappa}{8\pi G} \delta \mathcal{A} + \sum_{i=1}^n \Omega_i \delta J_i, \quad (5.40)$$

which leads to the interpretation of the area of (a cross section of) the horizon \mathcal{A} as the entropy of the black hole, with the celebrated formula $S = \mathcal{A}/(4G)$. (Of course, in a d -dimensional spacetime this area \mathcal{A} actually has the dimensions of length to the power $d - 2$.) The Killing symmetries of the MP metrics also allow us to construct a useful relation known as the integrated Smarr formula [26],

$$\frac{d-3}{d-2} M = \sum_{i=1}^n \Omega_i J_i + \frac{\kappa}{8\pi G} \mathcal{A}. \quad (5.41)$$

Following [26], the irreducible mass of the black hole may be identified from the first law. It is the mass associated with the area of the horizon, i.e., one integrates the area term in (5.40), obtaining

$$\begin{aligned} M_{\text{ir}} &= \frac{1}{8\pi G} \int_0^{\mathcal{A}} \kappa(\mathcal{A}', J_i = 0) d\mathcal{A}' \\ &= \frac{d-2}{16\pi G} \Omega_{d-2}^{1/(d-2)} \mathcal{A}^{(d-3)/(d-2)} \\ &= \frac{d-2}{d-3} \frac{\kappa \mathcal{A}}{8\pi G}. \end{aligned} \quad (5.42)$$

Hence $M - M_{\text{ir}}$ is the mass or energy due to the rotation of the black hole, and we expect that it can be removed through Penrose processes. In four dimensions this can be verified explicitly because the geodesics in the Kerr metric are completely soluble by quadratures. Given the recent developments described in section 5.2.6 above, it would be interesting to extend this analysis to higher dimensions.

To close this subsection, we note that the second law (i.e., $\delta \mathcal{A} \geq 0$) is also easily extended to higher dimensions, following the discussion in Chapter 1. One proof of the second law requires that the matter falling across the horizon satisfies the null energy condition and also that cosmic censorship holds [27]. While the former still seems a reasonable assumption in higher dimensions, the latter may appear more dubious given the recent results discussed in Chapter 3. However, the second law may also be proved by using the null energy condition and by demanding that the null generators of the horizon are complete [27]. The latter is consistent with our current understanding of the final state of the Gregory–Laflamme instability and hence it seems that the second law still rests on a firm foundation in higher dimensions.

5.2.8 Instabilities

While there is strong evidence for the stability of Kerr black holes in four dimensions, in fact the opposite is true for spinning black holes in higher dimensions. That is, we believe that in higher dimensions various instabilities arise for MP black holes when the angular momentum becomes large. In fact it has been argued that these instabilities are related to the appearance of a rich fauna of new black holes in higher dimensions [28, 29].

A precise understanding of instabilities would require an analysis of the linearized perturbations of the MP metrics (5.11) and (5.14). While this is possible in four dimensions, as noted in section 5.2.6, limited progress has been made in higher dimensions. However, insight into the situation in higher dimensions comes from making connections with the Gregory–Laflamme instability of black branes – see Chapter 2. As described below this approach has led to the conjecture that ultra-spinning black holes are unstable for $d \geq 6$ [7], and numerical evidence of this conjecture was recently found [30–34]. An interesting consequence is that it seems that general relativity in higher dimensions imposes a dynamical “Kerr bound” on the spin, of the form $J^{d-3} \lesssim GM^{d-2}$ in d dimensions.

To illustrate this point let us consider the spinning black hole solutions for a single nonvanishing spin parameter. With this restriction, for either odd or even d the metric reduces to

$$\begin{aligned} ds^2 = & -dt^2 + \frac{\mu}{r^{d-5}\rho^2} (dt + a \sin^2 \theta d\varphi)^2 + \frac{\Sigma}{\Delta} dr^2 \\ & + \Sigma d\theta^2 + (r^2 + a^2) \sin^2 \theta d\varphi^2 + r^2 \cos^2 \theta d\Omega_{d-4}^2, \end{aligned} \quad (5.43)$$

where

$$\Sigma = r^2 + a^2 \cos^2 \theta \quad \text{and} \quad \Delta = r^2 + a^2 - \frac{\mu}{r^{d-5}}. \quad (5.44)$$

Here we have set $a_1 = a$ and $\mu_1 = \sin \theta$ (as well as $a_{i>1} = 0$). Now the event horizon is determined as the largest root r_H of $\Delta(r) = 0$. That is,

$$r_H^2 + a^2 - \frac{\mu}{r_H^{d-5}} = 0. \quad (5.45)$$

In examining this equation it is not hard to see that, for $d = 4$ or 5 , there is an extremal limit (i.e., an upper bound on a) beyond which no horizon exists. However, as our discussion in section 5.2.3 indicated, the more interesting case is $d \geq 6$. For the latter we may note that the term r^2 makes the left-hand side of (5.45) large and positive as $r \rightarrow \infty$. The term $-\mu/r^{d-5}$ makes $\Delta(r)$, negative for small r , however, and hence there must be a (single) positive root, independently of the value of a . That is, we have the possibility of ultra-spinning solutions, for which a regular event horizon remains even when the angular momentum (per unit mass) grows arbitrarily large.

Let us examine the geometry of the horizon of (5.43) in this ultra-spinning regime. In the limit of very large a and fixed μ , the solution of (5.45) is given approximately by

$$r_H \simeq \left(\frac{\mu}{a^2} \right)^{1/(d-5)} \ll a. \quad (5.46)$$

Hence we observe that r_H shrinks as a grows (and μ is kept fixed). However, r_H is simply some coordinate expression and so one must instead examine the horizon in a covariant way to uncover the true geometry. Various approaches may be taken here, all with the same simple result. If we characterize the sizes of the horizon along and orthogonal to the plane of rotation as ℓ_{\parallel} and ℓ_{\perp} , respectively, then

$$\ell_{\parallel} \sim a \quad \text{and} \quad \ell_{\perp} \sim r_H. \quad (5.47)$$

That is, the horizon of these rapidly rotating black holes spreads out in the plane of rotation while contracting in the transverse directions, taking a “pancake” shape in this plane. Considering the area of the horizon, we find

$$\mathcal{A} = \Omega_{d-2} r_H^{d-4} (r_H^2 + a^2) \simeq \Omega_{d-2} r_H^{d-4} a^2 \simeq \Omega_{d-2} \left(\frac{\mu^{d-4}}{a^2} \right)^{1/(d-5)}. \quad (5.48)$$

Note that the area decreases as a grows because the contraction in the transverse directions overcomes the spreading in the plane of rotation. We emphasize that this result (5.48) only applies for $d \geq 6$. The horizon area also decreases with increasing a for $d = 4$ or 5 but only for larger d can we consider an ultra-spinning regime with $a \rightarrow \infty$, in which case the area shrinks to zero size.

Hence, from the perspective of an observer near the axis of rotation and near the horizon (i.e., near $\theta \sim 0$ and $r \sim r_H$), the horizon geometry appears similar to that of a black membrane,⁷ i.e., it has roughly the geometry $\mathbb{R}^2 \times S^{d-4}$. However, as we saw in Chapter 2, Gregory and Laflamme found that a black membrane would be classically unstable when the size in the brane directions is larger than that of the transverse sphere [35, 36]. Hence it is natural to expect that the ultra-spinning MP solutions are unstable in the limit $a \rightarrow \infty$ but also that the instability actually sets in at some finite value of a [7].

The transition between the regimes where the horizon behaves similarly to the Kerr black hole and where it behaves like a black membrane is easily seen using black hole thermodynamics. One simple quantity to consider is the black hole temperature of the metric (5.43). Beginning from zero spin, T decreases as a grows, just as in the familiar case of the Kerr black hole. For $d = 4$ and $d = 5$ the temperature continues to decrease, reaching zero at extremality; however, for $d \geq 6$ there is no extremal limit. Instead T reaches a minimum and then starts growing again, as expected for a black membrane. The minimum, where this behavior changes, can be determined exactly [7] as

$$\frac{a^2}{r_H^2} \Big|_{\text{crit}} = \frac{d-3}{d-5} \quad \text{or} \quad \frac{a^{d-3}}{\mu} \Big|_{\text{crit}} = \frac{d-3}{2(d-4)} \left(\frac{d-3}{d-5} \right)^{(d-5)/2}. \quad (5.49)$$

Following [30, 31] we can use this critical ratio (5.49) to define the boundary of the ultra-spinning regime. That is, ultra-spinning solutions are defined to be those for which the ratio a^{d-3}/μ exceeds the critical value given in (5.49). Explicitly evaluating (5.49) for the latter ratio, we find

$$\frac{a^{d-3}}{\mu} \Big|_{\text{crit}} = 1.30, 1.33, 1.34, 1.35 \quad \text{for } d = 6, 7, 8, 9, \text{ respectively}. \quad (5.50)$$

We note that these critical values are only weakly dependent on d . Further, these results would seem to indicate that the membrane-like behavior, and hence the instability, arises for relatively small values of the spin parameter a .

A further connection with black hole thermodynamics appears, because it is expected that the classical Gregory–Laflamme instabilities should correspond to the thermodynamic instabilities of the corresponding black branes [37, 38]. More precisely, it has been conjectured that the appearance of a negative “specific heat” for the black brane corresponds to the appearance of this classical instability. Applying this reasoning in the present context would suggest that the rotating black hole should become unstable at some point after $\partial^2 S / \partial J^2 > 0$ [28], i.e., after the point of inflection marked “x” in Fig. 5.3. Given the expression for the area (5.48),

⁷ This statement can be made mathematically precise in the limit $a \rightarrow \infty$ [7].

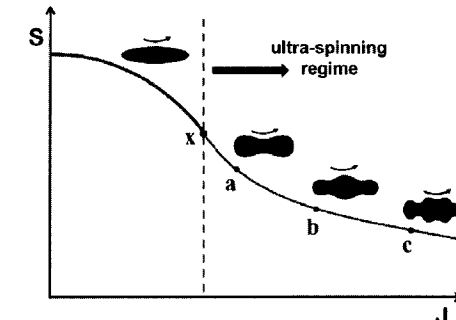


Figure 5.3 Phase diagram of entropy vs. angular momentum, at fixed mass, for MP black holes spinning in a single plane for $d \geq 6$. The point “x” indicates where $\partial^2 S / \partial J^2 = 0$. The subsequent points (a,b,c,...) correspond to the threshold of axisymmetric instabilities that introduce increasing numbers of ripples in the horizon. It is conjectured that a new class of black holes with rippled horizons branches from each of these points [28].

one finds that this point corresponds precisely to that identified above from the behavior of the temperature. That is, the critical point “x” where $\partial^2 S / \partial J^2 = 0$ is given precisely by (5.49).

While resolving these issues analytically remains intractable at present, there has been remarkable progress coming from numerical investigations in recent years [30, 31]. If one considers the instability just at threshold, i.e., precisely at the critical value of a , then the corresponding frequency is precisely zero and the unstable mode becomes a time-independent zero mode. In [30, 31], with a particular ansatz for such zero modes, the authors were able to locate numerically the corresponding critical values of a for singly spinning MP black holes (5.43) in $d = 6$ to 11. They found such a mode precisely where $\partial^2 S / \partial J^2 = 0$. However, the interpretation of this stationary mode is more subtle. Rather than corresponding to an instability, this perturbation simply corresponds to a shift in the solution space to a nearby MP black hole with a slightly larger spin. However, a small distance further into the ultra-spinning regime they also found a new zero mode, which “pinches” the horizon at the axis of rotation, as illustrated by point “a” in Fig. 5.3. It is believed that this zero mode does indeed correspond to the onset of a true instability for higher values of the angular momentum J . Further, this was only the first of a hierarchy of zero modes that introduce an increasing number of pinches or ripples in the event horizon along the θ direction. While these numerical searches identified only the stationary modes (by design), this provided strong evidence for the existence of a hierarchy of Gregory–Laflamme instabilities in the ultra-spinning regime.

These zero modes also provide evidence for a new class of stationary rotating black holes with spherical horizons but with a rippled profile in the polar angle θ .

The existence of these solutions was conjectured in [7, 28]. According to the phase diagram suggested in [28] there would be a new branch of solutions beginning at the point “a” and, as one moves along this branch, the pinch in the horizon at the axis of rotation would grow larger and larger. It is conjectured that this branch connects to yet another phase: the pinch produces a puncture in the horizon and the new phase would consist of spinning black rings, analogous to those discussed in Chapter 6 except that the horizon topology would be $S^1 \times S^{d-3}$. Similarly, it is conjectured that the branch starting from the point “b” would connect the spinning MP black holes to higher-dimensional versions of the “black Saturn” found in [39] for five dimensions. Hence the new spinning black holes with rippled spherical horizons appear to be only precursors to a rich fauna of new solutions with complex horizon topologies in higher dimensions.

Implicitly, in the above analysis we were considering only modes that respect all the rotational symmetries present in the original metric (5.43), i.e., $U(1) \times SO(d - 3)$. However, this restriction was only imposed to simplify the analysis. A priori, there is no reason why all the unstable modes should respect these symmetries. In fact recent numerical studies suggest that nonsymmetric modes play an important role in these instabilities. In [32, 33], full numerical simulations were carried out to describe the evolution of rapidly spinning MP black holes in higher dimensions – again with a single nonvanishing spin parameter, as in (5.43). In all the cases studied it was found that the solutions were unstable to nonaxisymmetric perturbations, with an initial profile proportional to $\sin 2\phi$. The critical value where this “bar-mode” instability set in was found to be

$$\left. \frac{a^{d-3}}{\mu} \right|_{\text{bar}} = 0.76, 0.41, 0.28, 0.27 \quad \text{for } d = 5, 6, 7, 8, \text{ respectively .} \quad (5.51)$$

We note that these values are considerably smaller than those in (5.50). Notably, these numerical simulations were able to find an instability of the $d = 5$ MP black hole, for which the previous discussion was unable to identify any instabilities. Further, following the nonlinear evolution of the unstable perturbation, the simulations [32, 33] found that the deformed black holes spontaneously emit gravitational waves, causing them to spin down and settle again to being a stable MP black hole, with spin parameter smaller than the critical value in (5.51). An open question is to determine when such “bar-mode” instabilities arise for MP black holes rotating in more than one plane. As an aside, let us note that in $d = 5$ with both spin parameters equal it was shown analytically that no instabilities appear [40].

In the preceding discussion we considered only MP black holes rotating in a single plane. However, this was only done to simplify the presentation and because this case was the focus of the numerical studies in [30–33]. As was discussed in section 5.2.3, ultra-spinning black hole solutions can also arise in which several

nonvanishing spin parameters grow large, as long as one (or two) of the spin parameters vanish in even (or odd) d . It is natural to expect that the ultra-spinning regime also extends to the regime where several a_i grow large while the remainder stay small. Guided by this intuition it is straightforward to extend the original discussion of the Gregory–Laflamme-like instabilities to the case where several spin parameters, say m , grow without bound while the remainder stay finite (or vanish) [7]. The limiting metric describes a (rotating) black $2m$ -brane, where the horizon topology is $\mathbb{R}^{2m} \times S^{d-2-2m}$. However, a Gregory–Laflamme-like instability is again expected to appear for these branes when the characteristic size in the planes with large spins is somewhat larger than the characteristic size in the transverse directions. In general, for many independent spins, the thermodynamic analysis mentioned above extends to determining if the Hessian $\partial^2 S / (\partial J_i \partial J_j)$ has negative eigenvalues [30, 31]. This expression provides a more refined definition of ultra-spinning black holes. In particular, following the discussion for a single nonvanishing J_i , we define the boundary of the ultra-spinning regime as the boundary at which this Hessian first acquires a zero eigenvalue.

Further insights into ultra-spinning instabilities have been found for one other example [29, 41, 42], namely, odd $d = 2n + 1$ with all n spin parameters equal. As noted in section 5.2.1, the rotational symmetry of these geometries is enhanced to $U(n)$, and it can be shown that the metric involves a fibration over the complex projective space CP^n [22]. Further, the metric perturbations of these spacetimes can be decomposed as harmonics on this space CP^n , and their analysis reduces to the study of an ordinary differential equation for the radial profile. Of course, in these metrics having all $a_i \neq 0$ there is an extremal limit and so it is not immediately obvious that one can reach an ultra-spinning regime or that any instabilities should appear. In fact, analysis of the above-mentioned Hessian reveals an ultra-spinning regime for any odd $d \geq 7$. Reference [29] explicitly identified unstable modes for $d = 9$, and supplementary work [41, 42] later found that unstable modes appeared very close to the extremal limit for $d = 7, 9, 11$, and 13. These results suggest that instabilities will arise in these cohomogeneity-1 black hole spacetimes for any odd $d \geq 7$. Recently these instabilities of cohomogeneity-1 black holes were connected to those of singly spinning black holes by the numerical work in [34]. The authors showed that the ultra-spinning instabilities in these two sectors are continuously connected by examining perturbations of MP black holes with all but one spin parameter equal. While their explicit calculations were made for $d = 7$, similar results are expected for higher odd d as well.

To close, we observe that the construction of the threshold zero modes for $d = 9$ suggests that there should be a new family of spinning black hole solutions characterized by 70 independent parameters [29]! Generically, these solutions would have only two Killing symmetries, i.e., time translations and one $U(1)$ rotation

symmetry. Hence, here again, the ultra-spinning instabilities open a window onto an exciting panorama of new black hole solutions in higher dimensions.

Acknowledgements

Research at Perimeter Institute is supported by the Government of Canada through Industry Canada and by the Province of Ontario through the Ministry of Research & Innovation. The author also acknowledges support from an NSERC Discovery grant and funding from the Canadian Institute for Advanced Research. I would also like to thank the Aspen Center for Physics for hospitality while preparing this paper and Roberto Emparan, Gary Horowitz, David Kubiznak, and Jorge Santos for their comments on this manuscript.

5.3 Appendix A: Mass and angular momentum

In this appendix we will consider the definitions of the mass and angular momentum of an isolated gravitating system in d dimensions. Our approach is simply to generalize the standard asymptotic analysis of four-dimensional solutions of Einstein's equations [43–45] to higher dimensions. In particular, the mass and angular momentum of any isolated gravitating system (e.g., a black hole) may be defined by comparison with a system that is both weakly gravitating and nonrelativistic. The result then provides a d -dimensional generalization of the ADM mass and angular momentum [43–45].

So, let us begin with the d -dimensional Einstein equations,

$$R_{\mu\nu} - \frac{1}{2}g_{\mu\nu}R = 8\pi G T_{\mu\nu}, \quad (5.52)$$

where we have included the stress-energy tensor for some matter fields, as it will be useful in the following discussion.⁸ We wish to consider solutions of these equations when the gravitating system is both weakly gravitating and nonrelativistic. First, for a weakly gravitating system the metric is everywhere only slightly perturbed from its flat-space form:

$$g_{\mu\nu} = \eta_{\mu\nu} + h_{\mu\nu}, \quad (5.53)$$

with $|h_{\mu\nu}| \ll 1$. Next, if the system is nonrelativistic, any time derivatives of fields will be much smaller than the corresponding spatial derivatives. Of course, this also implies that components of the stress energy tensor may be ordered as follows:

$$|T_{00}| \gg |T_{0i}| \gg |T_{ij}|. \quad (5.54)$$

⁸ In the following, the Greek indices μ, ν run over all the values $0, 1, \dots, d - 1$, while the Latin indices i, j run only over the spatial values $1, 2, \dots, d - 1$.

These inequalities indicate that the dominant source of the gravitational field is the energy density, while the momentum density provides the next most important source.

The solutions are most conveniently examined in the harmonic gauge

$$\partial_\mu \left(h^{\mu\nu} - \frac{1}{2}\eta^{\mu\nu}h^\alpha{}_\alpha \right) = 0. \quad (5.55)$$

With this choice, to leading order the Einstein equations (5.52) can be written as

$$\begin{aligned} \nabla^2 h_{\mu\nu} &= -16\pi G \left(T_{\mu\nu} - \frac{1}{d-2}\eta_{\mu\nu}T^\alpha{}_\alpha \right) \\ &= -16\pi G \tilde{T}_{\mu\nu}, \end{aligned} \quad (5.56)$$

where ∇^2 is the ordinary Laplacian in flat d -dimensional space, i.e., we have dropped the time derivatives of the metric perturbation. Note that $T^\alpha{}_\alpha \approx -T_{00}$ for nonrelativistic sources. Equation (5.56) is now readily solved by

$$h_{\mu\nu}(x^i) = \frac{16\pi G}{(N-2)\Omega_{d-2}} \int \frac{\tilde{T}_{\mu\nu}(y^i)}{|\vec{x} - \vec{y}|^{d-3}} d^{d-1}y, \quad (5.57)$$

where the integral extends only over the $d - 1$ spatial directions. Recall that Ω_{d-2} denotes the area of a unit $(d-2)$ -sphere, which was given in (5.3). Now evaluating (5.57) in the asymptotic region far from any sources, we have $r = |\vec{x}| \gg |\vec{y}|$, and so we may expand the result as

$$h_{\mu\nu}(x^i) = \frac{16\pi G}{(d-3)\Omega_{d-2}} \frac{1}{r^{d-3}} \int \tilde{T}_{\mu\nu} d^{d-1}y + \frac{16\pi G}{\Omega_{d-2}} \frac{x^k}{r^{d-1}} \int y^k \tilde{T}_{\mu\nu} d^{d-1}y + \dots \quad (5.58)$$

To simplify our results we will consider the system in its rest frame, and this implies that

$$\int T_{0i} d^{d-1}x = 0. \quad (5.59)$$

We choose the origin to sit at the center of mass, so that

$$\int x^k T_{00} d^{d-1}x = 0. \quad (5.60)$$

Now the total mass and angular momentum are defined as

$$M = \int T_{00} d^{d-1}x, \quad (5.61)$$

$$J^{\mu\nu} = \int (x^\mu T^{\nu 0} - x^\nu T^{\mu 0}) d^{d-1}x. \quad (5.62)$$

One further simplification comes from the conservation of stress-energy, which reduces to $\partial_k T^{k\mu} = 0$ in the case of interest and from which we can infer that

$$\int x^\ell T^{k\mu} d^{d-1}x = - \int x^k T^{\ell\mu} d^{d-1}x . \quad (5.63)$$

This result, along with (5.59) and (5.60), allows us to simplify the angular momentum to

$$\begin{aligned} J^{0k} &= 0 , \\ J^{kl} &= 2 \int x^k T^{\ell 0} d^{d-1}x . \end{aligned} \quad (5.64)$$

Applying these results to the expansion in (5.58) we find that, to leading order far from the system,

$$\begin{aligned} h_{00} &\approx \frac{16\pi G}{(d-2)\Omega_{d-2}} \frac{M}{r^{d-3}} , \\ h_{ij} &\approx \frac{16\pi G}{(d-2)(d-3)\Omega_{d-2}} \frac{M}{r^{d-3}} \delta_{ij} , \\ h_{0i} &\approx -\frac{8\pi G}{\Omega_{d-2}} \frac{x^k}{r^{d-1}} J^{ki} . \end{aligned} \quad (5.65)$$

While these results were derived for a system that is both weakly gravitating and nonrelativistic, the asymptotic behavior of the metric will be the same for any isolated gravitating system. In particular, then, we have used these expressions to identify the mass and angular momentum of the black hole solutions discussed in the main text.

5.4 Appendix B: A case study of $d = 5$

For $d = 5$ dimensions, we can write the metric (5.11) as

$$\begin{aligned} ds^2 &= -dt^2 + \frac{\mu}{\Sigma} (dt + a \sin^2 \theta d\phi_1 + b \cos^2 \theta d\phi_2)^2 + \frac{r^2 \Sigma}{\Pi - \mu r^2} dr^2 \\ &\quad + \Sigma d\theta^2 + (r^2 + a^2) \sin^2 \theta d\phi_1^2 + (r^2 + b^2) \cos^2 \theta d\phi_2^2 , \end{aligned} \quad (5.66)$$

where

$$\Sigma = r^2 + a^2 \cos^2 \theta + b^2 \sin^2 \theta , \quad (5.67)$$

$$\Pi = (r^2 + a^2)(r^2 + b^2) . \quad (5.68)$$

Comparing our notation here with that in the main text, we have $a_1 = a$, $a_2 = b$, $\mu_1 = \sin \theta$, and $\mu_2 = \cos \theta$.

Singularities Now, with some computer assistance one can easily calculate the Kretschmann invariant

$$R_{\mu\nu\rho\sigma} R^{\mu\nu\rho\sigma} = \frac{24\mu^2}{\Sigma^6} (4r^2 - 3\Sigma)(4r^2 - \Sigma) . \quad (5.69)$$

At $r = 0$, this expression yields

$$R_{\mu\nu\rho\sigma} R^{\mu\nu\rho\sigma} \Big|_{r=0} = \frac{72\mu^2}{(a^2 \cos^2 \theta + b^2 \sin^2 \theta)^4} . \quad (5.70)$$

Hence, if $b = 0$ above then we see that there is a divergence as $\theta \rightarrow \pi/2$, as described in case (b) in section 5.2.2. Further, with $b = 0$, if we examine the (r, ϕ_2) part of the metric near $r = 0$ but away from $\theta = \pi/2$, we find

$$ds^2 \simeq \frac{\cos^2 \theta}{1 - \mu/a^2} \left[dr^2 + \left(1 - \frac{\mu}{a^2}\right) r^2 d\phi_2^2 \right] + \dots . \quad (5.71)$$

Thus we see that there is an angular deficit $\Delta\phi_2 = 2\pi\mu/a^2$ on this axis.

If both a and b are nonvanishing, however, the curvature invariant in (5.70) remains finite. In this case, we introduce the radial coordinate $\rho = r^2$ and, assuming that $0 < a^2 \leq b^2$, we find

$$R_{\mu\nu\rho\sigma} R^{\mu\nu\rho\sigma} \Big|_{\rho=-a^2} = \frac{24\mu^2 [4a^2 + 3(b^2 - a^2) \sin^2 \theta] [4a^2 + (b^2 - a^2) \sin^2 \theta]}{(b^2 - a^2)^6 \sin^{12} \theta} . \quad (5.72)$$

In accordance with the discussion of case (c) in section 5.2.2, the surface $\rho = -a^2$ is entirely singular if $b^2 = a^2$. However, if $b^2 \neq a^2$ then the singularity in (5.72) appears only at $\theta = 0$. Thus in this case we can extend the geometry into the region $-b^2 \leq \rho \leq -a^2$, but one finds that for any value of ρ in this domain there are singularities at

$$\sin^2 \theta = \frac{|\rho| - a^2}{b^2 - a^2} , \quad (5.73)$$

where $\Sigma = 0$.

Horizons With $d = 5$, (5.22) for the horizon becomes a quadratic equation in r^2 and the roots are given by the relatively simple expressions

$$\begin{aligned} 2r_H^2 &= \mu - a^2 - b^2 + \sqrt{(\mu - a^2 - b^2)^2 - 4a^2b^2}, \\ 2r_C^2 &= \mu - a^2 - b^2 - \sqrt{(\mu - a^2 - b^2)^2 - 4a^2b^2}. \end{aligned} \quad (5.74)$$

Therefore the existence of a horizon requires that

$$\begin{aligned} \mu &\geq a^2 + b^2 + 2|ab|, \\ M^3 &\geq \frac{27\pi}{32G}(J_1^2 + J_2^2 + 2|J_1J_2|). \end{aligned} \quad (5.75)$$

Here, the definitions of the mass and angular momentum given in (5.15) have been inserted to yield the second equation, and we have set $J_1 \equiv J^{y_1x_1}$ and $J_2 \equiv J^{y_2x_2}$. Hence there are no ultra-spinning black holes in $d = 5$. Rather, if the angular momentum exceeds the above condition (5.75), the solution contains a naked “ring” singularity without any event horizon.

Ergosurfaces The equation for the ergosurface reduces to $\Sigma - \mu = 0$, or

$$r_E^2(\theta) = \mu - a^2 \cos^2 \theta - b^2 \sin^2 \theta. \quad (5.76)$$

When both a and b are nonvanishing, it is not hard to show that $r_E^2 > r_H^2$, i.e., the ergosurface nowhere touches the horizon.

Cohomogeneity-1 It is also interesting to observe the simplifications that arise when $b = a$. First note that, in this case, we have

$$\Sigma = r^2 + a^2 \quad \text{and} \quad \Pi = (r^2 + a^2)^2. \quad (5.77)$$

Next, we see that the angular components in the second line of (5.66) now combine to give $(r^2 + a^2)d\Omega_3^2$, i.e., the round metric on a three-sphere. Hence this portion of the metric is symmetric under $SO(4) \simeq SU(2) \times SU(2)$. This symmetry does not survive for the full metric, however, because there are other angular contributions in the first line of (5.66). These terms can be written in terms of the potential

$$A = i(\bar{z}_1 dz_1 + \bar{z}_2 dz_2) = \sin^2 \theta d\phi_1 + \cos^2 \theta d\phi_2, \quad (5.78)$$

where $z_1 = \sin \theta e^{i\phi_1}$ and $z_2 = \cos \theta e^{i\phi_2}$. Expressing A in these complex coordinates makes it clear that the surviving symmetry is $U(1) \times SU(2) = U(2)$, as discussed in section 5.2.1. The metric (5.66) with $b = a$ is said to be of cohomogeneity 1 because, after imposing this $U(2)$ symmetry, the metric components are entirely functions of the single (radial) coordinate r .

This enhanced symmetry also leads to a simplicity in other aspects of the geometry. For example, the Kretschmann invariant (5.69) is now a function only of r ,

$$R_{\mu\nu\rho\sigma} R^{\mu\nu\rho\sigma} = \frac{24\mu^2}{(r^2 + a^2)^6} (r^2 - 3a^2)(3r^2 - a^2) \underset{r \rightarrow 0}{\underset{\sim}{\rightarrow}} \frac{72\mu^2}{a^8}. \quad (5.79)$$

Hence the singularity at $\rho = -a^2$ in (5.72) simplifies to

$$R_{\mu\nu\rho\sigma} R^{\mu\nu\rho\sigma} \Big|_{\rho=-a^2+\varepsilon^2} = \frac{384\mu^2 a^2}{\varepsilon^{12}}, \quad (5.80)$$

where we are assuming that $\varepsilon \ll a$. We note also that for these black holes the location of the ergosurface (5.76) reduces to $r_E^2 = \mu - a^2$ and so the latter is now also independent of θ . Given this simple result, it is a straightforward exercise to write

$$r_E^2 - r_H^2 = \frac{\mu}{2} \left(1 - \sqrt{1 - \frac{4a^2}{\mu}} \right) > 0, \quad (5.81)$$

confirming that the ergosurface does not touch the horizon at any point in these cohomogeneity-1 black hole spacetimes.

References

- [1] R. C. Myers and M. J. Perry, Black holes in higher dimensional space-times, *Ann. Phys.* **172** (1986), 304.
- [2] W. Chen, H. Lu, and C. N. Pope, General Kerr–NUT–AdS metrics in all dimensions, *Class. Quant. Grav.* **23** (2006), 5323 [arXiv:hep-th/0604125].
- [3] F. R. Tangherlini, Schwarzschild field in n dimensions and the dimensionality of space problem, *Nuovo Cim.* **77** (1963), 636.
- [4] S. Hwang, A rigidity theorem for Ricci flat metrics, *Geometriae Dedicata* **71** (1998), 5.
- [5] G. W. Gibbons, D. Ida, and T. Shiromizu, Uniqueness and nonuniqueness of static vacuum black holes in higher dimensions, *Prog. Theor. Phys. Suppl.* **148** (2003), 284 [arXiv:gr-qc/0203004].
- [6] R. C. Myers, Higher dimensional black holes in compactified space-times, *Phys. Rev. D* **35** (1987), 455.
- [7] R. Emparan and R. C. Myers, Instability of ultra-spinning black holes, *JHEP* **0309** (2003), 025 [arXiv:hep-th/0308056].
- [8] J. M. Bardeen and G. T. Horowitz, The extreme Kerr throat geometry: a vacuum analog of $AdS_2 \times S^2$, *Phys. Rev. D* **60** (1999), 104030 [arXiv:hep-th/9905099].
- [9] H. K. Kunduri, J. Lucietti, and H. S. Reall, Near-horizon symmetries of extremal black holes, *Class. Quant. Grav.* **24** (2007), 4169 [arXiv:0705.4214 [hep-th]].
- [10] P. Figueras, H. K. Kunduri, J. Lucietti, and M. Rangamani, Extremal vacuum black holes in higher dimensions, *Phys. Rev. D* **78** (2008), 044042 [arXiv:0803.2998 [hep-th]].

- [11] R. P. Kerr, Gravitational field of a spinning mass as an example of algebraically special metrics, *Phys. Rev. Lett.* **11** (1963), 237.
- [12] M. Walker and R. Penrose, *Commun. Math. Phys.* **18** (1970), 265.
- [13] R. Penrose, Naked singularities, *Ann. N. Y. Acad. Sci.* **224** (1973), 125.
- [14] R. Floyd, The dynamics of Kerr fields, Ph.D. thesis, London University (1973).
- [15] V. P. Frolov and D. Kubiznak, Hidden symmetries of higher dimensional rotating black holes, *Phys. Rev. Lett.* **98** (2007), 011101 [arXiv:gr-qc/0605058].
- [16] D. N. Page, D. Kubiznak, M. Vasudevan, and P. Krtous, Complete integrability of geodesic motion in general Kerr–NUT–AdS spacetimes, *Phys. Rev. Lett.* **98** (2007), 061102 [arXiv:hep-th/0611083].
- [17] P. Krtous, D. Kubiznak, D. N. Page, and V. P. Frolov, Killing–Yano tensors, rank-2 Killing tensors, and conserved quantities in higher dimensions, *JHEP* **0702** (2007), 004 [arXiv:hep-th/0612029].
- [18] A. Sergeyev and P. Krtous, Complete set of commuting symmetry operators for Klein–Gordon equation in generalized higher-dimensional Kerr–NUT–(A)dS spacetimes, *Phys. Rev. D* **77** (2008), 044033 [arXiv:0711.4623 [hep-th]].
- [19] V. P. Frolov, P. Krtous, and D. Kubiznak, Separability of Hamilton–Jacobi and Klein–Gordon equations in general Kerr–NUT–AdS spacetimes, *JHEP* **0702** (2007), 005 [arXiv:hep-th/0611245].
- [20] T. Oota and Y. Yasui, Separability of Dirac equation in higher dimensional Kerr–NUT–de Sitter spacetime, *Phys. Lett.* **B659** (2008), 688 [arXiv:0711.0078 [hep-th]].
- [21] M. Cariglia, P. Krtous, and D. Kubiznak, Dirac equation in Kerr–NUT–(A)dS spacetimes: intrinsic characterization of separability in all dimensions, arXiv:1104.4123 [hep-th].
- [22] H. K. Kunduri, J. Lucietti, and H. S. Reall, Gravitational perturbations of higher dimensional rotating black holes: tensor perturbations, *Phys. Rev. D* **74** (2006), 084021 [arXiv:hep-th/0606076].
- [23] R. M. Wald, Black hole entropy is the Noether charge, *Phys. Rev. D* **48** (1993), 3427 [arXiv:gr-qc/9307038].
- [24] V. Iyer and R. M. Wald, Some properties of Noether charge and a proposal for dynamical black hole entropy, *Phys. Rev. D* **50** (1994), 846 [arXiv:gr-qc/9403028].
- [25] T. Jacobson, G. Kang, and R. C. Myers, On black hole entropy, *Phys. Rev. D* **49** (1994), 6587 [arXiv:gr-qc/9312023].
- [26] L. Smarr, Mass formula for Kerr black holes, *Phys. Rev. Lett.* **30** (1973), 71.
- [27] S. W. Hawking and G. F. R. Ellis, *The Large Scale Structure of Space–Time*, Cambridge University Press (1973).
- [28] R. Emparan, T. Harmark, V. Niarchos, N. A. Obers, and M. J. Rodriguez, The phase structure of higher-dimensional black rings and black holes, *JHEP* **0710** (2007), 110 [arXiv:0708.2181 [hep-th]].
- [29] O. J. C. Dias, P. Figueras, R. Monteiro, H. S. Reall, and J. E. Santos, An instability of higher-dimensional rotating black holes, *JHEP* **1005** (2010), 076 [arXiv:1001.4527 [hep-th]].
- [30] O. J. C. Dias, P. Figueras, R. Monteiro, J. E. Santos, and R. Emparan, Instability and new phases of higher-dimensional rotating black holes, *Phys. Rev. D* **80** (2009), 111701 [arXiv:0907.2248 [hep-th]].
- [31] O. J. C. Dias, P. Figueras, R. Monteiro, and J. E. Santos, Ultraspinning instability of rotating black holes, *Phys. Rev. D* **82** (2010), 104025 [arXiv:1006.1904 [hep-th]].
- [32] M. Shibata and H. Yoshino, Bar-mode instability of rapidly spinning black hole in higher dimensions: numerical simulation in general relativity, *Phys. Rev. D* **81** (2010), 104035 [arXiv:1004.4970 [gr-qc]].

- [33] M. Shibata and H. Yoshino, Nonaxisymmetric instability of rapidly rotating black hole in five dimensions, *Phys. Rev. D* **81** (2010), 021501 [arXiv:0912.3606 [gr-qc]].
- [34] O. J. C. Dias, R. Monteiro, and J. E. Santos, Ultraspinning instability: the missing link, *JHEP* **1108** (2011), 139 [arXiv:1106.4554 [hep-th]].
- [35] R. Gregory and R. Laflamme, Black strings and p-branes are unstable, *Phys. Rev. Lett.* **70** (1993), 2837 [arXiv:hep-th/9301052].
- [36] R. Gregory and R. Laflamme, The instability of charged black strings and p-branes, *Nucl. Phys.* **B428** (1994), 399 [arXiv:hep-th/9404071].
- [37] S. S. Gubser and I. Mitra, Instability of charged black holes in anti-de Sitter space, arXiv:hep-th/0009126.
- [38] H. S. Reall, Classical and thermodynamic stability of black branes, *Phys. Rev. D* **64** (2001), 044005 [arXiv:hep-th/0104071].
- [39] H. Elvang and P. Figueras, Black Saturn, *JHEP* **0705** (2007), 050 [arXiv:hep-th/0701035].
- [40] K. Murata and J. Soda, Stability of five-dimensional Myers–Perry black holes with equal angular momenta, *Prog. Theor. Phys.* **120** (2008), 561 [arXiv:0803.1321 [hep-th]].
- [41] J. E. Santos, unpublished.
- [42] M. Durkee and H. S. Reall, Perturbations of near-horizon geometries and instabilities of Myers–Perry black holes, *Phys. Rev. D* **83** (2011), 104044 [arXiv:1012.4805 [hep-th]].
- [43] R. Arnowitt, S. Deser, and C. Misner, Canonical variables for general relativity, *Phys. Rev.* **117** (1960), 1595.
- [44] R. Arnowitt, S. Deser, and C. Misner, Energy and the criteria for radiation in general relativity, *Phys. Rev.* **118** (1960), 1100.
- [45] R. Arnowitt, S. Deser, and C. Misner, Coordinate invariance and energy expressions in general relativity, *Phys. Rev.* **122** (1961), 997.

6

Black rings

ROBERTO EMPARAN AND HARVEY S. REALL

6.1 Introduction

A black ring is a D -dimensional black hole with horizon topology $S^1 \times S^{D-3}$. There is a simple heuristic way of understanding why such solutions might exist. Consider a black string, the product of the $(D-1)$ -dimensional Schwarzschild solution with a flat direction, with horizon topology $\mathbb{R} \times S^{D-3}$. Imagine bending the string into a loop, so the topology is now $S^1 \times S^{D-3}$. This loop would tend to contract owing to its tension and gravitational self-attraction. However, if the loop rotates then it might be possible to balance these forces with centrifugal repulsion. That this is indeed possible is proved by the existence of an explicit black ring solution of the five-dimensional vacuum Einstein equation [1, 2]. The existence of analogous solutions for $D > 5$ dimensions (or when a cosmological constant is included) is strongly suggested by the perturbative methods reviewed in Chapter 8.

The discovery of black rings revealed that higher-dimensional black holes can exhibit properties very different from those of four-dimensional holes. First, higher-dimensional black holes need not be topologically spherical. Second, higher-dimensional black holes are not uniquely parameterized by mass and angular momenta: there exist distinct black ring solutions with the same mass and angular momenta. Furthermore, there exist black ring and Myers–Perry solutions [3] with the same mass and angular momenta. Thus the topology and uniqueness theorems that underpin our understanding of four-dimensional black holes do not extend to higher dimensions in an obvious way.

The existence of black rings leads to further surprises. Imagine placing a topologically spherical black hole at the centre of a black ring. The gravitational attraction of the former will tend to contract the ring but this might be counteracted by

an increase in the ring’s angular momentum. This suggests the existence of stationary solutions describing a “superposition” of a black ring and a Myers–Perry black hole. Such a “black Saturn” solution has been found [4], demonstrating the existence of stationary multi-black-hole solutions of the five-dimensional vacuum Einstein equation. It is believed that such solutions do not exist in four dimensions.

In this chapter we will introduce explicit black ring solutions and describe their basic properties. We will consider only five-dimensional vacuum gravity. In more complicated theories there exist explicit solutions describing black rings with charges and/or dipoles. These are of considerable interest but we will not discuss them here. We refer the reader to our earlier review articles [5, 6] for more details.

This chapter is organized as follows. In section 6.2 we will motivate and interpret the coordinates used to describe black rings by constructing analogous coordinates for flat spacetime. Section 6.3 presents a black ring solution with a single nonvanishing angular momentum [1]. In section 6.4 we describe a more general solution, in which both angular momenta are nonzero [2]. In section 6.5 we discuss black Saturn and other solutions with disconnected horizons. Finally, section 6.6 reviews what is known about the stability of black rings.

6.2 Ring coordinates

As is often the case in general relativity, the description of black ring solutions is greatly facilitated when one works in adapted coordinates. A general way of finding them is to foliate flat space in terms of the equipotential surfaces of the field created by a source resembling the black hole that one is seeking. For black rings it turns out to be convenient to work with the equipotential surfaces of a 2-form potential $B_{\mu\nu}$. Thus we regard the ring as a circular string that acts as an electric source of the 3-form field strength $H = dB$, which satisfies the field equation

$$\partial_\mu(\sqrt{-g}H^{\mu\nu\rho}) = 0 \quad (6.1)$$

outside the ring source.

Let us write four-dimensional flat space by choosing polar coordinates in two orthogonal planes, (r_1, ϕ) and (r_2, ψ) :

$$d\mathbf{x}_4^2 = dr_1^2 + r_1^2 d\phi^2 + dr_2^2 + r_2^2 d\psi^2. \quad (6.2)$$

It is easy to construct the solution of (6.1) for a circular electric source at $r_1 = 0$, $r_2 = R$ and $0 \leq \psi < 2\pi$, using methods familiar in classical electrodynamics,

as

$$\begin{aligned} B_{t\psi} &= \frac{R}{2\pi} \int_0^{2\pi} d\psi \frac{r_2 \cos \psi}{r_1^2 + r_2^2 + R^2 - 2Rr_2 \cos \psi} \\ &= -\frac{1}{2} \left(1 - \frac{R^2 + r_1^2 + r_2^2}{\Sigma} \right), \end{aligned} \quad (6.3)$$

where

$$\Sigma = \sqrt{(r_1^2 + r_2^2 + R^2)^2 - 4R^2 r_2^2}. \quad (6.4)$$

We can just as easily find the electric–magnetic (Hodge) dual of this field. In five spacetime dimensions, $*H = F = dA$ where A is a 1-form potential, so the dual of an electric string is a magnetic monopole – in this case a circular distribution of monopoles. Surfaces of constant A_ϕ will be orthogonal to surfaces of constant $B_{t\psi}$. For the dual of the field (6.3) one finds

$$A_\phi = -\frac{1}{2} \left(1 + \frac{R^2 - r_1^2 - r_2^2}{\Sigma} \right). \quad (6.5)$$

Now define coordinates y and x that correspond to constant values of $B_{t\psi}$ and A_ϕ , respectively. A convenient choice is

$$y = -\frac{R^2 + r_1^2 + r_2^2}{\Sigma}, \quad x = \frac{R^2 - r_1^2 - r_2^2}{\Sigma}, \quad (6.6)$$

with inverse

$$r_1 = R \frac{\sqrt{1-x^2}}{x-y}, \quad r_2 = R \frac{\sqrt{y^2-1}}{x-y}. \quad (6.7)$$

The coordinate ranges are

$$-\infty \leq y \leq -1, \quad -1 \leq x \leq 1, \quad (6.8)$$

with $y = -\infty$ corresponding to the location of the ring source and asymptotic infinity recovered as $x \rightarrow y \rightarrow -1$. The axis of rotation around the ψ direction, $r_2 = 0$ (actually not a line but a plane), is at $y = -1$ and the axis of rotation around ϕ , $r_1 = 0$, is divided into two pieces: $x = 1$ is the disk $r_2 \leq R$ and $x = -1$ is its complement outside the ring, $r_2 \geq R$. In these coordinates the flat metric (6.2) becomes

$$d\mathbf{x}_4^2 = \frac{R^2}{(x-y)^2} \left((y^2-1)d\psi^2 + \frac{dy^2}{y^2-1} + \frac{dx^2}{1-x^2} + (1-x^2)d\phi^2 \right). \quad (6.9)$$

This is depicted in Fig. 6.1, where we present a section at constant ψ and ϕ . This quadrant is the quotient space $\mathbb{R}^4/(U(1)_\psi \times U(1)_\phi)$.

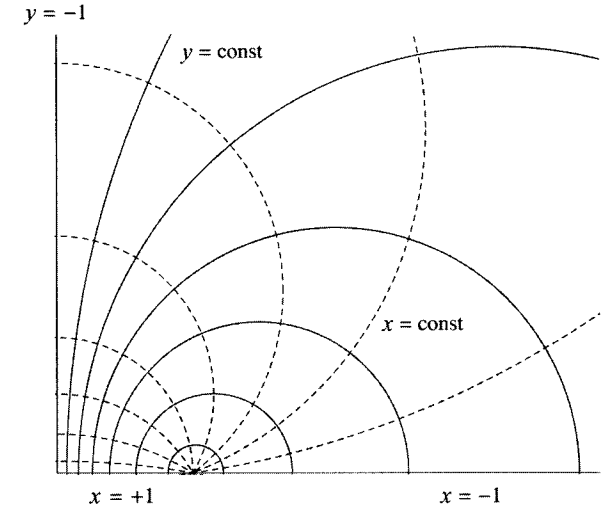


Figure 6.1 The “ring” coordinates (x, y) for flat four-dimensional space, on a section at constant ϕ and ψ . The angles ψ and ϕ rotate around the vertical and horizontal axes, respectively. The broken lines correspond to constant $x \in [-1, 1]$ and the solid lines to constant $y \in (-\infty, -1]$. In \mathbb{R}^4 the latter are surfaces with topology $S^1 \times S^2$, which for $y = -\infty$ collapse to a circle of radius R that divides the horizontal axis (a plane) into a disk at $x = +1$ and its complement at $x = -1$.

We can rewrite this same foliation of space in a manner that is particularly appropriate in the region near the ring. Define coordinates r and θ as

$$r = -\frac{R}{y}, \quad \cos \theta = x, \quad (6.10)$$

with

$$0 \leq r \leq R, \quad 0 \leq \theta \leq \pi. \quad (6.11)$$

The flat metric (6.9) becomes

$$d\mathbf{x}_4^2 = \left(1 + \frac{r \cos \theta}{R} \right)^{-2} \left[\left(1 - \frac{r^2}{R^2} \right) R^2 d\psi^2 + \left(1 - \frac{r^2}{R^2} \right)^{-1} dr^2 + r^2 (d\theta^2 + \sin^2 \theta d\phi^2) \right]. \quad (6.12)$$

The apparent singularity at $r = R$ corresponds to the ψ -axis of rotation.

It is now manifest that the surfaces at constant r , i.e., constant y , have a ring-like topology $S^2 \times S^1$, where the S^2 is parameterized by (θ, ϕ) and the S^1 by ψ . The black rings have their horizons and ergosurfaces at constant values of y , or r , so they will have topology $S^2 \times S^1$.

The coordinates r and θ are natural in the region of small r , where they recover their conventional interpretation as the radius and polar angle on spheres at constant r . However, they look bizarre at larger distances. In particular, asymptotic infinity corresponds to $r \cos \theta = -R$. The coordinates (x, y) are physically opaque, but they preserve a symmetry under the exchange $x \leftrightarrow y$ that is otherwise obscured and allow for more compact expressions.

Incidentally, $\Sigma^{-1} = (x - y)/(2R^2)$ solves the Laplace equation for a ring sourcing a scalar field: $\nabla^2 \Sigma^{-1} = 0$. Thus surfaces of constant scalar potential do not correspond to constant x or y and turn out to be less convenient for the construction of adapted coordinates.

6.3 Singly spinning black ring solution

6.3.1 Spacetime geometry

The metric for the black ring geometry preserves most of the basic structure of (6.9), but now it contains additional functions that encode the nonzero curvature produced by the black ring. In (x, y) coordinates these functions admit a particularly simple form, as they can be obtained by adding linear functions of x and y . The metric of a “singly spinning” black ring, with one nonvanishing angular momentum, is [1]

$$ds^2 = -\frac{F(y)}{F(x)} \left(dt - CR \frac{1+y}{F(y)} d\psi \right)^2 + \frac{R^2}{(x-y)^2} F(x) \left(-\frac{G(y)}{F(y)} d\psi^2 - \frac{dy^2}{G(y)} + \frac{dx^2}{G(x)} + \frac{G(x)}{F(x)} d\phi^2 \right), \quad (6.13)$$

where

$$F(\xi) = 1 + \lambda\xi, \quad G(\xi) = (1 - \xi^2)(1 + \nu\xi) \quad (6.14)$$

and

$$C = \sqrt{\lambda(\lambda - \nu)} \frac{1 + \lambda}{1 - \lambda}. \quad (6.15)$$

The dimensionless parameters λ and ν must lie in the range

$$0 < \nu \leq \lambda < 1. \quad (6.16)$$

When both λ and ν vanish we recover flat spacetime in the form (6.9). The scale for the solution is set by R , and λ and ν are parameters that characterize the shape and rotation velocity of the ring as we shall clarify presently.

Some intuition about the solution is obtained by recalling that the existence of black rings is motivated by regarding them as circular black strings. Then we should

expect to recover a black string in a limit in which the ring radius becomes infinite. To this effect, consider the (r, θ) coordinates introduced in (6.10), and redefine the parameters (ν, λ) in terms of (r_0, σ) , as follows:

$$\nu = \frac{r_0}{R}, \quad \lambda = \frac{r_0 \cosh^2 \sigma}{R}, \quad (6.17)$$

and $\psi = z/R$. Then take the limit $R \rightarrow \infty$ while keeping r_0 and σ and the coordinates r, θ and z finite. The solution for the metric becomes

$$ds^2 = -\hat{f} \left(dt + \frac{r_0}{r\hat{f}} \sinh \sigma \cosh \sigma dz \right)^2 + \frac{f}{\hat{f}} dz^2 + \frac{dr^2}{f} + r^2(d\theta^2 + \sin^2 \theta d\phi^2), \quad (6.18)$$

where

$$f = 1 - \frac{r_0}{r}, \quad \hat{f} = 1 - \frac{r_0 \cosh^2 \sigma}{r}. \quad (6.19)$$

This is the metric for a boosted black string, extended along the direction z , with boost parameter σ . The horizon is at $r = r_0$.

This limit gives an approximate interpretation to λ and ν . According to (6.17) the parameter ν measures the ratio of the radius of the S^2 at the horizon r_0 and the radius of the ring R . Therefore smaller values of ν correspond to thinner rings. Also, λ/ν is a measure of the speed of rotation of the ring. More precisely, $\sqrt{1 - \nu/\lambda}$ can be approximately identified with the local boost velocity $v = \tanh \sigma$.

We now turn to a general analysis of the metric. The coordinates x and y vary within the same ranges as in (6.8) and are interpreted in essentially the same manner as we saw in the previous section. An important difference, though, is that for general values of the parameters in (6.16) the orbits of $\partial/\partial\psi$ and $\partial/\partial\phi$ do not close off smoothly at their respective axes but in general have conical singularities there. To avoid such singularities at $x = -1$ and $y = -1$ the angular variables must be identified, with periodicity

$$\Delta\psi = \Delta\phi = 4\pi \frac{\sqrt{F(-1)}}{|G'(-1)|} = 2\pi \frac{\sqrt{1 - \lambda}}{1 - \nu}. \quad (6.20)$$

To avoid also a conical singularity at $x = +1$ we must have

$$\Delta\phi = 2\pi \frac{\sqrt{1 + \lambda}}{1 + \nu}. \quad (6.21)$$

This is compatible with (6.20) only if we take the two parameters λ, v to satisfy

$$\lambda = \frac{2v}{1+v^2}. \quad (6.22)$$

Fixing λ to this value leaves only two independent parameters in the solution, R and v . This is as expected on physical grounds: given, say, the mass and the radius of the ring, the angular momentum must be tuned so that the centrifugal force balances the tension and self-attraction of the ring, leaving only two free parameters. Demanding the absence of conical singularities, as in (6.22), actually corresponds to the condition that the system is balanced, without any external forces.

In terms of the boost parameter σ introduced in (6.17), in the limit of thin rings the equilibrium value from (6.22) becomes

$$|\sinh \sigma| \rightarrow 1 \quad (6.23)$$

or, equivalently, the velocity $|v| \rightarrow 1/\sqrt{2}$. This is the limiting velocity for keeping in mechanical equilibrium a circular black string of very large radius R . This value for the boost is rederived in the context of the blackfold approach in Chapter 8.

With the choices (6.20) and (6.22) for the parameters the solution becomes asymptotically flat as $x \rightarrow y \rightarrow -1$. Since the geometry is distorted by the presence of curvature, in order to go to manifestly asymptotically flat coordinates we have to modify (6.7) slightly. For x and y close to -1 , we set

$$\begin{aligned} \tilde{r}_1 &= \tilde{R} \frac{\sqrt{2(1+x)}}{x-y}, & \tilde{r}_2 &= \tilde{R} \frac{\sqrt{-2(1+y)}}{x-y}, \\ \tilde{R}^2 &= R^2 \frac{1-\lambda}{1-v}, & (\tilde{\psi}, \tilde{\phi}) &= \frac{2\pi}{\Delta\psi}(\psi, \phi). \end{aligned} \quad (6.24)$$

Then (6.13) asymptotes to the flat-space metric (6.2), now with “tilded” coordinates $\tilde{r}_{1,2}$ and $\tilde{\psi}, \tilde{\phi}$ with canonical periodicity 2π .

Note that $F(y)$ vanishes at $y = -1/\lambda$; nevertheless, it is easy to check that the metric and its inverse are smooth there. This locus corresponds to a timelike surface in spacetime at which $\partial/\partial t$ changes from being timelike to being spacelike, i.e., it is an *ergosurface*. A spatial cross section of this surface has topology $S^1 \times S^2$.

At $y = -1/v$ the metric becomes singular, but we can show that this is only a coordinate singularity by the transformation $(t, \psi) \rightarrow (v, \psi')$ defined by

$$dt = dv - CR \frac{1+y}{G(y)\sqrt{-F(y)}} dy, \quad d\psi = d\psi' + \frac{\sqrt{-F(y)}}{G(y)} dy. \quad (6.25)$$

In these coordinates the metric is

$$\begin{aligned} ds^2 &= -\frac{F(y)}{F(x)} \left(dv - CR \frac{1+y}{F(y)} d\psi' \right)^2 \\ &\quad + \frac{R^2}{(x-y)^2} F(x) \left(-\frac{G(y)}{F(y)} d\psi'^2 + \frac{2d\psi' dy}{\sqrt{-F(y)}} + \frac{dx^2}{G(x)} + \frac{G(x)}{F(x)} d\phi^2 \right), \end{aligned} \quad (6.26)$$

which is manifestly regular at $y = -1/v$. Let

$$V = \frac{\partial}{\partial t} + \Omega \frac{\partial}{\partial \tilde{\psi}} = \frac{\partial}{\partial v} + \Omega \frac{\partial}{\partial \tilde{\psi}'}, \quad (6.27)$$

where $\tilde{\psi}' = (2\pi/\Delta\psi)\psi'$ and

$$\Omega = \frac{1}{R} \sqrt{\frac{\lambda - v}{\lambda(1+\lambda)}} = \frac{1}{R} \sqrt{\frac{(1-v)(1+v^2)}{2(1+v)}}. \quad (6.28)$$

Then V is null at $y = -1/v$ where $V_\mu dx^\mu$ is a positive multiple of dy , from which it follows that $y = -1/v$ is a Killing horizon with angular velocity Ω . In the limit of a thin ring we recover $\Omega R = \tanh \sigma$.

This horizon has spatial topology $S^1 \times S^2$, although the S^2 is distorted away from perfect sphericity. At $y = -\infty$ the invariant $R_{\mu\nu\sigma\rho} R^{\mu\nu\sigma\rho}$ blows up, which corresponds to an inner spacelike singularity.

The Myers–Perry black hole with rotation in a single plane is contained within the family of solutions (6.13) as the particular limit in which $R \rightarrow 0$ and $\lambda, v \rightarrow 1$, while the parameters a, m are maintained at

$$m = \frac{2R^2}{1-v}, \quad a^2 = 2R^2 \frac{\lambda - v}{(1-v)^2}, \quad (6.29)$$

the coordinates (x, y) are changed to (r, θ) ,

$$\begin{aligned} x &= -1 + 2 \left(1 - \frac{a^2}{m} \right) \frac{R^2 \cos^2 \theta}{r^2 - (m-a^2) \cos^2 \theta}, \\ y &= -1 - 2 \left(1 - \frac{a^2}{m} \right) \frac{R^2 \sin^2 \theta}{r^2 - (m-a^2) \cos^2 \theta}, \end{aligned} \quad (6.30)$$

and (ψ, ϕ) are rescaled to $\sqrt{(m-a^2)/(2R^2)}(\psi, \phi)$, so they now have canonical periodicity 2π . Then we recover the metric

$$\begin{aligned} ds^2 &= - \left(1 - \frac{m}{\Sigma} \right) \left(dt + \frac{ma \sin^2 \theta}{\Sigma - m} d\psi \right)^2 + \Sigma \left(\frac{dr^2}{\Delta} + d\theta^2 \right) \\ &\quad + \frac{\Delta \sin^2 \theta}{1-m/\Sigma} d\psi^2 + r^2 \cos^2 \theta d\phi^2, \end{aligned} \quad (6.31)$$

$$\Delta \equiv r^2 - m + a^2, \quad \Sigma \equiv r^2 + a^2 \cos^2 \theta, \quad (6.32)$$

of the Myers–Perry black hole rotating in the ψ direction. The extremal limit $m = a^2$ of the Myers–Perry black hole actually corresponds to the same nakedly singular solution obtained as $v \rightarrow 1$ in (6.13).

In contrast with the Myers–Perry black hole, the geodesic equation is not separable in the black ring spacetime. Studies of geodesics have considered special cases, e.g., motion confined to submanifolds where $\partial/\partial\phi$ or $\partial/\partial\psi$ vanishes or geodesics with constant x, y [7–10].

6.3.2 Physical magnitudes and nonuniqueness

To demonstrate the absence of the uniqueness of this family of solutions, we need their two conserved charges, the mass and spin. These are obtained by examining the metric near asymptotic infinity, $x \rightarrow y \rightarrow -1$, in the more conventional coordinates of (6.24) and comparing it with the field of a source in linearized gravity (see e.g., [6]). We find

$$M = \frac{3\pi R^2}{2G} \frac{v}{(1-v)(1+v^2)}, \quad (6.33)$$

$$J = \frac{\pi R^3}{\sqrt{2}G} v \left(\frac{1+v}{(1-v)(1+v^2)} \right)^{3/2}. \quad (6.34)$$

The horizon area and temperature (from the surface gravity $\kappa = 2\pi T$) are

$$\mathcal{A}_H = 8\sqrt{2}\pi^2 R^3 \frac{v^2}{(1-v)(1+v^2)^{3/2}}, \quad (6.35)$$

$$T = \frac{1}{4\sqrt{2}\pi R} \frac{(1-v)\sqrt{1+v^2}}{v}. \quad (6.36)$$

We have imposed the equilibrium condition (6.22), so the solutions depend on only one dimensionless parameter. Since the Einstein equations in vacuum are scale invariant, the overall scale of the solutions can be fixed at one's convenience. For the purpose of comparing different solutions, instead of fixing R (which has no invariant meaning) we fix the mass M . Then all physical magnitudes can be rendered dimensionless by dividing out an appropriate power of M or of GM (which has dimension (length)²).

For the independent variable of the solutions we introduce a dimensionless “reduced spin” variable j , conveniently normalized as

$$j^2 \equiv \frac{27\pi}{32G} \frac{J^2}{M^3} \quad (6.37)$$

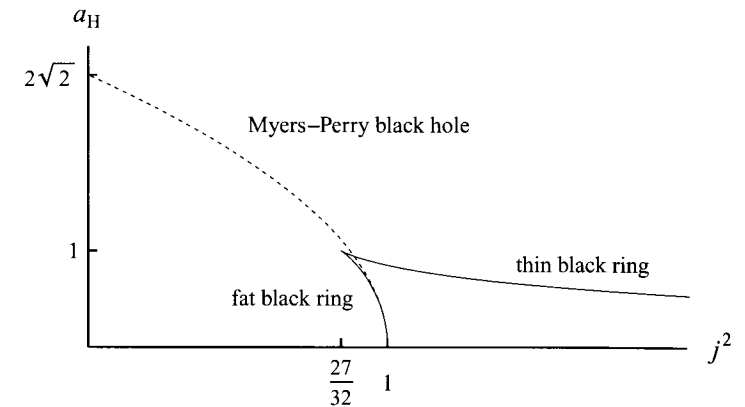


Figure 6.2 Horizon area a_H vs. j^2 , the square of the spin, for a given mass, for the neutral rotating black ring (solid) and the Myers–Perry black hole (dotted). Two branches of black rings, “thin” and “fat”, branch from the cusp at $(j^2, a_H) = (27/32, 1)$. In the range $27/32 < j^2 < 1$ there are two black rings and one Myers–Perry black hole with the same j , i.e., with the same mass and spin. The black ring at the minimum $j^2 = 27/32$ has a regular nondegenerate horizon. The Myers–Perry black hole and the black ring both limit at $(j^2, a_H) = (1, 0)$ to the same naked singularity.

(j^2 is often a more convenient variable than j). Then we characterize the equilibrium configurations by a curve $a_H(j)$ that gives the reduced area of the horizon,

$$a_H \equiv \frac{3}{16} \sqrt{\frac{3}{\pi}} \frac{\mathcal{A}_H}{(GM)^{3/2}} \quad (6.38)$$

as a function of the angular momentum for fixed mass. Using the results above this can be expressed in parametric form as

$$a_H = 2\sqrt{v(1-v)}, \quad j^2 = \frac{(1+v)^3}{8v} \quad (\text{black ring}), \quad (6.39)$$

with $0 < v \leq 1$.

For the Myers–Perry black hole (6.31), the corresponding relation is [3]

$$a_H = 2\sqrt{2(1-j^2)} \quad (\text{Myers–Perry black hole}). \quad (6.40)$$

The curves (6.39) and (6.40) are shown in Fig. 6.2. Contrary to what happens for rotating black holes in four dimensions and for the Myers–Perry black hole in five dimensions, the angular momentum of the black ring (for fixed mass) is bounded below but not above. Furthermore, in the range $27/32 \leq j^2 < 1$ there exist one Myers–Perry black hole and two black rings, all with the same values of the mass and the spin. Since the latter are the only conserved quantities carried by these objects, we have an explicit violation of black hole uniqueness. It is not possible to



Figure 6.3 A fat black ring ($v = 0.97$), a minimally spinning ring ($v = 0.5$) and a thin black ring ($v = 0.03$). The three rings shown have the same mass and the thin and fat rings have the same area. (These toroidal surfaces are the product of a constant- ϕ section of an isometric embedding in \mathbb{R}^3 of the S^2 of the horizon, times the S^1 at the inner rim of the ring.)

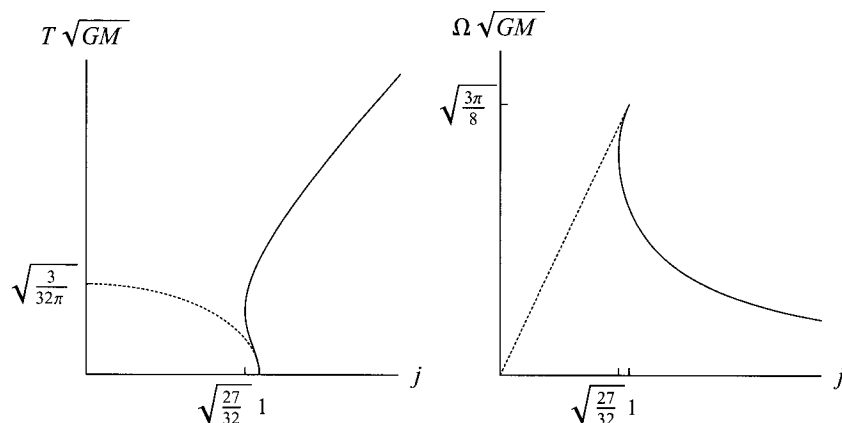


Figure 6.4 Temperature and angular velocity vs. angular momentum j for black rings (solid) and Myers–Perry black holes (dotted) of fixed mass. Both T and Ω have been rendered dimensionless by multiplying by \sqrt{GM} .

recover a notion of uniqueness by fixing the horizon topology, since there can be two black rings with the same M and J .

Figure 6.3 is a pictorial representation (after [7]) of different types of black rings: thin, fat, and minimally spinning. The figure suggests that fat black rings bear little resemblance to circular black strings. Instead, they may be better characterized as Myers–Perry black holes with a hole through their axis.

These interpretations are supported by an analysis of other physical properties. For instance, the temperature and angular velocity as a function of j are represented in Fig. 6.4. The two different qualitative behaviors for black rings are apparent. At large j , thin black rings are indeed very similar to black strings: the temperature

behaves like

$$T \rightarrow \frac{1}{4\pi\sqrt{2}r_0}, \quad (6.41)$$

where r_0 is the size of the S^2 at the horizon, as identified in (6.17). The behaviour $T \sim 1/r_0$ is as expected for a black string, with a Lorentz-boost factor for the limiting velocity $v = 1/\sqrt{2}$. Also, Ω decreases towards zero as j increases: for fixed mass, the longer the ring, the slower the rotation that is needed in order to achieve a given angular momentum. In contrast, for fat black rings T and Ω follow much more closely those of Myers–Perry black holes.

Thus, while the heuristic picture of a circular black string is an appropriate characterization of thin black rings, fat black rings are instead better regarded as Myers–Perry black holes with a piercing.

6.4 Black ring with two angular momenta

The exact solution for a black ring with rotation both along the S^1 direction ψ and along the ϕ direction of the S^2 was obtained by Pomeransky and Sen’kov [2]:

$$\begin{aligned} ds^2 = & -\frac{F(y, x)}{F(x, y)}(dt + \omega)^2 - \frac{H(x, y)}{F(y, x)}d\tilde{\psi}^2 - 2\frac{J(x, y)}{F(y, x)}d\tilde{\psi}d\tilde{\phi} + \frac{H(y, x)}{F(y, x)}d\tilde{\phi}^2 \\ & + \frac{\tilde{R}^2 F(x, y)}{(x - y)^2(1 - \alpha)^2} \left(\frac{dx^2}{G(x)} - \frac{dy^2}{G(y)} \right). \end{aligned} \quad (6.42)$$

The coordinates x and y retain essentially the same meaning as before, and the angles $\tilde{\phi}$ and $\tilde{\psi}$ have been already scaled to have canonical periodicity 2π .¹

The metric functions take a very complicated form in the general case, in which the black ring is not in equilibrium (their explicit forms can be found in [11]), but they simplify significantly when the balance of forces (i.e., the cancellation of conical singularities) is imposed. In this case the 1-form ω characterizing the rotation is given by

$$\begin{aligned} \omega = & -\frac{\sqrt{2}\tilde{R}v\sqrt{(1 + \alpha)^2 - v^2}}{H(y, x)} \left\{ (1 - x^2)y\sqrt{\alpha} d\tilde{\phi} \right. \\ & \left. + \frac{1 + y}{1 - v + \alpha} [1 + v - \alpha + x^2y\alpha(1 - v - \alpha) + 2\alpha x(1 - y)] d\tilde{\psi} \right\}, \end{aligned} \quad (6.43)$$

¹ In relation to [2] we have exchanged ϕ and ψ , and renamed λ as v , v as α , $2k^2$ as \tilde{R}^2 , Ω as ω and F as H to conform better to our notation for the single-spin black ring.

and the functions G, F, J, H become

$$\begin{aligned} G(\xi) &= (1 - \xi^2)(1 + v\xi + \alpha\xi^2), \\ F(x, y) &= 1 + v^2 - \alpha^2 + 2v\alpha(1 - x^2)y + 2xv(1 - y^2\alpha^2) \\ &\quad + x^2y^2\alpha(1 - v^2 - \alpha^2), \\ J(x, y) &= \frac{\tilde{R}^2(1 - x^2)(1 - y^2)v\sqrt{\alpha}}{(x - y)(1 - \alpha)^2} \\ &\quad \times [1 + v^2 - \alpha^2 + 2(x + y)v\alpha - xy\alpha(1 - v^2 - \alpha^2)], \\ H(x, y) &= \frac{\tilde{R}^2}{(x - y)^2(1 - \alpha)^2} \\ &\quad \times \left(G(x)(1 - y^2) \{[(1 - \alpha)^2 - v^2](1 + \alpha) + yv(1 - v^2 + 2\alpha - 3\alpha^2) \} \right. \\ &\quad \left. + G(y) \{2v^2 + xv[(1 - \alpha)^2 + v^2] + x^2[(1 - \alpha)^2 - v^2](1 + \alpha) \right. \\ &\quad \left. + x^3v(1 - v^2 - 3\alpha^2 + 2\alpha^3) - x^4(1 - \alpha)\alpha(-1 + v^2 + \alpha^2) \} \right). \end{aligned} \quad (6.44)$$

The solution now contains two dimensionless parameters v and α , and a scale \tilde{R} . In order to recover the metric (6.13), with λ fixed to the value (6.22) one must take $\alpha \rightarrow 0$ and make the identification $R^2 = \tilde{R}^2(1 + v^2)$. When $v = 0$ we find flat spacetime in coordinates that, for $\alpha \neq 0$, differ from (6.9) in a way that is familiar from a consideration of Boyer–Lindquist coordinates.

The parameters v and α are restricted to

$$0 \leq \alpha < 1, \quad 2\sqrt{\alpha} \leq v < 1 + \alpha, \quad (6.45)$$

for the existence of regular black hole horizons. The bound $v \geq 2\sqrt{\alpha}$ is actually a Kerr-like bound on the rotation of the S^2 . To see this, consider the equation for vanishing $G(y)$,

$$1 + vy + \alpha y^2 = 0, \quad (6.46)$$

which determines the position of the horizon within the allowed range $-\infty < y < -1$. If we make the identifications

$$y = -\frac{\tilde{R}}{r}, \quad v = \frac{2m}{\tilde{R}}, \quad \alpha = \frac{a^2}{\tilde{R}^2}, \quad (6.47)$$

this becomes the familiar expression $r^2 - 2mr + a^2 = 0$ (however, m and a are not the physical mass and angular momentum parameters, although they are related to them). Imposing the condition that the roots of (6.46) are real yields the required

bound, with an event horizon at

$$y_h = \frac{-v + \sqrt{v^2 - 4\alpha}}{2\alpha}. \quad (6.48)$$

When the bound is saturated, $v = 2\sqrt{\alpha}$, the horizon is degenerate, and when the bound is exceeded the horizon becomes a naked singularity.

The limit of a boosted rotating black string is obtained by changing coordinates and parameters as in (6.47), as well as using $x = \cos \theta$ and $\tilde{\psi} = z/\tilde{R}$ and then sending $\tilde{R} \rightarrow \infty$. The second angular momentum does not alter the limiting value of the boost, which is given by (6.23) again. The extremal Myers–Perry solution is recovered as a limit of the extremal solutions in which $\alpha \rightarrow 1$, $v \rightarrow 2$. However, in order to recover the general Myers–Perry solution as a limit, one needs to relax the equilibrium condition that has been imposed to obtain (6.44) and use the more general form of these functions given in [11].

The physical parameters of the solution are [2, 12]

$$M = \frac{3\pi \tilde{R}^2}{2G} \frac{v}{1 + \alpha - v}, \quad (6.49)$$

$$J_\psi = \frac{\pi \tilde{R}^3}{\sqrt{2}G} \frac{v(1 + v - 6\alpha + \alpha v + \alpha^2)\sqrt{(1 + \alpha)^2 - v^2}}{(1 + \alpha - v)^2(1 - \alpha)^2}, \quad (6.50)$$

$$J_\phi = \frac{2\pi \tilde{R}^3}{\sqrt{2}G} \frac{v\sqrt{\alpha[(1 + \alpha)^2 - v^2]}}{(1 + \alpha - v)(1 - \alpha)^2}, \quad (6.51)$$

$$\mathcal{A}_H = 8\sqrt{2}\pi^2 \tilde{R}^3 \frac{v(1 + v + \alpha)}{(y_h^{-1} - y_h)(1 - \alpha)^2}, \quad (6.52)$$

$$T = \frac{1}{4\sqrt{2}\pi \tilde{R}} \frac{(y_h^{-1} - y_h)(1 - \alpha)\sqrt{v^2 - 4\alpha}}{v(1 + \alpha + v)}, \quad (6.53)$$

$$\Omega_\psi = \frac{1}{\sqrt{2}\tilde{R}} \sqrt{\frac{1 + \alpha - v}{1 + \alpha + v}}, \quad (6.54)$$

$$\Omega_\phi = \frac{v(1 + \alpha) - (1 - \alpha)\sqrt{v^2 - 4\alpha}}{2\sqrt{2}\tilde{R}v\sqrt{\alpha}} \sqrt{\frac{1 + \alpha - v}{1 + \alpha + v}}. \quad (6.55)$$

To characterize the parameter region where black rings exist, i.e., their phase space, we fix the mass and employ dimensionless angular momentum variables j_ϕ, j_ψ , as implied by (6.37). The region of the (j_ψ, j_ϕ) -plane covered by doubly spinning black rings is shown in Fig. 6.5 for the region $j_\psi > j_\phi \geq 0$ (the rest of the plane can be obtained by iterating and by changing the signs of $j_{\psi,\phi}$). Extremal

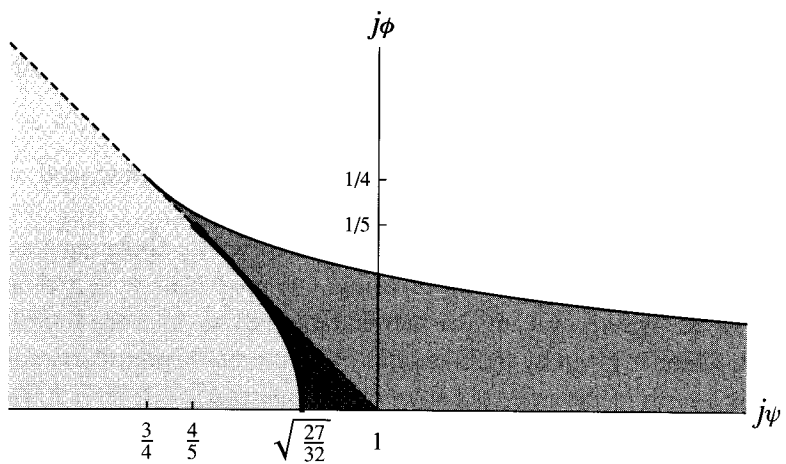


Figure 6.5 Phase space of doubly spinning black rings, restricted to the representative region $j_\psi > j_\phi \geq 0$. In the light-gray region there exist Myers–Perry black holes; in the medium-gray region there exist thin black rings; and in the dark-gray region there exist thin and fat black rings, and Myers–Perry black holes. The dashed line $j_\psi + j_\phi = 1$ corresponds to extremal Myers–Perry black holes. The thin solid curve corresponds to regular extremal black rings. The thick solid curve corresponds to regular nonextremal black rings with minimal j_ψ for a given j_ϕ .

black rings, with maximal J_ϕ for given J_ψ , lie along the curve [12, 13]

$$j_\psi = \frac{1 + 4\sqrt{\alpha} + \alpha}{4\alpha^{1/4}(1 + \sqrt{\alpha})}, \quad j_\phi = \frac{\alpha^{1/4}}{2(1 + \sqrt{\alpha})}, \quad 0 \leq \alpha \leq 1 \quad (6.56)$$

(the thin solid line in Fig. 6.5). This curve extends from $j_\psi = 3/4$, $j_\phi = 1/4$ (as $\alpha \rightarrow 1$) to $j_\psi \rightarrow \infty$, $j_\phi \rightarrow 0$ (as $\alpha \rightarrow 0$). The extremal Myers–Perry black holes lie along $j_\psi + j_\phi = 1$ (broken line in Fig. 6.5).

For doubly spinning black rings the angular momentum along the S^2 is always bounded above by that in the S^1 according to

$$|j_\phi| \leq \frac{1}{3}|j_\psi|. \quad (6.57)$$

This is saturated at the endpoint of the extremal black ring curve $j_\psi = 3/4$, $j_\phi = 1/4$.

6.5 Multiple black hole solutions

6.5.1 Black Satellites and multi-rings

In $D = 4$ it is believed that there are no stationary multi-black-hole solutions of vacuum gravity. However, such solutions do exist in $D = 5$. “Black Saturn”

solutions, in which a central Myers–Perry-type of black hole is surrounded by a concentric rotating black ring, have been constructed [4] using techniques of inverse scattering that exploit the complete integrability of the vacuum Einstein equations with $D - 2$ commuting isometries (as reviewed in [6]).

The existence of black Satellites is hardly surprising: since black rings can have arbitrarily large radius, it is clear that we can put a small black hole at the center of a very long black ring with very little interaction between the two objects. Similarly, we expect stationary configurations with multiple concentric black rings. Di-rings, with two concentric black rings rotating on the same plane, have been explicitly constructed [14] (see also [15]) and their physical properties have been investigated [16, 17].

While the metrics for these multi-black holes are rather complicated, intuitive discussions of their properties are presented in [18] and [16]. On the one hand, for a given mass, a Myers–Perry black hole maximizes its entropy by reducing its angular momentum to zero. On the other hand, a black ring can be made to carry any value of angular momentum while having arbitrarily low mass, by making it as thin and long as required. Then, in a black Satellite with given total M and J one can attain an entropy arbitrarily close to that of a static Myers–Perry black hole with the same mass, i.e., $a_H = 1$, by putting almost all this mass in a central, almost static, black hole and the angular momentum into a very thin and long black ring. Thus, black Satellites can take any value of j and a_H within the band

$$-\infty < j < \infty, \quad 0 < a_H < 1. \quad (6.58)$$

However, if we fix the total (M, J) of the black Satellite we can vary, say, the mass and spin of the black ring while adjusting the mass and spin of the central black hole to add up to the total values. Thus these configurations exhibit doubly continuous nonuniqueness.

These arguments can be made in greater generality for configurations with an arbitrary number of black rings, each new black object adding two more continuous parameters. More formally, for a general stationary multi-black hole solution for N black objects labelled by $i = 1, \dots, N$, each connected component of the horizon H_i is generated by a Killing vector

$$k_{(i)} = \xi + \Omega_i \psi, \quad (6.59)$$

where ξ and ψ are canonically normalized Killing vectors that generate unit-time translations and rotations at asymptotic infinity and Ω_i is the angular velocity on H_i . To each horizon component H_i we can assign an area and surface gravity, A_i and κ_i , and a (Komar) angular momentum

$$J_i = \frac{1}{16\pi G} \int_{H_i} \epsilon_{abcde} \nabla^d \psi^e. \quad (6.60)$$

The total ADM mass M is measured at infinity and, following a standard procedure, one can derive the Smarr relation

$$M = \frac{3}{2} \sum_i \left(\frac{\kappa_i}{8\pi G} \mathcal{A}_i + \Omega_i J_i \right) \quad (6.61)$$

and the first law of multi-black hole mechanics,

$$\delta M = \sum_i \left(\frac{\kappa_i}{8\pi G} \delta \mathcal{A}_i + \Omega_i \delta J_i \right). \quad (6.62)$$

Thus the phase space of multi-black hole configurations with up to N black objects has $2N$ variables (\mathcal{A}_i, J_i): there is a $2(N - 1)$ -parameter continuous nonuniqueness of solutions with given total M and J . In addition, for any N there can be discrete degeneracies, as we have seen for single ($N = 1$) black ring or Myers–Perry black hole configurations.

Perhaps the most interesting aspect of black Saturns is the way in which they exhibit the rotational dragging of one black object by the other. We can illustrate this by studying how the relation between the angular velocity Ω_{bh} and angular momentum J_{bh} of the central black hole is altered by the presence of the black ring. The effects can be dramatic: for instance, one can have configurations with $\Omega_{bh} \neq 0, J_{bh} = 0$, in which the black hole carries no intrinsic spin but the black ring forces it to rotate. But one can also have a central black hole with $\Omega_{bh} = 0, J_{bh} \neq 0$, such that, even if the black hole carries intrinsic angular momentum, it is made static by the counterrotational drag force of the ring. The dragging can be so extreme as to force the angular velocity and angular momentum of the central black hole into opposite directions, $\Omega_{bh} J_{bh} < 0$; they can even reach $\Omega_{bh} J_{bh} < -\kappa_{bh} \mathcal{A}_{bh}/(8\pi G) < 0$, so that the black hole makes a negative contribution to the total mass in (6.61)!

6.5.2 Phase diagram

In these multi-black hole configurations the surface gravities (i.e., temperatures) and angular velocities of disconnected components of the horizon are in general different. There is nothing to prevent a classical stationary configuration having these properties. However, if quantum effects are turned on, Hawking radiation will put these black holes in contact with each other and the radiation will tend to equilibrate both their temperatures and their angular velocities. Equality of these “intensive parameters” is a necessary condition for thermal equilibrium, and presumably also for mergers in phase space to solutions with connected horizon components. So these multi-black hole configurations cannot in general exist in

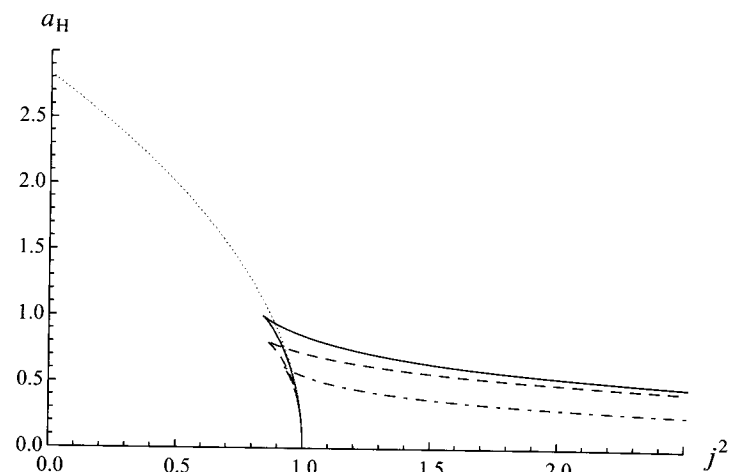


Figure 6.6 Phase diagram including Myers–Perry black holes (dotted curve), black rings (solid curve), black Saturns (broken curve) and black di-rings (broken-and-dotted curve), the last two being in thermodynamic equilibrium. All curves end on the same singular solution at $j = 1$. The asymptotic behaviour at large j depends only on the number of rings and follows (6.63).

thermal equilibrium (this problem is in addition to that of constructing a Hartle–Hawking state when ergoregions are present [19]).

Requiring equal temperatures and angular velocities for all the black objects imposes $2(N - 1)$ conditions on the parameters. This removes entirely the continuous nonuniqueness, leaving at most discrete degeneracies. Phases in thermodynamical equilibrium are therefore characterized by a curve in the (j, a_H) -plane. Figure 6.6 shows these curves for Myers–Perry black holes, black rings and black di-rings. For large values of j , generic multi-ring configurations can be regarded as consisting of very thin rings with radii that are much larger than the separation between rings, these separations being also much larger than the thickness of each ring [16]. Under these circumstances it can be shown that the curves $a_H(j)$ with n rings behave at large j as follows:

$$a_H^{(n\text{-ring})} \xrightarrow{j \rightarrow \infty} \frac{1}{n\sqrt{2} j}. \quad (6.63)$$

The asymptotic behaviour would be the same if there were a central black hole in the configuration (that was also in thermodynamic equilibrium), i.e., it depends only on the number of rings in the system. Thus the black Saturn and di-ring curves in Fig. 6.6 asymptote respectively to the black ring curve and to half the value of the black ring curve.

6.5.3 Bi-rings

It is also possible to have two black rings lying and rotating on orthogonal, independent, planes. Such *bicycling black rings* have been constructed using inverse scattering methods [12, 20] and provide a way of obtaining configurations with arbitrarily large values of both the angular momenta, for fixed mass; this cannot be achieved simultaneously for both spins either by Myers–Perry black holes or by doubly spinning black rings. In the solutions in [12, 20] each black ring possesses angular momentum only on its plane, along the S^1 , not in the orthogonal plane, on the S^2 . Nevertheless they drag each other, so that the two horizon angular velocities are nonzero on both the horizons. The solutions contain four free parameters, corresponding to, e.g., the masses of each ring and their two angular momenta. The more general six-parameter solution, in which each black ring has both angular momenta turned on, has not been constructed yet.

It is easy to argue, extending the arguments in [18], that multi-black hole solutions allow coverage of the entire phase plane (j_ψ, j_ϕ) of five-dimensional solutions.

6.6 Stability

Linearized perturbations of the black ring metric (6.13) have not yielded to analytical study. The apparent absence of a Killing tensor prevents the separation of variables even for massless scalar field perturbations. Also, the difficulties in decoupling the equations to find a master equation for linearized gravitational perturbations, already present for the Myers–Perry solutions, are if anything exacerbated for black rings.

Studies of the classical stability of black rings have therefore been mostly heuristic. We have seen that, locally, very thin black rings look like boosted black strings, which are prone to Gregory–Laflamme-type [21] instabilities [22]. Thus, thin black rings are expected to be unstable to the formation of ripples along their S^1 direction. In [7] it was found that thin black rings seem to be able to accommodate unstable Gregory–Laflamme modes down to values $j \sim O(1)$. Thus, it is conceivable that a large fraction of black rings in the thin branch, and possibly all the black rings in this branch, suffer from this instability. The ripples rotate with the black ring and then should emit gravitational radiation. However, the time scale for this emission is much longer than the time scale of the fastest Gregory–Laflamme mode, so that the pinch-down created by this instability will dominate the evolution at least initially. The later evolution of this instability is uncertain but, given that under the Gregory–Laflamme instability a black string pinches to a singularity and presumably breaks (through effects beyond the classical Einstein theory), it is conceivable, and compatible with an increment of the total area, that

the black ring also continues to pinch down until it fragments apart into smaller black holes that then fly away. Alternatively, the deformation of the horizon away from axial symmetry may grow so large and enhance the emission of gravitational waves so much that the angular momentum per unit mass is reduced to a value where the black ring can settle into a stable single-horizon black hole, which might be a stable Myers–Perry black hole.

The stability against variations of the S^1 radius can be analyzed by allowing for conical singularities and thus considering off-shell deformations of the black ring [7]. It is then possible to compute an effective potential for radial deformations of the black ring. Fat black rings sit at the maxima of this potential, while thin black rings sit at the minima. Thus, fat black rings are expected to be unstable to variations in their radius and presumably collapse to form Myers–Perry black holes. The analysis in [7] is in fact consistent with the previous, more abstract, analysis of local stability in [23]. This was based on the “turning-point” method of Poincaré, in which the equilibrium curves for phases near bifurcation points are studied. For the case of black rings, one focuses on the cusp where the two branches meet. One then assumes that these curves correspond to extrema of some potential, e.g., an entropy, that can be defined over all the plane (j, a_H). The cusp then corresponds to an inflection point of this potential where a branch of the maxima and a branch of the minima meet. By continuity, the branch with the higher entropy will be the most stable branch and the one with lower entropy will be unstable. Thus, for black rings an unstable mode is added when one goes from the upper (thin) branch to the lower (fat) branch. This is precisely as found from the mechanical potential for radial deformations [7].

Thus, a large fraction of all single-spin neutral black rings are expected to be classically unstable, and it remains an open problem whether a window of stability exists for thin black rings with $j \sim O(1)$. The stability, however, can improve greatly with the addition of charges and dipoles.

Doubly spinning black rings are expected to suffer from similar instabilities. Insofar as a fat ring branch exists that meets a thin ring branch at a cusp, the fat rings are expected to be unstable. Very thin rings are also expected to be unstable to Gregory–Laflamme perturbations that form ripples. The angular momentum on the S^2 may be redistributed nonuniformly along the ring, with the larger blobs concentrating more spin.

Much of what we can say about the classical stability of black Saturns and multi-rings follows from what we have said above for each of their components. For instance, if the rings are thin enough then they are expected to be Gregory–Laflamme-unstable. However, we know essentially nothing about what happens when the gravitational interactions among the black objects involved are strong.

Massive geodesics on the plane of a black ring (see [8]) show that a particle at the centre of the S^1 is unstable to migration towards the black ring. This suggests that a black Saturn with a small black hole at the centre of a larger black ring should be unstable. More speculatively, the peculiar effects that occur at large counterrotation, in particular when the central black hole contributes negatively to (6.61), may also be an indication of instability.

References

- [1] R. Emparan and H. S. Reall, A rotating black ring in five dimensions, *Phys. Rev. Lett.* **88** (2002), 101 101 [arXiv:hep-th/0110260].
- [2] A. A. Pomeransky and R. A. Sen'kov, Black ring with two angular momenta, arXiv:hep-th/0612005.
- [3] R. C. Myers and M. J. Perry, Black holes in higher dimensional space-times, *Ann. Phys.* **172** (1986), 304.
- [4] H. Elvang and P. Figueras, Black Saturn, *JHEP* **0705** (2007), 050 [arXiv:hep-th/0701035].
- [5] R. Emparan and H. S. Reall, Black rings, *Class. Quant. Grav.* **23** (2006), R169 [arXiv:hep-th/0608012].
- [6] R. Emparan and H. S. Reall, Black holes in higher dimensions, *Living Rev. Rel.* **11** (2008), 6 [arXiv:0801.3471 [hep-th]].
- [7] H. Elvang, R. Emparan, and A. Virmani, Dynamics and stability of black rings, *JHEP* **0612** (2006), 074 [arXiv:hep-th/0608076].
- [8] J. Hoskisson, Particle motion in the rotating black ring metric, *Phys. Rev. D* **78** (2008), 064 039 [arXiv:0705.0117 [hep-th]].
- [9] M. Durkee, Geodesics and symmetries of doubly-spinning black rings, *Class. Quant. Grav.* **26** (2009), 085 016 [arXiv:0812.0235 [gr-qc]].
- [10] T. Igata, H. Ishihara, and Y. Takamori, Stable bound orbits around black rings, *Phys. Rev. D* **82** (2010), 101 501 [arXiv:1006.3129 [hep-th]].
- [11] Y. Morisawa, S. Tomizawa, and Y. Yasui, Boundary value problem for black rings, *Phys. Rev. D* **77** (2008), 064 019 [arXiv:0710.4600 [hep-th]].
- [12] H. Elvang and M. J. Rodriguez, Bicycling black rings, *JHEP* **0804** (2008), 045 [arXiv:0712.2425 [hep-th]].
- [13] H. S. Reall, Counting the microstates of a vacuum black ring, *JHEP* **0805** (2008), 013 [arXiv:0712.3226 [hep-th]].
- [14] H. Iguchi and T. Mishima, Black di-ring and infinite nonuniqueness, *Phys. Rev. D* **75** (2007), 064 018 [arXiv:hep-th/0701043].
- [15] J. Evslin and C. Krishnan, The black di-ring: an inverse scattering construction, *Class. Quant. Grav.* **26** (2009), 125 018 [arXiv:0706.1231 [hep-th]].
- [16] R. Emparan and P. Figueras, Multi-black rings and the phase diagram of higher-dimensional black holes, *JHEP* **1011** (2010), 022 [arXiv:1008.3243 [hep-th]].
- [17] H. Iguchi and T. Mishima, Thermodynamic black di-rings, *Phys. Rev. D* **82** (2010), 084 009 [arXiv:1008.4290 [hep-th]].
- [18] H. Elvang, R. Emparan, and P. Figueras, Phases of five-dimensional black holes, *JHEP* **0705** (2007), 056 [arXiv:hep-th/0702111].
- [19] B. S. Kay and R. M. Wald, Theorems on the uniqueness and thermal properties of stationary, nonsingular, quasifree states on space-times with a bifurcate killing horizon, *Phys. Rept.* **207** (1991), 49.

- [20] K. Izumi, Orthogonal black di-ring solution, *Prog. Theor. Phys.* **119** (2008), 757 [arXiv:0712.0902 [hep-th]].
- [21] R. Gregory and R. Laflamme, Black strings and p-branes are unstable, *Phys. Rev. Lett.* **70** (1993), 2837 [arXiv:hep-th/9301052].
- [22] J. L. Hovdebo and R. C. Myers, Black rings, boosted strings and Gregory-Laflamme, *Phys. Rev. D* **73** (2006), 084 013 [arXiv:hep-th/0601079].
- [23] G. Arcioni and E. Lozano-Tellechea, Stability and critical phenomena of black holes and black rings, *Phys. Rev. D* **72** (2005), 104 021 [arXiv:hep-th/0412118].

Part IV

General properties

Constraints on the topology of higher-dimensional black holes

GREGORY J. GALLOWAY

7.1 Introduction

As discussed in the first chapter, black holes in four dimensions satisfy remarkable uniqueness properties. Of fundamental importance is the classical result of Carter, Hawking and Robinson that the Kerr solution, which is characterized by its mass M and angular momentum J , is the unique four-dimensional asymptotically flat stationary (i.e., steady state) solution to the vacuum Einstein equations.¹ A basic step in the proof is Hawking's theorem on the topology of black holes [2], which asserts that, for such black hole spacetimes, cross sections of the event horizon are necessarily spherical, i.e., they are topologically 2-spheres.² In short, for conventional black holes in four dimensions, the horizon topology is spherical.

However, as we saw in the previous chapter, in higher dimensions black hole horizons need not have spherical topology. With the remarkable discovery by Emparan and Reall [3] of the black ring solution, with its $S^1 \times S^2$ horizon topology, the question naturally arose as to what, if any, are the restrictions on horizon topology in higher-dimensional black holes. This issue was addressed in a paper of the author and Rick Schoen [4], in which we obtained a generalization of Hawking's theorem to higher dimensions. This generalization is discussed in sections 7.4 and 7.5. In preparation for that, we review Hawking's black hole topology theorem in section 7.2 and introduce some basic background material on marginally trapped

¹ Some recent progress has been made in removing the assumption of analyticity from the classical proof; see e.g., [1].

² Much later an entirely different proof of this fact was given based on topological censorship, as described in Chapter 1. However, topological censorship does not in general provide much information about horizon topology in higher dimensions; see the comments in section 7.8.2.

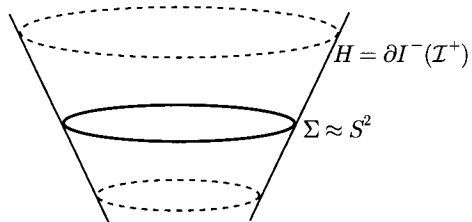


Figure 7.1

surfaces in section 7.3. Theorem 7.4.1 in section 7.4 leaves open the possibility of horizons with, for example, toroidal topology in vacuum black hole spacetimes. In section 7.6 we consider a refinement of Theorem 7.4.1 that rules out such “borderline” cases. In section 7.7 we address the effect of including the cosmological term in the Einstein equations. Further constraints on horizon topology are discussed in section 7.8, some based on quite different methods; concluding remarks are given in section 7.9.

7.2 Hawking’s theorem on black hole topology

In this section we will review Hawking’s theorem on black hole topology (as presented in [2]) and give a brief outline of its proof. At this point we wish to keep the discussion informal, and avoid any precise definitions until subsequent sections.

Theorem 7.2.1 ([2]) Let M^4 be a four-dimensional asymptotically flat stationary black hole spacetime obeying the dominant energy condition. Then cross sections of the event horizon are topologically 2-spheres.

Here asymptotically flat means that the spacetime admits a regular null infinity $\mathcal{I} = \mathcal{I}^+ \cup \mathcal{I}^-$. Then the (future) event horizon is the boundary of the past of future null infinity, $H = \partial I^-(\mathcal{I}^+)$ (see Fig. 7.1). By a cross section we mean a smooth compact (without boundary) 2-surface obtained, say, by intersecting H with a spacelike hypersurface. As we will recall later, the dominant energy condition is a positivity condition on the energy-momentum tensor of the spacetime.

Apart from one fact the proof of Theorem 7.2.1 is purely local. Assuming that there is a cross section Σ that is not spherical, Hawking’s proof involves deforming Σ outward to a surface Σ' that is *outer trapped*, that is to say, the future outward-directed null normal geodesics emanating from Σ' are converging along Σ' . But it is a basic fact that outer trapped surfaces cannot occur in the region outside the black hole; since the outgoing light rays are converging, such surfaces cannot be seen by distant observers and hence are necessarily contained within the black hole region.

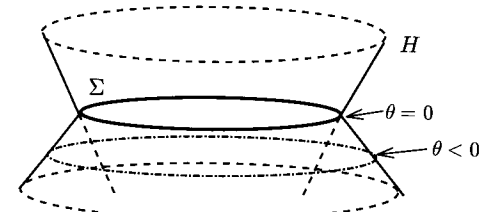


Figure 7.2

To construct the outer trapped surface, Hawking considers a specially chosen one-parameter deformation (or variation) $t \rightarrow \Sigma_t$ of $\Sigma = \Sigma_0$ to the past along the null hypersurface generated by the past outward-directed null normal geodesics of Σ (see Fig. 7.2). Let $\theta(t)$ denote the expansion of the future outward-directed null normal geodesics emanating from Σ_t . The event horizon H is a null hypersurface ruled by null geodesics, called the null generators of H . The assumption of stationarity implies that the congruence of the null generators of H has zero expansion.³ But the future outward directed null normal geodesics of Σ coincide with these generators, and this implies that $\theta(0) = 0$. If Σ is not a 2-sphere, and hence has genus (i.e., number of handles) $g \geq 1$, the Gauss–Bonnet theorem and the dominant energy condition are then used to show that $\partial\theta/\partial t|_{t=0} < 0$. It follows that, for sufficiently small $t > 0$, $\theta(t) < 0$, which implies that Σ_t is outer trapped. Hence, Σ must be a 2-sphere.

Actually, the torus T^2 ($g = 1$) arises as a borderline case in the proof. The arguments in [2] show that the torus could arise only under special circumstances, e.g., Σ would have to be flat and a certain energy-momentum tensor term would have to vanish along Σ . It is not quite clear to us, though, that the arguments succeed in eliminating the possibility of a torus altogether. In any case, as the proof relies on the Gauss–Bonnet theorem it does not directly generalize to higher dimensions.

In [5], Hawking showed how to extend his black hole topology result to *apparent horizons*, i.e., to outermost marginally outer-trapped surfaces. Here, “outermost” means with respect to a given spacelike hypersurface. Our generalization of Hawking’s theorem is carried out in this more general context. Moreover, like Hawking’s proof, our proof is variational in nature.

7.3 Marginally outer-trapped surfaces

The notion of a marginally outer-trapped surface was introduced early in the development of the theory of black holes. Under suitable circumstances the occurrence of a marginally outer-trapped surface in a time slice of spacetime signals the

³ By Hawking’s area theorem this expansion is, in general, nonnegative but goes to zero in the steady state limit.

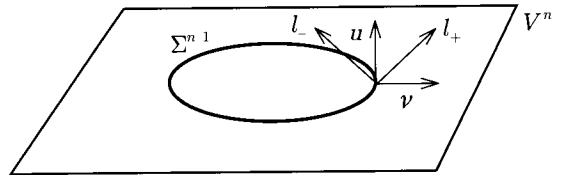


Figure 7.3

presence of a black hole [2]. For this and other reasons marginally outer-trapped surfaces have played a fundamental role in quasilocal descriptions of black holes; see e.g., [6]. They also play an important role in numerical simulations of black hole formation, black hole collisions etc., and many numerical algorithms have been developed to find them. The mathematical theory of marginally outer-trapped surfaces has been broadly developed in recent years; see e.g. the recent survey article [7].

Let (M^{n+1}, g) be a spacetime (a time-oriented Lorentzian manifold) of dimension $n+1, n \geq 3$. Let V^n be a spacelike hypersurface in M^{n+1} , with induced metric h and second fundamental form (extrinsic curvature tensor) K . Thus, for vectors X, Y tangent to V at a given point, $K(X, Y) = g(\nabla_X u, Y) = X^\mu Y^\nu \nabla_\mu u_\nu$, where ∇ is the Levi-Civita connection of M and u is the future-directed timelike unit vector field normal to V .

Let Σ^{n-1} be a compact hypersurface in V^n , and assume that Σ separates V into an ‘‘inside’’ and ‘‘outside’’; let v be the outward-pointing unit vector field normal to Σ in V . Then $l_+ = u + v$ (resp. $l_- = u - v$) is a future-directed outward-pointing (resp., future-directed inward-pointing) null normal vector field along Σ , unique up to positive scaling (see Fig. 7.3).

The second fundamental form of Σ , viewed as a submanifold of spacetime, can be decomposed into two scalar-valued *null second forms*, χ_+ and χ_- , associated with l_+ and l_- , respectively. At each point of Σ , χ_\pm is the bilinear form defined by

$$\chi_\pm(X, Y) = g(\nabla_X l_\pm, Y) = X^\mu Y^\nu \nabla_\mu (l_\pm)_\nu, \quad (7.1)$$

for pairs of vectors X, Y tangent to Σ . The *null expansion scalars* θ_\pm of Σ are obtained by tracing χ_\pm with respect to the induced metric γ on Σ ,

$$\theta_\pm = \text{tr}_\gamma \chi_\pm = \gamma^{AB} (\chi_\pm)_{AB} = \text{div}_\Sigma l_\pm. \quad (7.2)$$

It is easy to check that the sign of θ_\pm is invariant under positive rescaling of the null vector field l_\pm . The vector fields l_\pm correspond to the initial tangents of the future-directed null geodesics issuing orthogonally from Σ . Thus, physically ℓ_+ (resp., ℓ_-) measures the divergence of the outgoing (resp., ingoing) light rays emanating from Σ . One can express the null expansion scalars in terms of the *initial data* h, K

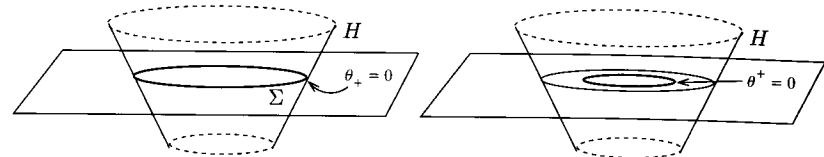


Figure 7.4 In stationary black hole spacetimes (left), cross sections of the event horizon are MOTSs. In dynamical black hole spacetimes (right), MOTSs typically occur inside the black hole.

on V^n , as follows:

$$\theta_\pm = \text{tr}_\gamma K \pm H, \quad (7.3)$$

where H is the mean curvature of Σ within V . Note, in particular, that in the time-symmetric case, $K \equiv 0$, θ_+ is just the mean curvature of Σ .

For round spheres in Euclidean slices of Minkowski space, with an obvious choice of inside and outside, one has $\theta_- < 0$ and $\theta_+ > 0$. In fact, this is the case in general for large ‘‘radial’’ spheres in *asymptotically flat* spacelike hypersurfaces. However, in regions of spacetime where the gravitational field is strong one may have both $\theta_- < 0$ and $\theta_+ < 0$, in which case Σ is called a *trapped surface*. Under appropriate energy and causality conditions the occurrence of a trapped surface signals the onset of gravitational collapse (this is the implication of the Penrose singularity theorem) and the existence of a black hole [2].

Focusing attention on the outward null normal only, we say that Σ is an outer-trapped surface if $\theta_+ < 0$. Finally, we define Σ to be a marginally outer-trapped surface (MOTS) if θ_+ vanishes identically.

Such surfaces arise naturally in a number of situations. Most basically, as pointed out in our discussion of the proof of Hawking’s black hole topology theorem, cross sections of the event horizon (obtained, say, as the smooth compact intersection of the event horizon with a spacelike hypersurface) in stationary black hole spacetimes are MOTSs (see Fig. 7.4, left-hand diagram).

In dynamical black hole spacetimes, MOTSs typically occur inside the event horizon (see the right-hand diagram in Fig. 7.4). (In fact they are forbidden to occur outside the black hole.) There are old heuristic arguments for the existence of MOTSs in this case, based on considering the boundary of the trapped region inside the event horizon. These heuristic ideas have recently been made rigorous, first by Andersson and Metzger [8] for three-dimensional initial-data sets and then by Eichmair [9, 10] for initial-data sets up to dimension seven. These results rely on a basic existence result for MOTSs under physically natural barrier conditions and imply the existence of outermost MOTSs, as will be described in the next section. We refer the reader to the survey article [7] for an excellent discussion

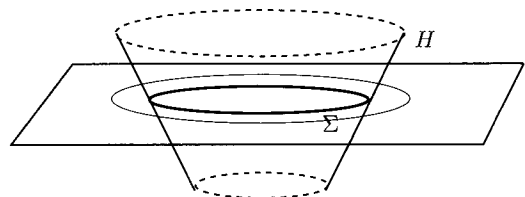


Figure 7.5 Cross sections of the event horizon in asymptotically flat stationary black hole spacetimes obeying the DEC are outermost MOTSs. Any surface that lies outside the event horizon H (like the outer surface shown in the figure) cannot have $\theta_+ \leq 0$.

of how the existence of MOTSs is established by inducing a blow-up of Jang's equation.

7.4 A generalization of Hawking's theorem and some topological restrictions

Let V^n be a spacelike hypersurface in the spacetime (M^{n+1}, g) , $n \geq 3$, as in the previous subsection. Henceforth, assume that spacetime satisfies the Einstein equations (without cosmological constant),

$$\text{Ric} - \frac{1}{2}Rg = \mathcal{T}.$$

Then M is said to obey the *dominant energy condition* (DEC) provided that the energy-momentum tensor \mathcal{T} satisfies $\mathcal{T}(X, Y) = T_{\mu\nu}X^\mu Y^\nu \geq 0$ for all future-directed causal vectors X, Y .

Our generalization of Hawking's theorem applies to outermost MOTSs. We say that a MOTS Σ in V is *outermost* provided that there are no outer-trapped ($\theta_+ < 0$) or marginally outer-trapped ($\theta_+ = 0$) surfaces outside of, and homologous to, Σ .⁴ It is a fact that a cross section Σ of the event horizon in an asymptotically flat black hole spacetime obeying the DEC⁵ is an outermost MOTS relative to any spacelike hypersurface whose intersection with the horizon is Σ . Again, the reason is that outer-trapped surfaces, or even marginally outer-trapped surfaces homologous to Σ , cannot occur outside the black hole region (see Fig. 7.5).

More generally, results of Andersson and Metzger [8] (in three spatial dimensions) and Eichmair [9, 10] (in up to seven spatial dimensions) guarantee the existence of outermost MOTSs under natural barrier conditions. More specifically, suppose that Σ_1 is an outer-trapped surface in V^n , $3 \leq n \leq 7$, and suppose also that

⁴ Here, “ Σ' homologous to Σ ” simply means that Σ and Σ' form the boundary of a compact region in V . We are not interested here in the occurrence of outer-trapped surfaces or MOTSs outside Σ that are not homologous to Σ .

⁵ Actually the *null energy condition*, $\text{Ric}(X, X) = R_{\mu\nu}X^\mu X^\nu \geq 0$ for all null vectors X , suffices for this.

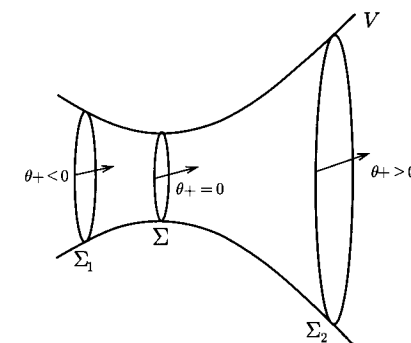


Figure 7.6

there is a surface Σ_2 outside and homologous to Σ_1 that is outer *untrapped*, i.e. which has outer null expansion $\theta_+ > 0$. (For example, Σ_2 might be a large sphere near infinity on an asymptotically flat end of V .) Then the results of Andersson and Metzger and of Eichmair imply the existence of an outermost MOTS Σ in the region bounded by Σ_1 and Σ_2 (see Fig. 7.6). For further details, see [7] and references therein.

We need to introduce one last piece of terminology. A smooth compact manifold is said to be of *positive Yamabe type* if it admits a Riemannian metric of positive scalar curvature. By the solution of the Yamabe problem, the conformal class of this metric will contain a metric of *constant* positive scalar curvature, but we shall not need that fact here.

We are now ready to state the generalization of Hawking's theorem.

Theorem 7.4.1 ([4]) Let V^n , $n \geq 3$, be a spacelike hypersurface in a spacetime obeying the DEC. If Σ^{n-1} is an outermost MOTS in V^n then Σ^{n-1} is of positive Yamabe type, unless Σ is Ricci flat (or flat if $n = 3, 4$), $\chi_+ \equiv 0$ and $\mathcal{T}(u, l_+) = T_{\mu\nu}u^\mu l_+^\nu \equiv 0$ on Σ .

Thus, apart from certain exceptional circumstances (that we ignore for now but will address later), Σ is of positive Yamabe type. The relevance of this for black hole topology is that there is an extensive literature concerning results which establish restrictions on the topology of manifolds that admit metrics of positive scalar curvature. We will consider two basic examples now and will discuss some further restrictions in section 7.8.1. For simplicity, in the present discussion we will assume that Σ is orientable.

Case 1: $\dim \Sigma = 2$ ($\dim M = 3 + 1$) In this case, Σ being of positive Yamabe type means that Σ admits a metric of positive Gaussian curvature. Hence, by the Gauss–Bonnet theorem, Σ is topologically a 2-sphere and we recover Hawking's theorem.

Case 2: $\dim \Sigma = 3$ ($\dim M = 4 + 1$) In this case we have the following result.

Theorem 7.4.2 If Σ is a compact orientable 3-manifold of positive Yamabe type then Σ must be diffeomorphic to (i) a spherical space, or (ii) $S^1 \times S^2$ or (iii) a connected sum of the previous two types.

By a spherical space we mean the 3-sphere S^3 or, more generally, a space covered by S^3 such as a lens space. Thus, the basic horizon topologies in the case $\dim \Sigma = 3$ are S^3 and $S^1 \times S^2$, the latter being realized by the black ring.

The proof of Theorem 7.4.2 goes briefly as follows. By the prime decomposition theorem [11], Σ can be expressed as a connected sum of (i) spaces covered by homotopy 3-spheres, (ii) $S^1 \times S^2$'s and (iii) $K(\pi, 1)$ spaces. We recall that a $K(\pi, 1)$ space is one whose universal cover is contractible, for example, a 3-torus. Now, by a result of Gromov and Lawson [12], a manifold that admits a metric of positive scalar curvature cannot have any $K(\pi, 1)$ spaces in its prime decomposition. Moreover, by the positive resolution of the Poincaré conjecture, the only homotopy 3-sphere is the 3-sphere. The theorem follows.

All the 3-manifolds listed in Theorem 7.4.2 admit metrics of positive scalar curvature, but so far only the S^3 and $S^1 \times S^2$ topologies have been realized by asymptotically flat stationary black hole spacetimes obeying the Einstein equations. Further restrictions on the horizon topology have been obtained under the assumption of additional symmetries. For example, in [13] it was shown that, for asymptotically flat stationary vacuum black holes in five dimensions with two commuting axial symmetries, the horizon must be topologically a 3-sphere, an $S^1 \times S^2$ or a lens space. If there is only one axial symmetry, which is guaranteed to be the case for analytic asymptotically flat stationary vacuum black holes [14, 15], some restrictions on the horizon topology beyond Theorem 7.4.2 can still be obtained. Roughly, in this case it was shown in [16] that the horizon is either a connected sum of lens spaces and $S^1 \times S^2$'s (with at least one $S^1 \times S^2$ present) or one of several possible quotients of S^3 by isometries. Topological censorship [17–19] and certain techniques used in our proof of Theorem 7.4.1 are two of the ingredients used in the proof in [16], which involves a detailed analysis of the quotient of a horizon cross section by the $U(1)$ action.

7.5 The proof of Theorem 7.4.1

Let the setting be as in the statement of Theorem 7.4.1. As noted earlier, the proof, like Hawking's, is variational in nature. We consider a one-parameter deformation (or variation) $t \rightarrow \Sigma_t$ of $\Sigma = \Sigma_0$ with initial deformation velocity $v = \partial/\partial t|_{t=0} = \phi v$, where we recall that v is the outward-pointing unit normal to Σ in V and ϕ is a smooth function on Σ . Such a deformation can be achieved by, for each $x \in \Sigma$,

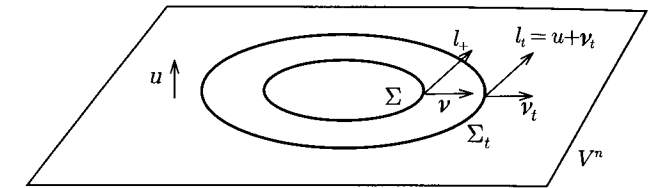


Figure 7.7

moving along the geodesic starting at x with initial velocity $\phi v|_x$ at time t . For t sufficiently small, this produces a smooth variation of Σ (see Fig. 7.7).

Let $\theta(t)$ denote the null expansion of Σ_t with respect to $l_t = u + v_t$, where v_t is the outward unit normal field to Σ_t in V . A computation shows that [20]

$$\frac{\partial \theta}{\partial t} \Big|_{t=0} = L(\phi), \quad (7.4)$$

where $L : C^\infty(\Sigma) \rightarrow C^\infty(\Sigma)$ is the operator given by

$$L(\phi) = -\Delta\phi + 2(X, \nabla\phi) + (\frac{1}{2}S - T(u, l_+) - \frac{1}{2}|\chi_+|^2 + \operatorname{div} X - |X|^2)\phi. \quad (7.5)$$

In the above, Δ , ∇ and div are the Laplacian, gradient and divergence operators respectively, on Σ ; S is the scalar curvature of Σ ; X is the vector field on Σ dual to the 1-form $K(v, \cdot)|_\Sigma$; $\langle \cdot, \cdot \rangle$ denotes the induced γ metric on Σ ; L is referred to as the stability operator associated with variations in the null expansion θ . In the time-symmetric case considered in [21], the vector field X vanishes, and L reduces to the classical stability operator of minimal surface theory.

Now consider the eigenvalue problem

$$L(\phi) = \lambda\phi. \quad (7.6)$$

Here L is a second-order linear elliptic operator that, owing to its first-order term, is not in general self-adjoint. As such it may have some nonreal eigenvalues. Nevertheless, as discussed in [20, 22], its *principal eigenvalue* λ_1 (i.e., the eigenvalue with smallest real part) is necessarily real and, moreover, one can choose a principal eigenfunction ϕ (hence satisfying $L(\phi) = \lambda_1\phi$) that is strictly positive: $\phi > 0$. Using the eigenfunction ϕ to define our variation, we have from (7.4)

$$\frac{\partial \theta}{\partial t} \Big|_{t=0} = \lambda_1\phi. \quad (7.7)$$

The eigenvalue λ_1 cannot be negative, for otherwise (7.7) would imply that $\partial\theta/\partial t < 0$ on Σ . Since $\theta = 0$ on Σ , this would mean that, for $t > 0$ sufficiently small, Σ_t would be outer trapped, contrary to our assumption that Σ is an outermost MOTS.

Hence $\lambda_1 \geq 0$, and we conclude for the variation determined by the positive eigenfunction ϕ that $\partial\theta/\partial t|_{t=0} = L(\phi) \geq 0$. By completing the square on the right-hand side of (7.5), we see that this implies that the following inequality holds:

$$-\Delta\phi + (Q + \operatorname{div} X)\phi + \phi|\nabla \ln \phi|^2 - \phi|X - \nabla \ln \phi|^2 \geq 0, \quad (7.8)$$

where, for notational convenience, we have put

$$Q = \frac{1}{2}S - T(u, l_+) - \frac{1}{2}|\chi_+|^2. \quad (7.9)$$

Setting $u = \ln \phi$ we obtain

$$-\Delta u + Q + \operatorname{div} X - |X - \nabla u|^2 \geq 0. \quad (7.10)$$

As a side remark, we see, on integrating this inequality, that the total scalar curvature of Σ is nonnegative and in fact is positive except under special circumstances. In four spacetime dimensions one may then apply the Gauss–Bonnet theorem to recover Hawking’s theorem; in fact this is essentially Hawking’s original argument. However, in higher dimensions the positivity of the total scalar curvature, in and of itself, does not provide any topological information.

To proceed, we first absorb the Laplacian term $\Delta u = \operatorname{div}(\nabla u)$ in (7.10) into the divergence term, to obtain

$$Q + \operatorname{div}(X - \nabla u) - |X - \nabla u|^2 \geq 0. \quad (7.11)$$

Setting $Y = X - \nabla u$, we arrive at the inequality

$$-Q + |Y|^2 \leq \operatorname{div} Y. \quad (7.12)$$

Now comes a simple but critical estimate, of a sort first considered in [23]. Given any $\psi \in C^\infty(\Sigma)$, we multiply through by ψ^2 and derive

$$\begin{aligned} -\psi^2 Q + \psi^2 |Y|^2 &\leq \psi^2 \operatorname{div} Y \\ &= \operatorname{div}(\psi^2 Y) - 2\psi \langle \nabla \psi, Y \rangle \\ &\leq \operatorname{div}(\psi^2 Y) + 2|\psi| |\nabla \psi| |Y| \\ &\leq \operatorname{div}(\psi^2 Y) + |\nabla \psi|^2 + \psi^2 |Y|^2. \end{aligned} \quad (7.13)$$

Integrating the above inequality yields

$$\int_\Sigma |\nabla \psi|^2 + Q\psi^2 \geq 0 \quad \text{for all } \psi \in C^\infty(\Sigma), \quad (7.14)$$

where Q is given in (7.9).

Now consider the eigenvalue problem

$$\hat{L}(\phi) = \lambda\phi, \quad (7.15)$$

where $\hat{L} : C^\infty(\Sigma) \rightarrow C^\infty(\Sigma)$ is the second-order linear elliptic operator given by

$$\hat{L}(\phi) = -\Delta\phi + Q\phi, \quad (7.16)$$

obtained formally from (7.5) by setting $X = 0$. For self-adjoint operators of the form (7.16), the Rayleigh formula [24] and an integration by parts gives the following standard characterization of the principal eigenvalue $\hat{\lambda}_1$ of \hat{L} ,

$$\begin{aligned} \hat{\lambda}_1 &= \inf_{\psi \neq 0} \frac{\int_\Sigma \psi \hat{L}(\psi) d\mu}{\int_\Sigma \psi^2 d\mu} \\ &= \inf_{\psi \neq 0} \frac{\int_\Sigma |\nabla \psi|^2 + Q\psi^2 d\mu}{\int_\Sigma \psi^2 d\mu}. \end{aligned} \quad (7.17)$$

It now follows from (7.14) that $\hat{\lambda}_1 \geq 0$. At this stage, the proof has reduced ‘morally’ to the time-symmetric case considered in [21], and the remainder of the argument can proceed in a similar fashion.

Let $\hat{\phi}$ be an eigenfunction associated with $\hat{\lambda}_1$; $\hat{\phi}$ can be chosen to be strictly positive: $\hat{\phi} > 0$. Consider Σ in the conformally related metric $\hat{\gamma} = \hat{\phi}^{2/n-2}\gamma$. By a standard formula for conformally related metrics, the scalar curvature \hat{S} of Σ in the metric $\hat{\gamma}$ is given by

$$\begin{aligned} \hat{S} &= \hat{\phi}^{-n/(n-2)} \left(-2\Delta\hat{\phi} + S\hat{\phi} + \frac{n-1}{n-2} \frac{|\nabla\hat{\phi}|^2}{\hat{\phi}} \right) \\ &= \hat{\phi}^{-2/(n-2)} \left(2\hat{\lambda}_1 + 2T(u, l_+) + |\chi_+|^2 + \frac{n-1}{n-2} \frac{|\nabla\hat{\phi}|^2}{\hat{\phi}^2} \right), \end{aligned} \quad (7.18)$$

where, for the second equation, we have used (7.15) and (7.16), with $\phi = \hat{\phi}$, and (7.9).

Since, by the dominant energy condition we have $T(u, l_+) \geq 0$, (7.18) implies that $\hat{S} \geq 0$. If $\hat{S} > 0$ at some point then by well-known results [25] one can conformally change $\hat{\gamma}$ to a metric of strictly positive scalar curvature, and the theorem follows. If \hat{S} vanishes identically then, by (7.18), $\hat{\lambda}_1 = 0$, $T(u, l_+) \equiv 0$, $\chi_+ \equiv 0$ and $\hat{\phi}$ is constant. Equations (7.15) and (7.16), with $\phi = \hat{\phi}$, and (7.9) then imply that $S \equiv 0$. By a result of Bourguignon (see [25]), it follows that Σ carries a metric of positive scalar curvature unless it is Ricci flat. Theorem 7.4.1 now follows.

Remark With regard to the assumption that Σ is an outermost marginally outer-trapped surface, the proof shows that it is sufficient to assume the existence of a positive ($v = \phi v$ with $\phi > 0$) variation $t \rightarrow \Sigma$, such that $\partial\theta/\partial t|_{t=0} \geq 0$. Such a MOTS is called stable in [20, 22], and arguments in [20, 22] show that Σ is stable if and only if $\lambda_1 \geq 0$, where λ_1 is the principal eigenvalue of the operator L given by (7.5). So, in other words, in Theorem 7.4.1 it is sufficient to assume that the MOTS Σ is stable.

7.6 The borderline case

A drawback of Theorem 7.4.1 is that if the dominant energy condition (DEC) along Σ does not hold strictly then this allows certain possibilities that one would prefer to rule out. For example, the possibility of a vacuum black hole spacetime with toroidal horizon topology remains. Eventually, however, we were able to remove the exceptional case (the “unless” clause) in Theorem 7.4.1 altogether, and hence prove the following.

Theorem 7.6.1 ([26]) Let V^n , $n \geq 3$, be a spacelike hypersurface in a spacetime obeying the DEC. If Σ^{n-1} is an outermost MOTS in V^n then Σ^{n-1} is of positive Yamabe type.

Thus, without exception, cross sections of the event horizon in asymptotically flat stationary black hole spacetimes obeying the DEC condition are of positive Yamabe type. In particular, there can be no toroidal horizons.

We remark that it is not sufficient to assume in Theorem 7.6.1 that Σ is stable, in the sense described at the end of section 7.5; there are counter examples in this case.

Theorem 7.6.1 is an immediate consequence of the following rigidity result.

Theorem 7.6.2 ([26]) Let V^n , $n \geq 3$, be a spacelike hypersurface in a spacetime obeying the DEC. Suppose that Σ is a MOTS in V such that there are no outer-trapped surfaces ($\theta_+ < 0$) outside and homologous to Σ . If Σ is not of positive Yamabe type then there exists an outer neighborhood $U \approx [0, \epsilon) \times \Sigma$ of Σ in V such that each slice $\Sigma_t = \{t\} \times \Sigma$, $t \in [0, \epsilon)$, is a MOTS.

Thus, if Σ is not of positive Yamabe type there would have to exist either an outer-trapped or marginally outer-trapped surface outside and homologous to Σ , and hence Σ would not be outermost.

We will make a brief comment about the proof of Theorem 7.6.2. The proof consists of two steps. In the first step one uses Theorem 7.4.1 and an inverse function

theorem to obtain an outer foliation $t \rightarrow \Sigma_t$, $0 \leq t \leq \epsilon$, of surfaces Σ_t of constant outer null expansion, $\theta(t) = c_t$. The second step involves showing that the constants c_t are zero. This latter step requires a reduction to the case where V has nonpositive mean curvature near Σ , which is achieved by a small spacetime deformation of V in a neighborhood of Σ . The proof makes use of the formula for the t -derivative $\partial\theta/\partial t$, not just at $t = 0$, where $\theta = 0$, but all along the foliation $t \rightarrow \Sigma_t$ where, a priori, $\theta(t)$ need not be zero. Thus, additional terms appear in the expression for $\partial\theta/\partial t$ beyond those in (7.4) and (7.5), including a term involving the mean curvature of V , and account needs to be taken of these terms. See [26] for details.

7.7 Effect of the cosmological constant

Now suppose that spacetime obeys the Einstein equation with cosmological term,

$$\text{Ric} - \frac{1}{2}Rg = \mathcal{T} - \Lambda g. \quad (7.19)$$

It is sufficient for the proof of Theorem 7.4.1 that the effective energy-momentum tensor $\mathcal{T}' = \mathcal{T} - \Lambda g$ should satisfy

$$\mathcal{T}'(u, l_+) = \mathcal{T}(u, l_+) + \Lambda \geq 0.$$

In particular, if the fields contributing to \mathcal{T} obey the DEC and $\Lambda \geq 0$ then Theorem 7.4.1 remains valid (similarly for Theorem 7.6.1).

However, if $\Lambda < 0$ then the effective DEC may fail to hold, and in this case Hawking’s arguments and the generalization of those arguments presented here do not yield any topological conclusions. Indeed, as discussed in Chapter 1, there are four-dimensional asymptotically locally anti-de Sitter vacuum black holes with horizon topology that of a surface of arbitrary genus. Higher-dimensional versions of these “topological” black holes were considered in, for example [27, 28].

Nevertheless, as Gibbons pointed out in [29], although Hawking’s theorem does not hold in the asymptotically locally anti-de Sitter setting, his basic argument still leads to an interesting conclusion. Gibbons showed that, for a time-symmetric ($K = 0$) spacelike hypersurface V in a four-dimensional spacetime M satisfying the Einstein equation (7.19), such that \mathcal{T} obeys the DEC and $\Lambda < 0$, an outermost MOTS Σ (which in this case is a minimal surface) must satisfy the area bound

$$\text{area}(\Sigma) \geq \frac{4\pi(g-1)}{|\Lambda|}, \quad (7.20)$$

where g is the genus of Σ . Woolgar [30] obtained a similar bound in the general, non-time-symmetric, case. Hence, for stationary black holes in this setting, the black hole entropy has a lower bound depending on a global topological invariant, namely, the Euler characteristic $\chi_\Sigma = 2 - 2g$.

In [21], Gibbon's result was extended to higher-dimensional spacetimes. There it was shown, in the time-symmetric case, that a bound similar to that obtained by Gibbons still holds, but in this bound the genus is replaced by the so-called σ -constant (or Yamabe invariant). The σ -constant is an invariant of smooth compact manifolds that in dimension 2 reduces to a multiple of the Euler characteristic. More recently, it was shown in [31] that, using arguments similar to those presented here to generalize Hawking's black hole topology theorem, this lower area bound can be extended to the non-time-symmetric case. We will take a moment to describe this result.

We begin by recalling the definition of the σ -constant. Let Σ^{n-1} , $n \geq 3$, be a smooth compact (without boundary) $(n-1)$ -dimensional manifold. If g is a Riemannian metric on Σ^{n-1} , let $[g]$ denote the class of metrics conformally related to g . The Yamabe constant with respect to $[g]$, which we denote by $\mathcal{Y}[g]$, is the number

$$\mathcal{Y}[g] = \inf_{\tilde{g} \in [g]} \frac{\int_{\Sigma} S_{\tilde{g}} d\mu_{\tilde{g}}}{(\int_{\Sigma} d\mu_{\tilde{g}})^{(n-3)/(n-1)}}, \quad (7.21)$$

where $S_{\tilde{g}}$ and $d\mu_{\tilde{g}}$ are respectively the scalar curvature and volume measure of Σ^{n-1} in the metric \tilde{g} . The quotient of integrals is just the volume-normalized total scalar curvature of (Σ, \tilde{g}) . The solution to the Yamabe problem due to Yamabe, Trudinger, Aubin and Schoen guarantees that the infimum in (7.21) is achieved by a metric of constant scalar curvature.

The σ -constant of Σ is defined as the supremum of the Yamabe constants over all conformal classes,

$$\sigma(\Sigma) = \sup_{[g]} \mathcal{Y}[g]. \quad (7.22)$$

As observed by Aubin, the supremum is finite and, in fact, bounded above in terms of the volume of the standard unit $(n-1)$ -sphere $S^{n-1} \subset \mathbb{R}^n$. The σ -constant divides the family of compact manifolds into three classes, according to: (i) $\sigma(\Sigma) > 0$, (ii) $\sigma(\Sigma) = 0$ and (iii) $\sigma(\Sigma) < 0$.

In the case $\dim \Sigma = 2$, the Gauss–Bonnet theorem implies that $\sigma(\Sigma) = 4\pi\chi(\Sigma) = 8\pi(1-g)$. Note that the inequality (7.20) gives information only when $\chi(\Sigma) < 0$. Correspondingly, in higher dimensions we shall be interested only in the case $\sigma(\Sigma) < 0$. It follows from the resolution of the Yamabe problem that $\sigma(\Sigma) \leq 0$ if and only if Σ does not carry a metric of positive scalar curvature. In this case, and with $\dim \Sigma = 3$, Anderson [32] showed, as an application of Perelman's work on the geometrization conjecture, that if Σ is hyperbolic, i.e. it carries a metric of constant curvature -1 , then the σ -constant is achieved for this metric and so $\sigma(\Sigma) < 0$.

Turning to the spacetime setting, we have the following result.

Theorem 7.7.1 ([31]) Let V^n , $n \geq 4$, be a spacelike hypersurface in a spacetime satisfying the Einstein equations (7.19), such that the fields giving rise to \mathcal{T} obey the DEC and $\Lambda < 0$. Let Σ^{n-1} be an outermost MOTS in V^n such that $\sigma(\Sigma) < 0$. Then the $(n-1)$ -volume of Σ satisfies

$$\text{vol}(\Sigma^{n-1}) \geq \left(\frac{|\sigma(\Sigma)|}{2|\Lambda|} \right)^{(n-1)/2}. \quad (7.23)$$

In fact, for this result it is sufficient that Σ be stable. We refer the reader to [31] for further details.

7.8 Further constraints on black hole topology

In section 7.8.1 we briefly describe some major developments in the study of manifolds of positive scalar curvature, which have led to restrictions on the topology of manifolds of positive Yamabe type. In section 7.8.2 we consider some restrictions on the horizon topology in six-dimensional black holes arising from cobordism theory. For the results on 4-manifolds referred to below, see, e.g., [33].

7.8.1 Obstructions to the existence of positive scalar curvature metrics

As we have shown, for spacetimes obeying the dominant energy condition, outermost MOTSs, in particular, cross sections of the event horizon in stationary black holes, must admit metrics of positive scalar curvature. In section 7.4 we described how this requirement restricts the horizon topology of five-dimensional black holes. The general problem of determining obstructions to the existence of positive scalar curvature metrics has been studied for many years. The first major result in this direction in higher dimensions was due to Lichnerowicz [34]. Using a Bochner-type argument he showed that if Σ is a compact spin manifold with a metric of positive scalar curvature then the kernel and cokernel of the Dirac operator vanish. In particular, if Σ has dimension $4k$ then the so-called \hat{A} -genus, which agrees with the index of the Dirac operator, must vanish, $\hat{A}(\Sigma) = 0$. In the case where Σ is four dimensional, the \hat{A} -genus is related to the intersection form $Q_{\Sigma} : H^2(\Sigma; \mathbb{Z}) \times H^2(\Sigma; \mathbb{Z}) \rightarrow \mathbb{Z}$ by $\hat{A}(\Sigma) = -\frac{1}{8}\sigma(\Sigma)$, where $\sigma(\Sigma)$ is the signature of Q_{Σ} .⁶ But there are known to be infinitely many smooth compact

⁶ By de Rham's theorem, modulo torsion, the classes $\alpha, \beta \in H^2(\Sigma; \mathbb{Z})$ can be represented by 2-forms α^*, β^* ; then $Q_{\Sigma}(\alpha, \beta) = \int_{\Sigma} \alpha^* \wedge \beta^*$.

spin-4 manifolds with nonzero signature, the $K3$ surface being one such example. Moreover, there are higher-dimensional analogues of the $K3$ surface that have nonzero \hat{A} -genus; see e.g., [35, p. 298]. As a consequence, all these examples fail to admit metrics of positive scalar curvature. In [36] Hitchin generalized the vanishing theorem of Lichnerowicz and obtained the surprising result that, in every dimension $k > 8$, there are smooth manifolds Σ^k , homeomorphic to the standard sphere S^k , that do not admit metrics of positive scalar curvature; these manifolds must be exotic spheres.

While these results are quite striking, they left open some very basic questions, for example, whether the k -torus, $k \geq 3$, admits a metric of positive scalar curvature. Then, in [37] Schoen and Yau made a major advance by proving, using minimal surface techniques, that if the fundamental group of a compact orientable 3-manifold contains a subgroup isomorphic to the fundamental group of a surface of genus $g \geq 1$ then the manifold does not admit a metric of positive scalar curvature. Hence, in particular, the 3-torus does not admit a metric of positive scalar curvature. In [38] Schoen and Yau generalized their techniques to higher dimensions, thereby establishing inductively the existence of a large class of compact manifolds, including tori, of dimension up to 7, that do not admit metrics of positive scalar curvature. The fundamental observation made in [38] is that if Σ^n , $3 \leq n \leq 7$, is a compact orientable manifold of positive scalar curvature then any nontrivial codimension-1 homology class can be represented by a manifold that admits a metric of positive scalar curvature. This was proved by choosing a manifold of least area in the homology class and making use of the positivity of the minimal surface stability operator, “rearranged” in an especially useful way.

Another very important development in the study of manifolds of positive scalar curvature was the introduction by Gromov and Lawson of the notion of *enlargability* [12, 39, 40]. In [12] they extended their methods to noncompact manifolds, which required an adaptation of Dirac operator methods to noncompact manifolds and which enabled them to strengthen some of their previous results. For example, using these improved techniques they were able to show that a compact 3-manifold that has a $K(\pi, 1)$ factor in its prime decomposition cannot admit a metric of positive scalar curvature, a result we used in section 7.4. They also proved the following.

Theorem 7.8.1 ([12]) A compact manifold of arbitrary dimension that admits a metric of nonpositive sectional curvature cannot admit a metric of positive scalar curvature.

In the context of the results discussed in sections 7.4 and 7.6, this rules out many obvious horizon topologies, including tori of all dimensions.

Finally, we mention that Seiberg–Witten theory provides further examples of compact simply connected 4-manifolds that do not admit metrics of positive scalar curvature. This relies on the following vanishing theorem (see e.g., [33]): if Σ is a compact 4-manifold with $b_2^+(\Sigma) \geq 2$, where $b_2^+(\Sigma)$ is the number of positive eigenvalues of the intersection form of Σ (or, equivalently, the dimension of the space of self-dual harmonic 2-forms), and Σ admits a metric of positive scalar curvature then the Seiberg–Witten invariants of Σ vanish. The proof is again a Bochner-type argument, now based on the *coupled* Lichnerowicz equation. This, in addition to the scalar curvature of Σ , includes a term involving the curvature of the connection on the determinant line bundle of the specified complex spin structure. At the same time, there are well-known classes of compact simply connected 4-manifolds that have nonvanishing Seiberg–Witten invariants (see e.g., [33]).

7.8.2 Cobordism constraints on four-dimensional horizons

Consider a six-dimensional asymptotically flat black hole spacetime M . One can imagine (and even construct under suitable circumstances) a smooth spacelike hypersurface V in M that meets the event horizon H in a smooth compact 4-manifold Σ and extends out to spatial infinity. In this situation Σ will be *cobordant* to a large sphere $\Sigma' \approx S^4$ out near infinity. That is, there is a compact region W in V whose boundary ∂W is the (appropriately oriented) union of Σ and Σ' . In [41] the authors examine, among other things, the consequences of the fact that Σ is cobordant to a 4-sphere, while taking advantage of the 4-manifold classification theorem of Freedman and subsequent work of Donaldson. (See [33] for a nice exposition of these results.) For this discussion, which refines that in [41], it is assumed that Σ is simply connected.

In addition to these classification results, the key fact is the following. If two compact oriented 4-manifolds are cobordant then they have the same signature. Hence, since Σ is cobordant to S^4 , $\sigma(\Sigma) = 0$.

Now, from Freedman’s classification of simply connected 4-manifolds in terms of intersection forms, the algebraic classification of intersection forms (as symmetric bilinear unimodular forms), and the restrictions on smooth 4-manifolds imposed by Donaldson’s work we know the following [33].

Theorem 7.8.2 Every smooth compact simply connected 4-manifold is homeomorphic to S^4 or to one of the following connected sums,

- (i) $(\#m\mathbb{CP}^2) \# (\#n\overline{\mathbb{CP}}^2)$,
- (ii) $(\#m S^2 \times S^2) \# (\#n\mathcal{E}_8)$ or $(\#m S^2 \times S^2) \# (\#n(-\mathcal{E}_8))$.

Recall that \mathbb{CP}^2 is the complex projective plane, $\overline{\mathbb{CP}}^2$ is the same as the latter but with the opposite orientation, \mathcal{E}_8 is the 4-manifold discovered by Freedman

with intersection-form the E_8 lattice and $-\mathcal{E}_8$ is the same as the latter but with the opposite orientation.

Using the fact that the signature is additive with respect to connected sums, i.e.,

$$\sigma(\Sigma_1 \# \Sigma_2) = \sigma(\Sigma_1) + \sigma(\Sigma_2),$$

along with the basic signature values $\sigma(\mathbb{CP}^2) = 1$, $\sigma(\overline{\mathbb{CP}}^2) = -1$, $\sigma(\pm \mathcal{E}_8) = \pm 8$ and $\sigma(S^2 \# S^2) = 0$, we see that the vanishing of the signature of Σ implies in (i) above that $m = n$ and in (ii) above that $n = 0$.

We conclude that, for our cross section of the event horizon Σ , if it is simply connected as well as cobordant to S^4 then it must be homeomorphic to S^4 or to a finite connected sum of $S^2 \times S^2$'s or to a finite connected sum of $\mathbb{CP}^2 \# \overline{\mathbb{CP}}^2$'s. In particular, Σ cannot be homeomorphic to \mathbb{CP}^2 (as observed in [42]) or to a $K3$ surface.

We obtain further restrictions on the topology of Σ if we assume in addition that Σ is a spin manifold. This would be the case for example if the spacelike hypersurface V is a spin manifold, for then Σ would inherit a spin structure from V . If Σ is a spin manifold then its second Stiefel–Whitney class $w_2 \in H^2(\Sigma, \mathbb{Z}_2)$, the obstruction to its being a spin manifold, must vanish. In turn it follows from Wu's formula [33] that the intersection form of Σ is even, i.e., for all classes α , $Q_\Sigma(\alpha, \alpha)$ is even. This rules out the connected sums of $\mathbb{CP}^2 \# \overline{\mathbb{CP}}^2$'s, and we finally arrive at the following. *The cross section of the event horizon Σ , if it is simply connected and a spin manifold, as well as cobordant to S^4 , must be homeomorphic to S^4 or to a finite connected sum of $S^2 \times S^2$'s.*

It is worth noting that black hole dimension 6 is the first dimension where cobordism theory becomes useful. This is due to the nontrivial fact, relevant to five-dimensional black holes, that any two compact 3-manifolds are (oriented) cobordant. In addition, it is a fact that the region “filling in” two k -dimensional (oriented) cobordant manifolds, $k \geq 3$, can be taken to be simply connected. It is for this reason that topological censorship, which would imply in the discussion above that V is simply connected, does not provide any general constraints on horizon topology in five or higher spacetime dimensions.⁷

7.9 Final remarks

In section 7.8.1 we focused on negative results concerning the existence of metrics of positive scalar curvature. There are also many positive results. For instance, there are the “gluing” (or surgery) results obtained independently, and using different methods, by Schoen and Yau [38] and Gromov and Lawson [40]. These show, in

particular, that the connected sum of manifolds admitting metrics of positive scalar curvature admits a metric of positive scalar curvature. That is, positive Yamabe type is preserved under connected sums. Using these surgery results and techniques and results from cobordism theory, Gromov and Lawson [40] were able to prove the following. Suppose that Σ is compact, simply connected, with dimension $k \geq 5$.

- (i) If Σ is not a spin manifold then Σ admits a metric of positive scalar curvature.
- (ii) If Σ is a spin manifold and is spin cobordant to a manifold that admits a metric of positive scalar curvature then Σ admits a metric of positive scalar curvature.

Since the spin cobordism groups are trivial in dimensions $k = 5, 6$ and 7 , it follows that every compact simply connected manifold of dimension 5, 6 or 7 admits a metric of positive scalar curvature.

We make one further completely elementary observation. Any manifold of the form $S^k \times M$, where $k \geq 2$ and M is any compact manifold, admits a metric of positive scalar curvature. Indeed, if g' is a round metric on S^k of radius r and g'' is any metric on M then the product metric $g' \oplus g''$ will have positive scalar curvature provided that one takes r to be sufficiently small.

Thus, while the requirement that the horizon be of positive Yamabe type puts rather strong restrictions on the topology of three-dimensional horizons (as discussed in section 7.4), the situation becomes considerably more flexible in higher dimensions. Indeed, the constraints on horizon topology described in this chapter still allow for a wide variety of possible topologies. The method of blackfolds to be discussed in Chapter 8 provides an approach to realizing many such topologies; see also [43]. The higher-dimensional near-horizon geometries constructed, for example, in [44], many of which satisfy both the constraint of being positive Yamabe and that of being cobordant to spheres, suggest even more possibilities.

References

- [1] S. Alexakis, A. D. Ionescu, and S. Klainerman, Uniqueness of smooth stationary black holes in vacuum: small perturbations of the Kerr spaces, *Commun. Math. Phys.* **299** (2010), 89–127.
- [2] S. W. Hawking and G. F. R. Ellis, *The Large Scale Structure of Space-Time*, Cambridge University Press (1973).
- [3] R. Emparan and H. S. Reall, A rotating black ring solution in five dimensions, *Phys. Rev. Lett.* **88** (2002), 101 101.
- [4] G. J. Galloway and R. Schoen, A generalization of Hawking's black hole topology theorem to higher dimensions, *Commun. Math. Phys.* **266** (2006), 571–576.
- [5] S. W. Hawking, The event horizon., in *Black Holes*, Les Houches Lectures, eds. H. C. DeWitt and B. S. DeWitt (1973), pp. 1–55.
- [6] A. Ashtekar and B. Krishnan, Isolated and dynamical horizons and their applications, *Living Rev. in Rel.* **7** (2004).

⁷ An exception to this can occur when symmetries permit dimensional reduction; cf., [16, 19].

- [7] L. Andersson, M. Eichmair, and J. Metzger, Jang's equation and its applications to marginally trapped surfaces, in *Complex Analysis and Dynamical Systems IV: Part 2. General Relativity, Geometry and PDE*, Contemporary Mathematics, vol. 554, American Mathematical Society (2011).
- [8] L. Andersson and J. Metzger, The area of horizons and the trapped region, *Commun. Math. Phys.* **290** (2009), 941–972.
- [9] M. Eichmair, The plateau problem for marginally outer trapped surfaces, *J. Differential Geom.* **83** (2009), 551–583.
- [10] M. Eichmair, Existence, regularity, and properties of generalized apparent horizons, *Commun. Math. Phys.* **294** (2010), 745–760.
- [11] J. Hempel, *3-Manifolds*, (1976) Princeton University Press, Ann. of Math. Studies, No. 86.
- [12] M. Gromov and H. B. Lawson, Positive scalar curvature and the Dirac operator on complete Riemannian manifolds, *Inst. Hautes Études Sci. Publ. Math.* **58** (1983), 83–196.
- [13] S. Hollands and S. Yazadjiev, Uniqueness theorem for 5-dimensional black holes with two axial Killing fields, *Commun. Math. Phys.* **283** (2008), 749–768.
- [14] S. Hollands, A. Ishibashi, and R. M. Wald, A higher dimensional stationary rotating black hole must be axisymmetric, *Commun. Math. Phys.* **271** (2007), 699–722.
- [15] V. Moncrief and J. Isenberg, Symmetries of higher dimensional black holes, *Class. Quant. Grav.* **25** (2008), 195015.
- [16] S. Hollands, J. Holland, and A. Ishibashi, Further restrictions on the topology of stationary black holes in five dimensions (2010), arXiv:1002.0490.
- [17] J. L. Friedman, K. Schleich, and D. M. Witt, Topological censorship, *Phys. Rev. Lett.* **71** (1993), 1486–1489.
- [18] G. J. Galloway, K. Schleich, D. M. Witt, and E. Woolgar, Topological censorship and higher genus black holes, *Phys. Rev.* **D60** (1999), 104039.
- [19] P. T. Chruściel, G. J. Galloway, and D. Solis, Topological censorship for Kaluza–Klein space-times, *Ann. Henri Poincaré* **10** (2009), 893–912.
- [20] L. Andersson, M. Mars, and W. Simon, Stability of marginally outer trapped surfaces and existence of marginally outer trapped tubes, *Adv. Theor. Math. Phys.* **12** (2008), 853–888.
- [21] M. Cai and G. J. Galloway, On the topology and area of higher-dimensional black holes, *Class. Quant. Grav.* **18** (2001), 2707–2718.
- [22] L. Andersson, M. Mars, and W. Simon, Local existence of dynamical and trapping horizons, *Phys. Rev. Lett.* **95** (2005), 111102.
- [23] R. Schoen and S.-T. Yau, Proof of the positive mass theorem. II, *Commun. Math. Phys.* **79** (1981), 231–260.
- [24] L. C. Evans, *Partial Differential Equations*, second edition, Graduate Studies in Mathematics, vol. 19, American Mathematical Society (2010).
- [25] J. L. Kazdan and F. W. Warner, Prescribing curvatures, in *Differential Geometry Proc. Sympos. Pure Math.*, vol. XXVII, American Mathematical Society (1975), pp. 309–319.
- [26] G. J. Galloway, Rigidity of marginally trapped surfaces and the topology of black holes, *Commun. Anal. Geom.* **16** (2008), 217–229.
- [27] D. Birmingham, Topological black holes in anti-de Sitter space, *Class. Quant. Grav.* **16** (1999), 1197–1205.
- [28] R. B. Mann, Topological black holes – outside looking in, in *Proc. Conf. on Internal Structure of Black Holes and Spacetime Singularities*, Haifa 1997, *Ann. Israel Phys. Soc.*, vol. 13, IOP (1997), pp. 311–342.

- [29] G. W. Gibbons, Some comments on gravitational entropy and the inverse mean curvature flow, *Class. Quant. Grav.* **16** (1999), 1677–1687.
- [30] E. Woolgar, Bounded area theorems for higher-genus black holes, *Class. Quant. Grav.* **16** (1999), 3005–3012.
- [31] G. J. Galloway and N. Ó Murchadha, Some remarks on the size of bodies and black holes, *Class. Quant. Grav.* **25** (2008), 105009.
- [32] M. T. Anderson, Canonical metrics on 3-manifolds and 4-manifolds, *Asian J. Math.* **10** (2006), 127–163.
- [33] A. Scorpan, *The Wild World of 4-Manifolds*, American Mathematical Society (2005).
- [34] A. Lichnerowicz, Spineurs harmoniques, *C. R. Acad. Sci. Paris* **257** (1963), 7–9.
- [35] H. B. Lawson, Jr. and M.-L. Michelsohn, *Spin Geometry*, Princeton Mathematical Series, vol. 38, Princeton University Press (1989).
- [36] N. Hitchin, Harmonic spinors, *Adv. Math.* **14** (1974), 1–55.
- [37] R. Schoen and S.-T. Yau, Existence of incompressible minimal surfaces and the topology of three-dimensional manifolds with nonnegative scalar curvature, *Ann. Math.* **110** (1979), 127–142.
- [38] R. Schoen and S.-T. Yau, On the structure of manifolds with positive scalar curvature, *Manuscripta Math.* **28** (1979), 159–183.
- [39] M. Gromov and H. B. Lawson, Spin and scalar curvature in the presence of a fundamental group. I, *Ann. Math.* **111** (1980), 209–230.
- [40] M. Gromov and H. B. Lawson, Jr., The classification of simply connected manifolds of positive scalar curvature, *Ann. Math.* **111** (1980), 423–434.
- [41] C. Helfgott, Y. Oz, and Y. Yanay, On the topology of stationary black hole event horizons in higher dimensions, *J. High Energy Phys.* (2006), 025 (electronic).
- [42] H. S. Reall, Higher dimensional black holes and supersymmetry, *Phys. Rev.* **D68** (2003), 024024.
- [43] F. Schwartz, Existence of outermost apparent horizons with product of spheres topology, *Commun. Anal. Geom.* **16** (2008), 799–817.
- [44] H. K. Kunduri and J. Lucietti, An infinite class of extremal horizons in higher dimensions, *Commun. Math. Phys.* **303** (2011), 31–71.

8

Blackfolds

ROBERTO EMPARAN

8.1 Introduction

The existence of black p -branes in higher-dimensional general relativity hints at the possibility of large classes of black holes without any four-dimensional counterpart. Black rings provide a nice explicit example; in Chapter 6 they were introduced as the result of the bending of a black string into the shape of a circle and spinning it up to balance forces. One can naturally expect that this heuristic construction extends to other black branes. If the worldvolume of a black p -brane could be similarly bent into the shape of a compact hypersurface, for instance that of a torus T^p or a sphere S^p , we would obtain many new geometries and topologies of black hole horizons.

Unfortunately, the techniques that allow one to construct *exact* black hole solutions in four and five dimensions have not been successfully extended to more dimensions. Still, one may want to hold on to the intuition that a long circular black string, or more generally a smoothly bent black brane, could be obtained as a perturbation of a straight one.

The experience with brane-like objects in other areas of physics suggests that such approximate methods may be efficiently applied to this problem. Consider, for instance, the Abelian Higgs theory and its familiar string-like vortex solutions. These are first obtained in the form of static straight strings, but one would expect that they can also bend and vibrate. It has been long recognized that, if the wavelength of these deformations is much longer than the thickness of the vortex, the dynamics of the full nonlinear theory is well approximated by the simpler Nambu–Goto worldsheet action. One can then use the latter for studying loops of strings of diverse shape. Another example is provided by D-branes in string theory, which are defined as surfaces where open strings can attach their endpoints (see Chapter 11).

Although the bending and vibrations of D-branes are generally intractable in an exact manner in string theory, they are again very efficiently captured by the Dirac–Born–Infeld worldvolume field theory, which is applicable as long as the scale of the deformations is sufficiently large that locally the brane can still be well approximated as a flat D-brane. In all these cases the full dynamics of the brane is replaced by an effective worldvolume theory for a set of “collective coordinates”.

Similarly, we seek an effective theory for describing black branes whose worldvolume is not exactly flat, or not in stationary equilibrium, but where the deviations from the flat stationary black brane occur on scales much longer than the brane thickness. Black branes whose worldvolume is bent into the shape of a submanifold of a background spacetime have been named *blackfolds*.

This chapter introduces the blackfold effective worldvolume theory for the dynamics of black branes, as well as its use as an approximate method for the construction of new black hole solutions [1–3]. Of special interest is a class of helical black rings that provide the first example of black holes in all dimensions $D \geq 5$ with the minimum of symmetry required by rigidity theorems. We also explain how the theory is useful for the analysis of dynamical nonstationary situations, in particular, of the Gregory–Laflamme instability of black branes reviewed in Chapter 2. The blackfold techniques connect it very directly to the instability of an effective “black brane fluid”, in a manner that shares features with the fluid–gravity correspondence considered in Chapter 13.

A word about notation in this chapter. When considering a p -brane with worldvolume \mathcal{W}_{p+1} embedded in a D -dimensional background spacetime, we write

$$n = D - p - 3. \quad (8.1)$$

Spacetime indices μ, ν run over $0, \dots, D$ and the covariant derivative compatible with the background metric $g_{\mu\nu}(x)$ is ∇_μ . Worldvolume indices a, b run over $0, \dots, p$, and the covariant derivative compatible with the metric $\gamma_{ab}(\sigma)$ induced on \mathcal{W}_{p+1} is D_a .

8.2 Effective theory for black hole motion

Above we motivated the blackfold effective approach by drawing analogies between black branes and the extended brane-like solutions of other nonlinear theories. However, the general-relativistic aspects of the effective theory of black p -brane dynamics are better introduced by considering first the simpler case $p = 0$, the effective dynamics of a black hole that moves in a background whose curvature radii $\sim R$ are large compared with the black hole horizon radius r_0 ,

$$r_0 \ll R. \quad (8.2)$$

This separation of scales implies the existence of two distinct regions in the geometry. First, there is a region around the black hole where the geometry is well approximated by the Schwarzschild(–Tangherlini) solution. If in this “near zone” we choose a coordinate r centered at the black hole, the Schwarzschild geometry is a good approximation as long as $r \ll R$, i.e.,

$$ds_{(\text{near})}^2 = ds^2(\text{Schwarzschild}) + O(r/R). \quad (8.3)$$

The corrections to the Schwarzschild metric are the (tidal) distortions that the background curvature creates on the black hole.

The second region is far enough from the black hole that its effect on the background geometry is very mild and can be treated as a small perturbation. This is the “far zone” where $r \gg r_0$ and in which we can make the expansion

$$ds_{(\text{far})}^2 = ds^2(\text{background}) + O(r_0/r). \quad (8.4)$$

Since we are too far from the black hole to resolve its size, effectively it is a point-like source whose gravitational effect on the background can be computed perturbatively. To this source we can assign an effective trajectory $X^\mu(\tau)$, with proper time τ and velocity $\dot{X}^\mu = \partial_\tau X^\mu$ such that $g_{\mu\nu}\dot{X}^\mu\dot{X}^\nu = -1$. We also ascribe to it an effective stress–energy tensor that encodes how the black hole affects the gravitational field in the far zone.

Let us determine the general form of this stress–energy tensor. We can assume in a natural way that the acceleration and other higher derivatives of the particle’s velocity are small, since they must be caused by deviations from flatness of the background in the region where the black hole moves. Since these variations occur on scales $\sim R$, these higher-derivative terms must be suppressed by powers of r_0/R . To leading order in this expansion, the stress–energy tensor of the effective source is determined by symmetry and worldline reparameterization invariance to have the form

$$T^{\mu\nu} = m \dot{X}^\mu \dot{X}^\nu. \quad (8.5)$$

In principle the coefficient m can also depend on τ . This tensor is understood to be localized at $x^\mu = X^\mu(\tau)$.

In effect we are replacing the entire near-zone geometry with a pointlike object. In the language of effective field theories, we are “integrating out” the short-wavelength degrees of freedom of the near zone and replacing them with an effective worldline theory of a point particle. The coefficient m must then be related through a matching calculation to a parameter of the “microscopic” configuration, which in this case can only be the horizon size r_0 . The matching condition is that the gravitational field of the effective source reproduces that of the black hole in the

far zone. Thanks to the separation of scales (8.2) the near and far zones overlap in

$$r_0 \ll r \ll R, \quad (8.6)$$

so we can match the fields there. On the one hand, in this region the near-zone Schwarzschild solution is in a weak-field regime and can be linearized around Minkowski spacetime. On the other hand, the background curvature of the far-zone geometry can be neglected in (8.6), so that the far field is the linear perturbation of Minkowski spacetime sourced by (8.5). It is now clear that these two fields are the same if m is equal to the ADM mass of the Schwarzschild solution with horizon radius r_0 , so that¹

$$m = \frac{(D-2)\Omega_{D-2}}{16\pi G} r_0^{D-3}, \quad (8.7)$$

where Ω_{D-2} is the volume of the unit $(D-2)$ -sphere. This result is the first step in the method of matched asymptotic expansions [4]. One can now proceed to solve the Einstein equations in a perturbative manner, first in the far zone, including the backreaction from the particle by means of suitable asymptotic conditions, and then in the near zone, where horizon regularity is imposed. At each step the solution in one zone provides boundary conditions for the equations to be solved in the other zone, through the matching of fields in the overlap region. Corrections involve higher derivatives of the velocity and of r_0 .

In this matching construction, a subset of the Einstein equations can be written as equations for $r_0(\tau)$ and $X^\mu(\tau)$. Their derivation is a well-understood but technically complicated procedure. Fortunately, if we are interested only in the leading-order equations then we can use a shortcut to them by applying the main guiding principles of effective theories: symmetry and conservation laws. In this case the principle is that of general covariance, which imposes that

$$\bar{\nabla}_\mu T^{\mu\nu} = 0. \quad (8.8)$$

This is indeed naturally required for a source of the gravitational field in the far zone. Put a bit more fancifully, this equation ensures the consistency of the coupling between the short- and long-wavelength degrees of freedom.

The overbar on the covariant derivative in (8.8) indicates that (8.8) makes sense only when projected along the effective particle trajectory:

$$\bar{\nabla}_\mu = -\dot{X}_\mu \dot{X}^\nu \nabla_\nu. \quad (8.9)$$

¹ Note that $m = \dot{X}^\mu \dot{X}^\nu T_{\mu\nu} = T_{\tau\tau}$ is proportional, but not necessarily equal, to the mass measured at asymptotic infinity in the background. The relation is given by the redshift between the particle’s proper time and the asymptotic time of the background.

Nevertheless, (8.8) has components in directions both orthogonal and parallel to the particle's velocity:

$$(g_{\rho\nu} + \dot{X}_\rho \dot{X}_\nu) \bar{\nabla}_\mu T^{\mu\nu} = 0 \quad \Rightarrow \quad m a^\mu = 0 , \quad (8.10)$$

$$\dot{X}_\nu \bar{\nabla}_\mu T^{\mu\nu} = 0 \quad \Rightarrow \quad \partial_\tau m(\tau) = 0 ; \quad (8.11)$$

here $a^\mu = D_\tau \dot{X}^\mu = \dot{X}^\nu \nabla_\nu \dot{X}^\mu$ is the effective-particle acceleration. The first equation is the geodesic equation determining the trajectory of a test particle.² The second equation implies that m is a constant along the trajectory.

Geodesic motion is so familiar that the effective theory for a black hole becomes of real interest only when it includes corrections to the leading-order equations [4]. In contrast, we will see that for black p -branes with $p > 0$ the effective theory already yields nontrivial results at leading order. The method of matched asymptotic expansions (or the closely related classical effective theory of [6]) provides the conceptual backdrop to the blackfold approach but at the practical level we will remain at the leading-order approximation, in which the black brane is a “test brane” in a background spacetime.

8.3 Effective blackfold theory

8.3.1 Collective field variables

Our aim is to extend the effective worldline theory of black holes to a worldvolume theory that describes the collective dynamics of a black p -brane.

The geometry of a flat static black p -brane in D spacetime dimensions is given by

$$ds^2 = - \left(1 - \frac{r_0^n}{r^n}\right) dt^2 + \sum_{i=1}^p (dz^i)^2 + \left(1 - \frac{r_0^n}{r^n}\right)^{-1} dr^2 + r^2 d\Omega_{n+1}^2 . \quad (8.12)$$

As in the previous example, the parameters of this solution include the “horizon thickness” r_0 and the $D - p - 1$ coordinates that parameterize the position of the brane in directions transverse to the worldvolume, which we denote collectively by X^\perp (making them explicit in the metric is possible but cumbersome). But now we must also include the possibility of a velocity u^i along the worldvolume of the brane. A covariant form of the boosted black brane metric is obtained by first introducing coordinates $\sigma^a = (t, z^i)$ that span the brane worldvolume having

² There is a long history of deriving the geodesic equation for a small particle (not necessarily a black hole) from the Einstein field equations; see [5] for a recent rigorous version. This can be taken as a confirmation of our generic symmetry argument.

Minkowski metric η_{ab} and a velocity u^a such that $u^a u^b \eta_{ab} = -1$. Then

$$ds^2 = \left(\eta_{ab} + \frac{r_0^n}{r^n} u_a u_b \right) d\sigma^a d\sigma^b + \left(1 - \frac{r_0^n}{r^n} \right)^{-1} dr^2 + r^2 d\Omega_{n+1}^2 . \quad (8.13)$$

Constant shifts of r_0 , of u^i , and of X^\perp still give solutions to the Einstein equations. In total, we have D zero modes, which yield D collective coordinates of the black brane. The long-wavelength effective theory describes fluctuations in which these variables change slowly on the worldvolume \mathcal{W}_{p+1} , over a large length scale $R \gg r_0$. Typically R is set by the smallest extrinsic curvature radius of \mathcal{W}_{p+1} or by the gradient of $\ln r_0$ along the worldvolume. Background curvatures may also be present but they are usually already accounted for by the extrinsic curvature they induce on \mathcal{W}_{p+1} .

With this variation the worldvolume metric deviates from the Minkowski metric η_{ab} , and the near-zone geometry is of the form

$$ds^2 = \left(\gamma_{ab}(X^\mu(\sigma)) + \frac{r_0^n(\sigma)}{r^n} u_a(\sigma) u_b(\sigma) \right) d\sigma^a d\sigma^b + \left(1 - \frac{r_0^n(\sigma)}{r^n} \right)^{-1} dr^2 + r^2 d\Omega_{n+1}^2 + \dots \quad (8.14)$$

where the dependence of γ_{ab} on the transverse coordinates gives rise to an extrinsic curvature of the worldvolume and the dots indicate that additional terms, of order $O(r_0/R)$, are required for this to be a solution to Einstein's equations.³

When $r \gg r_0$ this metric must match the geometry of the far-zone background with metric $g_{\mu\nu}$, in the region $r \ll R$ around the worldvolume of an infinitely thin brane at $x^\mu = X^\mu(\sigma)$. Thus we identify γ_{ab} with the metric induced on the effective brane worldvolume:

$$\gamma_{ab} = g_{\mu\nu} \partial_a X^\mu \partial_b X^\nu . \quad (8.15)$$

Again, we are replacing the near-zone geometry with an infinitely thin p -brane, with worldvolume \mathcal{W}_{p+1} , embedded in the background geometry.

8.3.2 Effective stress–energy tensor

The stress–energy tensor of the black brane is, like the mass m of the black hole in the previous example, computed in the overlap region $r_0 \ll r \ll R$ where the deviations away from Minkowski spacetime are small. It can be obtained as a generalization of the ADM mass or, equivalently, from the Brown–York quasilocal

³ This is very similar to the long-wavelength perturbation of anti-de Sitter black branes studied in Chapter 13.

stress-energy tensor [7]. This is computed on a timelike surface with induced metric $\tilde{h}_{\mu\nu}$ (not to be confused with $h_{\mu\nu}$ below) and extrinsic curvature $\Theta_{\mu\nu}$ as

$$T_{\mu\nu}^{(ql)} = \frac{1}{8\pi G} (\Theta_{\mu\nu} - \tilde{h}_{\mu\nu} \Theta) . \quad (8.16)$$

When measured at constant $r \gg r_0$, the divergent contributions to this tensor, which grow with r , can be subtracted in any conventional way; for instance, the method of background subtraction from Minkowski space is good enough for our purposes. Then, equivalently, this is the stress-energy tensor of a domain wall that encloses empty space and creates a field outside it equal to that of the black brane. This interpretation fits well with the idea that we are replacing the black brane with an effective source.

The surface at large constant r , where the quasilocal tensor $T_{\mu\nu}^{(ql)}$ is computed, has geometry $\mathbb{R}^{1,p} \times S^{n+1}$. We integrate the tensor over the sphere to obtain the stress-energy tensor of the black p -brane:

$$T_{ab} = \int_{S^{n+1}} T_{ab}^{(ql)} dS , \quad (8.17)$$

with components along the worldvolume directions.

For the boosted black p -brane (8.13) the result of this calculation is

$$T^{ab} = \frac{\Omega_{(n+1)}}{16\pi G} r_0^n (nu^a u^b - \eta^{ab}) . \quad (8.18)$$

This amounts to the stress-energy tensor of an isotropic perfect fluid,

$$T^{ab} = (\varepsilon + P)u^a u^b + P\eta^{ab} , \quad (8.19)$$

where the energy density ε and pressure P are given by

$$\varepsilon = \frac{\Omega_{(n+1)}}{16\pi G} (n+1)r_0^n , \quad P = -\frac{\Omega_{(n+1)}}{16\pi G} r_0^n . \quad (8.20)$$

In the rest frame of the fluid, and at any given point on the worldvolume, the Bekenstein–Hawking identification between horizon area and entropy applies to the black hole obtained by compactifying the p directions along the brane. Thus we identify an entropy density s from the horizon area density of (8.12):

$$s = \frac{\Omega_{(n+1)}}{4G} r_0^{n+1} . \quad (8.21)$$

Locally, we also have the conventional relation between surface gravity and temperature,

$$\mathcal{T} = \frac{n}{4\pi r_0} , \quad (8.22)$$

expressed in a way such that the first law of black hole thermodynamics applies in the local form

$$d\varepsilon = \mathcal{T}ds . \quad (8.23)$$

In addition, the Euler–Gibbs–Duhem relation,

$$\varepsilon + P = \mathcal{T}s , \quad (8.24)$$

is verified.

After introducing a slow variation of the collective coordinates the stress-energy tensor becomes

$$T^{ab}(\sigma) = \frac{\Omega_{(n+1)}}{16\pi G} r_0^n(\sigma) (nu^a(\sigma)u^b(\sigma) - \gamma^{ab}(\sigma)) + \dots , \quad (8.25)$$

where the ellipses stand for terms with gradients of $\ln r_0$, u^a , and γ_{ab} that are responsible for dissipative effects which we are taking to be small. We neglect them for now but will return to some of them in section 8.6.

8.3.3 Blackfold dynamics

In order to obtain equations for the collective variables we need to recall a few notions about the geometry of worldvolume embeddings. More details and proofs are provided in the appendix to this chapter.

Worldvolume geometry

The worldvolume \mathcal{W}_{p+1} is embedded in a background with metric $g_{\mu\nu}$, and its induced metric is (8.15). The indices μ, ν are raised and lowered using $g_{\mu\nu}$, and those of a, b using γ_{ab} . The first fundamental form of the submanifold,

$$h^{\mu\nu} = \partial_a X^\mu \partial_b X^\nu \gamma^{ab} , \quad (8.26)$$

acts as a projector onto \mathcal{W}_{p+1} (for a worldline, $h^{\mu\nu} = -\dot{X}^\mu \dot{X}^\nu$), and the tensor

$$\perp_{\mu\nu} = g_{\mu\nu} - h_{\mu\nu} \quad (8.27)$$

projects along directions orthogonal to it.

The background tensors $t^{\mu\dots v\dots}$ can be converted into worldvolume tensors $t^{a\dots b\dots}$ and vice versa using the pull-back map $\partial_a X^\mu$, a relevant example being the stress-energy tensor

$$T^{\mu\nu} = \partial_a X^\mu \partial_b X^\nu T^{ab} . \quad (8.28)$$

The covariant differentiation of these background tensors is well defined only along tangential directions, which we denote by an overbar:

$$\overline{\nabla}_\mu = h_\mu^\nu \nabla_\nu . \quad (8.29)$$

The divergence of the stress-energy tensor, projected parallel to \mathcal{W}_{p+1} , satisfies (see (8.138) below)

$$h^\rho_\nu \overline{\nabla}_\mu T^{\mu\nu} = \partial_b X^\rho D_a T^{ab} . \quad (8.30)$$

The *extrinsic curvature tensor*

$$K_{\mu\nu}^\rho = h_\mu^\sigma \overline{\nabla}_\nu h_\sigma^\rho = -h_\mu^\sigma \overline{\nabla}_\nu \perp_\sigma^\rho \quad (8.31)$$

is tangent to \mathcal{W}_{p+1} along its (symmetric) lower indices μ, ν and orthogonal to \mathcal{W}_{p+1} along ρ . Its trace is the *mean curvature vector*

$$K^\rho = h^{\mu\nu} K_{\mu\nu}^\rho = \overline{\nabla}_\mu h^{\mu\rho} . \quad (8.32)$$

A useful result is that, for any two vectors s^μ and t^μ tangent to \mathcal{W}_{p+1} ,

$$s^\mu t^\nu K_{\mu\nu}^\rho = \perp_\mu^\rho \nabla_s t^\mu = \perp_\mu^\rho \nabla_t s^\mu . \quad (8.33)$$

Blackfold equations

The classical dynamics of a generic brane was studied by Carter [8]. The equations are formulated in terms of a stress-energy tensor supported on, and tangent to, the $(p+1)$ -dimensional brane worldvolume \mathcal{W}_{p+1} :

$$\perp_\mu^\rho T^{\mu\nu} = 0 . \quad (8.34)$$

As in the $p=0$ example, general covariance implies that the stress-energy tensor must obey the equations

$$\overline{\nabla}_\mu T^{\mu\rho} = 0 . \quad (8.35)$$

This is a consequence of the underlying conservative dynamics of the full general relativity theory, but the effective worldvolume theory may be dissipative.

The expression on the left-hand side of (8.35) can be written as

$$\begin{aligned} \overline{\nabla}_\mu T^{\mu\rho} &= \overline{\nabla}_\mu (T^{\mu\nu} h_\nu^\rho) = T^{\mu\nu} \overline{\nabla}_\mu h_\nu^\rho + h_\nu^\rho \overline{\nabla}_\mu T^{\mu\nu} \\ &= T^{\mu\nu} K_{\mu\nu}^\rho + \partial_b X^\rho D_a T^{ab} , \end{aligned} \quad (8.36)$$

where in the last line we have used (8.30) and (8.31). Thus the D equations (8.35) separate into $D-p-1$ extrinsic equations in directions orthogonal to \mathcal{W}_{p+1} and

$p+1$ intrinsic equations parallel to \mathcal{W}_{p+1} :

$$T^{\mu\nu} K_{\mu\nu}^\rho = 0 \quad (\text{extrinsic equations}) , \quad (8.37)$$

$$D_a T^{ab} = 0 \quad (\text{intrinsic equations}) . \quad (8.38)$$

The extrinsic equations can be regarded as a generalization to p -branes of the geodesic equation (8.10) (where the acceleration is the extrinsic curvature of the worldline, $a^\rho = -K^\rho$). In other words, this is the generalization of Newton's equation “mass \times acceleration = 0” to relativistic extended objects. The second set of equations, (8.38), expresses energy-momentum conservation on the worldvolume. For a black hole this is a rather trivial equation, but for a p -brane we get all the complexity of the hydrodynamics of a perfect fluid.

If we insert the stress-energy tensor of the black brane, (8.18), and use (8.33) then the extrinsic equations (8.37) become

$$K^\rho = n \perp_\mu^\rho \dot{u}^\mu \quad (8.39)$$

and the intrinsic equations (8.38) become

$$\dot{u}_a + \frac{1}{n+1} u_a D_b u^b = \partial_a \ln r_0 . \quad (8.40)$$

Here $\dot{u}^\mu = u^\nu \nabla_\nu u^\mu$ and $\dot{u}^b = u^c D_c u^b$.

Equations (8.39) and (8.40) are the *blackfold equations*, a set of D equations that describe the dynamics of the D collective variables of a neutral black brane (a “test brane”) in the approximation where we neglect its backreaction on the background as well as the dissipative effects on its worldvolume.

8.3.4 Blackfold boundaries

The worldvolume of a black p -brane may have boundaries specified by a function $f(\sigma^a)$ such that $f|_{\partial\mathcal{W}_{p+1}} = 0$. If the effective fluid remains within these boundaries then the velocity must remain parallel to them,

$$u^a \partial_a f|_{\partial\mathcal{W}_{p+1}} = 0 . \quad (8.41)$$

If the boundary is “free”, i.e., there is no surface tension, then the Euler (force) equations for a generic perfect fluid require that the pressure vanishes at the boundary. For the black brane this requirement is given as

$$r_0|_{\partial\mathcal{W}_{p+1}} = 0 . \quad (8.42)$$

Geometrically, this means that the horizon must approach zero size at the boundary, so the horizon closes off at the edge of the blackfold.

8.3.5 Blackfold as a black hole

The blackfold construction puts, on any point in the worldvolume \mathcal{W}_{p+1} , a (small) transverse sphere s^{n+1} with Schwarzschild radius $r_0(\sigma)$. If \mathcal{B}_p is a spatial section of \mathcal{W}_{p+1} then the geometry of the horizon is the product of \mathcal{B}_p and s^{n+1} ; the product is warped since the radius $r_0(\sigma)$ of s^{n+1} varies along \mathcal{B}_p . If r_0 is nonzero everywhere on \mathcal{B}_p then the s^{n+1} are trivially fibered on \mathcal{B}_p and the horizon topology is the product topology of \mathcal{B}_p and the sphere.

The regularity of this horizon in the perturbative expansion, in which it is distorted by long-wavelength fluctuations, is believed to be satisfied when the blackfold equations, which incorporate local thermodynamic equilibrium, are satisfied. A complete proof is still lacking, but [9] and [10] provide evidence that this is true for, respectively, extrinsic and intrinsic deformations.

As we have seen, at the boundaries of \mathcal{B}_p the size of s^{n+1} vanishes, so the horizon topology will be different. The regularity of the horizon at these boundaries is not fully understood yet; it appears to depend on the specific type of boundary. We will return to this issue later.

8.4 Stationary blackfolds, action principle, and thermodynamics

Equilibrium configurations for blackfolds that remain stationary in time are of particular interest, since they correspond to stationary black holes. Requiring stationarity allows us to solve explicitly the intrinsic equations for the thickness r_0 and velocity u^a , so that one is left with only the extrinsic equations for the worldvolume embedding $X^\mu(\sigma)$.

8.4.1 Solution to the intrinsic equations

For a fluid configuration to be stationary, dissipative effects must be absent. In general this requires that the shear and expansion of its velocity field u vanish. One can then prove, using the fluid equations, that u must be proportional to a (worldvolume) Killing field $k = k^a \partial_a$. That is,

$$u = \frac{k}{|k|}, \quad |k| = \sqrt{-\gamma_{ab} k^a k^b}, \quad (8.43)$$

where k satisfies the worldvolume Killing equation $D_{(a} k_{b)} = 0$. Actually, we will assume that this Killing vector on the worldvolume is the pull-back of a timelike Killing vector $k^\mu \partial_\mu$ in the background,

$$\nabla_{(\mu} k_{\nu)} = 0, \quad (8.44)$$

such that $k_a = \partial_a X^\mu k_\mu$. The existence of this timelike Killing vector field is in fact a necessary assumption if we intend to describe stationary black holes.

The Killing equation (8.44) implies that

$$\nabla_{(\mu} u_{\nu)} = -u_{(\mu} \nabla_{\nu)} \ln |k|, \quad (8.45)$$

so the acceleration is

$$\dot{u}^\mu = \partial^\mu \ln |k|. \quad (8.46)$$

Since the expansion of u vanishes, the intrinsic equation (8.40) becomes

$$\partial_a \ln |k| = \partial_a \ln r_0, \quad (8.47)$$

so that

$$\frac{r_0}{|k|} = \text{constant}. \quad (8.48)$$

Expressed in terms of the local temperature T , (8.22), this equation says that the worldvolume variation of the temperature is dictated by the local redshift factor $|k|^{-1}$,

$$T(\sigma) = \frac{T}{|k|}. \quad (8.49)$$

This result can also be derived for a general fluid using the equations of fluid dynamics. The integration constant T can be interpreted, using the thermodynamic first law, which we will derive below, as the global temperature of the black hole. Equation (8.48) can be read as saying that the thickness

$$r_0(\sigma) = \frac{n}{4\pi T} |k| \quad (8.50)$$

adjusts its value along the worldvolume in such a way that T remains constant.

8.4.2 Extrinsic equations and action for stationary blackfolds

With the intrinsic solutions (8.46) and (8.48), the extrinsic equations (8.39) reduce to

$$\begin{aligned} K^\rho &= n \perp^{\rho\mu} \partial_\mu \ln r_0 \\ &= \perp^{\rho\mu} \partial_\mu \ln(-P). \end{aligned} \quad (8.51)$$

Using (8.145) from the chapter appendix, this equation can be equivalently found by varying, under deformations of the brane embedding, the action

$$I = \int_{\mathcal{W}_{p+1}} d^{p+1}\sigma \sqrt{-h} P. \quad (8.52)$$

This action, whose derivation actually does not assume any specific fluid equation of state, is a familiar one for branes with constant tension $-P$, whose worldvolume must be a minimal hypersurface so that $K^\rho = 0$ (an example is provided by Dirac–Born–Infeld branes with no gauge fields on their worldvolume). More generally, this is the action of a perfect fluid on \mathcal{W}_{p+1} .

Assume now that the background spacetime has a timelike Killing vector ξ , canonically normalized to generate unit time translations at asymptotic infinity and whose norm on the worldvolume is

$$-\xi^2|_{\mathcal{W}_{p+1}} = R_0^2(\sigma). \quad (8.53)$$

Let us assume further that ξ is hypersurface orthogonal, so that we can foliate the blackfold into spacelike slices \mathcal{B}_p normal to ξ . The unit normal to \mathcal{B}_p is

$$n^a = \frac{1}{R_0} \xi^a, \quad (8.54)$$

where R_0 measures the local gravitational redshift between worldvolume time and asymptotic time. Integrals over \mathcal{W}_{p+1} reduce, over an interval Δt of the Killing time generated by ξ , to integrals over \mathcal{B}_p with measure $dV_{(p)}$, so that

$$I = \Delta t \int_{\mathcal{B}_p} dV_{(p)} R_0 P. \quad (8.55)$$

Using (8.50) in (8.20) we get an expression for the action in terms of k that is very practical for deriving the extrinsic equations in explicit cases:

$$\tilde{I}[X^\mu(\sigma)] = \int_{\mathcal{B}_p} dV_{(p)} R_0 |k|^n. \quad (8.56)$$

The tilde distinguishes it from (8.55), since we have removed an overall constant factor (including a sign) that is irrelevant for obtaining the extrinsic equations.

8.4.3 Mass, angular momentum, entropy, and thermodynamics

Let k be given by a linear combination of orthogonal commuting Killing vectors of the background spacetime,

$$k = \xi + \sum_i \Omega_i \chi_i, \quad (8.57)$$

where ξ is the generator of time translations introduced above and the χ_i are generators of angular rotations in the background, normalized such that their orbits have periods 2π . Then the Ω_i are the angular velocities of the blackfold along these directions.

The mass and angular momenta of the blackfold are now given by the integrals of the energy and momentum densities over \mathcal{B}_p ,

$$M = \int_{\mathcal{B}_p} dV_{(p)} T_{ab} n^a \xi^b, \quad J_i = - \int_{\mathcal{B}_p} dV_{(p)} T_{ab} n^a \chi_i^b. \quad (8.58)$$

The total entropy is deduced from the entropy current $s^a = s(\sigma) u^a$,

$$S = - \int_{\mathcal{B}_p} dV_{(p)} s_a n^a = \int_{\mathcal{B}_p} dV_{(p)} \frac{R_0}{|k|} s(\sigma). \quad (8.59)$$

Let us now express the action (8.55) in terms of these quantities. Contracting the stress–energy tensor (8.19) with $n_a k_b$ and then using (8.24) and (8.49), we find

$$T_{ab} n^a \left(\xi^b + \sum_i \Omega_i \chi_i^b \right) + T s u^a n_a = n^a k_a P = -R_0 P, \quad (8.60)$$

and so, integrating over \mathcal{B}_p ,

$$I = -\Delta t \left(M - TS - \sum_i \Omega_i J_i \right). \quad (8.61)$$

This is an action in real Lorentzian time but, since we are dealing with time-independent configurations, we can rotate to Euclidean time with periodicity $1/T$ and recover the relation between the Euclidean action and the thermodynamic grand-canonical potential, $I_E = W[T, \Omega_i]/T$.

The identity (8.61) holds for any embedding, not necessarily one that is a solution to the extrinsic equations, so if we regard M , J_i , and S as functionals of the $X^\mu(\sigma)$ and consider variations where T and Ω_i are held constant then we have

$$\frac{\delta I[X^\mu]}{\delta X^\mu} = 0 \quad \Leftrightarrow \quad \frac{\delta M}{\delta X^\mu} = T \frac{\delta S}{\delta X^\mu} + \sum_i \Omega_i \frac{\delta J_i}{\delta X^\mu}. \quad (8.62)$$

Therefore the extrinsic equations are equivalent to the requirement that the first law of black hole thermodynamics holds for variations of the embedding.

Equation (8.61), Wick-rotated to $I_E[X^\mu]$, is therefore an effective worldvolume action that approximates, to leading order in r_0/R , the Euclidean gravitational action of the black hole. We might have taken this thermodynamic effective action as the starting point for the theory of stationary blackfolds, but we have preferred to work with the equations of motion. These allow us to consider situations away from stationary equilibrium and they also make more explicit the connection with worldvolume fluid dynamics.

Performing manipulations similar to those leading to (8.60) one finds that

$$(D-3)M - (D-2) \left(TS + \sum_i \Omega_i J_i \right) = \mathcal{T}_{\text{tot}} , \quad (8.63)$$

where

$$\mathcal{T}_{\text{tot}} = - \int_{\mathcal{B}_p} dV_{(p)} R_0 (\gamma^{ab} + n^a n^b) T_{ab} \quad (8.64)$$

is the total tensional energy obtained by integrating the local tension over the blackfold volume.

The Smarr relation for asymptotically flat vacuum black holes in D dimensions [11],

$$(D-3)M - (D-2) \left(TS + \sum_i \Omega_i J_i \right) = 0 , \quad (8.65)$$

must be recovered when the extrinsic equations for equilibrium are satisfied for a blackfold with compact \mathcal{B}_p in a Minkowski background where $R_0 = 1$. Thus, extrinsic equilibrium in Minkowski backgrounds implies that

$$\mathcal{T}_{\text{tot}} = 0 . \quad (8.66)$$

If the tensional energy did not vanish, this would imply the presence of sources of tension acting on the blackfold, e.g., in the form of conical or stronger singularities of the background space.

Another general identity is obtained by noticing that the blackfold fluid satisfies (see (8.49))

$$-P = \frac{1}{n} \mathcal{T} s . \quad (8.67)$$

Integrating (8.67) and using (8.61) we get

$$M - TS - \sum_i \Omega_i J_i = \frac{1}{n} TS , \quad (8.68)$$

or, in terms of the Euclidean action, $I_E = S/n$.

Note that, while the thermodynamic form of the action (8.61) and the Smarr relation (8.65) are exactly valid for neutral black holes, (8.63) and (8.68) hold only to leading order in the expansion in r_0/R .

8.4.4 Stationary blackfold boundaries

Let us now investigate what it means, for a stationary blackfold, that the thickness vanishes at its boundary, (8.42).

On the one hand, in section 8.4.2 we introduced the generators of unit time translations at asymptotic infinity, ξ^a , and on \mathcal{W}_{p+1} , n^a , which are related by the factor R_0 that measures the gravitational redshift between these two locations. On the other hand, relative to the worldvolume time generated by n^a , a fluid element on \mathcal{W}_{p+1} has a Lorentz-boost gamma factor

$$-n^a u_a = \frac{1}{\sqrt{1-v^2}} , \quad (8.69)$$

where v is the local fluid velocity,

$$v^2 = \sum_i v_i^2 , \quad v_i = \frac{\Omega_i |\chi_i|}{R_0} . \quad (8.70)$$

Since the velocity u^a is determined by (8.43) and (8.57), we have $\xi^a u_a = \xi^a \xi_a / |k| = -R_0^2 / |k|$ and

$$-n^a u_a = -\frac{1}{R_0} \xi^a u_a = \frac{R_0}{|k|} . \quad (8.71)$$

With (8.69), this implies that

$$|k| = R_0 \sqrt{1-v^2} . \quad (8.72)$$

At a blackfold boundary we must have $r_0 \rightarrow 0$. According to (8.48), if the blackfold is stationary then we must also have $|k| \rightarrow 0$. There are two possibilities.

- (i) $v \rightarrow 1$: the fluid velocity becomes null at the boundary. There is some evidence that in this case the full horizon is smooth; as we will see in section 8.5.1, there are blackfolds with this kind of boundary. We can compare these with the exact black hole solution for a regular horizon.
- (ii) $R_0 \rightarrow 0$: the blackfold encounters a horizon of the background, where the gravitational redshift diverges. This boundary can be regarded as an intersection of horizons, and the evidence from known exact solutions indicates that the intersection point, i.e., the blackfold boundary, is singular.

Nevertheless, the evidence for these two behaviours is largely circumstantial and it would be desirable to have a better understanding of horizon regularity at blackfold boundaries.

8.4.5 Ultra-spinning behaviour

Let us assume that all length scales along \mathcal{B}_p are of order $\sim R$ and that there are no large redshifts, of gravitational or Lorentz type, over most of the blackfold. This is satisfied naturally since redshifts become large only near the boundaries. Then,

temporarily setting $G = 1$, (8.58) and (8.59) generically give

$$M \sim R^p r_0^n, \quad J \sim R^{p+1} r_0^n, \quad S \sim R^p r_0^{n+1}. \quad (8.73)$$

This implies

$$\frac{J}{M} \sim R, \quad (8.74)$$

so that neutral blackfolds are always in an ultra-spinning regime, in which the angular momentum for fixed mass is very large. More precisely, in a neutral blackfold the length scale of angular momentum (8.74) is always much larger than the length scale of the mass $M^{1/(D-3)}$,

$$\frac{J/M}{M^{1/(D-3)}} \sim \left(\frac{r_0}{R}\right)^{(D-p-3)/(D-3)} \ll 1. \quad (8.75)$$

The entropy in (8.73) scales as

$$S(M, J) \sim J^{-p/(D-p-3)} M^{(D-2)/(D-p-3)}, \quad (8.76)$$

thus, in dimension D and for fixed mass, the most entropic solution for a given number of large angular momenta J is attained by blackfolds with the smallest p . The intuitive reason is that, for a given mass, the horizon is thicker if p is smaller – the horizon spreads out less. A thicker horizon has lower temperature and, since $TS \sim M$, the entropy is higher. In section 8.5.3 we will find that there is always a black 1-fold for any number of angular momenta, which therefore maximizes the entropy.

8.5 Examples of blackfold solutions

This formalism can be applied easily to the explicit construction of stationary black holes. Besides finding new solutions we will show that the blackfold method correctly recovers the limits in which known exact solutions become similar to black branes: the ultra-spinning regime of Myers–Perry black holes and the very-thin limit of the five-dimensional black ring, which provide nontrivial checks on the method.

8.5.1 Myers–Perry black hole as a blackfold disk

Myers–Perry black holes have ultra-spinning regimes where the geometry near the rotation axis approaches that of a black brane spread along the rotation plane [12]. This suggests that these regimes may be reproduced by blackfold constructions and indeed they are, in a rather nontrivial manner. Instead of studying the most general construction (see [3]), we will illustrate the blackfold construction in the

case of the six-dimensional black hole rotating along a single plane, which already exhibits all the relevant features.

Take $D = 6$ Minkowski spacetime as a background and a black 2-fold that extends along a plane within it (so that $n = 1$). The extrinsic equations are trivially solved, and we can restrict the analysis to the blackfold plane with polar coordinates (r, ϕ) and metric

$$ds^2 = -dt^2 + dr^2 + r^2 d\phi^2. \quad (8.77)$$

We set the blackfold in rotation along ϕ . Stationarity requires that the fluid rotates rigidly, see (8.43) and (8.57) with $\xi = \partial/\partial t$, $\chi = \partial/\partial\phi$, and angular velocity Ω , so the velocity is

$$u = \frac{1}{\sqrt{1 - \Omega^2 r^2}} \left(\frac{\partial}{\partial t} + \Omega \frac{\partial}{\partial \phi} \right). \quad (8.78)$$

The intrinsic equations are solved by appropriately redshifting the temperature, which determines the horizon thickness from (8.50) as

$$r_0(r) = \frac{1}{4\pi T} \sqrt{1 - \Omega^2 r^2}. \quad (8.79)$$

This implies that the extent of the blackfold along the rotation plane is limited to

$$0 \leq r \leq \Omega^{-1}. \quad (8.80)$$

Recall that, according to (8.42), the condition $r_0(\Omega^{-1}) = 0$ specifies a boundary of the blackfold. The effective fluid velocity becomes lightlike there and would be superluminal if we tried to go beyond this radius. Therefore the blackfold worldvolume is a disk.

It will be convenient to introduce two geometric parameters in place of T and Ω : the disk radius a and the blackfold thickness r_+ at the rotation axis:

$$a = \Omega^{-1}, \quad r_+ = r_0(0) = \frac{1}{4\pi T}. \quad (8.81)$$

What is the topology of the horizon of this blackfold? The disk is fibered at each point with a sphere S^2 of radius $r_0(r)$ that shrinks to zero at the disk's edge. Topologically, this is S^4 , the same as the topology of the horizon of the Myers–Perry black hole.

The mass and angular momentum of the blackfold are obtained from its energy and momentum densities. We have

$$T_{ab} n^a \xi^b = T_{tt} = \frac{r_+}{4G} \frac{2 - r^2/a^2}{\sqrt{1 - r^2/a^2}}, \quad (8.82)$$

$$-T_{ab} n^a \chi^b = T_{t\phi} = \frac{r_+}{4G} \frac{r^2/a}{\sqrt{1 - r^2/a^2}} \quad (8.83)$$

(since $n^a = \xi^a$). Then

$$M = \int_0^{2\pi} d\phi \int_0^a dr r T_{tt} = \frac{2\pi}{3G} r_+ a^2, \quad (8.84)$$

$$J = \int_0^{2\pi} d\phi \int_0^a dr r T_{t\phi} = \frac{\pi}{3G} r_+ a^3. \quad (8.85)$$

The entropy-density current $s^a = su^a$ gives

$$-s^a n_a = \frac{\pi}{G} r_+^2 \sqrt{1 - r^2/a^2}, \quad (8.86)$$

which integrates to

$$S = - \int_0^{2\pi} d\phi \int_0^a dr r s^a n_a = \frac{2\pi^2}{3G} r_+^2 a^2. \quad (8.87)$$

Let us now compare this result with ultra-spinning limit of the exact Myers–Perry black hole. The latter solution is specified by a mass parameter μ and a rotation parameter a . The horizon radius r_+ is obtained as the largest real root of

$$\mu = (r_+^2 + a^2)r_+. \quad (8.88)$$

In terms of these the exact mass, spin, and entropy are

$$M = \frac{2\pi}{3G} \mu, \quad J = \frac{1}{2} a M, \quad S = \frac{2\pi^2}{3G} r_+ \mu. \quad (8.89)$$

The ultra-spinning regime $J \rightarrow \infty$ with fixed M is obtained as $a \rightarrow \infty$. In this limit (8.88) becomes

$$\mu \rightarrow a^2 r_+, \quad (8.90)$$

and the physical quantities (8.89) become precisely the same as (8.84), (8.85), (8.87), after identifying the parameters r_+ and a .

This identification of parameters is in fact geometrically meaningful. For an ultra-spinning black hole the radii of the horizon in directions transverse and parallel to the rotation plane are [12]

$$r_\perp^{\text{MP}} \rightarrow r_+ \cos \theta, \quad r_\parallel^{\text{MP}} \rightarrow a, \quad (8.91)$$

where θ is the polar angle on the horizon. For the blackfold disk we have seen already that the radius in the plane parallel to the rotation is $r_\parallel^{\text{bf}} = a$. The square root in (8.79) suggests that we should introduce a polar angle $\theta = \arcsin(r/a)$ such that the thickness of the blackfold in directions transverse to the rotation plane is

$$r_\perp^{\text{bf}} = r_0(r) = r_+ \cos \theta. \quad (8.92)$$

Identifying this polar angle with that in the Myers–Perry solution, we find a perfect match of the two sides.

Since the horizon of the Myers–Perry solution is smooth, this example yields evidence of regularity at the boundary of the blackfold, where the fluid velocity becomes lightlike.

8.5.2 Curving black strings: black rings

We now consider stationary black one-folds (i.e., curved black strings) in a Minkowski background

$$ds^2 = -dt^2 + d\mathbf{x}_{(D-1)}^2 \quad (8.93)$$

with stationarity Killing vector $\xi = \partial/\partial t$, so that $R_0 = 1$.

Stationarity requires that the black string lies along a spatial Killing direction. Then the simplest way to solve the extrinsic equations is by imposing the condition that the tensional energy vanishes, (8.66). Since the string lies along an isometry, the integral in (8.64) is trivial and so the integrand, i.e., the tension measured relative to the frame defined by ξ , must vanish:

$$\text{tension} = -(\gamma^{ab} + \xi^a \xi^b) T_{ab} = 0. \quad (8.94)$$

Let us write

$$-\xi^a u_a = \cosh \sigma, \quad (8.95)$$

so that σ is the rapidity parameterizing the relative boost between the fluid and the background frame of observers along orbits of ξ . For a generic perfect fluid, the zero-tension condition (8.94) is

$$0 = (\gamma^{ab} + \xi^a \xi^b) \left[(\varepsilon + P) u_a u_b + P \gamma_{ab} \right] = \varepsilon \sinh^2 \sigma + P \cosh^2 \sigma. \quad (8.96)$$

Therefore, at equilibrium the fluid velocity $\tanh \sigma$ is fixed:

$$\tanh^2 \sigma = -\frac{P}{\varepsilon}. \quad (8.97)$$

Since $-P/\varepsilon$ is actually the square of the velocity of transverse elastic waves along the string, we see that the bending of the string can be regarded as the effect of its supporting a stationary elastic wave.

For the specific black string fluid (8.20), the condition (8.97) can be written as

$$\sinh^2 \sigma = \frac{1}{n}. \quad (8.98)$$

When $n = 1$, i.e., in $D = 5$, this is precisely the value for the boost found in Chapter 6 from the exact black ring solution, in the limit where the ring is very thin and long, $r_0/R \rightarrow 0$. In this case the black string lies along a circle of radius R on a plane within \mathbb{R}^4 .

It is straightforward to calculate (8.58) and (8.59) and to check that, with this value of the boost, the blackfold construction reproduces all the physical magnitudes of the exact black ring solution, to leading order in r_0/R . Beyond this order, in [9] the first corrections to the metric were computed; again, perfect agreement was found with the perturbative expansion of the exact solution in $D = 5$ and a check was made that horizon regularity is preserved for any $D \geq 5$.

8.5.3 Helical black rings and minimal rigidity

The previous construction did not specify the geometry of the curve along which the string lies. However, as we saw, this curve must lie along a spatial isometry of Euclidean space \mathbb{R}^{D-1} . If we are interested in blackfolds of finite extent, which correspond to asymptotically flat black objects, this isometry must be compact and therefore generated by rotational Killing vectors $\partial/\partial\phi_i$. Thus, if we write the subspace of \mathbb{R}^{D-1} in which the embedding of the string is nontrivial as

$$ds^2 = \sum_{i=1}^m (dr_i^2 + r_i^2 d\phi_i^2) \quad (8.99)$$

then the string lies along the curve

$$r_i = R_i, \quad \phi_i = n_i \sigma, \quad 0 \leq \sigma < 2\pi. \quad (8.100)$$

The upper limit

$$m \leq \left\lfloor \frac{D-1}{2} \right\rfloor = \left\lfloor \frac{n+3}{2} \right\rfloor$$

is set by the rank of the spatial rotation group in $D = n + 4$ spacetime dimensions. The $D - 2m - 2$ dimensions of space that are not explicit in (8.99) are orthogonal to the string and we will ignore them. They play a role only in providing, together with the m directions r_i , the $n + 2$ dimensions orthogonal to the worldsheet in which the horizon of the black string is “thickened” into a transverse S^{n+1} of radius r_0 .

The n_i must be integers in order that the curve is closed. Without loss of generality we may assume that $n_i \geq 0$. If we want to avoid multiple covering of the curve then the smallest n_i (which need not be unique), say n_1 , must be coprime with all the n_i . Thus the set of n_i can be specified by m positive rational numbers $n_i/n_1 \geq 1$.

If all $n_i = 1$ then we obtain a circular planar ring along an orbit of $\sum_i \partial_{\phi_i}$ with radius $\sqrt{\sum_i R_i^2}$. If, instead, at least two n_i are nonzero and are not both equal to 1 then we obtain *helical black rings*. Together with planar black rings, this exhausts all possible stationary black 1-folds in a Minkowski background with a spatially compact worldsheet.

The Killing generator of the worldsheet velocity field is

$$k = \frac{\partial}{\partial t} + \sum_i \Omega_i \frac{\partial}{\partial \phi_i}, \quad (8.101)$$

where the ratios of angular velocities must be rational,

$$\left| \frac{\Omega_i}{\Omega_j} \right| = \frac{n_i}{n_j} \quad \forall i, j, \quad (8.102)$$

and the equilibrium condition (8.98) implies that

$$\sum_{i=1}^m \Omega_i^2 R_i^2 = \frac{1}{n+1}. \quad (8.103)$$

The physical properties (mass, spins, entropy, etc.) of helical black rings in the approximation $r_0/R_i \ll 1$ were computed in [3]. It has been found that helical black rings are the solutions with the largest entropy among all blackfolds with given values of mass and angular momenta. Among helical black rings, the maximal entropy for a given set of values of the angular momenta is achieved by minimizing the n_i , since this makes the ring shorter and hence thicker. For a single angular momentum, the planar black ring maximizes the entropy.

Maximal symmetry breaking and saturation of the rigidity theorem

A spacetime containing a helical ring has the isometry generated by

$$\sum_i n_i \frac{\partial}{\partial \phi_i} \quad (8.104)$$

along the direction of the string. However, in general this string breaks other $U(1)$ isometries of the background, possibly leaving (8.104) as the only spatial Killing vector of the configuration.

In order to prove this point, observe that any additional $U(1)$ symmetry must leave the curve invariant, i.e., the curve must lie at a fixed point of the isometry. That is, the curve must be on a point in some plane in \mathbb{R}^{D-1} , so rotations in this plane around the point leave it invariant. Let us parameterize the most general

possible helical curve in \mathbb{R}^{D-1} as a curve in \mathbb{C}^m , with

$$m = \left\lfloor \frac{D-1}{2} \right\rfloor,$$

of the form

$$z_i = R_i e^{in_i \sigma}, \quad (8.105)$$

where possibly some n_i are zero. In order to find a plane in which rotations leave the curve invariant we must solve the equation

$$\sum_{i=1}^m a_i z_i = 0 \quad (8.106)$$

with complex a_i , for all values of σ . This equation admits a nontrivial solution only if some n_i are equal to each other (and possibly to zero).

Therefore, if (i) the string circles around in all the $m = \lfloor (D-1)/2 \rfloor$ independent rotation planes, i.e., all the possible n_i are nonzero, and (ii) all the n_i are different from each other then the only spatial Killing vector of the configuration is (8.104). In this case we obtain an asymptotically flat helical black ring with only one spatial $U(1)$ isometry.

The black hole rigidity theorem of [13, 14] requires that stationary non-static black holes have at least one such isometry, and in [15] it had been conjectured that black holes exist with not more than this symmetry. The construction of helical black rings that rotate in all possible planes and have exactly one spatial $U(1)$ proves this conjecture in any $D \geq 5$.

8.5.4 Odd-spheres

For our final example we describe a large family of solutions for black holes in D -dimensional flat space having the horizon topology

$$\left(\prod_{p_a=\text{odd}} S^{p_a} \right) \times S^{n+1}, \quad \sum_{a=1}^{\ell} p_a = p. \quad (8.107)$$

In this case the spatial section of the blackfold worldvolume \mathcal{B}_p is a product of odd-spheres.

S^{2k+1} blackfolds

We consider first a single odd-sphere S^{2k+1} , which contains a black ring as the particular case $k=0$. We embed the sphere S^{2k+1} into a $(2k+2)$ -dimensional flat

subspace of \mathbb{R}^{D-1} with metric

$$dr^2 + r^2 d\Omega_{2k+1}^2. \quad (8.108)$$

The unit metric on S^{2k+1} can be written as

$$d\Omega_{2k+1}^2 = \sum_{i=1}^{k+1} (d\mu_i^2 + \mu_i^2 d\phi_i^2), \quad \sum_{i=1}^{k+1} \mu_i^2 = 1, \quad (8.109)$$

where ϕ_i are the angles that parameterize the Cartan subgroup of the rotation group $SO(2k+2)$.

In the general stationary case we would consider the blackfold as embedded via $r = R(\mu_1, \dots, \mu_k)$. Then the extrinsic equations give a set of differential equations for $R(\mu_i)$ involving k angular velocities Ω_i . These are complicated to solve, but they simplify to algebraic equations in the still nontrivial instance in which the sphere is geometrically round with constant radius $r = R$ and rotates with the same angular velocity Ω in all angles. Then the stationarity Killing vector is

$$k = \frac{\partial}{\partial t} + \Omega \sum_{i=1}^{k+1} \frac{\partial}{\partial \phi_i}, \quad |k| = \sqrt{1 - \Omega^2 R^2}, \quad (8.110)$$

and the blackfold is homogeneous, so that the thickness r_0 is constant over the worldvolume.

The extrinsic equations for R can be easily (and consistently) obtained from the stationary blackfold action (8.56):

$$\tilde{I}[R] = \Omega(p) R^p (1 - R^2 \Omega^2)^{n/2}, \quad p = 2k+1. \quad (8.111)$$

This is extremized when

$$R = \frac{1}{\Omega} \sqrt{\frac{p}{n+p}}. \quad (8.112)$$

Equivalently, this value makes the local tension (8.94) vanish at each point. When $p=1$ we recover the result for black rings. Having found this equilibrium radius for round blackfolds, it is straightforward to compute their physical properties [3].

Products of odd-spheres

This construction can be extended easily to solutions where \mathcal{B}_p is a product of round odd-spheres, each labeled by an index $a = 1, \dots, \ell$. Denoting the radius of the S^{p_a} factor (p_a odd) by R_a , we take the angular velocities of the a th sphere as all equal to $\Omega^{(a)}$.

We embed the product of ℓ odd-spheres in a flat $(p + \ell)$ -dimensional subspace of \mathbb{R}^{D-1} with metric

$$\sum_{a=1}^{\ell} (dr_a^2 + r_a^2 d\Omega_{(p_a)}^2) , \quad \sum_{a=1}^{\ell} p_a = p , \quad (8.113)$$

and locate the blackfold at $r_a = R_a$. Note that, given $n \geq 1$, the number ℓ of spheres in the product is limited according to $\ell \leq n + 2$.

If the spheres are geometrically round then the stationary blackfold action (8.56) reduces to

$$\tilde{I}[R_a] = \prod_{b=1}^{\ell} \Omega_{(p_b)} R_b^{p_b} \left(1 - \sum_{a=1}^{\ell} (R_a \Omega^{(a)})^2 \right)^{n/2} , \quad (8.114)$$

whose variation with respect to each R_a gives the equilibrium conditions

$$R_a = \frac{1}{\Omega^{(a)}} \sqrt{\frac{p_a}{n+p}} . \quad (8.115)$$

A simple case is the p -torus, where all $p_a = 1$. This gives black holes with horizon topology $\mathbb{T}^p \times s^{n+1}$ that rotate simultaneously along all orthogonal 1-cycles of \mathbb{T}^p .

It is easy to see that, like Myers–Perry black holes and planar black rings, these odd-sphere solutions do not break any commuting isometry of the background.

To finish this subsection we note that, except for the case of black 1-folds, our analysis has not been systematic enough to be complete, and further classes of black holes can be expected in $D \geq 6$. But, for those we have presented, already one can see that black hole uniqueness is very badly violated in higher dimensions. Note also that all these horizon topologies admit metrics of positive scalar curvature and hence are compatible with the theorems in the previous chapter.

8.6 Gregory–Laflamme instability and black brane viscosity

The blackfold approach must capture the perturbative dynamics of a black hole when the perturbation along the horizon has long wavelength λ ,

$$\lambda \gg r_0 . \quad (8.116)$$

This includes in particular intrinsic fluctuations of the black brane in which the worldvolume geometry remains flat but r_0 and u^a are allowed to vary. A variation in the thickness of the brane, δr_0 , corresponds to a variation in the pressure and density of the effective fluid. Thus, for small fluctuations we expect to recover sound waves along the brane. These turn out to be unstable in an interesting way.

8.6.1 Sound waves on a black brane

Sound waves are easily derived for a generic perfect fluid. Introduce small perturbations in an initial uniform state at rest,

$$\varepsilon \rightarrow \varepsilon + \delta\varepsilon , \quad P \rightarrow P + \frac{dP}{d\varepsilon} \delta\varepsilon , \quad u^a = (1, 0, \dots) \rightarrow (1, \delta u^i) . \quad (8.117)$$

To linear order in the perturbations, the intrinsic fluid equations (8.38) give

$$\left(\partial_t^2 - \frac{dP}{d\varepsilon} \partial_i^2 \right) \delta\varepsilon = 0 , \quad (8.118)$$

so that longitudinal sound-mode oscillations of the fluid propagate with squared speed

$$v_s^2 = \frac{dP}{d\varepsilon} . \quad (8.119)$$

Neutral blackfolds have an imaginary sound speed squared,

$$v_s^2 = -\frac{1}{n+1} , \quad (8.120)$$

which implies that sound waves along the effective black brane fluid are unstable: under a density perturbation the fluid evolves to become more and more inhomogeneous. Thus the black brane horizon itself becomes inhomogeneous, the brane thickness r_0 varying along the brane as

$$\delta r_0 \sim e^{\Omega t + ik_i z^i} \quad (8.121)$$

with

$$\Omega = \frac{k}{\sqrt{n+1}} + O(k^2) \quad (8.122)$$

($k = \sqrt{k_i k^i}$). Unstable oscillations of the form (8.121) were the type of black brane instability discovered by Gregory and Laflamme (see Chapter 2). Using the blackfold effective theory, we have derived this instability in the regime of long wavelengths, $kr_0 \ll 1$. Many studies of the Gregory–Laflamme instability focus on the threshold mode, with $\Omega = 0$ at $k = k_{\text{GL}} \neq 0$, which has a “small” wavelength $2\pi/k_{\text{GL}} \sim r_0$ and typically needs numerical work for its determination. The blackfold approach reveals instead that the hydrodynamic modes, which have vanishing frequency as $k \rightarrow 0$, are much simpler to study. The slope of the curve $\Omega(k)$ near $k = 0$ is determined exactly using only the equation of state $P(\varepsilon)$ of the unperturbed static black brane.

8.6.2 Correlated dynamical and thermodynamical stability

It is conventional in fluid dynamics to express the speed of sound in terms of thermodynamic quantities. Using the Gibbs–Duhem relation $dP = s dT$ one finds that

$$\frac{dP}{d\varepsilon} = s \frac{dT}{d\varepsilon} = \frac{s}{c_v}, \quad (8.123)$$

where c_v is the isovolumetric specific heat. So, the black brane is dynamically unstable to long-wavelength hydrodynamical perturbations if and only if it is locally thermodynamically unstable, $c_v < 0$. The “correlated stability conjecture” of Gubser and Mitra [16] posits precisely this type of connection between dynamical and thermodynamic stability. The blackfold method not only shows very simply why this conjecture holds for hydrodynamic modes but also gives a quantitative expression for the unstable frequency in terms of local thermodynamics:

$$\Omega = \sqrt{\frac{s}{-c_v}} k + O(k^2). \quad (8.124)$$

8.6.3 Viscous damping

The analysis of the sound-wave instability in section 8.6.1 employed the stress–energy tensor of (8.18), which gives the perfect fluid approximation to the intrinsic dynamics of the black brane. This tensor was obtained from the stationary metric of the black brane. If we perturb this brane, it will vibrate in its quasinormal modes, with damped oscillations. The stress–energy tensor measured at large distance $r \gg r_0$ from the black p -brane will reflect this damping through the appearance of dissipative terms proportional to derivatives of u^a (the derivatives of r_0 are proportional to these), so that

$$T_{ab} = T_{ab}^{(\text{perfect})} - \zeta \theta P_{ab} - 2\eta \sigma_{ab} + O(D^2). \quad (8.125)$$

Here the orthogonal projector, expansion, and shear of the velocity congruence are

$$P_{ab} = \eta_{ab} + u_a u_b, \quad \theta = D_a u^a, \quad (8.126)$$

$$\sigma_{ab} = P_a^c P_b^d \left(D_{(c} u_{d)} - \frac{1}{p} \theta P_{cd} \right), \quad (8.127)$$

and the coefficients η and ζ are the effective shear and bulk viscosity of the black brane. They can be computed from a perturbative calculation very similar to those in the context of the fluid/gravity correspondence of Chapter 13. For a neutral black brane in asymptotically flat space this calculation was carried out in [10], and the

following results were obtained:

$$\eta = \frac{s}{4\pi}, \quad \zeta = \frac{s}{2\pi} \left(\frac{1}{p} - v_s^2 \right), \quad (8.128)$$

where s is the entropy density of the black brane, (8.21), and v_s is the speed of sound (8.120).

Now we can solve the fluid equations (8.38) for linearized sound-mode perturbations of the viscous fluid and obtain the leading corrections to the dispersion relation (8.122) at order k^2 . For the black brane fluid the result is

$$\Omega = \frac{k}{\sqrt{n+1}} \left(1 - \frac{n+2}{n\sqrt{n+1}} kr_0 \right) \quad (8.129)$$

and is valid up to corrections $O(k^3)$. We see that the viscosity has the expected effect of damping the sound waves. Figure 8.1 shows this dispersion relation along with the numerical results obtained by solving the linearized perturbations of a black string.

Equation (8.129) gives excellent agreement with the numerical data for small kr_0 , but it also shows a remarkable overall resemblance to them even when kr_0 is of order 1, which is beyond the expected range of validity of the approximation. The quantitative agreement improves with increasing n : in an expansion in $1/n$, (8.129) gives the exact leading-order value for the threshold wavenumber $k_{\text{GL}} \rightarrow \sqrt{n}/r_0$. In [10] it was suggested that this surprising agreement could be explained by noting that the thermal wavelength $\lambda_T = 1/T \sim r_0/n$ shrinks to zero as $n \rightarrow \infty$ for fixed r_0 . Quite plausibly, this effect extends the range of wavelengths that fall under the remit of fluid dynamics.

Let us emphasize how little has gone into the derivation of (8.129): only the equation of state $P(\varepsilon)$ and the viscosities η and ζ . Actually, for a black string, since the fluid is $1+1$ dimensional there is no shear and only ζ enters the calculations. The determination of these coefficients requires a study of perturbations of the black string, but this can be carried out analytically for all n and p and needs to be done only once. Furthermore, the result for η is known to be universal for black holes, and the value of ζ saturates a proposed bound [17], which may plausibly be proven in general. If there exists such a general argument for the value of ζ for a black brane then the entire expression for the curve (8.129) can be obtained, using simple algebra, from a knowledge of only $dP/d\varepsilon$.

Thus, the effective viscous fluid of the blackfold approach seems to capture in a strikingly simple manner some of the most characteristic features of black brane dynamics. This is a significant simplification of the complexity of Einstein’s equations.

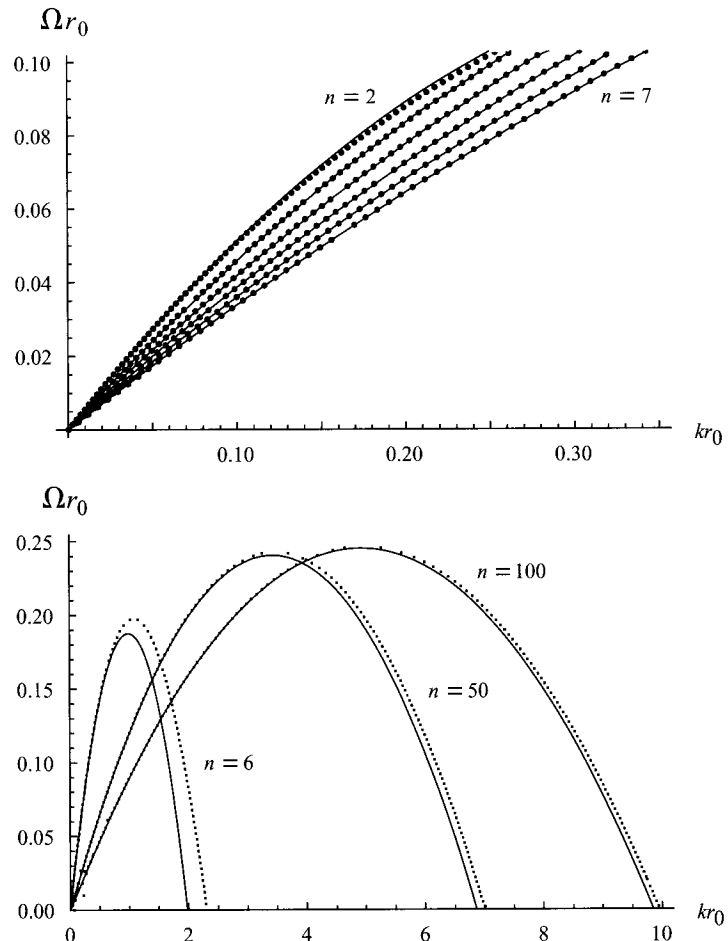


Figure 8.1 The angular velocity $\Omega(k)$ for unstable modes of black p -branes, in units of $1/r_0$ (the results depend only on n , (8.1)). The continuous curves are the analytical approximation (8.129), and the dotted curves are numerical solutions for the black brane perturbations. The upper diagram shows the results for $n = 2, \dots, 7$ at small k . The lower diagram shows the results for $n = 6, 50, 100$ at all k . For large n , (8.129) underestimates the wavenumber of the threshold mode by only an amount equal to $1/n$.

8.7 Extensions

Although in section 8.5 we considered only Minkowski backgrounds, the effective theory of blackfolds can be readily applied to the construction of black holes in curved backgrounds, such as de Sitter or anti-de Sitter spacetimes with cosmological constant Λ . In this case it is necessary that the thickness r_0 be much smaller than the curvature radius $|\Lambda|^{-1/2}$, so that the vacuum black brane solution is a good

approximation in the near zone. Black rings, odd-spheres, and other blackfolds with characteristic radii R that can be larger or smaller than $|\Lambda|^{-1/2}$ are easy to construct in these spacetimes [18, 19], as well as in other nontrivial backgrounds such as Kaluza–Klein monopoles [20].

Black p -branes can also carry on their worldvolumes the charges of q -branes, $0 \leq q \leq p$, which are sources of $(q+2)$ -form gauge field strengths F_{q+2} (see Chapter 11) [21, 22]. Then the worldvolume fluid includes a conserved q -brane number current. For $q = 0$ this amounts to a theory of an isotropic fluid with a conserved particle number, but when $q \geq 1$ the brane current makes the fluid anisotropic.

Blackfolds with a spatially compact worldvolume that supports these currents correspond to black holes that source the field F_{q+2} . When $q = 0$ they carry a conserved charge of a Maxwell field. When $q \geq 1$ they carry a dipole of the field. In contrast with neutral blackfolds, black holes constructed as charged blackfolds need not be ultra-spinning: the rotation may be small if the charge of the black brane is close to its upper extremal limit. The presence of charge close to extremality can also eliminate, in certain cases, the Gregory–Laflamme instability of the black brane. Then, the resulting black holes may be dynamically stable.

Of particular interest for string theory are blackfolds that carry Ramond–Ramond charges. In general, blackfold techniques are an appropriate tool for the study of configurations of D-branes in the probe approximation, in the case where the D-brane worldvolume theory has a thermal population of excitations. The blackfold gives a gravitational description of this thermally excited worldvolume, with a horizon which, on short scales, is like that of the straight black D-brane. As in the case of the AdS–CFT correspondence, this gravitational description of worldvolume theory is appropriate when there is a stack of a large number of D-branes (although not so large as to cause a strong backreaction on the background) and the theory is strongly coupled. In [23] these methods were developed to study a thermal version of the D3-brane bion, which is a configuration consisting of a D-brane and a parallel anti-D-brane connected by a wormhole.

8.8 Appendix: Geometry of submanifolds

Extrinsic curvature

For a submanifold \mathcal{W} embedded as $X^\mu(\sigma^a)$, the pull-back of the spacetime metric onto \mathcal{W} , γ_{ab} , is given by (8.15) and the first fundamental form of the surface, $h_{\mu\nu}$, is obtained as (8.26); it satisfies

$$h^\mu{}_\nu \partial_a X^\nu = \partial_a X^\mu, \quad h^\mu{}_\nu h^\nu{}_\rho = h^\mu{}_\rho. \quad (8.130)$$

Thus $h^\mu{}_\nu$ projects tensors onto directions tangent to \mathcal{W} . The tensor $\perp_{\mu\nu}$, introduced in (8.27), projects onto orthogonal directions:

$$\perp_{\mu\nu} \partial_a X^\mu = 0, \quad \perp_\mu{}^\nu \perp_\nu{}^\rho = \perp_\mu{}^\rho. \quad (8.131)$$

The shape of the embedding of the submanifold \mathcal{W} is captured by the second fundamental tensor, or extrinsic curvature tensor, (8.31). The symmetry of the first two indices of $K_{\mu\nu}{}^\rho$ is equivalent to the integrability of the subspaces orthogonal to $\perp_\mu{}^\nu$. To see this, let s and t be any two vectors in this subspace,

$$\perp_\mu{}^\nu t^\nu = 0, \quad \perp_\mu{}^\nu s^\nu = 0. \quad (8.132)$$

Then one can easily prove from the definition of $K_{\mu\nu}{}^\rho$ that

$$s^\mu t^\nu K_{\mu\nu}{}^\rho = \perp_\mu{}^\rho \nabla_s t^\mu, \quad (8.133)$$

so that

$$K_{[\mu\nu]}{}^\rho = 0 \quad \Leftrightarrow \quad 0 = \perp_\mu{}^\rho (\nabla_s t^\mu - \nabla_t s^\mu) = \perp_\mu{}^\rho [s, t]^\mu. \quad (8.134)$$

The vanishing of the last commutator is equivalent, through Frobenius' theorem, to the integrability of the subspace orthogonal to $\perp_\mu{}^\nu$. Therefore the extrinsic curvature tensor of the submanifold \mathcal{W} satisfies $K_{[\mu\nu]}{}^\rho = 0$.

Now, let N be any vector orthogonal to \mathcal{W} . Then

$$N_\rho K_{\mu\nu}{}^\rho = N_\rho h_\nu{}^\sigma \bar{\nabla}_\mu h_\sigma{}^\rho = -h_\nu{}^\rho \bar{\nabla}_\mu N_\rho. \quad (8.135)$$

Background tensors $t_{\mu_1\mu_2\dots}{}^{v_1v_2\dots}$ can be pulled back onto worldvolume tensors $t_{a_1a_2\dots}{}^{b_1b_2\dots}$ using $\partial_a X^\mu$ as follows:

$$t_{a_1a_2\dots}{}^{b_1b_2\dots} = \partial_{a_1} X^{\mu_1} \partial_{a_2} X^{\mu_2} \dots \partial^{b_1} X_{v_1} \partial^{b_2} X_{v_2} \dots t_{\mu_1\mu_2\dots}{}^{v_1v_2\dots}, \quad (8.136)$$

where

$$\partial^b X_v = \gamma^{bc} h_{v\rho} \partial_c X^\rho. \quad (8.137)$$

Even when the background tensor $t_{\mu_1\mu_2\dots}{}^{v_1v_2\dots}$ has all its indices parallel to \mathcal{W} , in general $\bar{\nabla}_\mu t_{\mu_1\mu_2\dots}{}^{v_1v_2\dots}$ has both parallel and orthogonal components. The parallel projection along all indices is related to the worldvolume covariant derivative $D_a t_{a_1a_2\dots}{}^{b_1b_2\dots}$ as in (8.136). Then, the divergences of background and worldvolume tensors are related as follows:

$$h^{v_1}_{\mu_1} \dots \bar{\nabla}_\rho t^{\rho\mu_1\dots} = \partial_{a_1} X^{v_1} \dots D_c t^{ca_1\dots}. \quad (8.138)$$

Variational calculus

Consider a congruence of curves, with tangent vector N , that intersect \mathcal{W} orthogonally,

$$N^\mu h_{\mu\nu} = 0, \quad N^\mu \perp_{\mu\nu} = N_\nu, \quad (8.139)$$

and Lie-drag \mathcal{W} along these curves. The congruence is arbitrary apart from the requirement that it should be smooth in a finite neighbourhood of \mathcal{W} , so this realizes arbitrary smooth deformations of the worldvolume $X^\mu \rightarrow X^\mu + N^\mu$.

Consider now the Lie derivative of $h_{\mu\nu}$ along N . In general,

$$\mathfrak{L}_N h_{\mu\nu} = N^\rho \nabla_\rho h_{\mu\nu} + h_{\rho\nu} \nabla_\mu N^\rho + h_{\mu\rho} \nabla_\nu N^\rho. \quad (8.140)$$

Using (8.135) one can derive

$$N_\rho K_{\mu\nu}{}^\rho = -\frac{1}{2} h_\mu{}^\lambda h_\nu{}^\sigma \mathfrak{L}_N h_{\lambda\sigma}. \quad (8.141)$$

Taking the trace, we have

$$N_\rho K^\rho = -\frac{1}{2} h^{\mu\nu} \mathfrak{L}_N h_{\mu\nu} = -\frac{1}{\sqrt{|h|}} \mathfrak{L}_N \sqrt{|h|}, \quad (8.142)$$

where $h = \det h_{\mu\nu}$. These equations generalize well-known expressions for the extrinsic curvature of a codimension-1 surface.

Consider now a functional of the embedding, of the form

$$I = \int_{\mathcal{W}} \sqrt{|h|} \Phi, \quad (8.143)$$

where Φ is a worldvolume function. Then

$$\delta_N I = \int_{\mathcal{W}} \mathfrak{L}_N \left(\sqrt{|h|} \Phi \right) = \int_{\mathcal{W}} \sqrt{|h|} (-N_\rho K^\rho \Phi + N^\rho \partial_\rho \Phi). \quad (8.144)$$

Since N is an arbitrary orthogonal vector we have

$$\delta_N I = 0 \quad \Leftrightarrow \quad K^\rho = \perp_\mu{}^\rho \partial_\mu \ln \Phi. \quad (8.145)$$

If Φ is constant then we recover the equation $K^\rho = 0$ for minimal-volume submanifolds.

References

- [1] R. Emparan, T. Harmark, V. Niarchos, and N. A. Obers, World-volume effective theory for higher-dimensional black holes (blackfolds), *Phys. Rev. Lett.* **102** (2009), 191301 [arXiv:0902.0427 [hep-th]].

- [2] R. Emparan, T. Harmark, V. Niarchos, and N. A. Obers, Essentials of blackfold dynamics, *JHEP* **1003** (2010), 063 [arXiv:0910.1601 [hep-th]].
- [3] R. Emparan, T. Harmark, V. Niarchos, and N. A. Obers, New horizons for black holes and branes, *JHEP* **1004** (2010), 046 [arXiv:0912.2352 [hep-th]].
- [4] E. Poisson, The motion of point particles in curved spacetime, *Living Rev. Rel.* **7** (2004), 6 [arXiv:gr-qc/0306052].
- [5] S. E. Gralla and R. M. Wald, A rigorous derivation of gravitational self-force, *Class. Quant. Grav.* **25** (2008), 205009 [arXiv:0806.3293 [gr-qc]].
- [6] W. D. Goldberger and I. Z. Rothstein, An effective field theory of gravity for extended objects, *Phys. Rev. D* **73** (2006), 104029 [arXiv:hep-th/0409156].
- [7] J. D. Brown and J. W. York, Quasilocal energy and conserved charges derived from the gravitational action, *Phys. Rev. D* **47** (1993), 1407 [arXiv:gr-qc/9209012].
- [8] B. Carter, Essentials of classical brane dynamics, *Int. J. Theor. Phys.* **40** (2001), 2099 [arXiv:gr-qc/0012036].
- [9] R. Emparan, T. Harmark, V. Niarchos, N. A. Obers, and M. J. Rodríguez, The phase structure of higher-dimensional black rings and black holes, *JHEP* **0710** (2007), 110 [arXiv:0708.2181 [hep-th]].
- [10] J. Camps, R. Emparan, and N. Haddad, Black brane viscosity and the Gregory–Laflamme instability, *JHEP* **1005** (2010), 042 [arXiv:1003.3636 [hep-th]].
- [11] T. Harmark and N. A. Obers, New phase diagram for black holes and strings on cylinders, *Class. Quant. Grav.* **21** (2004), 1709 [hep-th/0309116].
- [12] R. Emparan and R. C. Myers, Instability of ultra-spinning black holes, *JHEP* **0309** (2003), 025 [arXiv:hep-th/0308056].
- [13] S. Hollands, A. Ishibashi, and R. M. Wald, A higher dimensional stationary rotating black hole must be axisymmetric, *Commun. Math. Phys.* **271** (2007), 699 [arXiv:gr-qc/0605106].
- [14] V. Moncrief and J. Isenberg, Symmetries of higher dimensional black holes, *Class. Quant. Grav.* **25** (2008), 195015 [arXiv:0805.1451 [gr-qc]].
- [15] H. S. Reall, Higher dimensional black holes and supersymmetry, *Phys. Rev. D* **68** (2003), 024024 [hep-th/0211290].
- [16] S. S. Gubser and I. Mitra, The evolution of unstable black holes in anti-de Sitter space, *JHEP* **0108** (2001), 018 [arXiv:hep-th/0011127].
- [17] A. Buchel, Bulk viscosity of gauge theory plasma at strong coupling, *Phys. Lett. B* **663** (2008), 286–289 [arXiv:0708.3459 [hep-th]].
- [18] M. M. Caldarelli, R. Emparan, and M. J. Rodríguez, Black rings in (anti)-deSitter space, *JHEP* **0811** (2008), 011 [arXiv:0806.1954 [hep-th]].
- [19] J. Armas and N. A. Obers, Blackfolds in (anti)-de Sitter backgrounds, *Phys. Rev. D* **83** (2011), 084039 [arXiv:1012.5081 [hep-th]].
- [20] J. Camps, R. Emparan, P. Figueras, S. Giusto, and A. Saxena, Black rings in taub-NUT and D0–D6 interactions, *JHEP* **0902** (2009), 021 [arXiv:0811.2088 [hep-th]].
- [21] M. M. Caldarelli, R. Emparan, and B. Van Pol, Higher-dimensional rotating charged black holes, *JHEP* **1104** (2011), 013 [arXiv:1012.4517 [hep-th]].
- [22] R. Emparan, T. Harmark, V. Niarchos, and N. A. Obers, Blackfolds in supergravity and string theory, *JHEP* **1108** (2011), 154 [arXiv:1106.4428 [hep-th]].
- [23] G. Grignani, T. Harmark, A. Marini, N. A. Obers, and M. Orselli, Heating up the bion [arXiv:1012.1494 [hep-th]].

Algebraically special solutions in higher dimensions

HARVEY S. REALL

9.1 Introduction

At any point of a four-dimensional spacetime, the Weyl tensor (if nonzero) defines four *principal null directions* (PNDs) satisfying

$$\ell_{[\mu} C_{\nu\rho\sigma]\tau} \ell_\lambda] \ell^\rho \ell^\sigma = 0. \quad (9.1)$$

The Weyl tensor can be classified according to whether any of these null directions coincide. In general, the null directions are distinct and the Weyl tensor is said to be algebraically general. However, if two or more PNDs coincide then the Weyl tensor is algebraically special. An algebraically special *spacetime* is one whose Weyl tensor is everywhere algebraically special.

The algebraically special property has played an important role at several points in the history of black hole physics. The most important nontrivial solution of general relativity is the Kerr solution. The title of Kerr’s paper “Gravitational field of a spinning mass as an example of algebraically special metrics” [1] reveals the motivation for Kerr’s work: he was interested in finding new solutions having an algebraically special Weyl tensor. Assuming that the metric is algebraically special leads to a simplification of the Einstein equation, which helped Kerr find his solution.

Once the special importance of the Kerr solution came to be appreciated, the question of its classical stability was raised. Answering this question became possible only after Teukolsky exploited the algebraically special property to decouple the equations governing linearized-metric perturbations of the Kerr solution and to reduce them to a wave equation for a single complex scalar [2].

Another useful result closely related to the algebraically special property is the separability of the geodesic and Klein–Gordon equations in the Kerr spacetime.

There are other interesting algebraically special spacetimes in four dimensions, for example, the C-metric, which describes a pair of black holes being accelerated apart by a conical deficit singularity (i.e., a cosmic string) [3]. Its Weyl tensor is type D, i.e. there are two pairs of coincident PNDs, just as in the Kerr solution. It was this property that enabled the rotating generalization of the C-metric to be discovered [4]. The C-metric is relevant also to higher-dimensional black holes: the analytic continuation of a Kaluza–Klein generalization of the C-metric led to the discovery of black rings [5]. Further examples of interesting algebraically special vacuum spacetimes include pp-waves and the Taub–NUT spacetime.

Given the usefulness of the algebraically special property in four dimensions, it is natural to ask whether there is an analogous notion in $d > 4$ dimensions. If so, can it be exploited to solve the Einstein equation? Does it help in the study of perturbations of higher-dimensional black holes?

As we shall see, the algebraically special property can indeed be extended to $d > 4$ dimensions. However, there are several inequivalent ways of doing this. This stems from the fact that there are several different methods for performing the Petrov classification of the Weyl tensor in four dimensions. These methods look very different but in fact are equivalent. However, when extended to $d > 4$ dimensions they become inequivalent.

A classification of the Weyl tensor in higher dimensions based on generalizing the notion of PNDs was introduced by Coley, Milson, Pravda and Pravdova (CMPP) [6]. This classification has received most attention so far. We shall review it in section 9.2. In section 9.3 we review an alternative approach, due to De Smet [7], based on generalizing the spinorial approach to the four-dimensional classification. It turns out that this works only for the special case $d = 5$. In general there does not seem to be any simple relation between the CMPP and De Smet approaches. In particular, the De Smet approach does not lead to any notion of preferred null directions. Nevertheless, Myers–Perry black holes [8] are algebraically special with respect to both classifications. Other approaches to defining a notion of “algebraically special” in higher dimensions are discussed in section 9.4.

The emphasis in this chapter will be on applications, particularly those using the algebraically special property to construct new solutions of the Einstein equation or to study perturbations of known solutions. We will consider only solutions of the *vacuum* Einstein equation, allowing for a cosmological constant.

9.2 CMPP classification

9.2.1 The classification

Coley, Milson, Pravda and Pravdova (CMPP) developed a scheme for classifying the Weyl tensor that follows closely a four-dimensional approach based on principal

null directions [6, 9] (see [10] for an earlier review). Although their approach is in fact basis independent, it is most easily described by introducing a null basis $e_0 \equiv \ell$, $e_1 \equiv n$, $e_i \equiv m_i$ ($i = 2, \dots, d - 1$) where ℓ and n are null vectors and m_i are orthonormal spacelike vectors satisfying the scalar products

$$\ell^2 = n^2 = \ell \cdot m_i = n \cdot m_i = 0, \quad \ell \cdot n = 1, \quad m_i \cdot m_j = \delta_{ij}. \quad (9.2)$$

Different null bases at a point are related by Lorentz transformations. It is convenient to give names to particular kinds of Lorentz transformation. A *boost* is defined by

$$\ell \rightarrow \lambda \ell, \quad n \rightarrow \lambda^{-1} n, \quad m_i \rightarrow m_i, \quad (9.3)$$

with λ a scalar. A *spin* is a rotation of the spatial basis vectors

$$\ell \rightarrow \ell, \quad n \rightarrow n, \quad m_i \rightarrow X_{ij} m_j, \quad (9.4)$$

where X_{ij} is an orthogonal matrix. A *null rotation about ℓ* with parameters z_i is defined by

$$\ell \rightarrow \ell, \quad n \rightarrow n + z_i m_i - \frac{1}{2} z_i z_i \ell, \quad m_i \rightarrow m_i - z_i \ell. \quad (9.5)$$

Together these three special types of transformation generate the full Lorentz group.

A tensor component has *boost weight* b if it scales as λ^b under a boost. For example, consider the Weyl tensor components

$$C_{0i0j} = C_{\mu\nu\rho\sigma} \ell^\mu m_i^\nu \ell^\rho m_j^\sigma \rightarrow \lambda^2 C_{\mu\nu\rho\sigma} \ell^\mu m_i^\nu \ell^\rho m_j^\sigma = \lambda^2 C_{0i0j}; \quad (9.6)$$

the components C_{0i0j} have $b = 2$. In general, for a tensor with only “downstairs” indices, b is the number of 0 indices minus the number of 1 indices.

The symmetries of the Weyl tensor imply that it has components with b ranging from -2 to 2 . We say that the vector field ℓ is a *Weyl-aligned null direction* (WAND) iff the $b = 2$ components of the Weyl tensor vanish. This definition is independent of how the other basis vectors are chosen. Indeed it is equivalent to the condition (9.1). Hence, for $d = 4$, a WAND is the same as a principal null direction.

One reason for employing different terminology when $d > 4$ (i.e. “WAND” rather than “principal null direction”) is that WANDs behave rather differently when $d > 4$. When $d = 4$, there are four solutions of (9.1) (although some may coincide). However, for $d > 4$ this equation may admit no solutions, finitely many solutions or even a continuous family of solutions. For example, the static Kaluza–Klein bubble (the product of a flat time direction and the Euclidean Schwarzschild solution) admits no WAND [11]. The Schwarzschild solution admits two WANDs.

Table 9.1

Algebraic type	Vanishing Weyl components	Comment
O	$b = 2, 1, 0, -1, -2$	conformally flat
N	$b = 2, 1, 0, -1$	admits multiple WAND
III	$b = 2, 1, 0$	admits multiple WAND
II	$b = 2, 1$	admits multiple WAND
I	$b = 2$	admits WAND
G		admits no WAND

In the product spacetime $dS_3 \times S^2$ any null vector field tangent to dS_3 is a WAND, so there is a continuous family [11].

In four dimensions a spacetime is said to be algebraically special if everywhere it admits a *repeated* principal null direction (i.e. two or more null directions coincide). The higher-dimensional analogue of this is a *multiple WAND*. We say that the null vector field ℓ is a multiple WAND if all Weyl components with b equal to 2 or 1 vanish. Once again, this is a basis-independent statement. We define a spacetime to be algebraically special if it admits (everywhere) a multiple WAND.¹

The algebraic types of Weyl tensor are given in Table 9.1.

For example, we say that the Weyl tensor is type III if one can choose ℓ so that all the $b = 2, 1, 0$ components of the Weyl tensor vanish but one cannot choose ℓ so that all the $b = 2, 1, 0, -1$ components vanish. It is type I if there is a WAND but not a multiple WAND. Types II, III, N and O admit a multiple WAND. This classification can be made at any point. The algebraic type of a *spacetime* is defined to be the least special type of the Weyl tensor at any point in the spacetime.

This classification, based only on the vector ℓ , is the so-called primary classification. One can now ask, given an ℓ defined by the primary classification, whether one can choose n to be a WAND or a multiple WAND, corresponding respectively to the vanishing of either just the $b = -2$ or the $b = -2, -1$ Weyl components. This leads to a more refined secondary classification. For our purposes we shall be interested in the secondary classification only in the case for which both ℓ and n can be chosen to be multiple WANDs. In this case the spacetime must be of primary type II (if not conformally flat). Such a spacetime is referred to as a type D spacetime. Note that the algebraic type of a spacetime as defined above agrees with the standard definition when $d = 4$.

¹ Given that a spacetime might not admit even a WAND, CMPP defined a higher-dimensional spacetime to be algebraically special if it admits a WAND (everywhere). However, more recent papers have not maintained this nomenclature, for several reasons. First, it leads to tension with standard terminology in four dimensions. Second, there are examples of analytic spacetimes that admit a WAND in some open subset but not in some other open subset [11, 12]. Third, the existence of a WAND is not sufficiently restrictive to be a useful tool to address the problems discussed in the introduction.

9.2.2 Examples

The four-dimensional Schwarzschild and Kerr solutions are examples of type D spacetimes. Similarly, in $d > 4$ dimensions the Myers–Perry solution [8] (and its generalization to include a cosmological constant [13, 14] and NUT charge [15]) are type D [16, 17]. Black rings are not algebraically special: it was found in [12] that the singly spinning black ring solution is type I in one region and type G in another region.²

Consider a warped product spacetime of the form

$$ds^2 = A(y)^2 g_{MN}(x) dx^M dx^N + B(x)^2 g_{AB}(y) dy^A dy^B , \quad (9.7)$$

where g_{MN} is Lorentzian and g_{AB} is Riemannian. It was shown in [18] that such a spacetime is type D (or O) if the Lorentzian factor is (i) two-dimensional or (ii) a three-dimensional Einstein spacetime or (iii) a type D Einstein spacetime. Hence a black p -brane obtained from the product of the Schwarzschild (or Myers–Perry) solution with p flat dimensions must be type D. Similarly, product spacetimes such as $dS_p \times S^{d-p}$ ($p > 1$) are type D.

Note that the Wick rotation of a spacetime typically changes its algebraic type. For example, a five-dimensional Schwarzschild black string can be Wick-rotated to give a static Kaluza–Klein bubble spacetime (a product of the Euclidean Schwarzschild solution and a flat time direction). The former solution is type D but the latter is type G [11]. (An *expanding* KK bubble, given by Wick rotation of the five-dimensional Schwarzschild spacetime [19] is a warped product with a three-dimensional de Sitter factor and hence is type D by the above theorem.)

9.2.3 Goldberg–Sachs theorem

Probably the most important result concerning four-dimensional algebraically special solutions is the Goldberg–Sachs (GS) theorem:

In a vacuum spacetime (allowing for a cosmological constant) that is not conformally flat, a null vector field is a repeated principal null direction if, and only if, it is geodesic and shearfree.

² This emphasizes that the distinction between type I and type G is probably not useful (simpler examples of this behaviour were given in [11]). Given this example, one might wonder whether it is possible for a spacetime to be algebraically special in one open region and algebraically general in another open region. This seems unlikely: in simple examples the condition for the existence of a WAND reduces to an inequality involving the metric components. The type I or G behaviour just discussed corresponds to this inequality's being satisfied in one region but not in another. However, the criterion for the existence of a *multiple* WAND is that certain combinations of metric components should vanish. If this happens in some open region, and the spacetime is analytic, then it must happen everywhere. It would be nice to have a proof of this in general.

Generalizations of this theorem exist, for example, in which a Maxwell field is included. This theorem plays an important role in using the algebraically special property as a simplifying assumption to solve the Einstein equation. One introduces coordinates (r, x^i) , where r is an affine parameter along the null geodesics whose existence is guaranteed by the theorem. Using the algebraically special property and the Einstein equation, one can determine the full dependence of the metric on r [20]. The Einstein equation then reduces to equations governing the dependence of the metric on the other three coordinates x^i . This is a significant reduction in the difficulty of the problem, although the reduced equations are still sufficiently complicated to make one resort to extra assumptions in order to solve them.

The most spectacular use of the algebraically special property to solve the Einstein equation was Kinnersley's discovery of the most general type D solution [4]. In this case one has two principal null directions, both obeying the GS theorem, and this is sufficiently restrictive that the Einstein equations can be solved explicitly. Kinnersley's result provides significant motivation for the study of higher-dimensional algebraically special solutions. If we want to emulate his work then the first step is to generalize the Goldberg–Sachs theorem.

The GS theorem as stated above does not extend to higher dimensions. There are simple examples of spacetimes that admit nongeodesic multiple WANDs (e.g. $dS_3 \times S^2$: any null vector field tangent to dS_3 is a multiple WAND irrespective of whether it is a geodesic) and of spacetimes that admit geodesic but shearing multiple WANDs (e.g. a five-dimensional black string: the multiple WAND is a repeated PND of the four-dimensional Schwarzschild spacetime; this expands isotropically in the Schwarzschild directions but not in the string direction and hence is shearing). Nevertheless, it is clear that there *are* strong restrictions on the optical properties of a multiple WAND, and understanding precisely what these are, is the main problem in formulating a higher-dimensional generalization of the GS theorem.

A first step towards such a generalization is to understand how the “geodesic part” of the theorem must be modified in higher dimensions. This has now been completed. For vacuum spacetimes of type III or N it can be shown that the multiple WAND must be geodesic [21]. For type II (or D) it need not be geodesic. However, in the latter case it has been proved that there must exist another multiple WAND that *is* geodesic [22]. In other words, a vacuum spacetime admits a multiple WAND if and only if it admits a geodesic multiple WAND. The $dS_3 \times S^2$ example is a prototype for this behaviour. This result implies that there is no loss of generality in restricting our attention to geodesic multiple WANDs.

The next step is to understand the higher-dimensional analogue of the shearfree condition. This has not yet been achieved; however, there has been some progress. Recall that the expansion, rotation and shear are defined to be the trace, traceless

symmetric part and antisymmetric part of the matrix

$$\rho_{ij} = \nabla_j \ell_i = m_i^\mu m_j^\nu \nabla_\nu \ell_\mu . \quad (9.8)$$

The problem is to determine necessary (and, if possible, sufficient) conditions on ρ_{ij} for ℓ to be a multiple WAND. So far, progress has been made only with the more special algebraic types. For a type N vacuum spacetime, it was shown [21] that one can choose the spatial basis vectors m_i in such a way that ρ_{ij} is zero everywhere except for a 2×2 block in the upper-left corner, of the form

$$\begin{pmatrix} b & a \\ -a & b \end{pmatrix} . \quad (9.9)$$

Note that this 2×2 block has vanishing traceless symmetric part. However, the full $(d-2) \times (d-2)$ matrix ρ_{ij} is not shearfree except when $d=4$. The same result applies for type III spacetimes when $d=5$ and also when $d>5$, subject to a certain “genericity” assumption [21].

Results have also been obtained for the case of a Kerr–Schild spacetime. Such a spacetime has a metric of the form

$$g_{\mu\nu} = \eta_{\mu\nu} + H k_\mu k_\nu , \quad (9.10)$$

where k_μ is null with respect to the Minkowski metric $\eta_{\mu\nu}$ (which implies that it is null also with respect to $g_{\mu\nu}$) and H is a function. This class of spacetimes includes Myers–Perry black holes. Vacuum Kerr–Schild spacetimes are algebraically special for any $d \geq 4$, with k_μ a geodesic multiple WAND [23]. For these spacetimes it has been shown that one can choose the basis vectors m_i in such a way that ρ_{ij} is block diagonal, with 2×2 blocks of the form (9.9) along the diagonal (the parameters a, b can vary from block to block) and zeros elsewhere [23, 24].

These partial results are encouraging evidence that there does exist a simple canonical form for a matrix ρ_{ij} defined by a multiple WAND. This will provide a higher-dimensional generalization of the “only if” part of the Goldberg–Sachs theorem. It is less clear at present whether the “if” part of the theorem also will generalize, in other words, whether the canonical form for ρ_{ij} forces ℓ to be a multiple WAND. Some partial results in this direction are known. For example, if ℓ is geodesic with vanishing rotation and shear then it must be a multiple WAND [25, 26].

9.2.4 Peeling theorem

Some physical motivation for the study of algebraically special solutions in four dimensions comes from the peeling theorem. Consider a four-dimensional asymptotically flat spacetime and a null geodesic that approaches future null

infinity. Let ℓ denote the tangent to the geodesic. Then the Weyl tensor along this geodesic can be expanded in inverse powers of the affine parameter r along the geodesic:

$$C_{\mu\nu\rho\sigma} = \frac{1}{r} C_{\mu\nu\rho\sigma}^{(1)} + \frac{1}{r^2} C_{\mu\nu\rho\sigma}^{(2)} + \frac{1}{r^3} C_{\mu\nu\rho\sigma}^{(3)} + \frac{1}{r^4} C_{\mu\nu\rho\sigma}^{(4)} + \mathcal{O}\left(\frac{1}{r^5}\right), \quad (9.11)$$

where $C^{(1)}$ is type N, $C^{(2)}$ is type III, $C^{(3)}$ is type II (or D), in each case with repeated principal null direction ℓ , and $C^{(4)}$ is type I, with principal null direction ℓ . When first discovered, this suggested that the study of algebraically special spacetimes may be valuable for understanding the behaviour of spacetime far from a radiating source.

An argument in [27] suggests that this peeling property may not extend to higher dimensions. If an expansion of the above form does hold (with suitable powers of r) then the leading behaviour of $C_{\mu\nu\rho\sigma}$ near null infinity is type N. Therefore one would expect that, at large r , ρ_{ij} should have the form appropriate to a type N solution. As discussed above, this is a rank-2 matrix, i.e., it singles out a two-dimensional subspace. However, in the far field of a general radiating spacetime one might not expect such a preferred subspace to occur. If this were correct then the leading behaviour could not be type N. A similar argument excludes type III (at least for $d = 5$).³ Of course, this argument does not apply to asymptotically *locally* flat spacetimes, e.g. Kaluza–Klein (KK) asymptotics, for which one would expect ρ_{ij} to be degenerate near infinity. It seems likely that a peeling theorem would exist for spacetimes with boundary conditions appropriate to a KK reduction to four dimensions.

9.2.5 Finding new solutions

A main motivation for the study of algebraically special solutions in $d > 4$ dimensions is the hope that the algebraically special property will make the Einstein equation easier to solve, leading to the discovery of interesting new explicit solutions. In contrast with many other methods for solving the Einstein equation, this approach can cope with a nonzero cosmological constant. So far, there have been just a few investigations in this direction.

In four dimensions the Goldberg–Sachs theorem implies that a repeated principal null direction PND ℓ is geodesic and shearfree. In the simplest classes of algebraically special solutions the rotation of ℓ also vanishes. This implies that ℓ is orthogonal to a family of null hypersurfaces $u = \text{constant}$. One can introduce coordinates (r, y^i) on these surfaces, where r is an affine parameter along the

³ Alternatively, type N or type III might occur but with $\rho_{ij} = 0$.

geodesics with tangent ℓ and $i = 1, 2$. This gives a coordinate chart (u, r, y^i) on spacetime. Since the shear and rotation vanish, $\rho_{ij} = \frac{1}{2}\rho_{kk}\delta_{ij}$, where ρ_{kk} is the expansion. These spacetimes fall into two classes [20]: Robinson–Trautman spacetimes, for which $\rho_{kk} \neq 0$, and Kundt spacetimes for which $\rho_{kk} = 0$ (and hence $\rho_{ij} = 0$). In both classes the vacuum Einstein equation determines fully the r -dependence of the metric, and it reduces to nonlinear PDEs for a small number of functions of (u, y^i) . The Robinson–Trautman family contains the Schwarzschild solution and the C-metric and certain time-dependent generalizations of these spacetimes. The Kundt family describes various generalized gravitational wave solutions.

In $d > 4$ dimensions, some general properties of vacuum solutions with a hypersurface-orthogonal (geodesic) multiple WAND were investigated in [28]. The r -dependence of such solutions was fully determined. As discussed above, it is no longer true that the shear of the multiple WAND must vanish in general. However, if one makes the assumption that the shear *does* vanish then one can obtain higher-dimensional generalizations of the Robinson–Trautman and Kundt families of solutions.

The equations governing $d > 4$ vacuum Kundt solutions were obtained in [29]. The Robinson–Trautman case was investigated in [25]. Perhaps disappointingly, in the latter reference it was discovered that this class of solutions is considerably less rich in $d > 4$ dimensions; it contains the higher-dimensional Schwarzschild solution but no time-dependent generalizations. Furthermore, there is nothing that could be identified as a higher-dimensional C-metric. However, this lack of richness probably occurs because the shearfree condition is too restrictive in higher dimensions: we know that a multiple WAND need not be shearfree.

A promising avenue for future research would be to determine the canonical form for ρ_{ij} for the special case of a hypersurface-orthogonal multiple WAND; this is probably much easier than finding a full higher-dimensional generalization of the Goldberg–Sachs theorem. This could then be used as the starting point for integrating the Einstein equation using the above method.

A different approach would be to combine the algebraically special property with the assumption that the metric admits certain symmetries. In [11] the class of *axisymmetric* metrics, defined as those admitting a $SO(d - 2)$ isometry group with S^{d-3} orbits, was investigated. This includes the interesting class of *static* axisymmetric solutions, with isometry group $R \times SO(d - 2)$. Such solutions would include the solution describing a brane-world black hole in the Randall–Sundrum model, which is thought to be related to a higher-dimensional C-metric. Note that the general static axisymmetric solution of the Einstein equation is not known (except for $d = 4$ with vanishing cosmological constant). However, it was shown in [11] that if one demands that the metric be algebraically special as

well as axisymmetric (but not necessarily static) then the Einstein equation (with cosmological constant) can be solved. Most solutions discovered were already known (they were e.g. generalizations of the Schwarzschild black hole, black string or expanding KK bubble). However, one class (corresponding to axisymmetric Kundt solutions) was less familiar. It is specified by solutions of certain ODEs that cannot be solved analytically. Some spacetimes in this class have AdS–CFT applications, for example the gravitational dual of a CFT (vacuum state) in $R \times S^1 \times S^2$ [30] or in $\text{AdS}_2 \times S^2$ [31].

9.2.6 Perturbations

As discussed in the introduction, a major motivation for trying to exploit the algebraically special property in higher dimensions is its application to the study of linearized gravitational perturbations of black hole spacetimes. In four dimensions the Weyl tensor is encoded in the Newman–Penrose scalars Ψ_A , $A = 0, 1, \dots, 4$. The algebraically special property has two important consequences for perturbations [2].

First, one may choose the null basis so that ℓ is the repeated PND of the unperturbed spacetime and $\delta\Psi_0$ (the perturbation of Ψ_0) is gauge invariant under both infinitesimal diffeomorphisms and infinitesimal basis transformations. Note that this quantity is a complex scalar and therefore has two degrees of freedom, the same number as the gravitational field in four dimensions. It is therefore plausible that it captures all the information about generic metric perturbations. This is indeed the case: it can be shown that knowledge of the perturbation in Ψ_0 is sufficient to reconstruct the metric perturbation, up to the freedom to add a perturbation for which $\delta\Psi_0$ vanishes [32]. In the Kerr spacetime, it can be shown [33] that the only perturbations for which $\delta\Psi_0 = 0$ and which are regular at the future horizon and decay at infinity are the modes corresponding to infinitesimal changes in the mass and angular momentum of the black hole.

Second, $\delta\Psi_0$ can be *decoupled* from the other $\delta\Psi_A$. The perturbation $\delta\Psi_0$ satisfies a second-order linear homogeneous wave equation in the unperturbed spacetime. Remarkably, if one Fourier-analyzes this equation, i.e., assumes a dependence proportional to $\exp(-i\omega t + im\phi)$, then it can be separated and reduces to ODEs governing the r - and θ -dependences.

How much of this extends to perturbations of algebraically special vacuum solutions in $d > 4$ dimensions? Choose a null basis in which ℓ is a multiple WAND and let $\Omega_{ij} = C_{0i0j}$. This is a traceless symmetric matrix. In four dimensions it is equivalent to Ψ_0 . In [34] it was shown that the gauge-invariance properties of $\delta\Psi_0$ are satisfied also by $\delta\Omega_{ij}$. Note that this quantity has the same number of degrees of freedom as the linearized gravitational field. The four-dimensional case suggests

that knowledge of $\delta\Omega_{ij}$ will be sufficient to determine the metric perturbation, up to the freedom to add a small number of “nongeneric” modes. This remains to be shown. In any case, the fact that $\delta\Omega_{ij}$ is local and gauge invariant should make it useful in any study of perturbations of Myers–Perry black holes.

In [34] the conditions under which $\delta\Omega_{ij}$ satisfies a decoupled equation of motion were also analyzed. The result was that the conditions for decoupling in $d > 4$ dimensions are considerably stronger than in four dimensions. In four dimensions, one finds only that the multiple PND should be geodesic and shearfree, which is guaranteed by the Goldberg–Sachs theorem. But, for $d > 4$, one finds that the multiple WAND should be geodesic with vanishing expansion, rotation and shear, i.e., $\rho_{ij} = 0$. In other words, the decoupling of $\delta\Omega_{ij}$ occurs if and only if the spacetime is a Kundt spacetime. Unfortunately black hole spacetimes are not Kundt spacetimes, so decoupling does not occur even for the Schwarzschild spacetime in $d > 4$ dimensions.⁴

Although black holes are not Kundt spacetimes, the *near-horizon geometry* of an extreme black hole *is* a Kundt spacetime [34]. Therefore one can use the decoupled equation for $\delta\Omega_{ij}$ to study perturbations of near-horizon geometries. This was explored in [36].

It is conceivable that there is some other gauge-invariant quantity which does decouple and which reduces to $\delta\Psi_0$ when $d = 4$. That this might be possible is suggested by results for the Schwarzschild spacetime for which there exist additional local gauge-invariant combinations of Weyl components and connection components (e.g. ρ_{ij}) [34]. These combinations vanish identically for $d = 4$. Perhaps it is possible to add such a combination to $\delta\Omega_{ij}$ to obtain a quantity that does satisfy a decoupled equation.

9.2.7 NP and GHP formalisms

In four dimensions, the Newman–Penrose (NP) formalism [37] is a convenient framework for performing certain calculations in general relativity, particularly those involving preferred null directions. Therefore it plays a central role in the study of algebraically special solutions. The idea is simple: the components of any tensor with respect to a null basis are scalars (since they are defined by contraction of the tensor with the basis vectors). Hence, by contracting with basis vectors one can reduce tensorial equations, involving covariant derivatives, to scalar equations involving only partial derivatives. A higher-dimensional generalization of the NP

⁴ This is not in contradiction with the results in [35] for Schwarzschild perturbations, because in [35] the authors did not use the local quantity $\delta\Omega_{ij}$ but instead used a nonlocal scalar–vector–tensor decomposition exploiting spherical symmetry.

formalism has been developed [21, 26, 38]. For the special case $d = 5$, a spinor-based approach was presented in [39].

Often, and especially when studying algebraically special spacetimes, there exist one or more preferred null directions but no preferred spatial directions. The NP formalism has the drawback that it requires a specific choice of spatial basis vectors and does not maintain covariance with respect to spins (i.e. rotations of the spatial basis vectors). Furthermore, it does not maintain covariance with respect to boosts (which rescale the null basis vectors). These deficiencies were remedied in an improved formalism introduced by Geroch, Held and Penrose (GHP) [40]. A higher-dimensional generalization of this formalism was introduced in [41].

In the GHP approach we say that an object $T_{i_1 \dots i_s}$ is a *GHP scalar* if it transforms with a definite boost weight b under a boost (9.3) and transforms under a spin (9.4) as follows:

$$T_{i_1 \dots i_s} \rightarrow X_{i_1 j_1} \dots X_{i_s j_s} T_{j_1 \dots j_s}. \quad (9.12)$$

We say that such a quantity has *spin* s . For example, the quantity ρ_{ij} defined by (9.8), encoding the expansion, rotation and shear of ℓ , is a GHP scalar with $b = 1$ and $s = 2$. Another important GHP scalar is

$$\kappa_i = \nabla_0 \ell_i = m_i^\mu \ell^\nu \nabla_\nu \ell_\mu, \quad (9.13)$$

which has $b = 2$ and $s = 1$. This measures the failure of ℓ to be geodesic: ℓ is geodesic if and only if $\kappa_i = 0$. Not all NP scalars are GHP scalars. For example, the NP scalar $\nabla_0 \ell_1 = n^\mu \ell^\nu \nabla_\nu \ell_\mu$ transforms inhomogeneously under a boost and therefore is not a GHP scalar.

One can introduce derivative operators that map GHP scalars to GHP scalars and can write out components of e.g. the Bianchi identity using these derivatives [41]. The use of this formalism considerably simplifies the analysis of algebraically special solutions, e.g. of their perturbations [34].

9.3 De Smet classification

9.3.1 The classification

In four dimensions the most straightforward explanation of the Petrov classification makes use of the two-component spinor formalism.⁵ In this approach the Weyl tensor is equivalent to the Weyl spinor Ψ_{ABCD} , which is totally symmetric in

spinor indices. Therefore, specifying the Weyl tensor at a point is equivalent to specifying a homogeneous quartic polynomial in two complex variables (w, z) :

$$P = \Psi_{ABCD} \epsilon^A \epsilon^B \epsilon^C \epsilon^D, \quad (9.14)$$

where $\epsilon^A = (w, z)$. By the fundamental theorem of algebra, this polynomial can be factorized (e.g. we first divide through by w^4 to get a polynomial in z/w) and hence there exist (dual) spinors $\kappa_1, \dots, \kappa_4$ such that

$$\Psi_{ABCD} = (\kappa_1)_A (\kappa_2)_B (\kappa_3)_C (\kappa_4)_D. \quad (9.15)$$

In four dimensions a two-component spinor defines a null vector via $\ell^a = \bar{\kappa} \Gamma^a \kappa$. Hence $\kappa_1, \dots, \kappa_4$ define four null vectors. These are the principal null directions. The Petrov classification is equivalent to classifying the polynomial P by the multiplicity of its factors, e.g. a type N spacetime has a single factor of multiplicity 4 whereas a type D spacetime has two factors of multiplicity 2.

The De Smet classification is a five-dimensional generalization of this spinorial approach [7]. However, in contrast with the four-dimensional case the spinorial classification is not equivalent to the classification based on null directions.

In five dimensions one must work with Dirac spinors that have four complex components. One can choose a representation in which C and $C\Gamma^a$ are antisymmetric and $C\Gamma^{ab} = C\Gamma^{[a}\Gamma^{b]}$ are symmetric. From the Weyl tensor one can define a Weyl spinor

$$\Psi_{ABCD} = (C\Gamma^{ab})_{AB} (C\Gamma^{cd})_{CD} C_{abcd}. \quad (9.16)$$

This is manifestly symmetric in AB and in CD and under interchange of AB with CD . In fact it is totally symmetric. De Smet argued this using an “accidental” isomorphism of $Spin(1, 4)$ with a symplectic group. A more direct proof exploits the Fierz identity [42]. Either method works only for $d = 5$.

Just as in four dimensions, the symmetry of Ψ_{ABCD} implies that it is equivalent to a homogeneous quartic polynomial, as defined by (9.14). But there is an important difference from the four-dimensional case: ϵ^A now has four complex components, so P is a polynomial in four complex variables. No longer can the fundamental theorem of algebra be invoked to reduce it to a product of linear factors. Instead, De Smet proposed that one should attempt to factorize P into lower-degree polynomials and classify the Weyl tensor according to the degree and multiplicity of the factors. For example, if P factorizes into the product of two distinct quadratic polynomials then the Weyl tensor is said to be of type **22**. An underlining denotes a repeated factor, so **22** implies that P is the square of a quadratic polynomial. If P does not factorize then the Weyl tensor is algebraically general, denoted **4**. The

⁵ We shall use A, B, \dots to denote spinor indices for general d . A spinor is denoted with a superscript index: thus we write ϵ^A and dual spinors have subscript indices. The gamma matrices are denoted $(\Gamma^a)^A_B$, where a, b, c, \dots refer to an orthonormal basis. Spinor indices are lowered by the use of C_{AB} (the charge conjugation matrix) and raised with C^{-1} .

algebraic type of a *spacetime* is defined to be the least special type of the Weyl tensor in the spacetime.

Various vacuum spacetimes have been classified according to the De Smet scheme. The Schwarzschild [7] and Myers–Perry [43] solutions are type **22**. The Schwarzschild black string is type **22** [7]. Black rings are algebraically general (type **4**) [42].

The Weyl tensor has 35 independent real components whereas a symmetric spinor Ψ_{ABCD} has 35 complex components. Hence the equivalence of these objects implies that Ψ_{ABCD} must satisfy a reality condition worked out in [42]. This implies restrictions on the possible factorizations of P . For example, **1111** is not consistent with the reality condition.⁶ Incidentally, this counting of degrees of freedom shows that only for sufficiently small d can the Weyl tensor be equivalent to a valence-4 symmetric spinor, simply because the number of independent components of the latter grows much more rapidly with d than the number of components of the Weyl tensor.

In [42] relations between the CMPP and De Smet classifications were discussed. It was found that a Weyl tensor belonging to a given CMPP class must belong to a restricted set of possible De Smet classes, and vice versa.

9.3.2 Finding new solutions

De Smet's motivation for introducing his classification was that the resulting algebraically special property might assist in solving the Einstein equation. As discussed above, the general static axisymmetric vacuum solution is not known for $d > 4$. However, De Smet showed that if one imposes the additional condition that the spacetime is type **22** or **22** then a general solution can be found [7], including in the case with a cosmological constant [46]. Unfortunately, the list of solutions that results does not contain anything new.

In a different approach one tries to determine all vacuum solutions of a given De Smet type. This has been done for the simplest nontrivial type consistent with the reality condition, which is **1111** [42]. In this case, the Weyl spinor can be written, in terms of a single spinor ϵ , as $\Psi_{ABCD} = \epsilon_{(A}\epsilon_{B}\bar{\epsilon}_{C}\bar{\epsilon}_{D)}$. The existence of a globally defined spinor field makes the analysis reminiscent of the analysis of supersymmetric solutions of five-dimensional supergravity performed in [47]. One defines a real scalar $f = \bar{\epsilon}\epsilon$, a real vector $V_a = i\bar{\epsilon}\Gamma_a\epsilon$ and a real 2-form $F_{ab} = i\bar{\epsilon}\Gamma_{ab}\epsilon$. The Fierz identity implies various algebraic relations between these

⁶ A similar reality condition arises in four dimensions in the Riemannian signature. In general one can write a four-dimensional Weyl tensor in terms of Ψ_{ABCD} and $\bar{\Psi}_{A'B'C'D'}$. In the Lorentzian signature, the reality of the Weyl tensor implies that these objects are related by complex conjugation. In the Riemannian signature they are independent but must each obey a reality condition that restricts their types to *I*, *D* or *O* [44, 45].

objects, for example that $V^2 = -f^2$, such that V must be timelike or null. The Weyl tensor can be written as an expression quadratic in f , V and F . The Bianchi identity then imposes differential conditions on these objects. The idea is to exploit these conditions to help solve the Einstein equation (with Λ).

In the case in which V is globally null, the solutions must be Kundt solutions that are type *N* in the CMPP classification [42]. The more interesting case is when V is timelike. In this case, the solutions are of the form [42] $ds^2 = -dt^2 + A(t)^2 ds_4^2$, where ds_4^2 is a four-dimensional Einstein space of the Petrov type *(D, O)*⁷ and $A(t)$ is some simple function of t . This class includes the Kaluza–Klein monopole spacetime [48, 49].

This example illustrates how spacetimes that are algebraically special in the De Smet scheme admit various tensor fields globally defined in spacetimes. The types of field that arise are different for each De Smet class. Another example is type **22**, for which the Weyl tensor can be written entirely in terms of a certain 2-form [42]. The Bianchi identity imposes differential conditions on this 2-form. It will be interesting to see whether these kinds of condition are restrictive enough to enable one to determine the most general solution of the Einstein equation in various De Smet classes.

9.4 Other approaches

9.4.1 Bivector classification

The symmetries of the Weyl tensor imply that it can be used to map 2-forms (bivectors) to 2-forms:

$$\omega_{\mu\nu} \rightarrow \omega'_{\mu\nu} = \frac{1}{2} C_{\mu\nu}^{\rho\sigma} \omega_{\rho\sigma}. \quad (9.17)$$

If we introduce a basis for 2-forms and denote basis indices by capital letters then we can write this as

$$\omega'_A = C_A^B \omega_B. \quad (9.18)$$

In this approach, the idea is to classify the Weyl tensor by bringing the matrix C_A^B to a canonical form that depends on (but is not fully determined by) its eigenvalues. This was how Petrov performed the classification of the Weyl tensor in four dimensions.

The use of this method in higher dimensions was discussed in [50]. The resulting classification appears to be distinct from the CMPP (and De Smet) classifications.

⁷ Recall footnote 6: for a Riemannian manifold, the Petrov types of Ψ and $\bar{\Psi}$ are independent.

9.4.2 Hidden symmetries

The subject of the hidden symmetries of higher-dimensional black holes has received much attention recently; see [51] and references therein. In this section we shall discuss only how this topic relates to algebraic classification of the Weyl tensor.

We start with a definition: a *conformal Killing–Yano 2-form* is a 2-form ϕ satisfying

$$\nabla_\mu \phi_{\nu\rho} = \tau_{\mu\nu\rho} + \frac{2}{d-1} g_{\mu[\nu} K_{\rho]} \quad (9.19)$$

for some 3-form τ and 1-form K . If $K = 0$ then ϕ is a *Killing–Yano 2-form*. The remarkable fact that the geodesic equation, Klein–Gordon equation and Dirac equation are all separable in the Kerr spacetime is a consequence of the existence of a Killing–Yano 2-form in this spacetime.

Other four-dimensional type-D spacetimes, e.g., the C-metric, admit a conformal Killing–Yano 2-form (which leads to the separation of variables for *null* geodesics). In fact, in four dimensions the type-D property is equivalent to the existence of a *nondegenerate* conformal Killing–Yano 2-form. This led the authors of [52] to propose that one could take existence of such a 2-form as a higher-dimensional generalization of the type-D property. It was shown (subject to an assumption that the eigenvalues of $\phi^\mu{}_\nu$ are distinct) that this definition implies that the Weyl tensor must be type D in the CMPP classification. I am not aware of any results in the opposite direction.

There has been some progress in using the type-D property as defined by [52] to solve the Einstein equation. This starts from the additional assumption that ϕ should be closed, i.e. $\tau = 0$ in (9.19) (ϕ is then called a *principal* conformal Killing–Yano 2-form). It was shown [51, 53] that the most general solution of the vacuum Einstein equation that admits such a 2-form is the Myers–Perry solution, generalized to include NUT charge and cosmological constant [15]. Of course, this solution was already known. It would be interesting to know whether further progress could be made in solving the Einstein equation in the general case, for which $\tau \neq 0$.

9.4.3 Optical structures

The motivation here comes from the Goldberg–Sachs theorem: maybe the right approach to defining what we mean by “algebraically special” in higher dimensions is to discover a higher-dimensional generalization of the four-dimensional condition

that the spacetime should admit a shearfree null geodesic congruence. We shall refer to such a generalization as an optical structure. Given the existence of such a structure, one can ask what additional restrictions this imposes on the Weyl tensor.

This approach was adopted in [54] (see also [55]), in which it was proposed that an appropriate structure in $d = 2m$ dimensions is an m -dimensional distribution \mathcal{D} of the complexified tangent bundle of spacetime, which is integrable ($[\mathcal{D}, \mathcal{D}] \subset \mathcal{D}$) and totally null ($g(V, W) = 0$ for any $V, W \in \mathcal{D}$). The intersection $\mathcal{D} \cap \bar{\mathcal{D}}$ is then one-dimensional and consists of real null vectors. It can be shown that these are geodesic. In four dimensions this definition is equivalent to the existence of a shearfree null geodesic congruence. Definitions appropriate for odd d were given in [52, 56].

Optical structures are relevant for higher-dimensional black holes. In [52] it was shown that the Myers–Perry–(AdS) solution admits such structures. Indeed, they are closely related to the conformal Killing–Yano tensors that such solutions possess. Black rings do not possess an optical structure [56].

The existence of an optical structure imposes certain restrictions on the Weyl tensor [52, 56]. In order to obtain a generalization of the Goldberg–Sachs theorem, one might seek necessary and sufficient conditions on the Weyl tensor for the existence of an optical structure. It is not clear whether such conditions exist. However, some progress was made for $d = 5$ in [56], which presented conditions on the Weyl tensor sufficient⁸ for the existence of an optical structure. It was proposed that these conditions could be adopted as the definition of “algebraically special” for $d = 5$ and possibly $d > 5$. This appears to be distinct from the CMPP and De Smet definitions.

9.5 Outlook

Various approximate techniques point to the existence of large families of new black hole solutions in higher dimensions. If we are to go beyond perturbative methods to construct these solutions then we must either resort to numerics or develop new techniques for solving the Einstein equation analytically. Results in four dimensions suggest that exploiting the algebraically special property to simplify the Einstein equation is the most promising technique available for finding new analytic solutions. As discussed above, there are several different notions of “algebraically special” in higher dimensions and, therefore, possibly several different ways of simplifying the Einstein equation. It will be interesting to see what new solutions are discovered by these methods.

⁸ Subject to a “genericity” assumption.

Acknowledgements

I am grateful to Mahdi Godazgar, Vojtech Pravda and Alena Pravdova for comments on a draft of this chapter.

References

- [1] R. P. Kerr, Gravitational field of a spinning mass as an example of algebraically special metrics, *Phys. Rev. Lett.* **11** (1963), 237.
- [2] S. A. Teukolsky, *Astrophys. J.* **185** (1973), 635.
- [3] W. Kinnersley and M. Walker, Uniformly accelerating charged mass in general relativity, *Phys. Rev. D* **2** (1970), 1359.
- [4] W. Kinnersley, Type D vacuum metrics, *J. Math. Phys.* **10** (1969), 1195.
- [5] R. Emparan and H. S. Reall, A rotating black ring solution in five-dimensions, *Phys. Rev. Lett.* **88** (2002), 101 101 [arXiv:hep-th/0110260].
- [6] A. Coley, R. Milson, V. Pravda, and A. Pravdova, Classification of the Weyl tensor in higher-dimensions, *Class. Quant. Grav.* **21** (2004), L35 [arXiv:gr-qc/0401008].
- [7] P.-J. De Smet, Black holes on cylinders are not algebraically special, *Class. Quant. Grav.* **19** (2002), 4877–4896 [hep-th/0206106].
- [8] R. C. Myers and M. J. Perry, Black holes in higher dimensional space-times, *Ann. Phys.* **172** (1986), 304.
- [9] R. Milson, A. Coley, V. Pravda, and A. Pravdova, Alignment and algebraically special tensors in Lorentzian geometry, *Int. J. Geom. Meth. Mod. Phys.* **2** (2005), 41 [arXiv:gr-qc/0401010].
- [10] A. Coley, Classification of the Weyl tensor in higher dimensions and applications, *Class. Quant. Grav.* **25** (2008), 033 001 [arXiv:0710.1598 [gr-qc]].
- [11] M. Godazgar and H. S. Reall, Algebraically special axisymmetric solutions of the higher-dimensional vacuum Einstein equation, *Class. Quant. Grav.* **26** (2009), 165 009 [arXiv:0904.4368 [gr-qc]].
- [12] V. Pravda and A. Pravdova, WANDs of the black ring, *Gen. Rel. Grav.* **37** (2005), 1277 [arXiv:gr-qc/0501003].
- [13] S. W. Hawking, C. J. Hunter, and M. Taylor, Rotation and the AdS/CFT correspondence, *Phys. Rev. D* **59** (1999), 064 005 [arXiv:hep-th/9811056].
- [14] G. W. Gibbons, H. Lu, D. N. Page, and C. N. Pope, The general Kerr-de Sitter metrics in all dimensions, *J. Geom. Phys.* **53** (2005), 49 [arXiv:hep-th/0404008].
- [15] W. Chen, H. Lu and C. N. Pope, General Kerr-NUT-AdS metrics in all dimensions, *Class. Quant. Grav.* **23** (2006), 5323 [arXiv:hep-th/0604125].
- [16] V. P. Frolov and D. Stojkovic, Particle and light motion in a space-time of a five-dimensional rotating black hole, *Phys. Rev. D* **68** (2003), 064 011 [gr-qc/0301016].
- [17] N. Hamamoto, T. Houri, T. Oota, and Y. Yasui, Kerr-NUT-de Sitter curvature in all dimensions, *J. Phys. A* **40** (2007), F177–F184 [hep-th/0611285].
- [18] V. Pravda, A. Pravdova, and M. Ortaggio, Type D Einstein spacetimes in higher dimensions, *Class. Quant. Grav.* **24** (2007), 4407 [arXiv:0704.0435 [gr-qc]].
- [19] E. Witten, Instability of the Kaluza-Klein vacuum, *Nucl. Phys.* **B195** (1982), 481.
- [20] H. Stephani, D. Kramer, M. A. H. MacCallum, C. Hoenselaers, and E. Herlt, *Exact Solutions of Einstein's Field Equations*, Cambridge University Press (2003) 701 P.
- [21] V. Pravda, A. Pravdova, A. Coley, and R. Milson, Bianchi identities in higher dimensions, *Class. Quant. Grav.* **21** (2004), 2873 [Erratum: *ibid.* **24** (2007), 1691] [arXiv:gr-qc/0401013].
- [22] M. Durkee and H. S. Reall, A higher-dimensional generalization of the geodesic part of the Goldberg-Sachs theorem, *Class. Quant. Grav.* **26** (2009), 245 005 [arXiv:0908.2771 [gr-qc]].
- [23] M. Ortaggio, V. Pravda, and A. Pravdova, Higher dimensional Kerr-Schild spacetimes, *Class. Quant. Grav.* **26** (2009), 025 008 [arXiv:0808.2165 [gr-qc]].
- [24] T. Malek and V. Pravda, Kerr-Schild spacetimes with (A)dS background, *Class. Quant. Grav.* **28** (2011), 125 011 [arXiv:1009.1727].
- [25] J. Podolsky and M. Ortaggio, Robinson-Trautman spacetimes in higher dimensions, *Class. Quant. Grav.* **23** (2006), 5785–5797 [gr-qc/0605136].
- [26] M. Ortaggio, V. Pravda and A. Pravdova, Ricci identities in higher dimensions, *Class. Quant. Grav.* **24** (2007), 1657 [arXiv:gr-qc/0701150].
- [27] M. Ortaggio, V. Pravda, and A. Pravdova, On asymptotically flat algebraically special spacetimes in higher dimensions, *Phys. Rev. D* **80** (2009), 084 041 [arXiv:0907.1780 [gr-qc]].
- [28] A. Pravdova and V. Pravda, Newman-Penrose formalism in higher dimensions: vacuum spacetimes with a non-twisting multiple WAND, *Class. Quant. Grav.* **25** (2008), 235 008 [arXiv:0806.2423 [gr-qc]].
- [29] J. Podolsky and M. Zofka, General Kundt spacetimes in higher dimensions, *Class. Quant. Grav.* **26** (2009), 105 008 [arXiv:0812.4928 [gr-qc]].
- [30] K. Copsey and G. T. Horowitz, Gravity dual of gauge theory on $S^{**2} \times S^{**1} \times R$, *JHEP* **0606** (2006), 021 [arXiv:hep-th/0602003].
- [31] A. Kaus and H. S. Reall, Charged Randall-Sundrum black holes and $N = 4$ super Yang-Mills in $AdS(2) \times S^{**2}$, *JHEP* **0905** (2009), 032 [arXiv:0901.4236].
- [32] R. M. Wald, Construction of solutions of gravitational, electromagnetic, or other perturbation equations from solutions of decoupled equations, *Phys. Rev. Lett.* **41** (1978), 203.
- [33] R. M. Wald, On perturbations of a Kerr black hole *J. Math. Phys.* **14** (1973), 1453.
- [34] M. Durkee and H. S. Reall, Perturbations of higher-dimensional spacetimes, *Class. Quant. Grav.* **28** (2011), 035 011 [arXiv:1009.0015 [gr-qc]].
- [35] H. Kodama and A. Ishibashi, A master equation for gravitational perturbations of maximally symmetric black holes in higher dimensions, *Prog. Theor. Phys.* **110** (2003), 701 [arXiv:hep-th/0305147].
- [36] M. Durkee and H. S. Reall, Perturbations of near-horizon geometries and instabilities of Myers-Perry black holes, arXiv:1012.4805 [hep-th].
- [37] E. Newman and R. Penrose, An approach to gravitational radiation by a method of spin coefficients, *J. Math. Phys.* **3** (1962), 566.
- [38] A. Coley, R. Milson, V. Pravda, and A. Pravdova, Vanishing scalar invariant spacetimes in higher dimensions, *Class. Quant. Grav.* **21** (2004), 5519 [arXiv:gr-qc/0410070].
- [39] A. P. Gomez-Lobo and J. M. Martin-Garcia, Spinor calculus on 5-dimensional space-times, *J. Math. Phys.* **50** (2009), 122 504 [arXiv:0905.2846 [gr-qc]].
- [40] R. P. Geroch, A. Held, and R. Penrose, A space-time calculus based on pairs of null directions, *J. Math. Phys.* **14** (1973), 874.
- [41] M. Durkee, V. Pravda, A. Pravdova, and H. S. Reall, Generalization of the Geroch-Held-Penrose formalism to higher dimensions, *Class. Quant. Grav.* **27** (2010), 215 010 [arXiv:1002.4826 [gr-qc]].
- [42] M. Godazgar, Spinor classification of the Weyl tensor in five dimensions, *Class. Quant. Grav.* **27** (2010), 245 013 [arXiv:1008.2955 [gr-qc]].
- [43] P.-J. De Smet, The Petrov type of the five-dimensional Myers-Perry metric, *Gen. Rel. Grav.* **36** (2004), 1501–1504 [gr-qc/0312021].

- [44] S. Hacyan, *Phys. Lett.* **A75** (1979), 23.
- [45] A. Karlhede, Classification of Euclidean metrics, *Class. Quant. Grav.* **3** (1986), L1.
- [46] P.-J. De Smet, Five-dimensional metrics of Petrov type 22, *Class. Quant. Grav.* **20** (2003), 2541–2552 [gr-qc/0302081].
- [47] J. P. Gauntlett, J. B. Gutowski, C. M. Hull, S. Pakis, and H. S. Reall, All supersymmetric solutions of minimal supergravity in five dimensions, *Class. Quant. Grav.* **20** (2003), 4587 [arXiv:hep-th/0209114].
- [48] D. J. Gross and M. J. Perry, Magnetic monopoles in Kaluza–Klein theories, *Nucl. Phys.* **B226** (1983), 29.
- [49] R. D. Sorkin, Kaluza–Klein monopole, *Phys. Rev. Lett.* **51** (1983), 87.
- [50] A. Coley and S. Hervik, Higher dimensional bivectors and classification of the Weyl operator, *Class. Quant. Grav.* **27** (2010), 015 002 [arXiv:0909.1160 [gr-qc]].
- [51] P. Krtous, V. P. Frolov, and D. Kubiznak, Hidden symmetries of higher dimensional black holes and uniqueness of the Kerr–NUT–(A)dS spacetime, *Phys. Rev.* **D78** (2008), 064 022 [arXiv:0804.4705 [hep-th]].
- [52] L. Mason and A. Taghavi-Chabert, Killing–Yano tensors and multi-hermitian structures, *J. Geom. Phys.* **60** (2010), 907 [arXiv:0805.3756 [math.DG]].
- [53] T. Houri, T. Oota, and Y. Yasui, Closed conformal Killing–Yano tensor and Kerr–NUT–de Sitter spacetime uniqueness, *Phys. Lett.* **B656** (2007), 214 [arXiv:0708.1368 [hep-th]].
- [54] L. P. Hughston and L. J. Mason, A Kerr–Robinson, *Class. Quant. Grav.* **5** (1988), 275.
- [55] P. Nurowski and A. Trautman, *Diff. Geom. Appl.* **17** (2002), 175.
- [56] A. Taghavi-Chabert, Optical structures, algebraically special spacetimes, and the Goldberg–Sachs theorem in five dimensions, arXiv:1011.6168 [gr-qc].

10

Numerical construction of static and stationary black holes

TOBY WISEMAN

10.1 Introduction

Whilst black holes in four dimensions are well mannered, being spherically symmetric or having special algebraic properties which enable them to be found analytically, moving beyond four dimensions many solutions of interest appear to have no manners whatsoever. The problem of finding these unruly black holes becomes that of solving a nonlinear coupled set of partial differential equations (PDEs) for the metric components given by the Einstein equations. In general it is unlikely that closed-form analytic solutions will be found for many of the exotic black holes discussed earlier in this book. If we are to understand their properties then we must turn to numerical techniques to tackle the PDEs that describe them. It is the purpose of this chapter to develop general numerical methods to address the problem of finding static and stationary black holes.

Surely the phrase “the devil is in the detail” could not have a truer application than to numerics. The emphasis of this chapter will be to provide a road map in which we formulate the problem in as unified, elegant and geometric a way as possible. We will also discuss concrete algorithms for solving the resulting formulation, but the extensive details of implementation will not be addressed, probably much to the reader’s relief. Such details can be found in the various articles cited in this chapter.

Given the extensive efforts that have gone into understanding the dynamical numerical simulation of gravity, the most obvious approach to finding static and stationary solutions is to simulate a dynamical collapse of matter that is likely to form a solution of interest or, alternatively, to simulate vacuum gravity starting with initial data that appear to contain a black hole already. Such a dynamical approach is indeed possible but is not the approach we will develop here, for

several reasons. First, whilst such dynamical evolutions are well understood they are very complicated, typically requiring large computer resources. An important point is that in order to find an accurate stationary solution one would have to run a dynamical simulation for a long time to ensure that the resulting solution has indeed settled down, losing all its excitations to gravity waves, and this can be a serious challenge. Second, since of necessity one would be following the detailed evolution to the formation of a horizon and watching it radiate gravity waves and then ring down, one would certainly be doing far more work than is necessary if all that is required is the final stationary solution. Third, many of the families of exotic solutions that have been discussed are likely to be unstable, at least for certain ranges of parameters. It is still of interest to find such black holes, in order to elucidate the global structure of the space of solutions. For example, in Chapter 4 we discussed the fact that, in Kaluza–Klein theory, inhomogeneous black strings and some localised black holes are thought to be unstable. However, to confirm the elegant idea that these unstable solutions are continuously connected to each other requires us to find them. In principle one might try to tune the initial data in order to find an unstable solution, although in practice this is likely to be very difficult. We also mention a more speculative concern, namely that in higher dimensions it appears that cosmic censorship does not hold [1], and therefore it is unclear how generically one might expect to encounter singularity formation in dynamics.

For all these reasons, here we focus on finding static or stationary black holes by solving the static or stationary Einstein equations directly. Since these are PDEs, the most important question is what character they have, as this will determine how to approach the problem. In the context of dynamics the Einstein equations should be thought of as having a hyperbolic character, i.e. on small scales one has wave propagation along a light-cone. Consequently the dynamical Einstein equations are considered as an initial value problem, with data specified on a Cauchy surface or on a past light cone. In contrast, the static and stationary problem should be thought of as having an elliptic character. One solves elliptic systems as boundary value problems in which, for a second-order elliptic system, one piece of data, for example, a Dirichlet, Neumann, Robin or oblique condition is given on all boundaries. Physically, in a static or stationary context such boundary conditions will correspond to ensuring horizon regularity whilst also prescribing some particular asymptotic behaviour.

Our focus here is to present the problem in an elliptic framework, for which one requires only entirely conventional techniques and modest desktop computing resources. In particular we will discuss standard methods for solving elliptic systems, namely relaxation and Newton's method. In addition this approach is amenable to the full variety of methods for representing solutions, for example the

classical finite difference approach or the more modern spectral, pseudo-spectral and finite element methods.

Before embarking on our discussion of the numerical stationary problem for higher-dimensional black holes, some comments on the history of this problem are in order. Only with the rather recent revelation that black hole uniqueness breaks down in dimensions $D > 4$ did the numerical exploration of gravity in higher dimensions begin. Of course, in four dimensions the uniqueness of the Kerr solution meant that numerical work was not traditionally directed at vacuum black holes. Indeed, a key ingredient of the classical proofs of uniqueness was to formulate the four-dimensional stationary axisymmetric vacuum problem as an elliptic system [2]. However, the numerical stationary elliptic problem has featured prominently in the context of relativistic stars, particularly in the axisymmetric case, and there is a distinguished history of numerical work in this area beginning in the early 1970s (see for example the seminal works [3–5]). For a review of this fascinating field the reader is referred to [6]. In the context of nonvacuum static and stationary black holes such numerical methods were applied in [7] and [8] to find exotic four-dimensional charged solutions. In all these cases the approaches developed were based on the Weyl–Papapetrou form of the metric, exploiting the fact that the metric depends nontrivially on only two coordinates and has two commuting Killing vectors, so that solving the Einstein equations is consistently reduced to an elliptic problem. In the analytic context, recent uniqueness theorems for vacuum stationary black holes in higher dimensions [9, 10] also phrase the problem as an elliptic system and so far attention has been restricted to D -dimensional spacetimes with $D - 2$ commuting Killing vectors, where again the Weyl–Papapetrou form is used (see also [11]).

Numerical methods for metrics depending nontrivially on two coordinates but without the restriction of having $D - 2$ commuting Killing vectors were given in [12, 13] and applied to higher-dimensional black holes. An analogue of the Weyl form was employed for the metric. It was shown that a subset of the Einstein equations are elliptic in the metric components and may be solved by regarding the remaining Einstein equations as constraints. One must show that these constraints may be solved consistently by consideration of the various boundary conditions. Being based on this analogue Weyl form, these methods are manifestly noncovariant and by construction can only be applied to problems depending nontrivially on two coordinates. Whilst they have yielded interesting results, they give a rather unstable numerical scheme for solutions in $D > 4$ that have axes of rotational symmetry (such as localised Kaluza–Klein black holes), presumably owing to the lack of covariance, and are therefore hard to use in practice. We emphasise that the methods to be developed here will be fully covariant and may be applied to problems depending nontrivially on an arbitrary number of coordinates. In our

experience they are much better behaved in practice; for example, they have no difficulties regarding axes of symmetry.

For simplicity this chapter will focus entirely on finding vacuum black holes with no cosmological term and with a single-component nonextremal Killing horizon. We will concentrate on treating the case of static black holes, where most previous work has been directed. Indeed, the numerical solutions presented in [14] and discussed in Chapter 4 were found precisely using the methods we discuss. By the analytic continuation of time this problem has an elegant geometric formulation as finding Ricci-flat Riemannian solutions. We will study in detail the issue of its formulation as an elliptic boundary value problem and give two algorithms for solving the resulting PDEs. In the remainder of the chapter we will show that the stationary case, which must be treated directly in Lorentzian signature, can also be thought of as an elliptic boundary value problem.

10.2 Static vacuum black holes

In this section we treat the static vacuum case, following the approach of [14]. Let us consider a general nonextremal static black hole solution with a single component horizon, so that we may write the metric as

$$ds^2 = -N(x)^2 dt^2 + h_{ij}(x)dx^i dx^j , \quad (10.1)$$

where $\partial/\partial t$ is the static timelike Killing vector and at the horizon the norm of this vector vanishes, so that $N = 0$. The zeroth law implies that the surface gravity given by the function $\kappa = \partial_n N|_{N=0}$, where n is the unit vector normal to the horizon in a constant- t slice, is actually a constant. A standard result of Euclidean quantum gravity is that any such static black hole may be analytically continued to imaginary time $\tau = it$ to yield a Riemannian manifold with metric

$$ds^2 = +N(x)^2 d\tau^2 + h_{ij}(x)dx^i dx^j , \quad (10.2)$$

where, upon making τ an angular coordinate with period $\tau \sim \tau + 2\pi/\kappa$, the metric at the horizon becomes smooth with no boundary there. To manifest this we may take Gaussian coordinates normal to the horizon, where $x^i = \{r, x^a\}$ and the horizon is located at $r = 0$. Then near the horizon we have for the metric

$$ds^2 \sim (\kappa^2 r^2 d\tau^2 + dr^2) + \tilde{h}_{ab}(r, x)dx^a dx^b , \quad (10.3)$$

and we see that the shrinking Euclidean time circle forms the angle of polar coordinates in \mathbb{R}^2 , with r the radial coordinate. Whilst this polar coordinate system breaks down at the origin $r = 0$, simply by taking “Cartesian” coordinates $X = r \cos \kappa \tau$ and $Y = r \sin \kappa \tau$ one can write the metric in a chart that covers the horizon.

Thus a static black hole can be written as a smooth Euclidean geometry, where Euclidean time τ is periodic and $\partial/\partial\tau$ generates a $U(1)$ isometry. There is no boundary at the horizon and the geometry is perfectly smooth there. The horizon is marked by the vanishing of the vector $\partial/\partial\tau$, and consequently the horizon forms the fixed point set of the static isometry.

Solving the vacuum Einstein equation without the cosmological term is equivalent to finding a geometry that is Ricci flat, so that $R_{\mu\nu} = 0$. Finding a vacuum static black hole solution can then be viewed as part of the more general problem of finding Ricci-flat Riemannian geometries, the only special feature of a static black hole geometry being the $U(1)$ isometry generated by the hypersurface-orthogonal vector $\partial/\partial\tau$, which leaves a codimension-2 submanifold (the horizon) fixed.

There are several attractive features of this way of thinking. First, there is in principle no boundary at the horizon and, from the point of view of our boundary value problem, no boundary condition to impose there. The “in principle” qualification, which we will explain in more depth later, refers to the fact that if one wishes to use coordinates that manifest the $U(1)$ isometry then these will not cover the horizon, in exactly the same way that the polar coordinates do not cover the origin point. Whilst in practice it is sensible to adapt coordinates to any isometries, and we shall deal with this in detail later, for the present let us take a more formal view, ignoring issues of implementation such as which coordinates to take. In principle one can always take coordinates that are regular at the horizon (the “Cartesian” coordinates above) and then there is no boundary.

The second attractive feature is that Euclidean continuation is precisely what is done in semiclassical quantum gravity in considering a canonical ensemble, i.e., in order to work at fixed finite temperature. In particular the proper size of the Euclidean time circle has asymptotically an interpretation as the inverse temperature of the black hole. Far from the black hole horizon we will impose boundary conditions on the metric that involve fixing amongst other things the proper size of the time circle. This boundary value formulation thus leads us in a natural way to fix a very physical quantity, the temperature.

Third, the problem of finding Ricci-flat Riemannian metrics is one with wider application than just the finding of static black holes. For example, finding numerically the exotic Calabi–Yau geometries [15, 16] that underpin certain string theory compactifications is currently required in order to make detailed predictions of low-energy phenomenology. In addition, particularly in the case of such Kähler metrics, there may be new ways to think about the problem, inspired by the geometry [17, 18], which in the future might be useful in our black hole context.

Let us now consider how to formulate the problem of finding Ricci-flat Riemannian geometries as an elliptic boundary value problem.

10.2.1 The harmonic Einstein equation

The vacuum Einstein equation $R_{\mu\nu} = 0$ is a second-order quasilinear PDE in the metric components. Perturbing the metric about some background $g_{\mu\nu}$ by a perturbation $h_{\mu\nu}$, we have

$$\delta R_{\mu\nu} \equiv \Delta_R h_{\mu\nu} = \Delta_L h_{\mu\nu} + \nabla_{(\mu} v_{\nu)} , \quad (10.4)$$

where

$$\begin{aligned} \Delta_L h_{\mu\nu} &\equiv -\frac{1}{2}\nabla^2 h_{\mu\nu} - R_{\mu}{}^{\kappa}{}_{\nu}{}^{\lambda} h_{\kappa\lambda} + R_{(\mu}{}^{\kappa} h_{\nu)\kappa} , \\ v_{\mu} &\equiv \nabla_{\nu} h^{\nu}_{\mu} - \frac{1}{2}\partial_{\mu} h \end{aligned} \quad (10.5)$$

and Δ_L is the usual Lichnerowicz operator. The principal part of Δ_R , which we denote P_g , is given locally by the two derivative terms:

$$P_g h_{\mu\nu} = \frac{1}{2}(g^{\alpha\beta}\partial_{\mu}\partial_{\alpha}h_{\beta\nu} + g^{\alpha\beta}\partial_{\nu}\partial_{\alpha}h_{\beta\mu} - g^{\alpha\beta}\partial_{\alpha}\partial_{\beta}h_{\mu\nu} - g^{\alpha\beta}\partial_{\mu}\partial_{\nu}h_{\alpha\beta}) , \quad (10.6)$$

and this linear operator controls the very-short-wavelength behaviour of the perturbations, which determines the character of the equations $R_{\mu\nu} = 0$ about the background g . The condition that $R_{\mu\nu} = 0$ is elliptic about the background g gives the requirement that if one takes $h_{\mu\nu} = a_{\mu\nu} \exp(ik_{\alpha}x^{\alpha})$ for some constants $a_{\mu\nu}$ and any real nonzero k_{μ} then $P_g h_{\mu\nu} \neq 0$ everywhere. Physically this condition means that nowhere can we find a point where short-wavelength perturbations in a particular direction propagate as a wave.

We see that for perturbations of the form $h_{\mu\nu} = \partial_{(\mu}u_{\nu)}$, where u is some vector field, we have $P_g h_{\mu\nu} = 0$. Thus the Ricci-flatness condition $R_{\mu\nu} = 0$ is not an elliptic equation. Such a perturbation can be thought of as a short-wavelength infinitesimal diffeomorphism generated by u . This diffeomorphism is given by $h_{\mu\nu} = \nabla_{(\mu}u_{\nu)}$ but when u varies on very short scales, we have $\nabla_{(\mu}u_{\nu)} \sim \partial_{(\mu}u_{\nu)}$. Hence we may see the lack of ellipticity of $R_{\mu\nu} = 0$ as a consequence of gauge invariance. Without an elliptic set of PDEs we cannot treat the system as a boundary value problem as we might wish. In order to proceed we must therefore break this gauge invariance. However, lifting the gauge invariance need not imply breaking covariance. We emphasise that the method described below will indeed be fully covariant.

Instead of considering the vacuum Einstein equation $R_{\mu\nu} = 0$, we will consider what we term the *harmonic Einstein* equation,¹ $R_{\mu\nu}^H = 0$, where

$$R_{\mu\nu}^H \equiv R_{\mu\nu} - \nabla_{(\mu}\xi_{\nu)} , \quad \xi^{\alpha} \equiv g^{\mu\nu}(\Gamma_{\mu\nu}^{\alpha} - \bar{\Gamma}_{\mu\nu}^{\alpha}) . \quad (10.7)$$

¹ Note that this equation was referred to as the Einstein–DeTurck equation in [14, 19].

Here, Γ is our usual Levi–Civita connection of g and $\bar{\Gamma}$ is another connection that we are free to choose and to then consider as fixed. We term the reference connection as $\bar{\Gamma}$. Being constructed from the difference of two connections, the quantity ξ is a globally defined vector field. The equations $R_{\mu\nu}^H = 0$ have the great virtue of being elliptic. The principal part of the linearisation about a background g is simply

$$P_g^H h_{\mu\nu} = -\frac{1}{2}g^{\alpha\beta}\partial_{\alpha}\partial_{\beta}h_{\mu\nu} , \quad (10.8)$$

and thus for *any* Riemannian background g this is clearly elliptic. Taking $h_{\mu\nu} = a_{\mu\nu} \exp(ik_{\alpha}x^{\alpha})$, we have $P_g^H h_{\mu\nu} = a_{\mu\nu}k^{\alpha}k_{\alpha}$, which indeed only vanishes for vanishing $h_{\mu\nu}$ or k_{μ} , as required for ellipticity. An important point is that we have analytically continued to Euclidean signature. For a Lorentzian-signature metric g , $P_g^H h_{\mu\nu} = 0$ at a point x if we pick any nonzero but null vector k . In this Lorentzian case the harmonic Einstein equation has a hyperbolic character.

The harmonic Einstein equation has been used in the context of analysis for decades, for both the Riemannian elliptic problem and the Lorentzian dynamical hyperbolic problem (see for example [20]), with variations in the precise definition of the vector that nevertheless all lead to elliptic or hyperbolic equations, at least in the neighbourhood of a Ricci-flat solution.

The choice of vector field in (10.7) is due to DeTurck, who introduced it in the Riemannian context and later used it to show that Ricci flow is parabolic, as we will discuss later [21]. For simplicity, in what follows we will reduce the freedom in (10.7) by taking $\bar{\Gamma}$ to be the Levi–Civita connection of a reference metric \bar{g} that we are free to choose and then to consider as fixed. In this case we may write

$$\xi_{\mu} = g^{\alpha\beta}(\bar{\nabla}_{\alpha}g_{\beta\mu} - \frac{1}{2}\bar{\nabla}_{\mu}g_{\alpha\beta}) , \quad (10.9)$$

where $\bar{\nabla}$ is the covariant derivative of the metric \bar{g} .²

In D dimensions there are D local-coordinate degrees of freedom to fix, in order to lift the gauge invariance of the Ricci-flatness condition. The condition $\xi^{\mu} = 0$ precisely provides these D additional local conditions. The DeTurck choice of ξ can be thought of as a global version of the generalised harmonic coordinates introduced by Friedrich in the Lorentzian hyperbolic context, which were independently employed later by Garfinkle for numerical evolutions [23, 24] and have been used extensively since then. In generalised harmonic coordinates one writes $\xi^{\alpha} = g^{\mu\nu}\Gamma_{\mu\nu}^{\alpha} + H^{\alpha}$ in local coordinates for some choice of H^{α} , although we note

² We note this is close to, although not the same as, the Bianchi choice of vector field, used for example in [22]. In particular the Bianchi choice does not lead to the simple principal symbol (10.8) except for metrics g close to the reference metric \bar{g} .

that H^α is not a vector field globally. Locally this is the same as the definition above, where $H^\alpha = -g^{\mu\nu}\bar{\Gamma}_{\mu\nu}^\alpha$. The vanishing of ξ^μ can be thought of as a generalised harmonic gauge condition.³ Given a chart, the coordinates x^α are functions over the part of the manifold covered by the chart. If in this chart we took $\bar{\Gamma}_{\mu\nu}^\alpha = 0$ then the vanishing of ξ would imply $\nabla_S^2 x^\alpha = 0$, where ∇_S^2 is the scalar Laplacian, and hence the local coordinates would be harmonic functions – the so-called harmonic coordinates. For a general choice of reference connection we have $\nabla_S^2 x^\alpha = H^\alpha$, corresponding to the use of generalised harmonic coordinates. From now on we shall refer to a metric with $\xi = 0$ (our DeTurck choice of ξ in (10.7)) as being in the generalised harmonic gauge.⁴

A Ricci-flat solution in the generalised harmonic gauge $\xi = 0$ solves the harmonic Einstein equation $R_{\mu\nu}^H = 0$. However, the careful reader will notice that, whilst the PDEs $R_{\mu\nu}^H = 0$ are indeed elliptic for a Riemannian g (or indeed hyperbolic for a Lorentzian g), there is no reason to suspect a priori that a solution to $R_{\mu\nu}^H = 0$ has anything to do with a solution to the Ricci-flatness condition.

We now consider why solving $R_{\mu\nu}^H = 0$ might lead to a Ricci-flat solution presented in generalised harmonic coordinates. The situation is simplest in the Lorentzian hyperbolic context, where the answer lies in the contracted Bianchi identity applied to the harmonic Einstein equation. In either signature this yields the linear PDE

$$\nabla^2 \xi_\mu + R_\mu^\nu \xi_\nu = 0 \quad (10.10)$$

for the vector ξ^μ . If one ensures that ξ^μ and its normal derivative vanish on a Cauchy surface then, since the linear equation above is a wave equation, i.e. hyperbolic, for a Lorentzian g ξ^μ must remain zero under evolution of the metric in time. Hence in the dynamical hyperbolic context one simply imposes the vanishing of ξ and its time derivative as constraints on the initial data for the metric and then solves the hyperbolic harmonic Einstein equation. This procedure is guaranteed to recover a solution of the actual Einstein equation $R_{\mu\nu} = 0$ in coordinates defined by $\xi^\mu = 0$.

³ Note the subtle difference between the normal use of generalised harmonic coordinates, where one fixes H locally, and the DeTurck case here, where instead one fixes $\bar{\Gamma}$. These are inequivalent, as the relation between them involves the metric g .

⁴ Since $\xi = 0$ can be viewed as an elliptic equation for the coordinate functions we see that, whilst it is able to constrain the local degrees of freedom in the gauge, as with any elliptic equation one must specify the boundary data and this global gauge freedom must be fixed. When one specifies charts, one must specify the domain of these charts in \mathbb{R}^D , and this data precisely give these Dirichlet boundary conditions for the harmonic coordinate functions of the chart. The Dirichlet data for all the coordinate functions then imply that all the global data specifying the gauge are used up. Thus, in the elliptic context, harmonic coordinates are convenient as one has precisely the freedom to choose fixed charts on the manifold, and having made this choice there is no gauge freedom left. If the manifold has a boundary (or a fictitious boundary, as we discuss later) then one may freely use a chart adapted to this boundary, so that the boundary is at some constant coordinate location, without being concerned that the boundary position in the harmonic coordinates might be something that one must solve for, as in some other gauge choices.

In the Riemannian elliptic context in which we are interested, the situation is a little more complicated. As we shall see later we must supply data on any boundaries, give an initial guess and essentially hope for the best. Our initial guess and our reference metric will typically be far from a Ricci-flat solution. Hence we cannot consider the harmonic Einstein equation only in the neighbourhood of a Ricci flat solution, as the entire point of the problem is to find that solution. One might then imagine that the situation is hopeless in the elliptic context, in other words that solving $R_{\mu\nu}^H = 0$ is a problem unrelated to solving $R_{\mu\nu} = 0$. This is not the case, as we now discuss.

10.2.2 Ricci-flat solutions and Ricci solitons

A solution to the harmonic Einstein equation $R_{\mu\nu} = \nabla_{(\mu}\xi_{\nu)}$ with nonvanishing ξ is called a *Ricci soliton*. Obviously, we are interested in Ricci-flat solutions rather than solitons. As we now proceed to discuss, the existence of solitons is fortunately rather constrained provided that we choose our boundary conditions appropriately.

Suppose that we have boundaries or asymptotic regions in our problem and that we prescribe some data for the metric there that is compatible with the ellipticity of the harmonic Einstein equation. These data for the metric define a certain behaviour for the vector field ξ . Consider, as an example, a manifold with a boundary. Taking local coordinates near the boundary we may write the metric as

$$ds^2 = \alpha^2 dw^2 + \gamma_{ij}(dx^i + \beta^i dw)(dx^j + \beta^j dw), \quad (10.11)$$

where the boundary is located at $w = 0$. From a geometrical perspective, we might expect to try to fix some boundary condition involving the induced metric $\gamma_{ij}|_{w=0}$ and the extrinsic curvature $K_{ij} = (1/2\alpha)(\partial_w \gamma_{ij} - 2\nabla_{(i}\beta_{j)})|_{w=0}$, where the covariant derivatives and metric contractions are taken with respect to γ . We may regard γ_{ij} as the geometric Dirichlet data and K_{ij} , which involves the normal derivative of γ_{ij} , as the Neumann data. However, γ_{ij} and K_{ij} only have $D(D - 1)/2$ components whereas the full metric $g_{\mu\nu}$ has $D(D + 1)/2$. The harmonic Einstein equation requires elliptic data for all these components of $g_{\mu\nu}$. How should we fix the remaining D conditions? Since we are interested in Ricci-flat solutions of $R_{\mu\nu}^H = 0$, where $\xi^\mu = 0$, we had better enforce this. The additional conditions $\xi^\mu = 0$ precisely give the extra D conditions for the metric components.⁵

For the black holes discussed in this book, we are not concerned with manifolds with boundary, but, rather with asymptotic conditions. As we shall see

⁵ Very interestingly, Anderson showed [22] that one cannot impose $\xi = 0$ and require Dirichlet or Neumann boundary conditions (i.e. a fixed induced metric or extrinsic curvature), as these are not well-posed boundary conditions. Instead, one may fix the conformal class of γ_{ij} and the trace of K_{ij} , together with $\xi = 0$.

explicitly later, we may impose an asymptotically flat or Kaluza–Klein condition, so as to ensure that $\xi \rightarrow 0$ at infinity. However, this boundary example illustrates nicely that, in order to give data for the harmonic Einstein equation, one should ensure that the data are consistent not only with the geometric condition of interest but also ensuring with the vanishing of ξ . Obviously if one took boundary conditions that did not allow ξ to vanish then, although one might still be able to solve $R_{\mu\nu}^H = 0$, one should not expect to find Ricci-flat solutions, only solitons.

Consider a metric g and boundary or asymptotic conditions imposed on it that are consistent with ellipticity. These boundary conditions impose certain behaviours on ξ , for example $\xi = 0$ at a boundary as in the example above or $\xi \rightarrow 0$ in an asymptotically flat or Kaluza–Klein region. Then consider the action of the linear vector operator

$$\mathcal{D}_\mu^\nu \equiv \nabla^2 \delta_\mu^\nu + R_\mu^\nu \quad (10.12)$$

on this background, so that we may write the Bianchi identity (10.10) as $\mathcal{D} \cdot \xi = 0$. Take a vector field χ that has the same boundary or asymptotic behaviour as ξ , for example $\chi = 0$ on the boundary described above or $\chi \rightarrow 0$ in an asymptotically flat or Kaluza–Klein region. In order to find Ricci-flat solutions to the harmonic Einstein equation one should ensure that the metric boundary conditions lead to conditions on χ such that the linear elliptic vector problem $\mathcal{D} \cdot \chi = 0$ is well posed and admits the trivial solution $\chi = 0$.

Take the example of an asymptotically flat or Kaluza–Klein black hole. In the Riemannian signature with periodic time there are no boundaries, only the asymptotic region. The problem $\mathcal{D} \cdot \chi = 0$ with the condition $\chi \rightarrow 0$ asymptotically is indeed well posed and $\chi = 0$ is obviously a solution.

Note that we do not necessarily require the boundary condition $\xi \rightarrow 0$ on all boundaries. For example, at a “fictitious boundary” (see section 10.2.5 below) there are conditions, as we shall see later, where the tangential components of ξ have vanishing normal derivative (a Neumann condition) rather than themselves being forced to vanish. This still gives the well-posed problem $\mathcal{D} \cdot \chi = 0$, which is consistent with a trivial solution.

Now that we have boundary conditions consistent with obtaining a Ricci-flat solution, we may use the Bianchi identity to control the existence of solitons. A necessary condition for a soliton to exist is that $\mathcal{D} \cdot \chi = 0$ must admit a nontrivial solution for χ . Alternatively we may say that the vector operator \mathcal{D} with boundary conditions given by the behaviour of ξ must have a nontrivial kernel. Now, the kernel of such an operator should be finite dimensional and may certainly be trivial. The necessary condition that \mathcal{D} have a nontrivial kernel strongly constrains the possibility of the existence of Ricci solitons. Indeed, long ago Bourguignon [25]

showed that there are no Ricci solitons on a compact manifold without boundary for any choice of the vector ξ . In certain cases, such as for asymptotically flat or Kaluza–Klein metrics, as discussed later we can prove that the kernel is again trivial and that solitons cannot exist for the DeTurck choice of ξ in which we are interested. One arrives at the surprising conclusion that, despite the fact that one is solving the harmonic Einstein equation, which in a naive view is quite different from the Einstein equation itself, in certain situations of interest the only solutions are in fact Ricci-flat ones with the gauge condition $\xi = 0$ imposed.

Even if solitons do exist, this is in principle not a problem. Since the harmonic Einstein equation is elliptic, for well-posed boundary conditions on the metric we expect that solutions are locally unique. Hence a solution cannot be continuously deformed into another solution without suitably adjusting the boundary conditions. If there exists a Ricci-flat solution, then any Ricci soliton solutions cannot be arbitrarily “near” to it. Hence, numerically it should always be possible to distinguish the solution of interest from a soliton. An obvious test is to compute the vector field ξ and see whether it is zero. In particular let us define the scalar $\phi \equiv \xi^\mu \xi_\mu$ giving the norm of ξ . For a Riemannian manifold, the vanishing of ξ is necessary for the function ϕ to vanish. Hence we may check the magnitude of ϕ computed for our solution, and if it is anywhere nonzero then the solution is a soliton and we should try to find another solution. An important question, in practice, is how many soliton solutions there are. If one were trying to find a single Ricci-flat solution in a vast forest of solitons then such an approach may be impractical. If it is a single Ricci-flat solution in a small spinney then this approach is practical. Obviously, if no solitons exist then it is ideal.

10.2.3 Solutions that are asymptotically flat or Kaluza–Klein

Treating our static black hole problem as a Riemannian boundary value problem, we must impose boundary conditions asymptotically. Our discussion now follows that developed in [19]. We impose the condition that the Riemannian geometry has an asymptotic region such that the metric approaches the direct product $S_\beta^1 \times \mathcal{M}$. Here S_β^1 is the Euclidean time circle with length β (corresponding to temperature $T = 1/\beta$) and \mathcal{M} is a Ricci-flat manifold, the obvious choices for the latter being Euclidean space \mathbb{R}^{D-1} or $\mathbb{R}^{D-2} \times S_L^1$, the product of Euclidean space and a circle of length L . The former choice is appropriate for the Euclidean continuation of an asymptotically flat Lorentzian spacetime and the latter for an asymptotically Kaluza–Klein spacetime.

Let us consider the case where we require the black hole to be asymptotically flat. We require the manifold to have an asymptotic region where, for some large

R , the metric's behaviour is given by

$$\begin{aligned} ds^2 &= g_{\mu\nu}dx^\mu dx^\nu = d\tau^2 + \delta_{ij}dx^i dx^j + O(r^{-p}), \\ \partial_i g_{\mu\nu} &= O(r^{-p-1}), \quad \partial_i \partial_j g_{\mu\nu} = O(r^{-p-2}), \end{aligned} \quad (10.13)$$

for all $r > R$ and for some positive p . Here x^i are the usual Euclidean coordinates, with $r = \sqrt{\delta_{ij}x^i x^j}$. For a Ricci-flat solution we require that $p = D - 3$. We also require that the reference metric \bar{g} that defines the vector ξ as in (10.9) is asymptotically flat, so that in the same part of the manifold this reference metric also behaves as above.

In practice it is convenient to compactify the radial coordinate in this asymptotic region. Taking $\rho = 1/r$, we write the metric as

$$ds^2 = N^2 d\tau^2 + \frac{\alpha^2}{\rho^4} d\rho^2 + \frac{1}{\rho^2} h_{ab}(d\theta^a + w^a d\rho)(d\theta^b + w^b d\rho) \quad (10.14)$$

and require that $N = 1$, $\alpha = 1$, $w_a = 0$ and $h_{ab} = \Omega_{ab}$ at $\rho = 0$, where Ω_{ab} is the unit $(D - 2)$ -sphere metric. These appear as Dirichlet boundary conditions at $\rho = 0$ for the components of g , although we recall that $\rho = 0$ is really a regular singular point of the PDEs, since this is an asymptotic region rather than a boundary at a finite distance.

One may compute straightforwardly that, taking an asymptotically flat reference metric,

$$\xi^\tau = O(r^{-p-1}), \quad \xi^i = O(r^{-p-1}). \quad (10.15)$$

We see that the norm $\phi = \xi^\mu \xi_\mu \sim O(r^{-2p-2})$, so that the vector ξ goes to zero length asymptotically for any positive value of p . Thus these asymptotic boundary conditions are consistent with the proposition that the linear elliptic problem $\mathcal{D} \cdot \chi = 0$ discussed in the previous section is well posed and has a trivial solution. The asymptotically Kaluza–Klein case proceeds in exactly the same manner, but now one requires that the metric asymptotes to

$$\begin{aligned} ds^2 &= d\tau^2 + \delta_{ij}dx^i dx^j + dy^2 + O(r^{-p}), \\ \partial_i g_{\mu\nu} &= O(r^{-p-1}), \quad \partial_i \partial_j g_{\mu\nu} = O(r^{-p-2}), \end{aligned} \quad (10.16)$$

for some positive p ; y is the compact Kaluza–Klein circle and has period L . One obtains the same behaviour, $\phi \sim O(r^{-2p-2})$, as in the asymptotically flat case.

10.2.4 A maximum principle and the nonexistence of solitons

We have discussed above how a static asymptotically flat or Kaluza–Klein black hole may be thought of as a smooth Riemannian manifold with no boundary except for the asymptotic region. We showed that the vector ξ tends to zero in this

asymptotic region provided that the reference metric shares the same asymptotics. We now turn to the important question, raised earlier, of whether we can control the existence of Ricci solitons with such boundary conditions. Following [19], we will now show that, as we claimed earlier, solitons cannot exist. This implies that solving the harmonic Einstein equation is equivalent to solving the Einstein equation together with imposing the generalised harmonic gauge condition $\xi = 0$.

Contracting the Bianchi identity (10.10) with the vector and using the soliton equation yields

$$\nabla^2 \phi + \xi^\mu \partial_\mu \phi = (\nabla_\mu \xi_\nu)(\nabla^\mu \xi^\nu) \geq 0, \quad (10.17)$$

where again $\phi = \xi^\mu \xi_\mu$ is the norm of the vector field and we have used the fact that for a Riemannian geometry the right-hand side is nonnegative everywhere. Suppose, now, that we have a solution to the harmonic Einstein equation. Consider a function f obeying the linear elliptic equation,

$$\nabla^2 f + \xi^\mu \partial_\mu f \geq 0. \quad (10.18)$$

This equation enjoys a maximum principle, which states that if f is nonconstant then it must attain its maximum value on the boundary of the manifold.⁶ Furthermore, if a maximum exists at the boundary then the outer normal derivative of f at this maximum is strictly positive.

Since the function $\phi \geq 0$ and since a Ricci soliton must have $\phi \neq 0$ then a necessary condition for a solution to be a soliton is that ϕ is either constant and nonzero or it has a maximum somewhere. If ϕ is constant and nonzero then this implies that $\nabla_\mu \xi_\nu = 0$ and so the vector ξ is covariantly constant; thus, whilst the solution is a soliton it is also Ricci flat. Thus a challenge to Ricci flatness means that ϕ must be nonconstant and hence have a maximum somewhere. Since on replacing f with ϕ in (10.18) we obtain the condition (10.17), and for (10.18) we have a maximum principle, we see that if ϕ is nonconstant then its maximum must be at the boundary of the manifold, with positive normal outer gradient, or in an asymptotic region.

In the case of a compact manifold with no boundary we recover the result that a solution must be Ricci flat. For black hole solutions that necessarily have some form of boundary, either at finite proper distance from the horizon or asymptotically at infinite proper distance, we see that the existence of a soliton is intimately tied to the precise form of the boundary conditions imposed there.

Let us consider the asymptotically flat or asymptotically Kaluza–Klein boundary conditions discussed in the previous section. Assuming that we had found a solution to the harmonic Einstein equation compatible with those asymptotics, we calculated

⁶ See for example [26] or, for a statement of results specifically on Riemannian manifolds, see [27].

that $\phi = |\xi|^2 = O(r^{-2p-2})$; for the very weak requirement $p > 0$ this implies that $\phi \rightarrow 0$ asymptotically. Provided that there are no other boundaries, a simple application of the maximum principle rules out the existence of Ricci solitons, as we claimed earlier.⁷

10.2.5 Isometries and “fictitious” boundaries

Let us now turn to a more practical issue, namely the use of isometries to reduce the effective dimension of a PDE. A PDE problem in high dimensions rapidly becomes intractable. Thus, if we have isometries in our geometry, it is important to manifest them explicitly using adapted coordinates and hence benefit from the storage savings. The example of the five-dimensional Kaluza–Klein black holes discussed in Chapter 4 is a case in point. This five-dimensional problem is reduced to two effective dimensions when one takes into account the static $U(1)$ and rotational $SO(3)$ isometries.

Suppose we wish to represent numerically a function that has spherical symmetry in Euclidean space \mathbb{R}^n . Using Cartesian coordinates, so that $ds^2 = \delta_{ij}dx^i dx^j$, the origin of the symmetry, $x^i = 0$, is not a special point and the function is simply smooth there. If we use coordinates adapted to the symmetry, i.e., the spherical polar coordinates $ds^2 = dr^2 + r^2 d\Omega^2$, the function depends only on the radial coordinate r , giving the desired saving in storage. However, we find that the polar coordinate chart breaks down at the origin, and so now we must treat the point at the origin as effectively a boundary point – we term this a “fictitious boundary”. Of course, we may deduce the required boundary conditions in the polar chart simply from the requirement that in Cartesian coordinates the function be smooth, so that $f(x)$ is a C^∞ function. Then, using the fact that $r^2 = \delta_{ij}x^i x^j$, this implies a function that has only radial dependence must be a smooth function in r^2 , i.e. $f = f(r^2)$ is C^∞ .

There are two important fictitious boundaries that typically arise when one is considering static black holes. First, associated with the Euclidean static $U(1)$ isometry we have that the horizon is precisely the place where the time circle vanishes and hence the isometry has a fixed action. In this case we may write the metric in polar coordinates as

$$ds^2 = Adr^2 + r^2 Bd\tau^2 + rC_a drdx^a + h_{ab}dx^a dx^b, \quad (10.19)$$

⁷ Assume for contradiction that there is a Ricci soliton, so that $\phi \neq 0$. Consider some $R' > R$, so that on the closed surface $r = R'$ in the asymptotic region we have $\phi \leq C/R'^{2p+2}$ for some constant C . Then everywhere in the interior of this surface the maximum principle states that $\phi \leq C/R'^{2p+2}$. Under the assumption $\phi \neq 0$, we must be able to find a point p where ϕ is nonzero; we denote its value ϕ_0 , so that $\phi_0 = \phi(p)$. Choosing R' large enough, we may always ensure that the point p is in the interior of the portion of the manifold bounded by the surface $r = R'$ and also that $\phi_0 > C/R'^{2p+2}$. Since we know that in this interior $\phi \leq C/R'^{2p+2}$, we are led to a contradiction and must conclude that $\phi = 0$ everywhere as a consequence of the maximum principle.

where the component functions only depend on the radial and x coordinates and are independent of the time direction τ , which we recall has a period such that $\tau \sim \tau + 2\pi/\kappa$. Using the Cartesian coordinates X and Y mentioned above, for which $X = r \cos \kappa \tau$ and $Y = r \sin \kappa \tau$, one can show that the metric components in these coordinates are smooth functions of X and Y at the fixed point $r = 0$, provided that A, B, C_a, h_{ab} are smooth functions of $r^2 = X^2 + Y^2$ and of the coordinates x and, furthermore, that $\kappa^2 A = B$ at $r = 0$ for some constant $\kappa > 0$. Here the constant κ gives the surface gravity of the horizon with respect to $\partial/\partial\tau$.

Since there is no real boundary at the horizon, our maximum principle must ensure that no maximum of ϕ can occur there. Treating the horizon in static adapted coordinates we see the horizon as a fictitious boundary. We may simply compute that $\xi^r = \partial_r \xi^a = 0$ at $r = 0$. Now $\xi^r = 0$ everywhere, and hence $\partial_r \phi|_{r=0} = 0$. Recall that the maximum principle implies that a maximum at a boundary requires ϕ to have positive outer normal gradient. We see that, since $\partial_r \phi = 0$ at $r = 0$, the maximum principle does indeed rule out a maximum at this fictitious boundary.

Secondly, one typically has rotational axisymmetry in the problem and an associated $SO(n)$ isometry group. The axis of this symmetry is then the set of points fixed under the isometry. In this case we write the polar metric as

$$ds^2 = Adr^2 + r^2 Bd\Omega^2 + rC_a drdx^a + h_{ab}dx^a dx^b, \quad (10.20)$$

where $d\Omega^2$ is the line element on a unit $(n - 1)$ -sphere. Transforming to appropriate Cartesian coordinates one finds a smooth metric again, provided that A, B, C_a, h_{ab} are smooth functions of r^2 and that $A = B$ at $r = 0$. Note that there is no free constant as was the case for vanishing $U(1)$, since we have already chosen the sphere $d\Omega^2$ to have unit radius. As above, no maximum can reside here since $\partial_r \phi = 0$ at $r = 0$.

10.2.6 Solving the harmonic Einstein equation I: Ricci flow as local relaxation

We will now consider the canonical method for solving an elliptic system, and we shall find that for the harmonic Einstein equation this can be thought of in the continuum as the famous Ricci flow.

Suppose that we consider the Laplace equation, $\nabla^2 \psi = 0$, in some finite region U of D -dimensional Euclidean space and that we wish to solve this boundary value problem with some appropriate boundary conditions (e.g. Dirichlet). The simplest numerical approach is to represent the function ψ using real-space finite differences and to employ local relaxation to find a solution. Let us take the canonical coordinates (x_1, x_2, \dots, x_D) on \mathbb{R}^D and consider a rectangular lattice

of points with lattice spacing Δ at positions $(m_1\Delta, m_2\Delta, \dots, m_D\Delta)$ for integers m_1, m_2, \dots, m_D . Denote the set of points $\{p_i\}$ in this lattice that lie in the interior of the domain U as L , where $i = 1, \dots, N$ labels these points. The real-space, finite difference method represents the function ψ by storing the set of values $\{\psi_i\}$, where $\psi_i = \psi(p_i)$.

The simplest way to represent the Laplace equation is by second-order finite differences. Consider a point $p_i \in L$. We denote the $2D$ nearest neighbour points in this rectangular lattice as $p_{i \rightarrow j}$, where $j = 1, 2, \dots, 2D$. Then we may make the approximation

$$\nabla^2 \psi|_{p_i} \simeq \frac{1}{\Delta^2} \left(-(2D)\psi_i + \sum_{j=1}^{2D} \psi_{i \rightarrow j} \right). \quad (10.21)$$

By making Δ smaller, we approximate the Laplacian increasingly well, and we now have a finite representation of the continuum Laplace equation. Note that, for points in L that have nearest neighbour points in the boundary or are exterior to U , we consider the values of those neighbours to be fixed by the boundary conditions.

We then proceed by solving this finite problem. The classic method is that due to Jacobi, a local iterative procedure also known as relaxation. Let us imagine a sequence of guesses $\{\psi_i^{(A)}\}$, for integer $A = 0, 1, 2, \dots$, to the solution. The Jacobi method states that given a guess $\{\psi_i^{(A)}\}$ we can improve it by computing a new guess $\{\psi_i^{(A+1)}\}$ as

$$\psi_i^{(A+1)} = \frac{1}{2D} \left(\sum_{j=1}^{2D} \psi_{i \rightarrow j}^{(A)} \right) \quad (10.22)$$

The idea is that one takes an initial guess $\{\psi_i^{(0)}\}$ satisfying the boundary conditions and then iterates Jacobi's improvement method. For the simple Laplace equation one will reach a fixed point of this iteration that is a solution of the finite Laplace equation (10.21).

We may rearrange (10.22) above as

$$\frac{2D}{\Delta^2} \left(\psi_i^{(A+1)} - \psi_i^{(A)} \right) = \frac{1}{\Delta^2} \left(\sum_{j=1}^{2D} \psi_{i \rightarrow j}^{(A)} - (2D)\psi_i^{(A)} \right). \quad (10.23)$$

This may be viewed as a finite differencing of the diffusion equation, where now ψ is a function of x and of a flow time λ and

$$\frac{\partial \psi(\lambda, x)}{\partial \lambda} = \nabla^2 \psi(\lambda, x), \quad (10.24)$$

where we discretize time similarly to space, so that $\psi_i^{(A)} = \psi(A\delta)|_{p_i}$, with $\delta = \Delta^2/(2D)$ giving the discretization spacing in flow time. The right-hand side is approximated as above and the left-hand side is approximated using forward Euler differencing,

$$\frac{\partial \psi}{\partial \lambda} \Big|_{\lambda=A\delta} \simeq \frac{1}{\delta} \left(\psi_i^{(A+1)} - \psi_i^{(A)} \right). \quad (10.25)$$

Thus we see that the simplest local relaxation method used to solve the Laplace equation in fact amounts simply to diffusion on spatial and temporal scales much larger than the lattice scale Δ . Instead of thinking about Jacobi local relaxation and finite differences in an elliptic problem, we can describe this process more formally as a parabolic continuum diffusion problem. Then we can make an initial guess and act on it with diffusion until we reach a fixed point of the diffusion flow, and this will solve the original elliptic problem.

We may use the Jacobi method for the more complicated elliptic harmonic Einstein equation. Instead of a single function ψ , in a chart solutions must be found for all the components of the metric tensor $g_{\mu\nu}$. We may represent the metric in a chart by again taking the same lattice L in \mathbb{R}^D and storing the set of values $(g_{\mu\nu})_i \equiv g_{\mu\nu}(p_i)$. Recall that from (10.8) the harmonic Einstein equation has a second-derivative structure:

$$R_{\mu\nu}^H = -\frac{1}{2} g^{\alpha\beta} \partial_\alpha \partial_\beta g_{\mu\nu} + T_{\mu\nu}, \quad (10.26)$$

where $T_{\mu\nu}$ represents lower-order terms. Jacobi's method then proceeds by discretisation of the continuum equation

$$\frac{\partial g_{\mu\nu}(\lambda)}{\partial \lambda} = -2R_{\mu\nu}^H, \quad (10.27)$$

where the right-hand side is approximated using second-order finite difference and the left-hand side is differenced using the forward Euler method. We may think of Jacobi as approximating the harmonic Einstein equation as a set of Poisson equations, where the sources in the Poisson equations are the lower-derivative terms $T_{\mu\nu}$. It aims to solve the Poisson equations at each point in isolation by considering the neighbours and sources as fixed.

In fact there are many variants of the classical Jacobi relaxation method for elliptic systems. For example, the Gauss–Seidel method speeds up Jacobi by updating the values of the points *in situ* rather than storing a whole new approximation $\psi^{(A+1)}$ given a previous one $\psi^{(A)}$. This amounts to another discretisation of the continuum diffusion problem although with an exotic time-derivative differencing. Over-and-under relaxation schemes simply adjust the diffusion constant. Multi-grid methods work by concurrently solving the equation on multiple lattices, cascading

information from low to high resolution and back in order to allow it to propagate quickly over long distances. These methods give great enhancement of speed but, on scales larger than the lowest resolution lattice, are again acting as continuum diffusion.

Thus, whichever local relaxation method one chooses, on large enough scales one may consider the problem as continuum diffusion. For the harmonic Einstein equation, the canonical diffusion is the flow in time λ given in (10.27):

$$\frac{\partial g_{\mu\nu}(\lambda)}{\partial \lambda} = -2R_{\mu\nu} + 2\nabla_{(\mu}\xi_{\nu)} . \quad (10.28)$$

In fact this is precisely Ricci–DeTurck flow; the second term is an infinitesimal diffeomorphism generated by the vector field ξ , so that the flow is diffeomorphic⁸ to the Ricci flow

$$\frac{\partial g_{\mu\nu}(\lambda)}{\partial \lambda} = -2R_{\mu\nu} \quad (10.29)$$

introduced by Hamilton as a tool in geometric analysis, and which has gained fame for its role in proving the Poincaré conjecture. For an introduction to Ricci flow, see for example [28]. DeTurck proved that Ricci flow was a well posed parabolic flow by realising that one can add the diffeomorphism term and, with the choice in (10.7), explicitly render the flow equation parabolic.

Again on scales larger than the lattice resolution used in local relaxation, we may view the methods discussed above formally as Ricci–DeTurck flow. We may regard this parabolic flow as a continuum algorithm in order to solve the harmonic Einstein equation, making some initial guess for the parabolic flow. A fixed point of the flow is a solution of the harmonic Einstein problem. Hence, by simulating the flow for sufficient flow time, we hope to approach a fixed point as closely as we require.

One beautiful consequence is that, whilst we required some choice of reference metric to define the vector field ξ and render the harmonic Einstein equation elliptic, and hence well posed as a boundary value problem, in fact the Ricci–DeTurck flow is diffeomorphic to Ricci flow, which makes no reference to ξ . Thus, given some initial-guess metric, whilst different choices of reference metric will change the path taken in the space of metrics by the Ricci–DeTurck flow the path taken in the space of geometries (i.e. metrics modulo diffeomorphisms) is always the same.

Provided that one chooses a reference metric that shares the isometries of the metric of interest, for example static symmetry, the harmonic Einstein tensor is also

⁸ In the presence of boundaries we should ensure that the normal component of ξ at a boundary vanishes, in order for these two flows to be diffeomorphic. This ensures that the diffeomorphisms generated by ξ along the flow act to preserve the boundary points.

symmetric under these isometries. This implies that Ricci–DeTurck flow preserves the isometries of the metric.

Ricci flow has very nice geometrical properties. Essentially the diffusion applies to the geometry, and locally tries to smooth out curvature. Suppose that we have a Ricci-flat solution $g_{\mu\nu}$ and we wish to consider the Ricci flow of a perturbation to this, $h_{\mu\nu}$. Then from (10.4) we see that

$$\frac{\partial h_{\mu\nu}}{\partial \lambda} = -2\Delta_L h_{\mu\nu} - 2\nabla_{(\mu}v_{\nu)} , \quad (10.30)$$

where Δ_L is the Lichnerowicz operator on the background g and the second term on the right-hand side is simply an infinitesimal diffeomorphism generated by v . For Euclidean space this flow is then diffeomorphic to a flow where each component of the metric simply diffuses according to $\partial h_{\mu\nu}/\partial \lambda = \delta^{\alpha\beta}\partial_\alpha\partial_\beta h_{\mu\nu}$. Hence we see that Euclidean space is stable to linear perturbations. However, beyond this diffusive behaviour of linear perturbations the Ricci flow has very interesting nonlinear properties. For example, it wishes to collapse regions of positive curvature, as can be seen in the Ricci flow of a round sphere whose radius shrinks linearly in flow time, reaching zero size in finite time. Of relevance for us, it has been rigorously proven that Ricci flow exists and preserves asymptotic flatness for short times [29].

An important property of Ricci flow is that we see from the above that a Ricci-flat solution is a stable fixed point only if the operator Δ_L is positive. We may assume that there are no zero modes as these would be fixed appropriately by boundary conditions, which would ensure a locally unique solution. However, Δ_L may not be positive in general, so that there may exist one or more eigenfunctions with negative eigenvalues. At late times such eigenmodes grow exponentially in time, so that the perturbation will flow one away from the fixed point in these directions.

A fundamental property of static vacuum black holes is that the positivity of Δ_L for their Euclidean continuation is related to their thermodynamic behaviour since the Euclidean action is simply related to their free energy. In the asymptotically flat case this was made precise in [30]. In many cases, static black holes of interest (for example those in Kaluza–Klein theory, discussed in Chapter 4) possess negative modes of Δ_L , the canonical example being that of the asymptotically flat Euclidean Schwarzschild solution, which has the single negative mode discovered by Gross, Perry and Yaffe [31].

We have seen that standard local relaxation methods can be viewed as Ricci–DeTurck flow on large scales, which is diffeomorphic to Ricci flow. Thus, for all these methods, one cannot simply start with an initial guess and flow to the black hole fixed-point solution if it possesses negative modes. Starting with an initial guess close to the solution, one will flow towards the fixed point in nearly all

directions in the space of perturbations of the fixed point but generically will then veer off along the direction(s) tangent to the negative mode(s).

Since many solutions of interest have negative modes one might imagine that local relaxation completely fails to provide an algorithm for finding solutions of the elliptic harmonic Einstein problem. This conclusion, however, would have been reached too quickly; in principle Ricci flow and hence local relaxation may still be used but the method must be modified slightly. Suppose that the fixed point in which we are interested has a single negative mode of Δ_L and, up to diffeomorphisms, has no zero modes, so that the fixed point is locally unique. Examples of this include the small localised black holes in Kaluza–Klein theory discussed in Chapter 4. Let us call the fixed point g_0 . Then, locally about g_0 , the space of geometries (meaning metrics up to diffeomorphisms) is infinite dimensional. There are two special flows that emanate from g_0 along the negative-mode direction. Let us denote the negative-mode perturbation h at g_0 . Then these two special flows are $g_{\pm}(\lambda)$ such that $g_{\pm} \simeq g_0 \pm \exp(+2v^2\lambda)h$ as $\lambda \rightarrow -\infty$, where $\Delta_L h = -v^2 h$, so that v^2 is the magnitude of the negative eigenvalue. The perturbation h is a tangent vector to the space of geometries at g_0 . A basis for the tangent space at g_0 is given by h together with the positive eigenmodes of Δ_L . The positive eigenmodes are tangent to a codimension-1 surface Σ that contains g_0 and is closed under Ricci flow. Starting from any point in Σ near to g_0 , one remains within this surface under the action of the flow and flows to the fixed point, reaching it asymptotically.

The problem is then to generate an initial guess contained in Σ , since such an initial guess will flow to the fixed point. Consider a one-parameter family of geometries $g(\alpha)$, where α is the parameter. It is generic that the curve $g(\alpha)$ will intersect Σ . Suppose that this occurs at $\alpha = \alpha_*$. Then, for $\alpha > \alpha_*$ but close to α_* , one will initially flow towards g_0 and then be carried away in the direction of the negative mode. In the limit $\alpha \rightarrow \alpha_*$, the flow at late times will follow that of either g_+ or g_- . Let us assume it follows g_+ for $\alpha > \alpha_*$. Then, conversely, for $\alpha < \alpha_*$ one will approach g_0 and then deviate away in the opposite sense, flowing away close to the flow g_- .

Thus we see that, for α close to α_* , there is a critical behaviour associated with the unstable fixed point g_0 . By scanning the values of α one can hope to see this critical behaviour and, if one can identify whether one has flowed in the g_+ or the g_- direction, one can simply automate a tuning of α in order to get as close to α_* as required. Then one has achieved flows that get very close to g_0 for a long period of flow time before finally succumbing to the negative mode and flowing away. In principle one can get as close to the fixed point as desired.

For a Schwarzschild black hole the flows g_{\pm} generated by the negative mode either expand (say, g_+) or contract (g_-) the horizon. The flow g_- has been shown to continue to shrink the horizon to a finite time singularity, whilst under the flow

g_+ the horizon grows without stopping [32]. Thus, given a flow it is very simple to see on which side of Σ that flow is and hence to tune the parameter α to reach α_* . Similar behaviour is seen for the small Kaluza–Klein localised black holes, where one flow pinches the horizon to zero size and a finite time singularity and the other expands it until its poles touch and again a singularity is reached [14].

In principle this method may be extended to a case with N negative modes. Then an N -parameter family of initial data must be tuned in order to reach the fixed point. In the codimension-1 case, for which Σ partitions the space of geometries locally about g_0 , it is easy to see on which “side” of Σ one starts. This is not true in the higher-codimension case, and one must simply search the space of parameters until one locates the critical point α_* .

Let us summarise this discussion. Local relaxation is the simplest method for solving elliptic PDEs and can be applied to the harmonic Einstein equation. On large scales we may think of relaxation, from a continuum perspective, as Ricci–DeTurck flow, which is diffeomorphic to Ricci flow. Hence this approach has the beautiful geometric property that the trajectory taken by the flow is *independent* of the reference metric and hence of the gauge fixing. However, many black holes correspond to unstable fixed points of Ricci flow; for these, relaxation or Ricci flow may still be used to find solutions but, for a solution with N negative modes of its Lichnerowicz operator, one must find a suitable N -parameter set of initial data and tune the N parameters in order to flow or relax to a solution. We emphasise that there do exist interesting solutions with Killing horizons that are stable under Ricci flow, such as those in AdS/CFT where the boundary metric is a black hole [19].

10.2.7 Solving the harmonic Einstein equation II: Newton’s method

We have seen that, whilst the simplest relaxation methods for solving elliptic systems have an elegant geometric behaviour on large scales, it is difficult to find many black holes of interest that are unstable fixed points of these methods, owing to their having Euclidean negative modes. With one such negative mode these methods are still practical. For more they become increasingly hard to use.

Fortunately, there is a second standard technique for solving these elliptic systems, namely Newton’s method (also known as the Newton–Raphson method). As we shall see, this approach is considerably more complicated to implement and lacks the geometric elegance of relaxation; its behaviour depends explicitly on the choice of reference metric. However, the advantage of Newton’s method is that it is insensitive to the stability of the fixed point. In fact the basin of attraction of Newton’s method can be rather small, in practice; thus a combination of Ricci flow

or relaxation, to get close to the fixed point, followed by Newton's method to home in on it can be the best strategy.

Unlike relaxation, Newton's method is inherently nonlocal. Let us again imagine discretising our system using finite difference as above. At each lattice point in a chart we will have values for the various components of the metric. Globally there will be a finite set of numbers $\{g_M\}$ that will give the finite difference approximation to the metric $g_{\mu\nu}(x)$, where the index M includes both the lattice point in a given chart and the component of the tensor. Likewise we may represent the harmonic Einstein tensor in the interior of the manifold using the same index structure. Then the harmonic Einstein equation is given as $R_M^H(g) = 0$, which can be thought of as a finite set of coupled nonlinear equations in the variables g_M . The canonical way to solve such a system is by a multidimensional generalisation of Newton's method.

If we perturb the metric g to $g + \epsilon \delta g$, the harmonic Einstein tensor goes as

$$R_M^H(g + \epsilon \delta g) = R_M^H(g) + \epsilon \mathcal{O}(g)_M^N \delta g_N + O(\epsilon^2), \quad (10.31)$$

where the matrix $\mathcal{O}(g)_M^N$ is the linearisation of R_M^H . Begin with an initial guess $g_M^{(0)}$. Then Newton's method iteratively improves a trial metric $g_M^{(A)}$ as follows:⁹

$$g_M^{(A+1)} = g_M^{(A)} - (\mathcal{O}(g^{(A)})^{-1})_M^N R_N^H(g^{(A)}). \quad (10.32)$$

As with the one-dimensional Newton method this moves along the tangent of the equations to find a solution. Near a solution it will converge very quickly to that solution. However, the basin of attraction may be rather small in practice and, outside it, iterations of Newton's method will usually diverge and give singularities.

As for the Ricci-flow method, provided that the reference metric is chosen to have the same isometries as the metric, the harmonic Einstein tensor will be symmetric under these isometries and the Newton method will act to preserve them.

This method has the important advantage over the Ricci–DeTurck flow method that it is not sensitive to negative modes of the Lichnerowicz operator. However, it does assume that the linear problem $\mathcal{O} \cdot V = R^H$ can be solved for a vector V . In practice, robust methods, such as the biconjugate gradient method, exist for solving such (finite-dimensional) linear systems; these methods are insensitive to the spectrum of \mathcal{O} provided that there are no zero modes, which we can assume for well-posed boundary data. Thus a single initial guess will suffice, and one does not have to tune a family of initial guesses.

We see that the implementation of Newton's method is considerably more complicated than that of the relaxation–Ricci-flow methods. Another important

⁹ It is sometimes useful to take ‘smaller’ steps, with $g^{(A+1)} = g^{(A)} - \epsilon \mathcal{O}(g^{(A)})^{-1} R^H(g^{(A)})$ for some ϵ with $0 < \epsilon < 1$, particularly in the first iterations if the initial guess is not very close to the solution.

disadvantage of the Newton method as compared with the use of the Ricci–DeTurck flow is that the Newton method is not geometric, in the sense that the path taken by the algorithm in the space of geometries will depend explicitly on the choice of reference metric. This implies that the basin of attraction of a solution, which in practice may be rather small, will also depend on this choice of reference metric. Sometimes it is actually convenient to use a combination of the Ricci-flow method and the Newton method. The Ricci-flow method is rather robust and can quickly bring one reasonably close to a fixed point. It is tuning the flows very close to the fixed point that becomes difficult and time consuming. However, once one is reasonably close one can use the Newton method to find the precise fixed point quickly.

10.2.8 An illustrative example

In order to illustrate many of the points discussed above, we will now give a very simple example for which we already know the answer. We will consider finding the four-dimensional Schwarzschild solution using the various techniques above. We will assume spherical symmetry, so that the problem involves only ODEs, but we shall treat it in an identical manner to the much more complicated PDE problems in which we are really interested. This example is simple enough that we can be very explicit about the implementation, which we detail below.¹⁰

We note that our earlier maximum-principle argument states that, in this asymptotically flat case, no soliton solutions should exist and hence any solution to the harmonic Einstein equation must be Ricci flat. We will cover the manifold with one chart and use the fact that the solution is static and spherically symmetric, adapting our choice of coordinates to these symmetries. We will choose a radial coordinate r and assume that the horizon is located at $r = 0$ and infinity at $r = 1$. We continue to Euclidean time and write the smooth Riemannian metric as

$$ds^2 = r^2 A dt^2 + 4f^2 B dr^2 + f C d\Omega^2, \quad f = \frac{1}{(1-r^2)^2}, \quad (10.33)$$

where $d\Omega^2 = d\theta^2 + \sin^2 \theta d\phi^2$. Then A, B, C are functions of r and we have described the general static spherically symmetric metric. The above choice of factors means that, for the topology of the manifold we wish to describe, we have $A, B, C > 0$ on the domain $r \in [0, 1]$. At $r = 0$ we have a fictitious boundary, as we have adapted our coordinates to the static symmetry. From our previous discussion, the smoothness of the full Riemannian manifold implies that at $r = 0$

¹⁰ We have made available a very simple *Mathematica* notebook that implements the relaxation–Ricci-flow and Newton algorithms for this toy example. Hopefully this will provide an entry point for those interested in thinking about the more complicated problems of interest. This can be found at: www.cambridge.org/9781107013452.

we have $\kappa^2 = A/(4B)$, for surface gravity κ , and A, B, C are smooth functions of r^2 . At infinity, $r = 1$, we choose $A = B = C = 1$.

The harmonic Einstein tensor is determined by the components $R_{\tau\tau}^H$, R_{rr}^H and $R_{\theta\theta}^H$. We may discretise this system using finite differences by choosing a $(1 + N)$ -lattice of points at locations $r_i = i\Delta$ for $i = 0, 1, \dots, N$ with $\Delta = 1/N$, so that $A_i = A(r_i)$ and likewise for B and C . Our boundary conditions imply that $A_N = B_N = C_N = 1$. At the horizon we require smoothness in r^2 , which implies that we may deduce the boundary values A_0, B_0, C_0 in terms of the interior points. For small r the behaviour goes as a constant plus a quadratic in r , which gives $A_0 = (4A_1 - A_2)/3$ and likewise for B_0 and C_0 . We choose also to impose the regularity condition $A = B$ directly, by taking $A_0 = B_0$. This in turn determines B_1 from the smoothness requirement. In full, we have

$$\begin{aligned} A_0 &= \frac{1}{3}(4A_1 - A_2), & B_0 &= \frac{1}{3}(4A_1 - A_2), & C_0 &= \frac{1}{3}(4C_1 - C_2), \\ B_1 &= A_1 + \frac{1}{4}(B_2 - A_2), & A_N &= B_N = C_N = 1, \end{aligned} \quad (10.34)$$

and the vector $g_M \equiv \{A_1, \dots, A_{N-1}, B_2, \dots, B_{N-1}, C_1, \dots, C_{N-1}\}$ describes the metric subject to the above conditions. We finite-difference the derivative terms using simple second-order differencing:

$$\begin{aligned} \partial_r X_i &= \frac{1}{2\Delta} (X_{i+1} - X_{i-1}), \\ \partial_r^2 X_i &= \frac{1}{\Delta^2} (X_{i+1} + X_{i-1} - 2X_i); \end{aligned} \quad (10.35)$$

then we may evaluate $R_{\mu\nu i}^H \equiv R_{\mu\nu}^H(r_i)$.

Consider an initial guess $g_M^{(0)}$, and subsequent iterations of improvement $g_M^{(A)}$, for $A = 1, 2, \dots$. Then the Jacobi method or, equivalently, the Ricci–DeTurck flow discretised in time using forward Euler differencing, gives

$$r_i^2 A_i^{(A+1)} = r_i^2 A_i^{(A)} - 2\delta R_{\tau\tau}^H(g^{(A)})_i, \quad i = 1, \dots, N-1, \quad (10.36)$$

and similarly for B and C except that for B we have $i = 2, \dots, N-1$. The continuum Ricci-flow time λ for $g^{(A)}$ is then given as $\lambda = A\delta$ with $\delta = \Delta^2/2$. For the Newton method one creates the $(3N-4)$ -vector of equations

$$R_M^H \equiv \{R_{\tau\tau 1}^H, \dots, R_{\tau\tau N-1}^H, R_{rr 2}^H, \dots, R_{rr N-1}^H, R_{\theta\theta 1}^H, \dots, R_{\theta\theta N-1}^H\} \quad (10.37)$$

which is a function of the $(3N-4)$ -component vector g_M . Then the linearisation $\mathcal{O}_M^N \equiv \partial R_M^H / \partial g_N$ is a square matrix, which can be inverted to obtain the linear system required for the Newton method.

Without loss of generality we can choose $\kappa = 1/2$ by global scaling. Now, we note at this point that $A(r) = B(r) = C(r) = 1$ is the Schwarzschild solution for $\kappa = 1/2$. Whilst this has been presented as a toy example, it seems almost too trivial to find the solution in these coordinates and hence to challenge ourselves we will choose a background metric such that for the Schwarzschild solution the metric functions are not simply constant!

We know that Schwarzschild is unstable to Ricci flow with one negative mode. Thus let us choose the one-parameter family of initial metrics,

$$A = 1 - \alpha(1 - r^2)^2, \quad B = 1 - \alpha(1 - r^2)^2, \quad C = \frac{1}{2}(1 + r^2), \quad (10.38)$$

parameterised by the constant α , that satisfy our boundary conditions for $\kappa = 1/2$. We choose the metric at zero flow time to be given by A, B and C above and also take the fixed reference metric to be the same. We note that, since C is not constant, the actual Schwarzschild solution has nonconstant metric functions in the generalised harmonic coordinates imposed by the reference metric.

Under relaxation/Ricci flow we might hope that there is a critical value of α , say α_* , for which we approach the unstable Schwarzschild fixed point. Indeed, one finds that there is, with the critical value $\alpha_* \simeq 0.72$. In Fig. 10.1 we have plotted the size of the sphere at the horizon $R \equiv \sqrt{C}|_{r=0}$ against the flow time λ for a number of flows with various α values approaching α_* from above and below. We see that distinct behaviours are found for $\alpha > \alpha_*$ and $\alpha < \alpha_*$; these are straightforward to identify and hence to tune to the fixed point. Needless to say, the fixed point itself is Schwarzschild, and we see that for $\alpha \simeq \alpha_*$ the horizon does indeed tend to unit radius at late times, as it should for Schwarzschild with $\kappa = 1/2$.

The Newton method homes in efficiently on the Schwarzschild solution, provided that one is in the basin of attraction of the fixed point. In fact, for the choice of initial metric and reference metric given above, a rather wide range of values of α will lie in the basin of attraction. For example, simply taking $\alpha = 0$ for the initial guess will quickly find the Schwarzschild solution after a handful of Newton iterations.

10.3 Stationary vacuum solutions

Generally we wish to be able to tackle stationary solutions, and in this section we address how to extend the static methods discussed above to this case. We note that the classic four-dimensional uniqueness theorems rely on formulating the stationary axisymmetric problem as an elliptic system [2]. Our task here is to formulate the general stationary vacuum problem as an elliptic system using the

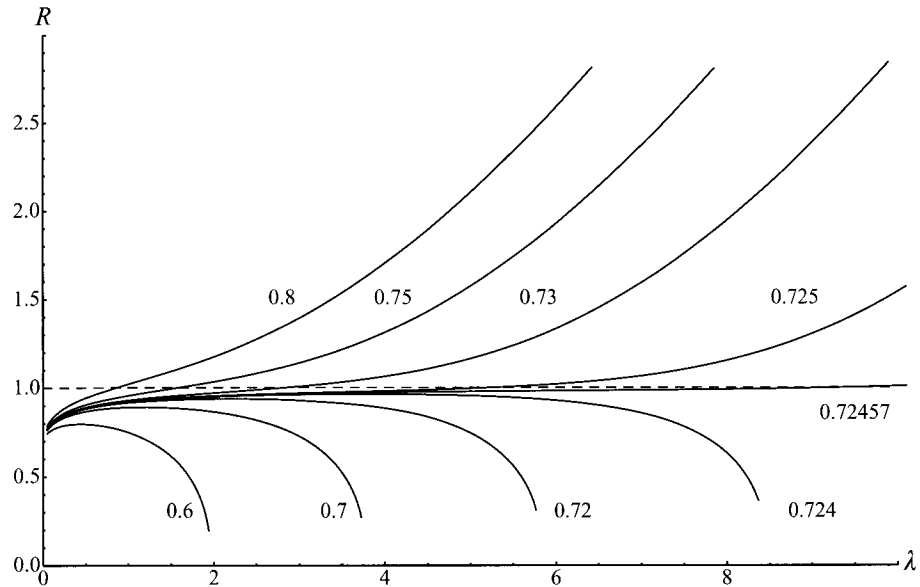


Figure 10.1 The use of relaxation or the Ricci-flow method to find the Schwarzschild solution. The plot shows the evolution of the radius of the horizon R as a function of the flow time λ , for flows with a variety of values of the parameter α . The values of α are labelled next to the corresponding curve. After initial transient behaviour we see that for $\alpha < \alpha_* \simeq 0.72$ the horizon shrinks (in fact to a singularity) in finite flow time. Conversely, for $\alpha > \alpha_*$ the horizon grows indefinitely. Tuning close to α_* one may approach the Schwarzschild solution as accurately as desired. We see that the quantity R plotted here does indeed tend to 1 (the Schwarzschild value for the chosen surface gravity) for a finely tuned flow. (The data presented were computed using a very modest number of lattice points, $N = 100$; we note that the value of α required to fine-tune the data will depend on this discretisation, giving α_* only in the continuum limit).

covariant harmonic Einstein equation approach and then to ensure that the Ricci-flow and Newton-method algorithms may still be applied. This will require us to tackle the problem from a manifestly Lorentzian point of view. This section is based on recent work [33].

10.3.1 Static solutions from a Lorentzian perspective

Instead of immediately considering stationary spacetimes, it is instructive to first consider static spacetimes from a Lorentzian perspective. The harmonic Einstein equation is not elliptic for a general Lorentzian manifold but, rather, is hyperbolic, and without ellipticity one would not expect to be able to impose the various boundary conditions physically required in a well-posed manner. However, consider a

chart away from any horizon that manifests the static symmetry

$$ds^2 = g_{\mu\nu}dx^\mu dx^\nu = -N(x)^2dt^2 + h_{ij}(x)dx^i dx^j , \quad (10.39)$$

so that $N^2 > 0$. With the choice that our reference metric is also static with respect to $\partial/\partial t$, so that

$$\bar{ds}^2 = \bar{g}_{\mu\nu}dx^\mu dx^\nu = -\bar{N}(x)^2dt^2 + \bar{h}_{ij}(x)dx^i dx^j , \quad (10.40)$$

again with $\bar{N}^2 > 0$ and \bar{h}_{ij} a smooth Euclidean metric, then $R_{\mu\nu}^H$ shares the static symmetry. Then, owing to this static symmetry, the harmonic Einstein equations $R_{\mu\nu}^H = 0$, considered as PDEs for the metric components of g , are invariant under an analytic continuation $t \rightarrow \tau = it$. Hence we immediately see that the harmonic Einstein equation restricted to Lorentzian static metrics and reference metrics is elliptic. The behaviour of the local-relaxation or Ricci-flow methods and of the Newton method will be precisely the same in either signature.

Under a Euclidean continuation, with Euclidean time taken to be periodic, we could remove the boundary associated with a horizon. However, we noted earlier that, in practice, one should take advantage of the static isometry and adapt coordinates to it; then, however, the horizon manifests itself as a fictitious boundary of such coordinates, analogous to the origin of polar coordinates. Boundary conditions at the horizon in these adapted coordinates are simply derived on transforming to regular coordinates that do not manifest the isometry but do manifest smoothness. In Lorentzian signature we have no option but to think of the horizon as a boundary. However, since the harmonic Einstein equations are signature independent, the boundary conditions for a regular Lorentzian horizon are precisely the same as those in Euclidean signature. Let us take coordinates in a base adapted to the horizon such that $x^i = (r, x^a)$ where $r = 0$ is the horizon. Then we write

$$ds^2 = -r^2Vdt^2 + Udr^2 + rU_a dr dx^a + h_{ab}dx^a dx^b , \quad (10.41)$$

where the metric components are functions of r and x^a . Changing to coordinates

$$a = r \cosh \kappa t , \quad b = r \sinh \kappa t \quad (10.42)$$

provides a good chart, covering the static Killing horizon, such that the metric components are smooth functions provided that V, U, U_a, h_{ab} are smooth (C^∞) functions of r^2 and x^a and

$$V = \kappa^2 U \quad (10.43)$$

at the horizon $r = 0$; κ is again the surface gravity. The same conditions will apply to the reference metric, which is also required to be smooth at $r = 0$. Of course,

we have exactly the same situation as in the Euclidean case in (10.19), with time continued back to Lorentzian signature.

In the Euclidean context it is clear that, since the metric is smooth and without boundary at the horizon, $R_{\mu\nu}^H$ must also be smooth there. The same is true in the Lorentzian case, where the tensor $R_{\mu\nu}^H$ shares the same regularity properties as the metric. This is easily seen by noting that in the coordinates (a, b, x^a) the metric and reference metric components are smooth functions, and hence so are those of $R_{\mu\nu}^H$. Transforming back to the static adapted coordinates (t, r, x^a) then gives

$$R^H = -r^2 f dt^2 + g dr^2 + r g_a dr dx^a + r_{ab} dx^a dx^b \quad (10.44)$$

where f, g, g_a and r_{ab} are smooth in r^2, x^a and, in addition, $f = \kappa^2 g$. Thus in the Lorentzian picture we have the nice property that Ricci flow and the Newton method will both preserve the regularity of the horizon boundary. Furthermore it will preserve the surface gravity of the horizon. Thus, we must now view the horizon as a boundary and we are naturally led to impose physical data there, namely the surface gravity with respect to $\partial/\partial t$.

10.3.2 Stationary spacetimes with globally timelike Killing vector

We begin our discussion of stationary spacetimes by considering the case of spacetimes with a globally timelike Killing vector, and we will argue that the harmonic Einstein equation for this case is elliptic. Of course we are ultimately interested in black hole spacetimes, which violate such a condition, since then the stationary Killing vector becomes null either on the horizon or outside the horizon at the boundary of an ergoregion. In the following subsection we consider more general stationary spacetimes that allow horizons and ergoregions.

Consider the most general stationary metric with Killing vector $T = \partial/\partial t$. We may write this using coordinates adapted to the stationary isometry as,

$$ds^2 = -N(x)[dt + A_i(x)dx^i]^2 + h_{ij}(x)dx^i dx^j. \quad (10.45)$$

Now, under our assumption that T is globally timelike we have $N > 0$, and we assume further that the function N is bounded. Physically this implies that our spacetime has no Killing horizons and also no ergoregions. Since $\det g_{\mu\nu} = -N \det h_{ij}$ we see that, provided the metric g is Lorentzian and smooth, so that $\det g_{\mu\nu} < 0$ and is bounded, this implies that $\det h_{ij} > 0$. We may then regard this metric as a smooth fibration of time over a base manifold \mathcal{M} such that (\mathcal{M}, h) is a smooth Riemannian manifold with Euclidean signature metric h_{ij} . It is worth

noting that this metric is not of the ADM form but, rather, takes the form of a Kaluza–Klein reduction ansatz with respect to time. Thus h_{ij} does not give the metric for a constant time slice of the Lorentzian geometry.

The second-order derivative terms acting on the metric components $g_{\mu\nu}$ in the stationary harmonic Einstein equation are written as

$$R_{\mu\nu}^H = -\frac{1}{2}g^{\alpha\beta}\partial_\alpha\partial_\beta g_{\mu\nu} + \dots = -\frac{1}{2}h^{ij}\partial_i\partial_j g_{\mu\nu} + \dots, \quad (10.46)$$

where the ellipses indicate lower-derivative terms. We see that, whilst the metric $g_{\mu\nu}$ is indeed Lorentzian, since there is no dependence on the coordinate t it is actually the metric h_{ij} that controls the character. We note that the above Kaluza–Klein form ensures that the inverse metric $g^{\mu\nu}$ in the base directions is given simply in terms of the inverse of h_{ij} . This immediately implies that the harmonic Einstein equation $R_{\mu\nu}^H = 0$ is elliptic, since h is smooth and of Euclidean signature.

We also require that $R_{\mu\nu}^H$ is a tensor that is invariant with respect to the stationary isometry T . Without this, Ricci–DeTurck flow and the Newton method will not consistently truncate to the class of stationary metrics (10.45). In order that $R_{\mu\nu}^H$ preserves the symmetry T , we choose the reference metric \bar{g} also to be a smooth Lorentzian metric that is stationary with respect to the vector field T :

$$\bar{g} = -\bar{N}(x)(dt + \bar{A}_i(x)dx^i)^2 + \bar{h}_{ij}(x)dx^i dx^j, \quad (10.47)$$

where again we have assumed that T is globally timelike and bounded with respect to \bar{g} , so that $\bar{N} > 0$ and bounded. Then \bar{h}_{ij} gives a second Riemannian metric on the same manifold \mathcal{M} . Since now $R_{\mu\nu}^H$ preserves the stationary symmetry, the Ricci–DeTurck flow can be consistently truncated to a parabolic flow on the space of Lorentzian stationary metrics. Since this flow remains diffeomorphic to Ricci flow (subject at least to the vanishing of the normal component of ξ on any boundaries), we arrive at the interesting result that we may apply parabolic Ricci flow to *stationary Lorentzian* spacetimes. Likewise, the Newton method will preserve the stationary symmetry and can be used to solve this elliptic stationary problem. We note that geometric flows of stationary metrics were first considered in [34].

In a situation where the solution we require has a stationary Killing vector that is globally timelike and bounded then, nearby that solution, the character of the harmonic Einstein equations will be elliptic. Subject to the imposition of suitable boundary conditions on any boundaries or asymptotic regions, one may use the Lorentzian stationary Ricci–DeTurck flow or the Newton method to solve for the solution. One must start with an initial guess that has a globally timelike bounded

stationary Killing field T and then, provided that guess is sufficiently good, one can hope that the subsequent Ricci–DeTurck flow or Newton iterations preserve the property that T is globally timelike.

10.3.3 Stationary black holes

We now proceed to consider the case of nonextremal black holes. In the context of the discussion above, now the norm of the Killing vector T will vanish either at the horizon itself, assuming that T is globally timelike outside the horizon (such as for certain Kerr–AdS black holes) or at the boundary of an ergoregion. Since we are interested in the exterior of the horizon, in the first case we may treat the system described above for globally timelike T and now regard the horizon as a boundary where suitable boundary conditions are required. However, in the second, more general, case, outside the horizon but inside the ergoregion we have the norm of $T > 0$ and hence $\det h_{ij} < 0$. Now the base manifold in the previous section fails to be Riemannian and so the argument, given above, that the harmonic Einstein equation is elliptic fails.

In order to make progress we use the rigidity property of stationary black holes, proved in $D > 4$ by Hollands, Ishibashi and Wald [35] for various asymptotics, including asymptotically flat solutions. Assume that there exists a stationary Killing vector T . Then the rigidity theorem states that for an asymptotically flat rotating black hole, for which T is not normal to the horizon, there exists a Killing vector K that commutes with T and which is normal to the horizon. Furthermore, there exist some number $N \geq 1$ of commuting Killing vectors R_a that also commute with T and asymptotically generate spatial rotation with closed orbits of period 2π . The theorem states that K may be written in terms of these: $K = T + \Omega^a R_a$, for some constants Ω^a . Consequently the horizon moves rigidly with respect to the orbits of K in its exterior and hence with respect to the asymptotic rotation generators R_a . Were this not the case, one would expect gravitational radiation to be emitted from the region near the horizon and this would presumably violate the assumption of stationarity.

Let us proceed by assuming that rigidity holds, so that there exists a stationary Killing vector T and Killing vectors R_a for $a = 1, \dots, N$, and that the vector fields T and R_a all commute. We take the vectors R_a to generate spatial isometries with either compact or noncompact orbits. In the compact case we take the period to be 2π and allow axes of this symmetry where the isometry has a fixed action. Rigidity implies that we may write the normal K to our Killing horizon as

$$K = T + \Omega^a R_a. \quad (10.48)$$

We may write the metric adapting coordinates to the isometries as

$$\begin{aligned} ds^2 = G_{AB}(x)[dy^A + A_i^A(x)dx^i][dy^B + A_j^B(x)dx^j] \\ + h_{ij}(x)dx^i dx^j, \end{aligned} \quad (10.49)$$

where $y^A = \{t, y^a\}$, $T = \partial/\partial t$ and $R_a = \partial/\partial y^a$. In analogy with the stationary case in the previous subsection we see that the geometry may be thought of as a fibration of the Killing vector directions over a base manifold \mathcal{M} with metric h_{ij} . Technically \mathcal{M} is the orbit space of the full Lorentzian spacetime with respect to the isometries T, R_a . We note that whilst, in four dimensions, for vacuum asymptotically flat solutions the circularity theorem implies that one can find a coordinate system where the cross terms between base and fibre, A_i^A , vanish this is not expected to hold for general stationary black holes in higher dimensions. At present, however, the only known solutions do in fact have vanishing A_i^A .

As with the analytic work on uniqueness, the aim now is to formulate the problem as an elliptic one on the orbit space \mathcal{M} . We emphasise that here we are seeking constructive numerical techniques to help us find black holes, rather than to prove the existence or uniqueness of such techniques. With this in mind we make our key assumption.

Assumption The manifold (\mathcal{M}, h) is smooth and Riemannian.

The full spacetime is Lorentzian and so, exterior to the horizon, $\det g_{\mu\nu} = \det G_{AB} \det h_{ij} < 0$. The chart breaks down at the horizon, where $\det G_{AB} = 0$ since the norm of K vanishes. It also breaks down at an axis of symmetry, where some R_a vanishes and again $\det G_{AB} = 0$. However, our assumption ensures that, exterior to all horizons and axes, $\det G_{AB} < 0$ and hence G_{AB} is of Lorentzian signature. We regard the horizon and axes of symmetry of the R_a as boundaries for the base manifold \mathcal{M} . We note that our assumption above ensures that the geometry of these boundaries is smooth. For simplicity we assume here that the boundaries are only due to the horizon and vanishing of the various R_a . However, more generally one might consider multiple Killing horizons and boundaries where linear combinations of the R_a vanish.¹¹

Harmark discussed the above form of metric in the context of classifying stationary spacetimes [36]. The structure of \mathcal{M} together with the data Ω^a at the horizon (or more generally horizons) and the data regarding which combination of the R_a vanishes at the axis boundaries defines a “rod structure” for stationary spacetimes and has been conjectured to classify higher-dimensional black holes.

¹¹ This was discussed in detail in the case of $D - 2$ commuting Killing vectors in [10].

It is instructive to consider the simple example of the Kerr solution from this perspective where the time and rotation Killing directions are fibred over a smooth base. In the conventional Boyer–Lindquist coordinates the Kerr metric takes the form

$$ds^2 = G_{tt}dt^2 + 2G_{t\phi}dtd\phi + G_{\phi\phi}d\phi^2 + h_{rr}dr^2 + h_{\theta\theta}d\theta^2 \quad (10.50)$$

with vanishing A_i^A (see (10.49)) and where

$$\begin{aligned} G_{tt} &= -\frac{\Delta - a^2 \sin^2 \theta}{\Sigma}, & G_{\phi\phi} &= \sin^2 \theta \frac{(r^2 + a^2)^2 - \Delta a^2 \sin^2 \theta}{\Sigma}, \\ G_{t\phi} &= -a \sin^2 \theta \frac{r^2 + a^2 - \Delta}{\Sigma}, & h_{rr} &= \frac{\Sigma}{\Delta}, & h_{\theta\theta} &= \Sigma, \end{aligned} \quad (10.51)$$

with $\Delta = r^2 + a^2 - 2Mr$ and $\Sigma = r^2 + a^2 \cos^2 \theta$. Here $T = \partial/\partial t$ and $R = \partial/\partial\phi$. The outer horizon and axis are the boundaries of the base manifold \mathcal{M} and are located at $r = r_h$ (where $\Delta = 0$) and $\theta = 0, \pi$ respectively. The Killing field $K = T + \Omega R$ is tangent to the horizon and timelike near there; the angular velocity of the horizon is given as $\Omega = a/(a^2 + r_h^2)$. One finds that $\det G_{AB} = -\Delta$, which vanishes at the horizon but not in its exterior. Whilst the θ coordinate is regular on the base at the rotation axes, the radial coordinate r is not regular at the horizon since Δ vanishes and so $h_{rr} \rightarrow \infty$ there. We therefore define a new radial coordinate, ρ , such that $d\rho = dr/\sqrt{\Delta}$ and $\rho = 0$ at the horizon, giving $r = M + \sqrt{M^2 - a^2} \cosh \rho$. Then the components of the base metric h_{ij} are smooth at the horizon boundary. In particular, in these coordinates, for the determinant of the base metric we have

$$h_{ij}dx^i dx^j = \frac{\Sigma}{\Delta} dr^2 + \Sigma d\theta^2 = \Sigma (d\rho^2 + d\theta^2) \implies \det h_{ij} = \Sigma^2 \geq r_h^2, \quad (10.52)$$

and thus we see that since $r_h > 0$ the base is indeed a smooth Riemannian manifold everywhere on and exterior to the horizon and the axis of symmetry.

10.3.4 Ellipticity of the stationary problem

It should be noted that we have not required the stationary Killing field T to be timelike. In the presence of horizons it will become null on the horizon or be spacelike if the horizon is surrounded by an ergoregion. We reiterate that in subsection 10.3.2 it is precisely where T fails to be timelike that ellipticity breaks down, since the base metric then fails to be Riemannian. The crucial observation

is that, for our class of stationary spacetimes (10.49),

$$\begin{aligned} R_{AB}^H &= -\frac{1}{2}g^{\alpha\beta}\partial_\alpha\partial_\beta g_{AB} + \dots = -\frac{1}{2}h^{mn}\partial_m\partial_n G_{AB} + \dots, \\ R_{Ai}^H &= -\frac{1}{2}g^{\alpha\beta}\partial_\alpha\partial_\beta g_{Ai} + \dots = -\frac{1}{2}h^{mn}\partial_m\partial_n (G_{AB}A_i^B) + \dots, \\ R_{ij}^H &= -\frac{1}{2}g^{\alpha\beta}\partial_\alpha\partial_\beta g_{ij} + \dots = -\frac{1}{2}h^{mn}\partial_m\partial_n (h_{ij} + G_{AB}A_i^A A_j^B) + \dots, \end{aligned} \quad (10.53)$$

where again the ellipses represent derivative terms lower than second order. We see that these equations have a character determined solely by the metric h_{ij} and, by our assumption above that the base \mathcal{M} is Riemannian, this system is indeed elliptic. Ergoregions may occur in which T is no longer timelike, but our assumption that the base is Riemannian implies that some linear combination of the Killing directions T, R_a is always timelike outside the horizons.

In analogy with the subsection 10.3.2, in order to ensure that $R_{\mu\nu}^H$ shares the symmetries of g we choose the reference metric \bar{g} in such a way that T, R_a are again Killing with respect to it and obey precisely the same assumptions as above for g . Thus we may write

$$\begin{aligned} \bar{ds}^2 &= \bar{g}_{\mu\nu}dX^\mu dX^\nu \quad (10.54) \\ &= \bar{G}_{AB}(x)[dy^A + \bar{A}_i^A(x)dx^i][dy^B + \bar{A}_j^B(x)dx^j] + \bar{h}_{ij}(x)dx^i dx^j, \end{aligned}$$

and we assume further that (\mathcal{M}, \bar{h}) is a smooth Riemannian manifold. Then the Ricci–DeTurck flow and the Newton method consistently truncate to Lorentzian stationary spacetimes of the form (10.49).

We must impose suitable boundary conditions at the boundaries of \mathcal{M} . Asymptotically we might impose the asymptotic flatness or Kaluza–Klein conditions mentioned above, which are compatible with $\xi \rightarrow 0$. The new feature is that we have additional boundaries on the base corresponding to the Killing horizons and axes of symmetry, and we will discuss this shortly. Using the Ricci–DeTurck flow or the Newton method, if we start from initial data in our stationary class then, for small flow times or updates, we expect to remain in this class. In particular we expect (\mathcal{M}, h) to remain a Riemannian manifold. Provided that this condition holds for the solution of interest and that our initial guess is sufficiently close to this then we might hope to reach this solution.

We note that the maximum principle discussed in the static context relies on the inequality in (10.17), which results from the positivity of $(\nabla_\mu\xi_\nu)(\nabla^\mu\xi^\nu)$ for a Riemannian manifold. Since the equations for the static case are independent of signature, the maximum principle must equally apply in the static Lorentzian context. However, one can check that in the stationary case this term has an indefinite sign, and it is unclear whether a maximum principle can be found that rules out solitons. This is not a problem in practice: one must simply check whether

a solution obtained is a soliton. However, the elegant property that in certain static cases there can be no solitons does not generalise in an obvious way to the stationary case.

10.3.5 Boundary conditions for the stationary problem

We conclude this chapter by giving explicitly boundary conditions for the metric components of our stationary spacetime (10.49) at the Killing horizon or symmetry axes. These are a generalisation of the boundary conditions required for the classical uniqueness theorems concerning four-dimensional stationary axisymmetric vacuum solutions [2]. These boundary conditions are derived and discussed in more detail in [33] and are consistent with the boundary conditions discussed by Harmark using particular coordinates on the base manifold [36]. Consider a Killing horizon with $K = T + \Omega^a R_a$. It is then convenient to change coordinates as follows:

$$t, y^a \rightarrow \tilde{t} = t, \tilde{y}^a = y^a - \Omega^a t, \quad (10.55)$$

so that $K = \partial/\partial\tilde{t}$ and $R_a = \partial/\partial\tilde{y}^a$. Note that if y^a is a periodic coordinate then \tilde{y}^a is also periodic with period 2π . Now consider a boundary, due either to the vanishing of K or to a compact R_a . We take base coordinates $x^i = (r, x^{\tilde{i}})$ adapted to the boundary, so that it lies at $r = 0$, and decompose the base metric:

$$h_{ij} dx^i dx^j = N dr^2 + r N_{\tilde{i}} dr dx^{\tilde{i}} + h_{\tilde{i}\tilde{j}} dx^{\tilde{i}} dx^{\tilde{j}}. \quad (10.56)$$

Horizon For a Killing horizon we write the following metric components:

$$G_{\tilde{t}A} = -r^2 f_A, \quad A_r^A = r g^A \quad (10.57)$$

for $A = (\tilde{t}, \tilde{y}^a)$. Then we let $X = \{f_A, g^A, G_{\tilde{y}^a \tilde{y}^b}, A_{\tilde{i}}^A, N, N_{\tilde{i}}, h_{\tilde{i}\tilde{j}}\}$ be the set of functions describing our metric. Now, by making the change of coordinates

$$a = r \cosh \kappa \tilde{t}, \quad b = r \sinh \kappa \tilde{t} \quad (10.58)$$

and requiring that in these Cartesian coordinates the components are smooth, we may deduce that the following behaviour is required in the stationary adapted chart: the functions X must be smooth functions of r^2 and $x^{\tilde{i}}$ at $r = 0$ and furthermore must obey the regularity condition

$$(f_{\tilde{t}} - \kappa^2 N)|_{r=0} = 0, \quad (10.59)$$

where κ is constant and gives the surface gravity with respect to K .

Axis Consider the axis associated with a vanishing compact R_a . Without loss of generality, choose this to be R_N . Then we choose to write

$$G_{\tilde{y}^N A} = r^2 f_A, \quad A_r^A = r g^A \quad (10.60)$$

and to let $Y = \{f_A, g^A, G_{\tilde{t}\tilde{t}}, G_{\tilde{y}^a \tilde{y}^b}, A_{\tilde{i}}^A, N, N_{\tilde{i}}, h_{\tilde{i}\tilde{j}}\}$ be the set of functions describing our metric (where $\tilde{a} = 1, \dots, N-1$). An analysis similar to that for the shrinking of the Euclidean time circle considered previously implies that, for a smooth metric, the metric functions Y must be smooth functions of r^2 and $x^{\tilde{i}}$ at $r = 0$; in addition we require that

$$(f_{\tilde{y}^N} - N)|_{r=0} = 0. \quad (10.61)$$

Of course, we will obtain analogous conditions for an axis with respect to a different R_a .

It is straightforward to check that the boundary conditions at the meeting of a horizon with an axis or two axes are compatible with each other. Take coordinates in the base $x^i = (r_1, r_2, x^{\tilde{i}})$, where $r_1 = 0$ gives the position of the first boundary and $r_2 = 0$ gives the position of the second boundary; hence the origin $r_1 = r_2 = 0$ is the meeting point. The boundary conditions near this origin are simply the union of the boundary conditions for each boundary. Note this implies that two boundaries (a horizon and an axis or two axes) meet in the base at right angles. We reiterate that we have only considered axes arising from fixed points of the R_a and, more generally, one could consider the vanishing of linear combinations of these.

A very important point is that, as discussed in section 10.2.1, having introduced boundary conditions we must check that these are compatible with finding Ricci-flat solutions. To investigate this we must consider our choice of reference metric, (10.54), which is also required to be regular and hence is subject to the same boundary conditions as above for its components on the various horizon and axis boundaries. In particular, we note that the surface gravity of the reference metric horizon must be the same as that of the actual metric. One can then explicitly check that

$$\xi^r|_{r=0} = 0, \quad \partial_r \xi^{\tilde{i}}|_{r=0} = 0, \quad \partial_r \xi^A|_{r=0} = 0 \quad (10.62)$$

both at a horizon and at an axis of symmetry, which is indeed consistent with the fact that the linear elliptic problem $\mathcal{D} \cdot \chi = 0$ discussed in section 10.2.2 is well posed and admits the trivial solution. Note that, since $\xi^r = 0$, the Ricci–DeTurck flow should be diffeomorphic to Ricci flow in the presence of such boundaries. Furthermore, the harmonic Einstein tensor will be regular at the horizon and axis boundaries. Thus in our adapted coordinates it will also obey the same regularity conditions as the metric above. In particular, Ricci–DeTurck flow and the Newton

method preserve regularity, and we have the elegant result that they leave the surface gravity constant.

This work is dedicated to my father.

Acknowledgements

I am greatly indebted to my collaborators Alexander Adam, Pau Figueras, Matthew Headrick, James Lucietti and Sam Kitchen.

References

- [1] L. Lehner and F. Pretorius, Black strings, low viscosity fluids, and violation of cosmic censorship, *Phys. Rev. Lett.* **105** (2010), 101–102.
- [2] B. Carter, Black hole equilibrium states: II general theory of stationary black hole states, in *Black Holes, Proc. 1972 Les Houches Summer School*, eds. B. and C. DeWitt (1973).
- [3] J. R. Wilson, Models of differentially rotating stars, *Astrophys. J.* **176** (1972), 195–204.
- [4] S. Bonazzola and J. Schneider, An exact study of rigidly and rapidly rotating stars in general relativity with application to the crab pulsar, *Astrophys. J.* **191** (1974), 273–286.
- [5] E. M. Butterworth and J. R. Ipser, On the structure and stability of rapidly rotating fluid bodies in general relativity. I. The numerical method for computing structure and its application to uniformly rotating homogeneous bodies, *Astrophys. J.* **204** (1976), 200–233.
- [6] N. Stergioulas, *Living Rev. Rel.* **6** (2003), 3.
- [7] B. Kleihaus and J. Kunz, Static black hole solutions with axial symmetry, *Phys. Rev. Lett.* **79** (1997), 1595–1598.
- [8] B. Kleihaus and J. Kunz, Rotating hairy black holes, *Phys. Rev. Lett.* **86** (2001), 3704–3707.
- [9] Y. Morisawa and D. Ida, A boundary value problem for the five-dimensional stationary rotating black holes, *Phys. Rev. D* **69** (2004), 124 005.
- [10] S. Hollands and S. Yazadjiev, Uniqueness theorem for 5-dimensional black holes with two axial Killing fields, *Commun. Math. Phys.* **283** (2008), 749–768.
- [11] T. Harmark, Stationary and axisymmetric solutions of higher-dimensional general relativity, *Phys. Rev. D* **70** (2004), 124 002.
- [12] T. Wiseman, Relativistic stars in Randall–Sundrum gravity, *Phys. Rev. D* **65** (2002), 124 007.
- [13] T. Wiseman, Static axisymmetric vacuum solutions and non-uniform black strings, *Class. Quant. Grav.* **20** (2003), 1137–1176.
- [14] M. Headrick, S. Kitchen, and T. Wiseman, A new approach to static numerical relativity, and its application to Kaluza–Klein black holes, *Class. Quant. Grav.* **27** (2010), 035 002.
- [15] M. Headrick and T. Wiseman, Numerical Ricci-flat metrics on K3, *Class. Quant. Grav.* **22** (2005), 4931–4960.

- [16] M. R. Douglas, R. L. Karp, S. Lukic, and R. Reinbacher, Numerical solution to the hermitian Yang–Mills equation on the Fermat quintic, *JHEP* **12** (2007), 083.
- [17] S. Donaldson, Some numerical results in complex differential geometry, *Pure Appl. Math. Q.* **5**, no. 2, special issue: in honor of Friedrich Hirzebruch, Part 1 (2009), 571–618.
- [18] M. Headrick and A. Nassar, Energy functionals for Calabi–Yau metrics, arXiv:0908.2635.
- [19] P. Figueras, J. Lucietti, and T. Wiseman, Ricci solitons, Ricci flow, and strongly coupled CFT in the Schwarzschild Unruh or Boulware vacua, arXiv:1104.4489.
- [20] Y Fourès-Bruhat, Théorème d’existence pour certains systèmes d’équations aux dérivées partielles non linéaires, *Acta Math.* **88** (1952), 141.
- [21] D. M. DeTurck, Deforming metrics in the direction of their Ricci tensors, *J. Diff. Geom.* **18** (1983), 157–162.
- [22] M. T. Anderson, On boundary value problems for Einstein metrics, *Geom. Topol.* **12** (2008), 2009–2045.
- [23] H. Friedrich, On the hyperbolicity of Einstein’s and other gauge field equations, *Commun. Math. Phys.* **100** (1985), 525–543.
- [24] D. Garfinkle, Harmonic coordinate method for simulating generic singularities, *Phys. Rev. D* **65** (2002), 044 029.
- [25] J. P. Bourguignon, in *Proc. Conf. on Global Differential Geometry and Global Analysis*, Berlin 1979, vol. 838 of Lecture Notes in Mathematics, Springer (1981), pp. 42–63.
- [26] M. H. Protter and H. F. Weinberger, *Maximum Principles in Differential Equations*, Prentice-Hall (1967).
- [27] T. Aubin, Non-linear analysis on manifolds. Monge–Ampere equations, Springer-Verlag (1982).
- [28] P. M. Topping, *Lectures on the Ricci Flow*, LMS Lecture Note Series, vol. 325 Cambridge University Press (2006).
- [29] T. A. Oliynyk and E. Woolgar, Asymptotically flat Ricci flows, arXiv:math/0607438v2.
- [30] O. J. C. Dias, P. Figueras, R. Monteiro, H. S. Reall, and J. E. Santos, An instability of higher-dimensional rotating black holes, *JHEP* **05** (2010), 076.
- [31] D. J. Gross, M. J. Perry, and L. G. Yaffe, Instability of flat space at finite temperature, *Phys. Rev. D* **25** (1982), 330–355.
- [32] M. Headrick and T. Wiseman, Ricci flow and black holes, *Class. Quant. Grav.* **23** (2006), 6683–6708.
- [33] A. Adam, S. Kitchen, and T. Wiseman, A numerical approach to finding general stationary vacuum black holes, arXiv:1105.6347.
- [34] M. M. Akbar and E. Woolgar, Ricci solitons and Einstein-scalar field theory, *Class. Quant. Grav.* **26** (2009), 05 5015 [arXiv:0808.3126 [gr-qc]].
- [35] S. Hollands, A. Ishibashi, and R. M. Wald, A higher dimensional stationary rotating black hole must be axisymmetric, *Commun. Math. Phys.* **271** (2007), 699–722.
- [36] T. Harmark, Domain structure of black hole space-times, *Phys. Rev. D* **80** (2009), 024 019.

Part V

Advanced topics

Black holes and branes in supergravity

DONALD MAROLF

11.1 Introduction

The goal of the present chapter is to introduce black holes and branes in supergravity in the simplest possible manner. As a result, we make no attempt to be complete and, in fact, we will intentionally omit many points dear to the hearts of practising string theorists and supergravity experts. In particular, spinors and supersymmetry will make only a passing appearance, in section 11.2.3, which can be skipped if the material seems too technical (though be sure to read the “executive summary” at the end of that section). Instead, we focus on bosonic spacetime solutions and the dynamics of the associated bosonic fields.

Even within this limited scope, our referencing of the original works will be rather sporadic. The interested reader can consult [1] for a more encyclopedic review of branes and black holes in string theory (as of 1997), with numerous references to the original works. We also refer the reader to [2] for a more recent review of black holes in four- and five-dimensional supergravity and for complementary material in ten and eleven dimensions, to [3] for a partial guide to the literature as of 2004, and to various textbooks [4–9] for further reading.

Our treatment will focus on supergravity theories in ten and eleven dimensions, which are in many ways simpler than their lower-dimensional counterparts and which allow us to make direct contact with string theory. We draw heavily on Polchinski’s treatment [5], though the style is (hopefully) more adapted to the current readership. We begin in section 11.2 with a discussion of both the kinematics and dynamics of eleven-dimensional supergravity and then introduce the associated branes in section 11.3. We follow tradition in referring to eleven-dimensional supergravity as “M theory.”¹

¹ The origin of this term seems to be lost in the mists of history.

The case of ten-dimensional supergravity is also central to our mission. We choose to approach this subject via the Kaluza–Klein reduction of eleven-dimensional supergravity. Section 11.4 thus begins with some introductory remarks on Kaluza–Klein compactifications and then constructs a supergravity theory (type IIA theory) in 9+1 dimensions. Section 11.5 introduces the branes of type IIA theory and then discusses both the very similar case of type IIB supergravity and the so-called T-duality symmetry that relates the two theories. The type I and heterotic theories are mentioned only briefly. We close with some brief remarks on D-brane perturbation theory and with a few words about black hole entropy via D-branes in section 11.6. We hope that this will provide a useful basis for the later chapters in this volume.

11.2 Supergravity in eleven dimensions

Before diving into the details, a few words of orientation are in order. We will shortly see that supergravity in eleven (10+1) dimensions is really not much more complicated than the 3+1 Einstein–Maxwell theory of Einstein–Hilbert gravity coupled to Maxwell electrodynamics. The same is not true of supergravity in lower dimensions. In ten (9+1) dimensions and below, many interesting supergravity theories contain a so-called dilaton field, which couples nonminimally to the Maxwell-like gauge fields. As a result, the equivalence principle does not hold in such theories, and different fields couple to distinct metrics that differ by a conformal factor. However, in eleven dimensions properties of the supersymmetry algebra guarantee that any supergravity theory containing no fields with spin higher than 2 has no dilaton.² In fact, there is a unique supergravity theory in eleven dimensions and it contains only three fields: the metric, a U(1) (i.e., abelian, Maxwell-like) gauge field, and a spin-3/2 gravitino.

In contrast, in $D > 11$ spacetime dimensions there are *no* supergravity theories without fields of spin $s > 2$. The basic reason for this property is that supersymmetry is associated with generators having spin 1/2. The action of such “supercharges” on a given field thus returns a field of different spin. Working through the details one finds that, in any dimension D , theories with spin s equal only to 2 or less can accommodate no more than 32 supercharges. In asymptotically flat settings, asymptotic Lorentz symmetry implies that each supercharge is associated with some component of a spinor of the associated Lorentz group. It turns out that eleven-dimensional Majorana spinors have precisely 32 components, so that

precisely the number of supercharges found in one $D = 11$ spinor is allowed. Any supergravity theory with 32 supercharges is called maximally supersymmetric.

Another reason to begin in eleven dimensions is that lower-dimensional supergravity theories can generally be obtained through the Kaluza–Klein mechanism, in which some subset of the dimensions are taken to be compact and small (and also through using certain so-called “dualities”). This mechanism will be discussed in sections 11.4.1 and 11.4.2 below.

11.2.1 On n -form gauge fields

We first address just the bosonic part of eleven-dimensional supergravity, setting the fermionic fields to zero. The differences between this truncated theory and 3+1 Einstein–Maxwell theory are the result simply of the differing numbers of dimensions. There are two reasons for this. The first is the obvious fact that the theory lives in a 10+1 spacetime instead of a 3+1 spacetime. The second is that the gauge field is itself slightly “larger” than that of Maxwell theory. Instead of having a *vector* (or, equivalently, a 1-form) potential, the potential is a 3-form, A_3 .

We will encounter a number of n -form potentials below. Although they may at first seem unfamiliar, they are in fact a very natural (and very slight) generalization of Maxwell fields. An n -form gauge potential A_n is associated with an $(n + 1)$ -form field strength of the form $F_{n+1} = dA_n$, where d is the exterior derivative. As a result, the field strength satisfies the Bianchi identity $dF_{n+1} = 0$. As with the familiar Maxwell field, there is an associated set of gauge transformations

$$A_n \rightarrow A_n + d\Lambda_{n-1}, \quad (11.1)$$

where Λ_{n-1} is an arbitrary $(n - 1)$ -form. Such gauge transformations leave the field strength F_{n+1} invariant. For reference purposes, we will record our convention for differential forms (which agrees with [5]):

$$A_n = \frac{1}{p!} A_{\alpha_1 \dots \alpha_n} dx^{\alpha_1} \wedge \dots \wedge dx^{\alpha_n}. \quad (11.2)$$

Thus we have

$$\int A_n = \int A_{012\dots(n-1)} d^n x. \quad (11.3)$$

In D spacetime dimensions (generally taken to be eleven in this section), the equation of motion for such a gauge field is typically of the form

$$d \star F_{D-(n+1)} = \star J_{D-n}, \quad (11.4)$$

² One can have antisymmetric tensor fields, which propagate on curved manifolds without the constraints associated with other higher-spin fields. Because of these constraints, theories with spin higher than 2 are generally believed to be inconsistent unless they include an infinite number of such fields.

where, in a slight abuse of notation, $\star F_{D-(n+1)}$ denotes the $(D - (n + 1))$ -form that is the Hodge-dual of $F_{(n+1)}$ and is defined by

$$\star F_{\alpha_1 \dots \alpha_{d-p}} = \frac{1}{p!} \epsilon_{\alpha_1 \dots \alpha_{d-p}}^{\beta_1 \dots \beta_p} F_{\beta_1 \dots \beta_p}; \quad (11.5)$$

ϵ is the Levi-Civita tensor. Similarly, $\star J_{D-n}$ is the Hodge-dual of some n -form current J_n . These conventions are consistent with taking the natural coupling, in an action between an n -form gauge field and its current, to be of the form $\int_{\mathcal{M}} A_n \wedge \star J_{D-n} \propto \int_{\mathcal{M}} \sqrt{-g} A_{\alpha_1 \dots \alpha_n} J^{\alpha_1 \dots \alpha_n}$, where \mathcal{M} denotes the spacetime manifold.

As usual, gauge symmetry implies that the current is conserved. However, current conservation for a $(D - n)$ -form current with $D - n > 1$ is, in a certain sense, a much stronger statement than current conservation in 3+1 Maxwell theory. Note that the analogue of Gauss' law in the present context is found by defining the charge Q_B contained in a $(D - n)$ -ball B by the integral $Q_{D-n} = \int_{\partial B} \star F_{D-(n+1)}$ over the boundary ∂B of that ball. Now, suppose that the current J_{D-n} in fact vanishes in a neighborhood of the surface ∂B . Then by Stokes' theorem and equation (11.4) we can deform the surface ∂B in any way we like and, as long as the surface does not encounter any current, the total charge Q_{D-n} does not change.

In the familiar 3+1 Maxwell theory, electric charge is measured by integrals over 2-surfaces. This is associated with the fact that an electrically charged particle sweeps out a worldline in spacetime. Note that any sphere that can be collapsed to a point without encountering the worldline of the particle must enclose zero net charge. The important fact is that, in four dimensions, there are 2-spheres that "link" with any curve and which cannot be shrunk to a point without encountering the particle's worldline. In contrast, circles do not link with worldlines in 3+1 dimensions. For this reason, particles in 3+1 dimensions cannot be electrically charged under any gauge field whose field strength is, for example, a 3-form. This illustrates a general relation between a gauge field and the associated charges: unless the worldvolume of an object can link with surfaces of dimension $D - (n + 1)$, the object cannot be electrically charged under an n -form gauge potential A_n .

While we are at this point we may as well work out the relevant counting in the general case. Let us suppose that we have an n -form gauge field A_n in D spacetime dimensions. Then, we must integrate $\star F_{D-(n+1)}$ over a $D - (n + 1)$ surface in order to calculate the charge. Now, in D dimensions surfaces of dimensions k and m can link without intersecting if $k + m + 1 = D$ (i.e., curves in three dimensions, 2-surfaces and worldlines in four dimensions, etc.). Thus, a nonzero electric charge of A_n is associated with n -dimensional worldvolumes. Such objects are generically known as " p -branes" (as higher-dimensional generalizations of the term membrane). Here, p is the number of spatial dimensions of the object, i.e., the electric charge of an n -form gauge potential is carried by $(n - 1)$ -branes,

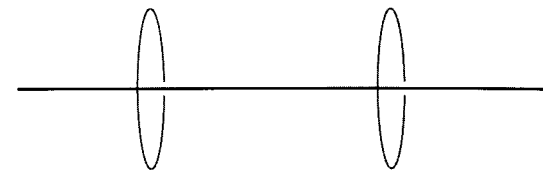


Figure 11.1 A 1-brane. By charge conservation, both circles necessarily capture the same flux.

whose worldvolume has $n - 1$ spatial dimensions and time. This is how strings, membranes, and other branes arise in our discussion of supergravity.

Note that, although p -branes are extended objects, the concept of a charge density of A_{p+1} -charge on a p -brane is not appropriate. Recall that the charge is measured by any $(D - (p + 2))$ -surface surrounding the brane and that, by the above charge conservation argument, smooth deformations of the surface do not change the charge so measured. Thus, the equations of motion tell us that moving the $(D - (p + 2))$ -surface *along* the brane cannot *ever* change the flux through the surface; see Fig. 11.1. Thus, nonuniform "pure" p -branes cannot exist! The proper approach here is to assign to such a p -brane only one number, the total charge. It simply happens that the particular type of charge being measured is somewhat less local than the familiar electric charge; it is fundamentally associated with $(p + 1)$ -dimensional hypersurfaces in the spacetime.³

As a small complication, we will be interested not only in electric charges but also in magnetic charges. Indeed, in supersymmetric string theory both electric and magnetic charges appear to be on an equal footing. A useful point of contact for the present discussion is to realize that, in a certain sense, both electrically and magnetically charged "objects" can occur in pure Einstein-Maxwell theory without any matter fields. These are just the electrically and magnetically charged eternal black hole solutions. Although the Maxwell field satisfies both $dF = 0$ and $d\star F = 0$ at every nonsingular point of such spacetimes, the black holes can still be said to "carry charge," owing to topological effects; the electric or magnetic flux starts in one asymptotic region, funnels through the Einstein-Rosen bridge at the "throat" of the black hole, and continues out into the other asymptotic region.⁴ Note that black holes (i.e., point-like or 0-brane objects) may carry both electric and magnetic charge for a Maxwell field in 3+1 dimensions.

³ Of course, it is possible for a p -brane to also carry A_n -form charges with $n < p + 1$. For example, a string can carry point charges in addition to some intrinsic string charge. In this case the proper concept is of a density of A_n -charge per unit $(p - n - 1)$ -dimensional volume. Such charge densities need not be homogeneous.

⁴ As a result, the electric charge of the black hole measured in one asymptotic region is the opposite of the charge measured in the other asymptotic region. However, this need not trouble us so long as we understand that we must first orient ourselves by picking an asymptotic region in order to discuss the notion of charge.

The counting of dimensions for magnetic charges proceeds much like the counting for electric charges. To define what we mean by a magnetic charge, we recall that the hodge duality $F \rightarrow \star F$ in Maxwell theory interchanges electric and magnetic charge. Thus, since electric charge is associated with integrals of $\star F_{D-(n+1)}$, magnetic charge is defined by integrating the field strength F_{n+1} itself over an $(n+1)$ -surface. In D dimensions, an $(n+1)$ -surface can link with $(D-n-2)$ -worldvolumes, or $(D-n-3)$ -branes. As a check, for 3+1 Maxwell theory we have magnetic $(4-1-3=0)$ -branes.

Let us take a look at the eleven-dimensional context. Without knowing anything more about supergravity than we already do at this stage in our discussion, we can expect two types of “objects” to be of particular interest from the point of view of the 3-form gauge field A_3 . There may be $(2+1)$ -dimensional electrically charged objects (2-branes) and $((D-n-3)+1 = (11-3-3)+1 = 5+1)$ -dimensional magnetically charged objects (5-branes). Since there are no explicit charges in the theory, these “objects” (if they exist) must be black-hole-like “solitonic” solutions. We will see below that black 2-brane and black 5-brane solutions carrying the proper charges do indeed exist in eleven-dimensional supergravity. What is more, and what is different from lower-dimensional supergravity, is that the horizons of these black branes remain smooth in the extreme limit of maximal electric or magnetic charge. The extremal versions of these brane solutions are what are usually referred to as the M-theory 2-brane or M2-brane, and the M-theory 5-brane or M5-brane. We will discuss these in more detail in section 11.3.2.

11.2.2 Dynamics

The discussion of section 11.2.1 should have provided some orientation to supergravity in eleven dimensions. Now, however, it is time to fill in a few details. For example, it is appropriate to write down the full dynamics of the system. This is conveniently summarized by the action [10]:

$$\begin{aligned} S = & \frac{1}{2\kappa_{11}^2} \int d^{11}x e \left[(R - \frac{1}{2}|F_4|^2) \right. \\ & - \frac{1}{2^3 \times 4!} (\bar{\psi}_\alpha \Gamma^{\alpha\beta\gamma\delta\sigma\lambda} \psi_\lambda + 12 \bar{\psi}^\beta \Gamma^{\gamma\delta} \psi^\sigma) (F + \hat{F})_{\beta\gamma\delta\sigma} \\ & - \bar{\psi}_\alpha \Gamma^{\alpha\beta\gamma} D_\beta (\frac{1}{2}(\omega + \hat{\omega})) \psi_\gamma \Big] \\ & - \frac{1}{12\kappa_{11}^2} \int A_3 \wedge F_4 \wedge F_4, \end{aligned} \quad (11.6)$$

where

$$|F_m|^2 = \frac{1}{m!} g^{\alpha_1\beta_1} \cdots g^{\alpha_m\beta_m} F_{\alpha_1\dots\alpha_m} F_{\beta_1\dots\beta_m}. \quad (11.7)$$

Here R is the Ricci scalar of the metric $g_{\alpha\beta}$, e_α^a is the vielbein (orthonormal basis) which squares to $g_{\alpha\beta}$ (e is its determinant), A_3 is the 3-form field discussed in the previous section, and ψ is the spin-3/2 gravitino. We use the notation

$$\begin{aligned} \hat{\omega}_{\alpha ab} &= \omega_{\alpha ab} + \frac{1}{8} \bar{\psi}^\beta \Gamma_{\beta\alpha ab\gamma} \psi^\gamma, \\ \hat{F}_{\alpha\beta\gamma\delta} &= F_{\alpha\beta\gamma\delta} - 3 \bar{\psi}_{[\alpha} \Gamma_{\beta\gamma} \psi_{\delta]} . \end{aligned} \quad (11.8)$$

In the above, Greek letters (α, β, \dots) denote spacetime indices and Latin letters (a, b, \dots) denote internal indices. The square brackets indicate a completely anti-symmetric sum over permutations of the indices, divided by the number of terms in this sum. Our conventions for spinors and Γ -matrices are those of [4]. We will not state them explicitly here, as spinors make appearances only in this section and in section 11.2.3, and, in both cases, the details can be safely glossed over.

Expression (11.6) looks a little complicated, but we will consider the various terms separately. We begin with the least familiar part: the gravitino. Since our attention here will be focused on classical solutions, we can largely ignore the gravitino. The main point here is that the gravitino is a fermion and, owing to the Pauli exclusion principle, fermion fields do not have semiclassical states of the same sort that bosonic fields do. It is helpful here to think about the electron field as an example. There are, of course, states with a large number of electrons that are well described by a classical charged fluid. However, because of the exclusion principle, there are no semiclassical coherent states of the electron field itself, i.e., no states for which the dynamics is well described by a *classical spinor field*. In the same way, we might expect that there are states of the gravitino field that are well described by some sort of classical fluid, but we should only expect the classical action (11.6) to be a good description of the dynamics when the gravitino field vanishes. Thus, we will set $\psi = 0$ throughout most of our discussion. This is self-consistent at the classical level, as setting $\psi = 0$ in the initial data is enough to guarantee $\psi = 0$ for all time.

A study of (11.6) shows that the dynamics of the solutions for which $\psi = 0$ can be obtained by simply setting ψ to zero in the action. This simplifies the situation sufficiently that it is worth rewriting the action as follows:

$$S_{\text{bosonic}} = \frac{1}{2\kappa_{11}^2} \int d^{11}x (-g)^{1/2} \left(R - \frac{1}{2}|F_4|^2 \right) - \frac{1}{12\kappa_{11}^2} \int A_3 \wedge F_4 \wedge F_4 . \quad (11.9)$$

This sort of presentation, giving only the bosonic terms, is quite common in the literature and is sufficient for most solutions of interest.⁵ Now that we have set the gravitino to zero, we see that our action contains only three terms: the Einstein (scalar curvature) term R , the Maxwell-like term $|F_4|^2$, and the remaining so-called “Chern–Simons term.”

Note that, although the Chern–Simons term contains the gauge potential A_3 , it is invariant under gauge transformations $A_3 \rightarrow A_3 + d\Lambda_2$, at least under “small” gauge transformations for which Λ is a well-defined smooth 2-form and $\Lambda_2 \rightarrow 0$ sufficiently rapidly at any boundaries. This term is very interesting and turns out to significantly modify the picture outlined in section 11.2.1.

Though we will be able to ignore these modifications for our purposes below, it is worth saying just a few words about them here. To this end, suppose that we couple a 3-form source J_3 to (11.9) via a term of the form $\int A_3 \wedge \star J_3$. The F_4 equation of motion is then of the form

$$d(\star F_4 + \text{const} \times A_3 \wedge F_4) = \star J_3, \quad (11.10)$$

suggesting that the relevant conserved 2-brane charge Q_2 is given by integrating $\star F_4 + \text{const} \times A_3 \wedge F_4$ over some closed 7-surface. The Bianchi identity on F_4 means that Q_2 is invariant under “small” gauge transformations, though, like the action, Q_2 does change under the action of “large” gauge transformations where Λ_2 is not single valued. In fact, in units of the fundamental charge (discussed below), one can show that Q_2 changes by an integer multiple of an associated 5-brane charge Q_5 defined by integrating F_4 over a 4-surface. This feature allows M2-branes to end on M5-branes. See e.g. [15] for a review of this phenomenon and [16] for further comments on charge in the presence of Chern–Simons terms.

The reason why we can ignore the Chern–Simons term below is that we will be considering only relatively simple configurations of branes. Specifically we note that, since $dF = 0$, the Chern–Simons contribution to (11.10) is proportional to $F_4 \wedge F_4$. Furthermore, the Chern–Simons term makes no contribution to the equation of motion for the metric. Thus, whenever there are at each point four or more linearly independent vectors k such that $k^\alpha F_{\alpha\beta\gamma\delta} = 0$, we have $F_4 \wedge F_4 = 0$ and the Chern–Simons term does not affect the equations of motion. For the cases we consider below, this property is satisfied as the nonvanishing components of F will lie in a subspace of dimension 7 or less.

⁵ Typically, an interesting bosonic solution in fact corresponds to a quantum state in some supersymmetry multiplet. The supersymmetry algebra can often be used to construct spacetime solutions corresponding to other states in the multiplet in which the fermions are excited. See for example [11–14].

11.2.3 Supersymmetry and BPS states

Some comments are now in order on the subject of supersymmetry, so that we may introduce (and then use!) the concept of Bogomoln’yi–Prasad–Sommerfeld (BPS) states. Again, I will begin with a few heuristics to provide a rough perspective for students of 3+1 general relativity. We will see below that BPS solutions are closely related to extremal solutions, in particular, to extremely charged solutions. As a result, most of our intuition from extreme Reissner–Nordström solutions carries over to the general BPS case.

The setting for any discussion of BPS solutions is the class of supergravity solutions that satisfy either asymptotically flat or asymptotically Kaluza–Klein boundary conditions. We thus require the topology of the asymptotic region to be of the form $(\mathbb{R}^n - \Sigma) \times Y$ for some compact set $\Sigma \subset \mathbb{R}^n$ and some homogeneous manifold Y , though we will not specify further details of the boundary conditions here.

In the setting of pure gravity, one would expect such spacetimes to exhibit asymptotic symmetries that correspond to the Poincaré group in the appropriate number of spacetime dimensions together with the symmetries of Y . Some particular solutions in this class will even have Killing vectors that make some subgroup of the Poincaré group into an *exact* symmetry of the spacetime, e.g., the rotation subgroup in spherically symmetric cases.

Now, supersymmetry is best thought of as an (anticommuting) extension of the diffeomorphism group. Indeed, diffeomorphisms form a subgroup of the supersymmetry gauge transformations and, in the asymptotically flat setting just described, the asymptotic Poincaré transformations will be a subgroup of the asymptotic supersymmetry transformations. Solutions that are invariant under a subgroup of the supersymmetry transformations containing nontrivial anticommuting elements are said to have a “Killing spinor” η and are known as BPS (Bogomoln’yi–Prasad–Sommerfeld) solutions.

It turns out that $\bar{\eta}\Gamma^\mu\eta$ is then a Killing vector field of the solution. Furthermore, it is everywhere nonspacelike (i.e., timelike or null).⁶ Since for nonextreme black holes any stationary Killing field becomes spacelike behind the horizon, it follows that any BPS black hole must be extreme.

Having oriented ourselves with this intuitive introduction, it is now time to examine the details of the eleven-dimensional supersymmetry transformations and their algebra. The infinitesimal supersymmetry transformations are in one-to-one

⁶ When the spacetime is asymptotically flat in all directions (i.e., the fields decay in an asymptotic region diffeomorphic to \mathbb{R}^n minus some compact set), this Killing field is in fact timelike except perhaps on a Killing horizon [17]. The structure of the argument is very much like the Witten proof of the positive energy theorem [18].

correspondence with Grassmann valued (Majorana⁷) spinor fields $\eta(x)$. The transformation associated with η is given by

$$\begin{aligned}\delta e_\alpha^a &= \frac{1}{2}\bar{\eta}\Gamma^a\psi_\alpha, \\ \delta A_{\alpha\beta\gamma} &= -\frac{3}{2}\bar{\eta}\Gamma_{[\alpha\beta}\psi_{\gamma]}, \\ \delta\psi_\alpha &= D_\alpha(\hat{\omega})\eta + \frac{\sqrt{2}}{(4!)^2}(\Gamma_\alpha^{abcd} - 8e_\alpha^a\Gamma^{bcd})\eta\hat{F}_{abcd} \equiv \hat{D}_\alpha\eta,\end{aligned}\quad (11.11)$$

where the last line defines the supercovariant derivative \hat{D}_α acting on the spinor η .

The details of the supersymmetry transformations are not particularly important for our purposes. What is important is the general structure. Note that the variation of the vielbein e involves the gravitino ψ , but then the variation of the gravitino involves the connection $\hat{\omega}$, which contains derivatives of the vielbein. Similarly, taking two variations of the gauge field A_3 , we find terms involving derivatives of the gauge field. As a result, the proper second variations give just diffeomorphisms of the spacetime.

Recalling that the variation of A_3 contains ψ , we also note that the first variation of the gravitino field involves a derivative of the spinor η . Thus, the second variation of A_3 is something that involves the derivative of η . With a proper choice of spinors η , one can construct a second supersymmetry variation that gives just the usual gauge transformation $A_3 \rightarrow A_3 + d\Lambda_2$ on the gauge field, where this Λ_2 is built from the relevant η 's. Thus, both diffeomorphisms and gauge transformations are in fact contained in the spacetime supersymmetry algebra. The supersymmetry algebra can be thought of as a sort of “square root” of the diffeomorphism and gauge algebras. The fact that diffeomorphisms and gauge transformations are expressed as squares leads to extremely useful positivity properties.

While we will not need the details of the local supersymmetry algebra below, it is useful to display the algebra of the asymptotic supercharges. Just as for diffeomorphisms and gauge transformations, the asymptotic supersymmetries lead, in the asymptotically flat context, to conserved “supercharges.” In fact, for the eleven-dimensional case there are several relevant notions of the asymptotic algebra. The reason is that there are interesting p -branes for several values of p . There are thus several interesting classes of asymptotically Kaluza–Klein structures associated with different choices of the homogeneous manifold $Y = \mathbb{R}^{11-p}$.

However, all these algebras are rather similar. If Q is the generator of supersymmetry transformations, so that the asymptotic versions of the transformations above are generated by taking (super)Poisson brackets with $Q\bar{\eta}$, then the algebra

associated with the p -brane case has the general form (see e.g. [19])

$$\{Q_A^I, \overline{Q}^{JB}\}_+ = -2P_\mu\Gamma_A^{\mu B}\delta^{IJ} - 2iZ^{IJ}\delta_A^B, \quad (11.12)$$

where we have used A, B for the internal spinor indices. Here P_μ are the momenta per unit p -volume and Z^{IJ} is an antisymmetric real matrix associated with the asymptotic gauge transformations. In particular the eigenvalues of Z are of the form $\pm iq$, where q is the appropriately normalized charge carried by the p -brane. Our notation reflects the fact that it is natural to split the SUSY generator Q , which is an eleven-dimensional Majorana fermion, into a set of $(11-p)$ -dimensional fermions Q^I . Thus, the indices A, B take values appropriate to spinors in $(11-d)$ dimensions.

The most important property of this algebra is that it implies the so-called BPS bound on masses and charges. To get an idea of how this arises, recall that, while $\overline{Q}Q$ is a Lorentz invariant, it is $Q^\dagger Q$ that is a positive definite operator. Thus, a positivity condition should follow by writing the algebra in terms of Q^\dagger and Q . For simplicity, let us also choose an asymptotic Lorentz frame such that the energy-momentum of the spacetime is aligned with the time direction, that is, $P_\mu = T\delta_{\mu 0}$, where T is the brane tension or mass per unit p -volume.⁸ The algebra then takes the form

$$\{Q_A^I, Q^{\dagger JB}\}_+ = 2T\delta^{IJ}\delta_A^B + 2iZ^{IJ}\Gamma_A^{0B}. \quad (11.13)$$

It is useful to adopt the notation of quantum mechanics even though we are considering classical spacetimes. Thus, we will describe a spacetime by a state $|\psi\rangle$ and let the generators Q act on that state as $Q|\psi\rangle$. Contracting the above relation (11.13) with η_{JB} and $\eta_I^{\dagger A}$ for a set of spinor fields η_I , taking the expectation value in any state, and using the positivity of the inner product and the fact that the eigenvalues of Γ_A^{0B} are ± 1 yields the relation

$$T \geq |q|. \quad (11.14)$$

See [20] for a full classical supergravity derivation in the context of magnetic charge in eleven dimensions and [17] for a complete derivation in classical $N = 2$ supergravity in four dimensions. See also [21, 22] for details of the argument above in a four-dimensional context.

This is the BPS bound. A spacetime in which this bound is saturated is called a BPS spacetime and the corresponding quantum states are known as BPS states. Note that, from our above argument, a state is BPS only if it is annihilated by a

⁸ Simple relativistic branes have a fixed value of T . As a result, stretching the brane over an additional p -volume V_p increases the energy by TV_p and requires a corresponding amount of work. Thus T is also the tension in the more familiar sense of the force density (the force per unit $(p-1)$ -volume) required to stretch the brane.

⁷ That is, satisfying the reality condition $\eta^* = B\eta$ where $B = \Gamma^3\Gamma^5\dots\Gamma^9$ and $*$ denotes complex conjugation.

supersymmetry generator, that is, if the spacetime is invariant under the transformation (11.11) for some spinor η . The converse is also true: any asymptotically flat spacetime that is invariant under some nontrivial supersymmetry transformation is BPS. Given a solution s and a spinor η for which the transformation (11.11) vanishes on s , one says that η is a *Killing spinor* of s . Since the gravitino ψ vanishes for a bosonic solution, in this context we see from (11.11) that η is a Killing spinor whenever it is supercovariantly constant, i.e., when it satisfies $\hat{D}_\alpha \eta = 0$.

The bound (11.14) is reminiscent of the extremality bound for Reissner–Nordström black holes. It turns out that the relationship is a strong one. Given the similarity of eleven-dimensional supergravity to Einstein–Maxwell theory, it will come as no surprise that there is a supergravity theory in 3+1 dimensions that contains Einstein–Maxwell theory, together with a few extra fields. When the extra fields vanish on an initial slice, they remain zero for all time. Thus, Einstein–Maxwell theory is a “consistent truncation” of the supergravity. In this context, the BPS bound and the extremality bound for charge coincide when there is no angular momentum. Thus, any asymptotically flat solution of Einstein–Maxwell theory with extremal charge and vanishing angular momentum can be lifted to a BPS solution of the supergravity.

In general, any BPS black hole solution will be extremal, though the converse is not always true. An important example occurs in four dimensions where all BPS states must have zero angular momentum. Thus, the 3+1 extreme Kerr solution is not BPS.

Now, in familiar 3+1 Einstein–Maxwell gravity, we are used to thinking of extreme black holes as being some sort of marginal and perhaps unphysical case. Indeed, it is an important part of black hole thermodynamics that one cannot by any finite (classical) process transform a nonextreme black hole into an extreme black hole. Moreover, a real astrophysical black hole will quickly lose its charge, owing to interactions with the interstellar medium. Even in a pure vacuum, quantum field theory effects in the real world cause black holes to lose their charge and to evolve toward neutral black holes. However, this last statement is a consequence of the large charge-to-mass ratio of the electron. Owing to the BPS bound discussed above, objects like the familiar electron do not exist in a theory with sufficient supersymmetry. As a result, BPS black holes do not discharge. Instead, nonextreme black holes decay *toward* extremality through the emission of Hawking radiation and (assuming that black holes have only a finite number of internal states) any nonextreme black hole will decay to an extreme black hole in a very large but finite time. Thus, extreme black holes are of central importance in understanding supersymmetric theories as they represent stable “ground states” for black holes.

Now that we have come to terms with supersymmetry, we will proceed to ignore fermions completely in the sections below.

Executive summary If you decided to skip over the material involving spinors, the key point is that theories with enough supersymmetry have a so-called **BPS bound**. This means that (in appropriate units) the mass per unit volume of a p -brane must be greater than or equal to the associated A_{p+1} -form charge. Solutions that saturate this bound are called BPS solutions and have special properties. In particular, any BPS black hole or brane is extremal.

11.3 M-branes: the BPS solutions

Although we wish to focus on the eleven-dimensional case, supersymmetry and supergravity can also be considered in less than eleven dimensions. For example, in 3+1 dimensions any asymptotically flat solution of Einstein–Maxwell theory with extremal charge and zero angular momentum can be lifted to a BPS solution of 3+1 supergravity. But this is just the class of Majumdar–Papapetrou solutions [23, 24], which consist of some number of extreme Reissner–Nordström black holes in static equilibrium. Since the Majumdar–Papapetrou solutions are a more familiar analogue of the eleven-dimensional M-brane solutions that we wish to discuss, we present a brief review in section 11.3.1 as an introduction to the world of M-branes. This material overlaps with and extends the discussion of Chapter 1. We then examine the M-branes themselves in section 11.3.2.

11.3.1 The 3+1 Majumdar–Papapetrou solutions

Recall that the Reissner–Nordström solution with mass M and charge Q takes the form

$$ds^2 = - \left(1 - \frac{2GM}{R} + \frac{GQ^2}{R^2} \right) dt^2 + \left(1 - \frac{2GM}{R} + \frac{GQ^2}{R^2} \right)^{-1} dR^2 + R^2 d\Omega_2^2, \quad (11.15)$$

where R is the usual Schwarzschild radial coordinate, t is the Killing time, and $d\Omega_2^2$ is the metric on the unit 2-sphere; Q and M are the charge and mass of the black hole, with Q measured in units of $\sqrt{(\text{mass})(\text{length})}$, as is natural in classical mechanics with $c = 1$ but $G \neq 1$, so that Coulomb’s law is $F = Q^2/r^2$. The factors of Newton’s constant G have been left explicit for consistency with the rest of this exposition. The extremal situation occurs when $GM^2 = Q^2$ and, in this case, the solution is controlled by a single length scale $r_0 = GM = \sqrt{GQ}$. The metric simplifies to

$$ds^2 = - \left(1 - \frac{r_0}{R} \right)^2 dt^2 + \left(1 - \frac{r_0}{R} \right)^{-2} dR^2 + R^2 d\Omega_2^2. \quad (11.16)$$

Let us take this opportunity to recall that the horizon at $r = r_0$ lies an infinite proper distance away from any $r > r_0$ along any surface of constant t . Since the size of the sphere is approximately a constant (r_0) over the entire region near the horizon one says that an extreme black hole has “an infinite throat”. In fact, the region near the horizon is just the so-called Bertotti–Robinson universe, two-dimensional anti-de Sitter space (AdS_2) times S^2 . A simple way to see this is to set $z = r_0(1 - r_0/R)^{-1}$ and to expand the metric in powers of $1/z$. One finds that

$$ds^2 = \frac{-dt^2 + dz^2}{z^2} + r_0^2 d\Omega_2^2 + O(z^{-4}). \quad (11.17)$$

The leading terms shown give precisely $\text{AdS}_2 \times S^2$ in so-called Poincaré coordinates.

We now return to the full metric (11.16) and change to so-called isotropic coordinates in which the spatial part of the metric is conformally flat. Let $r = R - r_0$, so that the horizon lies at $r = 0$. Introducing the Cartesian coordinates x^i as usual on \mathbf{R}^3 , we have

$$ds^2 = -f^{-2} dt^2 + f^2 \sum_{i=1}^3 dx^i dx^i, \quad (11.18)$$

where $f = 1 + r_0/r$. Similarly, the electromagnetic potential is given by $A_t = f^{-1}$ with the spatial components of A vanishing. As the function f satisfies Poisson’s equation with a delta function source,

$$\partial_x^2 f := \sum_{i=1}^3 \partial_i \partial_i f = -4\pi \delta^{(3)}(x), \quad (11.19)$$

the solution for the extreme black hole takes a form similar to that in electrodynamics (except that the Poisson equation is for the *inverse* of the electrostatic potential). Note that the relevant differential operator is the Laplacian on a *flat* 3-space and not that directly defined by the metric. Such differential operators will often appear below, and we will use the convention that ∂_x^2 will always denote the flat-space Laplacian associated with the coordinates x . Similarly, we will write $dx^2 := \sum_i dx^i dx^i$.

The analogy with electrostatics is quite strong. The metric (11.18) and the associated electric field define the class of Majumdar–Papapetrou solutions [23, 24]. These are, in general, solutions of the Einstein–Maxwell system coupled to so-called extremal dust. This dust is characterized by the property that, when two grains of dust are at rest, their electrostatic repulsion is exactly sufficient to balance their gravitational attraction and they remain at rest. Modulo the conditions below, any choice of the function f in (11.18) yields a static solution of the field equations

corresponding to some distribution of this dust. For an asymptotically flat solution, we should take f to be of the form $1 + Q/r$ near infinity. The one restriction on f is that $\rho = -(1/4\pi)\nabla^2 f$ must be everywhere positive. In particular, we will take it to be of the form $\rho_0 + \sum_{k=1}^N r_k \delta(x - x_k)$, where ρ_0 is continuous. The density (defined with respect to the Cartesian coordinate system x_i) of extremal dust is given by ρ_0 and each delta function will result in the presence of an extremal black hole.

Extremality is quite important for the simple form of this class of solutions. It is only in the extreme limit that the repulsion induced by the electric charge can “cancel” the gravitational attraction so that the solution can remain static. If one adds any additional energy to the solution, the nonlinearities of gravity become more directly manifest.

Note that the source in (11.19) lies at the origin of the x -coordinates, that is, at the horizon of the black hole. However, since the horizon of the black hole is in fact not just a single point in space, $x = 0$ is clearly a coordinate singularity. This means that although the support of the delta function lies at $x = 0$, this should not be interpreted as the location of the black hole charge. Rather, the role of this delta function is to enforce a boundary condition on the electric flux emerging from the black hole such that the hole does indeed carry the proper charge.

Of course, in 3+1 dimensions we can also have magnetically charged black holes. In fact we can have dyons, carrying both electric and magnetic charge. The corresponding extremal solutions are given directly by electromagnetic duality rotations of the above solution.

For future reference we note that there is a similar set of solutions in 4+1 dimensions, though black holes in five dimensions can carry only electric charge. These solutions take the form

$$ds^2 = -f^{-2} dt^2 + f \sum_{i=1}^4 dx^i dx^i = -f^{-2} dt^2 + f dx^2, \quad (11.20)$$

where $\partial_x^2 f = -2\Omega_3[\rho_0 + \sum_{k=1}^N r_k^2 \delta(x - x_k)]$, Ω_3 is the volume of the unit 3-sphere, ρ_0 is the charge per unit $d^4 x$ cell, and r_k is a length scale parameterizing the charge of the k th extremal black hole. The fact that r_k^2 , as opposed to r_k , appears as the source reflects the fact that the fundamental solution of Poisson’s equation in four dimensions is of the form r^{-2} .

As we have already noted, there is a coordinate singularity at the black hole horizon. Thus, the isotropic form of the metric does not allow us to see to what extent the black hole, or even the horizon, is nonsingular. However, if the black hole is to have a smooth horizon then a necessary condition is that the horizon have nonzero (and finite) area. That this is true of the above metrics is easy to read off

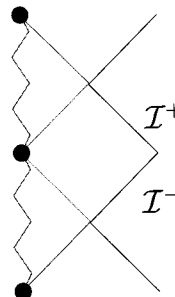


Figure 11.2 Conformal diagram for extreme Einstein–Maxwell black holes.

from (11.18) and (11.20) by noting that the divergence of f^2 or f cancels the r^2 factor that arises in writing dx^2 in spherical coordinates (i.e., $dx^2 = dr^2 + r^2 d\Omega^2$). While this is certainly not a sufficient condition for the smoothness of the horizon, it will serve as a useful guide below.⁹

For completeness, we display conformal diagrams for the above solutions in Fig. 11.2. The 3+1 and 4+1 cases are identical except for the dimension of the (suppressed) spheres of symmetry. Here \mathcal{I}^+ , \mathcal{I}^- denote the past and future null infinities of a particular asymptotic region and the zigzag line denotes the (timelike) singularity. The black circles mark the “internal infinities”. These points lie at an infinite affine parameter along any geodesic (spacelike, timelike, or null) from the interior.

However, Fig. 11.2 does not tell the entire story. For charged nonextreme black holes it is known that, while the exterior solution is quite stable, the simple analytic textbook Reissner–Nordström solution is in fact unstable near the inner horizon. Perturbations transform what would be the inner horizon into a curvature singularity; see e.g. [28–30]. Now, recall that the inner horizon coincides with the event horizon in the extreme limit. Though there are some subtleties, this turns out to imply that extreme black holes (produced, say, by the emission of Hawking radiation from non-extreme black holes) have a singularity lurking just below their event horizon [31, 32]. Specifically, in the limit where an observer enters the black hole long after it was formed, no proper time passes for that observer between the horizon and the singularity. We say that such black holes have an “effective spacetime diagram” with a singular horizon given by Fig. 11.3. We expect that the same is true of the higher-dimensional extreme black holes discussed below, where by black hole we mean that the horizon is compactly generated. Black branes with

⁹ Interestingly, while the 3+1 Majumdar–Papapetrou solutions (11.18) are smooth (and in fact analytic [25]), the 4+1 solutions (11.20) are not [20, 26]. In even higher dimensions the corresponding solutions have curvature singularities on the would-be horizon (i.e., they have curvature singularities at locations that would have been a horizon in lower-dimensional cases) [27].

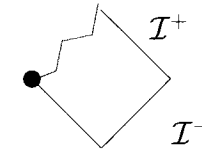


Figure 11.3 Effective conformal diagram for perturbed extreme Einstein–Maxwell black holes, as seen by late-time observers.

noncompactly generated horizons can be quite different, owing to the extra need to impose boundary conditions in the directions along the branes.

11.3.2 Brane solutions in eleven dimensions

There are four (basic) solutions of eleven-dimensional supergravity that are of particular importance in string/M theory. They are known as the (eleven-dimensional) Aichelburg–Sexl metric [33], the M2-brane [34] (electrically charged under A_3), the M5-brane (magnetically charged under A_3), and the eleven-dimensional version of the Kaluza–Klein monopole [35, 36]. Although it may not be obvious from the names, all four basic solutions are associated with branes in string/M theory. Below, we discuss only the extreme versions of these basic solutions, which turn out to be BPS. In particular they each have 16 Killing spinors, preserving half the supersymmetry. The nonextremal forms of the M-branes may be found in, e.g., [20].

It is sometimes said that an arbitrary BPS solution can be built from these basic solutions. The point here is that the above “basic” solutions are in one-to-one correspondence with the types of charge present in eleven-dimensional supergravity. Since the charges are additive, one is tempted to say that any solution with arbitrary amounts of the various charges can be built up by “combining” these basic solutions. We will see below that certain simple solutions carrying multiple charge are in fact built from the basic solutions in a simple way. However, there is as yet no known method for writing down a general BPS solution, much less one in terms of the basic solutions.

Let us begin with the BPS M2- and M5-branes, as these are straightforward supergravity analogues of the extreme Reissner–Nordström black holes discussed above.¹⁰ There is a corresponding notion of isotropic coordinates, in which the multi-black-hole solutions are given by solving a flat-space Poisson equation with

¹⁰ Interestingly, the global structure of the non-extreme M2- and M5-brane solutions is much like that of the Schwarzschild black hole, as opposed to that of non-extreme Reissner–Nordström solutions. In particular, there is no inner horizon and the singularity is spacelike as opposed to timelike.

delta function sources. The solutions of this Poisson equation are typically denoted H_2 for the M2-brane and H_5 for the M5-brane and are referred to as “harmonic” functions. The details are different for the two branes, but both should seem quite familiar from our review of the Majumdar–Papapetrou solutions.

For the M2-brane we introduce a set of three coordinates x_{\parallel} that should be thought of as labeling the directions along the brane and a set of eight coordinates x_{\perp} that should be thought of as labeling the directions orthogonal to the brane. As one of the x_{\parallel} directions is the time direction, we define $dx_{\parallel}^2 = -(dx_{\parallel}^0)^2 + (dx_{\parallel}^1)^2 + (dx_{\parallel}^2)^2$. The solution takes the form

$$\begin{aligned} A_3 &= H_2^{-1} dt \wedge dx_{\parallel,1} \wedge dx_{\parallel,2} \\ ds^2 &= H_2^{-2/3} dx_{\parallel}^2 + H_2^{1/3} dx_{\perp}^2, \end{aligned} \quad (11.21)$$

with $\partial_{\perp}^2 H_2$ equal to a sum of delta functions. Note that, near the delta function source, H_2 will diverge as r^{-6} , where r is the x_{\perp} coordinate distance from the source. As a result, $H_2^{1/3}$ diverges as r^{-2} , and the sphere at the horizon will have nonzero (finite) area. This suggests that the horizon of at least a single BPS M2-brane is smooth, and a careful investigation [20] showed that this is indeed the case. In fact, by a direct analogue of our discussion for 3+1 extreme Einstein–Maxwell black holes, one can show that the region near the horizon is just $\text{AdS}_4 \times S^7$.

This is rather interesting, as the extremal limits of black branes in lower-dimensional supergravity theories tend, because of the dilaton, to have singular horizons. The global structure of the M2-brane is in fact much like that of the extreme Reissner–Nordström black holes discussed above. The conformal diagram is just that of Fig. 11.2, except that each point on the diagram now represents a surface with both the topology and metric of $\mathbb{R}^2 \times S^7$ rather than just that of a sphere.

For the M5-brane we introduce a set of six coordinates x_{\parallel} along the brane and a set of five coordinates x_{\perp} orthogonal to the brane. Again, the x_{\parallel} directions include the time t . The solution takes the form

$$\begin{aligned} dA &= F = -\frac{1}{4!} \partial_{x_{\perp}}^4 H_5 \epsilon^i{}_{jklm} dx^j \wedge dx^k \wedge dx^l \wedge dx^m, \\ ds^2 &= H_5^{-1/3} dx_{\parallel}^2 + H_5^{2/3} dx_{\perp}^2, \end{aligned} \quad (11.22)$$

with $\partial_{\perp}^2 H_5$ equal to a sum of delta functions. The different form of the gauge field as compared with (11.21) is associated with the fact that this solution carries a magnetic charge instead of an electric charge. Now, the field H_5 diverges at a delta function source as r^{-3} , so that $H_5^{2/3}$ diverges as r^{-2} and again the area of the spheres is finite at the horizon. Once again, a detailed study shows that the

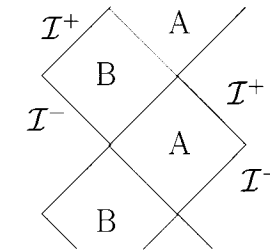


Figure 11.4 Conformal diagram for the extreme M5-brane.

horizon is completely smooth and, as one might guess, the near-horizon geometry is $\text{AdS}_7 \times S^4$.

The surprise [20] is that this solution turns out to have no singularities at all, even inside the horizon! Its conformal diagram is thus rather different from those we have encountered so far and is shown in Fig. 11.4. The regions marked A and B (“in front of” and “behind”) the horizon are exactly the same. In familiar cases, the singularity theorems guarantee that something of this kind does not occur: compact trapped surfaces imply a singularity in their future [37]. However, the fact that we are dealing with a black brane and not a black hole means that the trapped surfaces are not in fact compact. The point here is that the horizon is extended in the x_{\parallel} directions. What happens when the solution is toroidally compactified by making identifications in the x_{\parallel} coordinates is an interesting story, which will be discussed below.

The remaining two solutions have the noteworthy property of being BPS despite the fact that the gauge field A_3 is identically zero. It can be seen that this is not really a contradiction to the condition of extremality when one notes (see section 11.4.2) that under Kaluza–Klein reduction a momentum can act like a charge. Another useful perspective results from recalling that two parallel beams of light (or two parallel gravitational waves) do not interact gravitationally. The same is true for any null particles. Thus, one may say that spatial components of the momentum (of like sign) provide a gravitational repulsion and that the case of null momentum is like the case of extremal charge, in which this repulsion exactly balances the gravitational attraction due to the energy of the particles.

The Aichelberg–Sexl metric carries just such a null momentum. This solution was originally constructed [33] (in 3+1 dimensions) by boosting a Schwarzschild solution, while rescaling its mass parameter M in order to keep the total energy E finite in some asymptotic frame. This explains the null momentum of the resulting solution. It too can be described in terms of a “harmonic function” H_{AS} . The Aichelberg–Sexl metric may be thought of as the gravitational field of a null particle, such as a graviton or a quantum of the A_3 field in the short-wavelength

(WKB) approximation. We introduce a time coordinate t , a coordinate z in the direction of motion of the particle, and a set of nine additional coordinates x_\perp . In isotropic coordinates, the solution takes the form

$$ds^2 = -dt^2 + dx_\perp^2 + dz^2 + (H_{\text{AS}} - 1)(dt - dz)^2, \quad (11.23)$$

where $H_{\text{AS}}(x_\perp)$ is a solution of $\partial_\perp^2 H_{\text{AS}} = -7\Omega_9\rho$, ρ is again a source, and Ω_9 is the volume of the unit 9-sphere. When ρ is a delta function, this solution is in fact singular at the source.

Let us now turn to the Kaluza–Klein monopole. This solution was originally constructed [35, 36] by using the fact that the metric product of any two Ricci flat spaces is Ricci flat. Thus, one can make a static solution of 4+1 Einstein gravity out of any solution to four-dimensional Euclidean gravity. Such a solution is Ricci flat, so the metric product with a line is also Ricci flat. The metric product of Euclidean Taub–NUT space [38] with a line gives the 4+1 Kaluza–Klein monopole. The eleven-dimensional solution of interest here is simply the metric product of Euclidean Taub–NUT space with a 6+1 Minkowski space. Recall that the Taub–NUT solution is not asymptotically flat. Rather, although it is asymptotically flat in three directions (to which we assign coordinates x_\perp), the fourth direction (which we will call θ) is an angular coordinate for which the associated S^1 twists around the 2-sphere to make a nontrivial asymptotic structure. Introducing coordinates x_\parallel on the 6+1 Minkowski space, the solution takes the form

$$ds^2 = dx_\parallel^2 + H_{\text{KK}}dx_\perp^2 + H_{\text{KK}}^{-1}(d\theta + a_i dx_\perp^i)^2, \quad (11.24)$$

with, of course, a vanishing 3-form potential A_3 . Again, H_{KK} satisfies an equation of the form $\partial_\perp^2 H_{\text{KK}} = -4\pi\rho$ and a_k is determined from H_{KK} via $\partial_{x_\perp^i} H_{\text{KK}} = \epsilon_{ijk} \partial_{x_\perp^j} a_k$. As usual we find a coordinate singularity at the location of the delta function sources.

But the story of this singularity is just that of Taub–NUT space. Suppose that θ is periodic with period L . Then the spacetime is in fact smooth in the neighborhood of a “source” of the form $\rho = L/(4\pi)\delta^{(3)}(x_\perp)$; in this case, (11.24) actually represents a smooth, geodesically complete, solution to the *source-free* 10+1 Einstein equations. A source of this sort is referred to as a monopole of unit charge. A multi-center solution¹¹ is smooth whenever each separate center has this charge. Now, if we take the limit of a multi-center solution in which several centers coalesce into a single center with charge greater than 1, the resulting spacetime has a timelike singularity at the source. However, this singularity (with an integer n number of units of the above fundamental charge) has a particularly simple form.

¹¹ One with several delta function sources.

It is a quotient of flat space, and in this sense it is a higher-dimensional version of a conical singularity.

A favorite topic to include in discussions of black holes is that of black hole entropy. It is therefore natural to ask about the entropy of the branes that we have discussed above. Similar thermodynamic arguments hold for black branes as for black holes, suggesting that one should associate an entropy of $A/(4G_{11})$ with such objects, where A is the area (volume) of the horizon and $1/(16\pi G_{11}) = 1/(2\kappa_{11}^2)$ is the coupling constant that stands in front of the supergravity action. However, the Kaluza–Klein monopole and Aichelberg–Sexl metric have no Killing horizons and so presumably carry no such entropy.

The M2- and M5-branes are a bit more subtle. On the one hand, their horizons are homogeneous surfaces that are noncompact. As such, one might be tempted to assign them infinite entropy. Some further insight into the issue is gained by using the fact that the solutions are invariant under translations in the spatial x_\parallel coordinates to make toroidal identifications and compactify the horizons. We can then calculate the horizon area and, because the norms of the Killing fields ∂_{x_\parallel} vanish on the horizon, the result is zero. Thus, at least when compactified in this way, M2- and M5-branes have vanishing horizon volumes and again carry no entropy. This is another sense in which such solutions are “basic”.

One might guess that there is something singular about the zero-area horizons of compactified M2- and M5-branes. However, since those solutions were constructed by making discrete identifications of spacetime with smooth horizons, the curvature and field strength cannot diverge at the zero-area horizon. It turns out that the situation is essentially the same as that which arises [39, 40] when AdS_3 is identified to make the $M = 0$ Banados, Teitelboim, and Zanelli (BTZ) black hole. The initially spacelike Killing fields ∂_{x_\parallel} become null on the horizon but also have fixed points. Thus, the horizon of the compactified solution has both closed null curves and a “Lorentzian conical singularity”.

11.3.3 Brane engineering

Before leaving eleven dimensions, a few words are in order on two basic techniques in “brane engineering,” the construction of new brane solutions from old ones. The particular techniques to be discussed are known as smearing and combining charges. Together, they will allow us to build BPS black branes with finite entropy.

Smearing is particularly straightforward. It is based on the observation that each type of “basic” solution above is related to the solution of a linear differential equation. Using a delta function source gives a solution that preserves some set of translation symmetries (in the x_\parallel directions) and breaks another set (in the x_\perp directions). However, a solution can be obtained that preserves more translational

symmetries by using a more symmetric source, e.g., one supported on a line, plane, or higher-dimensional surface. Constructing such a solution can be thought of as “smearing out” the charge of a less symmetric solution. Smearing out a given brane solution often results in a spacetime with a singular horizon. However, this need not be especially worrying if one regards the smeared solution as merely an effective description that is analogous to a description of a collection of discrete atoms as a continuous fluid. One imagines an array of branes in which a large number of unsmeared basic branes are placed in the spacetime with a small spacing between the branes.

The next technique to discuss is that of combining the basic types of charge. As mentioned above, this is in general rather difficult. If, however, two solutions preserve some of the same supersymmetries *and* they have been engineered to have the same translation symmetries (for example, by smearing) then they tend to be rather easy to combine. Making a simple guess as to the way in which the relevant harmonic functions (H_2, H_5, H_{AS}, H_M) should enter the metric and gauge fields tends to lead to a solution to the supergravity equations that preserves the common supersymmetries.

So far as I know there are no general theorems available on this subject. We will thus content ourselves with a few simple examples that fall into the class discussed in [41, 42]; see also [2]. We have already discussed the solution (11.21) corresponding to a set of parallel M2-branes. This solution preserves half the original 32 supersymmetries of 10+1 supergravity. The particular supersymmetries that are broken relate to the plane in space along which the M2-branes are oriented. Let us call the spatial coordinates along these branes x_{\parallel}^1 and x_{\parallel}^2 . We could also consider another set of M2-branes oriented along a plane associated with two other coordinates y_{\parallel}^1 and y_{\parallel}^2 , which are orthogonal to the x_{\parallel} coordinates. A set of solutions containing both types of brane and separately preserving the eight supersymmetries common to both sets of M2-branes is given by

$$\begin{aligned} A &= H_x^{-1} dt \wedge dx_{\parallel,1} \wedge dx_{\parallel,2} + H_y^{-1} dt \wedge dy_{\parallel,1} \wedge dy_{\parallel,2}, \\ ds^2 &= -H_x^{-2/3} H_y^{-2/3} dt^2 + H_x^{-2/3} H_y^{1/3} dx_{\parallel}^2 + H_x^{1/3} H_y^{-2/3} dy_{\parallel}^2 \\ &\quad + H_x^{1/3} H_y^{1/3} dx_{\perp}^2, \end{aligned} \quad (11.25)$$

where H_x, H_y are functions only of the six spatial coordinates x_{\perp} that are transverse to both sets of branes. The functions H_x and H_y are, as usual, related to source distributions through $\partial_{x_{\perp}}^2 H_x = -7\Omega_8 \rho_x$ and $\partial_{x_{\perp}}^2 H_y = -7\Omega_8 \rho_y$, and the distributions ρ_x and ρ_y may be arbitrary functions of x_{\perp} .

Note that the form (11.25) is just like that of (11.21) except that we have included two harmonic functions. A given term in the metric (11.25) is multiplied by a power of each harmonic function, which is determined by whether the term

refers to distances along or transverse to the corresponding brane. These powers are identical to those in (11.21).

In the solution (11.25) we have taken the two sets of branes to be completely orthogonal. However, other choices of the relative angle still preserve the same amount of supersymmetry. If one considers the coordinates $x_{\parallel}, y_{\parallel}$ as two sets of holomorphic coordinates on \mathbb{C}^2 then the requirement for a supersymmetric solution is that the x_{\parallel} - and y_{\parallel} -planes are related by a $U(2)$ transformation [43–45] as opposed to a more general $O(4)$ transformation. The metric in this case takes a similar form, with the part of the metric on the 4-space spanned by $x_{\parallel}, y_{\parallel}$ taking a certain Hermitian form.

However, combining the two sets of branes without first smearing them to generate four translation symmetries is more difficult. It turns out that, when one or both sets of branes is “localized” (i.e., not completely spread out along the other set of branes) then the supergravity equations no longer divide cleanly into parts describing each set of branes separately. The case where only one set of M2-branes is localized (and thus two translational symmetries remain) is still tractable, however. The solution still takes the same basic form (11.25) and the construction of the solution still splits into two parts. One can first solve a standard flat-space Poisson equation for the harmonic function H_x associated with the delocalized set of branes. One then has a linear differential equation to solve for the localized-brane harmonic function H_y , where H_x appears in the particular differential operator to be inverted. Such solutions exhibit an interesting phenomenon. While localized solutions exist when the branes are separated (in the x_{\perp} directions), the y -branes effectively delocalize along the x -branes in the limit where this separation is removed.¹²

Let us now return to the smeared solution (11.25) and consider the case for which $\rho_x = \rho_y = r_0^4 \delta^{(6)}(x_{\perp})$. We then find that H_x and H_y diverge at $x_{\perp} = 0$ as $|x_{\perp}|^{-4}$. As a result, the 5-spheres at $x_{\perp} = 0$ are infinite in volume and the solution is singular. However, adding a third M2-brane in another completely orthogonal ($z_{\parallel}^1, z_{\parallel}^2$) plane yields a nonsingular solution. The gauge field and the metric,

$$\begin{aligned} A &= H_x^{-1} dt \wedge dx_{\parallel,1} \wedge dx_{\parallel,2} + H_y^{-1} dt \wedge dy_{\parallel,1} \wedge dy_{\parallel,2} + H_z^{-1} dt \wedge dz_{\parallel,1} \wedge dz_{\parallel,2}, \\ ds^2 &= -H_x^{-2/3} H_y^{-2/3} H_z^{-2/3} dt^2 + H_x^{-2/3} H_y^{1/3} H_z^{1/3} dx_{\parallel}^2 + H_x^{1/3} H_y^{-2/3} H_z^{1/3} dy_{\parallel}^2 \\ &\quad + H_x^{1/3} H_y^{1/3} H_z^{-2/3} dz_{\parallel}^2 + H_x^{1/3} H_y^{1/3} H_z^{1/3} dx_{\perp}^2, \end{aligned} \quad (11.26)$$

for $\partial_{x_{\perp}}^2 H_{x,y,z}(x_{\perp}) = -2\Omega_3 \rho_{x,y,z}(x_{\perp})$ yield a BPS solution of the supergravity equations that preserves one-eighth of the supersymmetry (i.e., four supercharges) and

¹² This behavior is also typical of other BPS intersecting branes when the intersection (i.e., the set of directions common to both branes) is either 0+1 or 1+1 dimensional, though fully localized solutions exist for higher-dimensional intersections. See [46–48] for details and [49–51] for examples of such fully localized solutions.

has a smooth horizon. Moreover, this solution has the property that the translational Killing fields ∂x_{\parallel}^i , ∂y_{\parallel}^i , ∂z_{\parallel}^i have norms that do not vanish on the horizon.

In contrast, recall that, while the solution (11.21) for a single M2-brane has a smooth horizon, the spatial translational Killing fields have vanishing norm there. As mentioned above, on the one hand this means that compactifying a single M2-brane by, for example, taking the coordinate x_{\parallel}^1 as living on a circle, yields a solution with a conical singularity at the horizon and vanishing entropy. On the other hand, because the norms of the spatial translations do not vanish for the solution (11.26), it compactifies nicely into a black object with finite horizon area.¹³ This is the simplest BPS black brane solution with a finite entropy and, as a result, it is the simplest solution for which a microscopic accounting of the entropy has been given in string theory. A straightforward calculation shows that the horizon area is

$$A = \Omega_3 r_x r_y r_z L_{1x} L_{2x} L_{1y} L_{2y} L_{1z} L_{2z}, \quad (11.27)$$

where Ω_3 is the volume of the unit 3-sphere and the L 's are the lengths of the various circles on which the solution has been compactified.

Now, charges are quantized in string/M theory, and it is useful to express the entropy in terms of the number of charge quanta Q_x , Q_y , Q_z carried by the various branes. The tension of a single M2-brane is $(2\pi)^3 l_p^{-3}$, where l_p is the eleven-dimensional Planck length, defined by $16\pi G_{11} = 2\kappa_{11}^2 = (2\pi)^8 l_p^9$. Note that r_x^2 is a measure of the charge *density* of the x -type branes per unit cell of the y , z 4-space. As such, r_x^2 is proportional to $Q_x / (L_{1y} L_{2y} L_{1z} L_{2z})$. Inspection of the area formula (11.27) thus shows that rewriting the area in terms of the integer charges will remove the L factors. Putting in the proper normalization coefficients, the result turns out to be

$$\frac{A}{4G_{11}} = 2\pi \sqrt{Q_x Q_y Q_z}. \quad (11.28)$$

We will comment briefly on the corresponding microscopic counting of states in section 11.6.2.

11.4 Kaluza–Klein and dimensional reduction

So far, we have dealt almost exclusively with eleven-dimensional supergravity. However, it is the ten-dimensional supergravity theories that admit self-consistent

¹³ As given by (11.26) this horizon is in fact smooth. We expect the compactified black hole to be subject to an instability similar to that of extreme Reissner–Nordstrom, so that the perturbed conformal diagram is given by Fig. 11.3. Recall, however, that this instability affects only the black hole interior and so does not change the horizon area.

perturbative quantizations in terms of strings.¹⁴ This means that the powerful technology of perturbative quantum field theory can be brought to bear on questions concerning quantum dynamics. This perturbative technology can be applied in particular to certain branes in 9+1 supergravity. It is through this fusion of supergravity and perturbative field theory that string/M theory has been revolutionized in recent years via studies of duality, black hole entropy, and more recently of the Maldacena conjecture, i.e., AdS–CFT correspondence.

This is not the place to enter into a detailed discussion of string perturbation theory, though we will comment briefly on the subject in section 11.6. The reader interested in learning that subject should consult the standard references (e.g. [4–9]). Our purpose here is to provide a clear picture of the supergravity side of BPS-brane physics, and in particular to discuss the relationship of BPS-branes with the eleven-dimensional theories. As the so-called type IIA ten-dimensional theory can be obtained by Kaluza–Klein reduction from M theory, we will warm up by discussing Kaluza–Klein compactification in nongravitational theories in section 11.4.1. We then address the reduction of M theory to the IIA theory in detail in section 11.4.2, setting the stage for our discussion of 9+1 branes in section 11.5.

11.4.1 Some remarks on Kaluza–Klein reduction

The idea of the Kaluza–Klein mechanism is that, at low energies, a *quantum* field theory on an $(n + d)$ -dimensional spacetime in which d dimensions are compact behaves essentially like a quantum field theory on an n -dimensional spacetime. To see why, consider a free scalar field on $M^n \times S^1$, where M^n is n -dimensional Minkowski space. Normal modes of the field are labeled by an n -vector momentum p and an integer k corresponding to the momentum around the S^1 . Suppose that the length of the S^1 is L , so that the dispersion relation associated with one-particle excitations is $E^2 = p^2 + (k/L)^2$. If we now consider the theory at energy scales less than $1/L$, the only states with such a low energy have $k = 0$, i.e., they are translationally invariant around the S^1 .

In this way, our scalar field reduces at low energies to a quantum field on n -dimensional Minkowski space. Note that this is an intrinsically quantum mechanical effect, associated with both the quantization of energy and with the discrete spectrum of the Laplacian on a circle. Since the Laplacian has a discrete spectrum on any compact space, the same basic mechanism operates with any choice of compact manifold. The simplest cases to analyze are those in which the spacetime of interest is a direct product of a noncompact spacetime M with a compact manifold K and

¹⁴ It should be mentioned that string theory is not a quantization of pure 9+1 supergravity; string theory modifies the physics even at the classical level, though only by adding heavy fields with masses of order $1/l_s$ where l_s is the string scale. See section 11.6.1 for (a few) more details.

in which K is a homogeneous space. In that case, the lower-dimensional (reduced) theory is typically obtained from the higher-dimensional one simply by taking the fields to be invariant under the symmetry group that acts transitively on the compact manifold. On a general manifold of the form $M \times K$, the reduced theory is given by considering the zero modes of the Laplacian (or other appropriate differential operator) on K . Similar, but less clean, mechanisms may apply even when the spacetime is not a direct product of a compact and a noncompact spacetime.

The effect of compactification on interacting fields is similar. At the perturbative level the story is exactly the same, and nonperturbative effects seldom change the picture significantly.

11.4.2 Kaluza–Klein in (super)gravity

We now turn to Kaluza–Klein reduction in a theory with gravity. Since the spacetime metric is dynamical this case is perhaps not as clean cut as the scalar field example just discussed. However, at the perturbative level one may treat gravity just as any other field. Our general experience with quantum mechanics and the uncertainty principle also makes it reasonable on more general grounds to expect that excitations associated with a small compact space will be expensive in terms of energy. Thus, at least at first glance, we expect that gravity on a manifold of the form $M \times K$ reduces at low energies to a theory on the noncompact manifold M .

We are most interested in the Kaluza–Klein reduction of eleven-dimensional supergravity on $\mathcal{M} = M \times S^1$, where M is a (9+1)-dimensional asymptotically flat spacetime. We expect the reduced theory to be obtained by considering the class of eleven-dimensional field configurations that are translationally invariant around the S^1 . Let us therefore assume that our eleven-dimensional spacetime \mathcal{M} has a spacelike Killing vector field λ^μ whose orbits have the topology S^1 . It is convenient to normalize this Killing field to have norm +1 at infinity and to denote the length of the Killing orbits there by L . The Killing field is not necessarily hypersurface orthogonal.

Since the translation group generated by the Killing field acts nicely (technically, “properly discontinuously” [37–39]) on our eleven-dimensional spacetime \mathcal{M} , we may consider the quotient of the smooth topological space \mathcal{M} and the action of this group. The result is a new topological space M which is a ten-dimensional smooth manifold. This is the manifold on which our (10 = 9 + 1)-dimensional reduced theory will live.

By using the metric, we define a set of projection operations on the various 10+1 fields with each projection providing a different field in the (9+1)-dimensional spacetime. Recall that a field is an object that transforms in a certain way under local Lorentz transformations, (i.e., diffeomorphisms) of the manifold. The

diffeomorphisms of the 9+1 manifold will be that subgroup of the eleven-dimensional diffeomorphisms that leaves the killing field λ^μ invariant. Thus, the transformations that become the diffeomorphisms of the 9+1 manifold are a proper subgroup of the 10+1 diffeomorphisms and a single 10+1 field can contain several 9+1 fields.

To see how the 9+1 fields are constructed, consider any coordinate patch U (with coordinates x^a) on the 9+1 manifold M . If $V \subset \mathcal{M}$ is the preimage of U under the above quotient construction, then each x^a defines a function on V . Since no linear combination of the gradients of the x^a functions can be proportional to the Killing field λ^μ , we can complete this set of functions to a coordinate patch on V by adding a (periodic) coordinate θ that is proportional to the Killing parameter along any orbit of λ^μ , i.e., satisfying $\theta_{,\mu}\lambda^\mu = \lambda^\mu\lambda_\mu$.

This coordinate system gives an explicit realization of the natural decomposition of the 10+1 fields into a set of 9+1 fields. The set of gradients $x_{,\mu}^a$ of the 9+1 coordinates define a projection operation on any contravariant (upper) index, as does the gradient $\theta_{,\mu}$ of the coordinate θ . Thus, from the 10+1 contravariant metric $g^{\mu\nu}$, we can define the 9+1 metric $g^{ab} = x_{,\mu}^a x_{,\nu}^b g^{\mu\nu}$, a 9+1 abelian vector field $A_1^a = -x_{,\mu}^a \theta_{,\nu} g^{\mu\nu}$, and a 9+1 scalar field ϕ through $Le^{4\phi/3} = \lambda^\mu g_{\mu\nu} \lambda^\nu$. The particular coefficient of ϕ is chosen so that it is canonically normalized.¹⁵ This ϕ is the famous dilaton of string theory, and it is this field that is responsible for many differences between supergravity in less than eleven dimensions and familiar Einstein–Maxwell theory. It is clear that all these fields transform in an appropriate way under 9+1 diffeomorphisms.

We now make several important observations. The first is that nondegeneracy of the 10+1 metric implies nondegeneracy of the 9+1 metric. Thus g^{ab} has an inverse that gives the covariant metric g_{ab} .

The second is that the scalar has been defined by the norm of the Killing field and not by the norm of $\theta_{,\mu}$ as one might expect. The point is that these two objects are related. To see this, let us first note that the coordinates x^a are constant along the orbits of the Killing field. Thus, the Lie derivative of x^a along λ^μ vanishes and we have $x_{,\nu}^a g^{\nu\mu} \lambda_\mu = 0$. This means that the gradients $x_{,\mu}^a$ span the space orthogonal to λ_μ at each point. But, by definition, $\lambda^\mu \theta_{,\mu} = \lambda^\mu \lambda_\mu$. Thus, we find that $\theta_{,\mu} - \lambda_\mu$ is of the form $c_a x_{,\mu}^a$ where c_a is some function on the 9+1 spacetime. This fact, together with the definition of A_1 , can be used to derive the relation

$$c_a = -g_{ab} A_1^b; \quad (11.29)$$

thus, we have

$$\theta_{,\mu} \theta^{\mu} = \lambda^\mu \lambda_\mu + A_{1a} A_1^a. \quad (11.30)$$

¹⁵ When $2\kappa_{10}^2$ is set to 1; see below.

We see that the definition of ϕ differs from the seemingly more natural one only by a function of the vector field A_1 . Choosing to write ϕ directly in terms of the Killing field λ^μ removes a mixing between the vector field and scalar that would otherwise obscure the physics. Note that we have related the scalar field ϕ to the logarithm of the norm of the Killing field and that this norm is positive by assumption.

Finally, let us consider the vector field A_1 . Although we have $x_{,\nu}^a g^{\nu\mu} \lambda_\mu = 0$, the vector field A_1 need not vanish. There is a freedom to redefine the zero of θ at each value of the x^a . This amounts to the transformation $\theta \rightarrow \theta - \Lambda(x)$. Under this operation we see that the 9+1 metric g^{ab} is not affected, and neither is the scalar (since it depends only on the norm of the Killing field), while the vector field transforms as $A_1^a \rightarrow A_1^a + \Lambda_{,b} g^{ab}$, i.e., $A_{1a} \rightarrow A_{1a} + \Lambda_{,a}$. Thus we see that A_1 is in fact an abelian gauge field. The associated field strength $F_2 = dA_1$ (with A_1 considered as a 1-form) is just the “twist” of the Killing field λ^μ , which measures the failure of λ^μ to be hypersurface orthogonal.

It is interesting to ask about the charge to which this gauge field couples, as the field itself arises directly from the reduction of the gravitational field in eleven dimensions. To this end, consider a “gauge” transformation of the above form with constant Λ . In familiar Maxwell theory, this global $U(1)$ rotation is generated by the total electric charge operator. But, in terms of \mathcal{M} it is a shift in θ , which is just a translation along λ^μ . We therefore identify the total A_1 -charge on M with the corresponding momentum on \mathcal{M} . One may check that any timelike total energy-momentum for \mathcal{M} becomes a charge and a ten-dimensional energy-momentum vector on M satisfying a BPS bound.

In performing calculations, it is often useful to express the above decomposition in terms of the eleven-dimensional covariant metric ds_{11}^2 . The reader may check that we have

$$ds_{11}^2 = g_{ab} dx^a dx^b + e^{4\phi/3} (d\theta + A_{1a} dx^a)^2. \quad (11.31)$$

One might think that it is natural to decompose the antisymmetric 3-form A_3 into a (9+1)-dimensional 3-form $\hat{A}_3^{abc} = A_3^{\mu\nu\rho} x_{,\mu}^a x_{,\nu}^b x_{,\rho}^c$ and 2-form $A_2^{ab} = A_3^{\mu\nu\rho} x_{,\mu}^a x_{,\nu}^b \lambda_\rho$, in order that both are invariant under the gauge transformation $A_1 \rightarrow A_1 + d\Lambda_0$. However, it turns out that the 3-form \hat{A}_3 then transforms nontrivially under the gauge transformations associated with the 2-form potential A_2 . The various gauge transformations cannot be completely disentangled and in fact the standard choice is instead to define \tilde{A}_3, A_2 by

$$A_3 = \frac{1}{3!} \tilde{A}_{3abc} dx^a \wedge dx^b \wedge dx^c + \frac{1}{2!} A_{2ab} dx^a \wedge dx^b \wedge d\theta. \quad (11.32)$$

As a result, the 3-form \tilde{A}_3 is *not* invariant under $A_1 \rightarrow A_1 + d\Lambda_0$ but instead transforms as $A_3 \rightarrow A_2 \wedge d\Lambda_0$. In addition, the gauge symmetry of the

eleven-dimensional A_3 implies that there are 9+1 gauge symmetries $A_3 \rightarrow A_3 + d\Lambda_2$ and $A_2 \rightarrow A_2 + d\Lambda_1$ where Λ_n are arbitrary n -forms. From here on we will drop the tilde on \tilde{A}_3 . The decomposition of the fermionic fields is similar, but we will not go into this in detail.

11.4.3 On 9+1 dynamics: here comes the dilaton

The dynamics for the 9+1 theory follows from that of eleven dimensions by insertion of the relations between the 9+1 fields and the 10+1 fields into the action. The result is an action principle for the 9+1 theory, which takes the form

$$\begin{aligned} S_{9+1, \text{bosonic}} = & \frac{1}{2\kappa_{10}^2} \int d^{10}x \sqrt{-g} (e^{2\phi/3} R - \frac{1}{2} e^{2\phi} |F_2|^2) \\ & - \frac{1}{4\kappa_{10}^2} \int d^{10}x \sqrt{-g} (e^{-2\phi/3} |F^2|_3 + e^{2\phi/3} |\tilde{F}_4|^2) \\ & - \frac{1}{4\kappa_{10}^2} \int A_2 \wedge F_4 \wedge F_4. \end{aligned} \quad (11.33)$$

Here all quantities refer to the (9+1)-dimensional fields and we have set $F_n = dA_{n-1}$ and $\tilde{F}_4 = dA_3 - A_1 \wedge F_3$. As opposed to F_4 itself, the new field strength \tilde{F}_4 is invariant under gauge transformations of the A_1 potential. We have also set $\kappa_{10}^2 = \kappa_{11}^2/L$.

An important feature of (11.33) is that the field ϕ appears in several places, with factors $e^{\alpha\phi}$ for different values of α appearing in different terms. The upshot is that the various gauge fields do not couple minimally to the metric g . Of course, we have the freedom to mix the metric with ϕ by rescaling it by some power of e^ϕ . This can be used to make any gauge field couple minimally to the new metric or to remove the factors involving e^ϕ in front of the scalar curvature term and put the action in a form more like that of familiar Einstein–Hilbert gravity. However, because different factors $e^{\alpha\phi}$ appear in the different terms, this cannot be done for all the fields at once. Thus, we may think of each different gauge field as coupling to a different metric.

A short calculation shows that the gauge fields F_2 and F_4 couple minimally to $e^{2\phi/3} g$ while the gauge field F_3 couples minimally to $e^{-\phi/3} g$. In doing this calculation it is important to realize that terms like $|F_2|^2$ contain implicit factors of the metric g (see 11.7), which has been used to contract the indices. However, it is for the “Einstein metric” $e^{\phi/6} g$ that the gravitational part of the action takes the standard Einstein–Hilbert form (the integral of the scalar curvature density) without any extra factors involving e^ϕ .

The choice of a particular metric in the class $e^{\alpha\phi}g$ is known as the choice of conformal frame. One can make a choice of frame that simplifies a given calculation, if one desires. It is interesting to note that in the conformal frame defined by (11.31) the field ϕ has no explicit kinetic term, so that its variation leads to a constraint. It turns out that this is just a combination of the usual constraints that one would expect in a gravitating theory and that a term of the form $\partial_a\partial^a\phi$ does appear in the equations of motion obtained by varying the metric in that frame.

The two most useful choices of conformal frame are the Einstein frame (defined by the Einstein metric $g_E = e^{\phi/6}g$ mentioned above) and the so-called string frame. The action in the Einstein frame is a handy thing to have on hand, so we will write it down here. If we now let g_E denote the metric in the Einstein frame and let R_E be the associated curvature, the action is given by

$$\begin{aligned} S_{\text{IIA,bosonic}} = & \frac{1}{2\kappa_{10}^2} \int d^{10}x \sqrt{-g_E} (R_E - \frac{1}{2}\partial_a\phi\partial^a\phi) \\ & - \frac{1}{4\kappa_{10}^2} \int d^{10}x \sqrt{-g_E} (e^{3\phi/2}|F_2|^2 + e^{-\phi}|F^2|_3 + e^{\phi/2}|\tilde{F}_4|^2) \\ & - \frac{1}{4\kappa_{10}^2} \int A_2 \wedge F_4 \wedge F_4. \end{aligned} \quad (11.34)$$

Note that in the Einstein frame the gauge fields are all sources for the dilaton but the metric is not. Also, since the kinetic term for the dilaton now takes the standard form we can see that the dilaton would be canonically normalized if we set $2\kappa_{10}^2$ to 1. Finally, since it is in this frame that the gravitational dynamics takes the familiar Einstein–Hilbert form, this is the frame in which the standard ADM formulas for energy and momentum may be applied and in which the entropy of black holes is given by $A/4$ in Planck units.

The string frame is defined by taking the metric to be $e^{2\phi/3}g$, where g is the original metric appearing in (11.31). Thus the string metric g_S and the Einstein metric g_E are related by $ds_E = e^{-\phi/2}ds_S$, and the action in the string frame takes the form

$$\begin{aligned} S_{\text{IIA,bosonic}} = & \frac{1}{2\kappa_{10}^2} \int d^{10}x \sqrt{-g_S} e^{-2\phi} (R_S + 4\partial_a\phi\partial^a\phi - \frac{1}{2}|F_3|^2) \\ & - \frac{1}{4\kappa_{10}^2} \int d^{10}x \sqrt{-g_S} (|F_2|^2 + |\tilde{F}_4|^2) \\ & - \frac{1}{4\kappa_{10}^2} \int A_2 \wedge F_4 \wedge F_4. \end{aligned} \quad (11.35)$$

After setting $c = \hbar = 1$, the parameter κ_{10}^2 has units of (length)⁸. It is useful to write $2\kappa_{10}^2 = (2\pi)^7 g_s^2 l_s^8$, where l_s is the “string length” and g_s is the “string coupling”. For more on the separate roles of g_s and l_s see section 11.6.

Note that two gauge fields (F_2 and F_4) couple minimally to the string metric g_S . These two gauge fields are known as Ramond–Ramond (R–R) gauge fields while F_3 is known as the Neveu–Schwarz Neveu–Schwarz (NS–NS) gauge field or sometimes just as the Neveu–Schwarz (NS) gauge field.¹⁶ For an explanation of how this terminology arose in string perturbation theory, see e.g. [5–7, 9]. The potential A_2 for this field is commonly written as B_2 (and its field strength F_3 is written as H_3) and, when string theorists discuss “the B -field,” it is this potential to which they are referring.

What makes the string metric especially useful is that it turns out to be the metric to which fundamental strings (which we have not yet discussed) couple minimally, and thus in which one makes the most direct contact with string perturbation theory. We cannot pursue this point further here.

In the above we have discussed only the compactification of eleven-dimensional supergravity on a circle. One can, of course, consider further compactifications to smaller-dimensional manifolds. The story in that case is much the same except that the number of lower-dimensional fields generated increases rapidly. In particular, further compactification generates large numbers of massless scalars, which couple nonminimally to the various gauge fields. These cousins of the dilaton are generally referred to as *moduli*.

All these moduli have a tendency to diverge at the horizon of an extreme black hole, making the solution singular. One may think of the situation as follows: the moduli, like the dilaton, couple to the gauge fields, so that the squared field strengths F^2 act as sources. This can be seen from the action (11.34) in the Einstein frame. Nonsingular extremal black hole solutions typically have an infinite throat, as in the four- and five-dimensional Einstein–Maxwell examples discussed earlier. This means that a smooth such solution would have an infinite volume of space near the horizon in which the gauge field strengths are approximately constant. Unless these gauge fields are tuned to have $F^2 = 0$, or the various gauge fields are somehow played off against one another, this provides an infinite source for the moduli. As a result, smooth solutions are obtained only when the charges of the black hole are such that the potential for the moduli provided by the various F^2 terms has a stationary point. In the spacetime solution, the moduli then approach this stationary point as one approaches the horizon. This phenomenon is known as the attractor mechanism for extreme black holes; see e.g. [52–55, 59–61]. As a result of this effect some care is required in constructing an extremal black hole solution with a smooth horizon, and such solutions necessarily carry more than one charge. For a brane solution, the norm of each spacelike Killing field acts like

¹⁶ In a confusing piece of terminology, it is sometimes also called the Kalb–Ramond gauge field.

a modulus whose sources must be properly tuned (as the norm would define a new dilaton-like scalar under further Kaluza–Klein reduction).

This is essentially the issue encountered at the end of section 11.3.3, where it was found that three charges (in that case, three different types of M2-brane) were required to obtain a brane solution in which the norms of the spacelike Killing fields do not vanish on the horizon. Recall that a Killing field with positive norm allows us to Kaluza–Klein-reduce the spacetime to a solution of lower-dimensional supergravity. Because the three-charge solution (11.26) has six Killing vector fields whose norms do not vanish on the horizon, it may be reduced all the way down to a solution of 4+1 gravity. In this context, it represents an extreme black *hole*. In fact, it reduces to just the standard 5+1 extremal black hole (11.20) of Einstein–Maxwell theory.

It should be noted that the theory discussed above is far from the only supergravity theory in ten dimensions. It is a particular kind called type IIA, originally constructed in [59–61]. The “II” refers to the fact that there are two independent gravitino fields; as a result, the number of supercharges is equal to that in two ten-dimensional spinors. Each ten-dimensional spinor has 16 components, so this theory is maximally supersymmetric, just like the eleven-dimensional theory. In type IIA theory these gravitinos have opposite chirality. This in turn allows type IIA theory to be defined even on nonorientable manifolds. There is also a type IIB theory, which also has two gravitinos (and is thus also maximally supersymmetric) but of the same chirality. Thus, type IIB theory can only be defined on manifolds with a global notion of chirality and, in particular, only on orientable spacetimes. We will discuss type IIB theory further in section 11.5.3 below. Two other supergravity theories with less supersymmetry (only 16 supercharges) are known as the type I and heterotic theories. Each type of supergravity in ten dimensions is associated with its own version of string theory. We will not discuss type I or heterotic supergravity here, but discussions of these theories and how they are related to the type II theories can be found in [5–9].

11.5 Branes in 9+1 type II supergravity

We will now discuss the basic brane solutions of type II supergravity in 9+1 dimensions. Since any solution of type IIA theory is really a solution of eleven-dimensional supergravity in disguise, any brane solution of type IIA theory immediately defines a brane solution of eleven-dimensional supergravity. Thus, we should be able to construct the basic brane solutions of type IIA theory by working with the basic brane solutions of section 11.3.2. For this reason we address the type

IIA solutions first, in section 11.5.1. Next follows a short aside on brane singularities in section 11.5.2. We then briefly discuss type IIB supergravity and its relation, through so-called T-duality with the type IIA theory, in section 11.5.3. In what follows, we will discuss only branes that become BPS in the extreme limit, although intrinsically non-BPS D-branes can also be of interest (see e.g. [62–68]).

11.5.1 Type IIA branes

In our decomposition of the eleven-dimensional metric and gauge field into the various fields of ten-dimensional supergravity, we proceeded by projecting the fields along directions both parallel and transverse to the Kaluza–Klein Killing field λ^μ . In order to get brane solutions of type IIA theory that are charged under all the type IIA gauge fields, a similar operation will need to be performed on the eleven-dimensional branes. For any given brane in eleven dimensions, we will need to reduce both a basic brane solution in which the Killing field acts along the brane (i.e., is a symmetry of the brane) and one in which it acts transversely to the basic brane.

One may at first wonder what it means for the brane to be transverse to the Killing field, since translations along a Killing field must leave the solution invariant and therefore must preserve the brane. The answer to this puzzle is the smearing mentioned in section 11.3.3. One can take a basic brane solution, pick a direction transverse to the brane, smear the brane in that direction, and then reduce to 9+1 dimensions along the smearing direction.

Performing the required reductions amounts to no more than using the relations between the 9+1 fields and the 10+1 fields given in section 11.4 to write down the 9+1 solutions from the branes given in section 11.3.2. We leave the details of the calculations to the reader but we provide a list here of the various 9+1 brane solutions. Below, we group together those branes charged under the Ramond–Ramond gauge fields and those charged under the NS–NS gauge fields. This grouping is natural from the point of view of the type IIA theory (and of string perturbation theory), though we will see that it is somewhat less natural from the eleven-dimensional point of view.

Let us begin with the Ramond–Ramond branes. It turns out that the type IIA theory has p -brane solutions, with Ramond–Ramond charge, for every even p . What is very nice is that, in terms of the string metric, all these solutions take much the same simple form. In order to treat all the branes at once, it is useful to introduce a uniform notation for both electrically and magnetically charged branes. For each gauge field A_n we can introduce (at least locally) a magnetic dual gauge

field A_{9-n} through¹⁷ $dA_{8-n} = \star F_{n+1}$. A brane that couples magnetically to A_n then couples electrically to A_{9-n} , and vice versa. In type IIA theory this notation should introduce no confusion, as the standard gauge fields have $n = 1, 2, 3$ while these new (dual) gauge fields have $n = 5, 6, 7$.

Introducing the usual set of $p + 1$ coordinates x_{\parallel} along the brane and $9 - p$ coordinates x_{\perp} transverse to the brane we have, for all even p ,

$$\begin{aligned} ds_{\text{string}}^2 &= H_p^{-1/2} dx_{\parallel}^2 + H_p^{1/2} dx_{\perp}^2, \\ A_{p+1} &= H_p^{-1} dx_{\parallel}^0 \wedge \cdots \wedge dx_{\parallel}^p, \\ e^{2\phi} &= H_p^{(3-p)/2}, \end{aligned} \quad (11.36)$$

where H_p is a function only of the x_{\perp} coordinates and satisfies

$$\partial_{\perp}^2 H_p = -(7-p)\Omega_{8-p} r_0^{7-p} \delta^{(9-p)}(x_{\perp}) \quad (11.37)$$

for the basic brane solution. Here Ω_{8-p} is the volume of the unit $(8-p)$ -sphere and r_0 is a length scale parameterizing the strength of the source. These solutions are known as extreme R-R p -branes or, in a slight abuse of language, as (extreme) D p -branes, where the notation ‘‘D’’ comes from the way in which these objects are described in string perturbation theory (where they are associated with Dirichlet boundary conditions for strings; see section 11.6.2). As usual, we can also obtain a solution by considering more general source terms on the right-hand side of (11.37). For odd p there are no gauge fields A_{p+1} in type IIA supergravity, so (11.36) does not yield a solution to this theory for such cases.¹⁸

Let us briefly mention that the nonextreme R-R brane solutions (for $p \leq 6$) take the rather simple form [69]

$$\begin{aligned} ds_{\text{string}}^2 &= H_p^{-1/2} \left(-fdt^2 + \sum_{i=1}^p (dx_{\parallel}^i)^2 \right) + H_p^{1/2} \left(\frac{dr^2}{f} + r^2 d\Omega_{8-p}^2 \right), \\ A_{p+1} &= [1 + \coth \beta (H_p^{-1} - 1)] dx_{\parallel}^0 \wedge \cdots \wedge dx_{\parallel}^p, \\ e^{2\phi} &= H_p^{(3-p)/2}, \end{aligned} \quad (11.38)$$

where

$$H_p = 1 + \frac{\sinh^2 \beta r_+^{7-p}}{r^{7-p}}, \quad f = 1 - \frac{r_+^{7-p}}{r^{7-p}}, \quad (11.39)$$

¹⁷ Here we again ignore the Chern–Simons terms, which modify and complicate this simple uniform expression. As usual, this suffices for the solutions to be discussed below.

¹⁸ One might also ask about the case $p = 8$, since we have not discussed a 9-form gauge potential. It turns out that there is in fact a Ramond–Ramond 8-brane in type IIA theory and that its existence is tied to the Chern–Simons term in the type IIA action. In this work, we follow a policy of considering only the asymptotically flat brane solutions, which restricts us to branes of codimension 3 or higher; i.e., to $p \leq 6$ in ten-dimensions.

and r_+ , β specify the charge Q , mass M per unit p -volume V_p , temperature T , and entropy density S/V_p , through

$$\begin{aligned} Q &= \frac{(7-p)\Omega_{8-p}}{2\kappa_{10}^2} r_+^{7-p} \sinh \beta \cosh \beta, \\ \frac{M}{V_p} &= \frac{(8-p)\Omega_{8-p} r_+^{7-p}}{2\kappa_{10}^2} \left(1 + \frac{7-p}{8-p} \sinh^2 \beta \right), \\ T &= \frac{7-p}{4\pi r_+ \cosh \beta}, \\ \frac{S}{V_p} &= \frac{4\pi \Omega_{8-p}}{2\kappa^2} \cosh \beta r_+^{(8-p)}. \end{aligned} \quad (11.40)$$

In particular, the extremal limit is $\beta \rightarrow \infty$, $r_+ \rightarrow 0$ with M/V_p fixed, so that $M/V_p \rightarrow Q$ and $S \rightarrow 0$. For $p < 5$ the temperature also vanishes in the extremal limit. However, for $p = 5$, T remains nonzero, and for $p = 6$ it diverges. Here we allow only a single brane (which is analogous to having a single delta-function source in (11.37)), as nonextremal branes attract each other and solutions with more than one such brane are not stationary. As for the M-branes, their global structure, (11.38), is like that of the Schwarzschild solution as opposed to that of nonextremal Reissner–Nordström.

Although all these R-R branes take the same simple form (11.36), they proceed by quite different routes from those taken by the eleven-dimensional branes. A short list follows. The D0-brane solution follows by reducing the smeared Aichelberg–Sexl metric along the smearing direction. The D2-brane follows by reducing the smeared M2-brane along the smearing direction. The D4-brane is the reduction of the unsmeared M5-brane in a direction along the brane. Finally, the D6-brane is the reduction of the unsmeared Kaluza–Klein monopole along the S^1 fibers.

Next, there are the Neveu–Schwarz branes. Since the only Neveu–Schwarz gauge field is A_2 , we expect to find two types of Neveu–Schwarz brane. The gauge field A_2 should couple electrically to a 1-brane (a string) and it should couple magnetically to a 5-brane. The 1-brane follows by reducing the M2-brane in a direction along the brane. The resulting solution,

$$\begin{aligned} ds_{\text{string}}^2 &= H_F^{-1} dx_{\parallel}^2 + dx_{\perp}^2, \\ A_2 &= H_F^{-1} dx_{\parallel}^0 \wedge dx_{\parallel}^1, \\ e^{2\phi} &= H_F^{-1}, \end{aligned} \quad (11.41)$$

is known as the *fundamental string*. The reason for this is that this solution represents the classical limit of a long straight version of the same string as that appearing in string perturbation theory.

The Neveu–Schwarz 5-brane (NS5-brane) is constructed by smearing the M5-brane in a transverse direction and then reducing along the smearing direction. The result is

$$\begin{aligned} ds_{\text{string}}^2 &= dx_{\parallel}^2 + H_5 dx_{\perp}^2, \\ F_3 &= -\frac{1}{3!} \partial_{x_{\perp}^i} H_5 \epsilon_{ijkl} dx_{\perp}^j \wedge dx_{\perp}^k \wedge dx_{\perp}^l, \\ e^{2\phi} &= H_5. \end{aligned} \quad (11.42)$$

An interesting property of the NS5-brane is that, in the string metric, the timelike Killing field has no horizon; its norm is constant across the spacetime. What would have been the horizon at $x_{\perp} = 0$ has receded to infinite proper distance in all directions, not just along a Killing slice as for the extreme Reissner–Nordström black hole. As a result, the coordinate patch discussed above actually covers a manifold that, in the string frame, is geodesically complete.¹⁹

Finally, there are the purely gravitational “branes” given by the 9+1 versions of the Aichelburg–Sexl metric and of the Kaluza–Klein monopole with all gauge fields set to zero and a constant dilaton. These may be either written down directly by analogy with (11.23) and (11.24) or constructed by reducing the 10+1 solutions to 9+1 dimensions (and first smearing the Aichelburg–Sexl metric in some x_{\perp} direction).

This exhausts the possible ways to make extremal 9+1 branes by reducing (and perhaps smearing once) the basic eleven-dimensional branes. Below, we provide a few words on their global structure and singularities.

11.5.2 Brane singularities

We have constructed the D-brane spacetimes from what (in most cases) are smooth eleven-dimensional solutions (at least outside some horizon). However, the reduced solutions contain new singularities. Of the 9+1 branes, only the NS 5-brane does not have a naked singularity.²⁰ For the D4- and D6-branes and the fundamental string, this happens because the Killing field used in the reduction has fixed points, so that $\lambda^{\mu} \lambda_{\mu}$ and thus e^{ϕ} vanish (and $\phi \rightarrow -\infty$).

For the D6-brane, the (6+1)-plane of fixed points at $x_{\perp} = 0$ is manifest in (11.24) and results in a (6+1)-dimensional timelike singularity in the (9+1)-dimensional

¹⁹ However, it is not geodesically complete either in the Einstein frame or as viewed from the eleven-dimensional perspective. In each of these cases there is a null singularity at the horizon.

²⁰ This statement refers to the metric in the string frame. In the Einstein frame there is a naked singularity on the horizon. Its story is much like that of the D2-brane to be discussed below.

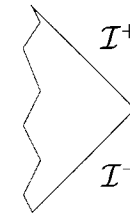


Figure 11.5 Conformal diagram for the extreme D6-brane.

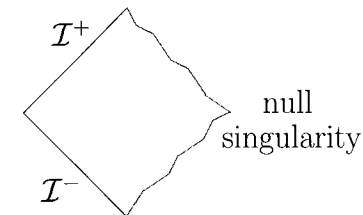


Figure 11.6 Conformal diagram for the extreme D4-brane or the fundamental string.

D6-brane solution. The conformal diagram for the D6-brane is therefore the one given in Fig. 11.5.

Turning to the D4-brane, the fixed points of the Kaluza–Klein Killing field in the compactified M5-brane solution are found less obviously from (11.22) but were briefly discussed in section 11.3.2. There we saw that the fixed-point set consisted of certain horizon generators and so defined a null plane. As a result, the singularity of the D4-brane is null and lies on the would-be horizon. Because $\phi \rightarrow -\infty$, in terms of the 9+1 metric this turns out to be a (null) curvature singularity. The story of the fundamental string is much the same. See Fig. 11.6 for both.

Let us now consider the D2-brane solution, which is the reduction of a smeared M2-brane. Although smearing the M2-brane in a transverse direction makes the horizon of the eleven-dimensional solution singular, one may take the perspective that the smeared solution represents the approximate solution for an array of M2-branes for which the length scale associated with the charge of each brane is much larger than the spacing between the branes. In this case one interprets the D2-brane horizon as being nonsingular²¹ from the eleven-dimensional point of view. However, from the 9+1 perspective we clearly have $\phi \rightarrow +\infty$ on the horizon. The metric (11.36) with $p = 2$ also has a null curvature singularity on the horizon, though all curvature scalars are finite. The simplest way to detect the singularity

²¹ Actually, as consisting of many separate nonsingular horizons.

from the metric (11.36) is to note that the spheres around the brane shrink to zero size at the horizon so that, if the solution were smooth then the horizon could have only a single null generator, which is impossible. Thus the conformal diagram of the 9+1 D2-brane solution is again given by Fig. 11.6.

With an eleven-dimensional perspective in mind, the singularities of the D2-, D4-, and D6-brane solutions might not be considered especially troubling. Nevertheless, from the 9+1 perspective the singularities are quite real and represent places where the 9+1 equations of motion break down. Let us recall that the Aichelberg–Sexl metric (the lift of the D0-brane solution to eleven dimensions) is singular and should be thought of as describing the approximate field produced by some “source.” For the Aichelberg–Sexl metric, one may think of this source as being a short-wavelength graviton; the solution (11.23) itself represents just the Coulomb part of the field. Similarly, looking at the way in which the D-brane singularities interact with the equations of motion through (11.37), it is natural to think of the singularities as representing bits of matter, like a braney form of extremal dust, that are coupled to the supergravity. It should be noted that this dual perspective of thinking of branes either as solitonic objects intrinsic to some basic version of the theory (such as supergravity or string theory) or as external objects or sources coupled to such a theory is pervasive in string/M theory.

11.5.3 The type IIB theory and S- and T-dualities

The other type of maximally supersymmetric gravity theory in 9+1 dimensions is called type IIB theory (originally constructed in [70–72]). It is not given by the dimensional reduction of a 10+1 theory though it has many of the same properties as the type IIA theory. For example, both theories consist of a metric, a dilaton, and a B_2 -field (which together form the so-called Neveu–Schwarz sector of the theory), together with various Ramond–Ramond gauge fields. The theories are identical in the Neveu–Schwarz sectors, so that the Aichelberg–Sexl, fundamental-string, NS5-brane, and Kaluza–Klein-monopole solutions are the same in both cases. The main difference is that while IIA supergravity has (electric and magnetic) Ramond–Ramond gauge fields A_p of every odd rank, the type IIB theory has Ramond–Ramond gauge fields A_p of every even rank. As in IIA, the Ramond–Ramond fields are minimally coupled to the string-frame metric. As a result, the Dp -brane solutions in IIB are again given by (11.36) though now p is odd; that is, the IIB theory has D1-, D3-, D5-, D7-, and D9-branes.²²

The D3-brane has particularly noteworthy features. Since the Ramond–Ramond fields are minimally coupled in the string frame, the kinetic term of A_4 is of the form $\sqrt{-g_S}|F_5|^2$. Note that this term is conformally invariant in ten dimensions (just as the usual Maxwell kinetic term $\sqrt{-g}|F_2|^2$ is conformally invariant in four dimensions). As a result, A_4 remains minimally coupled in any conformal frame and in particular in the Einstein frame, where the kinetic terms of the graviton and the dilaton are diagonal. Thus, in contrast with all other IIB gauge fields, the 5-form F_5 does not act as a source for the dilaton! Indeed, consulting (11.36) one finds that $\phi = \text{constant}$ for $p = 3$. As a result the D3-brane has a smooth horizon. In fact the solution is very similar to that of the M5-brane, having the same singularity-free conformal diagram (Fig. 11.4). The near-horizon geometry is $\text{AdS}_5 \times S^5$.

Clearly the D3-brane is the marginal case that separates Dp -branes with $p < 3$ from those with $p > 3$. As one might expect, the D1 (and D(−1)) solution resembles that of the IIA D0, D2 solutions (with a null singularity where $\phi \rightarrow +\infty$), while the D5 resembles the D4 (with a null singularity where the Ricci scalar diverges). Branes with large values of p ($p = 7, 9$) are special cases, which we ignore here as they are not asymptotically flat.

To understand fully the relations between the various brane solutions it is important to understand certain symmetries known as S- and T-duality. We begin with S-duality, which is a symmetry of IIB supergravity alone. To study this symmetry, it is useful to define a complex scalar $\tau = A_0 + i e^{-\phi}$, a 2×2 matrix

$$\mathcal{M}_{ij} = \frac{1}{\text{Im } \tau} \begin{bmatrix} |\tau|^2 & -\text{Re } \tau \\ -\text{Re } \tau & 1 \end{bmatrix},$$

and a vector of 2-form potentials

$$A_2^i = \begin{bmatrix} B_2 \\ A_2 \end{bmatrix},$$

where the Neveu–Schwarz gauge field is denoted B_2 (with field strength H_3) to distinguish it from the Ramond–Ramond gauge field A_2 (with field strength F_3). In terms of these fields the Einstein-frame action²³ takes the form [7]

$$S_{\text{IIB, bosonic}} = \frac{1}{2\kappa_{10}^2} \int d^{10}x \sqrt{-g_E} (R_E - \frac{1}{12} F_{abc}^i \mathcal{M}_{ij} F^{jabc} + \frac{1}{4} (\partial^a \mathcal{M}_{ij} \partial_a \mathcal{M}^{-1ij})) - \frac{1}{8\kappa_{10}^2} \int d^{10}x \sqrt{-g_S} |\tilde{F}_5|^2 - \frac{1}{4\kappa_{10}^2} \int A_4 \wedge H_3 \wedge F_3, \quad (11.43)$$

where $F_3^i = \frac{1}{3!} F_{abc}^i dx^a \wedge dx^b \wedge dx^c = dA_2^i$ and $\tilde{F}_5 = F_5 + \frac{1}{2} \epsilon_{ij} A_2^i \wedge F_3^j$ with ϵ_{ij} antisymmetric and $\epsilon_{12} = 1$.

²² If one is interested in Euclidean solutions then it also makes sense to consider D(−1)-branes (D-instantons) in the IIB theory.

²³ The equations of motion that follow from this action must be supplemented by the constraint that the 5-form $F_5 = dA_4$ is self-dual, i.e., that $\star F_5 = F_5$.

The action (11.43) makes manifest an invariance under the $SL(2, \mathbb{R})$ symmetry

$$\tau \rightarrow \frac{a\tau + b}{c\tau + d}, \quad F_3^i \rightarrow \Lambda_j^i F_3^j, \quad \tilde{F}_5 \rightarrow \tilde{F}_5, \quad g_E \rightarrow g_E, \quad (11.44)$$

for

$$\Lambda_j^i = \begin{bmatrix} d & c \\ b & a \end{bmatrix}$$

with $\det \Lambda = 1$. The transformation with

$$\Lambda_j^i = \begin{bmatrix} 0 & 1 \\ -1 & 0 \end{bmatrix}$$

is of particular interest and gives rise to what is known as S-duality. For solutions with $A_0 = 0$ it acts as $\phi \rightarrow -\phi$ and interchanges F_3 and H_3 . As a result, it maps D1-branes to fundamental strings and maps D5-branes to NS5-branes (and vice versa). However, it leaves the D3-brane and all purely gravitational branes invariant.

Finally, we turn to T-duality, which is a symmetry that relates the full type IIA and type IIB string theories. At the level of supergravity, this is a symmetry that maps solutions of type IIA theory with a Killing field into solutions of type IIB theory with a Killing field. It appears that T-duality is an exact symmetry of the underlying string/M theory even with no Killing field, but then it maps a nearly classical spacetime into a complicated highly quantum mechanical state.

It is useful first to write down the explicit action of T-duality on the metric and Neveu–Schwarz fields. Let us introduce a coordinate z such that translations in z have Killing symmetry. Let x^α be any other collection of coordinates that makes (z, x^α) a coordinate patch. Again writing the antisymmetric Neveu–Schwarz field as B_2 instead of A_2 , if the original solution is (g, B) then the transformed solution (\tilde{g}, \tilde{B}) is given [73, 74] by

$$\begin{aligned} \tilde{g}_{zz} &= 1/g_{zz}, & \tilde{g}_{z\alpha} &= B_{z\alpha}/g_{zz}, & \tilde{g}_{\alpha\beta} &= g_{\alpha\beta} - (g_{z\alpha}g_{z\beta} - B_{z\alpha}B_{z\beta})/g_{zz}, \\ \tilde{B}_{z\alpha} &= g_{z\alpha}/g_{zz}, & \tilde{B}_{\alpha\beta} &= B_{\alpha\beta} - (g_{z\alpha}B_{\beta z} - g_{z\beta}B_{\alpha z})/g_{zz}, \\ \tilde{\phi} &= \phi + \log g_{zz}. \end{aligned} \quad (11.45)$$

Note that T-duality essentially interchanges the $g_{z\alpha}$ part of the metric with the $B_{z\alpha}$ part of the gauge field.²⁴ Now, in the asymptotically flat context, the g_{z0} component of the metric is associated with momentum in the z direction while the B_{z0} component of the gauge field is associated with electrically charged strings

²⁴ In fact, in the case where the z direction is compactified into an S^1 , (11.45) can be described geometrically by noting that the Kaluza–Klein reduction to 8+1 dimensions has two 1-form gauge fields, one from the ten-dimensional metric and one from the ten-dimensional field B_2 . In the Neveu–Schwarz sector, T-duality simply interchanges the two circle bundles associated with these gauge fields.

that extend in the z direction. Thus one finds [75] that T-duality interchanges momentum and charge and in particular maps the (one-smeared) Aichelburg–Sexl solutions to fundamental string solutions (which carry the electric charge to which B couples).

Strictly speaking, the T-duality of string theory requires a Killing field with compact (S^1) orbits, though (11.45) maps solutions to solutions even if the orbits are noncompact. The original spacetime should be asymptotically Kaluza–Klein and, if the original z coordinate is identified to be such that the length of the S^1 at infinity is L , the z coordinate of the transformed spacetime should be identified such that the length of the S^1 at infinity is $4\pi^2 l_s^2/L$. The point is that if the orbits of the Killing field are compact then quantum mechanics implies that the momentum component around the compact direction is quantized. Proper normalization then guarantees that T-duality takes a solution with one quantum of momentum to a solution containing a single fundamental string.

The effect of T-duality on the Ramond–Ramond fields is as follows:

$$\begin{aligned} \tilde{F}_{n,\alpha_1\dots\alpha_n} &= (\text{const})F_{n+1,z\alpha_1\dots\alpha_n}, \\ \tilde{F}_{n,z\alpha_1\dots\alpha_{n-1}} &= (\text{const})F_{n-1,\alpha_1\dots\alpha_{n-1}}. \end{aligned} \quad (11.46)$$

Thus, if one takes a Dp -brane and T-dualizes in some direction along the brane, one obtains a $D(p-1)$ -brane solution that is smeared along the T-duality direction. In string theory D -brane charge is quantized. The normalization constants in (11.46) are chosen so that the transformed solution has one unit of $D(p-1)$ -brane charge when the original solution has one unit of Dp -brane charge. Similarly, if one smears a unit charge Dp -brane solution in a transverse direction, keeping the total charge equal to one quantum, then the T-dual solution is a unit charge $D(p+1)$ -brane. See [5–9] for a discussion of D -brane tensions, charge quantization, etc. In any given direction one may check that the T-duality transformation squares to the identity.

11.6 Some remarks on string perturbation theory

In the preceding sections we have discussed the supergravity aspects of various string-theoretic branes, including D-branes. However, the real power of D-branes, and thus their importance, stems from the fact that there is a renormalizable (in fact, order-by-order finite) quantum perturbation theory to complement the classical supergravity description. This perturbation theory describes both the internal dynamics of D-branes and also their interactions with the supergravity fields. In particular, it is the key to the famous counting of states of BPS and near-BPS black holes. Thus, although we will not discuss the details, it is worthwhile to say a few

words here about this perturbation theory. We hope this gives a useful complement to standard presentations, which concentrate more on the perturbation theory details.

11.6.1 Background field expansions and perturbative string theory

A useful framework from which to view string perturbation theory is that of the background field expansion (see e.g. [76]). Let us first review this idea in the context of standard quantum field theory. For definiteness, the reader may choose to focus on a familiar low-dimensional interacting scalar field theory or on even quantum mechanics. We will use ϕ to denote the scalar field or, more generally, as a schematic notation for the collection of all relevant fields.

Let us begin by supposing that there is some complete quantum theory of this field, consisting of a set of field operators $\hat{\phi}(x)$ and an associated set of composite operators acting on a Hilbert space. Exact calculations for interacting quantum field theories are seldom possible, and one must resort to various approximation schemes and expansions in small parameters in order to obtain results. For situations where the field is nearly in its vacuum state, standard perturbation theory (see e.g. [77, 78]) can be a useful technique.

However, this is not the only case of interest. For example, it may be that a laboratory device (or a star, black hole, or astrophysical event) produces a large, essentially classical, disturbance in the field ϕ and that one wishes to study small quantum effects in the resulting behavior. It is in such a regime that background field methods are useful. One first considers the solution ϕ_0 to the classical field equations that would describe the situation if \hbar were set to zero. One then rewrites the theory in terms of the field $\widehat{\delta_0\phi}(x) = \hat{\phi}(x) - \phi_0(x)$. Assuming that there is in fact a set of semiclassical states in which the expectation value of $\hat{\phi}(x)$ is close to $\phi_0(x)$ and in which the fluctuations are “small,” it makes sense to attempt a perturbative treatment in terms of the field $\widehat{\delta_0\phi}$.

This is the basic idea behind the background field expansion. However, there is an additional subtlety. Although one expects any differences to vanish as $\hbar \rightarrow 0$, there need not be any state in which the expectation value of $\hat{\phi}(x)$ is exactly $\phi_0(x)$. In a perturbative framework, one assumes that the difference between the actual expectation value and the classical solution ϕ_0 can be expanded in powers of \hbar and simply solves for it at each order of perturbation theory. It is useful to take the expectation value calculated at order n , which we write as $\overline{\phi}_n$, to be an effective “classical field” and to work at order n with the perturbation $\widehat{\delta_n\phi} = \phi(x) - \overline{\phi}_n$.

Within the range of validity of this perturbation theory, one can ([76]) expand about a general classical solution ϕ_0 and obtain, at order n in perturbation theory, an

“effective action” for the “effective classical background field” $\overline{\phi}$. The variations of the effective action with respect to the effective field yield the classical equations of motion for ϕ , corrected by terms of up to order n in \hbar such that the solutions of these equations yield the expectation value of $\hat{\phi}(x)$ (to order n) in a semiclassical state.

One could also attempt to follow the same general framework but to expand around some arbitrary field ϕ_0 that is not a solution of the classical equations of motion. In this case the field $\widehat{\delta_0\phi}(x)$ is not small and the perturbation theory will not contain anything like a stable vacuum. Because the variation of the action does not vanish at the chosen background the action contains a term linear in $\widehat{\delta_0\phi}(x)$ that acts as a source. This typically leads to various infrared divergences in the perturbation theory since, when integrated over all time, this source will produce an infinite number of particles. Thus if, for some reason, someone had handed us not the full classical dynamics of the field but only the equations of the perturbation theory around an arbitrary background then the classical solutions of the theory would still be recognizable.

String perturbation theory is in fact a version of background field theory in which the “strings” correspond to excitations of the field $\widehat{\delta_0\phi}(x)$. However, the logical order of the background field framework is reversed or, perhaps more accurately, turned inside out. Instead of starting with a classical theory, quantizing, and performing the background field expansion, one instead postulates a perturbative expansion²⁵ about any background field and then reconstructs the “classical” dynamics of the background field, in the manner discussed above, from the condition that the perturbation theory is well defined.

This seemingly odd logical structure makes more sense when one recalls that string theory is not, at present, a complete theory based on any particular set of fundamental principles or axioms. Rather, it is an accidentally discovered set of self-consistent mathematical phenomena related to quantum gravity, the unification of forces, and so on. The way in which string perturbation theory arose historically was through interest in QCD and possible “strings” of gauge field flux that would connect the quarks in hadrons. In the course of the study of such strings, it was discovered that they defined a perturbation theory which was finite order by order and which contained a spin-2 particle that could be interpreted as a graviton. Since finding a perturbative treatment of quantum gravity, or even constructing a new theory of gravity that could be treated perturbatively, had been a question of interest for some time, string theory presented a solution to this technical problem, as follows. Simply take this accidentally discovered perturbation theory and use it to construct an associated theory of quantum (and classical) gravity. In the case

²⁵ More accurately, the S-matrix corresponding to such an expansion.

of string theory, the postulated perturbation theory was used to construct not only the classical dynamics of the various fields, but also to deduce the classical field content itself. The rest, as they say, is history.

Our story of supergravity discussed in the previous sections is relevant here because the dynamics of string theory reduces in a certain limit to classical supergravity. A few finer points are worth mentioning briefly. The first is that, when viewed as a background field theory of the sort just discussed, classical string theory actually contains not only the fields of classical supergravity but also an infinite tower of massive fields. The masses of these *classical* fields are, however, of order l_s^{-1} (and therefore considered to be large). Thus, one expects there to be a large regime in which these fields are not independently excited. Instead, the heavy (massive) fields are “locked” to the values of the massless fields. At the extreme end of this regime the massive fields are completely irrelevant. However, as one pushes toward the boundaries of this regime the massive fields may still have some effect on the dynamics. If one solves the classical equations of motion for the heavy fields, one finds that they are disturbed slightly by the massless fields and then in turn provide small sources for the massless fields. This analysis, known in path integral terminology as “integrating out” the massive fields, leads to additional effective interactions between the massless fields. Such interactions are nonlocal, on a scale set by the masses of the heavy fields, i.e., on the scale of the string length. When expanded in a power series they lead to a series of higher-derivative terms in the action, suppressed by powers of the string scale. These are the so-called α' -corrections, where $\alpha' \propto l_s^2$.

In this way the string scale appears explicitly in the dynamics of classical string theory. Now, it is true that in the “real world” the string length is likely to be within a few orders of magnitude of the Planck scale. In principle, however, the two scales are completely independent and should not be confused. The string scale controls the corrections to classical supergravity caused by the tower of massive fields and the 9+1 Planck scale is the true quantum scale. Their ratio defines the string coupling g_s . The regime in which string perturbation theory is useful is $g_s \ll 1$, in which the string length is much greater than the 9+1 Planck length.

11.6.2 Strings and D-branes

In order to describe how D-branes fit into this picture, we should say just a few more words about the relation of strings to supergravity. As mentioned above, strings provide rules for constructing the perturbation theory about a given 9+1 supergravity background. Roughly speaking, one replaces the Feynman diagrams (related to particles) of familiar perturbation theory with a new sort of diagram

related to strings. For details, the reader should consult [4–9]. For our purposes below, it will mostly suffice to think about the strings as classical objects.

One can conceive of two basic types of string. The first are the so-called closed strings, which at any moment of time have the topology S^1 and resemble a classical rubber band. It turns out that closed strings define a consistent perturbation theory in and of themselves and that it is this case that leads to the type II supergravities on which we have focused. Another version of the closed string leads to heterotic supergravity, which has half as much supersymmetry as the type II theories.

One might also consider so-called open strings, which, at any instant of time, have the topology of an interval. In order for the dynamics of such strings to be well defined one must specify boundary conditions at the ends. A natural choice is to impose Neumann boundary conditions to describe free ends. Such strings are similar to classical rubber bands that have been cut open. It turns out that this type of string does not yield a consistent perturbation theory by itself, as two open strings can join together to produce a closed string. When open and closed strings are taken together, a consistent perturbation theory does result. This theory is associated with type I supergravity, having half as much supersymmetry as the type II theories.

The other type of boundary condition that one can impose at the end of a string is the Dirichlet boundary condition, requiring the end of the string to remain fixed at some point in space. One can also consider a mixture of Dirichlet and Neumann boundary conditions, insisting that the end of the string remains attached to some submanifold of spacetime but is otherwise free to roam around the surface. Surfaces associated with such Dirichlet boundary conditions are known as Dirichlet submanifolds, or D-branes. Again, for a consistent perturbation theory one must consider closed strings in addition to these open strings. Since we have singled out this submanifold as a special place in the spacetime, such a perturbation theory should not describe an expansion about empty space. However, there remains the possibility that it can describe an expansion about a background in which certain submanifolds are picked out as special, i.e., a background that includes certain brane-like features. Recall that, as a background field expansion, this perturbation theory should tell us about all the dynamics of the background, including any dynamics of the branes.

To make a long story short, it turns out that the Dirichlet submanifolds are sources of the Ramond–Ramond gauge fields and of the gravitational field. That is, they carry both stress–energy and Ramond–Ramond charge. Thus one might expect that they have something to do with the branes, discussed earlier, that carry Ramond–Ramond charge. In fact, this D-brane perturbation theory is intended to give an expansion about a background that includes such a charged gravitating R–R brane in the regime of asymptotically small string coupling g_s , the coupling

that controls the strength of all interactions. The perturbation theory describes both the dynamics of the bulk fields (roughly speaking, through the closed strings) and of the brane itself (roughly speaking, through the open strings). The two parts are coupled and interact.

Let us briefly comment on how this picture meshes with the supergravity point of view. To do so, we must consider the strength of the above-mentioned interaction. This is determined by the source provided by the brane for the various supergravity fields. However, a simple brane has only one charge, which is necessarily equal to its mass per unit volume if the brane is BPS. As a result, the strength of the source is governed by GT , where $16\pi G = 2\kappa_{10}^2 = (2\pi)^7 g_s^2 l_s^8$ and T is the brane tension.

Now, in string theory, as in any theory with both electric and magnetic charges, the charge (and thus T for BPS branes) is quantized in integer multiples of some fundamental unit. It turns out that on the one hand the charge of any R–R brane (with n units of charge) is proportional to n/g_s . Thus, $GT \sim ng_s$ goes to zero at weak coupling. As a result, the supergravity fields go over to flat empty space in this limit and the field generated by a fixed number n of such branes is indeed perturbative at small g_s . On the other hand, since the mass per unit volume of the D-brane is diverging, any internal dynamics associated with motion of the D-brane is frozen out in this limit. Thus the picture from supergravity agrees with the string perturbation theory described above: up to perturbations, it consists of flat empty space with a preferred submanifold in spacetime occupied by a largely nondynamical brane. This suggests that the D-branes of perturbation theory should be identified with the Ramond–Ramond branes of supergravity. Additional evidence for this picture comes from the great success of D-brane perturbation theory in reproducing the entropy of black holes [79–89], Hawking radiation [90–92], and the so-called gray-body factors [93] associated with Ramond–Ramond branes.

In contrast, Neveu–Schwarz branes do not admit simple descriptions as backgrounds for string perturbation theory. For the fundamental string, the reason is that (with n units of charge) the tension is proportional to n and does not depend on the string coupling. These branes therefore remain fully dynamical at small g_s , while the spacetime solution again becomes just Minkowski space. For the NS5-brane (with n units of charge) the tension is proportional to n/g_s^2 . Thus, $GT \sim n$ and the supergravity fields remain unchanged as we take $g_s \rightarrow 0$; consequently the fields cannot be described as small perturbations about Minkowski space.

11.6.3 A few words on black hole entropy

This is not the place for an in-depth discussion of just how D-brane perturbation theory can be used to reproduce the properties of supergravity solutions. Such treatments can be found in [88] and in [5–7, 9]. They involve the fact that the

open strings associated with D-branes describe, in the low-energy limit, a certain nonabelian Yang–Mills theory. The low-energy limit of that theory can then be analyzed and used to study the low-energy limit of the brane dynamics. Since BPS branes have the minimal possible energy for their charge, this means that BPS and nearly BPS branes can be addressed by such techniques.

We will close, however, by giving some parts of the entropy calculation for a particular case. As already mentioned, the solution (11.26) with three mutually orthogonal sets of M2-branes is the simplest BPS black brane solution with nonzero entropy. Let us compactify a circle along one M2-brane (say, that associated with the $z_{||}$ coordinates) and Kaluza–Klein-reduce to 9+1 type-IIA supergravity. Then, as we have seen, the z -type M2-branes (which are wrapped around this circle) become fundamental strings in the IIA description while the x - and y -type M2-branes (which do not wrap around the compact circle) become D2-branes. It turns out that a simple description of the microscopic perturbative states can be obtained by T-dualizing this solution to the IIB theory along the direction in which the fundamental strings point. This turns the fundamental strings into momenta and the two sets of D2-branes into D3-branes.

Let us now T-dualize twice more in, say, the two $y_{||}$ directions. This again yields a solution of IIB theory. The momentum remains momentum in the same direction, but one set of D3-branes has become a set of D1-branes and the other has become a set of D5-branes. The D1-branes (D-strings) are stretched in the same direction as that in which the momentum is flowing, and this all happens in a D5-brane direction. These T-dualities do not change the integer charges Q_x , Q_y , Q_z associated with the various types of brane: Q_x is now the number of D5-branes, Q_y the number of D-strings, and Q_z the number of momentum quanta. One can check that these T-dualities do not change the Bekenstein–Hawking entropy and, as presumed symmetries of the underlying string theory, they cannot change the number of microstates.

The case of a single D5-brane is particularly simple to discuss. It turns out that the low-energy dynamics reduces to what is effectively just a collection of D-strings²⁶ that are stuck to the D5-brane but free to oscillate within it. The momentum in the solution is just the momentum carried by these oscillations, and the energy of the solution is a linear sum of contributions from the D5-brane rest energy, the D-string rest energy, and the momentum. For a supersymmetric solution, all the oscillations must move in the same direction along the D-string and so are described by, say, right-moving fields on a (1+1)-dimensional spacetime. Oscillations of D-strings propagate at the speed of light and so the associated energy–momentum vector is null.

²⁶ Or, even better, to a single D-string wrapped Q_y times around the direction in which the momentum flows. See, e.g., [94].

Thus, for each string, there are four massless 1+1 right-moving scalar fields corresponding to the four internal directions of the 5-brane. Supersymmetry implies that there are also four massless 1+1 right-moving fermionic fields for each D-string. A fermion acts roughly like half a boson, so we may think of this as $6Q_y$ massless right-moving scalars on $S^1 \times R$ (the worldvolume of a 1-brane). A standard formula tells us that, given n massless right-moving scalars with Q_z units of momentum, the entropy at large Q_z is $S = 2\pi\sqrt{Q_z n/6}$. Thus we have $S = 2\pi\sqrt{Q_y Q_z}$, in agreement with the Bekenstein–Hawking entropy $S = A/(4G_{11})$ (see (11.28) with $Q_x = 1$) for the associated black hole.

This gives an idea of the way in which D-brane perturbation theory provides a microscopic accounting of the entropy of this BPS black hole. The other BPS and near-BPS cases are similar in many respects. It is quite satisfying to arrive at exactly the Bekenstein–Hawking entropy formula without having to adjust any free parameters. However, one is certainly struck by the qualitative differences between the regime in which we are used to thinking about black holes and the regime in which the string calculation is performed. We usually consider black holes with large smooth horizons; in contrast, the perturbative calculation is done in the asymptotic regime of small g_s , where spacetime is flat and the horizon has degenerated to zero size. The belief is that supersymmetry guarantees the entropy of the quantum system to be independent of g_s , as it does for other nongravitational systems.²⁷ However, there is much room for speculation and investigation in trying to match these pictures more closely and in understanding just what form these states take in the black hole regime of finite g_s .

Acknowledgements

The author wishes to thank Gary Horowitz, Clifford Johnson, Rob Myers, Amanda Peet, and especially Joe Polchinski for innumerable discussions on string theory and stringy black holes, as well as Tomas Andrade and Tony Zee for spotting numerous typos in an earlier version of this chapter. This work was supported in part by the US National Science Foundation under grant PHY08-55415 and in part by funds from the University of California.

References

- [1] D. Youm, Black holes and solitons in string theory, *Phys. Rept.* **316** (1999), 1 hep-th/9710046.

²⁷ As supporting evidence, recall that the Bekenstein–Hawking entropy of our BPS black hole does not depend on g_s when written in terms of the integer charges (11.28).

- [2] K.-I. Maeda and M. Nozawa, Black hole solutions in string theory, arXiv:1104.1849 [hep-th].
- [3] D. Marolf, Resource letter: the nature and status of string theory, *Am. J. Phys.* **72** (2004), 730–741 [hep-th/0311044].
- [4] M. Green, J. Schwarz, and E. Witten, *Superstring Theory*, Cambridge University Press (1987).
- [5] J. Polchinski, *String Theory*, Cambridge University Press (1998).
- [6] C. V. Johnson, *D-branes*, Cambridge University Press (2003).
- [7] K. Becker, M. Becker, and J. H. Schwarz, *String Theory and M-Theory: A Modern Introduction*, Cambridge University Press (2007).
- [8] M. Dine, *Supersymmetry and String Theory: Beyond the Standard Model*, Cambridge University Press (2007).
- [9] E. Kiritsis, *String Theory in a Nutshell*, Princeton University Press (2007).
- [10] E. Cremmer, B. Julia, and J. Scherk, Supergravity theory in eleven-dimensions, *Phys. Lett.* **B76** (1978), 409.
- [11] P. C. Aichelburg and F. Embacher, Exact superpartners of $N = 2$ supergravity solitons, *Phys. Rev.* **D34** (1986), 3006.
- [12] M. J. Duff, J. T. Liu, and J. Rahmfeld, Dipole moments of black holes and string states, *Nucl. Phys.* **B494** (1996), 161 [hep-th/9612015].
- [13] M. J. Duff, J. T. Liu, and J. Rahmfeld, $g = 1$ for Dirichlet 0-branes, *Nucl. Phys.* **B524** (1998), 129 [hep-th/9801072].
- [14] V. Balasubramanian, D. Kastor, and J. Traschen, The spin of the M2-brane and spin–spin interactions via probe techniques, *Phys. Rev.* **D59** (1999), 984007.
- [15] P. K. Townsend, Brane surgery, *Nucl. Phys. Proc. Suppl.* **58** (1997), 163.
- [16] D. Marolf, Chern–Simons terms and the three notions of charge, in *Quantization, Gauge Theory, and Strings, Proc. Int. Conf. dedicated to the memory of Professor Efim Fradkin*, eds. A. Semikhatov, M. Vasiliev, and V. Zaiken, Scientific World (2001), [hep-th/0006117].
- [17] G. W. Gibbons and C. M. Hull, A Bogomolny bound for general relativity and solitons in $N = 2$ supergravity, *Phys. Lett.* **109B** (1982), 190.
- [18] E. Witten, A simple proof of the positive energy theorem, *Commun. Math. Phys.* **80** (1981), 381.
- [19] J. A. de Azcarraga, J. P. Gauntlett, J. M. Izquierdo, and P. K. Townsend, Topological extensions of the supersymmetry algebra for extended objects, *Phys. Rev. Lett.* **63** (1989), 2443.
- [20] G. W. Gibbons, G. T. Horowitz, and P. K. Townsend, Higher-dimensional resolution of dilatonic black-hole singularities, *Class. Quant. Grav.* **12** (1995), 297.
- [21] E. Witten and D. Olive, Supersymmetry algebras that include topological charges, *Phys. Lett.* **78B** (1978), 97.
- [22] S. Ferrara, C. A. Savoy, and B. Zumino, General massive multiplets in extended supersymmetry, *Phys. Lett.* **100B** (1981), 393.
- [23] S. Majumdar, *Phys. Rev.* **72** (1947), 930.
- [24] A. Papapetrou, *Proc. Roy. Irish Acad.* **A51** (1947), 191.
- [25] J. B. Hartle and S. W. Hawking, Solutions of the Einstein–Maxwell equations with many black holes, *Commun. Math. Phys.* **26** (1972), 87–101.
- [26] D. L. Welch, On the smoothness of the horizons of multi-black hole solutions, *Phys. Rev.* **D52** (1995), 985 [arXiv:hep-th/9502146].
- [27] G. N. Candlish and H. S. Reall, On the smoothness of static multi-black hole solutions of higher-dimensional Einstein–Maxwell theory, *Class. Quant. Grav.* **24** (2007), 6025–6040 [arXiv:0707.4420 [gr-qc]].

- [28] E. Poisson and W. Israel, Internal structure of black holes, *Phys. Rev.* **D41** (1990), 1796.
- [29] M. Dafermos, The interior of charged black holes and the problem of uniqueness in general relativity, *Commun. Pure Appl. Math.* **58** (2005), 445–504 [arXiv:gr-qc/0307013].
- [30] P. R. Brady and J. D. Smith, Black hole singularities: a numerical approach, *Phys. Rev. Lett.* **75** (1995), 1256 [arXiv:gr-qc/9506067].
- [31] D. Marolf, The dangers of extremes, *Gen. Rel. Grav.* **42** (2010), 2337–2343 [arXiv:1005.2999 [gr-qc]].
- [32] D. Marolf and A. Ori, to appear. Pre-print [arXiv:1109.5139 [gr-qc]].
- [33] P. C. Aichelburg and R. U. Sexl, On the gravitational field of a massless particle, *Gen. Rel. Grav.* **2** (1971), 303.
- [34] E. Bergshoeff, E. Sezgin, and P. K. Townsend, Supermembranes and eleven-dimensional supergravity, *Phys. Lett.* **B189** (1987), 75.
- [35] R. Sorkin, Kaluza–Klein monopole, *Phys. Rev. Lett.* **51** (1983), 87.
- [36] D. Gross and M. Perry, Magnetic monopoles in Kaluza–Klein theories, *Nucl. Phys.* **B226** (1983), 29.
- [37] S. Hawking and G. F. R. Ellis, *The Large-Scale Structure of Space-Time*, Cambridge University Press (1973).
- [38] E. T. Newman, L. Tamburino, and T. Unti, *J. Math. Phys.* **4** (1963), 915.
- [39] M. Bañados, C. Teitelboim, and J. Zanelli, The black hole in three-dimensional space–time, *Phys. Rev. Lett.* **69** (1992), 1849 [hep-th/9204099].
- [40] M. Bañados, M. Henneaux, C. Teitelboim, and J. Zanelli, Geometry of the (2+1) black hole, *Phys. Rev.* **D48** (1993), 1506 [gr-qc/9302012].
- [41] A. A. Tseytin, Harmonic superpositions of M-branes, *Nucl. Phys.* **B475** (1996), 149 [arXiv:hep-th/9604035].
- [42] J. P. Gauntlett, D. A. Kastor, and J. H. Traschen, Overlapping branes in M theory, *Nucl. Phys.* **B478** (1996), 544–560 [hep-th/9604179].
- [43] K. Behrndt and M. Cvetic, BPS saturated bound states of tilted p-branes in type II string theory, *Phys. Rev.* **D56** (1997), 1188–1193 [hep-th/9702205].
- [44] J. C. Breckenridge, G. Michaud, and R. C. Myers, New angles on D-branes, *Phys. Rev.* **D56** (1997), 5172–5178 [hep-th/9703041].
- [45] V. Balasubramanian, F. Larsen, and R. G. Leigh, Branes at angles and black holes, *Phys. Rev.* **D57** (1998), 3509–3528 [hep-th/9704143].
- [46] S. Surya and D. Marolf, Localized branes and black holes, *Phys. Rev.* **D58** (1998), 124013 [hep-th/9805121].
- [47] D. Marolf and A. W. Peet, Brane baldness versus superselection sectors, *Phys. Rev.* **D60** (1999), 105007 [hep-th/9903213].
- [48] A. Gomberoff, D. Kastor, D. Marolf, and J. H. Traschen, Fully localized brane intersections – the plot thickens, *Phys. Rev.* **D61** (2000), 024012 [hep-th/9905094].
- [49] S. A. Cherkis and A. Hashimoto, Supergravity solution of intersecting branes and AdS/CFT with flavor, *JHEP* **0211** (2002), 036 [hep-th/0210105].
- [50] E. D’Hoker, J. Estes, and M. Gutperle, Exact half-BPS type IIB interface solutions. II. Flux solutions and multi-Janus, *JHEP* **0706** (2007), 022 [arXiv:0705.0024 [hep-th]].
- [51] E. D’Hoker, J. Estes, and M. Gutperle, Exact half-BPS type IIB interface solutions. I. Local solution and supersymmetric Janus, *JHEP* **0706** (2007), 021 [arXiv:0705.0022 [hep-th]].
- [52] S. Ferrara, R. Kallosh, and A. Strominger, $N = 2$ extremal black holes, *Phys. Rev.* **D52** (1995), 5412 [arXiv:hep-th/9508072].

- [53] S. Ferrara and R. Kallosh, Supersymmetry and attractors, *Phys. Rev.* **D54** (1996), 1514 [arXiv:hep-th/9602136].
- [54] S. Ferrara, G. W. Gibbons, and R. Kallosh, Black holes and critical points in moduli space, *Nucl. Phys.* **B500** (1997), 75 [arXiv:hep-th/9702103].
- [55] S. Ferrara, K. Hayakawa, and A. Marrani, Lectures on attractors and black holes, *Fortsch. Phys.* **56** (2008), 993 [arXiv:0805.2498 [hep-th]].
- [56] S. Bellucci, S. Ferrara, M. Gunaydin, and A. Marrani, SAM lectures on extremal black holes in $d = 4$ extended supergravity, arXiv:0905.3739 [hep-th].
- [57] T. Ortin, Supersymmetric solutions of 4-dimensional supergravities, in *Proc. AIP Conf.*, vol. 1318 (2010), p. 175 [arXiv:1010.1383 [gr-qc]].
- [58] S. Kachru, R. Kallosh, and M. Shmakova, Generalized attractor points in gauged supergravity, arXiv:1104.2884 [hep-th].
- [59] I. C. G. Campbell and P. C. West, $N = 2, D = 10$ nonchiral supergravity and its spontaneous compactification, *Nucl. Phys.* **B243** (1984), 112.
- [60] M. Huq and M. A. Namazie, Kaluza–Klein supergravity in ten-dimensions, *Class. Quant. Grav.* **2** (1985), 293.
- [61] F. Giani and M. Pernici, $N = 2$ supergravity in ten-dimensions, *Phys. Rev.* **D30** (1984), 325–333.
- [62] O. Bergman and M. R. Gaberdiel, A nonsupersymmetric open string theory and S-duality, *Nucl. Phys.* **B499** (1997), 193 hep-th/9701137.
- [63] O. Bergman and M. R. Gaberdiel, Stable non-BPS D-particles, *Phys. Lett.* **B441** (1998), 133, hep-th/9806155.
- [64] O. Bergman and M. R. Gaberdiel, Non-BPS states in heterotic type IIA duality, *JHEP* **9903** (1999), 013.
- [65] A. Sen, Stable non-BPS states in string theory, *JHEP* **9806** (1998), 007, hep-th/9803194.
- [66] A. Sen, Stable non-BPS bound states of D-branes, *JHEP* **9808** (1998), 010, hep-th/9805019.
- [67] A. Sen and B. Zwiebach, Stable non-BPS states in F theory, hep-th/9907164.
- [68] M. R. Gaberdiel and A. Sen, Nonsupersymmetric D-brane configurations with Bose–Fermi degenerate open string spectrum, hep-th/9908060.
- [69] G. T. Horowitz and A. Strominger, Black strings and P-branes, *Nucl. Phys.* **B360** (1991), 197–209.
- [70] J. H. Schwarz and P. C. West, Symmetries and transformations of chiral $N = 2, D = 10$ supergravity, *Phys. Lett.* **B126** (1983), 301.
- [71] P. S. Howe and P. C. West, The complete $N = 2, D = 10$ supergravity, *Nucl. Phys.* **B238** (1984), 181.
- [72] J. H. Schwarz, Covariant field equations of chiral $N = 2, D = 10$ supergravity, *Nucl. Phys.* **B226** (1983), 269.
- [73] T. Buscher, Path integral derivation of quantum duality in nonlinear sigma models, *Phys. Lett.* **B201** (1988), 466.
- [74] T. Buscher, A symmetry of the string background field equations, *Phys. Lett.* **B194** (1987), 59.
- [75] J. H. Horne, G. T. Horowitz, and A. R. Steif, An equivalence between momentum and charge in string theory, *Phys. Rev. Lett.* **68** (1992), 568–571, hep-th/9110065.
- [76] B. DeWitt, in *Relativity, Groups, and Topology II*, Proc. 1983 Les Houches Summer School, eds. B. DeWitt and R. Stora, Elsevier (1984).
- [77] C. Itzykson and J.-B. Zuber, *Quantum Field Theory*, McGraw-Hill (1980).
- [78] S. Weinberg, *The Quantum Theory of Fields*, Cambridge University Press (1995).

- [79] A. Strominger and C. Vafa, Microscopic origin of the Bekenstein–Hawking entropy, *Phys. Lett.* **B379** (1996), 99–104 [hep-th/9601029].
- [80] C. Callan and J. Maldacena, D-brane approach to black hole quantum mechanics, *Nucl. Phys.* **B472** (1996), 591–610 [hep-th/9602043].
- [81] G. Horowitz and A. Strominger, Counting states of near extremal black holes, *Phys. Rev. Lett.* **77** (1996), 2368 [hep-th/9602051].
- [82] J. Breckenridge, R. Myers, A. Peet, and C. Vafa, D-branes and spinning black holes, *Phys. Lett.* **B391** (1997), 93–98 [hep-th/9602065].
- [83] J. Maldacena and A. Strominger, Statistical entropy of four-dimensional extremal black holes, *Phys. Rev. Lett.* **77** (1996), 428–429 [hep-th/9603060].
- [84] C. Johnson, R. Khuri, and R. Myers, Entropy of 4-D extremal black holes, *Phys. Lett.* **B378** (1996), 78–86 [hep-th/9603061].
- [85] J. Breckenridge, D. Lowe, R. Myers, A. Peet, A. Strominger, and C. Vafa, Microscopic entropy of near extremal spinning black holes, *Phys. Lett.* **B381** (1996), 423–426 [hep-th/9603078].
- [86] I. R. Klebanov and A. A. Tseytlin, Intersecting M-branes as four-dimensional black holes, *Nucl. Phys.* **B475** (1996), 179–192 [hep-th/9604166].
- [87] J. M. Maldacena, $N = 2$ extremal black holes and intersecting branes, *Phys. Lett.* **B403** (1997), 20–22 [hep-th/9611163].
- [88] G. T. Horowitz and D. Marolf, Counting states of black strings with traveling waves, *Phys. Rev.* **D55** (1997), 835–845 [hep-th/9605224].
- [89] G. T. Horowitz and D. Marolf, Counting states of black strings with traveling waves II, *Phys. Rev.* **D55** (1997), 846–852 [hep-th/9606113].
- [90] A. Dhar, G. Mandal, and S. Wadia, Absorption vs. decay of black holes in string theory and T symmetry, *Phys. Lett.* **B388** (1996), 51 [hep-th/9605234].
- [91] S. R. Das and S. D. Mathur, Comparing decay rates for black holes and D-branes, *Nucl. Phys.* **B478** (1996), 561–576 [hep-th/9606185].
- [92] S. R. Das and S. D. Mathur, Interactions involving D-branes, *Nucl. Phys.* **B482** (1996), 153–172 [hep-th/9607149].
- [93] J. Maldacena and A. Strominger, Black hole greybody factors and D-brane spectroscopy, *Phys. Rev.* **D55** (1997), 861–870 [hep-th/9609026].
- [94] J. Maldacena, Black holes in string theory, Ph.D. thesis, [hep-th/9607235].

12

The gauge/gravity duality

JUAN MALDACENA

In this chapter we explain the gauge/gravity duality [1–3], which is a motivation for studying black hole solutions in various numbers of dimensions. The gauge/gravity duality is an equality between two theories. On one hand we have a quantum field theory in d spacetime dimensions. On the other hand we have a gravity theory on a $(d + 1)$ -dimensional spacetime that has an asymptotic boundary which is d -dimensional. It is also sometimes called AdS/CFT, because the simplest examples involve anti-de Sitter spaces and conformal field theories. It is often called gauge/string duality, because the gravity theories are string theories and the quantum field theories are gauge theories. It is also referred to as “holography” because one is describing a $(d + 1)$ -dimensional gravity theory in terms of a lower-dimensional system, in a way that is reminiscent of an optical hologram, which stores a three-dimensional image on a two-dimensional photographic plate. This duality is called a “conjecture”, but by now there is considerable evidence that it is correct. In addition, there are some derivations based on physical arguments.

The simplest example involves an anti-de Sitter spacetime. So, let us start by describing this spacetime in some detail. Anti-de Sitter is the simplest solution of Einstein’s equations with a negative cosmological constant. It is the Lorentzian analogue of hyperbolic space, which was historically the first example of a non-Euclidean geometry. In a similar way, AdS/CFT gives the simplest example of a quantum mechanical spacetime.

The metric in AdS space can be written as

$$ds_{\text{AdS}_{d+1}}^2 = L^2 \left[-(r^2 + 1)dt^2 + (r^2 + 1)^{-1}dr^2 + r^2 d\Omega_{d-1}^2 \right], \quad (12.1)$$

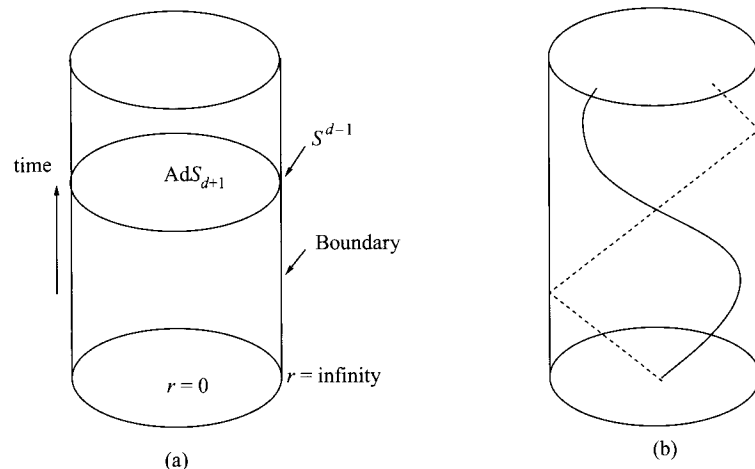


Figure 12.1 (a) Penrose diagram for anti-de Sitter space. It is a solid cylinder. The vertical direction is time. The boundary contains the time direction and the sphere S^{d-1} , represented here as a circle. (b) Massive geodesic (solid line) and a massless geodesic (broken line).

where the last term is the metric of the unit sphere S^{d-1} and L is the radius of curvature. Note that near $r = 0$ the metric looks like flat space. As we go to larger values of r we see that g_{00} and the metric on the sphere grow. The growth of g_{00} can be viewed as a rising gravitational potential. In fact, a slowly moving massive particle feels a gravitational potential $V \sim \sqrt{-g_{00}}$. If a particle is set at rest at a large value of r , it will execute an oscillatory motion in the r direction, very much like a particle in a harmonic oscillator potential. This gravitational potential confines particles to a region around the origin. A massive particle with finite energy cannot escape to infinity, $r = \infty$. However, a massless geodesic can go to infinity and back in finite time. One way to see this is to look at the Penrose diagram of AdS. We can factor out $1 + r^2$ from the metric (12.1) and define a new radial coordinate x via $dx = dr/(1 + r^2)$, which now has a finite range. Thus, the Penrose diagram of AdS space is a solid cylinder; see Fig. 12.1(a). Time is in the vertical direction and the boundary is at $r = \infty$, which corresponds to a finite value of x . The S^{d-1} is the spatial section of the surface of the cylinder. The metric (12.1) has an obvious $\mathbb{R} \times SO(d)$ symmetry, but AdS has more symmetries. The full symmetry group is $SO(2, d)$. These symmetries can be made more manifest by viewing AdS as the hyperboloid

$$-Y_{-1}^2 - Y_0^2 + Y_1^2 + \cdots + Y_d^2 = -L^2 \quad (12.2)$$

in $\mathbb{R}^{2,d}$. This description is useful for realizing the symmetries explicitly; however, in this hyperboloid the time direction, t in (12.1), is compact (it is just the angle in

the $(-1, 0)$ -plane). In all physical applications we want to take this time direction to be noncompact.

These isometries of AdS are very powerful. Let us recall the situation in flat space. If we have a massive geodesic in flat space then we can always boost to a frame where the particle is at rest. In AdS it is the same: if we consider the oscillating trajectory of a massive particle then we can “boost” to a frame where that particle is at rest. Thus, the moving particle does not know that it is moving and, despite appearances, there is no “center” in AdS. The Hamiltonian is part of the symmetry group (as in the Poincaré group) and there are several choices of Hamiltonian. Once we choose a Hamiltonian, for example one that shifts t in (12.1), then we have chosen a “center” and a notion of the lowest-energy state, in which a particle sits at this “center.”

In some applications it is useful to focus on a small patch of the boundary and treat it as $\mathbb{R}^{1,d}$. In fact, there is a choice of coordinates in which the AdS metric takes the form

$$ds^2 = L^2 \frac{-dt^2 + d\vec{x}_{d-1}^2 + dz^2}{z^2}. \quad (12.3)$$

Here the boundary is at $z = 0$ and we have slices that display the Poincaré symmetry group in d dimensions (one time dimension and $d - 1$ spatial dimensions). In fact, if we take $t \rightarrow ix_0$ then we get hyperbolic space, now sometimes called Euclidean AdS! In these coordinates we can also see clearly another isometry, which rescales the coordinates, so that $(t, \vec{x}, z) \rightarrow \lambda(t, \vec{x}, z)$. These coordinates have a horizon at $z = \infty$ and cover only a portion of (12.1). They are convenient when we want to consider a CFT living in Minkowski space, $\mathbb{R}^{1,d-1}$.

The AdS/CFT relation postulates that all the physics in an asymptotically anti-de Sitter spacetime can be described by a local quantum field theory that lives on the boundary. The boundary is given by $\mathbb{R} \times S^{d-1}$. The isometries of AdS act on the boundary. They send points on the boundary to points on the boundary. This action is simply that of the conformal group in d dimensions, $SO(2, d)$. Thus the quantum field theory is a conformal field theory. In fact, the rescaling symmetry of (12.3) translates into a dilatation on the boundary. The boundary theory is thus scale invariant. It has no dimensionful parameter. Usually theories that are scale invariant are also conformal invariant. These are theories where the stress–energy–momentum tensor is traceless. The conformal group includes the Poincaré group, the dilatation, and “special conformal transformations”, which will not be important for us here. Notice that the conformal symmetry ensures that we can choose an arbitrary radius for the boundary S^{d-1} , so we can set it to 1. In fact, if we have a conformal field theory then the tracelessness of the stress tensor implies that field theories on a space with a metric that is either $g_{\mu\nu}^b$ or $\omega^2(x)g_{\mu\nu}^b$ are basically the

same (up to a well-understood conformal anomaly). Here we are talking about the metric on the boundary, where the field theory lives. This metric is not dynamical; it is fixed.

How can it be that a $(d+1)$ -dimensional bulk theory is equivalent to a d -dimensional one? In fact, let us attempt to disprove such an equivalence. A skeptic would argue as follows. Let us do a simple count of the number of degrees of freedom. Since the bulk has one extra dimension, we seem to have a contradiction. In fact, we could consider the number of degrees of freedom at large energies, in a microcanonical ensemble. To compute this number we can introduce an effective temperature. On the one hand, in a theory with massless fields (or a theory with no scale) we expect that the entropy S should behave as $V_{d-1}T^{d-1}$. So, if the boundary theory is a CFT on $\mathbb{R} \times S^3$ then for temperatures large compared with the radius of S^3 (i.e., for $T \gg 1$), we expect that the entropy should grow as follows:

$$S \propto c T^{d-1}, \quad (12.4)$$

where c is a dimensionless constant that measures the effective number of fields in the theory; for free fields it can be explicitly computed, as we will do later in an example. On the other hand, from the bulk point of view it seems that we also have a theory with massless particles, which are gravitons. We could have extra fields, but, for the time being, let us include only gravitons, which give a lower bound to the entropy. The entropy of these gravitons is certainly larger than the entropy from the region where $r \sim 1$. In that region, which has a volume of order 1, we get

$$S_{\text{graviton gas}} > T^d, \quad (12.5)$$

because it has d spatial dimensions. For large enough T we see that (12.5) is larger than (12.4). So we appear to have a contradiction with the basic claim of AdS/CFT. However, we are forgetting something essential: the bulk theory contains *gravity*. And gravity gives rise to black holes. And black holes give rise to bounds on entropy. Black holes in AdS have the form

$$ds_{\text{AdS}_{d+1}}^2 = L^2 \left[- \left(r^2 + 1 - \frac{2gm}{r^{d-2}} \right) dt^2 + \left(r^2 + 1 - \frac{2gm}{r^{d-2}} \right)^{-1} dr^2 + r^2 d\Omega_{d-1}^2 \right] \quad (12.6)$$

where m is proportional to the mass and g is proportional to Newton's constant in units of the AdS radius:

$$g \propto \frac{G_{N,d+1}}{L^{d-1}} \quad (12.7)$$

The gas of gravitons extends up to $r_z \sim T$ and has a mass of order $m \sim T^{d+1}$. For large T we can neglect the 1 in (12.6) and so obtain, for the Schwarzschild radius,

$r_s^d \sim gm \sim gT^{d+1}$. We see that the Schwarzschild radius is larger than the size of the system for temperatures that are large enough, $T > 1/g$. Thus, the result (12.5) breaks down for such large temperatures. At large enough energies we compute the entropy in terms of the black hole entropy. This entropy grows as the area of the horizon $S \sim r_s^{d-1}/g$. One can see that the Hawking temperature for big black holes is $T \propto r_s$. The entropy of the black hole is $S_{BH} \sim T^{d-1}/g$. This is now of the expected form (12.4), with

$$c \propto \frac{1}{g} \propto \frac{L^{d-1}}{G_{N,d+1}}. \quad (12.8)$$

Thus, AdS/CFT connects the entropy of a black hole with the ordinary thermal entropy of a field theory. This has two very important applications. First, regarding conceptual issues, it gives a statistical interpretation for black hole entropy; in addition, since it displays the black hole as an ordinary thermal state in a unitary quantum field theory, we see that these black holes are consistent with quantum mechanics and unitary evolution. Second, it allows us to compute the thermal free energy, and other thermal properties, in quantum field theories that have gravity duals.

The number of fields scales as the inverse of Newton's constant. Notice that g from (12.8) measures the effective gravitational coupling at the AdS scale. It is the dimensionless constant measuring the effective nonlinear interactions among gravitons. Thus, *if we want a weakly coupled bulk theory then we require that the field theory has a large number of fields*. This is a necessary but not sufficient condition. One important feature of a weakly coupled theory is the existence of a Fock space structure in the Hilbert space. Namely, we can talk about a single particle, two particles, etc. Their energies are, up to small corrections, proportional to the sum of the energies of each particle. The dual quantum field theory has to have a similar structure. In fact, this structure emerges quite naturally in large- N gauge theories. A large- N gauge theory is based on the gauge group $SU(N)$ (or $U(N)$), with fields in the adjoint representation. In this case we can form gauge-invariant operators by taking traces of the fundamental fields, i.e., $\text{Tr}(F_{\mu\nu}F^{\mu\nu})$, $\text{Tr}(F_{\mu\nu}D_\rho F^{\mu\nu})$, etc. These traces are local operators, where the fields are all evaluated at the same point in spacetime. In addition, one could have double trace operators, such as the product of the above two operators. When we act with one such operator on the field theory vacuum we create a state in the field theory. In a general CFT (even if it does not have a known gravity dual) we have a map between states on the cylinder $\mathbb{R} \times S^{d-1}$ and operators on the plane \mathbb{R}^d . The dimension of the operator is equal to the energy of the corresponding state. (The scaling dimension tells us how the operator scales under the scaling transformation mentioned after (12.3).) This follows from the fact that we can go to a Euclidean cylinder; the

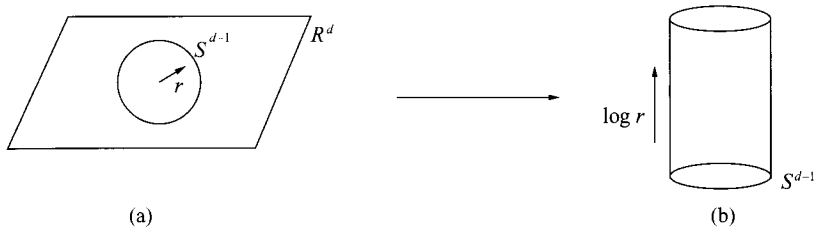


Figure 12.2 (a) A conformal field theory on the Euclidean plane, \mathbb{R}^d . We can act with various operators at $r = 0$. These create certain states on S^{d-1} , which are given by performing the path integral of the field theory in the interior of the S^{d-1} with the operators inserted. (b) Owing to the Weyl symmetry of the theory we can rescale the metric and view it as a metric on a cylinder $\mathbb{R} \times S^{d-1}$. States of the theory on this cylinder are in one-to-one correspondence with operators on the plane. This is a general property of CFTs and is completely independent of AdS/CFT.

Euclidean cylinder and the plane differ by an overall Weyl transformation of the metric

$$d(\log r)^2 + d\Omega^2 = \frac{1}{r^2}(dr^2 + r^2 d\Omega^2).$$

Thus, they are equivalent in a CFT. An operator at the origin of the plane creates a state at fixed r that can be viewed as a state of the field theory on the cylinder; see Fig. 12.2. This state-operator mapping is valid for any conformal field theory. The AdS/CFT equivalence relates a state of the field theory on the cylinder to a state of the bulk theory in the global coordinates (12.1). Since the symmetries are the same on both sides, we can divide the states, or operators, according to their transformation laws under the conformal group. Such representations are characterized by the spin of the operator and its scaling dimension, Δ . A simple example is the stress-tensor operator, $T_{\mu\nu}$. This operator creates a graviton in AdS. The dimension of the stress tensor is d . Single-trace operators are associated with single-particle states in the bulk. Multitrace operators correspond to multiparticle states in the bulk. There exists a general argument, based on a simple analysis of Feynman diagrams, that shows that the dimension of a multitrace operator is the sum of the dimensions of each single-trace component, up to $1/N^2$ corrections. In fact the same analysis of Feynman diagrams shows that the large- N limit of general gauge theories gives a string theory [4]. The argument does not specify precisely the kind of string theory that we will get, it only says that we can organize the diagrams of interest in terms of diagrams we can draw on a sphere plus those on a torus, etc. Each time we increase the genus of the surface we get an additional power of $1/N^2$. This looks like a string theory with string coupling $g_s \sim 1/N$. The strings that we have in the bulk are precisely the strings suggested by this argument.

The preceding argument says that a large- N limit is necessary in a weakly coupled gravity theory. This does not mean that we are restricted to linearized solutions. In a weakly coupled gravity theory we can consider full classical nonlinear solutions of the equations, such as the black hole solutions we discussed above. Weak coupling means that we can neglect quantum gravity corrections or loop diagrams.

In string theory the graviton is the lowest oscillation mode of a string. The gravitational coupling discussed above is related to the interaction strength between strings. However, we have another condition for the validity of the gravity approximation. In gravity we treat the graviton as a point-like particle and ignore all the massive string states. The typical size of the graviton is given by the string length l_s , an additional parameter beyond the Planck scale. In order to ignore the rest of the string states we need

$$\frac{L_{\text{AdS}}}{l_s} \gg 1, \quad (12.9)$$

i.e., we need (12.9) to hold for gravity to be a good approximation. This condition is simply saying that the typical size of the space should be much bigger than the intrinsic size of the graviton in string theory. This condition is important because in many concrete examples we have to make sure that this condition is met, otherwise gravity would give the wrong answers even if we had a large number of fields! If (12.9) is not valid then we should consider the full string theory in AdS. A salient feature of string theory is that there are massive string states of higher spin, $S > 2$. In fact, in a large- N gauge theory we can easily write down single-trace operators with higher spin, such as $\text{Tr}(F_{\mu\nu} D_+^S F^{\mu\nu})$, with D_+ a derivative along a null direction. Such operators have relatively small scaling dimensions Δ at weak coupling; in this case $\Delta = 4 + S$. These give rise to particles of spin S , whose bulk mass is comparable to the inverse AdS radius. Such light string states render the Einstein gravity approximation invalid. Thus, *in order to trust the gravity approximation the field theory should necessarily be strongly interacting*. This is a necessary but not sufficient condition. The coupling should be strong enough to give a large dimension to all the higher-spin single-trace operators of the theory. Such masses are set by the parameter (12.9). In concrete examples we find that the quantity (12.9) is proportional to a positive power of the effective 't Hooft coupling of the theory, $g_{\text{YM}}^2 N$, where g_{YM} is the coupling constant of the gauge theory. The extra factor N enters because color-correlated particles can exchange N gluons, which enhances their interactions at large N . By taking a large value of $g_{\text{YM}}^2 N$ it is possible to give a large dimension to the higher-spin states. We are left with a light graviton and other lower-spin states. In this case we expect that their interactions are those of Einstein gravity.

12.1 Scalar field in AdS

In order to be more precise about the correspondence between states in AdS and states in the boundary, it is necessary to do the quantum mechanics of a particle in AdS. Equivalently, we will quantize the corresponding field in AdS. In this subsection we consider a massive scalar field in AdS with action

$$S = - \int d^{d+1}x \sqrt{g} [(\nabla\phi)^2 + m^2\phi^2]. \quad (12.10)$$

Let us compute the energy spectrum in AdS in the global coordinates of (12.1). Let us focus on the ground state. We expect that it should have zero angular momentum. So, we make an ansatz for the wavefunction $\phi = e^{-i\omega t} F(r)$, with the boundary condition that $F(r) \rightarrow 0$ at infinity. By setting $\nabla^2\phi - m^2\phi = 0$ we get an ω -dependent equation for $F(r)$ with two boundary conditions, one at infinity and one at the origin. It is an eigenvalue problem, which gives quantized frequencies. It is possible to check that

$$\phi = e^{-i\Delta t} \frac{1}{(1+r^2)^{\Delta/2}} \quad (12.11)$$

with

$$\Delta = \frac{d}{2} + \sqrt{\frac{d^2}{4} + (mL)^2} \quad (12.12)$$

is a solution of the equation of motion with the correct boundary conditions. We identify this solution as the ground state, since it has no oscillations in the radial direction. The energy is $\omega = \Delta$. The energies of all other states differ from this by an integer, $\omega_n = \Delta + n$. This is due to the fact that we can get all the other states from the action of the conformal generators; thus, their energies are determined by the conformal algebra.

We get a wavefunction localized near the center of AdS. In the large-mass limit $mL \gg 1$, we see that it becomes sharply localized at $r = 0$, as we expect for a classical particle in AdS. For mL of order 1, the wavefunction is extended over a region of order 1 in r , which corresponds to proper distances of order the AdS radius. A particle of zero mass, $m = 0$, has an integer energy $\Delta = d$. The case of the graviton gives an equation similar to that of a massless field and also leads to $\Delta = d$, as expected from the dimension of the stress tensor.

It would seem from (12.12) that the dimensions of the operators are bounded below by d , which is the dimension of a marginal operator in the field theory. However, there are two effects that allow us to go to lower dimensions. First, there are some allowed “tachyons” in AdS. Namely, it is possible for a field to have $-d^2/4 \leq (mL)^2 < 0$. In other words, if a field is only slightly tachyonic, this relation is allowed [5]. The reason that it does not lead to an instability is due to

the boundary conditions. These boundary conditions force the field to have some kinetic energy in the radial direction, which overwhelms the negative energy of the mass term. In fact, we can check from (12.12) that such states have positive energies. A second fact is that in the range $-d^2/4 \leq (mL)^2 < 1 - d^2/4$ we can have a second quantization prescription [6]. To understand this, note that if we choose the other sign for the square root in (12.12) then (12.11) is another solution of the equation of motion. For fields with $m^2 < 0$, both solutions decay as $r \rightarrow \infty$. So we can set boundary conditions that remove either of these solutions. The quantization leading to (12.12) corresponds to removing the solution that decay more slowly as $r \rightarrow \infty$.

Let us now do a different computation, which will further elucidate the relation between bulk fields and boundary operators. It is convenient to go to Euclidean space and to choose the Poincaré coordinates (12.3). We will consider the problem of computing the path integral of this scalar field theory with fixed boundary conditions at the boundary. The quantum gravity problem in AdS contains such a problem: we have to do this for all the fields of the theory, including the graviton.

Let us consider the classical, or semiclassical, contribution to this problem. This is given by finding a classical solution that obeys the boundary condition and evaluating the action for this solution. If we set zero boundary conditions then the field is zero and the action is zero. If we set non-zero boundary conditions, the classical action gives us something interesting. Since we have translation symmetry along the boundary directions, we will go to Fourier space and write $\phi = e^{ikx} f(k, z)$. The wave equation becomes

$$\frac{d^2 f}{dz^2} + (1-d) \frac{1}{z} \frac{df}{dz} - \left(k^2 + \frac{(mL)^2}{z^2} \right) f = 0. \quad (12.13)$$

Near the boundary, for small z there are two independent solutions, behaving as $f = z^\Delta$ or $f \sim z^{d-\Delta}$. We will put a boundary condition on the larger component of the general solution. Since that component of the solution depends on z , we take a boundary condition at $z = \epsilon$, i.e.,

$$\phi(x, z)|_{z=\epsilon} = \phi_0(x) \epsilon^{d-\Delta}. \quad (12.14)$$

The solution of (12.13) that decays at $z \rightarrow \infty$ is

$$f(k, z) = e^{ikz} z^{d/2} K_v(kz), \quad v = \sqrt{\frac{d^2}{4} + (mL)^2}, \quad (12.15)$$

where K is a Bessel function. In order to obey the boundary conditions we set

$$\phi(k, z) = \phi_0(k) \epsilon^{d-\Delta} \frac{f(k, z)}{f(k, \epsilon)}. \quad (12.16)$$

We now insert this into the action (12.10). We can integrate by parts and use the equations of motion. The computation then reduces to a boundary term. For each Fourier mode we get [7]

$$\begin{aligned} S &= \phi_0(-\vec{k}) \epsilon^{d-\Delta} \frac{1}{\epsilon^d} z d_z \phi(k, z)|_{z=\epsilon} = \phi_0(-k) \phi_0(\vec{k}) \epsilon^{d-2\Delta} \frac{z d_z f(k, z)}{f(k, \epsilon)} \\ S &= \phi_0(-k) \phi_0(\vec{k}) \left(\epsilon^{-2\nu} P(k^2 \epsilon^2) - |k|^{2\nu} 2^{-2\nu} \frac{\Gamma(-\nu)}{\Gamma(\nu)} 2\nu \right), \end{aligned} \quad (12.17)$$

where P is a polynomial. Note that the first term contains divergent terms when $\epsilon \rightarrow 0$. These terms are analytic in momentum and, upon Fourier transformation, give terms that are local in position space. These terms were to be expected since the boundary conditions that we are considering are such that the field grows towards the boundary; from the field theory point of view they can be viewed as UV divergences. However, the last term in (12.17) gives a nonlocal contribution in position space and represents the interesting part of the correlator. Transformed back to position space this gives

$$S = -\frac{2\nu \Gamma(\Delta)}{\pi^{d/2} \Gamma(\nu)} L^{d-1} \int d^d x d^d y \frac{\phi_0(x) \phi_0(y)}{|x - y|^{2\Delta}}. \quad (12.18)$$

The AdS/CFT correspondence “dictionary” states that this computation with fixed boundary conditions is related to the generating function of correlation functions for the corresponding operator in the field theory [2, 3]. In other words, for a field ϕ related to the single-trace operator \mathcal{O} we have the equality

$$Z_{\text{gravity}}[\phi_0(x)] = Z_{\text{field theory}}[\phi_0(x)] = \left\langle \exp \left(\int d^d x \phi_0(x) \mathcal{O}(x) \right) \right\rangle. \quad (12.19)$$

The leading approximation to the gravity result is then given by evaluating the classical action; it is given by e^{-S} , with S as in (12.18). The correlation functions of the operators are then given by

$$\langle \mathcal{O}(x_1) \cdots \mathcal{O}(x_n) \rangle = \frac{\delta}{\delta \phi_0(x_1)} \cdots \frac{\delta}{\delta \phi_0(x_1)} Z_{\text{gravity}}[\phi_0(x)]. \quad (12.20)$$

In the quadratic approximation the gravity result is given by (12.18), and the correlation functions factorize into products of two-point functions. We can include interactions in the bulk. For example, we can have a ϕ^3 bulk interaction. Then the leading approximation is given by taking the classical but nonlinear solution with these boundary conditions and evaluating the corresponding action. It can be computed perturbatively by evaluating Feynman–Witten diagrams in the bulk [3].

For each single-trace operator we have a corresponding field in the bulk with a certain boundary condition. Among these fields is the graviton, associated with the

stress tensor. The generating function of correlation functions of the stress tensor is obtained by considering the field theory on a general boundary geometry $g_{\mu\nu}^b(x)$. At the classical level we find a solution of Einstein’s equations, $R_{\mu\nu} \propto g_{\mu\nu}$, with $g_{\mu\nu}^b$ as a boundary condition. We insert this into the action and obtain the quantity $Z_{\text{gravity}}[g_{\mu\nu}^b(x)] \sim \exp\{-S_E[g_{cl}]\}$. We can also view this quantity as the Hartle–Hawking wavefunction of the universe in the Euclidean region. As a first step, one can expand Einstein’s equations to quadratic order and compute the two-point function. The action for each polarization component is similar to that of a massless scalar field. In this case, the ϵ -dependent factor in (12.14) drops out. So, it makes sense to compute the absolute normalization of the two-point function. This two-point function of the stress tensor is another measure of the degrees of freedom of the theory. It is proportional to the overall coefficient in the Einstein action, which is the quantity c introduced earlier, in (12.8). In other words, we schematically have $T_{\mu\nu}(x) T_{\sigma\delta}(0) = c(t_{\mu\nu\sigma\delta}/|x|^{2d})$, where $t_{\mu\nu\sigma\delta}$ is an x -dependent tensor, taking into account the fact that the stress tensor is traceless and conserved. In fact, since the classical gravity action contains c as an overall factor, we conclude that, to leading order in $1/c$ and in the gravity approximation, all stress-tensor correlators are proportional to c . They are universal for any field theory that has a gravity dual for each spacetime dimension. Such correlators are not universal in quantum field theory (except in two dimensions, $d = 2$). The universality arises only in the gravity approximation and is removed by higher-derivative corrections to the action. Stringy corrections give rise to these higher-derivative corrections. Similarly, the coefficient that appears in this computation is equal to the coefficient appearing in the computation of the thermal free energy (up to universal constants). Again, this does not hold for general field theories in $d > 2$, but it does hold in $d = 2$.

Another interesting case is a gauge field in AdS. This corresponds to a conserved current on the boundary theory. Thus a gauge symmetry in the bulk corresponds to a global symmetry on the boundary. We have an exactly conserved charge in the boundary theory. Owing to the presence of black holes, the only way to ensure that we have a conserved charge is to have a gauge symmetry in the bulk.

12.2 The $\mathcal{N} = 4$ super Yang–Mills/AdS₅ × S⁵ example

The previous discussion was completely general. In order to be specific, let us discuss one particular example of a dual pair. We will first discuss the field theory and then the gravity theory and show how various objects match in the two theories.

We will consider a four-dimensional field theory that is similar to quantum chromodynamics. In quantum chromodynamics we have a gauge field A_μ that is a (traceless) 3×3 matrix in the adjoint representation of $SU(3)$. The

action is

$$S = -\frac{1}{4g_{\text{YM}}^2} \int d^4x \text{Tr}(F_{\mu\nu}F^{\mu\nu}), \quad F_{\mu\nu} = [\partial_\mu + A_\mu, \partial_\nu + A_\nu] \quad (12.21)$$

We can consider the generalization of this theory to a gauge group $SU(N)$ or $U(N)$, where A_μ is now an $N \times N$ matrix. In QCD we also have fermions that transform in the fundamental representation. Here we will do something different: we will add fermions that transform in the adjoint representation. The reason is that we would like to construct a theory that is supersymmetric. Supersymmetry is a powerful tool for checking many predictions of the gauge/gravity duality. The existence of this duality does not rely on supersymmetry but is easier to find a dual pair when we have supersymmetry. Supersymmetry relates bosons and fermions. In a supersymmetric theory the bosons and their fermionic partners are in the same representation of the gauge group. If we simply add a Majorana fermion to the adjoint we get an $\mathcal{N} = 1$ supersymmetric theory. This theory is not conformal quantum mechanically. It has a beta function, as in the theory with no fermions. If instead we add four fermions χ_α and six scalars ϕ^I , all in the adjoint and with special couplings, we get a theory that has maximal supersymmetry, an $\mathcal{N} = 4$ supersymmetric theory [8]. The Lagrangian of this theory is completely determined by supersymmetry and the choice of the gauge group. It has the schematic form

$$\begin{aligned} S = & -\frac{1}{4g_{\text{YM}}^2} \int d^4x \text{Tr} \left(F^2 + 2(D_\mu \Phi^I)^2 + \chi \not{D} \chi + \chi [\Phi, \chi] - \sum_{IJ} [\Phi^I, \Phi^J]^2 \right) \\ & + \frac{\theta}{8\pi^2} \int \text{Tr}(F \wedge F). \end{aligned} \quad (12.22)$$

We have two constants, the coupling constant g_{YM}^2 and the angle θ . All relative coefficients in the Lagrangian are determined by supersymmetry. The fields are all in a single supermultiplet under supersymmetry. This theory is classically and *quantum mechanically* conformal invariant. In other words, its beta function is zero. Thus, unlike QCD, it does not become more weakly coupled as you go to high energies: the coupling is set once and for all. If it is weak, it is weak at all energies; if it is strong, it is strong at all energies. The effective coupling constant is

$$\lambda = g_{\text{YM}}^2 N. \quad (12.23)$$

The extra factor N arises as follows. If we have two fields whose color and anticolor are entangled or summed over then there are N gluons that can be exchanged between them to preserve this entanglement. The theory has an $SO(6)$ or $SU(4)$ R-symmetry that rotates the six scalars into each other and also rotates the fermions. An R-symmetry does not commute with supersymmetry. This is the case here because bosons and fermions are in different representations of $SU(4)$.

Now let us discuss the gravity theory. It is a string theory, which gives rise to a quantum mechanically consistent gravity theory. Since we started from a supersymmetric gauge theory, we also expect to have a supersymmetric string theory. There are well-known supersymmetric string theories in ten dimensions. In particular there is a theory that contains only closed oriented strings, called type IIB. This string theory reduces at long distances to a gravity theory. It is a supergravity theory called, not surprisingly, type-IIB supergravity [9]. This is a theory that contains the metric plus other massless fields required by supersymmetry. In particular, it contains a five-form field strength $F_{\mu_1 \dots \mu_5}$ that is completely antisymmetric in its indices (see Chapter 11). It is also constrained to be self-dual: $F_5 = *F_5$. It is analogous to the two-form field strength $F_{\mu\nu}$ of electromagnetism. In four dimensions we can have charged black hole solutions that involve the metric and the electric (or magnetic) two-form field strength. In particular, the near-horizon solution of an extremal black hole has the geometry $\text{AdS}_2 \times S^2$ with a two-form flux on the AdS_2 (resp. S^2) for an electrically (resp. magnetically) charged black hole. Something similar arises in ten dimensions. There is a solution of the equations of the form $\text{AdS}_5 \times S^5$ with a five-form along both the AdS_5 and S^5 directions. We have both electric and magnetic fields, owing to the self-duality constraint on F_5 . The Dirac quantization condition says that magnetic fluxes on an S^2 are quantized. In the string theory case the flux on the S^5 is also quantized:

$$\int_{S^5} F_5 \propto N. \quad (12.24)$$

This number is the same as the number of colors of the gauge theory.

The equations of motion of ten-dimensional supergravity that are relevant for us follow from the action

$$S = \frac{1}{(2\pi)^7 l_p^8} \int d^{10}x \sqrt{g} (R - F_5^2) \quad (12.25)$$

plus the self-duality constraint $F_5 = *F_5$. The equations of motion relate the radii of AdS_5 and S^5 to N . In fact, we find that both radii are given by $L^4/l_p^4 = 4\pi N$. In string theory we also have the string length, given by $l_s = g_s^{-1/4} l_p$. This sets the string tension, $T = 1/2\pi l_s^2$. The coupling constant g_s determines the interaction strength between strings. It is given by the vacuum expectation value of a massless field of the ten-dimensional theory, $g_s = \langle e^\phi \rangle$. The gravity theory has another massless scalar field, χ . This second field is an axion, with periodicity $\chi \rightarrow \chi + 2\pi$. These two fields are associated with the two parameters g_{YM}^2 and θ in the Lagrangian. It is natural to identify θ with the expectation value, or boundary condition, for χ and g_{YM}^2 with the string coupling g_s : $g_{\text{YM}}^2 = 4\pi g_s$. The precise numerical coefficient can be set by the physics of D-branes [10] or by using the

S-duality of both theories. After doing this, one can write the AdS_5 and S^5 radii in terms of the Yang–Mills quantities

$$\frac{L^4}{l_s^4} = 4\pi g_s N = g_{\text{YM}}^2 N = \lambda, \quad \frac{L^4}{l_p^4} = 4\pi N. \quad (12.26)$$

As we discussed in a general way, in order to have a weakly coupled bulk theory we need $N \gg 1$. In addition, in order to trust the Einstein gravity approximation we need a large effective coupling. Thus, we have the following situation:

$$\begin{aligned} g_{\text{YM}}^2 N \gg 1, & \quad \text{gravity is good, gauge theory is strongly coupled;} \\ g_{\text{YM}}^2 N \ll 1, & \quad \text{gravity is not good, gauge theory is weakly coupled.} \end{aligned}$$

In these two extreme regimes it is easy to do computations using one of the two descriptions.

The 't Hooft limit [4], which gives planar diagrams, corresponds to $N \rightarrow \infty$ with $g_{\text{YM}}^2 N$ fixed. It is sometimes useful to take the 't Hooft limit first and obtain a free string theory in the bulk and then vary the 't Hooft coupling λ from weak to strong, so that we change the AdS radius in string units. The string is governed by a two-dimensional field theory whose target space is AdS (plus the S^5 and some fermionic dimensions). This two-dimensional field theory is weakly coupled if the AdS radius is large and strongly coupled when the radius is small or the gauge theory is weakly coupled. For values of order 1, $g_{\text{YM}}^2 N \sim 1$, one needs to use the full string-theory description or solve the full planar gauge theory.

The $\mathcal{N} = 4$ super Yang–Mills theory has an S-duality symmetry, which exchanges weak and strong coupling. One is tempted to go to strong coupling and then use S-duality in order to get a weakly coupled theory again. This does not work. The bulk theory also has an S-duality symmetry. These two S-duality symmetries are in one-to-one correspondence. So, in order to test whether we can trust the gravity description, first we apply S-duality to both sides to send $g_s < 1$ and then we apply the criterion stated above.

It is interesting to return to the problem of comparing the thermal free energies of the gauge theory and of the gravity theory. This time we will keep track of the numerical coefficients. We consider the field theory in $\mathbb{R}^3 \times S_\beta^1$. The free energy at weak coupling is given by the usual formula,

$$\begin{aligned} -\beta F &= V \int \frac{d^3 k}{(2\pi)^3} \left(n_{\text{bosons}} \log \frac{1}{(1 - e^{-\beta|\vec{k}|})} + n_{\text{fermions}} \log(1 + e^{-\beta|\vec{k}|}) \right) \\ &= \frac{\pi^2}{6} V N^2 T^3, \quad \beta = \frac{1}{T}, \end{aligned} \quad (12.27)$$

where we have used $n_{\text{bosons}} = n_{\text{fermions}} = 8N^2$. At strong coupling we take the Euclidean black brane solution, with $\tau \sim \tau + \beta$,

$$ds^2 = \frac{L^2}{z^2} \left[\left(1 - \frac{z^4}{z_0^4} \right) d\tau^2 + \left(1 - \frac{z^4}{z_0^4} \right)^{-1} dz^2 + dx^2 \right], \quad (12.28)$$

which is simply related to the large-mass limit of (12.6). We can obtain $\beta = \pi z_0$ by demanding that there should be no singularity at $z = z_0$, as usual. The entropy is given by the Bekenstein–Hawking formula [11]

$$S = \frac{\text{area}}{4G_N} = \frac{L^8 V_{S^5}}{4G_{N,10} z_0^3} = \frac{\pi^2}{2} V N^2 T^3. \quad (12.29)$$

From the entropy we can simply compute the free energy. We get

$$-\beta F = \frac{S}{4} = \frac{\pi^2}{8} V N^2 T^3. \quad (12.30)$$

We see that there is a factor of 3/4 difference between (12.30) and (12.27). This does *not* represent a disagreement with AdS/CFT. On the contrary, it is a prediction of how the free energy changes between weak and strong coupling. Under general large- N arguments we expect the free energy to have the form

$$\frac{F(\lambda, N)}{F(\lambda = 0, N)} = f_0(\lambda) + \frac{1}{N^2} f_1(\lambda) + \dots \quad (12.31)$$

We expect that $f_0(\lambda)$ behaves smoothly between $f_0 = 1$ at $\lambda = 0$ and $f_0 = 3/4$ at $\lambda \gg 1$. In fact, the leading corrections from both values have been computed and they go in the direction naively expected [12, 13]. In this example the function f_0 approaches a constant at large λ . There are examples where $f_0 \sim 1/\sqrt{\lambda}$ for large λ , [14, 15].

If we are interested in computing the free energy of super Yang–Mills at strong coupling, we can do it using the gravity result (12.30).

The existence of the S^5 is related to the $SO(6)$ symmetry of the theory. The Killing vectors generating the S^5 isometries give rise to gauge fields in AdS_5 . These are the gauge fields associated with global symmetries that we expected in general. Of course, in other gauge/gravity duality examples one can also have global symmetries that are not associated with a Kaluza–Klein gauge field.

Many observables have a simple geometric description at strong coupling. In fact, the strings (and the branes) of string theory can end on the boundary, and they correspond to various types of operator in the boundary theory. For example, a Wilson loop operator $\text{Tr}[P \exp(\oint_C A)]$ can be computed in terms of a string in the

bulk, that ends on the boundary along the contour \mathcal{C} . At strong coupling the leading approximation is given just by the area of the surface that ends on this contour. At finite coupling we need to perform a worldsheet quantization of this theory, in other words, we need to sum over all surfaces that end on this contour. Certain Wilson loops can be computed exactly using techniques that rely on supersymmetry, confirming the predictions of gauge/gravity duality [16].

The gauge theory contains scalar fields. The potentials for these scalar fields have flat directions. Namely, it is possible to give expectation values to the fields in such a way that the vacuum energy continues to be zero. This spontaneously breaks the conformal symmetry. At high energies the conformal symmetry is restored, but it is broken at low energies. These flat directions correspond to expectation values for the scalar fields that are diagonal matrices. As a simple example we can set $\Phi^1 = \text{diag}(a, 0, \dots, 0)$ and all the other scalar fields to zero. This breaks the gauge group from $U(N) \rightarrow U(1) \times U(N-1)$. In the gravity dual, it corresponds to setting a D3-brane at a position $z \sim 1/a$ in the Poincaré coordinates (12.3). One would expect that the gravitational potential pushes the brane towards the horizon. However, this force is precisely balanced by an electric repulsion provided by the electric five-form field strength. The massless fields living on this D3-brane correspond to the fields in the $U(1)$ factor. The massive W bosons arising from the Higgs mechanism correspond to strings that go from the brane to the horizon. It is interesting that one can write down solutions that correspond to general vacuum expectation values:

$$ds^2 = f^{-1/2}(-dt^2 + d\vec{x}^2) + f^{1/2}(d\vec{y}^2), \quad (12.32)$$

$$f = 4\pi \sum_i \frac{l_p^4}{|\vec{y} - \vec{y}_i|^4}.$$

Here \vec{x} is a three-dimensional vector and \vec{y} is a six-dimensional vector. The \vec{y}_i are related to the vacuum expectation values of the scalar fields, $\vec{\Phi} = \text{diag}(\vec{y}_1, \vec{y}_2, \dots, \vec{y}_N)$. This solution looks like a multicentered black brane. In principle, we cannot trust the solution near a single center since the curvature is very large. However, in situations where we have many coincident centers we can trust the solution. For example, if we break $U(2N)$ into $U(N) \times U(N)$ by giving the expectation value $\Phi^1 = \text{diag}(a, \dots, a, 0, \dots, 0)$, with N as, we can trust the solution everywhere. In the UV, for large $|\vec{y}|$ we have a single AdS geometry, which splits into two AdS throats with smaller radii as we go to lower values of $|\vec{y}|$. This describes the corresponding flow in the gauge theory from the UV to the IR, where we have two decoupled conformal field theories. This is an example of a geometry that is asymptotically AdS near the boundary but is not AdS in the interior.

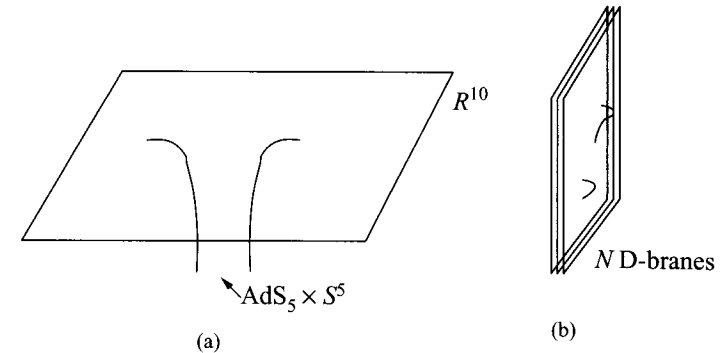


Figure 12.3 (a) The geometry of the black three-brane solution given by (12.32) with (12.33). Far away we have ten-dimensional flat space. Near the horizon we have $\text{AdS}_5 \times S^5$. (b) The D-brane description: D-brane excitations are described by open strings living on them. They can start and end on any of N D-branes so we have N^2 of them. At low energies they give rise to a $U(N)$ gauge theory, $\mathcal{N} = 4$ super Yang–Mills.

It is instructive to consider the solution (12.32) with [17]

$$f = 1 + \frac{4\pi N l_p^4}{|y|^4}. \quad (12.33)$$

This enables us to give a physical derivation of the gauge/gravity duality for this example [1]. This solution goes to ten-dimensional flat space for $|\vec{y}| \gg N^{1/4} l_p$. It represents an extremal black three-brane; see Fig. 12.3. It is extended along 1+3 of the spacetime dimensions, labeled by t and \vec{x} , and it is localized in six of them, labeled by \vec{y} . The near-horizon geometry of this black D3-brane is obtained by going to small values of y and dropping the 1 in (12.33). When the string coupling is very small, $g_s N \ll 1$, this system can be described as a set of N D3-branes. A D3-brane is a solitonic defect that exists in string theory [18]. It is described in terms of an extremely simple string theory construction. This construction tells us that we get $N = 4$ super Yang–Mills at low energies. In fact, it is easy to understand the scalar fields: they come from the motion of the branes in the six transverse dimensions. We can view the gauge fields as arising from supersymmetry. A system of N identical branes is expected to have an ordinary S_N permutation symmetry. However, for these branes this symmetry is enlarged into a full $U(N)$ gauge symmetry. Thus, we have two descriptions for the brane: first as a black brane and second as a set of D-branes. We can now take the low-energy limit of each description. The low-energy limit of the D-brane description gives us the $\mathcal{N} = 4$ $U(N)$ super Yang–Mills theory. The low-energy limit on the gravity side corresponds to going very close to the horizon of the black three-brane. There, the large redshift

factor (i.e., the fact that $f^{-1/2} \rightarrow 0$) gives a very low energy to all the particles living in that near-horizon region. This region is simply $\text{AdS}_5 \times S^5$. Assuming that these two descriptions are equivalent we get the gauge/gravity duality.

12.3 The spectrum of states or operators

In this case we can make a complete correspondence between the massless fields in the bulk and operators in the field theory. The massless ten-dimensional fields can be expanded in spherical harmonics on the S^5 . In addition, they fill supermultiplets. It is interesting to note that we have 32 supercharges in the bulk theory. With this large number of supercharges, a generic supermultiplet would contain states with spins bigger than 2. However, we can have special BPS multiplets with spins only up to 2. Thus all the massless particles of the ten-dimensional theory should be in special BPS multiplets. In ten flat dimensions this is only possible if the particles are massless. In $\text{AdS}_5 \times S^5$, it is only possible if the AdS energy is fixed in terms of the $SO(6)$ charge. In the field theory these are in multiplets that contain the operators $\text{Tr}[\Phi^{I_1}\Phi^{I_2}\dots\Phi^{I_J}]$, where the $SO(6)$ indices are symmetrized and the traces extracted. These operators are in the same representation as the spherical harmonics on S^5 with angular momentum J . Their dimension is $\Delta = J$ at all values of the coupling, because it is a BPS state. Here we see the power of supersymmetry: it allows us to compute these dimensions for all values of the coupling. The above operators correspond to a special field, in the bulk theory, which is a deformation of the S^5 and the five-form field strength. The rest of the supergravity fields are related to this field by supersymmetry.

It is interesting to consider the fate of other operators. As mentioned above, we can consider higher-spin operators. It is simpler to understand the mechanism that gives them a large dimension by considering operators with large charges. Let us take $Z = \Phi^1 + i\Phi^2$ and the operator $\text{Tr}(Z^J)$. If we now add some derivatives, obtaining $\text{Tr}(D_+ Z Z D_+ Z Z \dots)$, then at weak coupling the dimension of the operator is the same independently of the order. As we turn on the coupling, the Hamiltonian or the dilatation operator starts moving these derivatives. In some sense, we can view the chain of Z s as defining a lattice. The fact that only planar diagrams contribute implies that the interactions are short range on this lattice. The range increases as we increase the perturbation theory order: the derivatives start moving around and gain a kinetic energy that depends on their “momentum” along the chain of Z s. More explicitly, the operators that diagonalize the Hamiltonian (or the dilatation operator) have the schematic form

$$\mathcal{O} \sim \sum_l e^{ipl} \text{Tr}(D_+ Z Z^l D_+ Z Z^{J-l-2}) + \dots . \quad (12.34)$$

We have used the cyclicity of the trace to set a derivative in the first position. The ellipses represent the extra terms that can appear when l or $J - l - 2$ are small, and they are needed to quantize the momentum precisely. The momentum p is quantized with an expression of the form $p_n \sim 2\pi n/J + o(1/J^2)$, where the subleading term depends on the extra terms that appear when the two derivatives are near each other. A derivative with zero momentum can be pulled out of the trace and acts as an ordinary derivative. This is just an element of the conformal group and it does not give rise to spin but to ordinary orbital angular momentum in AdS. Thus, in order to get spin we need derivatives that have some momentum and thus some kinetic energy. This kinetic energy increases as λ increases. Thus, for large λ , all the states that have nonzero momentum acquire a large energy. This is especially true for a short string (small J), where the momentum has to be relatively large owing to the momentum quantization condition.

This is just a qualitative argument. The exact computation of these energies requires considerable technology and it employs a deep “integrability” symmetry of the planar gauge theory or of the corresponding string theory [19]. For the lightest spin-4 state (a Konishi multiplet), these energies were computed for any λ in [20]. They behave as expected and are in complete agreement with AdS/CFT. Namely, they go from a value of order one at weak coupling to the strong coupling result, which is $\Delta = 2\lambda^{1/4}$. This strong coupling value is computed as follows. When the AdS radius is large, in string units, the massive string states feel almost as if they were in flat space. The lightest massive string state in flat space has mass $m^2 = 4/l_s^2$ [21]. Using (12.12) and (12.26) this gives $\Delta \sim Lm \sim 2\lambda^{1/4}$.

12.4 The radial direction

One of the crucial elements of gauge/gravity duality is the emergence of an extra “radial” dimension, the z coordinate in (12.3). Let us discuss this in more detail and in some generality. In ordinary physics we are used to particles that typically are massive. Such a particle has a quantum state described by the three spatial positions. Even if it has internal constituents, as does a proton or an atom (ignoring spin), we can describe the particle’s state by simply giving its spatial momentum or position. Of course, its energy is determined by its mass. In a scale-invariant theory we cannot have massive particles. Naively, we would therefore say that all the particles are massless. However, these massless particles interact in a nontrivial way and they cannot be viewed as good asymptotic states. This is true even in large- N gauge theories. However, in such theories we have some weakly interacting excitations. They are objects created by the action of single-trace operators on the vacuum. These objects are characterized by the four-momentum of the operator. Notice that we have one more component of the momentum than for an ordinary

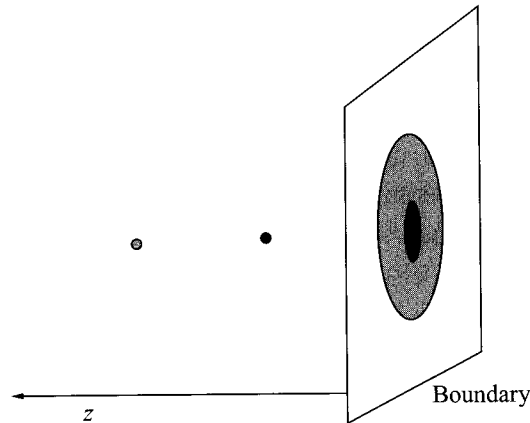


Figure 12.4 The size–radius correspondence. In the CFT we have excitations that have a size. The same object has two different sizes, related by a dilatation. This corresponds to two particles with the same proper size in AdS but located at different values of the radial position of AdS.

massive particle. For a simple operator, such as $\text{Tr}(F_{\mu\nu} F^{\mu\nu})$, the state created at zero coupling with a given four-momentum is a pair of gluons that sum up to the total four-momentum. As we increase the coupling we start producing more and more gluons via a showering process. For these CFT states we can specify arbitrarily the value of $k^2 = k_\mu k^\mu$. In the CFT we can view these as objects that have a position and, in addition, a size. The size is one more continuous variable that we need to specify in order to characterize the state. This is the reason why we need to give four continuous quantum numbers to specify a state in the four-dimensional CFT. These states are not particles in the CFT; they are particles in AdS. We can say that the size of the state in the CFT is related to the position along the radial direction in AdS; see Fig. 12.4. In the coordinates (12.3) the size is proportional to z . In fact, the sizes of particles in AdS provide a simple way to parameterize the representations of the conformal group. In other words, unitary representations of the conformal group correspond, in a one-to-one mapping, to particles, or fields, in AdS together with a boundary condition. This is a completely general mathematical result. We saw this explicitly above for the case of a scalar field. A representation is characterized by the value of the scaling dimension, which in turn determines the mass of the field.

Now, if this is so general, why don't all theories have gravity duals? Well, to some extent we can say that they all do. However, the gravity dual could be a strongly coupled theory in the bulk. Large- N theories give weakly coupled string duals; however, they can be highly stringy. We need some additional conditions that ensure an approximate locality of the interactions in the bulk. In particular, we

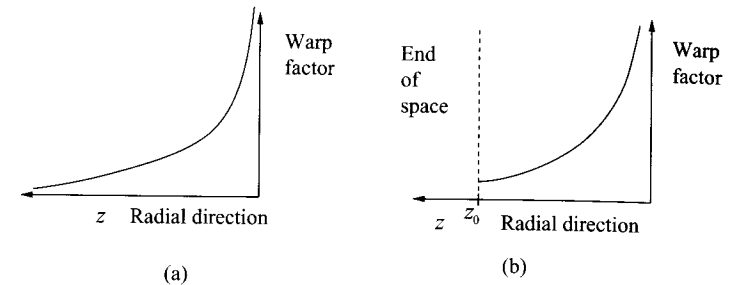


Figure 12.5 (a) The behavior of the warp factor, or gravitational potential, in the AdS case. It rises to infinity at the boundary and goes to zero towards the interior. A particle is pushed towards ever larger values of z . In the field theory this corresponds to an excitation that is expanding in size. (b) Warp factor in a theory with a mass gap. Now the warp factor has a minimum and excitations minimize their energy by sitting at z_0 . Typically the space ends, in a smooth way, at $z = z_0$. In the dual field theory excitations have a preferred size, as does a proton in QCD.

need locality within an AdS radius. A necessary condition is that all the higher-spin fields have large anomalous dimensions. It might be the case that this is a sufficient condition, but this has not been clearly demonstrated from the axioms of conformal field theories. The condition is, of course, expected to hold if we assume bulk locality.

Even though we have focused on conformal field theories, the gauge/gravity duality is also valid for nonconformal theories [22–24]. In those cases the metric has the form $ds^2 = w(z)^2(dx^2 + dz^2)$. As in the conformal case, w rises rapidly when we approach the boundary and the size is also related to the z direction. However, since we do not have a precise scaling symmetry, the physical behavior of boundary objects of different sizes is different. The same happens in the bulk: particles at different positions in the z direction see a geometry with different properties. In some cases the geometric description fails either for small z or for large z . In particular, this happens when the gauge theory coupling becomes weak in the UV or the IR [22]. In such examples the gravity description is a good approximation only for distance scales (or energy scales) such that the gauge theory coupling is large. One can consider quantum field theories with a mass gap. The corresponding gravity configurations are such that the warp factor has a minimum value at some position z_0 . In several examples one finds that the space ends at z_0 because some other dimensions (similar to the S^5 , above) are shrinking smoothly at $z = z_0$. A massive particle minimizes its energy by sitting at z_0 . Therefore its wavefunction is concentrated around z_0 , see Fig. 12.5. The precise shape of the warp factor has to be computed by solving the bulk equations.

References

- [1] J. M. Maldacena, The large N limit of superconformal field theories and supergravity, *Adv. Theor. Math. Phys.* **2** (1998), 231–252 [hep-th/9711200].
- [2] S. S. Gubser, I. R. Klebanov, and A. M. Polyakov, Gauge theory correlators from noncritical string theory, *Phys. Lett.* **B428** (1998), 105–114 [hep-th/9802109].
- [3] E. Witten, Anti-de Sitter space and holography, *Adv. Theor. Math. Phys.* **2** (1998), 253–291 [hep-th/9802150].
- [4] G. 't Hooft, A planar diagram theory for strong interactions, *Nucl. Phys.* **B72** (1974), 461.
- [5] P. Breitenlohner and D. Z. Freedman, Positive energy in anti-de Sitter backgrounds and gauged extended supergravity, *Phys. Lett.* **B115** (1982), 197.
- [6] I. R. Klebanov and E. Witten, AdS/CFT correspondence and symmetry breaking, *Nucl. Phys.* **B556** (1999), 89–114 [hep-th/9905104].
- [7] D. Z. Freedman, S. D. Mathur, A. Matusis, and L. Rastelli, Correlation functions in the CFT(d)/AdS(d+1) correspondence, *Nucl. Phys.* **B546** (1999), 96–118 [hep-th/9804058].
- [8] M. B. Green, J. H. Schwarz, and L. Brink, $N = 4$ Yang–Mills and $N = 8$ supergravity as limits of string theories, *Nucl. Phys.* **B198** (1982), 474–492.
- [9] J. H. Schwarz, Covariant field equations of chiral $N = 2$, $D = 10$ supergravity, *Nucl. Phys.* **B226** (1983), 269.
- [10] J. Polchinski, S. Chaudhuri, and C. V. Johnson, Notes on D-branes, hep-th/9602052.
- [11] S. S. Gubser, I. R. Klebanov, and A. W. Peet, Entropy and temperature of black 3-branes, *Phys. Rev.* **D54** (1996), 3915–3919 [hep-th/9602135].
- [12] S. S. Gubser, I. R. Klebanov, and A. A. Tseytin, Coupling constant dependence in the thermodynamics of $N = 4$ supersymmetric Yang–Mills theory, *Nucl. Phys.* **B534** (1998), 202–222 [hep-th/9805156].
- [13] A. Fotopoulos and T. R. Taylor, Comment on two loop free energy in $N = 4$ supersymmetric Yang–Mills theory at finite temperature, *Phys. Rev.* **D59** (1999), 061701 [hep-th/9811224].
- [14] O. Aharony, O. Bergman, D. L. Jafferis, and J. Maldacena, $N = 6$ superconformal Chern–Simons–matter theories, M2-branes and their gravity duals, *JHEP* **0810** (2008), 091 [arXiv:0806.1218 [hep-th]].
- [15] N. Drukker, M. Marino, and P. Putrov, From weak to strong coupling in ABJM theory, arXiv:1007.3837 [hep-th].
- [16] V. Pestun, Localization of gauge theory on a four-sphere and supersymmetric Wilson loops, arXiv:0712.2824 [hep-th].
- [17] G. T. Horowitz and A. Strominger, Black strings and P-branes, *Nucl. Phys.* **B360** (1991), 197–209.
- [18] J. Polchinski, Dirichlet branes and Ramond–Ramond charges, *Phys. Rev. Lett.* **75** (1995), 4724–4727 [hep-th/9510017].
- [19] N. Beisert *et al.*, Review of AdS/CFT integrability: an overview, arXiv:1012.3982 [hep-th].
- [20] N. Gromov, V. Kazakov, and P. Vieira, Exact spectrum of planar $\mathcal{N} = 4$ supersymmetric Yang–Mills theory: Konishi dimension at any coupling, *Phys. Rev. Lett.* **104** (2010), 211601, arXiv:0906.4240 [hep-th].
- [21] J. Polchinski, *String Theory*, vol. 1, *An Introduction to the Bosonic String*, Cambridge University Press (1998).

- [22] N. Itzhaki, J. M. Maldacena, J. Sonnenschein, and S. Yankielowicz, Supergravity and the large N limit of theories with sixteen supercharges, *Phys. Rev.* **D58** (1998), 046004 [hep-th/9802042].
- [23] E. Witten, Anti-de Sitter space, thermal phase transition, and confinement in gauge theories, *Adv. Theor. Math. Phys.* **2** (1998), 505–532 [hep-th/9803131].
- [24] I. R. Klebanov and M. J. Strassler, Supergravity and a confining gauge theory: duality cascades and chi SB resolution of naked singularities, *JHEP* **0008** (2000), 052 [arXiv:hep-th/0007191 [hep-th]].

13

The fluid/gravity correspondence

VERONIKA E. HUBENY, SHIRAZ MINWALLA,
MUKUND RANGAMANI

13.1 Introduction

In this chapter we will study a particular long-wavelength limit of Einstein's equations with a negative cosmological constant in $d + 1$ dimensions. In such a limit we find that Einstein's equations reduce to the equations of fluid dynamics (relativistic generalizations of the famous Navier–Stokes equations) in d dimensions. While the motivation for our study lies within the AdS/CFT correspondence of string theory, the fluid/gravity correspondence stands on its own and can be viewed as a map between two classic dynamical systems.

13.1.1 Prelude: CFT stress tensor dynamics from gravity

An important consequence of the AdS/CFT correspondence (see Chapter 12) is that the dynamics of the stress(–energy–momentum) tensor in a large class of d -dimensional strongly coupled quantum field theories is governed by the dynamics of Einstein's equations with negative cosmological constant in $d + 1$ dimensions. To begin with, we shall try to provide the reader with some intuition for this statement and argue that searching for a tractable corner of this connection leads one naturally to the fluid/gravity correspondence.

In its most familiar example, the AdS/CFT correspondence asserts that $SU(N)$ $\mathcal{N} = 4$ super Yang–Mills (SYM) theory is dual to type-IIB string theory on $\text{AdS}_5 \times S^5$. It has long been known that in the 't Hooft limit, which involves taking $N \rightarrow \infty$ while keeping the coupling λ fixed, the gauge theory becomes effectively classical. However, it was widely believed that for any nontrivial gauge theory the resulting classical system would be too complicated to be tractable. The remarkable observation of Maldacena in 1997 was that this field theory intuition

is spectacularly wrong. Indeed, not only is the classical system governing $\mathcal{N} = 4$ SYM tractable, it is actually a well-known theory, viz., classical type IIB string theory.

Now, even classically, string theory has complicated dynamics; however, in the strong gauge coupling ($\lambda \rightarrow \infty$) regime, it reduces to the dynamics of type IIB supergravity (by the decoupling of the massive string states). More interestingly, type IIB supergravity on $\text{AdS}_5 \times S^5$ admits several consistent truncations. The simplest and most universal of these is the truncation to Einstein's equations with negative cosmological constant,

$$E_{\mu\nu} \equiv R_{\mu\nu} - \frac{1}{2}R g_{\mu\nu} + \Lambda g_{\mu\nu} = 0, \quad \Lambda \equiv -\frac{d(d-1)}{2L_{\text{AdS}}^2}. \quad (13.1)$$

(Note that the AdS curvature radius L_{AdS} can be scaled away by a change of units; we therefore set L_{AdS} to unity in the rest of this chapter.) Having thus motivated the study of the most beautiful equation of physics, namely Einstein's equation of general relativity, we now confront the question, what does this imply for the field theory?

Recall that according to the AdS/CFT correspondence “dictionary” there is a one-to-one map between single-particle states in the classical Hilbert space of string theory and single-trace operators in the gauge theory. For instance, the bulk graviton maps to the stress tensor of the boundary theory. Taking the collection of such single-trace operators as a whole, one can try to formulate dynamical equations for their quantum expectation values in the field theory. While this can be done in principle, the resulting system is nonlocal in terms of the intrinsic field theory variables themselves.

However, because we can associate the quantum operators (and their expectation values) of the gauge theory at strong coupling with the classical fields of string theory or supergravity, we know that the set of classical equations for which we are looking are just the local equations of type IIB supergravity on $\text{AdS}_5 \times S^5$. This reduction, whilst retaining much interesting physics, still turns out to be too complicated from the field theory perspective. For one thing, the space of single-trace operators is still infinite dimensional (at infinite N), and relatedly attempting to classify the solution space of type IIB supergravity is a challenging problem. However, the fact that on the string side we can reduce the system to (13.1) implies that there is a decoupled sector of stress tensor dynamics in $\mathcal{N} = 4$ SYM at large λ .¹

Actually, there is an infinite number of conformal gauge theories which have a gravitational dual that truncates consistently at the two-derivative level to

¹ While this is always true in two-dimensional field theories, such a decoupling is not generic in higher-dimensional field theories (in fact it is not true of $\mathcal{N} = 4$ Yang–Mills at weak coupling), and is in itself a surprising and interesting fact about the $\mathcal{N} = 4$ dynamics at strong coupling.

Einstein's equations with a negative cosmological constant; $\mathcal{N} = 4$ SYM theory is just a particularly simple member of this class. Thus (13.1) describes the *universal decoupled* dynamics of the stress tensor for an infinite number of different gauge theories. In the first part of this chapter we will focus on the study of this universal sector. Later we will generalize to the study of bulk equations with more fields, thereby obtaining a richer dynamics at the expense of universality.

Given this association between the dynamics of quantum field theory stress tensors with the dynamics of gravity in negatively curved backgrounds, it is natural to ask, can we do more? Can we for instance classify all possible behaviors of stress tensors? On the gravity side we would have to classify all possible solutions to (13.1); this is a laudable goal and various chapters in this book address this question using different approaches. We are going to focus on an aspect that naturally follows from the basic organizing principle of physics: the separation of scales.

It is well known that in many situations in physics (as well as in chemistry, biology, etc.), complicated UV dynamics results in relatively simple IR dynamics. Perhaps the first systematic exposition of this ubiquitous fact was in the context of finite-temperature physics. It has been known for almost 200 years that the dynamics of nearly equilibrated systems at high enough temperatures may be described by an effective theory called hydrodynamics. The key dynamical equation of hydrodynamics is the conservation of the stress tensor,

$$\nabla_a T^{ab} = 0, \quad (13.2)$$

where ∇_a is the covariant derivative compatible with the background metric γ_{ab} on which this fluid lives. As this equation is an autonomous dynamical system involving just the stress tensor, it should lie within the sector of universal decoupled stress tensor dynamics.

Given that the AdS/CFT correspondence asserts that this universal sector is governed by (13.1), we are led to conclude that (13.1) must, in an appropriate high-temperature and long-distance limit to which we refer as the *long-wavelength regime*, reduce to the equations of d -dimensional hydrodynamics. Indeed, this expectation has been independently verified in [1], and the resulting map between gravity and fluid dynamics has come to be known as the *fluid/gravity correspondence*. In particular, the specific fluid dynamical equations dual to long-wavelength gravity in the universal sector have been determined up to the second order in a gradient expansion (cf. section 13.4.4). Given any solution to these fluid dynamical equations, the fluid/gravity map *explicitly* determines a solution to Einstein's equations (13.1) to the appropriate order in the derivative expansion. The solutions in gravity are simply inhomogeneous time-dependent black holes, with slowly varying but otherwise generic horizon profiles.

The main focus of the present chapter is to explain and present the fluid/gravity map at the full nonlinear level, following [1] and subsequent work. The connection between these two systems was established and extensively studied much earlier at the linearized level in the AdS/CFT context (following the seminal work [2]). The first hints of a connection between fluid dynamics and gravity at the nonlinear level were obtained in attempts to construct nonlinear solutions dual to a particular boost-invariant flow [3], which provided inspiration for the fluid/gravity map. Such a map was also suggested by the observation that the properties of large rotating black holes in global AdS space are reproduced by the equations of nonlinear fluid dynamics [4]. We refer the reader to [5] for a list of developments and references.

13.1.2 Preview of the fluid/gravity correspondence

Having provided the reader with a broad, albeit abstract, rationale for associating the dynamics of Einstein's equations with that of a quantum field-theoretic stress tensor, we now provide some specifics that set the stage for our discussion.

According to the gauge/gravity “dictionary”, distinct asymptotically AdS bulk geometries correspond to distinct states in the boundary gauge theory. Pure AdS geometry, i.e., maximally symmetric negatively curved spacetime, corresponds to the vacuum state of the gauge theory. A large² Schwarzschild–AdS black hole corresponds to a thermal density matrix in the gauge theory. This can be easily conceptualized in terms of the late-time configuration to which a generic state evolves: in the bulk, the combined effect of gravity and negative curvature tends to make a generic configuration collapse to form a black hole, which settles down to the Schwarzschild–AdS geometry, while, in the field theory, a generic excitation will eventually thermalize. Note that although the underlying theory is supersymmetric, the correspondence applies robustly to nonsupersymmetric states such as the black holes mentioned above. In this sense, supersymmetry is *not* needed for the correspondence.

On the boundary, the essential physical properties of the gauge theory state (such as local energy density, pressure, temperature, entropy current, etc.) are captured by the expectation value of the *boundary stress tensor*, which in the bulk is related to normalizable metric perturbations about a given state. It can be extracted via a well-defined Brown–York-type procedure [6], as we review later (see (13.39)).

At the risk of being repetitive we urge the reader to note the distinction between the two separate stress tensors that will enter our analysis. In our framework, on the

² Recall that AdS is a space of constant negative curvature, which introduces a length scale, called the AdS scale L_{AdS} , corresponding to the radius of curvature. Black hole size is then measured in terms of this AdS scale; large black holes have horizon radius $r_+ > L_{\text{AdS}}$. We will focus on the large black hole limit $r_+ \gg L_{\text{AdS}}$ and therefore will be considering *planar* Schwarzschild–AdS black holes.

one hand the *bulk* stress tensor appearing on the right-hand side of the bulk Einstein equation is zero if we are interested only in the universal subsector discussed above. On the other hand, the *boundary* stress tensor T^{ab} is nonzero; it is a measure of the normalizable fall-off of the bulk metric at the boundary. Note that the boundary stress tensor does not curve the boundary spacetime in accordance with Einstein's equations since the boundary metric γ_{ab} is non-dynamical and fixed. We will discuss generalizations that allow for nontrivial bulk matter in section 13.6 when we move outside the universal stress tensor sector.

To describe the gravity duals of fluid flows, a useful starting point is the map between the boundary and bulk dynamics in global thermal equilibrium. In the field theory, one characterizes thermal equilibrium by a choice of static frame and a temperature field. On the gravity side, the natural candidates to characterize the equilibrium solution are static (or more generally stationary) black hole spacetimes, as can be seen if one demands regular solutions with periodic Euclidean time circle. The temperature of the fluid is given by the Hawking temperature of the black hole, while the fluid dynamical velocity is captured by the horizon boost velocity of the black hole. For planar Schwarzschild–AdS black holes the temperature grows linearly with horizon size; the AdS asymptotics thus ensures thermodynamic stability as well as providing a natural long-wavelength regime.

Now let us try to move gently away from the equilibrium configuration. Starting with the stationary black hole (namely the boosted planar Schwarzschild–AdS_{d+1}) solution, we wish to use it to build solutions where the fluid dynamical temperature and velocity are slowly varying functions of the boundary directions. Intuitively, this mimics patching together pieces of black holes with slightly different temperatures and boosts in a smooth way so as to get a regular solution of (13.1). In order to obtain a true solution of Einstein's equations, the patching-up procedure cannot be done arbitrarily; one is required at the leading order to constrain the velocity and temperature fields to obey the equations of ideal fluid dynamics.³ Further, the solution itself is corrected order by order in a derivative expansion, a process that likewise corrects the fluid equations. All these steps may be implemented⁴ in detail in a systematic boundary gradient expansion. The final output is a map between solutions to negative-cosmological-constant gravity and the equations of fluid dynamics in one lower dimension, i.e. the fluid/gravity map.

A noteworthy aspect of this construction is that Einstein's equations become tractable, because we are in the long-wavelength regime, without losing nonlinearity. From the boundary standpoint one encounters domains of nearly constant fluid

³ These constraints are actually the radial momentum constraints for gravity in AdS and imply (13.2). In contrast with the conventional ADM decomposition, we imagine foliating the spacetime with timelike leaves and “evolving” into the AdS bulk radially.

⁴ In the technical implementation of this program, it is important that one respects boundary conditions. We require that the bulk metric should asymptote to γ_{ab} (up to a conformal factor) and further be manifestly regular in the part of the spacetime outside any event horizon.

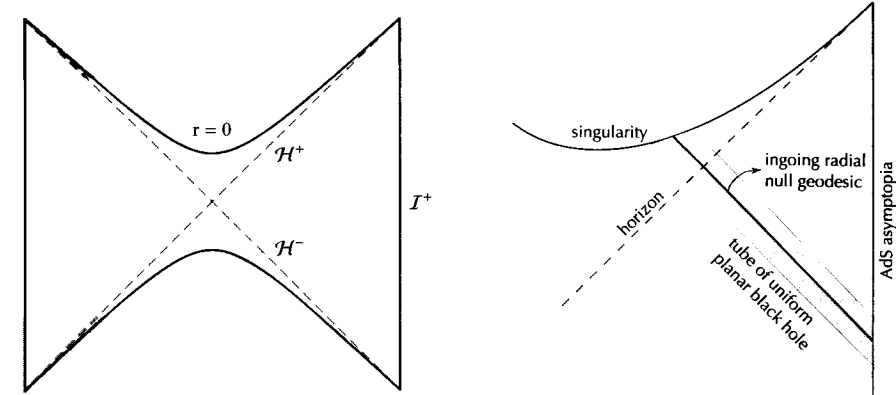


Figure 13.1 Penrose diagram of the uniform planar black hole (13.17) and the causal structure of the spacetimes dual to fluid dynamics, illustrating the tube structure. The broken line in the right-hand figure denotes the future event horizon, while the shaded area indicates the region of spacetime over which the solution is well approximated by a corresponding uniform black hole.

variables; these domains can then be extended radially from the boundary into the bulk and, in each such bulk ‘tube’, illustrated in Fig. 13.1, we are guaranteed to have a solution that is close to the equilibrium form. Lest the reader be led astray, we should note that the solutions we are constructing are perturbative and hence approximate. Nevertheless, they are “generic” slowly varying asymptotically-AdS black hole geometries, with no Killing fields.

A remarkable outcome of the association between generic black holes and fluid flows is that it automatically provides a sensible entropy current with nonnegative divergence for hydrodynamics. On the gravitational side, entropy is naturally associated with the area of the event horizon; by pulling back this area form to the boundary, we can equip our fluid with a canonical entropy current.

We now turn to the technical aspects of the fluid/gravity map. Following a review of fluid dynamics and the perturbative construction of gravitational solutions, we present the main results (in particular the bulk metric and the boundary stress tensor, to second order in boundary derivatives) in section 13.4. The subsequent sections are devoted to describing some implications and extensions of the basic construction.

13.2 Relativistic fluid dynamics

To set the stage, let us start by reviewing fluid dynamics, explicating the use of the gradient expansion as an organizational principle. At high temperatures every nontrivial quantum field theory (and every experimentally realizable system)

equilibrates into a fluid phase, i.e., a translationally invariant phase in which the adiabatic displacement of neighboring elements requires no force.

Weakly interacting fluids are composed of a collection of a large number of long-lived partonic excitations that continually collide. The time and space intervals between the successive collisions of a given parton are called the mean free time t_m and the mean free length ℓ_m , respectively.⁵ Such fluids are characterized by a parton density function in phase space, and the time evolution of this function is governed by the well-known Boltzmann transport equations of statistical physics. These equations have an interesting property: arbitrary initial density functions relax to local thermal equilibrium over a time scale of order the mean free time. In other words, for $t \gg t_m$ the parton distribution in momentum space approximately reduces, at every point x , to an equilibrium distribution. However, the parameters⁶ characterizing this equilibrium configuration, i.e., the temperature field $T(x)$ and fluid velocity field $u^a(x)$, vary on a length scale that is large compared with ℓ_m ; $T(x)$ and $u^a(x)$ are the effective dynamical variables of the system at later times, and their evolution as a function of time is governed by the equations of fluid dynamics.

Now, it turns out that the equations of fluid dynamics may also be derived in a much simpler and more general manner, and so they apply even at strong coupling. The main assumption that underlies fluid dynamics is that systems always equilibrate locally over a finite time scale, to which we will continue to refer as t_m . While this assumption is true of the Boltzmann transport equations, it is believed to hold also for strongly coupled fluids. It follows immediately that $T(x)$ and $u^a(x)$ are the effective variables for dynamics at length and time scales large compared with ℓ_m and t_m . As we will now see, the equations of fluid dynamics follow inevitably from this conclusion.

13.2.1 The equations of fluid dynamics and constitutive relations

The stress tensor in any d -dimensional quantum field theory on a background with metric γ_{ab} obeys the d conservation equations

$$\nabla_a T^{ab} = 0. \quad (13.3)$$

These equations do not constitute a well-defined initial value problem for the stress tensor in general, since in $d \geq 2$ we have more variables (the $\frac{1}{2}d(d+1)$ independent

⁵ In a relativistic system of massless particles, such as $\mathcal{N} = 4$ SYM, $t_m \sim \ell_m$. We will assume this to be the case in our discussions below.

⁶ For simplicity, in this discussion we assume that the system has no conserved charges other than the stress-energy-momentum tensor, and no other Goldstone-like light degrees of freedom. We discuss generalizations below.

components of the stress tensor) than equations.⁷ In the fluid dynamical limit, however, the stress tensor is determined as a function of d variables $T(x)$ and $u^a(x)$. Consequently (13.3), supplemented by a formula for T^{ab} as a function of the thermodynamical fields, constitutes a complete set of dynamical equations. These are the equations of fluid dynamics.

A constitutive relation that expresses T^{ab} as a function of $T(x)$, $u^a(x)$, and their derivatives turns (13.3) into a concrete set of fluid dynamical equations. In thermal equilibrium the stress tensor T^{ab} is given by

$$T^{ab} = (P + \rho) u^a u^b + P \gamma^{ab}, \quad (13.4)$$

where P is the pressure of the fluid and ρ is its energy density. Recall that both ρ and P are known functions of temperature (determined by the thermodynamic equation of state of the fluid). For a fluid in *local* thermal equilibrium, (13.4) generalizes to

$$T^{ab}(x) = [P(x) + \rho(x)] u^a(x) u^b(x) + P(x) \gamma^{ab} + \Pi^{ab}(x), \quad (13.5)$$

where $P(x) = P(T(x))$, $\rho(x) = \rho(T(x))$, and $\Pi^{ab}(x)$ represents the contributions of derivatives of $T(x)$ and $u^a(x)$ to the stress tensor. This dissipative part Π^{ab} may then be expanded as follows:

$$\Pi^{ab} = \sum_{n=1}^{\infty} \ell_m^n \Pi_{(n)}^{ab}, \quad (13.6)$$

where $\Pi_{(n)}^{ab}$ is defined to be of n th order in derivatives of the fluid dynamical fields. Note that the magnitude of $\Pi_{(n)}^{ab}$ relative to the ideal fluid stress tensor is approximately $(\ell_m/L)^n$, where L characterizes the length scale of variation of the temperature and velocity fields; consequently terms at higher values of n are increasingly subdominant in the fluid dynamical limit.

The explicit form of the functions $\Pi_{(n)}^{ab}$ can be derived only from a detailed study of the dynamics of the specific system. However, the allowed forms for constitutive relations are significantly constrained by symmetry and other general considerations. At first order, for instance, it is possible to assert on very general grounds that

$$\begin{aligned} \Pi_{(1)}^{(ab)} &\equiv P_c^a P_d^b \Pi_{(1)}^{cd} - \frac{1}{d-1} P^{ab} P_{cd} \Pi_{(1)}^{cd} = -2\eta \sigma^{ab}, \\ \frac{1}{d-1} \Pi_{(1)}^{ab} P_{ab} - \frac{\partial P}{\partial \rho} (u_a u_b \Pi_{(1)}^{ab}) &= -\zeta \theta, \end{aligned} \quad (13.7)$$

⁷ For the special case of conformal field theories the number of variables is reduced by one, as the trace of the stress tensor vanishes. In this case, at $d = 2$, we have as many variables as equations. This observation underlies the special simplicity of CFTs in $d = 2$.

where

$$P^{ab} \equiv u^a u^b + \gamma^{ab} \quad (13.8)$$

is the projector onto space in the local fluid rest frame,

$$\sigma^{ab} = \nabla^{\langle a} u^{b \rangle} \equiv P^{ac} P^{bd} \left(\nabla_{(c} u_{d)} - \frac{1}{d-1} P_{cd} \theta \right) \quad (13.9)$$

is the fluid shear tensor, $\theta \equiv \nabla_c u^c$ is the expansion, and the superscript angle brackets around the indices a and b denote the symmetric transverse traceless part of the expression. Here η and ζ are arbitrary functions of the temperature referred to as the shear and bulk viscosity, respectively.

Equation (13.7) is a physically complete specification of the constitutive relations at first order even though it leaves $P_c^a \Pi_{(1)}^{cd} u_d$ and one linear combination of $\Pi_{(1)}^{ab} P_{ab}$ and $u_a u_b \Pi_{(1)}^{ab}$ unspecified. The reason is that $T(x)$ and $u^a(x)$ have no intrinsic definition away from equilibrium. All equations of fluid dynamics must be “field redefinition invariant” (invariant under redefinitions of $T(x)$ and $u^a(x)$ that reduce to identity in equilibrium), and it turns out that the left-hand sides in (13.7) are the only field-redefinition-invariant data in $\Pi_{(1)}^{ab}$. The other components of $\Pi_{(1)}^{ab}$ can be modified at will by an appropriate field redefinition and have no physical significance.

The right-hand sides of the two equations in (13.7) represent the most general inequivalent “tensor” and “scalar” data that can be constructed from a single derivative of fluid dynamical fields in a way that is compatible with the conservation equation at first order which implies that $u^a \nabla_a T \propto \theta$.

It is sometimes convenient to address the field redefinition ambiguity by giving the fields $u^a(x)$ and $T(x)$ unambiguous (but arbitrary) meanings. In the so-called ‘Landau frame’ this is achieved by asserting that, at each point,

$$T_b^a(x) u^b(x) = -\rho(x) u^a(x). \quad (13.10)$$

This relation defines u^a by identifying it with the unique timelike eigenvector of the stress tensor at any point and defines the temperature by identifying the corresponding eigenvalue with the energy density.⁸ In the Landau frame, which we adopt for most of this chapter, equations (13.7) simplify to

$$\Pi_{(1)}^{ab} = -2\eta \sigma^{ab} - \zeta \theta P^{ab}. \quad (13.11)$$

As the equations of fluid dynamics are both local and thermodynamical in nature, they must respect a local form of the second law of thermodynamics. It follows that the equations of fluid dynamics must be accompanied by an entropy current

whose divergence is pointwise nonnegative in every conceivable fluid flow. At first order, for a charge-free fluid, the constraints imposed by this requirement comprise a relatively mild set of inequalities on η and ζ . It turns out that the entropy current is constrained to take the form

$$J_s^a = s u^a - \frac{1}{T} u_b \Pi_{(1)}^{ab}, \quad (13.12)$$

where s is the entropy density. It is possible to demonstrate that the current in (13.12) is field redefinition invariant to first order. Note that the second term on the right-hand side of (13.12) vanishes in the Landau frame. Using the Euler relation $\rho + P = sT$ and the Gibbs–Duhem relation $dP = s dT$ of thermodynamics along with the equations of motion, it follows that the divergence of this entropy current is given by

$$\nabla_a J_s^a = -\nabla_a \left(\frac{u_b}{T} \right) \Pi_{(1)}^{ab}. \quad (13.13)$$

Using (13.7) (or more simply (13.11), in the Landau frame), it is easy to verify that positivity of the entropy current requires that $\eta \geq 0$ and $\zeta \geq 0$. At higher orders in the derivative expansion (for uncharged fluids) and even at first order for more complicated fluids (e.g. charged fluids and superfluids) the requirement of positivity of the entropy current imposes more than a set of inequalities on transport coefficients; it forces linear combinations of otherwise arbitrary transport coefficients to vanish [7].

In the rest of this chapter we will be especially interested in the fluid dynamics of conformal field theories. These theories enjoy three key simplifications. First, as they have no dimensionless parameters, the dependence of all physical quantities (e.g. P , ρ , η) on temperature follows on dimensional grounds. In particular,

$$P = \alpha T^d, \quad \rho = (d-1)\alpha T^d, \quad \eta = \eta' T^{d-1}, \quad (13.14)$$

where α and η' are dimensionless constants. Second, the stress tensor in any CFT is necessarily traceless; in particular, it follows from this condition that $\zeta = 0$. Finally, the stress tensor in such theories must transform covariantly under Weyl transformations. This imposes additional restrictions on the stress tensor at higher orders in the derivative expansion. In summary, for a conformal fluid the stress tensor up to first order has the form

$$T^{ab} = \alpha T^d (du^a u^b + \gamma^{ab}) - \eta' T^{d-1} \sigma^{ab}, \quad (13.15)$$

where α and η' are pure numbers and $\eta' \geq 0$.

The constraints on allowed forms of the constitutive relations at higher order are more complicated. The most general allowed equations of second-order fluid dynamics were largely (but perhaps not completely) worked out in [8]. In the

⁸ Note that the equations (13.10) are true in equilibrium.

following we will determine the second-order fluid equations for $\mathcal{N} = 4$ Yang-Mills at strong coupling using the fluid/gravity duality.

13.2.2 The Navier–Stokes scaling limit

An interesting fact about the equations of relativistic (or any other compressible) fluid dynamics is that they reduce to a universal form under a combined low-amplitude and long-wavelength scaling. Consider a uniform fluid at rest, perturbed in such a way that the amplitude of velocity fluctuations is small (scaling as ϵ) and the amplitude of temperature fluctuations is smaller (scaling as ϵ^2). We also require that the wavelength of spatial fluctuations is large (scaling as $1/\epsilon$) and that the temporal scale of these fluctuations is even larger (scaling as $1/\epsilon^2$). We then take the strict $\epsilon \rightarrow 0$ limit. In this limit:

- (i) The fluid is non-relativistic, as all velocities are parametrically smaller than the speed of light.
- (ii) The fluid is incompressible, as all velocities are parametrically smaller than the speed of sound (recall that sound is a compression wave and that fluid flows at velocities smaller than the speed of sound are effectively incompressible).
- (iii) The temporal component of the energy conservation equations reduces, at leading order $\mathcal{O}(\epsilon^2)$ to the continuity equation $\vec{\nabla} \cdot \vec{v} = 0$. We use the symbol \vec{v} for the nonrelativistic spatial velocity.
- (iv) The spatial component of the energy conservation equations reduce at leading order, $\mathcal{O}(\epsilon^3)$, to the famous (nonrelativistic) Navier–Stokes equations

$$\dot{\vec{v}} + \vec{v} \cdot \vec{\nabla} \vec{v} = -\vec{\nabla} P + \nu \nabla^2 \vec{v}, \quad (13.16)$$

with kinematic viscosity

$$\nu = \frac{\eta}{\rho_0 + P_0},$$

where ρ_0 and P_0 are the background values of the density and pressure of the fluid.

Note that the Navier–Stokes equations are homogeneous neither in amplitude of fluctuations (the convective term is nonlinear) nor in derivatives (the viscous term is quadratic in derivatives). All terms retained in (13.16) are equally important in the $\epsilon \rightarrow 0$ limit; in particular, the parameter ν may be set to unity by a uniform rescaling of space and time. In contrast, the viscosities η, ζ give a subleading correction to ideal fluid dynamics in the derivative expansion of relativistic fluid dynamics.

Taking the spatial divergence of (13.16) one sees that the pressure may be obtained in terms of the velocity field *on any given time slice*, so the pressure is not an independent degree of freedom. The initial data of the Navier–Stokes equations comprise just the components of a divergence-free velocity field specified on any time slice. This reduction is not surprising, since the sound waves are being projected out in this limit.

The incompressible Navier–Stokes equations (13.16) describe a wide variety of sometimes extremely complicated phenomena such as turbulence. Despite the fact that these equations have been studied for almost 200 years, their nonlinear phenomenology remains rather poorly understood. It is hoped that the fluid/gravity correspondence will shed a new (geometric) light on some of these issues.

13.3 Perturbative construction of gravity solutions

We have seen that fluid dynamics can be treated systematically as a theory of long-wavelength fluctuations about thermal equilibrium. We are now going to construct gravitational solutions dual to fluid flows by formalizing this intuition: we will set up an algorithmic procedure to construct slowly varying dynamical black hole spacetimes as solutions to (13.1).

13.3.1 Global thermal equilibrium from gravity

The starting point from the gravitational perspective is a solution that corresponds to global thermal equilibrium. For the moment let us consider a conformal field theory on Minkowski space, for which $\gamma_{ab} = \eta_{ab}$. From the gauge/gravity correspondence we know that the dual geometry in the bulk is the planar Schwarzschild–AdS_{d+1} geometry, whose metric in static coordinates (with $x^a = \{t, y^i\}$) is given by

$$ds^2 = -r^2 f(r/T) dt^2 + \frac{dr^2}{r^2 f(r/T)} + r^2 \delta_{ij} dy^i dy^j, \quad f(r) \equiv 1 - \left(\frac{4\pi}{dr} \right)^d. \quad (13.17)$$

This is a one-parameter family of solutions, parameterized in terms of the black hole temperature T , which determines the horizon radius, $r_+ \equiv 4\pi T/d$, where f vanishes. It is easy to generate a d -parameter family of solutions by boosting (13.17) along the translationally invariant spatial directions y^i ; this leads to a solution parameterized by a (normalized) timelike velocity field u^a . The parameters that characterize the bulk solution are precisely the basic hydrodynamical degrees of freedom, viz., the temperature T and velocity u^a of the black hole. It is easy to see that the solution induces, on the Minkowski boundary of the AdS_{d+1} spacetime, a stress tensor that precisely takes the ideal-fluid form (13.4) with thermodynamic

parameters specified by (13.14). The normalization constant α is fixed by the gravitational theory as $\pi^d/(16\pi G_N^{(d+1)})$.

Now we consider this d -parameter family of boosted planar Schwarzschild–AdS _{$d+1$} geometries, each of which holographically maps to an ideal (conformal) fluid living on $\mathbb{R}^{d-1,1}$ (which is endowed with the Minkowski metric). This fluid is in global thermal equilibrium and one should be able to describe the long-wavelength but arbitrary-amplitude fluctuations away from equilibrium via hydrodynamics. This class of fluctuations has a bulk geometric ‘‘avatar’’; we now describe an algorithmic procedure that enables us to construct such asymptotically locally AdS _{$d+1$} black hole geometries, which are generically inhomogeneous and dynamical. This procedure relies crucially on the fact that hydrodynamics, as indeed any effective field theory, can be systematically studied in a gradient expansion.

13.3.2 The perturbation theory

We start by considering perturbations to the ‘‘seed’’ geometry characterizing equilibrium. We take the boosted planar Schwarzschild–AdS _{$d+1$} spacetime (13.17), for convenience rewritten in ingoing coordinates so as to remove the coordinate singularity on the horizon, and replace the parameters u_a and T by functions of the boundary coordinates x^a , obtaining

$$\begin{aligned} ds^2 = & -2u_a(x)dx^a dr - r^2 f(r/T(x))u_a(x)u_b(x)dx^a dx^b \\ & + r^2 P_{ab}(x)dx^a dx^b. \end{aligned} \quad (13.18)$$

Here $f(r)$ is as specified in (13.17) and P_{ab} is found from (13.8) with $\gamma_{ab} = \eta_{ab}$. The metric (13.18), which we henceforth denote as $g_{\mu\nu}^{(0)}(T(x), u^a(x))$, is not a solution to Einstein’s equations. It has, however, two felicitous features: (i) it is regular for all $r > 0$; (ii) if the functions $T(x)$ and $u^a(x)$ are chosen so as to have small derivatives then it can be approximated in local domains by a corresponding boosted black hole solution. These observations lead us to consider an iterative procedure to correct (13.18) order by order in a gradient expansion. We will find, however, that we cannot specify just any slowly varying $T(x)$ and $u^a(x)$ (recall that x^a includes the temporal direction). A true solution to Einstein’s equations is obtained only when the functions $T(x)$ and $u^a(x)$, in addition to being slowly varying, satisfy a set of equations that happen to be precisely the conservation equations of fluid dynamics. Let us record that we have fixed the gauge by setting $g_{rr} = 0$ and $g_{ra} = -u_a$.

Since we want to keep track of the derivatives with respect to the boundary coordinates, it is useful to introduce a book-keeping parameter ε and regard the variables of the problem as functions of rescaled boundary coordinates εx^a . At the

end of the day ε can be set to unity. With this in mind, let us consider the corrections to the ‘‘seed’’ metric in a gradient expansion:

$$\begin{aligned} g_{\mu\nu} &= \sum_{k=0}^{\infty} \varepsilon^k g_{\mu\nu}^{(k)}(T(\varepsilon x), u^a(\varepsilon x)), \\ u^a &= \sum_{k=0}^{\infty} \varepsilon^k u^a{}^{(k)}(\varepsilon x), \quad T = \sum_{k=0}^{\infty} \varepsilon^k T^{(k)}(\varepsilon x), \end{aligned} \quad (13.19)$$

where the corrections $g_{\mu\nu}^{(k)}$, $u^a{}^{(k)}$, and $T^{(k)}$ are to be determined by solving Einstein’s equations to the k th order in the gradient expansion. The ansatz (13.19) is therefore inserted into Einstein’s equations (13.1) and the result expanded in powers of ε .

Let us first examine the resulting structure in an abstract way. For the sake of argument, assume that we have determined $g_{\mu\nu}^{(m)}$ for $m \leq n-1$ and $T^{(m)}$ and $u^a{}^{(m)}$ for $m \leq n-2$. At order ε^n one finds that Einstein’s equations reduce to a set of *inhomogeneous linear differential equations*, whose structure can be written schematically as the operator equation

$$\mathbb{H}[g^{(0)}(T^{(0)}, u^a{}^{(0)})] g^{(n)} = s_n, \quad (13.20)$$

where we have dropped the spacetime indices for notational clarity (cf. [1, 5] for the explicit equations). Since each derivative with respect to x^a is accompanied by a power of ε , it follows that the linear operator \mathbb{H} is constructed purely from the data of the equilibrium Schwarzschild–AdS _{$d+1$} geometry. This means that \mathbb{H} is at most a second-order differential operator with respect to the radial variable r . Moreover, it has to be independent of n . Thus the perturbation theory in ε is ultra-local in the boundary coordinates, implying that we can solve the equations of motion of the bulk spacetime point by point on the boundary!

On the right-hand side of (13.20) we have collected into a source term s_n all order- ε^n terms that do not have explicit radial derivatives. This source term is thus a complicated construct involving contributions from different orders in perturbation theory. It is a local expression of $(n-m)$ th order in boundary derivatives of $T^{(m)}$ and $u^a{}^{(m)}$ for $m \leq n-1$, and determining it is the most substantial part of the computation.

The reader may be puzzled by the following aspect of (13.20): while we have $d(d+1)/2$ equations, we have only $d(d-1)/2$ variables after allowing for the gauge redundancy. This implies that a subset of Einstein’s equations has a distinguished status as constraint equations, while the remainder are the physical dynamical equations.

To understand this, let us examine the differential equations (13.20) by invoking the canonical split of our bulk coordinates $X^\mu = (r, x^a)$. The E_{ra} equations (13.1)

are the momentum-constraint equations for “evolution” in the radial direction. These equations are special in several ways. To start with, they need to be satisfied only on a single r -slice; the “dynamical” equations E_{ab} then ensure that they will be solved on every r -slice. For this reason, it is consistent to study these equations just at the boundary, where they turn out to reduce to the equations of conservation of the boundary stress tensor,

$$\nabla_a T_{(n-1)}^{ab} = 0. \quad (13.21)$$

(See section 13.4.4 for the definition of the boundary stress tensor.) Note that at n th order the equations (13.21) depend only on the boundary stress tensor built from the spacetime metric at order $n - 1$. The reason is that (13.21) has an explicit boundary derivative, which carries its own effective power of ε . The net upshot is that the unknown metric $g^{(n)}$ does not enter the equations (13.21); the operator \mathbb{H} in (13.20) vanishes for these solutions. Hence (13.21) is instead a constraint on the solution already obtained at one order lower in perturbation theory. As we will see below, the solution for $g^{(n)}$ of the dynamical equations at each order in perturbation theory is uniquely obtained in terms of the previous-order solution and so, ultimately, in terms of the velocity and temperature fields that enter the starting ansatz (the zeroth-order term in perturbation theory). Consequently, (13.21) constrains the starting velocity and temperature fields, and it turns out to be the equation of boundary fluid dynamics.

The remaining equations E_{rr} (the “Hamiltonian constraint” for radial evolution) and E_{ab} are dynamical equations; the operator \mathbb{H} is a second-order differential operator in r . Exploiting the spatial rotational symmetry of the seed solution, these equations can be decoupled and solved by quadratures:

$$g^{(n)} = \text{particular}(s_n) + \text{homogeneous}(\mathbb{H}). \quad (13.22)$$

A unique solution to the dynamical equations is obtained upon specification of the boundary conditions, i.e., normalizability at infinity and regularity in the interior for all $r > 0$. These turn out to define the solution completely,⁹ and one ends up with a regular black hole geometry at each given order in the ε -expansion.

In summary, at any order in the perturbative expansion one solves the constraint equations, enforcing fluid dynamical equations on the “initial” data. One then solves for the corrected metric. This correction feeds into the constraint equations, giving the corrected equations of fluid dynamics and so on. The process may be iterated to any desired order, thereby yielding a systematic derivative expansion of the equations of fluid dynamics.

⁹ Apart from fact that the operator \mathbb{H} has zero modes, which are accounted for by redefinition of the background values of T and u^a .

13.4 Results at second order

Having seen in an abstract form the iterative procedure that perturbatively corrects the “seed” metric to obtain a solution to Einstein’s equations at arbitrary order in the gradient expansion, we now turn to the results of this construction (for now still considering energy–momentum transport only on the boundary). While our discussion so far has been restricted to the case of a flat boundary metric $\gamma_{ab} = \eta_{ab}$, the observation we made about the ultra-locality of the perturbation theory allows us to generalize immediately to slowly varying curved boundary metrics. Given a metric γ_{ab} on the boundary, we can exploit the freedom to pass over to a Gaussian normal coordinate chart about the point under consideration and account for the curvatures that begin to arise at second order in the ε expansion by computing the appropriate source terms. We will therefore present the results below for this more general setting. Before we do so, we will take the opportunity to review a beautiful technical framework developed in [9] that simplifies the results for conformal fluids.

13.4.1 Weyl-covariant formalism

The vacuum AdS_{d+1} spacetime is dual to the vacuum state of a conformal field theory. If we are interested in a hydrodynamic description of the latter on a background manifold \mathcal{B}_d then, rather than focusing on the metric γ_{ab} of this geometry, we can consider the conformal class of metrics $(\mathcal{B}_d, \mathcal{C})$. On this conformal class there is a natural derivative operator, defined through a Weyl connection, which keeps track efficiently of the Weyl transformation properties of various operators. This is all the more natural in the context of fluid dynamics, where there is a distinguished vector field, the velocity u^a , defined to be the (normalized) timelike eigenvector of the stress tensor.

Let us first start with local Weyl rescalings of the boundary metric, which transforms homogeneously, i.e.,

$$\gamma_{ab} = e^{2\phi} \tilde{\gamma}_{ab} \quad \Leftrightarrow \quad \gamma^{ab} = e^{-2\phi} \tilde{\gamma}^{ab}. \quad (13.23)$$

We will call a tensor \mathcal{Q} with components $\mathcal{Q}_{a_1 \dots a_n}^{b_1 \dots b_m}$ conformally covariant and of weight w if it transforms homogeneously under Weyl rescalings of the metric, i.e., if $\mathcal{Q} = e^{-w\phi} \tilde{\mathcal{Q}}$ under (13.23). The velocity field u^a transforms as a weight-1 tensor while the stress tensor T^{ab} of a conformal fluid has weight $d + 2$ in d spacetime dimensions.

One defines a class of torsionless connections, called Weyl connections, characterized by a connection one-form \mathcal{A}_a , whose associated covariant derivative ∇^{Weyl} captures the fact that the metric transforms homogeneously under conformal

transformations (with weight -2). In particular, for every metric in the conformal class \mathcal{C} , we have

$$\nabla_a^{\text{Weyl}} \gamma_{bc} = 2\mathcal{A}_a \gamma_{bc}. \quad (13.24)$$

Given this derivative structure, we can define a Weyl covariant derivative $\mathcal{D}_a = \nabla_a^{\text{Weyl}} + w\mathcal{A}_a$ that is metric compatible and whose action on tensors transforming homogeneously with weight w (i.e., $\mathcal{Q}_{b...}^{a...} = e^{-w\phi} \tilde{\mathcal{Q}}_{b...}^{a...}$) is given by

$$\begin{aligned} \mathcal{D}_c \mathcal{Q}_{b...}^{a...} &\equiv \nabla_c \mathcal{Q}_{b...}^{a...} + w \mathcal{A}_c \mathcal{Q}_{b...}^{a...} \\ &+ (\gamma_{cd} \mathcal{A}^d - \delta_c^a \mathcal{A}_d - \delta_d^a \mathcal{A}_c) \mathcal{Q}_{b...}^{d...} + \dots \\ &- (\gamma_{cb} \mathcal{A}^d - \delta_c^d \mathcal{A}_b - \delta_b^d \mathcal{A}_c) \mathcal{Q}_{d...}^{a...} - \dots. \end{aligned} \quad (13.25)$$

The connection has been defined in such a way that the Weyl covariant derivative of a conformally covariant tensor transforms homogeneously, with the same weight as the tensor itself.

In hydrodynamics we will require that the Weyl-covariant derivative of the fluid velocity be transverse and traceless,

$$u^a \mathcal{D}_a u^b = 0, \quad \mathcal{D}_a u^a = 0; \quad (13.26)$$

this enables one to determine uniquely the connection one-form \mathcal{A}_a as the distinguished vector field

$$\mathcal{A}_a = u^c \nabla_c u_a - \frac{1}{d-1} u_a \nabla_c u^c = a_a - \frac{1}{d-1} \theta u_a \quad (13.27)$$

built from the fluid velocity field.

One can rewrite the various quantities appearing in the gradient expansion of the stress tensor in this Weyl-covariant notation. For instance, at first order in derivatives the shear and vorticity are derived from the velocity field:

$$\sigma^{ab} = \mathcal{D}^{[a} u^{b]}, \quad \omega^{ab} = -\mathcal{D}^{[a} u^{b]}. \quad (13.28)$$

Both have weight $w = 3$. The fluid dynamical equations, expressing stress tensor conservation, are simply $\mathcal{D}_a T^{ab} = 0$ in this Weyl-covariant language (they are equivalent to (13.3) since (13.25) with $w = d+2$ gives $\mathcal{D}_a T^{ab} = \nabla_a T^{ab} + T_a^a \mathcal{A}^b$ and the conformal fluid stress tensor must be traceless).

13.4.2 Generic asymptotically AdS black hole metric

We now have at our disposal all the technical machinery necessary to present the results for the gravity dual of nonlinear fluid dynamics. By a suitable choice of

gauge (a slight generalization of the Eddington–Finkelstein coordinates), one can express the bulk metric $g_{\mu\nu}$ in the form

$$ds^2 = -2u_a(x) dx^a (dr + \mathfrak{V}_b(r, x) dx^b) + \mathfrak{G}_{ab}(r, x) dx^a dx^b, \quad (13.29)$$

where the fields \mathfrak{V}_a and \mathfrak{G}_{ab} are functions of r and x^a that admit an expansion in the boundary derivatives. In the parameterization used in [10] one finds that the metric functions are given up to second order in derivatives as follows:

$$\begin{aligned} \mathfrak{V}_a &= r\mathcal{A}_a - \mathcal{S}_{ac} u^c - \mathfrak{v}_1 \left(\frac{r}{T} \right) P_a^b \mathcal{D}_c \sigma_b^c \\ &+ u_a \left\{ \frac{1}{2} r^2 f \left(\frac{r}{T} \right) + \frac{1}{4} \left[1 - f \left(\frac{r}{T} \right) \right] \omega_{cd} \omega^{cd} + \mathfrak{v}_2 \left(\frac{r}{T} \right) \frac{\sigma_{cd} \sigma^{cd}}{d-1} \right\}, \end{aligned} \quad (13.30)$$

$$\begin{aligned} \mathfrak{G}_{ab} &= r^2 P_{ab} - \omega_a^c \omega_{cb} + 2 \left(\frac{r}{T} \right)^2 \mathfrak{g}_1 \left(\frac{r}{T} \right) \left[\frac{4\pi T}{d} \sigma_{ab} + \mathfrak{g}_1 \left(\frac{r}{T} \right) \sigma_a^c \sigma_{cb} \right] \\ &- \mathfrak{g}_2 \left(\frac{r}{T} \right) \frac{\sigma_{cd} \sigma^{cd}}{d-1} P_{ab} - \mathfrak{g}_3 \left(\frac{r}{T} \right) \left(\mathfrak{T}_{1ab} + \frac{1}{2} \mathfrak{T}_{3ab} + 2 \mathfrak{T}_{2ab} \right) \\ &+ \mathfrak{g}_4 \left(\frac{r}{T} \right) (\mathfrak{T}_{1ab} + \mathfrak{T}_{4ab}). \end{aligned}$$

Here

$$\mathcal{S}_{ab} = \frac{1}{d-2} \left(\mathcal{R}_{ab} - \frac{\mathcal{R}}{2(d-1)} \gamma_{ab} \right)$$

is the Schouten tensor of the boundary metric, where the Weyl-covariant curvature tensors are

$$\begin{aligned} \mathcal{R}_{ab} &= R_{ab} - (d-2)(\nabla_a \mathcal{A}_b + \mathcal{A}_a \mathcal{A}_b - \mathcal{A}^2 \gamma_{ab}) - g_{ab} \nabla_c \mathcal{A}^c - \mathcal{F}_{ab}, \\ \mathcal{R} &\equiv \mathcal{R}_a^a = R - 2(d-1) \nabla_c \mathcal{A}^c + (d-2)(d-1) \mathcal{A}^2, \end{aligned} \quad (13.31)$$

with $\mathcal{F}_{ab} \equiv \nabla_a \mathcal{A}_b - \nabla_b \mathcal{A}_a$. As well as the shear and vorticity tensors (13.28) constructed from the fluid velocity, we also encounter four of the five second-order tensors that form a Weyl-covariant basis,

$$\begin{aligned} \mathfrak{T}_1^{ab} &= 2u^c \mathcal{D}_c \sigma^{ab}, & \mathfrak{T}_2^{ab} &= C^{acbd} u_c u_d, \\ \mathfrak{T}_3^{ab} &= 4\sigma^{c[a} \sigma_c^{b]}, & \mathfrak{T}_4^{ab} &= 2\sigma^{c[a} \omega_c^{b]}, & \mathfrak{T}_5^{ab} &= \omega^{c[a} \omega_c^{b]}. \end{aligned} \quad (13.32)$$

Note that the tensor \mathfrak{G}_{ab} is clearly transverse since it is built out of operators that are orthogonal to the velocity, and it can be inverted via the relation $(\mathfrak{G}^{-1})^{ac} \mathfrak{G}_{cb} = P_a^a$.

The induced metric on the boundary in these coordinates takes the form

$$\gamma_{ab} = \lim_{r \rightarrow \infty} \frac{1}{r^2} (\mathfrak{G}_{ab} - 2u_{(a} \mathfrak{V}_{b)}) , \quad (13.33)$$

which, crucially, is used to raise and lower the boundary indices.

Finally, the various functions \mathfrak{g}_i and \mathfrak{v}_i appearing in the metric are given in terms of definite integrals once one has inverted the operator \mathbb{H} :

$$\begin{aligned} \mathfrak{g}_1(y) &= \int_y^\infty d\xi \frac{\xi^{d-1} - 1}{\xi(\xi^d - 1)} , \\ \mathfrak{g}_2(y) &= 2y^2 \int_y^\infty \frac{d\xi}{\xi^2} \int_\xi^\infty d\xi \xi^2 \mathfrak{g}'_1(\xi)^2 , \\ \mathfrak{g}_3(y) &= y^2 \int_y^\infty d\xi \frac{\xi^{d-2} - 1}{\xi(\xi^d - 1)} , \\ \mathfrak{g}_4(y) &= y^2 \int_y^\infty \frac{d\xi}{\xi(\xi^d - 1)} \int_1^\xi d\xi \xi^{d-3} \left(1 + (d-1)\xi \mathfrak{g}_1(\xi) + 2\xi^2 \mathfrak{g}'_1(\xi) \right) \\ \mathfrak{v}_1(y) &= \frac{2}{y^{d-2}} \int_y^\infty d\xi \xi^{d-1} \int_\xi^\infty d\xi \frac{\xi - 1}{\xi^3(\xi^d - 1)} , \\ \mathfrak{v}_2(y) &= \frac{1}{2y^{d-2}} \int_y^\infty \frac{d\xi}{\xi^2} \left[1 - \xi(\xi - 1) \mathfrak{g}'_1(\xi) - 2(d-1)\xi^{d-1} \right. \\ &\quad \left. + (2(d-1)\xi^d - (d-2)) \int_\xi^\infty d\xi \xi^2 \mathfrak{g}'_1(\xi)^2 \right] . \end{aligned} \quad (13.34)$$

The asymptotic behavior of these functions $\mathfrak{g}_i(r/T)$ and $\mathfrak{v}_i(r/T)$ is important for the stress tensor computation of section 13.4.4 and can be found in [10].

13.4.3 Event horizon and entropy current

The metric (13.29), (13.30) solves Einstein's equations to second order in the gradient expansion, provided that the first-order stress tensor (which takes the form (13.15) with coefficients extracted from the first-order bulk metric and given explicitly below in section 13.4.4) satisfies the hydrodynamic conservation equations. While this already establishes a firm connection between solutions of Einstein's equations and those of fluid dynamics (in one lower dimension), it is imperative to establish that the bulk geometry that we describe is regular everywhere outside the curvature singularity at $r = 0$.

Although one can utilize the behavior of the metric functions and iteratively argue that the sources are regular order by order in perturbation theory, it is convenient to establish once and for all that what one has constructed is a black hole spacetime with a regular event horizon. Doing this involves ascertaining the location of the event horizon. A priori, this sounds formidable, especially given that explicit solution is contingent on having solved the fluid equations. Moreover, as is well known, the event horizon is a teleological concept (it is the boundary of the past of future null infinity) whose determination requires one to know the entire future history of the spacetime. However, with the one key assumption of late-time relaxation, which is natural from fluid dynamics, it turns out to be possible to determine the location of the event horizon *locally* within our gradient expansion. Apart from showing the regularity of the event horizon, this has the additional virtue of enabling us to determine a natural entropy current for fluid dynamics [11].

Since generic flows of dissipative fluids tend to approach global equilibrium at late times, it follows that the corresponding event horizon has to approach the radial position determined by the local late-time temperature of the fluid. In particular, we look for the null co-dimension-1 surface given by the equation $S_{\mathcal{H}}(r, x) = r - r_{\mathcal{H}}(x) = 0$ with the correct asymptotics. The function $r_{\mathcal{H}}(x)$ should be parameterized within the gradient expansion

$$r_{\mathcal{H}}(x) = \frac{4\pi T(x)}{d} + \sum_k \varepsilon^k r_{(k)}(x).$$

The corrections $r_{(k)}(x)$ are determined by solving the null condition $g^{\mu\nu} \partial_\mu S_{\mathcal{H}} \partial_\nu S_{\mathcal{H}} = 0$. The resulting equations are algebraic for $r_{(k)}$ and, to second order in the gradients, one finds that, for the solution (13.29)–(13.34),

$$r_{\mathcal{H}}(x) = \frac{4\pi T(x)}{d} + \frac{d}{4\pi T(x)} (\aleph_1 \sigma_{ab} \sigma^{ab} + \aleph_2 \omega_{ab} \omega^{ab} + \aleph_3 \mathcal{R}) \quad (13.35)$$

with

$$\begin{aligned} \aleph_1 &= \frac{2(d^2 + d - 4)}{d^2(d-1)(d-2)} - \frac{2\mathfrak{v}_2(1)}{d(d-1)} , \\ \aleph_2 &= -\frac{d+2}{2d(d-2)} , \quad \aleph_3 = -\frac{1}{d(d-1)(d-2)} . \end{aligned} \quad (13.36)$$

This indeed establishes that the solutions to second order constructed in section 13.4.2 qualify to be called inhomogeneous dynamical black holes.

Note that, in general, beyond the leading order the horizon position and generators are not simply given by the corresponding fluid temperature and velocity (for example, while the horizon generators must be vorticity-free, ω_{ab} need not vanish for the boundary fluid). In some sense, while the black hole horizon is distinguished

in the bulk, the physics appears simpler when expressed in terms of the fluid data living on the boundary.

Having determined the event horizon of the gravity solution, we immediately have access to an important hydrodynamic quantity, viz., the *entropy current*. For a black hole spacetime it is natural to view the area of the event horizon as an entropy in the sense of Bekenstein [12] and Hawking [13]. In fact, by suitably foliating the event horizon with spatial slices (propagated forward by the null generator), we can equivalently talk about an area $(d-1)$ -form $a_{\mathcal{H}}$ on these slices. Since we imagine the dual fluid as living on the boundary of the spacetime, it is natural to pull back this area-form out to the boundary. A canonical choice is to pull back along radially ingoing null geodesics [11], and this is quite easy to implement for the metric (13.29), where the lines of $x^a = \text{constant}$ are precisely such geodesics. We then have a $(d-1)$ -form on the boundary that can be dualized to a one-form or equivalently a current J_s^a , which is the entropy current on the boundary. Not only does this definition agree with the equilibrium notion of entropy of the fluid but also, thanks to the area theorem of black hole horizons, we are immediately guaranteed that this current has a manifestly nonnegative divergence as demanded by the second law. The hydrodynamic entropy current takes the general form

$$\begin{aligned} J_s^a &= su^a + \frac{sd^2}{(4\pi T)^2} u^a (A_1 \sigma_{cd} \sigma^{cd} + A_2 \omega_{cd} \omega^{cd} + A_3 \mathcal{R}) \\ &\quad + \frac{sd^2}{(4\pi T)^2} (B_1 \mathcal{D}_c \sigma^{ac} + B_2 \mathcal{D}_c \omega^{ac}) + \dots, \end{aligned} \quad (13.37)$$

where s is the entropy density and $A_{1,2,3}, B_{1,2}$ are a priori arbitrary numerical coefficients. While $\mathcal{D}_a J_s^a \geq 0$ only demands that $B_1 + 2A_3 = 0$, the gravity solution (13.29) determines the coefficients in (13.37) explicitly. In particular, we obtain

$$\begin{aligned} s &= \frac{1}{4G_N^{(d+1)}} \left(\frac{4\pi T}{d} \right)^{d-1}, \quad A_1 = \frac{2}{d^2} (d+2) - \left(\frac{1}{2} \mathfrak{g}_2(1) + \frac{2}{d} \mathfrak{v}_2(1) \right), \\ A_2 &= -\frac{1}{2d}, \quad B_1 = -2A_3 = \frac{2}{d(d-2)}, \quad B_2 = \frac{1}{d-2}. \end{aligned} \quad (13.38)$$

We should note here that there is an ambiguity in pulling back the area-form from the event horizon to the boundary since one can supplement the pull-back map with a boundary diffeomorphism, and this affects the coefficient A_1 above. Because this just relabels boundary points in the gradient expansion, one is tempted to think of this ambiguity as unphysical. However, it is rather curious that, if one tries to pull back the area form from quasilocal horizons, one encounters a shifted

value of A_1 [14], which suggests that there is perhaps more to this ambiguity than meets the eye.

13.4.4 Stress tensor of dissipative fluid

Given an asymptotically locally AdS_{d+1} metric, one can construct a quasilocal boundary tensor that is manifestly conserved and is associated with the stress-energy-momentum tensor of the conformal field theory [6, 15]. To perform the computation one regulates the bulk spacetime by introducing an explicit cut-off at $r = r_\infty$. The boundary stress tensor is given in terms of the extrinsic curvature K_{ab} of this surface, defined in terms of its unit outward-pointing normal n^a as $K_{ab} = \gamma_{ac} \nabla^c n_b$. In addition to the extrinsic curvature, one also has contributions from the counter-terms necessary to obtain a finite boundary stress tensor. Denoting the curvatures of the boundary metric by ${}^\gamma R$ etc., this tensor is given (to second order) by

$$\begin{aligned} T_{ab} &= \lim_{r_\infty \rightarrow \infty} \frac{-r_\infty^d}{8\pi G_N^{(d+1)}} \left[K_{ab} - K \gamma_{ab} + (d-1)\gamma_{ab} \right. \\ &\quad \left. - \frac{1}{d-2} \left({}^\gamma R_{ab} - \frac{1}{2} {}^\gamma R \gamma_{ab} \right) \right]. \end{aligned} \quad (13.39)$$

For the gravity duals to fluid dynamics constructed in section 13.4.2, one finds that the boundary stress tensor takes the form (13.5) with the dissipative parts, at first and second order, given by this gravitational construction as

$$\begin{aligned} \Pi_{(1)}^{ab} &= -2\eta \sigma^{ab}, \\ \Pi_{(2)}^{ab} &= \tau_\pi \eta \mathfrak{T}_1^{ab} + \kappa \mathfrak{T}_2^{ab} + \lambda_1 \mathfrak{T}_3^{ab} + \lambda_2 \mathfrak{T}_4^{ab} + \lambda_3 \mathfrak{T}_5^{ab}, \end{aligned} \quad (13.40)$$

where the tensors \mathfrak{T}_i^{ab} were defined earlier in (13.32). With the tensor structure determined, one is just left with determining the six transport coefficients, η , τ_π , κ , and λ_i for $i = \{1, 2, 3\}$; these completely characterize the flow of a nonlinear viscous fluid with a gravitational dual. The transport coefficients for conformal fluids in a d -dimensional boundary turn out to be

$$\begin{aligned} \eta &= \frac{1}{16\pi G_N^{(d+1)}} \left(\frac{4\pi}{d} T \right)^{d-1}, \\ \tau_\pi &= \frac{d}{4\pi T} \left[1 + \frac{1}{d} \text{Harmonic} \left(\frac{2}{d} - 1 \right) \right], \quad \kappa = \frac{d}{2\pi(d-2)} \frac{\eta}{T}, \\ \lambda_1 &= \frac{d}{8\pi} \frac{\eta}{T}, \quad \lambda_2 = \frac{1}{2\pi} \text{Harmonic} \left(\frac{2}{d} - 1 \right) \frac{\eta}{T}, \quad \lambda_3 = 0, \end{aligned} \quad (13.41)$$

where $\text{Harmonic}(x)$ is the harmonic number function. Setting $d = 4$ in the above expressions and using the fact that $\text{Harmonic}(-\frac{1}{2}) = -2 \log(2)$ together with the replacement

$$\frac{1}{16\pi G_N^{(5)}} = \frac{N^2}{8\pi^2},$$

one can obtain the transport coefficients for $SU(N)$ $\mathcal{N} = 4$ super Yang–Mills theory [1, 16]. This has been used for real data analysis from e.g. the Relativistic Heavy Ion Collider (RHIC).

One immediate consequence of (13.41) and (13.38) is that our fluid saturates the famous bound on the viscosity-to-entropy density ratio, $\eta/s \geq 1/(4\pi)$, [17]. This bound is saturated by a large class of two-derivative theories of gravity, and it is indeed experimentally satisfied by all presently known systems in nature. Intriguingly, cold atoms at unitarity and quark–gluon plasmas both come near to saturating this bound [18]. Its status in more general theories is currently under active debate [19].

Moreover, (13.41) reveals further intriguing relations between the coefficients that hint at the specific nature of any conformal fluid which admits a gravitational dual. For example, the result $\lambda_3 = 0$ is universal but nontrivial from the fluid standpoint. We also see that $2\eta\tau_\pi = 4\lambda_1 + \lambda_2$ for all d ; this was shown to hold quite generally in a large class of two-derivative theories of gravity (including matter couplings) [20].

13.5 Specific fluid flows and their gravitational analogue

The construction presented above can be generalized in many interesting ways; however, before indicating the most important of these in section 13.6, we first pause to discuss some special cases of the framework explained in the preceding section. One reason to discuss these special cases is that, while we have demonstrated the existence of a map from the equations governing fluid dynamics to those governing the dynamics of gravity, we have not at any stage solved the fluid equations explicitly. The felicitous feature of our construction was the ultra-locality along the boundary directions that allowed us to implement the construction in terms of local solutions to the conservation equations. Construction of novel fluid flows and the generic behavior of the relativistic conservation equations are interesting (and perhaps hard) questions. Nevertheless there are some corners in which we can gain an analytic control that serves not only as a check that the fluid/gravity solution set is nonempty but also provides a point of contact with previous studies of the hydrodynamic regime in the AdS/CFT literature.

13.5.1 Linearized setting: quasinormal modes

Above we established a map between any solution of the equations of fluid dynamics and long-wavelength solutions of Einstein gravity with a negative cosmological constant. In order to find explicit gravitational solutions we need a class of explicit solutions to the equations of fluid dynamics. In this subsection and the next we will study such examples.

It is of course easy to solve the equations of fluid dynamics, derived above, when they are linearized about static equilibrium. Utilizing translational invariance, we search for solutions of the form

$$u^a = \delta_t^a + \delta_j^a \delta v^j e^{i(\omega t + k^i y_i)}, \quad T = T_0 + \delta T e^{i(\omega t + k^i y_i)},$$

with purely spatial velocity fluctuations δv^j . The resulting linear equations require that the matrix of coefficients $M(\omega, k)$ annihilates the length- d column vector with entries δv^i and δT . So the spectrum $\omega(k)$ is obtained as the roots of the d th-order polynomial $\det(M) = 0$. At leading (ideal-fluid) order, the d roots to this equation turn out to be $\omega = \pm k/\sqrt{d-1}$ (the sound modes of the fluid) and $\omega = 0$ with degeneracy $d-2$ (the shear modes of the fluid). These modes and their corresponding eigenvectors receive corrections at higher orders in the derivative expansion; in particular the shear modes pick up a nontrivial k -dependence, $\omega \propto ik^2$, at first order. The explicit solutions are easily determined (see [1]). Employing the fluid/gravity map then yields explicit linearized solutions of the Einstein equations (13.1) about the planar black hole background, whose study in fact predates the fluid/gravity map by almost 10 years.

The spectral problem of the linearized fluctuations about a black hole solution is of course a well-studied topic [21]. It is known that, owing to the presence of a horizon, black holes admit no normal modes. Instead, by imposing regularity at the future event horizon one finds quasinormal modes, i.e., modes that have complex frequencies characterizing the decay of perturbations at late times. Mathematically these are related to the poles of the retarded Green's function computed in the black hole background.

In terms of the gauge/gravity perspective, such quasinormal modes describe the time scale for return to thermal equilibrium in the field theory [22]. Asymptotically AdS black holes host an infinite family of quasinormal modes. All except d of these are “massive”; their frequency remains finite (and has a finite imaginary part or decay rate $\propto T$) even in the limit $k \rightarrow 0$. However, planar black holes admit exactly d special “massless” quasinormal modes. These so-called hydrodynamic modes can have arbitrarily low frequency at long spatial wavelengths and therefore fall within the long-wavelength regime. These are precisely the sound and shear modes described above.

The fact that the dispersion relations of the massless quasinormal modes agree with the hydrodynamic dispersion relations was first demonstrated in the pioneering works [23, 24], in which the Schwarzschild–AdS quasinormal modes were mapped to sound and shear modes of the dual field theory (perturbed from thermal equilibrium).

13.5.2 Rotating black holes in global AdS space

A second class of examples that accord one analytic control are the explicit solutions corresponding to stationary configurations in hydrodynamics. While on flat space there are no interesting stationary flows other than a uniformly boosted fluid (whose dual is the seed solution with which we started), it turns out that by a suitable choice of background geometry one can derive nontrivial flows. We now describe one such flow on the Einstein static universe ($\mathbb{R} \times S^{d-1}$), whose existence allows one to make contact with rotating black holes in asymptotically (globally) AdS spacetimes.

The fluid flows of a conformal relativistic d -dimensional fluid on a spatial S^{d-1} conserve angular momentum in addition to energy. The angular momentum on the S^{d-1} is a rank- d antisymmetric matrix, which can be brought to canonical form by an $SO(d)$ similarity transform (a rotation) and is therefore labeled by its $\lfloor d/2 \rfloor$ inequivalent eigenvalues. For every physically allowed choice of these $\lfloor d/2 \rfloor$ angular momenta and of the energy, an arbitrary fluid flow eventually settles down into an equilibrium stationary configuration.

The stationary configurations of viscous conformal fluids on spheres turn out to be extremely simple. The velocity field is simply that of a rigid rotation. Focusing on the case $d = 2n$ for concreteness, the metric of a unit S^{2n-1} may be written in terms of the direction cosines μ_i as

$$ds_{S^{2n-1}}^2 = \sum_{i=1}^n \mu_i^2 d\phi_i^2 + d\mu_i^2, \quad \text{where} \quad \sum_{i=1}^n \mu_i^2 = 1. \quad (13.42)$$

In these coordinates the velocity and temperature fields of stationary flows take the forms

$$u_s^a \partial_a = \gamma \left(\partial_t + \sum_{i=1}^n \omega_i \partial_{\phi_i} \right), \quad T_s = \gamma T_0, \quad \gamma = \left(1 - \sum_{i=1}^m \omega_i^2 \mu_i^2 \right)^{-1/2}. \quad (13.43)$$

This flow is Weyl-equivalent to a uniform velocity and temperature configuration on a conformally rescaled spacetime [4], i.e.,

$$ds^2 = \gamma^2 (-dt^2 + ds_{S^{2n-1}}^2), \quad u_s^a \partial_a = \partial_t + \sum_{i=1}^n \omega_i \partial_{\phi_i}, \quad T_s = T_0. \quad (13.44)$$

It is not difficult to verify that (13.44) provides a nondissipative solution to the equations of fluid dynamics at least to second order (the solution is nondissipative because it is stationary; equivalently, the divergence of the entropy current vanishes). The constant parameters ω_i and T_0 of this solution turn out to have thermodynamical significance: they are simply the angular velocity (i.e., the chemical potential for the angular momentum) and the temperature of the fluid configuration.

According to the AdS/CFT correspondence, the dual description of a conformal field theory on $\mathbb{R} \times S^{d-1}$ is simply asymptotically global AdS _{$d+1$} space. If we pump a large amount of energy and angular momentum into global AdS _{$d+1$} space and let the system relax, we expect the eventual equilibrium configuration to be that of a large rotating black hole. This reasoning leads to a prediction: the fluid/gravity map applied to (13.44) should produce the (independently known) metric of a large rotating AdS _{$d+1$} black hole, expanded to second order in the derivative expansion. This prediction¹⁰ has been verified in detail in the following manner. It is possible to transform the exactly known metric of rotating AdS _{$d+1$} black holes to the fluid/gravity gauge described in section 13.3 above. This maneuver in fact turns out to simplify greatly the rotating black hole metric, which takes the form (13.29) with

$$\begin{aligned} \mathfrak{V}_a(r, x) &= r \mathcal{A}_a - \mathcal{S}_{ac} u^c - \frac{(4\pi T)^d r^2 u_a}{2d^2 \det(r \delta_c^b - \omega_c^b)}, \\ \mathfrak{G}_{ab}(r, x) &= r^2 P_{ab} - \omega_a^c \omega_{cb}. \end{aligned} \quad (13.45)$$

The above is an exact rewriting of the rotating AdS black holes (in even dimensions) of [26]. The metric (13.45) may be expanded in derivatives simply by expanding the inverse determinant in powers of ω . By truncating this expansion at second order we recover exactly the metric dual to the fluid flow (13.44). It is rather remarkable that the full black hole solution can be written economically within the fluid/gravity metric ansatz, perhaps suggesting that there is a greater utility for metrics of the form (13.29).

13.5.3 Nonrelativistic fluids

While relativistic fluids are interesting in astrophysical or high-energy plasma physics contexts, most fluids encountered in everyday situations are nonrelativistic. Furthermore, for many practical applications one is interested in their dynamics

¹⁰ The first observation that the properties of large rotating black holes should be reproduced from fluid dynamics was made in [4]; this observation was a precursor to the fluid/gravity map. Rotating black holes were studied further in [25] in four dimensions and fully analyzed in d dimensions in [10]. Here for illustration we give the general result found in [10], i.e., the explicit coordinate transformation for rewriting the rotating black hole solution in AdS _{$d+1$} given in [26] in fluid variables.

in the incompressible regime, which is attained by projecting out the sound mode. It is natural to ask whether this regime is accessible to fluid/gravity; an affirmative answer is suggested by the discussion in section 13.2.2, namely, one only needs to implement the Navier–Stokes scaling limit directly in the fluid/gravity solutions. This procedure was carried out in [27] to obtain the gravitational dual of nonrelativistic incompressible fluid flows. In principle this provides a geometric window to explore phenomenologically interesting fluid flows.

13.6 Extensions beyond conformal fluids

The fluid/gravity correspondence was originally derived for the case of conformal fluids, which are related to the gravitational dynamics in an asymptotically AdS spacetime. Conformal theories are rather special; the “ordinary” fluids that one encounters every day deviate significantly from this behavior. Hence it would be useful to look for extensions of the basic framework which allow for these generalizations. As already indicated earlier, this can be done at the expense of complicating the system of gravitational equations, with the accompanying loss of universality. Nevertheless, forays into these areas have revealed very interesting lessons about fluid dynamics in general that transcend the fluid/gravity correspondence. In this section we take stock of some of these developments.

13.6.1 Nonconformal fluids

The first generalization we consider is provided by a handy trick that can be used to obtain a particular class of nonconformal theories. It turns out that by exploiting the gauge/gravity duality for a special class of theories, viz., theories that naturally arise on the worldvolume of Dp -branes, one finds a surprisingly tractable class of nonconformal fluids.

Let us first consider the special case of the D4-brane which is a solution of the equations of ten-dimensional type IIA supergravity; type IIA supergravity is the dimensional reduction of eleven-dimensional supergravity on an S^1 and the D4-brane solution is the dimensional reduction of an M5-brane solution that wraps the S^1 . The near-horizon geometry of the M5-brane solution is $\text{AdS}_7 \times S^4$, and the eleven-dimensional equations admit a consistent truncation to the seven-dimensional equations of motion (13.1) for gravitational dynamics with a negative cosmological constant. Compactifying further on an S^1 and restricting to the zero-momentum sector on this circle yields a further consistent truncation of this seven-dimensional set of equations. The resulting six-dimensional equations are simply the Einstein-dilaton equations about the D4-brane background. It follows that the Einstein-dilaton equations constitute a consistent truncation of the equations of

type IIA supergravity about the D4 near-horizon background (as one can easily verify independently).

It turns out that the fluid dynamics dual to the long-wavelength fluctuations about the thermal M5-brane solution is simply that computed in section 13.3, for the special case $d = 6$. We want to focus on gravitational solutions corresponding to fluid flows independent of one of the boundary directions x^i (the direction of the S^1 in the paragraph above). These lie within the six-dimensional consistent truncation described above. However, these are simply the gravitational solutions dual to fluid flows on the worldvolume theory of the D4-brane. In other words, the fluid dynamics of the D4-brane worldvolume theory is a dimensional reduction of the conformal fluid dynamics on the worldvolume of the M5-brane. Moreover the gravitational duals to D4-brane fluid flows are very easily obtained from the Kaluza–Klein reduction of the results of section 13.3. Note that the dimensional reduction of conformal fluid dynamics results in nonconformal fluid dynamics (e.g., the dimensional reduction of a traceless stress tensor generically has a nonvanishing trace).

It is an interesting and surprising fact that the discussion of the previous paragraph generalizes to Dp -branes for all p at the purely algebraic level. In every case, one can find a consistent truncation of the Einstein-dilaton system, which, in a purely formal manner, can be regarded as the reduction of negative-cosmological-constant Einstein gravity in a higher (sometimes fractional) dimension [28]. This observation immediately yields the fluid descriptions of arbitrary Dp -brane backgrounds as a dimensional reduction of the conformal fluid dynamics derived in section 13.3.

13.6.2 Theories with a deconfinement transition

So far we have studied the fluid dynamical description of field theories that are “deconfined” at every temperature, i.e., the free energy is $\mathcal{O}(N^2)$. Consider, however, a theory like pure Yang–Mills at large N , which undergoes a first-order deconfinement phase transition at finite temperature. Such a system has a dual description in terms of a black hole only above the deconfinement temperature; the low-temperature phase is given by a gas of glueballs and is thermodynamically indistinguishable from the vacuum at leading order in N (the free energy is $\mathcal{O}(1)$).

The Scherk–Schwarz reduction of $\mathcal{N} = 4$ Yang–Mills on a circle of radius R (with antiperiodic boundary conditions for fermions) is a simple example of such a theory. At strong coupling this theory undergoes a first-order deconfinement transition at $TR = 2\pi$. The gravity dual of the high-temperature phase is simply the S^1 compactification of the AdS_5 planar black hole. The gravity dual of the low-temperature phase is a so-called AdS soliton (i.e., a double analytic continuation

of the planar Schwarzschild–AdS black hole, in which the role of time and the S^1 direction are interchanged). At temperatures much higher than the phase transition, the effective three-dimensional low-energy theory is simply a dimensional reduction of the four-dimensional conformal fluid system derived in earlier subsections (just as we found in section 13.6.1).

However, at the phase transition temperature we have a new phenomenon; there exists a new static solution of the equations of motion, a co-dimension-1 domain wall that interpolates between the AdS soliton and the S^1 compactification of the planar AdS_5 black hole. Unfortunately this solution has been constructed only numerically [29]. The domain wall is static in these solutions because of a pressure balance on the two sides (recall that the free energies, and hence the pressures, of the two phases are equal at a phase transition temperature). This configuration is that of a fluid with a boundary; the effective low-energy fluctuations of this system consist of boundary modes (like waves on the surface of water) in addition to the bulk modes discussed so far in this chapter. At the ideal-fluid level, the action for boundary degrees of freedom is captured by a single parameter, i.e., the surface tension of the boundary (computed from a numerical solution).

Already, using the ideal-fluid action including boundary terms, it has proved possible to construct many stationary solutions of the fluid equations. These solutions, called plasma balls and plasma rings, have dual descriptions as black holes, black rings, and (in higher dimensions) black objects of more exotic topology [30]. The effective action for surface degrees of freedom has not been worked out at higher orders in the derivative expansion, and this would appear to be an interesting exercise.

One particularly interesting static solution of the equations of ideal-fluid dynamics including boundary terms is the plasma tube, a configuration consisting of a domain wall that interpolates from the vacuum to the high-temperature phase at the phase transition temperature followed by a second, parallel, domain wall at separation L that interpolates back to the vacuum. Such a fluid configuration is the two-dimensional analogue of a three-dimensional cylindrical tube of fluid and, as is well known, undergoes a famous fluid dynamical instability (to droplet formation) called the Rayleigh instability. For real fluids such as water, the endpoint of the Rayleigh instability is a series of disconnected droplets. Now, the gravitational dual of the plasma tube is an infinitely long black string in five-dimensional gravity. This solution has the well-known Gregory–Laflamme instability (see Chapter 2), which, apparently, is dual to the Rayleigh instability in the long-wavelength limit. The boundary dual of a series of disconnected droplets, however, is a series of disconnected black holes. This discussion, at least, strongly suggests that the endpoint of the Gregory–Laflamme instability consists of localized black holes [31]. Note that the fluid description breaks down near the “pinch off” point; the actual

description of the topology change in this process requires the use of the full field theory (e.g. details of the interactions between water molecules in the case of water).

13.6.3 Charged fluids and anomalies

Under the AdS/CFT correspondence, a global symmetry in the boundary maps to a gauge symmetry in the bulk. This suggests that there should be a duality between the long-wavelength asymptotically-AdS planar black hole solutions of the Einstein–Maxwell theory (with negative cosmological constant) and the equations of charged fluid dynamics. This is a useful extension, as the fluids of interest in experimental situations conserve one or more $U(1)$ charges in addition to energy and momentum. For instance, the flow of air in the atmosphere conserves air molecule number.

It is conceptually straightforward to generalize the set-up of section 13.3 to the study of locally thermalized charged planar black holes. The starting point is the construction of spacetimes that tubewise approximate Reissner–Nordström AdS black hole solutions with locally varying temperature, chemical potential, and velocity. A perturbation expansion entirely analogous to that outlined in section 13.3 then constructs the gravitational solutions to the Einstein–Maxwell–Chern–Simons theory (which forms a consistent truncation of type IIB supergravity on $\text{AdS}_5 \times S^5$) dual to charged fluid flows, order by order in a derivative expansion [32, 33]. This procedure also determines the equations of charged fluid dynamics order by order in the derivative expansion. The results of this analysis turn out to produce a surprise purely from the viewpoint of charged first-order fluid dynamics, as we now explain.

The equations of charged fluid dynamics are the conservation of the charge current

$$\nabla_a J^a = 0 , \quad (13.46)$$

together with the conservation of the stress tensor (13.3). Concrete fluid dynamical equations require constitutive relations that express the field-redefinition-invariant parts of the stress tensor and charge current in terms of expressions of first order in the derivatives of the fluid fields. The charge current for charge density q takes the form

$$J^a = q u^a + J_{\text{diss}}^a , \quad (13.47)$$

where J_{diss}^a represents the dissipation contribution of terms with one or more derivatives of the fluid fields to the charge current and is to be viewed as the charge current

analogue of Π^{ab} ; expanding, we obtain a form similar to (13.6):

$$J_{\text{diss}}^a = \sum_{n=1}^{\infty} \ell_m^n j_{(n)}^a . \quad (13.48)$$

Standard textbook analyses assert that the most general allowed forms at first order for the constitutive relations of a relativistic charged fluid are the first equation of (13.7) along with

$$P_c^a \left(j_{(1)}^c + \frac{q}{\rho + P} (u_b \Pi_{(1)}^{bc}) \right) = \kappa V_1^a , \quad V_1^a \equiv -P^{ab} \nabla_b \frac{\mu}{T} + \frac{F^{ab} u_b}{T} , \quad (13.49)$$

while the second equation of (13.7) is modified to

$$\frac{1}{d-1} \Pi_{(1)}^{ab} P_{ab} - \frac{\partial P}{\partial \rho} (u_a u_b \Pi_{(1)}^{ab}) + \frac{\partial P}{\partial q} (u_a j_{(1)}^a) = -\beta \nabla_c u^c . \quad (13.50)$$

In (13.49), F^{ab} is the nondynamical background electromagnetic field, which couples to the $U(1)$ current J^a in (13.46), and μ is the chemical potential of the fluid. Provided that

$$\eta \geq 0 , \quad \kappa \geq 0 , \quad \beta \geq 0 ,$$

these expressions are consistent with the positivity of the divergence of the canonical fluid entropy current

$$J_{\text{can}}^a = s u^a - \frac{1}{T} u_b \Pi_{(1)}^{ab} - \frac{\mu}{T} j_{(1)}^a , \quad (13.51)$$

using the relation, commonly alleged to hold,

$$\nabla_a J_{\text{can}}^a = -\nabla_a \left(\frac{u_b}{T} \right) \Pi_{(1)}^{ab} - \left[\nabla_a \left(\frac{\mu}{T} \right) - \frac{F_{ab} u^b}{T} \right] j_{(1)}^a . \quad (13.52)$$

However, it was found by explicit computation that the fluid dual to the asymptotically AdS–Einstein–Maxwell–Chern–Simons system has constitutive relations that differ from those of (13.49) in the following way: the right-hand relation in (13.49) includes new terms proportional to the fluid vorticity ω^a and the rest-frame magnetic field B^a , where

$$\omega^a = \frac{1}{2} \epsilon^{abcd} u_b \partial_c u_d , \quad B^a = \frac{1}{2} \epsilon^{abcd} u_b F_{cd} .$$

In a beautiful paper [34], the authors pointed out the reason for the appearance of these new terms. When the $U(1)$ current has a global $U(1)^3$ triangle anomaly (as is

true of the field theory dual to a bulk system with a five-dimensional Chern–Simons term), (13.52) has an additional term on its right-hand side that is proportional to this anomaly. This term spoils the positivity of the divergence of the canonical entropy current; it is, however, consistent with the positivity of the divergence of a modified entropy current, provided that modifications are also made to the right-hand side of (13.49). More concretely, the positivity of the entropy current in every conceivable circumstance requires that, in addition to the first equation of (13.7) and to (13.50),

$$J_S^a = J_{\text{can}}^a + \sigma_\omega \omega^a + \tilde{\sigma}_B B^a , \quad (13.53)$$

$$P_c^a \left(j_{(1)}^c + \frac{q}{\rho + P} (u_b \Pi_{(1)}^{bc}) \right) = \kappa V_1^a + \tilde{\kappa}_\omega \omega^a + \tilde{\kappa}_B B^a ,$$

where

$$\sigma_\omega = c \frac{\mu^3}{3T} + T \mu k_2 + T^2 k_1 ,$$

$$\sigma_B = c \frac{\mu^2}{2T} + \frac{T}{2} k_2 ,$$

$$\tilde{\kappa}_\omega = c \left(\mu^2 - \frac{2}{3} \frac{q}{\rho + P} \mu^3 \right) + T^2 \left(1 - \frac{2q}{\rho + P} \mu \right) k_2 - \frac{2q}{\rho + P} k_1 ,$$

$$\tilde{\kappa}_B = c \left(\mu - \frac{1}{2} \frac{q}{\rho_n + P} \mu^2 \right) - \frac{T^2}{2} \frac{q}{\rho + P} k_2 ,$$

and k_1 and k_2 are integration constants. Further, the imposition of *CPT* invariance forces k_2 to vanish.

This explanation accounts for the additional transport coefficients in the AdS/CFT duality but in fact applies more generally to every fluid flow with a $U(1)^3$ anomaly. The effect of these new transport coefficients may well turn out to have experimentally measurable effects in relativistic heavy-ion collisions or in neutron or quark stars.

13.6.4 Holographic superfluid hydrodynamics

It was pointed out in [35] that charged asymptotically AdS_5 planar black holes are sometimes unstable in the presence of charged scalar fields. The endpoint of this instability is a hairy black hole, a black hole immersed in a charged scalar condensate. The AdS/CFT correspondence maps the hairy black hole to a phase in which a global $U(1)$ symmetry is spontaneously broken by the vacuum expectation value of a charged scalar operator (see Chapter 14 for further discussion). In condensed

matter physics, a phase with a spontaneously broken global $U(1)$ symmetry is referred to as a superfluid.

The variables of relativistic superfluid dynamics consist of two velocity fields, the normal fluid velocity u^a and a superfluid velocity field u_s^a , together with a temperature and a chemical potential field. The superfluid velocity is the unit vector in the direction of $-\xi_a$, where ξ_a is the gradient of the phase of the scalar condensate. The conservation of the stress tensor and of the charge current, together with the assertion that ξ_a is curl free, constitute the equations of superfluid dynamics. These equations form a closed dynamical system once they are supplemented by constitutive relations that express the stress tensor, charge current, and the component of ξ_a along the normal velocity as functions of the fluid dynamical variables.

It has proved possible to apply the fluid/gravity map to hairy black holes to derive the constitutive relations for holographic superfluids, with interesting results. The theory of perfect superfluids was worked out by Landau and Tisza in the 1940s. In a recent work [36], the authors used the equations of Einstein gravity to rederive the Landau–Tisza equations for superfluids, which admit a holographic description. The theory of first-order dissipative corrections to the equations of Landau–Tisza superfluidity was most completely spelled out in [37]. These calculations, made within the fluid/gravity framework, have led to the realization that the 13-parameter Clark–Puterman equations derived within this framework are missing one parameter (under the assumption of parity invariance for the superfluids) or six parameters (if the superfluids are not assumed to preserve parity). A completely satisfactory framework for superfluid hydrodynamics was developed only very recently [7], and the fluid/gravity map has played a major role in this development.

13.7 Relation to other developments

Finally, having surveyed the fluid/gravity correspondence and its various applications, we describe connections with other approaches.

13.7.1 Implications for Israel–Stewart formalism

One useful application of the fluid/gravity correspondence is an improvement on the “causal relativistic hydrodynamics”, also known as the Israel–Muller–Stewart formalism [38, 39]. To appreciate the context, recall that a conventional theory of relativistic dissipative (i.e., irreversible) hydrodynamics, which is first order in time derivatives, is described in terms of a parabolic system of differential equations leading to the instantaneous propagation of signals. While these apparently acausal

modes lie outside the long-wavelength regime of validity of the hydrodynamical formulation, as discussed in [40], they nevertheless lead to conceptual and computational problems. To capture the dissipative physics, in [38] it was observed that second-order terms are needed in the entropy current. These render the system hyperbolic, thereby providing a good initial value formulation. However, the particular terms added were not all possible ones consistent with the symmetries, so, as such, the construction appears somewhat ad hoc. Indeed, in [16] it was observed, in the context of a conformal fluid, that the terms added do not maintain conformal invariance of the system, manifesting the incompleteness of the approach. The fluid/gravity construction in effect prescribes the correct completion to render the full system causal as well as manifestly consistent with the symmetries. We expect that, owing to the gravitational dual, causality will be guaranteed at all orders in the derivative expansion.

13.7.2 The black hole membrane paradigm

Perhaps the most salient feature of the fluid/gravity correspondence is the fact that the horizon dynamics (which in this case prescribes the dynamics of the entire spacetime) is governed by hydrodynamics. On the face of it, such a type of relation is not new; in fact, for several decades relativists have explored the idea that spacetime, or important aspects thereof such as black hole horizons, might resemble a fluid. Early indications include the black hole thermodynamics [12, 13] developed in the 1970s, analogue models of black holes [41] initiated in the early 1980s, and, most strikingly, the black hole membrane paradigm [42, 43] formulated in the late 1970s. The latter realizes the idea that, for external observers, black holes behave much like a fluid membrane endowed with physical properties such as viscosity, conductivity, and so forth. In particular, the dynamics of this membrane is governed by the familiar laws of fluid dynamics, namely the compressible Navier–Stokes equations.

Motivated by the superficial similarity between the membrane paradigm and the fluid/gravity correspondence, recently authors [44, 45] have attempted to formulate a precise derivation of the former. In [44] Einstein’s equations in the bulk are projected onto a null hypersurface and then expanded in gradients along the hypersurface. However, in [45] it was shown that one can systematically find a solution to the vacuum Einstein equations that describes the near-horizon geometry of a generic nondegenerate black hole in the long-wavelength regime.

Within the fluid/gravity correspondence, the entire spacetime evolution is mapped to the dynamics of a conformal fluid, which, although reminiscent of the membrane paradigm, has one important twist: the membrane lives on the *boundary* of the spacetime (which is unambiguously defined and admits a fluid description

with well-defined dynamics) and gives a perfect mirror of the full bulk physics. This “membrane at the end of the universe” picture is a natural consequence of the holographic nature of the fluid/gravity correspondence.

13.7.3 Blackfolds

As in the fluid/gravity correspondence and membrane-paradigm-type ideas, the blackfold approach to constructing higher-dimensional black holes (discussed in Chapter 8) likewise asserts that an effective theory describing the long-wavelength dynamics of black hole horizons can be expressed in terms of fluid dynamics. However, there are several important differences between these descriptions. Since the blackfold “fluid” pertains to the effective worldvolume dynamics of an extended black object as seen from far away, the intrinsic dynamics typically has to be supplemented by extrinsic dynamics describing how the blackfold embeds in the ambient spacetime. However, in the fluid/gravity correspondence the fluid resides on the boundary of asymptotically (locally) AdS spacetime, so there is no difficulty regarding the extrinsic dynamics.

Moreover, although the blackfold formalism is most naturally formulated in asymptotically flat spacetime, by a suitable separation of scales one can in principle consider blackfolds with any asymptotics. In contrast, the fluid/gravity correspondence concerns asymptotically-AdS black holes. Unlike all the above-mentioned approaches, only in the fluid/gravity correspondence does the fluid have a known physical microscopic origin: the effective behavior of the dual field theory residing on the AdS boundary.

13.8 Summary

The fluid/gravity correspondence provides a natural way to map solutions of fluid dynamics into those of gravity, enabling one to construct time-dependent inhomogeneous black hole solutions to Einstein’s equations, while retaining the full nonlinearity of the latter. An interesting aspect of this construction is the manner in which classical gravity can be molded to fit naturally with effective field theory intuition in order to extract approximate solutions. While the construction itself arose from the gauge/gravity correspondence, it is clear that it can be implemented in greater generality.

Apart from providing interesting insights into the dynamics of gravity, the map has played an important role in clarifying various issues in fluid dynamics. The role of quantum anomalies in hydrodynamical transport, and generalizations of fluid dynamics to systems with spontaneously broken symmetries, are two examples where the fluid/gravity map has served to elucidate the underlying physics. The

physical points seem much simpler to understand from the gravitational perspective; aided by this intuition one can re-evaluate the hypotheses of traditional descriptions of fluids.

The fluid/gravity map suggests several extremely interesting technical, as well as conceptual, questions for the future. Some of these are as follows. Does the gravitational viewpoint shed any light on turbulent fluid flows or on singularities that can develop in finite time from smooth initial data in fluid dynamics? Is there a path integral formulation of fluid dynamics at finite N , and how does it map to the path integral of bulk gravity? Are the corrections to the classical equations of gravity constrained by the requirement of the positivity of divergence of an “entropy current” on an event horizon (analogously to, and perhaps even dual to, the situation in fluid dynamics)? It seems likely that many interesting results remain to be discovered in this general area.

13.9 Epilogue: Einstein and Boltzmann

As we have emphasized throughout, the equations of fluid dynamics, for which we have an independent field theory intuition, are dual to a long-wavelength limit of Einstein’s equations (13.1). It is then natural to ask, what is the field-theoretic interpretation of the full dynamical system of equations (13.1)? We believe that these equations may be conceptually thought of as the strong coupling analogue of (a decoupled sector of) the Boltzmann transport equations.

It is well known that the linearization of the Boltzmann transport equations about equilibrium yields an infinite set of “quasinormal modes”, i.e., solutions to the equations of motion that decay to zero (returning the system back to equilibrium) at late times. Exactly d of these quasinormal modes are massless (in the sense that they are static in the infinite-wavelength limit). In textbooks on statistical mechanics, fluid dynamics is sometimes derived as the non-linear theory of this finite set of Boltzmann “quasinormal modes”. The remaining quasinormal modes are “fast modes,” which decay away on a time scale set by the mean free path of kinetic theory.

Similarly, the linearization of the equations of gravity about the planar black hole gives d massless quasinormal modes and an infinite set of massive quasinormal modes. In direct analogy with the work on the Boltzmann equations, the fluid/gravity correspondence constructs the equations of fluid dynamics as the non-linear theory of these massless modes (effectively by integrating out the massive modes, order by order). For this reason it is natural to think of the full set of Einstein’s equations in the presence of an event horizon (including all quasinormal mode degrees of freedom) as the strong-coupling analogue of the Boltzmann transport equations.

An important property of the Boltzmann transport equations is that they are irreversible: they obey the Boltzmann H -theorem (which asserts that a certain functional of kinetic variables called H always increases in time and is maximum in equilibrium). In direct analogy, Einstein's equations, together with the assumption of the regularity of future event horizons (and physical energy conditions), always obey the classic area-increase theorem of general relativity. This suggests that a better analogy exists between the Boltzmann transport equations and Einstein's equations *plus the condition of regularity of the future event horizon*. The last condition breaks the time-reversal invariance of Einstein's equations. In fact, the requirement that the future event horizon stays regular was a crucial element in our implementation of the fluid/gravity map. The Boltzmann theorem has a local analogue in fluid dynamics; it maps to the statement that the equations of fluid dynamics are accompanied by a local entropy current whose divergence is everywhere nonnegative. The area-increase theorem of general relativity can be used to construct such an entropy current for the fluid dynamics generated from the fluid/gravity map.

Just like the Boltzmann equations, the system of gravitational equations (13.1) can be used to study the approach to equilibrium from a highly nonequilibrated starting point. In simple studies of equilibration using Einstein's equations [46, 47], the equilibration time, measured by the time taken for fluid dynamics to take over as an effective description, turns out to be extremely rapid. In more complicated situations the equilibration process displays sharp phase transitions associated with Choptuik phenomena. Indeed the equations (13.1) undoubtedly contain a host of dynamical delights for the intrepid gravitational and statistical physicist; it seems clear that the fluid/gravity map is merely the tip of an iceberg of connections between gravity and statistical physics.

References

- [1] S. Bhattacharyya, V. E. Hubeny, S. Minwalla, and M. Rangamani, Nonlinear fluid dynamics from gravity, *JHEP* **0802** (2008), 045 [arXiv:0712.2456 [hep-th]].
- [2] G. Policastro, D. T. Son, and A. O. Starinets, The shear viscosity of strongly coupled $N = 4$ supersymmetric Yang–Mills plasma, *Phys. Rev. Lett.* **87** (2001), 081601 [arXiv:hep-th/0104066].
- [3] R. A. Janik and R. B. Peschanski, Asymptotic perfect fluid dynamics as a consequence of AdS/CFT, *Phys. Rev. D* **73** (2006), 045013 [arXiv:hep-th/0512162].
- [4] S. Bhattacharyya, S. Lahiri, R. Loganayagam, and S. Minwalla, Large rotating AdS black holes from fluid mechanics, *JHEP* **09** (2008), 054 [arXiv:0708.1770 [hep-th]].
- [5] M. Rangamani, Gravity and hydrodynamics: lectures on the fluid–gravity correspondence, *Class. Quant. Grav.* **26** (2009), 224003 [arXiv:0905.4352 [hep-th]].
- [6] V. Balasubramanian and P. Kraus, A stress tensor for anti-de Sitter gravity, *Commun. Math. Phys.* **208** (1999), 413–428 arXiv:hep-th/9902121.

- [7] J. Bhattacharya, S. Bhattacharyya, S. Minwalla, and A. Yarom, A theory of first order dissipative superfluid dynamics, arXiv:1105.3733 [hep-th].
- [8] P. Romatschke, Relativistic viscous fluid dynamics and non-equilibrium entropy, *Class. Quant. Grav.* **27** (2010), 025006 [arXiv:0906.4787 [hep-th]].
- [9] R. Loganayagam, Entropy current in conformal hydrodynamics, *JHEP* **0805** (2008), 087, arXiv:0801.3701 [hep-th].
- [10] S. Bhattacharyya, R. Loganayagam, I. Mandal, S. Minwalla, and A. Sharma, Conformal nonlinear fluid dynamics from gravity in arbitrary dimensions, *JHEP* **0812** (2008), 116 [arXiv:0809.4272 [hep-th]].
- [11] S. Bhattacharyya, V. E. Hubeny, R. Loganayagam, et al., Local fluid dynamical entropy from gravity, *JHEP* **0806** (2008), 055 [arXiv:0803.2526 [hep-th]].
- [12] J. D. Bekenstein, Black holes and entropy, *Phys. Rev. D* **7** (1973), 2333–2346.
- [13] S. W. Hawking, Particle creation by black holes, *Commun. Math. Phys.* **43** (1975), 199–220.
- [14] I. Booth, M. P. Heller, G. Plewa, and M. Spalinski, On the apparent horizon in fluid–gravity duality, arXiv:1102.2885 [hep-th].
- [15] M. Henningson and K. Skenderis, The holographic Weyl anomaly, *JHEP* **07** (1998), 023 [arXiv:hep-th/9806087].
- [16] R. Baier, P. Romatschke, D. T. Son, A. O. Starinets, and M. A. Stephanov, Relativistic viscous hydrodynamics, conformal invariance, and holography, *JHEP* **0804** (2008), 100 [arXiv:0712.2451 [hep-th]].
- [17] P. Kovtun, D. T. Son, and A. O. Starinets, Viscosity in strongly interacting quantum field theories from black hole physics, *Phys. Rev. Lett.* **94** (2005), 111601 [arXiv:hep-th/0405231].
- [18] T. Schafer and D. Teaney, Nearly perfect fluidity: from cold atomic gases to hot quark gluon plasmas, *Rept. Prog. Phys.* **72** (2009), 126001 [arXiv:0904.3107 [hep-ph]].
- [19] A. Buchel, R. C. Myers, and A. Sinha, Beyond eta/s = 1/4 pi, *JHEP* **0903** (2009), 084 [arXiv:0812.2521 [hep-th]].
- [20] M. Haack and A. Yarom, Nonlinear viscous hydrodynamics in various dimensions using AdS/CFT, *JHEP* **0810** (2008), 063 [arXiv:0806.4602 [hep-th]].
- [21] E. Berti, V. Cardoso, and A. O. Starinets, Quasinormal modes of black holes and black branes, *Class. Quant. Grav.* **26** (2009), 163001 [arXiv:0905.2975 [gr-qc]].
- [22] G. T. Horowitz and V. E. Hubeny, Quasinormal modes of AdS black holes and the approach to thermal equilibrium, *Phys. Rev. D* **62** (2000), 024027 [arXiv:hep-th/9909056].
- [23] G. Policastro, D. T. Son, and A. O. Starinets, From AdS/CFT correspondence to hydrodynamics, *JHEP* **09** (2002), 043 [arXiv:hep-th/0205052].
- [24] G. Policastro, D. T. Son, and A. O. Starinets, From AdS/CFT correspondence to hydrodynamics. II: Sound waves, *JHEP* **12** (2002), 054 [arXiv:hep-th/0210220].
- [25] S. Bhattacharyya, R. Loganayagam, S. Minwalla, et al., Forced fluid dynamics from gravity, *JHEP* **0902** (2009), 018 [arXiv:0806.0006 [hep-th]].
- [26] G. Gibbons, H. Lu, D. N. Page, and C. Pope, The general Kerr–de Sitter metrics in all dimensions, *J. Geom. Phys.* **53** (2005), 49–73 [arXiv:hep-th/0404008 [hep-th]].
- [27] S. Bhattacharyya, S. Minwalla, and S. R. Wadia, The incompressible non-relativistic Navier–Stokes equation from gravity, *JHEP* **0908** (2009), 059 [arXiv:0810.1545 [hep-th]].
- [28] I. Kanitscheider and K. Skenderis, Universal hydrodynamics of non-conformal branes, *JHEP* **0904** (2009), 062 [arXiv:0901.1487 [hep-th]].

- [29] O. Aharony, S. Minwalla, and T. Wiseman, Plasma-balls in large N gauge theories and localized black holes, *Class. Quant. Grav.* **23** (2006), 2171–2210 [arXiv:hep-th/0507219].
- [30] S. Lahiri and S. Minwalla, Plasmarrings as dual black rings, *JHEP* **05** (2008), 001 [arXiv:0705.3404 [hep-th]].
- [31] V. Cardoso and O. J. Dias, Rayleigh–Plateau and Gregory–Laflamme instabilities of black strings, *Phys. Rev. Lett.* **96** (2006), 181601 [arXiv:hep-th/0602017 [hep-th]].
- [32] J. Erdmenger, M. Haack, M. Kaminski, and A. Yarom, Fluid dynamics of R-charged black holes, *JHEP* **0901** (2009), 055 [arXiv:0809.2488 [hep-th]].
- [33] N. Banerjee, J. Bhattacharya, S. Bhattacharyya, *et al.*, Hydrodynamics from charged black branes, *JHEP* **1101** (2011), 094 [arXiv:0809.2596 [hep-th]].
- [34] D. T. Son and P. Surowka, Hydrodynamics with triangle anomalies, *Phys. Rev. Lett.* **103** (2009), 191601 [arXiv:0906.5044 [hep-th]].
- [35] S. S. Gubser, Breaking an Abelian gauge symmetry near a black hole horizon, *Phys. Rev.* **D78** (2008), 065034 [arXiv:0801.2977 [hep-th]].
- [36] J. Sonner and B. Withers, A gravity derivation of the Tisza–Landau model in AdS/CFT, *Phys. Rev.* **D82** (2010), 026001 [arXiv:1004.2707 [hep-th]].
- [37] S. J. Puterman, *Superfluid Hydrodynamics*, vol. 3, North-Holland (1974).
- [38] W. Israel, Nonstationary irreversible thermodynamics: a causal relativistic theory, *Ann. Phys.* **100** (1976), 310–331.
- [39] W. Israel and J. M. Stewart, Transient relativistic thermodynamics and kinetic theory, *Ann. Phys.* **118** (1979), 341–372.
- [40] R. P. Geroch, On hyperbolic “Theories” of relativistic dissipative fluids, gr-qc/0103112.
- [41] W. G. Unruh, Experimental black hole evaporation, *Phys. Rev. Lett.* **46** (1981), 1351–1353.
- [42] K. S. Thorne, R. H. Price, and D. A. MacDonald, *Black Holes: The Membrane Paradigm*, New Haven: Yale University Press (1986).
- [43] T. Damour, Black hole eddy currents, *Phys. Rev.* **D18** (1978), 3598–3604.
- [44] C. Eling and Y. Oz, Relativistic CFT hydrodynamics from the membrane paradigm, *JHEP* **1002** (2010), 069 [arXiv:0906.4999 [hep-th]].
- [45] I. Bredberg, C. Keeler, V. Lysov, and A. Strominger, From Navier–Stokes to Einstein, arXiv:1101.2451 [hep-th].
- [46] P. M. Chesler and L. G. Yaffe, Horizon formation and far-from-equilibrium isotropization in supersymmetric Yang–Mills plasma, *Phys. Rev. Lett.* **102** (2009), 211601 [arXiv:0812.2053 [hep-th]].
- [47] S. Bhattacharyya and S. Minwalla, Weak field black hole formation in asymptotically AdS spacetimes, *JHEP* **0909** (2009), 034 [arXiv:0904.0464 [hep-th]].

14

Horizons, holography and condensed matter

SEAN A. HARTNOLL

14.1 Introduction

Consistent theories of quantum gravity in spacetimes that asymptote to anti-de Sitter (AdS) spacetime are equivalent to quantum field theories defined on the conformal boundary of the spacetime [1]. A pedagogical discussion of this “holographic correspondence” may be found in [2, 3] and in Chapter 12 of this volume. While some deeper questions arising from the correspondence remain to be understood from first principles, the conceptual “Gestalt switch” involved in viewing physical processes simultaneously from a gravitational and a field-theoretic perspective has provided an invaluable source of physical intuition as well as computational power. In particular, in the large- N limit of quantum field theories, to be recalled shortly, the gravitational description becomes weakly curved and the tools of general relativity may be harnessed.

This chapter will be concerned with black holes in four-dimensional asymptotically AdS spacetimes. By focusing on charged planar black holes, we will establish an interface with the rich phenomenology of (2+1)-dimensional quantum field theories that has been widely studied in condensed matter physics. Planarity of the horizon will translate into the statement that the dual quantum field theory propagates on a background Minkowski spacetime in 2+1 dimensions. The perhaps more familiar spherical foliation of asymptotically AdS spacetimes would correspond to considering quantum field theories on a spatial sphere; this complicates the field-theoretic physics by introducing a scale, the radius of the sphere, and also does not correspond to a situation of significant interest in condensed matter physics at present. The charge of the black hole will translate into the fact that the field theory is in a state with a nonzero charge density. This charge density is to be

thought of as the “stuff” of condensed matter physics, a proxy for, e.g., the fluid of electrons in a metal.

In this chapter we will pursue a gravitational approach to the following fundamental field-theoretic question. Consider a general quantum field theory in a state with a finite charge density. How might one attempt to classify all the gapless low-temperature phases of matter that can arise? Free field theories exhibit two well-known low-temperature phases. Free charged bosons will undergo Bose-Einstein condensation, spontaneously breaking the charge symmetry. The gapless degree of freedom is consequently a Goldstone boson. Free charged fermions, in contrast, cannot macroscopically occupy their ground state but, rather, build up a Fermi surface. The gapless degrees of freedom are then particle-hole excitations of the Fermi surface. The dynamics of Goldstone bosons and Fermi surface excitations is tightly constrained by kinematics and is well understood. Beyond free or weakly interacting theories, however, the question of possible phases of matter becomes more difficult – this is where a gravitational perspective may be useful.

After a brief review of the holographic correspondence and of some challenges and expectations from condensed matter theory, we will translate our guiding question into gravitational terms. Take a gravitational theory with some specific matter content that admits asymptotically AdS solutions. Require the spacetime to have a net asymptotic electric flux, i.e., require the spacetime to be charged. What, then, is the thermodynamically dominant spacetime that sources this charge? The basic dichotomy that we will discuss is whether the electric flux emanates from behind a charged horizon in the interior of the spacetime or whether it is explicitly sourced by charged matter. The gravitational physics resolving this tension will be that of charged superradiance instabilities. Returning to a field theory perspective at the end of the chapter, we will argue that this distinction is the gravitational realisation of the field theoretic distinction between “fractionalised” phases and “mesonic” phases. The precise meaning of these terms will be made clear in what follows.

14.2 Preliminary holographic notions

There exist certain quantum field theories in which the locality of the renormalisation group (RG) flow can be geometrically realised in a useful way. This is a feature of the holographic correspondence that will be central to our discussion. The basic idea is to append an extra spatial dimension to the spacetime of the quantum field theory. This extra dimension will correspond to the RG scale, as illustrated in Fig. 14.1. In contrast to the fixed “boundary” field theory spacetime, the “bulk” spacetime with an extra dimension will be dynamical. The boundary conditions set at infinity in the bulk correspond to the UV values of couplings in the field theory.

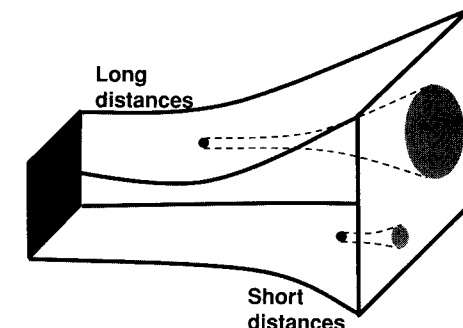


Figure 14.1 The extra radial dimension in holography corresponds to the renormalisation group scale. Processes in the interior determine long-distance physics, the IR of the dual field theory, while processes near the boundary control the short-distance, or UV, physics.

Solving the gravitational equations of motion is dual to following the RG flow down in energy scales. A modern presentation of the holographic renormalisation group may be found in [4, 5]. For our purposes we need the picture in Fig. 14.1 only as a way of organising our thoughts about asymptotically AdS spacetimes. The asymptotic spacetime describes the UV of the quantum field theory while the interior of the spacetime describes the IR.

At this point we can understand why AdS spacetime plays a privileged role in discussions of holography. The simplest quantum field theories are those that exhibit no RG flow at all, i.e., that are scale invariant; AdS spacetime is the geometrisation of this invariance for a relativistic quantum field theory. In our planar coordinates, AdS spacetime takes the form (cf. (12.1))

$$ds^2 = \frac{L^2}{r^2} (-dt^2 + dr^2 + dx^2 + dy^2) . \quad (14.1)$$

This spacetime is invariant under

$$r \rightarrow \lambda r , \quad \{t, x, y\} \rightarrow \lambda \{t, x, y\} . \quad (14.2)$$

Therefore if we follow an RG flow in the boundary theory, by rescaling the field theory coordinates $\{t, x, y\}$, it must be that we move simultaneously into the bulk.¹ When we do this, the spacetime does not change. More generally, spacetimes will not be scale invariant but, rather, only asymptotically AdS, so that the dual field theory approaches a fixed point at high energies.

¹ In the coordinates of (14.1), and throughout this chapter, the conformal boundary of spacetime is at $r \rightarrow 0$, and r increases as one moves into the space. This is essentially the inverse of the radial coordinate used elsewhere in this book. Such a coordinate is more conventionally denoted by z . We need, however, to keep z free to denote the dynamical critical exponent below. We note that the coordinate r has units of length.

One must ask exactly which class of quantum field theories admits a holographic description, with the renormalisation group classically geometrised. Insofar as the answer to this question is known, two properties are key. First, the theory must admit a large- N expansion. Second, in this large- N limit “most” operators in the theory must acquire parametrically large anomalous dimensions [6]. The role of the large- N limit is that it implies an underlying “master” classical field configuration, which dominates the path integral [7]. The expectation values of operators must factorise into products of the expectation values of single-trace operators, the effective classical fields, to leading order at large N . These single-trace operators will correspond to classical single-particle states in the bulk description. In general, one must still deal with infinitely many such classical fields, as occurs for example with the large- N limit of the $O(N)$ model [8]. The additional condition that all except a small handful of the single-trace operators acquire parametrically large anomalous dimensions will translate into the bulk statement that all except a handful of the classical bulk fields become parametrically heavy and may therefore be ignored for many questions. It is clear that this additional fact requires the large- N field theory to be strongly interacting. A finite number of classical fields in the bulk can then be described by a local classical action, whose “radial” local equations of motion have a chance of realising the local renormalisation group flow equations for finitely many single-trace operators and the multitrace operators they generate [4–6].

Many theories are known for which the two properties of the previous paragraph hold true. Some, such as $\mathcal{N} = 4$ super Yang–Mills theory in 3+1 dimensions [1], the Aharony, Bergman, Jafferis and Maldacena (ABJM) class of $\mathcal{N} = 6$ gauge theories in 2+1 dimensions [9] and their many cousins with less supersymmetry, have explicitly known Lagrangian descriptions. The schematic form of these Lagrangians is

$$\mathcal{L} \sim \text{Tr} (F^2 + (\partial\Phi)^2 + i\bar{\Psi}\Gamma \cdot \partial\Psi + g^2[\Phi, \Phi]^2 + ig\bar{\Psi}[\Phi, \Psi]) . \quad (14.3)$$

This expression is intended to convey the following features. The theory has a large- N nonabelian gauge group with field strength F . The theory contains adjoint bosonic (Φ) and fermionic (Ψ) matter. The matter typically comes in multiple flavours and with various patterns of interactions. The matter fields can be charged under global symmetries. Throughout this chapter we will assume the existence of a global $U(1)$ symmetry in the theory. We will add a chemical potential for this symmetry and thereby induce a charge density.

For the vast majority of quantum field theories having classical gravity duals, however, we do not know the field theory Lagrangian explicitly. Any consistent theory of quantum gravity with a superselection sector described by

asymptotically AdS spacetimes will define a dual quantum field theory. Very many such constructions are believed to exist. These form the “landscape” of string vacua; see e.g. [10]. Rather than via a Lagrangian, the dual field theories are characterised by their spectrum of operators and the correlation functions of these operators. One can argue cogently that such a description of a theory, in terms of operators and correlators, is better suited to strongly interacting theories than a Lagrangian description, which employs somewhat fictitious weakly interacting fields.

As this chapter is a gravitational perspective on holographic physics, we shall look at general features of charged asymptotically AdS spacetimes without concerning ourselves with the specific dual field theories involved. Some results that we discuss have been embedded into actually existing concrete holographic dualities, while others remain to be so realised.

We have stated that the large- N field theory limit is a classical limit and that the bulk gravitational description provides the anticipated classical description. Let us briefly see how this works out. The simplest theory that has the AdS metric (14.1) as a solution is Einstein gravity with a negative cosmological constant, for which the Lagrangian is

$$\mathcal{L} = \frac{1}{2\kappa^2} \left(R + \frac{6}{L^2} \right) . \quad (14.4)$$

To exhibit the large number of degrees of freedom of the large- N limit in a universal way, we can heat up the field theory. This is achieved by considering a (planar) black hole in the interior of an AdS spacetime. The Schwarzschild–AdS solution is

$$ds^2 = \frac{L^2}{r^2} \left(-f(r)dt^2 + \frac{dr^2}{f(r)} + dx^2 + dy^2 \right) . \quad (14.5)$$

Here the metric function and corresponding field theory temperature are

$$f(r) = 1 - \left(\frac{r}{r_+} \right)^3 , \quad T = \frac{3}{4\pi r_+} . \quad (14.6)$$

As usual the temperature can be determined as the inverse period of the Euclidean time circle that renders the Euclidean Schwarzschild–AdS solution regular at the horizon $r = r_+$. A nonzero temperature is an IR phenomenon. Consequently we see in (14.6) that the UV metric ($r \rightarrow 0$) is not altered by the presence of a horizon, while the IR interior of the spacetime is qualitatively changed. From the Euclidean solution we can compute the free energy of the field theory by evaluating the gravitational path integral on the Euclidean saddle point, so that, with $Z = e^{-S_E}$,

$$F = -T \log Z = TS_E = -\frac{(4\pi)^3 L^2}{2 \times 3^3 \kappa^2} V_2 T^3 . \quad (14.7)$$

In evaluating the on-shell action one must ‘‘holographically renormalise’’ volume divergences (see e.g. [11]). In the above expression V_2 is the spatial volume of the field theory. The temperature dependence is determined by dimensional analysis – we started with a scale-invariant theory and so the temperature is the only scale. The coefficient of the temperature scaling gives a measure of the number of degrees of freedom of the theory. In the large- N limit we therefore expect that

$$\frac{L^2}{\kappa^2} \gg 1 , \quad (14.8)$$

and, indeed, this is the classical gravitational limit in which the AdS curvature is small in Planck units.

14.3 Brief condensed matter motivation

This section will introduce the quantum field theory problem of a nonzero density of fermions coupled to a gapless boson. We will firstly explain why such a system is of interest in condensed matter physics and secondly why it is a challenging system to study in 2+1 spacetime dimensions.

Consider the conduction electrons in a metal. At the lattice energy scale we are faced with a strongly interacting many body problem. Landau argued that the solution to this many body problem would simplify for physics at the lowest energy scales; see e.g. [12]. One step in Landau’s argument followed from the Pauli exclusion principle obeyed by the fermion density. The conduction electrons would be forced to build up a Fermi surface in momentum space, and consequently the lowest-energy fermionic excitations would correspond to removing or adding a fermion to the top of the Fermi sea. These excitations would not live at the origin of momentum space but rather at the Fermi momentum $k = k_F$. The reduced phase space available to fermions to scatter close to the Fermi surface then results in a suppression of the effects of interactions. In modern renormalisation group language, the Fermi-liquid theory of the low-energy excitations of fermions about a Fermi surface turns out to be an IR free fixed point, independently of the strength of electron interactions at the UV lattice scale [13, 14]. It therefore provides a robust weakly interacting starting point from which physical questions such as superconducting pairing instabilities may be studied.

In recent years, a large number of experiments on many different families of materials, including several families of nonconventional superconductors, have indicated that, in many situations of significant interest, Fermi-liquid theory does not adequately describe low-energy electronic physics. One famous indication of

this fact is that the observed electrical resistivity is larger than in Fermi-liquid theory, often scaling as T rather than the predicted T^2 at low temperatures.² See e.g. [15] for an overview of such measurements. This may suggest the presence of additional low-energy excitations capable of efficiently scattering the low-energy current-carrying fermions. As we have just recalled that fermions are unable to scatter efficiently near the Fermi surface, we are led to consider the existence of additional gapless bosonic degrees of freedom, taking the system outside the low-energy universality class of Fermi-liquid theory.

Bosonic excitations can arise as collective modes of the UV electrons. However, in order for the bosons to be gapless the system must either be tuned to a ‘‘quantum critical point’’ at which the mass of the boson vanishes or else there must be a kinematical constraint leading to a ‘‘critical phase’’ where the boson can remain massless over a range of parameter space. A quantum critical point separates different zero-temperature phases of matter. If one phase is characterised by an order parameter then, at the critical point, fluctuations of the order parameter will become massless, and these are the modes that can scatter fermions [16, 17]. Critical phases are perhaps more closely related to the types of theory with a holographic dual, and so we will discuss them in a little more detail. They will also connect directly to our later discussion of spacetimes with and without charged event horizons.

A natural way to describe the more robust gapless bosons of critical phases is as deconfined gauge fields, whose masslessness is protected by gauge invariance. Gauge fields can emerge as collective excitations of electrons when the microscopic lattice theory contains constraints, e.g. the forbidding of the double occupancy of lattice sites [18]. In terms of the creation operator $c_{i\sigma}^\dagger$ for an election with spin $\sigma = \uparrow, \downarrow$, the no-double-occupancy constraint at each site i reads

$$\sum_\sigma c_{i\sigma}^\dagger c_{i\sigma} \leq 1 . \quad (14.9)$$

Such constraints can be elegantly recast as equalities rather than inequalities by using a redundant mathematical description of the electron as the composite of a spinon particle $f_{i\sigma}^\dagger$ and a holon particle b_i^\dagger . The constraint (14.9) becomes the statement that at each site there must either be an up spin, a down spin, or a hole (i.e. a missing electron). Let us write this as

$$\sum_\sigma f_{i\sigma}^\dagger f_{i\sigma} + b_i^\dagger b_i = 1 . \quad (14.10)$$

² For completeness we should note that, to obtain a nonzero resistivity, translational invariance must be broken by adding e.g. contact ‘‘umklapp’’ interactions to the Fermi-liquid theory.

This is equivalent to “fractionalising” the electron into its spin and charge degrees of freedom by writing

$$c_{i\sigma} = f_{i\sigma} b_i^\dagger. \quad (14.11)$$

This description is redundant because the local (in time and space) transformation

$$f_{i\sigma}(t) \rightarrow e^{i\theta(t)} f_{i\sigma}(t), \quad b_i(t) \rightarrow e^{i\theta(t)} b_i(t), \quad (14.12)$$

leaves the physical field $c_{i\sigma}$ invariant. This redundancy must be cancelled out of the theory by gauging the symmetry (14.12). Upon gauging, the constraint (14.10) appears as the local Gauss law for the total gauge charge at each site.

The main purposes of the previous paragraph were, first, to explain how local microscopic constraints motivate the emergence of gauge fields and, second, to introduce the notion of fractionalisation, in which a gauge-invariant fermion c is expressed as a composite of a gauge-charged fermion f and a gauge-charged boson b . A description of the system in terms of an emergent gauge boson and gauge-charged bosons and fermions starts to take us close to the class of theories discussed just before (14.3). The substantial difference between the continuum limit of the theory discussed here and that of (14.3) is that here we are discussing an emergent $U(1)$ gauge field while holographic theories typically have $SU(N)$ gauge fields, with N large. Such will be the price of theoretical control over computations.

Suppose that we are granted a critical phase described by an emergent photon. A simple low-energy effective theory describing the interaction of this photon with the fermionic excitations of a Fermi surface is quantum electrodynamics at finite chemical potential μ :

$$\mathcal{L} = -\frac{1}{4}F^2 + \bar{\psi} [\gamma \cdot (i\partial + A) + \gamma^0 \mu] \psi. \quad (14.13)$$

While (2+1)-dimensional Maxwell theories tend to confine [19], it is believed that the presence of a Fermi surface dynamically suppresses the instantons responsible for confinement; see e.g. [20, 21]. Therefore the theory (14.13) is an example of a (2+1)-dimensional theory that, at energy scales well below the chemical potential scale, should describe the excitations of a Fermi surface interacting with a gapless boson.

A useful recent discussion of the theory (14.13) at the lowest energy scales, including references to an extensive earlier literature, can be found in [22]. It had been known for some time that the theory flowed to strong coupling, but it was believed that the RG flow could be reigned in by means of a large- N expansion in which the number of fermion fields was taken to be large (this is quite different from the 't Hooft matrix large- N expansion that will be discussed in the rest of

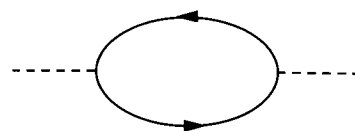


Figure 14.2 One-loop correction to the boson propagator from fermions.

this chapter). An important result in [22] was that this large- N expansion breaks down at high loop order, owing to the particular kinematic effects associated with the presence of a Fermi surface. This has the consequence that controlling the low-energy physics seems to require one to directly confront strong interactions. It was subsequently observed that such effects occur also in other models of bosons coupled to (2+1)-dimensional Fermi surfaces, in which the boson describes gapless order-parameter fluctuations rather than an emergent gauge field [23, 24]. Obtaining a controlled description of the low-energy dynamics of a finite density of fermions coupled to a gapless boson remains a formidable quantum-field-theoretic problem, with potentially important consequences for exotic states of matter. Attempts to address this problem using more conventional, field-theoretic, frameworks than holography include [25].

While field-theoretic computations in the model (14.13) are not controlled at low energies, it is possible to gain qualitative insight from uncontrolled perturbative computations. A basic quantity to consider is the propagator for the bosonic field. In the QED example (14.13) this is the transverse gauge field \vec{A} (the temporal component becomes gapped owing to screening by the density of the fermions). In general it is best to consider gauge-invariant quantities, but this correlator has the same form in theories at quantum critical points in which the gapless boson is gauge invariant. Classically, the inverse boson propagator has the schematic form $D(\omega, k)^{-1} = \omega^2 + k^2$. The leading correction is given by the loop of fermions shown in Fig. 14.2. Evaluating this self-energy diagram, the inverse propagator to leading order at low (Euclidean) energies ω and momenta k becomes

$$D(\omega, k)^{-1} = \gamma \frac{|\omega|}{|k|} + k^2. \quad (14.14)$$

This rather nonanalytic structure of the low-energy propagator is possible because the chemical potential μ breaks Lorentz invariance. The main point is that, while the UV propagator has the Lorentzian scale invariance $\{t, |x|\} \rightarrow \lambda \{t, |x|\}$, the emergent IR scaling of the propagator (14.14) is

$$t \rightarrow \lambda^3 t, \quad |x| \rightarrow \lambda |x|. \quad (14.15)$$

We are simplifying a little here; the correct scaling is locally anisotropic in momentum owing to the presence of a Fermi surface. The interested reader is referred to

[22]. The scaling (14.15) is said to correspond to a dynamical critical exponent $z = 3$. In general, z denotes the relative scaling of space and time. The one-loop result $z = 3$ is not typically protected from order-1 corrections at higher loop orders. The phenomenon whereby the interaction of the boson with a finite density of fermions causes a strong frequency dependence in the boson propagator is called Landau damping.

To summarise this brief motivation from condensed matter physics: it is of interest to understand the behaviour of gapless bosons coupled to the excitations of a Fermi surface. One example of this occurs when a metallic system exhibits an emergent gauge symmetry. Quantum field theories describing such bosons and fermions are typically strongly interacting at low energies in 2+1 dimensions and resilient to conventional field-theoretic techniques. An important quantity characterising the emergent strongly interacting low-energy theory is the dynamical critical exponent z .

14.4 Holography with a chemical potential

The upshot of the previous section is that we would like to have a controlled framework to study the low-energy physics of gapless bosons coupled to a finite density of fermions. We have seen that field theories with holographic gravity duals typically have the ingredients necessary to approach this question, i.e., $SU(N)$ gauge fields that are massless and matter charged under a global symmetry that can be placed at a chemical potential to induce a charge density. In this section we will describe how to set up the gravitational version of this field-theoretic problem.

We wish to consider finite-density states of matter. This means that $\langle J^t \rangle \neq 0$, where J^t is the charge density operator for a global $U(1)$ symmetry in the field theory. A finite charge density is induced by holding the system at a nonzero chemical potential. Recall that this means that we add to the Lagrangian of the theory the term $\Delta\mathcal{L} = \mu J^t$. The most basic explicit entry in the holographic “dictionary” is that single-trace operators in the quantum field theory are in one-to-one correspondence with fields in the gravitating bulk. In particular, see e.g. [11], the charge density operator J^t is dual to the time component of a Maxwell field A_t in the bulk. The connection between bulk and field theory quantities works as follows. In our classical limit, the gauge potential will obey Maxwell’s equations in the bulk. For a given solution to the bulk equations of motion, the corresponding values of μ and $\langle J^t \rangle$ can be read from the asymptotic near-boundary ($r \rightarrow 0$) behaviour of the solution as

$$A_t(r) = \mu + \langle J^t \rangle r + \dots \quad (14.16)$$

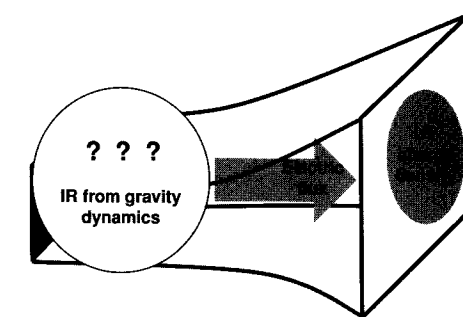


Figure 14.3 The basic aim in finite-density holography: use the gravitational equations of motion to find the interior IR geometry, given the boundary condition that there is an electric flux at infinity.

Thus the chemical potential and charge density are the boundary values of the Maxwell potential and electric flux, respectively:

$$\mu = \lim_{r \rightarrow 0} A_t, \quad \langle J^t \rangle = \lim_{r \rightarrow 0} F_{rt}. \quad (14.17)$$

Therefore to impose that the quantum field theory is at nonzero density, we must impose that the dual spacetime has an electric flux at infinity.

As explained in section 14.2 above, the asymptotic boundary conditions on the spacetime correspond to the UV starting point of the field-theoretic RG flow. Integrating the bulk equations of motion into the interior of the spacetime corresponds to flowing down to the low-energy IR limit of the theory. This is the regime where traditional field-theoretic approaches run into difficulties, and so we would like to understand what holography has to say. The holographic framework is illustrated in Fig. 14.3 and will guide the remainder of this chapter. We will find that the question of how to “fill in” the spacetime, given electric flux at the boundary, leads to gravitational physics that is interesting in its own right.

14.5 The planar Reissner–Nordström–AdS black hole

The minimal framework capable of describing the physics of electric flux in an asymptotically AdS geometry is Einstein–Maxwell theory with a negative cosmological constant [26]. The Lagrangian density can be written as

$$\mathcal{L} = \frac{1}{2\kappa^2} \left(R + \frac{6}{L^2} \right) - \frac{1}{4e^2} F_{\mu\nu} F^{\mu\nu}. \quad (14.18)$$

Here κ and e are respectively the Newtonian and Maxwell constants while L sets the cosmological constant length scale.

[22]. The scaling (14.15) is said to correspond to a dynamical critical exponent $z = 3$. In general, z denotes the relative scaling of space and time. The one-loop result $z = 3$ is not typically protected from order-1 corrections at higher loop orders. The phenomenon whereby the interaction of the boson with a finite density of fermions causes a strong frequency dependence in the boson propagator is called Landau damping.

To summarise this brief motivation from condensed matter physics: it is of interest to understand the behaviour of gapless bosons coupled to the excitations of a Fermi surface. One example of this occurs when a metallic system exhibits an emergent gauge symmetry. Quantum field theories describing such bosons and fermions are typically strongly interacting at low energies in 2+1 dimensions and resilient to conventional field-theoretic techniques. An important quantity characterising the emergent strongly interacting low-energy theory is the dynamical critical exponent z .

14.4 Holography with a chemical potential

The upshot of the previous section is that we would like to have a controlled framework to study the low-energy physics of gapless bosons coupled to a finite density of fermions. We have seen that field theories with holographic gravity duals typically have the ingredients necessary to approach this question, i.e., $SU(N)$ gauge fields that are massless and matter charged under a global symmetry that can be placed at a chemical potential to induce a charge density. In this section we will describe how to set up the gravitational version of this field-theoretic problem.

We wish to consider finite-density states of matter. This means that $\langle J^t \rangle \neq 0$, where J^t is the charge density operator for a global $U(1)$ symmetry in the field theory. A finite charge density is induced by holding the system at a nonzero chemical potential. Recall that this means that we add to the Lagrangian of the theory the term $\Delta\mathcal{L} = \mu J^t$. The most basic explicit entry in the holographic “dictionary” is that single-trace operators in the quantum field theory are in one-to-one correspondence with fields in the gravitating bulk. In particular, see e.g. [11], the charge density operator J^t is dual to the time component of a Maxwell field A_t in the bulk. The connection between bulk and field theory quantities works as follows. In our classical limit, the gauge potential will obey Maxwell’s equations in the bulk. For a given solution to the bulk equations of motion, the corresponding values of μ and $\langle J^t \rangle$ can be read from the asymptotic near-boundary ($r \rightarrow 0$) behaviour of the solution as

$$A_t(r) = \mu + \langle J^t \rangle r + \dots \quad (14.16)$$

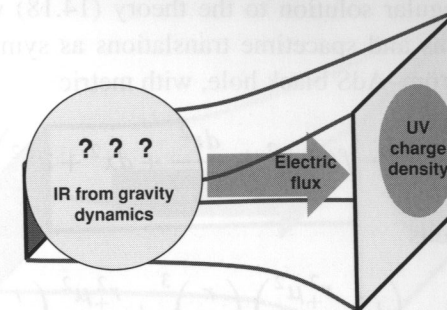


Figure 14.3 The basic aim in finite-density holography: use the gravitational equations of motion to find the interior IR geometry, given the boundary condition that there is an electric flux at infinity.

Thus the chemical potential and charge density are the boundary values of the Maxwell potential and electric flux, respectively:

$$\mu = \lim_{r \rightarrow 0} A_t, \quad \langle J^t \rangle = \lim_{r \rightarrow 0} F_{rt}. \quad (14.17)$$

Therefore to impose that the quantum field theory is at nonzero density, we must impose that the dual spacetime has an electric flux at infinity.

As explained in section 14.2 above, the asymptotic boundary conditions on the spacetime correspond to the UV starting point of the field-theoretic RG flow. Integrating the bulk equations of motion into the interior of the spacetime corresponds to flowing down to the low-energy IR limit of the theory. This is the regime where traditional field-theoretic approaches run into difficulties, and so we would like to understand what holography has to say. The holographic framework is illustrated in Fig. 14.3 and will guide the remainder of this chapter. We will find that the question of how to “fill in” the spacetime, given electric flux at the boundary, leads to gravitational physics that is interesting in its own right.

14.5 The planar Reissner–Nordström–AdS black hole

The minimal framework capable of describing the physics of electric flux in an asymptotically AdS geometry is Einstein–Maxwell theory with a negative cosmological constant [26]. The Lagrangian density can be written as

$$\mathcal{L} = \frac{1}{2\kappa^2} \left(R + \frac{6}{L^2} \right) - \frac{1}{4e^2} F_{\mu\nu} F^{\mu\nu}. \quad (14.18)$$

Here κ and e are respectively the Newtonian and Maxwell constants while L sets the cosmological constant length scale.

There is a unique regular solution to the theory (14.18) with electric flux at infinity that has rotations and spacetime translations as symmetries. This is the planar Reissner–Nordström–AdS black hole, with metric

$$ds^2 = \frac{L^2}{r^2} \left(-f(r)dt^2 + \frac{dr^2}{f(r)} + dx^2 + dy^2 \right). \quad (14.19)$$

The metric function here is

$$f(r) = 1 - \left(1 + \frac{r_+^2 \mu^2}{2\gamma^2} \right) \left(\frac{r}{r_+} \right)^3 + \frac{r_+^2 \mu^2}{2\gamma^2} \left(\frac{r}{r_+} \right)^4. \quad (14.20)$$

We introduced the dimensionless ratio of the Newtonian and Maxwell couplings

$$\gamma^2 = \frac{e^2 L^2}{\kappa^2}. \quad (14.21)$$

The Maxwell potential of the solution is

$$A = \mu \left(1 - \frac{r}{r_+} \right) dt. \quad (14.22)$$

We have required the Maxwell potential to vanish on the horizon, $A_t(r_+) = 0$. The simplest argument for this condition is that otherwise the holonomy of the potential around the Euclidean time circle would remain nonzero when the circle collapses at the horizon, indicating a singular gauge connection. The planar Reissner–Nordström–AdS solution is characterised by two scales, the chemical potential $\mu = \lim_{r \rightarrow 0} A_t$ and the horizon radius r_+ . From the dual field theory perspective, it is more physical to think in terms of the temperature than the horizon radius. The temperature is given by

$$T = \frac{1}{4\pi r_+} \left(3 - \frac{r_+^2 \mu^2}{2\gamma^2} \right). \quad (14.23)$$

The black hole is illustrated in Fig. 14.4. This black hole, which can additionally carry a magnetic charge, was the starting point for holographic approaches to finite-density condensed matter [27, 28].

Because the underlying UV theory is scale invariant, the only dimensionless quantity that we can discuss is the ratio T/μ . In order to answer our basic question about the IR physics at low temperatures, we must take the limit $T/\mu \ll 1$ of the solution. We thereby obtain the extremal Reissner–Nordström–AdS black hole, with

$$f(r) = 1 - 4 \left(\frac{r}{r_+} \right)^3 + 3 \left(\frac{r}{r_+} \right)^4. \quad (14.24)$$

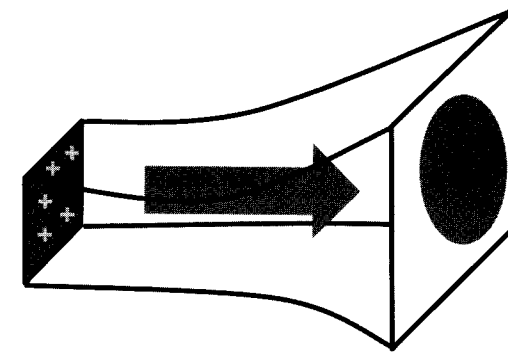


Figure 14.4 The planar Reissner–Nordström–AdS black hole. The charge density is sourced entirely by flux emanating from the black hole horizon.

The near-horizon extremal geometry, capturing the field theory IR, follows by expanding the solution near $r = r_+$. Setting $r = r_+(1 - r_+/\rho)$, taking ρ as large and rescaling $\{t, x, y\}$ by dimensionless constants gives

$$ds^2 = \frac{L^2}{6} \left(\frac{-d\bar{t}^2 + d\rho^2}{\rho^2} \right) + d\bar{x}^2 + d\bar{y}^2, \quad A = \frac{\gamma}{\sqrt{6}} \frac{d\bar{t}}{\rho}. \quad (14.25)$$

The near-horizon geometry is seen to be the famous Bertotti–Robinson-like spacetime $\text{AdS}_2 \times \mathbb{R}^2$ [29].

Consistently with the field theory intuition following from our discussion in section 14.3 above, the interior geometry (14.25) exhibits an emergent IR scaling invariance:

$$\rho \rightarrow \lambda \rho, \quad t \rightarrow \lambda t, \quad \{x, y\} \rightarrow \{x, y\}. \quad (14.26)$$

Under this scaling, however, time scales but space does not. We will see shortly that such a scaling is a degenerate limit of possible scalings that are anisotropic in time and space, with dynamical critical exponent $z = \infty$. This fact is directly related to the following two statements. First, the entropy density remains finite at zero temperature:

$$s = \frac{S}{V_2} = \frac{2\pi}{\kappa^2} \frac{A}{V_2} = \frac{\pi \mu^2}{3e^2} \quad (T = 0). \quad (14.27)$$

Here V_2 is the field theory spatial volume, A is the event horizon area and the second equality gives Hawking’s formula for the black hole entropy. Second, the density of states is IR divergent [30]. The IR scaling (14.26) implies that $\rho(E) \sim e^S \delta(E) + E^{-1}$. The first term is the zero-temperature entropy density, while the second gives an IR divergence upon integrating.

The implication of the previous paragraph is that the near-horizon geometry of extremal Reissner–Nordström–AdS black holes is unlikely to survive beyond the bulk classical large- N limit. The entropy density suggests a fine tuning while the divergent number of states suggests an instability. In the following sections we will discuss two circumstances in which the near-horizon $\text{AdS}_2 \times \mathbb{R}^2$ has instabilities at leading order in large N . The first involves bosons and leads to superconductivity and the second involves fermions. We then discuss the effects of incorporating dilaton couplings; in these cases $\text{AdS}_2 \times \mathbb{R}^2$ is not even a solution to the equations of motion. The new IR geometry in all cases captures physics analogous to Landau damping with finite z .

14.6 Holographic superconductors

Despite the concerns expressed at the end of the previous section, a near-horizon AdS_2 geometry is a robust feature of extremal black holes; see e.g. [31]. One way to evade this conclusion is to add charged matter fields to our Einstein–Maxwell theory. This is a natural extension; a consistent microscopic theory in the bulk will certainly have fields carrying the Maxwell charge. We will find that extremal black holes can become thermodynamically disfavoured in relation to new solutions to the equations of motion in which the asymptotic electric flux is explicitly supported by charged fields rather than emanating from behind an extremal horizon. If the charged matter is bosonic then we obtain so-called ‘‘holographic superconductors’’ [32, 33], while in the case of charged fermions we obtain ‘‘electron stars’’ [34, 35]. Consider first the bosonic case. A simple Lagrangian density to consider is

$$\mathcal{L} = \frac{1}{2\kappa^2} \left(R + \frac{6}{L^2} \right) - \frac{1}{4e^2} F_{\mu\nu} F^{\mu\nu} - |\nabla\phi - iA\phi|^2 - m^2|\phi|^2 - V(|\phi|). \quad (14.28)$$

We have taken the charge of the scalar to be unity, without loss of generality.

The question is whether there are circumstances under which it is favourable for the charged scalar field ϕ to condense. The Maxwell potential A_t of the Reissner–Nordström background acts like a space-dependent chemical potential for the scalar. We might therefore anticipate the Bose–Einstein condensation of ϕ [36]. Counteracting this possibility, we can recall that the gravitational well of asymptotically AdS spacetimes acts like a covariant box and is capable of stabilising potential tachyons [37]. Furthermore, the propensity of matter to fall into black hole horizons can be formalised into ‘‘no hair’’ theorems forbidding the presence of scalar fields outside black holes in a range of circumstances; see e.g. [38].

The conditions for instability simplify at zero temperature. Here stability is determined by the behaviour of the scalar field in the near-horizon $\text{AdS}_2 \times \mathbb{R}^2$ geometry [33, 39, 40]. The scalar field will condense if its effective mass squared in

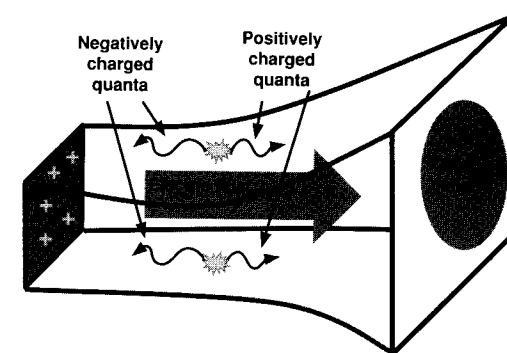


Figure 14.5 The onset of the superconducting instability. Pair-produced waves are repelled or attracted to the black hole depending on their charge.

the near-horizon region is below the AdS_2 Breitenlohner–Freedman bound ($m_{\text{BF}}^2 = -1/(4L_{\text{AdS}_2}^2)$; see e.g. [41]), i.e.

$$L_{\text{AdS}_2}^2(m^2 + g^{tt}A_t A_t) = \frac{1}{6}(m^2 L^2 - \gamma^2) \leq -\frac{1}{4}. \quad (14.29)$$

Here we have used the near-horizon solution (14.25). This expression can be understood physically as the condition for the classical field analogue of Schwinger pair production in AdS_2 [42]. The spacetime becomes unstable to the production of pairs of classical waves, as illustrated in Fig. 14.5. The physics here can also be understood as the charged analogue of superradiance. It is more than an analogy, as Reissner–Nordström–AdS black holes can be uplifted to higher-dimensional rotating black holes [26]. Superradiance leads to a genuine instability in the present context as the AdS_4 ‘‘box’’ reflects the waves back towards the black hole, leading to exponential growth in the mode.

Rather than the dynamical evolution of the instability at fixed energy, we are interested in determining the dominant saddle point of the asymptotically AdS_4 Euclidean path integral at fixed temperature and chemical potential. It has been shown that, in the model (14.28), if the mass satisfies the inequality (14.29) then it is thermodynamically favourable for the scalar field ϕ to condense, below a critical temperature $T < T_C \propto \mu$. The condensation occurs via a second-order phase transition [32, 33]. The condensate describes a macroscopically occupied bosonic ground state with a definite phase. It thereby spontaneously breaks the $U(1)$ symmetry of the theory. For this reason these solutions are known as holographic superconductors.

The objective of this chapter is to characterise phases of matter with gravity duals at low temperatures such that $T/\mu \ll 1$. We therefore omit a review of the many properties of holographic superconductors in order to focus on their low-energy

behaviour at low temperatures. The interested reader is referred to the discussions in [11, 43, 44].

The problem becomes to determine the IR behaviour (i.e. in the far interior of the spacetime) of solutions to the equations of motion following from (14.28). This behaviour depends strongly on the choice of potential V . The cleanest behaviours to consider are those in which the scalar field ϕ tends to a constant, ϕ_∞ , in the IR. Preserving rotational and spacetime translational invariance implies that the holographic superconductor spacetime, Maxwell potential and scalar may be taken to have the general form

$$\frac{1}{L^2}ds^2 = -f(r)dt^2 + g(r)dr^2 + \frac{dx^2 + dy^2}{r^2}, \quad A = \gamma h(r)dt, \quad \phi = \phi(r). \quad (14.30)$$

In these coordinates, a zero-temperature IR spacetime without a finite-size horizon will be at $r \rightarrow \infty$. If the scalar field does not stabilise as $r \rightarrow \infty$, as occurs for instance for $m^2 < 0$ and no potential V [45], then corrections to the leading-order gravity action (14.28) will be necessary in order to access the true far IR of the theory at zero temperature. When the scalar does stabilise we can hope for a scale-invariant solution. Suppose that we find such an IR fixed point. A useful quantity to consider is the IR scaling dimension of the field theory charge density operator J^t dual to A_t in the bulk [46]. The renormalisation group flow described by the spacetime (14.30) is being driven by the UV insertion of μJ^t . Lorentz invariance is broken along this flow and the bulk $U(1)$ Maxwell symmetry is Higgsed. The operator J^t therefore typically acquires an anomalous dimension. If it becomes irrelevant in the IR theory then we can expect that Lorentz symmetry will be restored and that we will obtain an emergent AdS_4 spacetime. This phenomenon has been observed in various models, starting with [47] and including cases that can be uplifted to consistent nonlinear solutions of string theory [48, 49].

More generally, the operator J^t will not be irrelevant in the IR and we have reason to anticipate a non-Lorentz-invariant fixed point. Correspondingly, in [45, 46] so-called Lifshitz [50] geometries were found in the far IR. These take the form

$$\frac{1}{L^2}ds^2 = -\frac{dt^2}{r^{2z}} + g_\infty \frac{dr^2}{r^2} + \frac{dx^2 + dy^2}{r^2}, \quad A = \gamma h_\infty \frac{dt}{r^z}, \quad \phi = \phi_\infty. \quad (14.31)$$

Without loss of generality we have rescaled the time coordinate to remove any constant term in g_{tt} . The Lifshitz solution has the scaling symmetry

$$r \rightarrow \lambda r, \quad t \rightarrow \lambda^z t, \quad \{x, y\} \rightarrow \lambda \{x, y\}. \quad (14.32)$$

The variable z is called the dynamical critical exponent. Setting $r = \rho^{1/z}$ in the Lifshitz geometry (14.31) and then comparing with the $AdS_2 \times \mathbb{R}^2$ near-horizon

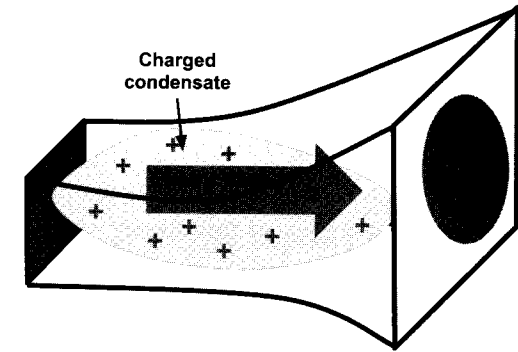


Figure 14.6 The zero-temperature holographic superconductor. The electric flux is sourced entirely by the scalar field condensate.

geometry of the extremal black hole (14.25), we see that the extremal black hole corresponds to the limit $z \rightarrow \infty$. The relativistic case AdS_4 is given by $z = 1$. An immediate property of the solution (14.31) is that, unlike for the $AdS_2 \times \mathbb{R}^2$ case, there is no electric flux emanating from the horizon: $\lim_{r \rightarrow \infty} \int_{\mathbb{R}^2} \star F = 0$. All the field theory charge density is therefore sourced by the condensate in the bulk, as illustrated in Fig. 14.6.

Substituting the Lifshitz ansatz (14.31) into the equations of motion, one finds that the theory (14.28) admits Lifshitz solutions, with the dynamical critical exponent z given by

$$8(V_T - 3) + 4(V'_T)^2 - 4V_T + 12z + (V'_T)^2 + 8V_T - 24z^2 + V'_T z^3 = 0. \quad (14.33)$$

Here we have introduced

$$V_T = \kappa^2 L^2 [V(\phi_\infty) + m^2 \phi_\infty^2], \quad V'_T = \frac{\kappa^2 L}{e} [V'(\phi_\infty) + 2m^2 \phi_\infty]. \quad (14.34)$$

Thus the dynamical critical exponent is determined by the values of the potential and its first derivative at ϕ_∞ , which are in turn determined by the equations of motion. In order for the scaling (14.32) to have a straightforward interpretation as a renormalisation transformation, one should have $z > 0$. The null energy condition in the bulk furthermore implies that $z > 1$ [46]. Even if (14.33) gives physical solutions for z , it is not guaranteed that the corresponding Lifshitz solution is realised as the near-horizon geometry. An instructive simple case to consider is $m^2 > 0$ and $V = 0$. One obtains in this case [45, 46]

$$z = \frac{\gamma^2}{\gamma^2 - L^2 m^2}, \quad \phi_\infty^2 = \frac{1}{e^2 L^2} \frac{6z}{(1+z)(2+z)}. \quad (14.35)$$

behaviour at low temperatures. The interested reader is referred to the discussions in [11, 43, 44].

The problem becomes to determine the IR behaviour (i.e. in the far interior of the spacetime) of solutions to the equations of motion following from (14.28). This behaviour depends strongly on the choice of potential V . The cleanest behaviours to consider are those in which the scalar field ϕ tends to a constant, ϕ_∞ , in the IR. Preserving rotational and spacetime translational invariance implies that the holographic superconductor spacetime, Maxwell potential and scalar may be taken to have the general form

$$\frac{1}{L^2}ds^2 = -f(r)dt^2 + g(r)dr^2 + \frac{dx^2 + dy^2}{r^2}, \quad A = \gamma h(r)dt, \quad \phi = \phi(r). \quad (14.30)$$

In these coordinates, a zero-temperature IR spacetime without a finite-size horizon will be at $r \rightarrow \infty$. If the scalar field does not stabilise as $r \rightarrow \infty$, as occurs for instance for $m^2 < 0$ and no potential V [45], then corrections to the leading-order gravity action (14.28) will be necessary in order to access the true far IR of the theory at zero temperature. When the scalar does stabilise we can hope for a scale-invariant solution. Suppose that we find such an IR fixed point. A useful quantity to consider is the IR scaling dimension of the field theory charge density operator J^t dual to A_t in the bulk [46]. The renormalisation group flow described by the spacetime (14.30) is being driven by the UV insertion of μJ^t . Lorentz invariance is broken along this flow and the bulk $U(1)$ Maxwell symmetry is Higgsed. The operator J^t therefore typically acquires an anomalous dimension. If it becomes irrelevant in the IR theory then we can expect that Lorentz symmetry will be restored and that we will obtain an emergent AdS_4 spacetime. This phenomenon has been observed in various models, starting with [47] and including cases that can be uplifted to consistent nonlinear solutions of string theory [48, 49].

More generally, the operator J^t will not be irrelevant in the IR and we have reason to anticipate a non-Lorentz-invariant fixed point. Correspondingly, in [45, 46] so-called Lifshitz [50] geometries were found in the far IR. These take the form

$$\frac{1}{L^2}ds^2 = -\frac{dt^2}{r^{2z}} + g_\infty \frac{dr^2}{r^2} + \frac{dx^2 + dy^2}{r^2}, \quad A = \gamma h_\infty \frac{dt}{r^z}, \quad \phi = \phi_\infty. \quad (14.31)$$

Without loss of generality we have rescaled the time coordinate to remove any constant term in g_{tt} . The Lifshitz solution has the scaling symmetry

$$r \rightarrow \lambda r, \quad t \rightarrow \lambda^z t, \quad \{x, y\} \rightarrow \lambda \{x, y\}. \quad (14.32)$$

The variable z is called the dynamical critical exponent. Setting $r = \rho^{1/z}$ in the Lifshitz geometry (14.31) and then comparing with the $AdS_2 \times \mathbb{R}^2$ near-horizon

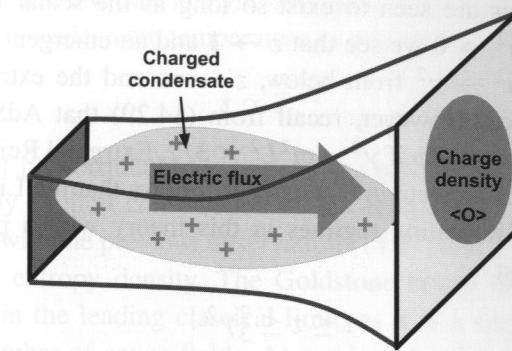


Figure 14.6 The zero-temperature holographic superconductor. The electric flux is sourced entirely by the scalar field condensate.

geometry of the extremal black hole (14.25), we see that the extremal black hole corresponds to the limit $z \rightarrow \infty$. The relativistic case AdS_4 is given by $z = 1$. An immediate property of the solution (14.31) is that, unlike for the $AdS_2 \times \mathbb{R}^2$ case, there is no electric flux emanating from the horizon: $\lim_{r \rightarrow \infty} \int_{\mathbb{R}^2} \star F = 0$. All the field theory charge density is therefore sourced by the condensate in the bulk, as illustrated in Fig. 14.6.

Substituting the Lifshitz ansatz (14.31) into the equations of motion, one finds that the theory (14.28) admits Lifshitz solutions, with the dynamical critical exponent z given by

$$8(V_T - 3) + 4(V'_T)^2 - 4V_T + 12z + (V'_T + 8V_T - 24)z^2 + V'^2_T z^3 = 0. \quad (14.33)$$

Here we have introduced

$$V_T = \kappa^2 L^2 [V(\phi_\infty) + m^2 \phi_\infty^2], \quad V'_T = \frac{\kappa^2 L}{e} [V'(\phi_\infty) + 2m^2 \phi_\infty]. \quad (14.34)$$

Thus the dynamical critical exponent is determined by the values of the potential and its first derivative at ϕ_∞ , which are in turn determined by the equations of motion. In order for the scaling (14.32) to have a straightforward interpretation as a renormalisation transformation, one should have $z > 0$. The null energy condition in the bulk furthermore implies that $z > 1$ [46]. Even if (14.33) gives physical solutions for z , it is not guaranteed that the corresponding Lifshitz solution is realised as the near-horizon geometry. An instructive simple case to consider is $m^2 > 0$ and $V = 0$. One obtains in this case [45, 46]

$$z = \frac{\gamma^2}{\gamma^2 - L^2 m^2}, \quad \phi_\infty^2 = \frac{1}{e^2 L^2} \frac{6z}{(1+z)(2+z)}. \quad (14.35)$$

The Lifshitz solutions are seen to exist so long as the scalar is not too heavy, $L^2 m^2 < \gamma^2$. As $L^2 m^2 \rightarrow 0$ we see that $z \rightarrow 1$ and an emergent relativistic AdS_4 is obtained. As $L^2 m^2 \rightarrow \gamma^2$ from below, $z \rightarrow \infty$ and the extremal $\text{AdS}_2 \times \mathbb{R}^2$ geometry is recovered. However, recall from (14.29) that $\text{AdS}_2 \times \mathbb{R}^2$ is stable against the condensation of ϕ if $\gamma^2 - m^2 L^2 \leq 3/2$. Extremal Reissner–Nordström is likely to be the ground state in this case. It follows that the Lifshitz geometries (14.35) realised as IR scaling regimes in this theory with a positive quadratic potential have at most

$$1 \leq z \leq \frac{2}{3}\gamma^2. \quad (14.36)$$

Thus the dynamical critical exponent is bounded by the relative strengths of the Maxwell and Newtonian couplings.

A few words about the near-horizon Lifshitz geometry (14.31) are appropriate at this point. As befits a scale-invariant solution, all local curvature invariants constructed from the Riemann tensor are constant and small in Planck units when $\kappa/L \ll 1$ [50]. Furthermore, the geometry is robust against higher-derivative corrections, which can only renormalise the overall curvature scale L and the dynamical critical exponent z [51]. Nonetheless, Lifshitz spacetimes are geodesically incomplete. For $z \neq 1$, an infalling observer experiences divergent tidal forces as $r \rightarrow \infty$ [11, 52]. Thus, strictly speaking, the spacetime does not end at a horizon in the interior but, rather, at a null singularity. In the classical gravity limit $\kappa/L \ll 1$, a parametrically small nonzero temperature $0 < T/\mu \ll 1$ will lead to a regular finite-temperature horizon and is sufficient to safely bound all observables. In practice this will suffice for many purposes. However, the spirit of the investigations in this chapter is to access the lowest possible energy scales in the dual field theory. In this sense we would like to be able to set $T = 0$ and probe all the way into the interior. It remains to be seen, then, whether this singularity has interesting consequences for the IR of the dual field theory, via for instance the overproduction of excited string states near the singularity, owing to the large tidal forces [53].

The emergent low-energy Lifshitz scaling (14.32) reminds us, of course, of the field theory scaling (14.15). The holographic superconductor setting is different from that field theory case because it describes a symmetry-breaking phase. In the holographic superconductor it is the bosonic superfluid density, rather than the finite density of fermions, that is ‘‘Landau damping’’ the transverse gauge fields of the dual field theory and leading to the Lifshitz scaling (14.32). The Lifshitz IR geometry indicates that, as well as the necessary Goldstone boson, owing to spontaneous symmetry breaking there are additional (neutral) gapless excitations at the lowest energy scales. We argue that these are (a gauge-invariant version of) Landau-damped $SU(N)$ gauge fields. This presence of gapless degrees of freedom is seen, for instance, in the power-law scaling of the entropy density at

low temperatures. Dimensional analysis and the Lifshitz scaling (14.32) imply that the entropy density scales with temperature as follows:

$$s \propto T^{2/z}. \quad (14.37)$$

The coefficient of proportionality is large in the bulk classical limit. This scaling can be verified by explicit construction of low-temperature black hole solutions and is consistent with the previous observation (14.27) that $z = \infty$ leads to a finite zero-temperature entropy density. The Goldstone boson itself does not appear in the geometry in the leading classical limit, as it is a single mode in contrast with the large number of gauge fields. At one-loop level in the bulk, fluctuations of the Goldstone mode lead to IR divergences in our case of a 2+1 dimensional field theory. These randomise the phase of the condensate and restore the $U(1)$ symmetry, in accordance with the Coleman–Mermin–Wagner theorem [54]. A general framework for incorporating the low-energy physics of the Goldstone mode may be found in [55].

14.7 Electron stars

Charged fermions in the bulk can qualitatively alter the interior of zero-temperature finite-charge-density spacetimes. The physics is similar to that of the charged bosons we have just discussed but has important differences. Pauli exclusion implies that fermions cannot macroscopically occupy their ground state. The state will therefore not have a coherent phase and the $U(1)$ symmetry remains unbroken. As is familiar from solid state physics, the presence of a sufficiently large background Maxwell potential A_t does not cause Bose–Einstein condensation but, rather, the build-up of a Fermi surface. The filled Fermi sea is a specific quantum vacuum of the fermions in the presence of a chemical potential that is stable in the absence of interactions. Gravitating Fermi surfaces are also familiar; they are the neutron stars of astrophysics. The solutions that we discuss in the following are charged planar cousins of neutron stars and therefore we will call them electron stars.

Consider a free charged Dirac field added to the Einstein–Maxwell action, so that

$$\mathcal{L} = \frac{1}{2\kappa^2} \left(R + \frac{6}{L^2} \right) - \frac{1}{4e^2} F_{\mu\nu} F^{\mu\nu} - \bar{\psi} \Gamma \cdot \left(\partial + \frac{1}{4} \omega_{\mu\nu} \Gamma^{\mu\nu} - iA \right) \psi - m^2 \bar{\psi} \psi. \quad (14.38)$$

Here $\Gamma^{\mu\nu}$ is an antisymmetrised gamma matrix and $\omega_{\mu\nu}$ is the spin connection. As we did for charged scalars in the previous section, we can ask about the fate of extremal Reissner–Nordström black holes in presence of charged fermions. Because fermion statistics prevents the macroscopic occupation of states, fermionic

instabilities should not be seen as an exponentially growing classical solution to the Dirac equation. Indeed such classical instabilities do not occur [56]. However, the Schwinger pair production of fermions will occur in the near-horizon $\text{AdS}_2 \times \mathbb{R}^2$ geometry if the fermion mass is sufficiently low [42], i.e.

$$m^2 L^2 \leq \gamma^2. \quad (14.39)$$

This is the fermionic analogue of the inequality (14.29) for bosons. In the fermionic case, while satisfying this inequality does not lead to a classical instability, it is manifested in solutions to the Dirac equation by the fermion acquiring an imaginary scaling dimension in the $\text{AdS}_2 \times \mathbb{R}^2$ spacetime [56, 57]. Analogously to the discussion for bosons, illustrated in Fig. 14.5, we might expect that pair production will lead to neutralisation of the black hole and a Fermi sea outside the horizon carrying the charge.

A further, logically separate, indication that a Fermi sea will become populated and backreact on the spacetime is the presence of Fermi-surface singularities in fermion Green's functions in the extremal Reissner–Nordström background [56–59]. In the textbook case of fermions in flat space with a constant chemical potential, the residue of the Fermi-surface singularity in the Green's function is related to the density of fermions via the Migdal relation. A similar relation should be anticipated in our curved spacetime [60], where now the density of fermions will gravitate.

Extremal Reissner–Nordström–AdS can be quantum mechanically unstable to population of the Fermi sea by the above two mechanisms. This amounts to saying that the unpopulated extremal Reissner–Nordström fermion vacuum is thermodynamically unstable. We will show this by constructing solutions with a populated Fermi sea and will find that they have a lowered free energy.

It is in general difficult to find solutions to the Einstein–Maxwell–Dirac system (14.38) with a populated and gravitating Fermi sea. The reason is that one must find all the eigenstates of the Dirac operator in a given background whose energies are below the chemical potential, sum their contributions to the bulk energy-momentum tensor and then self-consistently backreact this energy-momentum tensor on the geometry to solve the equations of motion. The problem simplifies in a coarse-grained limit in which the fermions may be treated as an ideal fluid [34, 35]. In our charged and gravitating context, this can be called the Thomas–Fermi–Oppenheimer–Volkov limit. Mathematically, the limit is a WKB limit in which the Dirac eigenstates become very localised in the geometry and are therefore locally not sensitive to variations in the curvature and Maxwell field.

The WKB electron star limit requires the mass m of a fermion to be large in units of the overall curvature length scale L of the spacetime. Furthermore, a consistent

solution requires the attractive gravitational force and the repulsive electrostatic forces between the fermions making up the star to be comparable. Thus we impose

$$mL \sim \frac{eL}{\kappa} \equiv \gamma \gg 1. \quad (14.40)$$

In addition to this WKB limit, by working in the classical limit throughout this chapter we have already been assuming that the Maxwell and Newton couplings are small: $e \ll 1$ and $\kappa/L \ll 1$. The notion that a large density of noninteracting fermions, with Compton wavelength much smaller than the scale at which the background varies, can be described as an ideal fluid is intuitively plausible and so we will not support this claim here. The process of coarse graining is discussed from various angles in [35, 61–64].

The action for a charged gravitating ideal fluid can be written as

$$\mathcal{L} = \frac{1}{2\kappa^2} \left(R + \frac{6}{L^2} \right) - \frac{1}{4e^2} F_{\mu\nu} F^{\mu\nu} + p(\mu_{\text{loc}}, s). \quad (14.41)$$

This is Schutz's form of the action for an ideal fluid [65], generalised to allow the fluid to be charged [35]. To obtain the expected ideal fluid equations of motion, one must write down the local chemical potential:

$$\mu_{\text{loc}} = |d\phi + \alpha d\beta + \theta ds + A|.$$

Then one varies μ_{loc} with respect to the fluid potential variables $\{\phi, \alpha, \beta\}$ as well as the local entropy density s and “thermasy” θ . We will only consider zero-temperature irrotational fluids, for which $\alpha = \beta = \theta = s = 0$ and ϕ can be absorbed into A by a gauge transformation. The potential A will only have a time component. Thus we have that

$$\mu_{\text{loc}} = \frac{A_t}{\sqrt{g_{tt}}}. \quad (14.42)$$

This is, of course, simply the chemical potential as seen in the local rest frame of the fermions. The pressure p is determined by the local chemical potential via the charge density σ and the energy density ρ :

$$-p = \rho - \mu_{\text{loc}}\sigma, \quad \rho = \int_m^{\mu_{\text{loc}}} Eg(E)dE, \quad \sigma = \int_m^{\mu_{\text{loc}}} g(E)dE, \quad (14.43)$$

where the density of states is given by

$$g(E) = \frac{1}{\pi^2} E \sqrt{E^2 - m^2}. \quad (14.44)$$

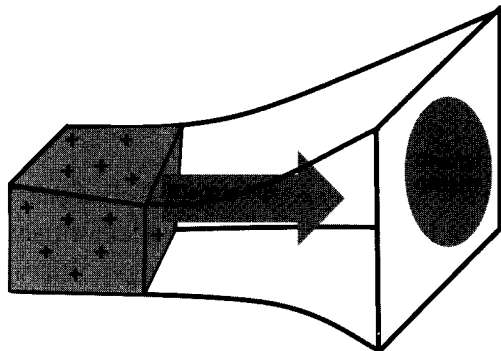


Figure 14.7 The electron star. The electric flux is sourced entirely by a fluid of fermions. The fluid is present at all radii for which the local chemical potential is greater than the fermion mass.

To find the electron star solution, one makes the same ansatz (14.30) as above for holographic superconductors. Now there is no scalar field ϕ , but rather the fluid tracks the background metric and Maxwell fields via (14.43). It is straightforward to solve the Einstein–Maxwell ideal-fluid equations of motion numerically to find the profile of the star [35]. Before concentrating on the interior IR geometry, we can make two qualitative comments. First, it is clear from the equations of state (14.43) that the fluid is present only if the local chemical potential (14.42) is larger than the rest mass energy of the fermions,

$$\mu_{\text{loc}} > m . \quad (14.45)$$

This is the condition for populating the local Fermi sea. Looking for extremal solutions, without a finite-temperature horizon, one finds that the condition (14.45) is satisfied from the deep IR up to a specific radius. This radius is the boundary of the star. Outside the star, the geometry becomes Reissner–Nordström–AdS with a mass and charge determined by integrating over the fermions in the star. This type of solution is illustrated in Fig. 14.7. Analogously to the holographic superconductors, at zero temperature all the charge is carried by the fermions rather than lying behind a horizon.

Second, consider heating up the system. At leading order in the semiclassical limit, this means placing a finite-temperature black hole horizon in the interior of the spacetime. The fluid remains at zero temperature, as it must be in thermal equilibrium with the Hawking radiation of the black hole, the effects of which are negligible in the semiclassical limit. At finite temperature, a fraction of the charge is carried by the black hole horizon, which subsequently pushes the fermion fluid a finite distance away from the horizon. The star becomes a band of fluid with an inner and an outer radius [66, 67]. At nonzero temperature we can adjust the

ratio T/μ . We can expect that, at sufficiently high values of this ratio, the star will collapse to form a black hole. This will be analogous to the maximal mass of spherical neutron stars; in global rather than planar AdS the mass scale can be compared with the radius of the spatial boundary sphere. In that case there is a first-order phase transition: above a critical mass the degeneracy pressure cannot sustain the star [62, 63]. In our planar set-up we might anticipate a second-order transition similar to that of the holographic superconductors discussed above. In fact, the transition turns out to be third order [66, 67]. The reason for the softness of the transition is that the free energy of the fluid is given by its pressure, and the pressure turns on relatively slowly when $\mu_{\text{loc}} = m + \delta\mu$ is only slightly above the fermion mass: from the formulae in (14.43) one obtains $p \sim (\delta\mu)^{5/2}$ [66]. In contrast, the energy and charge densities ρ, σ go as $(\delta\mu)^{3/2}$.

Electron stars are found to exist whenever the fermion mass satisfies the condition (14.39) for Schwinger pair production to occur in what would, in the case of a black hole, be the near-horizon $\text{AdS}_2 \times \mathbb{R}^2$ region. In these cases, for all temperatures $T < T_C \propto \mu$ the electron star has a lower free energy than the corresponding Reissner–Nordström–AdS black hole [35, 66, 67]. It is thermodynamically favourable to populate the Fermi sea.

We now return to our main focus, regarding the emergent IR geometry at zero temperature. Despite preserving the $U(1)$ symmetry, electron stars obey similar equations to holographic superconductors. We can again make a Lifshitz scaling ansatz (14.31) for the $r \rightarrow \infty$ IR geometry. Substituting the ansatz (14.31) into the equations of motion following from the action (14.41) gives the dynamical critical exponent z in terms of the pressure and energy density in the interior of the star:

$$\frac{2(6 + 3\hat{p}_\infty + \hat{\rho}_\infty)}{\hat{p}_\infty + \hat{\rho}_\infty} - \frac{12 + \hat{p}_\infty - 3\hat{\rho}_\infty}{\hat{p}_\infty + \hat{\rho}_\infty} z + z^2 = 0 . \quad (14.46)$$

Here $\{\hat{p}, \hat{\rho}\} = L^2 \kappa^2 \{p, \rho\}$. This expression is general; it will continue to hold for an equation of state for the fermion fluid that is different from that for free fermions. The local chemical potential (14.42) in the interior of the star is found to be, again independently of the equation of state,

$$L^2 \mu_\infty^2 = \gamma^2 \frac{z - 1}{z} . \quad (14.47)$$

Here we see that the star will have $z \geq 1$. For the case of free fermions, we can perform the integrals in (14.43) with the value (14.47) for the local chemical potential. Substituting the results of the integrals into (14.46) gives a formula that can be solved numerically to obtain z . By scaling the integrals in (14.46) and using (14.47) one finds that $\hat{p}, \hat{\rho} \sim e^2 \gamma^2$. Thus, from (14.46), for z to be of order 1 requires that $e^2 \gamma^2 \sim 1$. Curiously, this is a regime in which the gravitational coupling is the

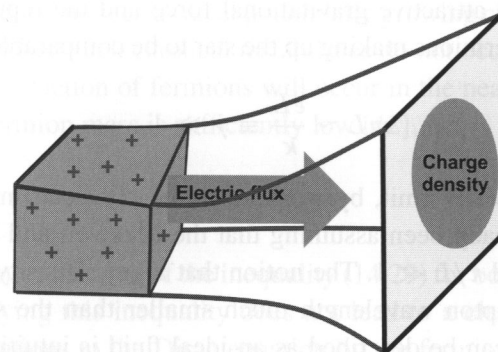


Figure 14.7 The electron star. The electric flux is sourced entirely by a fluid of fermions. The fluid is present at all radii for which the local chemical potential is greater than the fermion mass.

To find the electron star solution, one makes the same ansatz (14.30) as above for holographic superconductors. Now there is no scalar field ϕ , but rather the fluid tracks the background metric and Maxwell fields via (14.43). It is straightforward to solve the Einstein–Maxwell ideal-fluid equations of motion numerically to find the profile of the star [35]. Before concentrating on the interior IR geometry, we can make two qualitative comments. First, it is clear from the equations of state (14.43) that the fluid is present only if the local chemical potential (14.42) is larger than the rest mass energy of the fermions,

$$\mu_{\text{loc}} > m. \quad (14.45)$$

This is the condition for populating the local Fermi sea. Looking for extremal solutions, without a finite-temperature horizon, one finds that the condition (14.45) is satisfied from the deep IR up to a specific radius. This radius is the boundary of the star. Outside the star, the geometry becomes Reissner–Nordström–AdS with a mass and charge determined by integrating over the fermions in the star. This type of solution is illustrated in Fig. 14.7. Analogously to the holographic superconductors, at zero temperature all the charge is carried by the fermions rather than lying behind a horizon.

Second, consider heating up the system. At leading order in the semiclassical limit, this means placing a finite-temperature black hole horizon in the interior of the spacetime. The fluid remains at zero temperature, as it must be in thermal equilibrium with the Hawking radiation of the black hole, the effects of which are negligible in the semiclassical limit. At finite temperature, a fraction of the charge is carried by the black hole horizon, which subsequently pushes the fermion fluid a finite distance away from the horizon. The star becomes a band of fluid with an inner and an outer radius [66, 67]. At nonzero temperature we can adjust the

ratio T/μ . We can expect that, at sufficiently high values of this ratio, the star will collapse to form a black hole. This will be analogous to the maximal mass of spherical neutron stars; in global rather than planar AdS the mass scale can be compared with the radius of the spatial boundary sphere. In that case there is a first-order phase transition: above a critical mass the degeneracy pressure cannot sustain the star [62, 63]. In our planar set-up we might anticipate a second-order transition similar to that of the holographic superconductors discussed above. In fact, the transition turns out to be third order [66, 67]. The reason for the softness of the transition is that the free energy of the fluid is given by its pressure, and the pressure turns on relatively slowly when $\mu_{\text{loc}} = m + \delta\mu$ is only slightly above the fermion mass: from the formulae in (14.43) one obtains $p \sim (\delta\mu)^{5/2}$ [66]. In contrast, the energy and charge densities ρ, σ go as $(\delta\mu)^{3/2}$.

Electron stars are found to exist whenever the fermion mass satisfies the condition (14.39) for Schwinger pair production to occur in what would, in the case of a black hole, be the near-horizon $\text{AdS}_2 \times \mathbb{R}^2$ region. In these cases, for all temperatures $T < T_C \propto \mu$ the electron star has a lower free energy than the corresponding Reissner–Nordström–AdS black hole [35, 66, 67]. It is thermodynamically favourable to populate the Fermi sea.

We now return to our main focus, regarding the emergent IR geometry at zero temperature. Despite preserving the $U(1)$ symmetry, electron stars obey similar equations to holographic superconductors. We can again make a Lifshitz scaling ansatz (14.31) for the $r \rightarrow \infty$ IR geometry. Substituting the ansatz (14.31) into the equations of motion following from the action (14.41) gives the dynamical critical exponent z in terms of the pressure and energy density in the interior of the star:

$$\frac{2(6 + 3\hat{p}_\infty + \hat{\rho}_\infty)}{\hat{p}_\infty + \hat{\rho}_\infty} - \frac{12 + \hat{p}_\infty - 3\hat{\rho}_\infty}{\hat{p}_\infty + \hat{\rho}_\infty}z + z^2 = 0. \quad (14.46)$$

Here $\{\hat{p}, \hat{\rho}\} = L^2 \kappa^2 \{p, \rho\}$. This expression is general; it will continue to hold for an equation of state for the fermion fluid that is different from that for free fermions. The local chemical potential (14.42) in the interior of the star is found to be, again independently of the equation of state,

$$L^2 \mu_\infty^2 = \gamma^2 \frac{z-1}{z}. \quad (14.47)$$

Here we see that the star will have $z \geq 1$. For the case of free fermions, we can perform the integrals in (14.43) with the value (14.47) for the local chemical potential. Substituting the results of the integrals into (14.46) gives a formula that can be solved numerically to obtain z . By scaling the integrals in (14.46) and using (14.47) one finds that $\hat{p}, \hat{\rho} \sim e^2 \gamma^2$. Thus, from (14.46), for z to be of order 1 requires that $e^2 \gamma^2 \sim 1$. Curiously, this is a regime in which the gravitational coupling is the

square of the Maxwell coupling, $e^4 \sim \kappa^2/L^2$, which is reminiscent of the relation between closed and open string couplings. The explicit dependence of z on $e^2\gamma^2$ can be found numerically [35]. Somewhat analogously to the expression (14.35) for a class of holographic superconductors, it is found that, at fixed mass m , if $e^2\gamma^2 \rightarrow \infty$ then $z \rightarrow 1$ from above, while if $e^2\gamma^2 \rightarrow 0$ then $z \rightarrow \infty$. The possible interior geometries of electron stars range from AdS_4 to $\text{AdS}_2 \times \mathbb{R}^2$.

As previously for the holographic superconductors, it is gratifying to see the emergence of an IR scaling regime, due to finite density at strong coupling, that mirrors the one-loop Landau-damping physics discussed in section 14.3. The fermions and bosons of the current and previous sections, respectively, can in fact be combined to give an emergent scaling due partially to a symmetry-breaking condensate and partially to a density of fermions [68]. One potential limitation of the perturbative computation is the controlled determination of z . In the gravitational framework that we have explored, we see that z is tied to the ratio of the Newton and Maxwell couplings and to the mass of the charged fields. In field theoretic language these quantities translate respectively into the ‘‘central charges’’ characterising the two-point function of the energy-momentum tensor and electric current and the anomalous scaling dimension of the gauge-invariant charged operator carrying the charge density.

14.8 Dilatonic scalars: Lifshitz and beyond

The bottom line following from the previous two sections is that, whenever it is possible to pair-produce fermions or bosons in the vicinity of a planar extremal Reissner–Nordström–AdS horizon, the extremal black hole is not the thermodynamically preferred zero-temperature finite charge density spacetime. The dominant ground states that we have found are distinguished from extremal Reissner–Nordström–AdS by two properties. First, all the electric flux is sourced explicitly by charged bosonic and fermionic fields rather than emanating from behind an event horizon. Second, the emergent IR scaling geometry has a finite- z Lifshitz scaling, rather than the $z = \infty$ scaling of $\text{AdS}_2 \times \mathbb{R}^2$. We might ask whether it is possible to decouple these two effects, that is, whether it is possible to have an emergent finite- z scaling together with a flux carried by a horizon rather than charged fields.

We can think heuristically of the $\text{AdS}_2 \times \mathbb{R}^2$ near-horizon geometry as being ‘‘pushed open’’ by the flux it carries. In the Lifshitz solutions of the previous sections, the flux is consumed by the charged fermions and bosons as we move towards the ‘‘horizon’’ and therefore the spatial metric is able to collapse. In the absence of charged sources, the solution has nowhere to dump the electric flux and so we need an alternate mechanism to violate Gauss’s law. A simple way to do this

is to introduce a dilaton field. A minimal Einstein–Maxwell–dilaton–AdS action takes the form

$$\mathcal{L} = \frac{1}{2\kappa^2} \left(R + \frac{6}{L^2} \right) - \frac{1}{4e^2} e^{2\alpha\phi} F_{\mu\nu} F^{\mu\nu} - \frac{1}{2} (\nabla\phi)^2. \quad (14.48)$$

Without loss of generality, consider $\alpha > 0$. If the dilaton ϕ is not constant in the near-horizon region then the effective Maxwell coupling $e_{\text{eff}} = e \exp(-\alpha\phi)$ will continue running and we may be able to escape landing at an $\text{AdS}_2 \times \mathbb{R}^2$ attractor point.

Indeed it is found that the IR geometry of the dilaton theory (14.48), with an asymptotic electric flux, takes the Lifshitz form (14.31), with $z > 1$ generically [69, 70]. The important difference in relation to (14.31) is that, as we anticipated, the dilaton is not constant but rather grows logarithmically as $r \rightarrow \infty$:

$$\phi = k \log r, \quad (14.49)$$

with $k > 0$. The effective Maxwell coupling therefore vanishes in the far interior. Within a string theoretic framework, this leads us to be concerned about large stringy effects in the near-horizon geometry. Higher-derivative corrections may be expected to stabilise the dilaton at a constant value, leading again to an $\text{AdS}_2 \times \mathbb{R}^2$ near-horizon geometry [31]. If this occurs, the semiclassical gravitational limit has nonetheless provided a parametrically large window of IR energy scales controlled by a $z > 1$ scaling. The dilaton itself is covariant rather than invariant under this scaling.

Once we are accustomed to the logarithmic running of the dilaton in (14.49), we can expect that allowing couplings other than the Maxwell coupling to run with the dilaton may induce new effects in the near-horizon geometry. For instance, consider a potential for the dilaton. Assume that the potential is dominated by an exponential term in the near-horizon region, where, the dilaton is growing according to (14.49). Thus we write the Lagrangian density as

$$\mathcal{L} = \frac{1}{2\kappa^2} (R - V_0 e^{2\beta\phi}) - \frac{1}{4e^2} e^{2\alpha\phi} F_{\mu\nu} F^{\mu\nu} - \frac{1}{2} (\nabla\phi)^2. \quad (14.50)$$

The cosmological constant term has been replaced by the potential $V_0 e^{2\beta\phi}$, which is not constant in the near-horizon limit. Note that the action (14.50) only applies to leading order for a large dilaton. In order for the theory to have e.g. an asymptotic AdS_4 vacuum, there must be additional terms in the potential to asymptotically stabilise the dilaton.

The near-horizon scaling solutions of (14.50) take a more general form than the Lifshitz geometry. The metric must generically be written as [71–73]

$$ds^2 = r^{2\delta} \left(-\frac{dt^2}{r^{2z}} + g_\infty \frac{dr^2}{r^2} + \frac{dx^2 + dy^2}{r^2} \right). \quad (14.51)$$

Table 14.1

gravity	field theory
$g_{\mu\nu} = T^{\mu\nu}$	
$A_\mu = J^\mu$	
$\phi \sim \text{Tr}(\Phi\Phi), \text{tr}(\Psi\Psi)$	
$\psi \sim \text{Tr}(\Phi\Psi)$	
ϕ (dilaton) $\sim \text{Tr}(F_{\mu\nu}F^{\mu\nu})$	

The extra term compared with (14.31) implies that now the metric itself transforms covariantly under scalings rather than being invariant. This fact has immediate consequences for the thermodynamics of the system. For instance, while Lifshitz invariance implies the entropy density scaling of (14.37) with temperature for all the systems considered thus far, heating up the Lifshitz-covariant spacetime (14.51) leads to a low-temperature dependence of the entropy density [71–73]:

$$s \propto T^{2(1-\delta)/z}. \quad (14.52)$$

This scaling can be recovered from a dimensional analysis that imparts an “anomalous” scaling dimensionality to the spatial volume while keeping the relative scaling between space and time, determined by z . Another consequence is that the curvature scalars of the spacetime (14.51) are no longer constant, and one must worry once more about stringy and quantum gravity effects in the far IR of the geometry. The reader is referred to discussions in [72, 73].

A summary of this section is that, within the semiclassical regime at least, dilaton spacetimes with an asymptotic electric flux have near-horizon geometries characterised by a finite- z scaling symmetry. This is achieved without explicit charged matter. All the flux, as defined by $\int_{\mathbb{R}^2} \star (e^{2\alpha\phi} F)$, emanates from behind the IR “horizon”.

14.9 Horizons, fractionalisation and black hole information

In this last section we will tie together the various solutions discussed into an interpretational framework. To start, recall the correspondence between the basic ingredients at our disposal in the gravitational and field theoretic descriptions of the system; this is the connection between bulk fields and gauge-invariant operators mentioned in section 14.4 above. See Table 14.1.

For the last three rows in this table, the precise matching between gauge-invariant observables and bulk fields depends on the particular instance of duality being considered. The schematic correspondence indicated for these cases shows roughly the types of simple operator that will correspond to our bulk fields. However, the

“elementary” field theoretic operators $\Phi, \Psi, F_{\mu\nu}$ are not directly accessible in the bulk, as they are not gauge invariant. In a slight abuse of terminology, we will refer to the gauge-invariant operators dual to ϕ, ψ as “mesonic”. The name is intended to remind us that these operators are composite in terms of the fields appearing in a “microscopic” field theory Lagrangian.

Next, some general comments about horizons. The physics of horizons in holography is overdetermined (in the Freudian rather than the mathematical sense of the word); they seem to play multiple independent yet crucial roles simultaneously. These range from providing a mechanism for dissipation at leading order in the large- N expansion to geometrically realising, for instance, the IR temperature scale and associated physics such as thermal screening. Here we wish to argue that horizons at finite charge density have the additional role of enabling a gauge-invariant description of “fractionalised” phases where microscopically the electric charge would seem to be carried by gauge-charged operators. Very loosely speaking, the gauge variance is hidden behind the horizon. The word “fractionalised” is used here in analogy with the condensed matter construction (14.11). We can think of the gauge-invariant fermion c as being analogous to the mesonic field ψ , while the gauge-charged fermion and boson f and b are analogous to the “microscopic” fields Ψ and Φ .

The identification of horizons with deconfined phases, as defined for instance through an expectation value for the Polyakov loop, is a seminal result in holography [74]. The spirit of the physics here will be similar, except that we are primarily interested in the charged sector at zero temperature.

One route to understanding the ubiquity of horizons in holography is the following. Recall from section 14.2 above that two key ingredients of holography are, first, that the large- N limit enables the correlators of certain single-trace operators to factorise and, second, that there should only be a handful of such single-trace operators with an anomalous dimension of order one. The second statement requires the theory to be strongly interacting, as otherwise there will be an infinite tower of single-trace operators with roughly evenly spaced dimensions. Taking these statements together, one is led to the notion of a “generalised free field”, i.e., operators that factorise but do not obey free wave equations in the field theory Minkowski space. Examples are the gauge-invariant operators appearing in (14.53). One can then show that generalised free fields can only arise as a small subsector of a larger theory [75], consistent with the large central charge (14.8) in the holographic context. This means that, to reconstruct the full theory, the set of gauge-invariant operators that we have been considering must be completed with a large number ($\sim N^2$, say) of operators with large anomalous dimensions. These operators will not (typically) have a classical geometric description in the bulk but will appear, rather, as “black hole microstates”. The fact that this large number of “heavy”

states, with fixed mass and charges, is indistinguishable to most bulk probes leads to the finite entropy density of black hole horizons.

We see, therefore, that the elegant distinction between “mesonic” phases, where the flux is sourced by charged fields in the bulk dual, and “fractionalised” phases, where the flux is sourced by horizons, is made possible by the holographic large- N limit. The reason is, as we explained above, that this limit creates a hierarchy in the anomalous dimensions of operators in the theory, and it is this hierarchy that allows the distinction between black hole states and classical bulk fields. The same mechanism underlies holographic descriptions of finite-temperature deconfinement transitions.

Seemingly independently of holography, the mean field limit of the fractionalised Fermi-liquid phase of the lattice Anderson model [76] was also found to lead to a zero-temperature entropy density and consequently an effective $\text{AdS}_2 \times \mathbb{R}^2$ -like IR scaling regime. Taken together with the holographic results, this may suggest that, in classical limits, charge fractionalisation is closely tied to a finite entropy density (a similar conclusion is argued in [77]). An obstacle to such a general conclusion is the charged dilatonic near-horizon geometries of section 14.8. While the running dilaton of these solutions is presumably stabilised at an $\text{AdS}_2 \times \mathbb{R}^2$ attractor point, once higher-derivative corrections are included [31], this is not visible in the leading classical bulk limit. The probable lesson here is that the generalised free field/black hole microstate dichotomy does not guarantee that there are sufficiently many charged black hole microstates to generate classical charged black hole horizons. Consequently, to leading order in N the low-energy physics need not have a $z = \infty$ scaling symmetry.

So far we have not defined fractionalisation in a system-invariant way. One way to make the notion more precise is via the “Luttinger count” [78]. Under quite general circumstances, compressible finite-density phases of matter, in which the $U(1)$ symmetry is unbroken, are expected to obey the Luttinger theorem. This theorem says that the total charge density is equal to the sum of the momentum space volumes of all Fermi surfaces in the theory weighted by the charge of the corresponding fermionic operators:

$$\langle J^t \rangle = \sum_{\ell \in \text{fermions}} q_\ell V_\ell . \quad (14.53)$$

The Fermi surfaces are defined as the singular loci of the fermion Green’s function at zero energy, e.g. $G_\ell^{-1}(k = k_F, \omega = 0) = 0$. An essential feature of a “fractionalised Fermi liquid” [79] is that, while the Luttinger count (14.54) remains true in the presence of gauge fields, the corresponding gauge-charged Fermi surfaces may not be detectable by gauge-invariant fermion probes of the system. Thus, when we sum over all Fermi surfaces of gauge-invariant operators, we may encounter a deficit

in the Luttinger count. Thus the difference between the right- and left-hand sides of (14.54), with the sum restricted to gauge-invariant mesonic fermions, gives a measure of the fractionalised nature of the system.

Using the Luttinger count, let us compare a stable extremal Reissner–Nordström spacetime, i.e. one with all charged bosons and fermions heavier than the bounds (14.29) and (14.39), with an electron star. In a WKB limit for the fermions, one can establish that the field theory charge density equals the flux emanating from the horizon plus the charge carried by a fermion fluid outside the black hole; see e.g. [66]. The bulk fermions obey a bulk Luttinger theorem at each radius [35], and therefore one might anticipate that the flux emanating from the horizon will equal the “missing” contribution to the gauge-invariant Luttinger count. That is, we expect that

$$\text{flux from} \begin{array}{l} \text{Fermi surface} \\ \text{horizon} \end{array} = \langle J^t \rangle - \sum \text{volumes of } \psi . \quad (14.54)$$

This relation was made precise in [64, 77], where it was shown that, in field theory phases dual to an electron star, i.e. where all the charge is sourced by bulk fermions, the Luttinger equality (14.54) holds when the sum is restricted to gauge-invariant Fermi surfaces. Conversely, an extremal Reissner–Nordström spacetime that is stable against the condensation of WKB fermions will have no associated gauge-invariant Fermi surfaces.³ The Luttinger relation (14.54) is therefore maximally violated in this case. At the time of writing, only these limiting cases of “fully mesonic” electrons stars and “fully fractionalised” extremal black holes have been constructed. No doubt, before this book is published, intermediate cases will also have been realised holographically. The important point is that a deficit in the gauge-invariant Luttinger count gives a direct connection between charged horizons and fractionalised phases of matter.

References

- [1] J. M. Maldacena, The large N limit of superconformal field theories and supergravity, *Adv. Theor. Math. Phys.* **2** (1998), 231–252 [hep-th/9711200].
- [2] J. Polchinski, Introduction to gauge/gravity duality, arXiv:1010.6134 [hep-th].
- [3] J. McGreevy, Holographic duality with a view toward many-body physics, *Adv. High Energy Phys.* **2010** (2010), 723105 [arXiv:0909.0518 [hep-th]].
- [4] I. Heemskerk, J. Polchinski, Holographic and Wilsonian renormalization groups, arXiv:1010.1264 [hep-th].

³ Away from the WKB limit there is a small window of bulk fermion charges and masses where it is possible to have a gauge-invariant Fermi surface without pair-producing fermions near the horizon in accordance with the criterion (14.39). See Figure 6 of [56]. In these cases, extremal Reissner–Nordström will coexist with a parametrically small amount of charge carried by fermions outside the horizon.

- [5] T. Faulkner, H. Liu, and M. Rangamani, Integrating out geometry: holographic Wilsonian RG and the membrane paradigm, arXiv:1010.4036 [hep-th].
- [6] I. Heemskerk, J. Penedones, J. Polchinski, and J. Sully, Holography from conformal field theory, *JHEP* **0910** (2009), 079 [arXiv:0907.0151 [hep-th]].
- [7] E. Witten, The $1/N$ expansion in atomic and particle physics, in *Recent Developments in Gauge Theories*, ed. G. 't Hooft, Plenum Press (1980), p. 403.
- [8] I. R. Klebanov and A. M. Polyakov, AdS dual of the critical O(N) vector model, *Phys. Lett.* **B550** (2002), 213–219 [hep-th/0210114].
- [9] O. Aharony, O. Bergman, D. L. Jafferis, and J. Maldacena, $N = 6$ superconformal Chern–Simons–matter theories, M2-branes and their gravity duals, *JHEP* **0810** (2008), 091 [arXiv:0806.1218 [hep-th]].
- [10] F. Denef, in *Les Houches Lectures on Constructing String Vacua*, arXiv:0803.1194 [hep-th].
- [11] S. A. Hartnoll, Lectures on holographic methods for condensed matter physics, *Class. Quant. Grav.* **26** (2009), 224 002 [arXiv:0903.3246 [hep-th]].
- [12] P. W. Anderson, *Basic Notions of Condensed Matter Physics*, Addison-Wesley (1984).
- [13] J. Polchinski, Effective field theory and the Fermi surface, arXiv:hep-th/9210046.
- [14] R. Shankar, Renormalization-group approach to interacting fermions, *Rev. Mod. Phys.* **66** (1994), 129.
- [15] S. Sachdev and B. Keimer, Quantum criticality, *Physics Today* **64** (2011), 29 [arXiv:1102.4628 [cond-mat.str-el]].
- [16] H. v. Löhneysen, A. Rosch, M. Vojta, and P. Wölfle, Fermi-liquid instabilities at magnetic quantum phase transitions, *Rev. Mod. Phys.* **79** (2007), 1015 [arXiv:cond-mat/0606317 [cond-mat.str-el]].
- [17] S. Sachdev, *Quantum Phase Transitions*, Cambridge University Press (1999).
- [18] P. A. Lee, N. Nagaosa, and X.-G. Wen, Doping a Mott insulator: physics of high-temperature superconductivity, *Rev. Mod. Phys.* **78** (2006), 17 [arXiv:cond-mat/0410445 [cond-mat.str-el]].
- [19] A. M. Polyakov, Quark confinement and topology of gauge groups, *Nucl. Phys.* **B120** (1977), 429–458.
- [20] S.-S. Lee, Stability of the U(1) spin liquid with a spinon Fermi surface in 2+1 dimensions, *Phys. Rev.* **B78** (2008), 085 129.
- [21] M. Unsal, Topological symmetry, spin liquids and CFT duals of Polyakov model with massless fermions, arXiv:0804.4664 [cond-mat.str-el].
- [22] S.-S. Lee, Low energy effective theory of Fermi surface coupled with a U(1) gauge field in 2+1 dimensions, *Phys. Rev.* **B80** (2009), 165 102 [arXiv:0905.4532 [cond-mat.str-el]].
- [23] M. A. Metlitski and S. Sachdev, Quantum phase transitions of metals in two spatial dimensions: I. Ising-nematic order, arXiv:1001.1153 [cond-mat.str-el].
- [24] M. A. Metlitski and S. Sachdev, Quantum phase transitions of metals in two spatial dimensions: II. Spin density wave order, *Phys. Rev.* **B82** (2010), 075 128 [arXiv:1005.1288 [cond-mat.str-el]].
- [25] D. F. Mross, J. McGreevy, H. Liu, and T. Senthil, A controlled expansion for certain non-Fermi liquid metals, arXiv:1003.0894 [cond-mat.str-el].
- [26] A. Chamblin, R. Emparan, C. V. Johnson, and R. C. Myers, Charged AdS black holes and catastrophic holography, *Phys. Rev.* **D60** (1999), 064 018 [hep-th/9902170].
- [27] S. A. Hartnoll, P. K. Kovtun, M. Muller, and S. Sachdev, Theory of the Nernst effect near quantum phase transitions in condensed matter, and in dyonic black holes, *Phys. Rev.* **B76** (2007), 144 502 [arXiv:0706.3215 [cond-mat.str-el]].

- [28] S. A. Hartnoll and C. P. Herzog, Ohm's law at strong coupling: S duality and the cyclotron resonance, *Phys. Rev.* **D76** (2007), 106 012 [arXiv:0706.3228 [hep-th]].
- [29] G. W. Gibbons, Aspects of supergravity theories, in *Supersymmetry, Supergravity and Related Topics*, eds. F. del Aguila, J. de Azcárraga, and L. Ibáñez, World Scientific (1985), p. 147.
- [30] K. Jensen, S. Kachru, A. Karch, J. Polchinski, and E. Silverstein, Towards a holographic marginal Fermi liquid, arXiv:1105.1772 [hep-th].
- [31] A. Sen, Black hole entropy function and the attractor mechanism in higher derivative gravity, *JHEP* **0509** (2005), 038 [hep-th/0506177].
- [32] S. A. Hartnoll, C. P. Herzog, and G. T. Horowitz, Building a holographic superconductor, *Phys. Rev. Lett.* **101** (2008), 031 601 [arXiv:0803.3295 [hep-th]].
- [33] S. A. Hartnoll, C. P. Herzog, and G. T. Horowitz, Holographic superconductors, *JHEP* **0812** (2008), 015 [arXiv:0810.1563 [hep-th]].
- [34] S. A. Hartnoll, J. Polchinski, E. Silverstein, and D. Tong, Towards strange metallic holography, *JHEP* **1004** (2010), 120 [arXiv:0912.1061 [hep-th]].
- [35] S. A. Hartnoll and A. Tavanfar, Electron stars for holographic metallic criticality, *Phys. Rev.* **D83** (2011), 046 003 [arXiv:1008.2828 [hep-th]].
- [36] S. S. Gubser, Breaking an Abelian gauge symmetry near a black hole horizon, *Phys. Rev.* **D78** (2008), 065 034 [arXiv:0801.2977 [hep-th]].
- [37] P. Breitenlohner and D. Z. Freedman, Positive energy in anti-de Sitter backgrounds and gauged extended supergravity, *Phys. Lett.* **B115** (1982), 197.
- [38] T. Hertog, Towards a novel no-hair theorem for black holes, *Phys. Rev.* **D74** (2006), 084 008 [gr-qc/0608075].
- [39] S. S. Gubser and A. Nellore, Low-temperature behavior of the Abelian Higgs model in anti-de Sitter space, *JHEP* **0904** (2009), 008 [arXiv:0810.4554 [hep-th]].
- [40] F. Denef and S. A. Hartnoll, Landscape of superconducting membranes, *Phys. Rev.* **D79** (2009), 126 008 [arXiv:0901.1160 [hep-th]].
- [41] I. R. Klebanov and E. Witten, AdS/CFT correspondence and symmetry breaking, *Nucl. Phys.* **B556** (1999), 89–114 [hep-th/9905104].
- [42] B. Pioline and J. Troost, Schwinger pair production in AdS(2), *JHEP* **0503** (2005), 043 [hep-th/0501169].
- [43] C. P. Herzog, Lectures on holographic superfluidity and superconductivity, *J. Phys.* **A42** (2009), 343 001 [arXiv:0904.1975 [hep-th]].
- [44] G. T. Horowitz, Introduction to holographic superconductors, arXiv:1002.1722 [hep-th].
- [45] G. T. Horowitz and M. M. Roberts, Zero temperature limit of holographic superconductors, *JHEP* **0911** (2009), 015 [arXiv:0908.3677 [hep-th]].
- [46] S. S. Gubser and A. Nellore, Ground states of holographic superconductors, *Phys. Rev.* **D80** (2009), 105 007 [arXiv:0908.1972 [hep-th]].
- [47] S. S. Gubser and F. D. Rocha, The gravity dual to a quantum critical point with spontaneous symmetry breaking, *Phys. Rev. Lett.* **102** (2009), 061 601 [arXiv:0807.1737 [hep-th]].
- [48] J. P. Gauntlett, J. Sonner, and T. Wiseman, Holographic superconductivity in M-theory, *Phys. Rev. Lett.* **103** (2009), 151 601 [arXiv:0907.3796 [hep-th]].
- [49] S. S. Gubser, S. S. Pufu, and F. D. Rocha, Quantum critical superconductors in string theory and M-theory, *Phys. Lett.* **B683** (2010), 201–204 [arXiv:0908.0011 [hep-th]].
- [50] S. Kachru, X. Liu, and M. Mulligan, Gravity duals of Lifshitz-like fixed points, *Phys. Rev.* **D78** (2008), 106 005 [arXiv:0808.1725 [hep-th]].
- [51] A. Adams, A. Maloney, A. Sinha, and S. E. Vazquez, $1/N$ effects in non-relativistic gauge-gravity duality, *JHEP* **0903** (2009), 097 [arXiv:0812.0166 [hep-th]].

- [52] K. Copsey and R. Mann, Pathologies in asymptotically Lifshitz spacetimes, *JHEP* **1103** (2011), 039 [arXiv:1011.3502 [hep-th]].
- [53] G. T. Horowitz and A. R. Steif, Space-time singularities in string theory, *Phys. Rev. Lett.* **64** (1990), 260.
- [54] D. Anninos, S. A. Hartnoll, and N. Iqbal, Holography and the Coleman–Mermin–Wagner theorem, *Phys. Rev.* **D82** (2010), 066 008 [arXiv:1005.1973 [hep-th]].
- [55] D. Nickel and D. T. Son, Deconstructing holographic liquids, arXiv:1009.3094 [hep-th].
- [56] T. Faulkner, H. Liu, J. McGreevy, and D. Vegh, Emergent quantum criticality, Fermi surfaces, and AdS(2), arXiv:0907.2694 [hep-th].
- [57] H. Liu, J. McGreevy, and D. Vegh, Non-Fermi liquids from holography, *Phys. Rev.* **D83** (2011), 065 029 [arXiv:0903.2477 [hep-th]].
- [58] S.-S. Lee, A non-Fermi liquid from a charged black hole: a critical Fermi ball, *Phys. Rev.* **D79** (2009), 086 006 [arXiv:0809.3402 [hep-th]].
- [59] M. Cubrovic, J. Zaanen, and K. Schalm, String theory, quantum phase transitions and the emergent Fermi liquid, *Science* **325** (2009), 439–444 [arXiv:0904.1993 [hep-th]].
- [60] M. Cubrovic, J. Zaanen, and K. Schalm, Constructing the AdS dual of a Fermi liquid: AdS black holes with Dirac hair, arXiv:1012.5681 [hep-th].
- [61] R. Ruffini and S. Bonazzola, Systems of selfgravitating particles in general relativity and the concept of an equation of state, *Phys. Rev.* **187** (1969), 1767–1783.
- [62] J. de Boer, K. Papadodimas, and E. Verlinde, Holographic neutron stars, *JHEP* **1010** (2010), 020 [arXiv:0907.2695 [hep-th]].
- [63] X. Arsiwalla, J. de Boer, K. Papadodimas, and E. Verlinde, Degenerate stars and gravitational collapse in AdS/CFT, *JHEP* **1101** (2011), 144 [arXiv:1010.5784 [hep-th]].
- [64] S. A. Hartnoll, D. M. Hofman, and D. Vegh, Stellar spectroscopy: fermions and holographic Lifshitz criticality, arXiv:1105.3197 [hep-th].
- [65] B. F. Schutz, Perfect fluids in general relativity: velocity potentials and a variational principle, *Phys. Rev.* **D2** (1970), 2762–2773.
- [66] S. A. Hartnoll and P. Petrov, Electron star birth: a continuous phase transition at nonzero density, *Phys. Rev. Lett.* **106** (2011), 121 601 [arXiv:1011.6469 [hep-th]].
- [67] V. G. M. Puletti, S. Nowling, L. Thorlacius, and T. Zingg, Holographic metals at finite temperature, *JHEP* **1101** (2011), 117 [arXiv:1011.6261 [hep-th]].
- [68] M. Edalati, K. W. Lo, and P. W. Phillips, Neutral order parameters in metallic criticality in $d = 2 + 1$ from a hairy electron star, arXiv:1106.3139 [hep-th].
- [69] M. Taylor, Non-relativistic holography, arXiv:0812.0530 [hep-th].
- [70] K. Goldstein, S. Kachru, S. Prakash, and S. P. Trivedi, Holography of charged dilaton black holes, *JHEP* **1008** (2010), 078 [arXiv:0911.3586 [hep-th]].
- [71] S. S. Gubser and F. D. Rocha, Peculiar properties of a charged dilatonic black hole in AdS_5 , *Phys. Rev.* **D81** (2010), 046 001 [arXiv:0911.2898 [hep-th]].
- [72] C. Charmousis, B. Gouteraux, B. S. Kim, E. Kiritsis, and R. Meyer, Effective holographic theories for low-temperature condensed matter systems, *JHEP* **1011** (2010), 151 [arXiv:1005.4690 [hep-th]].
- [73] N. Iizuka, N. Kundu, P. Narayan, and S. P. Trivedi, Holographic Fermi and non-Fermi liquids with transitions in dilaton gravity, arXiv:1105.1162 [hep-th].
- [74] E. Witten, Anti-de Sitter space, thermal phase transition, and confinement in gauge theories, *Adv. Theor. Math. Phys.* **2** (1998), 505–532 [hep-th/9803131].
- [75] S. El-Showk and K. Papadodimas, Emergent spacetime and holographic CFTs, arXiv:1101.4163 [hep-th].

- [76] S. Sachdev, Holographic metals and the fractionalized Fermi liquid, *Phys. Rev. Lett.* **105** (2010), 151 602 [arXiv:1006.3794 [hep-th]].
- [77] N. Iqbal, H. Liu, and M. Mezei, Semi-local quantum liquids, arXiv:1105.4621 [hep-th].
- [78] L. Huijse and S. Sachdev, Fermi surfaces and gauge–gravity duality, arXiv:1104.5022 [hep-th].
- [79] T. Senthil, S. Sachdev, and M. Vojta, Fractionalized Fermi liquids, *Phys. Rev. Lett.* **90** (2003), 216 403 [arXiv:cond-mat/0209144].

Index

AdS/CFT correspondence, *see gauge/gravity duality*
 Aichelberg–Sexl metric, 76, 291–293, 307–308, 310
 algebraically special solution, 213–229
 angular momentum, 10, 80, 104–106, 126–128, 149, 192
 angular velocity, 11, 12, 80, 116, 141, 149–150, 197, 373
 anti-de Sitter (AdS) spacetime, 14, 171, 325–327
 planar black hole, 15, 339, 359, 391, 398
 soliton, 375
 spherical black hole, 15, 328
 apparent horizon, 53–58, 161
 area theorem, 21, 120
 attractor mechanism, 303
 background field expansion, 314
 bicycling black rings, 152
 bifurcate Killing horizon, 23, 114, 119
 Birkhoff’s theorem, 16, 102
 black brane, 40, 122, 181, 184–187, 204–209, 339–342
 with Ramond–Ramond charge, 306
 black hole microstates, 318–320, 329, 338–339, 414
 black hole thermodynamics, 20–24, 32, 118–120, 122–123, 192–194, 284
 entropy, 24, 33, 73, 80, 119, 149, 192, 196, 293, 307, 318, 328–329, 339, 399, 405, 412
 first law, 23, 119, 150, 187, 193
 temperature, 24, 119, 142, 144, 186, 191, 307, 329, 398
 black ring, 124, 134–154, 199–201
 di-ring, 149–151
 doubly spinning, 145–148
 helical, 200–201
 singly spinning, 138–145
 black Saturn, 135, 148–151
 black string, 31–42, 45–65, 73, 139, 144, 199–200
 inhomogeneous, 85–95
 blackfolds, 180–209, 382

boost weight, 215
 Bose–Einstein condensate, 400, 405
 boundary stress tensor, 351, 362, 369–370
 BPS bound, 283
 BPS states, 281–285, 318–320, 342
 Breitenlohner–Freedman bound, 401
 bubble of nothing, 71, 215–217
 C-metric, 214
 Calabi–Yau geometry, 237
 Cauchy horizon, 7, 11, 114, 288
 causality violation, *see* closed timelike curves
 chemical potential, 395–398, 407
 Chern–Simons term, 280, 379
 closed timelike curves, 12, 111
 cobordism, 175
 Coleman–Mermin–Wagner theorem, 405
 conformal field theory (CFT), 327, 330, 357
 conformal Killing–Yano 2-form, 116, 228
 constraint damping, 50
 constraint equations, 47, 361
 correlated stability conjecture, 206
 cosmic censorship, 19–20, 42, 44, 59, 120, 234
 D-brane, 180–181, 209, 306, 317–318, 341–342
 de Sitter spacetime, 14, 90, 217
 deconfinement transition, 375–377
 dilaton, 299, 301–302, 311, 410–412
 dragging of inertial frames, 11
 dynamical critical exponent, 396, 402–405, 409
 Eddington–Finkelstein coordinates, 4, 48, 112–116, 365
 electron stars, 405–410
 energy condition
 dominant, 70, 160, 164
 null, 18, 21, 120, 164
 entropy, *see* black hole thermodynamics, entropy
 entropy current, 193, 357, 368–369, 378
 ergoregion, 12, 110–112, 130, 140, 260–262
 Euler characteristic, 171

Euler–Gibbs–Duhem relation, 187, 357
 excision, 47
 extremal limit, 8, 13, 75, 80, 114, 284, 398
 extrinsic curvature, 47, 185, 188, 209–210, 241, 369
 Fermi liquid theory, 392
 Fermi sea, 406
 Fermi surface, 388, 392, 394, 415
 fictitious boundary, 246–247, 259
 fluid/gravity correspondence, 348–384
 fractal, 58–60
 fractionalisation, 394, 414–415
 free energy, 338–339, 375, 391
 fundamental string, 307, 309
 gauge/gravity duality, 325–345, 388–392, 412
 geodesic congruence
 expansion, 21, 219
 rotation, 219
 shear, 21, 219
 Geroch–Held–Penrose (GHP) formalism, 224
 Gibbs–Duhem relation, 206, 357
 Goldberg–Sachs theorem, 217
 Goldstone boson, 388, 405
 Gregory–Laflamme instability, *see* instability, black string
 harmonic coordinates, 50, 239
 harmonic Einstein equation, 238–268
 Hartle–Hawking wavefunction, 335
 holographic superconductors, 400–405
 holography, *see* gauge/gravity duality
 Hopf fibration, 77
 horizon topology, 15, 18, 89–90, 101, 124–125, 134, 141, 159–177, 196–204
 hydrodynamics, 350–384
 superfluid, 379–380
 inner horizon, *see* Cauchy horizon
 instability
 black brane, 40, 205–207
 black ring, 152–154
 black string, 32–42, 54–65, 89
 spherical black hole, 94, 120–126
 Israel–Stewart formalism, 380
 Jacobi method, 248
 Kaluza–Klein monopole, 77, 292, 307
 Kerr solution, 10–13, 116, 213, 222, 228, 264
 Kerr–Schild metric, 115, 219
 Killing spinor, 281, 284
 Killing tensor, 117
 Kruskal coordinates, 5, 37–38, 40
 Kundt spacetimes, 221, 223
 Landau damping, 396
 Landau frame, 356
 large- N gauge theory, 329–331, 390–392
 lens space, 166
 Lichnerowicz operator, 34, 238
 negative mode, 251
 Lifshitz geometries, 402–405, 410–412
 Luttinger count, 414–415
 M2-brane, 290, 295
 M5-brane, 290, 374
 conformal diagram, 291
 Majumdar–Papapetrou solutions, 9, 285–288
 marginally outer-trapped surface (MOTS), 163–173
 mass, 69, 102, 126–128
 matched asymptotic expansion, 82, 183
 maximum principle, 245–247
 mean free length, 354
 mean free time, 354
 membrane paradigm, 381
 moduli, 303
 Myers–Perry black holes, 101–131, 196–199
 in anti-de Sitter, 101, 373
 in five dimensions, 128–131, 141–145
 Navier–Stokes equations, 358–359
 Neveu–Schwarz (NS) 5-brane, 308
 Neveu–Schwarz gauge field, 303
 Newman–Penrose (NP) formalism, 223
 Newton’s method, 253
 nonsingular solutions, 77, 291, 311
 nonuniqueness, 31, 142–145, 149
 null expansion scalars, 162–163
 null rotation, 215
 p-brane, 184, 186, 276
 peeling theorem, 219
 Penrose diagram, 5, 6, 7–10, 113, 115, 288, 291, 309, 326, 353
 Penrose inequality, 20
 phase transition
 first-order, 375, 409
 second-order, 401
 third-order, 409
 plasma ball, 376
 plasma tube, 376
 positive energy theorem, 70
 pressure, 186, 355, 359, 407
 principal null direction (PND), 213, 225
 quantum critical point, 393
 quasinormal modes, 17, 371–372, 383
 R-symmetry, 336
 Ramond–Ramond (RR) gauge fields, 303, 310

- Raychaudhuri equation, 21
 Rayleigh–Plateau instability, 46, 64, 376
 relativistic fluid dynamics, 353–359
 Ricci flow, 250–257
 Ricci soliton, 241–243
 Ricci–DeTurck flow, 250, 261
 rigidity of stationary black holes, 202, 262
 Robinson–Trautman spacetimes, 221
 S-duality, 311–312, 338
 singularity, 106–108, 129
 - conical, 71, 108, 139, 214, 293
 - coordinate, 4
 - curvature, 4
 - naked, 10, 13, 19, 59, 110, 114
 - null, 8, 309, 311, 404
 - ring, 11, 107, 113
 - spacelike, 4, 75, 115, 141
 - timelike, 7, 75, 113
 Smarr formula, 119, 150, 194
 smearing, 293
 sound waves, 205, 359, 371
 spinor, 224, 282–284
 stability, 17, 93–95, 124, 153, 206, 209, 400
 - of a surface, 170
 stability operator, 167
 string coupling, 302, 316, 330, 337
 string frame, 302
 string length, 302, 316, 331, 337
 string theory, 277, 297, 313–320, 330–331, 337–343, 348–349
 - closed strings, 317
 - open strings, 317
 super Yang–Mills (SYM) theory, 335, 390
 supercharges, 282
 superradiance, 13, 111, 401
 supersymmetry, 274, 281–285, 336
 surface gravity, 22, 84, 90, 119, 236
 T-duality, 312–313
 Tangherlini solution, 55, 102
 Taub–NUT instanton, 77, 292
 temperature, *see* black hole thermodynamics, temperature
 't Hooft coupling, 331
 't Hooft limit, 338, 348
 topological censorship, 18
 topology of horizon, *see* horizon topology
 transverse tracefree gauge, 34
 trapped surface, 19, 160–163
 ultra-spinning black hole, 109, 120–126, 195
 viscosity
 - bulk, 46, 206, 356
 - shear, 46, 206, 356, 370
 vorticity, 364, 378
 Weyl aligned null direction (WAND), 215–224
 Weyl covariant derivative, 364
 Wilson loop, 339
 Yamabe constant, 172
 Yamabe type, 165–166, 170, 177
 Yang–Mills theory, *see* super Yang–Mills theory